

Semi-Local Exchange-Correlation Approximations in Density Functional Theory

Fabien Tran,^{*,†} Susi Lehtola,^{*,‡} Stefano Pittalis,^{*,¶} and Miguel A. L. Marques^{*,§}

[†]*VASP Software GmbH, Berggasse 21/14, A-1090 Vienna, Austria*

[‡]*Department of Chemistry, University of Helsinki, P.O. Box 55 (A. I. Virtasen aukio 1), FI-00014 University of Helsinki, Finland*

[¶]*Istituto Nanoscienze, Consiglio Nazionale delle Ricerche, Via Campi 213A, I-41125 Modena, Italy*

[§]*Research Center Future Energy Materials and Systems of the University Alliance Ruhr and Interdisciplinary Centre for Advanced Materials Simulation, Ruhr University Bochum, Universitätsstraße 150, D-44801 Bochum, Germany*

E-mail: fabien.tran@vasp.at; susi.lehtola@alumni.helsinki.fi; stefano.pittalis@cnr.it; miguel.marques@rub.de

Abstract

Density functional theory has become the workhorse of modern electronic structure calculations, with wide-ranging applications in chemistry, physics, materials science, biochemistry, etc. At its heart lies the exchange-correlation functional, a quantity which exactly encapsulates the many-body effects stemming from the quantum mechanical interactions between the electrons. Yet, the exact functional is unknown, and computationally tractable approximations are therefore necessary for practical applications. Over the past six decades, hundreds of density functional approximations have been proposed with varying degrees of accuracy and computational efficiency.

This review surveys the theoretical foundations of semi-local functionals, including local density approximations, generalized gradient approximations, and meta-generalized gradient approximations. We provide a comprehensive, consistently organized discussion that consolidates both historical developments and recent advances in this field. Beginning with the essential concepts of Kohn–Sham density functional theory, we present the construction prin-

ciples of semi-local exchange-correlation functionals. Special attention is given to the physical motivations underlying functional development, the mathematical properties that guide their construction, and the practical considerations that determine their applicability across different chemical and physical systems. For each class of functionals, we trace their evolution from early prototypes to modern sophisticated forms, highlighting key innovations and the interplay between theoretical rigor and empirical fitting. We examine how successive rungs of Jacob’s ladder, from the local density approximation through generalized gradient approximations to meta-generalized gradient approximations, incorporate additional ingredients to improve accuracy while maintaining computational efficiency.

This work is intended to serve as both a introduction for newcomers to the field and a comprehensive reference for practitioners. By consolidating the extensive literature on semi-local functionals and providing a unified framework for understanding their construction and application, we aim to facilitate further developments in density functional approximations and their use in tackling the diverse challenges

of modern computational chemistry and condensed matter physics.

Abbreviations

1D	one-dimensional
2D	two-dimensional
3D	three-dimensional
DFT	density functional theory
EXX	exact exchange
GGA	generalized gradient approximation
HEG	homogeneous electron gas
HF	Hartree–Fock
KLI	Krieger–Li–Iafrate
KS	Kohn–Sham
LDA	local density approximation
LO	Lieb–Oxford
MC	Monte Carlo
MGGA	meta generalized gradient approximation
OEP	optimized effective potential
RPA	random-phase approximation
TDDFT	time-dependent density functional theory

Contents

Abstract	1
Abbreviations	2
1 Introduction	3
1.1 Preamble	3
1.2 Kohn–Sham DFT: The essentials	4
1.3 Hierarchy of functional approximations	7
1.4 Libxc: a libraries of exchange, correlation, and kinetic functionals	8

2 A dive into DFT	9
2.1 Units, constants and variables . . .	9
2.1.1 Units	9
2.1.2 Constants	9
2.1.3 Variables	10
2.2 Density functionals via constrained search	14
2.3 Bounds	15
2.4 Adiabatic connection formula . .	16
2.5 Hole functions	16
2.6 Correlation energy via response functions	18
2.7 Short-range behavior of the exchange-hole function and related quantities	19
2.8 Self-interaction free conditions . .	20
2.9 Scaling in DFT	21
2.10 High- and low-density limits of the homogeneous electron gas . .	22
2.11 Gradient-expansion approximations	23
2.12 Semiclassical expansion in the Lieb–Simon limit	25
2.13 From local to non-local xc potentials	25
2.14 Fundamental gaps	26
2.15 Electron-electron interaction in low-dimensional systems	28
2.16 Thermal DFT	28
2.17 Non-collinear spin-DFT	30
2.18 Enhancement factors and spin-resolved energies	31
2.18.1 Enhancement factors . . .	31
2.18.2 Spin resolved exchange and kinetic energy	32
2.18.3 Spin-resolved correlation energy	32
2.18.4 Systematic fits of density functionals	33
3 Semi-local xc approximations	33
3.1 Local-density approximation . . .	33
3.1.1 Exchange	34
3.1.2 Correlation	35
3.1.3 Exchange and correlation .	47
3.2 Generalized-gradient approximation	51
3.2.1 Exchange	51
3.2.2 Correlation	77

3.2.3 Exchange and correlation	91
3.3 Meta-generalized gradient approximation	97
3.3.1 Exchange	98
3.3.2 Correlation	127
3.3.3 Exchange and correlation	140
4 Conclusions and Outlook	142
CRedit statement	144
References	144

1 Introduction

1.1 Preamble

Density functional theory (DFT)^{1,2} has emerged as one of the most powerful and widely used computational methods in quantum chemistry and condensed matter physics due to its remarkable success in calculating ground-state properties, while maintaining a favorable balance between computational cost and accuracy. DFT has enabled unprecedented insights into electronic structure across an extensive range of systems. It is nowadays routinely used to guide experimental design and provide a fundamental understanding of chemical bonding and reactivity. The profound impact of DFT is evidenced by its widespread adoption across disciplines ranging from materials science to biochemistry.

The exchange-correlation (xc) energy functional^{2,3} is at the heart of DFT. This is a functional of the electron density that embodies the quantum mechanical many-body effects of the electron-electron interaction. Although the exact form of the xc functional remains unknown, it can be successfully approximated by assuming a semi-local dependence on the electron density. Advancements in the development of such approximations have expanded the applicability and accuracy of DFT calculations. The careful balance between physical insight and (more or less) empirical parameterization in these functionals has enabled systematic improvements in the description of electronic structure, which have given rise to the

celebrated status of DFT as an indispensable tool in modern computational science.

The development of xc functionals began with the local density approximation (LDA) in the 1960s,² relying on the known properties of the homogeneous electron gas (HEG).^{4,5} The LDA is the simplest and most fundamental type of functional: It approximates the xc energy at each point in space by that of the HEG of that local density. LDAs perform remarkably well for many properties despite their conceptual simplicity, and still remain used nowadays in some applications.

Generalized gradient approximations (GGAs), which incorporate the electron density gradient to better describe inhomogeneous systems, were proposed in the 1980s.⁶ GGAs were found early on to lead to good agreement with experiment for harmonic vibrational frequencies as well as excellent agreement for atomization energies,^{7,8} laying the ground for their later popularity. Crucially, Pople’s implementation of DFT in the GAUSSIAN program⁹ around the same time¹⁰ made DFT accessible to the broader chemistry community, catalyzing its widespread adoption. This combination of improved accuracy through GGAs and increased availability through user-friendly software established DFT as a practical tool for mainstream computational chemistry.

The 1990s saw the introduction of hybrid functionals, which combine exact exchange from Hartree–Fock (HF) theory with a semi-local xc term.^{11,12} These hybrid functionals marked a crucial step forward in accuracy (particularly for molecular systems), and established a new paradigm in functional design.

Recent years have witnessed the emergence of even more sophisticated approaches, including meta-GGA (MGGA) functionals^{13,14} that incorporate kinetic-energy density; range-separated hybrids¹⁵ that use a different fraction of exact exchange at short and long range, leading to an improved description of long-range interactions; local hybrids^{16,17} that adjust the fraction of exact exchange at each point in space; as well as double hybrid functionals^{18,19} that include correlation effects from wavefunction theory. More recent developments such as

machine-learning functionals^{20–24} have renewed the promise of increased accuracy and transferability.

Despite all of the aforementioned advances, the fundamental challenge of developing a truly universal functional remains. In this review, we examine the rich 60-year history of the development of xc approximations. Although several articles have reviewed xc functionals of DFT,^{25–31} we believe that there is still a need for an updated, comprehensive, and consistently organized review that consolidates the old and new developments and addresses the evolving landscape of this dynamic field.

Given the vast scope of the field, we restrict our discussion to semi-local xc functionals, specifically the LDA, GGA, and MGGA families, as semi-local functionals remain in many cases the workhorses of modern DFT calculations, especially for extended systems and large-scale applications. Although hybrid functionals, range-separated methods, double hybrids, etc. have demonstrated impressive accuracy for many applications, their inclusion would expand this review beyond practical bounds.

This review is organized as follows. We introduce some preliminary concepts that are important for constructing functionals in section 2.1.3. We begin with a brief introduction to DFT, outlining some relevant quantities and define our notation. Then, we present a collection of exact results that are referenced in subsequent sections.

We present an extensive listing of functionals in section 3, which is organized into the LDA, GGA and MGGA families. For clarity, we distinguish between exchange functionals, correlation functionals, and combined xc functionals, as the development of exchange functionals has often pursued paradigms that differ from those for correlation functionals. We present the functionals in chronological order, highlighting the historical connections between the various approximations. For each functional, we briefly explain the motivation behind its development, provide its definition, and offer a concise discussion of its applicability, usually summarizing results from the original work.

Unless otherwise stated, comments regarding the performance of each functional follow the original literature. We note, however, that many early assessments were conducted on the same data sets used during development, which can limit their generality from a modern perspective. Data sets were also rather small, covering only a restricted portion of chemical space, and sometimes not reflecting the true accuracy of certain functionals.³² Readers may wish to keep this context in mind when interpreting historical claims, particularly for more empirical approaches. Ideally, performance evaluations should be made close to the complete-basis-set limit so that conclusions reflect intrinsic functional behavior. Comparisons to experiment also depend on choices such as the relativistic treatment^{33–35} (non-relativistic, scalar-relativistic, four-component, pseudopotentials) and the numerical discretization.^{36–39} These issues, however, lie beyond the scope of this review and will not be discussed further.

We conclude in section 4 with a few remarks on the genealogy of the various functionals, their popularity, and future directions in the field.

1.2 Kohn–Sham DFT: The essentials

The conceptual foundations for density functional theory can be traced back to the seminal works of Thomas⁴⁰ and Fermi⁴¹, who proposed that the electron density could serve as the fundamental variable for describing quantum systems, eliminating the need for the many-body wavefunction. Although their original model that employed a local approximation for the kinetic energy and the classical electrostatic interaction proved too crude for practical chemistry, it established the revolutionary idea that the electron density contains all information about the ground state of a quantum system. Slater⁴² likewise realized that the HF exchange energy has a simple closed-form expression for the case of free electrons, and successfully applied this *approximate* scheme to atoms, molecules, and solids.

The breakthrough of DFT came in 1964,

when Hohenberg and Kohn¹ showed that the ground-state energy of a quantum-mechanical system of interacting electrons could indeed be determined in terms of a functional of the electronic density only. Shortly after, a paper by Kohn and Sham² (KS) proposed a way to determine this density and the corresponding energy in a way that is in principle exact.

The KS scheme turns out to be evocative of the HF approximation, and especially its approximated form by Slater⁴². The approach is deceptively simple, it exploits the fact that an interacting many-electron problem can be mapped onto an effective single-particle problem defined by a local potential $v_s(\mathbf{r})$:

$$\left[-\frac{1}{2}\nabla^2 + v_s(\mathbf{r}) \right] \psi_i(\mathbf{r}) = \varepsilon_i \psi_i(\mathbf{r}) \quad (1)$$

Above is the KS equation in the form it is usually written in DFT papers that deal with non-degenerate closed-shell systems. In this case, there is an equal number of spin-up and spin-down electrons $N_\uparrow = N_\downarrow$. Spin-up and spin-down here refer to the z -projection \hat{S}_z , which shares common eigenstates with the total spin (\hat{S}^2) operator. The description of degenerate ground states is possible in DFT as well^{43–47}, but this goes beyond the scope of this introduction.

Although practical, this implicit description of spin can make unclear the generalization of the expressions from DFT to *collinear* spin-DFT (see section 2.17); the more general (non-collinear) spin-polarized case will be discussed in sections 2.17 and 2.18. In particular, since we shall report most functional approximations directly for collinear spin-DFT, it is useful to include the spin index explicitly from the start.¹ Therefore, we rewrite eq. (1) as

$$\left[-\frac{1}{2}\nabla^2 + v_s(\mathbf{r}) \right] \psi_{i\sigma}(\mathbf{r}) = \varepsilon_{i\sigma} \psi_{i\sigma}(\mathbf{r}) \quad (2)$$

where $\sigma = \uparrow, \downarrow$.

Equation (2) stems from the assumption that

¹This also eliminates the laborious and error-prone task of tracing various factors of two and powers thereof in actual implementations.

the particle density for the ground state of the real system, $n(\mathbf{r})$, may be obtained from the ground state of a non-interacting system in the form of a single Slater determinant.² Therefore,

$$n(\mathbf{r}) = \sum_{\sigma} \sum_i f_{i\sigma} |\psi_{i\sigma}(\mathbf{r})|^2 \quad (3)$$

where $f_{i\sigma}$ are the occupation numbers of $\psi_{i\sigma}(\mathbf{r})$. Equation (2) also stresses that the original DFT of Hohenberg and Kohn has a single potential, v_s , which acts on both spin channels; as will become clear below, v_s is a functional of the *total* particle density. Therefore, $\varepsilon_{i\uparrow} = \varepsilon_{i\downarrow} = \varepsilon_i$ are the eigenvalues of the orbitals $\psi_{i\uparrow} = \psi_{i\downarrow} = \psi_i$.

The energy of the ground state is expressed as

$$E[n] = T_s[n] + \int d^3r n(\mathbf{r}) v_{\text{ext}}(\mathbf{r}) + E_{\text{Hxc}}[n] \quad (4)$$

Notice that here and below, the notation $[n]$ is used to denote a functional of the density n . For brevity this dependence is not stressed wherever not absolutely necessary; for example, we write $\psi_{i\sigma}(\mathbf{r})$ instead of $\psi_{i\sigma}[n](\mathbf{r})$ even though the solutions to eq. (2) carry the self-consistent dependence on n .

The first term on the right hand side of eq. (4),

$$T_s[n] = -\frac{1}{2} \sum_{\sigma} \sum_i \int d^3r f_{i\sigma} \psi_{i\sigma}^*(\mathbf{r}) \nabla^2 \psi_{i\sigma}(\mathbf{r}) \quad (5)$$

is the kinetic energy of the non-interacting KS system of eq. (2). The second term is the energy due to an external scalar potential acting on the electrons. The function $v_{\text{ext}}(\mathbf{r})$ usually contains the electrostatic potential exerted by the nuclei on the electrons in a molecule, but can also contain external electric or magnetic fields, or the confining potential in a quantum dot, for example. Next, we arrive to the crucial term in eq. (4),

$$E_{\text{Hxc}}[n] = E_{\text{H}}[n] + E_{\text{xc}}[n] \quad (6)$$

where

$$E_{\text{H}}[n] = \frac{1}{2} \int d^3r \int d^3r' \frac{n(\mathbf{r})n(\mathbf{r}')}{|\mathbf{r} - \mathbf{r}'|} \quad (7)$$

provides the classical electrostatic electron-electron interaction, commonly referred to as the Hartree (H) energy, and $E_{\text{xc}}[n]$ accounts for all the quantum mechanical many-body contributions beyond $E_{\text{H}}[n]$ and $T_{\text{s}}[n]$ (see eq. (106)).

Like $T_{\text{s}}[n]$, also $E_{\text{x}}[n]$ has an exact expression in terms of the KS orbitals $\psi_{i\sigma}$,

$$E_{\text{x}}[n] = -\frac{1}{2} \sum_{\sigma} \int d^3r \int d^3r' \frac{|\gamma_{\sigma}(\mathbf{r}, \mathbf{r}')|^2}{|\mathbf{r} - \mathbf{r}'|} \quad (8)$$

where

$$\gamma_{\sigma}(\mathbf{r}, \mathbf{r}') = \sum_i f_{i\sigma} \psi_{i\sigma}(\mathbf{r}) \psi_{i\sigma}^*(\mathbf{r}') \quad (9)$$

is the (spin-resolved) one-body reduced-density matrix of the KS determinant.

Even though the exact expression for $E_{\text{x}}[n]$ is known, it is often convenient to approximate both the exchange and correlation energies. This convenience is often not only numerical, but also theoretical: the artificial division between exchange and correlation is not really physical, and only arises due to our inability to solve the many-particle Schrödinger equation. In fact, semi-local approximations to both the exchange and correlation contributions often lead to significantly more accurate predictions than those obtained by using a semi-local correlation functional in combination with fully non-local exact exchange of eq. (8).

The potential felt by the KS electrons is obtained by combining the variational condition for the KS system with the one for the energy functional in eq. (4). As a result,

$$v_{\text{s}}(\mathbf{r}) = v_{\text{ext}}(\mathbf{r}) + v_{\text{H}}(\mathbf{r}) + v_{\text{xc}}(\mathbf{r}) \quad (10)$$

where the second term is the Hartree potential

$$v_{\text{H}}(\mathbf{r}) = \frac{\delta E_{\text{H}}[n]}{\delta n(\mathbf{r})} = \int d^3r' \frac{n(\mathbf{r}')}{|\mathbf{r} - \mathbf{r}'|} \quad (11)$$

and

$$v_{\text{xc}}(\mathbf{r}) = \frac{\delta E_{\text{xc}}[n]}{\delta n(\mathbf{r})} \quad (12)$$

is the xc potential. Since the KS equations, eq. (2), depend non-linearly on the density, they must be solved self-consistently: one starts with an initial guess for $v_{\text{s}}(\mathbf{r})$ or $\{\psi_i\}$ and iterates the scheme until convergence is reached.

Far away from the center of a neutral finite system, the xc potential decays as $-1/r$:^{48,49} a property that is already observed at the level of the exact exchange optimized effective potential (EXX-OEP).^{50,51} Exceptions are found along the nodal planes of the highest occupied orbitals in molecules.^{52,53}

We stress that the formulation of DFT discussed in this review is the one within the Born–Oppenheimer⁵⁴ approximation: the solution of the nuclear problem is decoupled from the solution of the many-electron problem. Thus, for brevity, we do not explicitly write the energy due to the interactions among the nuclei.² We note that DFT can be extended to approaches beyond the Born–Oppenheimer approximation, as well;⁵⁵ however, such theories are beyond the scope of the present review.

The KS approach is not the only way to use the framework of DFT. In fact, one can take its basic idea even further, and approximate T_{s} of eq. (4) as an *explicit* functional of the density and its derivatives. In this way, when combined with an LDA or a GGA for E_{xc} , the total energy E becomes an explicit functional of the density. The Rayleigh–Ritz variational principle then leads to a partial differential equation where the only unknown is n . The resulting scheme, usually called orbital-free DFT, is extraordinarily efficient, and can therefore be used to model huge systems. However, the kinetic energy term $T_{\text{s}}[n]$ is dominant in typical systems, and is similar in absolute value to that of the exactly known external potential term. Because of this, it is extremely difficult to develop sufficiently accurate approximations for

²For finite systems at *fixed* nuclear configuration, this energy is a trivial constant. The term must however be included in the optimization of the geometry and also be taken into account to retrieve the correct thermodynamic limit.

$T_s[n]$ only via n , but progress is ongoing.^{56–58}

1.3 Hierarchy of functional approximations

Except for a handful of toy systems, such as the ones studied in refs. 59 and 60, we do not know the *exact* expression for $E_{xc}[n]$ or $T_s[n]$ explicitly in terms of *solely* the particle density. In principle, one can calculate the exact functional from an exact solution of the many-particle Schrödinger equation,⁶¹ but since these solutions are prohibitively hard and expensive to calculate, approximations of $E_{xc}[n]$ are necessary for any practical usage. The importance of developing such approximations can hardly be exaggerated: the quality of the approximation to the xc terms effectively determines if DFT is a useful computational tool or not. More than 600 approximations for E_{xc} have been developed so far, forming what some researchers call the *zoo of xc functionals*.^{62,63}

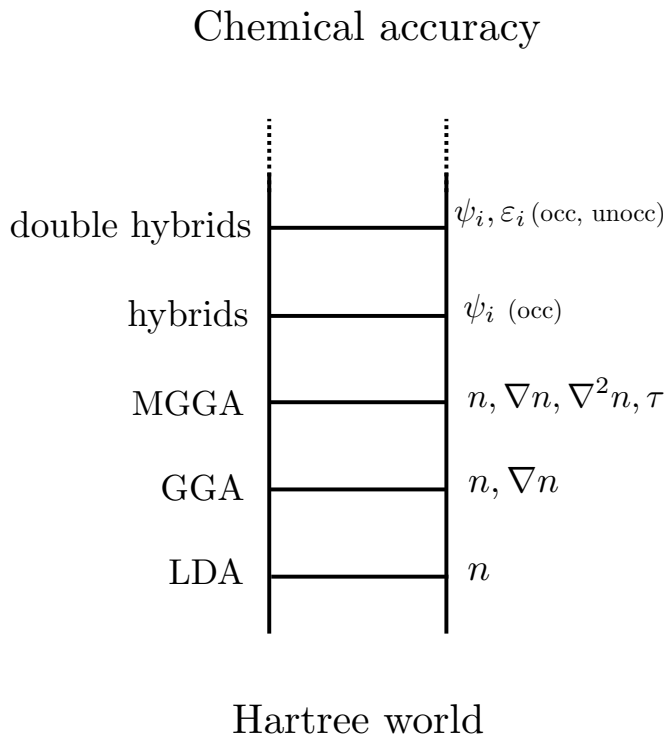


Figure 1: Jacob’s ladder of density functional approximations for the xc energy.

Expressions for $E_{xc}[n]$ are often given in terms

of xc-energy per electron, $e_{xc}(\mathbf{r})$,

$$E_{xc}[n] = \int d^3r n(\mathbf{r}) e_{xc}(\mathbf{r}) \quad (13)$$

or alternatively in terms of the xc-energy per volume, $\epsilon_{xc} = ne_{xc}$. $E_{xc}[n]$ can also be given via xc-hole functions or, more frequently, by a combination of the energy densities and enhancement factors (see more details below).³

Approximate functionals can be divided into families, depending on how they depend on the particle density and on the KS orbitals. In 2001, Perdew and Schmidt³ suggested to organize these families as successive rungs of a ladder (see fig. 1). At the bottom of the ladder we find the Hartree world, where the interaction between the electrons is approximated solely by the classical repulsion energy $E_H[n]$ defined in eq. (7), while $E_{xc}[n]$ is ignored. Climbing each rung leads to an increase in the complexity and computational cost of the functional, but should in principle also lead to higher accuracy. However, one should notice that it is not given that a functional belonging to a higher rung is *systematically* better than a functional from a lower rung. At the top of the ladder, one arrives at the *heaven of chemical accuracy*, defined as an error of 1 kcal/mol (43 meV/atom).⁶⁴ With this image in mind, Perdew and Schmidt³ baptized it *Jacob’s ladder* after the biblical dream of Jacob.

The first rung introduces the LDA, a functional that depends locally on the density only: $e_{xc}^{\text{LDA}}(\mathbf{r}) = e_{xc}(n(\mathbf{r}))$. Typically this utilizes estimations of the xc-energy of the HEG—a surprisingly good choice already proposed by Kohn and Sham² in 1965. This was the standard xc functional in the early decades of DFT, and even though its popularity has waned over the years, it still finds relevant applications in solid-state physics.

The second rung is occupied by the GGA, which sets $e_{xc}^{\text{GGA}}(\mathbf{r}) = e_{xc}(n(\mathbf{r}), \nabla n(\mathbf{r}))$. As compared to the LDA, the GGA adds the gra-

³There is, however, a large degree of ambiguity in the definition of the energy densities, as we can add any function $f(\mathbf{r})$ that satisfies $\int d^3r f(\mathbf{r}) = 0$ to ϵ_{xc} without changing the physical quantity E_{xc} . The choice of $f(\mathbf{r})$ is a *gauge freedom*.

cient of the density ∇n , a semi-local quantity that samples an infinitesimal region around \mathbf{r} , as a parameter to the energy density. There is a considerable amount of craftsmanship and physical/chemical intuition going into the creation of the function $e_{xc}^{GGA}(\mathbf{r})$, but also a fair extent of arbitrariness. It is therefore not surprising that a large number of forms have been proposed over the years.

Next, we find the MGGAs: $e_{xc}^{MGGa}(\mathbf{r}) = e_{xc}(n(\mathbf{r}), \nabla n(\mathbf{r}), \nabla^2 n(\mathbf{r}), \tau(\mathbf{r}))$. This form adds to the GGA a dependence on the Laplacian of the density $\nabla^2 n(\mathbf{r})$ and/or the kinetic-energy density $\tau = (1/2) \sum_{i\sigma} f_{i\sigma} \nabla \psi_{i\sigma}^* \cdot \nabla \psi_{i\sigma}$. Often, the dependence on $\nabla^2 n$ is omitted, and the functional only depends on τ . The MGGAs have become increasingly popular especially in the last two decades, as evidence has accumulated that they may be competitive against higher-level approximations. Subcategories of the MGGAs are discussed in section 3.3.

The next rung is populated by functionals that combine a semi-local functional and exact (or HF) exchange (see eq. (8)). These functionals can include the whole HF exchange term, or only a part of it. Moreover, the interaction kernel can be the bare Coulomb interaction or a screened version of it. Notorious examples of approximations belonging to this rung are the (global) hybrid functionals, range-separated hybrid functionals, and local hybrid functionals.

Finally, on the highest rung of Jacob’s ladder one finds functionals that depend on all (occupied and empty) KS orbitals and their eigenvalues.^{65,66} Perhaps the best known examples are the random-phase approximation^{67–71} (RPA), as well as double hybrids^{18,19}.

1.4 Libxc: a libraries of exchange, correlation, and kinetic functionals

The implementation and standardization of xc functionals has evolved significantly over the past decades. Earlier computational chemistry libraries provided access to only a few selected functionals but often suffered from inconsistent naming conventions and limited reusabil-

ity⁷² between different programs. Despite several earlier attempts at modularized DFT libraries,^{73–75} none became widely used and fell out of maintenance.

The situation improved considerably with the development of Libxc.^{76,77} Libxc is a comprehensive, portable library of xc and kinetic functionals for DFT calculations, now providing implementations of over 600 functionals ranging from LDAs to sophisticated MGGAs and global and range-separated hybrid functionals.⁴ Libxc has become the de facto standard in the computational chemistry and materials science communities, and is now used by over 50 electronic structure programs, including ABACUS,⁷⁸ ABINIT,⁷⁹ ACE-molecule,⁸⁰ ADF,⁸¹ APE,⁸² AtomPAW,⁸³ BAGEL,⁸⁴ BigDFT,⁸⁵ CASTEP,⁸⁶ ChronusQ,⁸⁷ CONQUEST,⁸⁸ CP2K,⁸⁹ CPMD,⁹⁰ deMon2k,⁹¹ DFT-FE,⁹² DFTK,⁹³ Elk,⁹⁴ ERKALE,⁹⁵ exciting,⁹⁶ FHI-aims,⁹⁷ FLEUR,⁹⁸ GAMESS (US),⁹⁹ GPAW,¹⁰⁰ HelFEM,¹⁰¹ HORTON,¹⁰² INQ,¹⁰³ JDFTx,¹⁰⁴ MADNESS,¹⁰⁵ MOLGW,¹⁰⁶ Molpro,¹⁰⁷ MRCC,¹⁰⁸ NWChem,¹⁰⁹ Octopus,¹¹⁰ OpenMolcas,¹¹¹ ORCA,¹¹² PROFESS,¹¹³ Psi4,¹¹⁴ PySCF,¹¹⁵ QuantumATK,¹¹⁶ Quantum Espresso,¹¹⁷ RMG,¹¹⁸ Serenity,¹¹⁹ Siam Quantum 2,¹²⁰ SIESTA,¹²¹ SIRIUS,¹²² TURBOMOLE,¹²³ VASP,¹²⁴ VeloxChem,¹²⁵ WIEN2k,¹²⁶ and yambo¹²⁷, for instance. The success of Libxc can be attributed to its rigorous implementation, extensive testing, and seamless integration with most electronic structure codes. Beyond simply providing functional implementations, Libxc serves as a crucial standardization tool by establishing consistent naming conventions and interfaces, thereby enhancing reproducibility and facilitating comparison of results across different computational frameworks. For example, it has been recently shown that the DFT literature is full of ambiguities that can lead to errors in the energy that can be detected in benchmark studies.¹²⁸

Libxc is the *raison d’être* of this review: the present effort is deeply tied to over a decade of Libxc development, which has resulted in an

⁴Note that Libxc only evaluates the semi-local component of the hybrid functionals.

extensive bibliography of functionals and a catalogue of functional forms. In this review we have aligned our nomenclature as closely as possible with that used in Libxc to provide a direct correspondence between the theoretical definitions presented here, their numerical implementations, and their practical usage in DFT codes.

2 A dive into DFT

In this section, we aim at fixing the notation and introducing DFT in relation to the construction of xc approximations. Our selection of the topics and the depth of the discussion is inspired by several excellent reviews^{25,31,129–135} and our own experience in the field. Although our presentation is somewhat tailored towards semi-local functionals, the concepts and results discussed herein have general valor. Note that pedagogical reviews of advanced mathematical topics not discussed in this review, such as the convex formulations of DFT and discussions of differentiability and v -representability, can be found elsewhere.^{136–140}

2.1 Units, constants and variables

The purpose of this section is to provide a glossary of the most common physical constants and variables used in the construction of xc functionals. This also provides us with the opportunity to unify the notation used in the definition of the approximate xc functionals. Before proceeding with this discussion, we need to specify the units employed in the work; these are specified in section 2.1.1. Next, constants that are frequently used across functionals are defined in section 2.1.2. The dependence of the various functionals on the density and the kinetic-energy density is usually expressed via intermediate variables, and the variables that are recurrently used are defined in section 2.1.3. Useful relations between these variables are also provided.

Sections 2.1.2 and 2.1.3 report quantities that are commonly used in the description of xc functionals. Quantities that are not comprised

in the aforementioned sections, but are necessary to specify functionals, are defined locally, as needed. Numerical values of parameters beyond the common ones are shown in the specific parts devoted to each approximations, if their number is relatively small; otherwise, the relevant references are cited.

2.1.1 Units

First of all, let us specify that we work in atomic units within the usual Hartree atomic units, i.e., the vacuum dielectric constant is set to be $\epsilon_0 = 1/4\pi$ and has no dimensions. In this unit system the numerical values of the Bohr radius (a_B), the (negative) of the electronic charge ($|e|$), the electronic mass (m_e), and the reduced Planck's constant (\hbar) are set to one:

$$a_B = 1, e^2 = 1, m_e = 1, \hbar = 1 \quad (14)$$

This sets three fundamental units, the atomic units (au) of length, mass, and charge:¹⁴¹

$$\text{au}_{\text{length}} = a_B = 5.29177210544(82) \times 10^{-11} \text{ m} \quad (15a)$$

$$\text{au}_{\text{mass}} = m_e = 9.1093837139(28) \times 10^{-31} \text{ kg} \quad (15b)$$

$$\text{au}_{\text{charge}} = e = 1.602176634 \times 10^{-19} \text{ C} \quad (15c)$$

Finally, we work in a system of units in which temperature is measured in energy units, i.e., $k_B = 1$.

2.1.2 Constants

The factor in the exchange energy of the HEG (eq. (257)) is^{142–144}

$$A_x = \frac{3}{4} \left(\frac{3}{2\pi} \right)^{2/3} \approx 0.458165 \quad (16)$$

When writing the exchange in the form given in eq. (256), the numerical prefactor is changed to^{142,143}

$$C_x = \frac{3}{2} \left(\frac{3}{4\pi} \right)^{1/3} = \frac{3}{4} \left(\frac{6}{\pi} \right)^{1/3} \approx 0.930526 \quad (17)$$

The factor in the exchange energy of the 2D HEG (eq. (264)) is¹⁴²⁻¹⁴⁵

$$A_x^{2D} = \frac{4\sqrt{2}}{3\pi} \approx 0.600211 \quad (18)$$

When writing the 2D exchange in the form given in eq. (263), the numerical prefactor is changed to:^{142,143,145}

$$C_x^{2D} = \frac{8}{3\sqrt{\pi}} \approx 1.504506 \quad (19)$$

The proportionality constant between the reduced density gradients $s_{(\sigma)}$ and $x_{(\sigma)}$ (eqs. (46) and (48)) is:

$$C_s = \frac{1}{2(6\pi^2)^{1/3}} \approx 0.128278 \quad (20)$$

C_s^2 is the proportionality constant between $q_{(\sigma)}$ and $u_{(\sigma)}$ in eqs. (61) and (62).

The proportionality constant between s_{σ}^{2D} and x_{σ}^{2D} in eq. (52) is

$$C_s^{2D} = \frac{1}{2\sqrt{4\pi}} \approx 0.141047 \quad (21)$$

The factor in the kinetic energy of the HEG (eqs. (68) and (70)) is^{40,41}

$$C_F = \frac{3}{10} (6\pi^2)^{2/3} \approx 4.557800 \quad (22)$$

The coefficient of the second-order s_{σ}^2 -term in the density-gradient expansion of screened exact exchange is¹⁴⁶

$$\mu^{\text{Sham}} = \frac{7}{81} \approx 0.086420 \quad (23)$$

The coefficient of the second-order s_{σ}^2 -term in the density-gradient expansion of exact exchange is¹⁴⁷

$$\mu^{\text{GE}} = \frac{10}{81} \approx 0.123457 \quad (24)$$

The coefficient of the second-order s_{σ}^2 -term in the density-gradient expansion of `gga_x_pbe` exchange is^{148,149}

$$\mu^{\text{PBE}} = \frac{\pi^2}{3} \beta^{\text{MB}} \approx 0.219515 \quad (25)$$

where $\beta^{\text{MB}} \approx 0.066725$ (see below). The parameter in `gga_x_pbe`^{148,149} derived from the Lieb–Oxford (LO) bound¹⁵⁰ is

$$\kappa^{\text{PBE}} = 0.804 \quad (26)$$

The Ma and Brueckner¹⁵¹ high-density limit of the coefficient of the second-order t^2 -term in the density-gradient expansion of exact correlation^{151,152} is

$$\beta^{\text{MB}} \approx 0.0667 \quad (27)$$

Note that there is some uncertainty in the literature about the precise value of β^{MB} . From refs. 152 and 151, $\beta^{\text{MB}} = 16(3/\pi)^{1/3} C_c(0) \approx 0.066726$, where $C_c(r_s = 0) = 0.004235$ (see `gga_c_p86`), while $\beta^{\text{MB}} \approx 0.066725$ is often quoted.

2.1.3 Variables

The electron density n in the spin-unpolarized case is given by

$$n(\mathbf{r}) = 2 \sum_i |\psi_i(\mathbf{r})|^2 \quad (28)$$

where we set $f_{\sigma i} = 1$ in eq. (3) and used the fact that the up and down channel share the same set of spatial orbitals ψ_i . In the spin-polarized case

$$n = n_{\uparrow} + n_{\downarrow} \quad (29)$$

where

$$n_{\sigma} = \sum_i f_{i\sigma} |\psi_{i\sigma}|^2 \quad (30)$$

and

$$n_{\uparrow} = n_{\downarrow} = \frac{n}{2} \quad (31)$$

when there is no spin-polarization. The spin-polarization ζ is defined as

$$\zeta = \frac{n_{\uparrow} - n_{\downarrow}}{n} \quad (32)$$

Conversely, the spin-up and spin-down densities can be solved from the total density n and spin-

polarization ζ as

$$n_{\uparrow} = \frac{n}{2}(1 + \zeta) \quad (33a)$$

$$n_{\downarrow} = \frac{n}{2}(1 - \zeta) \quad (33b)$$

Note that eqs. (33a) and (33b) yield

$$1 - \zeta^2 = 4 \frac{n_{\uparrow} n_{\downarrow}}{n^2} \quad (34)$$

The Wigner–Seitz radius r_s ¹⁴⁴ in the spin-unpolarized cases in 1D, 2D, and 3D are given by

$$r_s^{1D} = \frac{1}{2n} \quad (35a)$$

$$r_s^{2D} = \frac{1}{\sqrt{\pi n}} \quad (35b)$$

$$r_s^{3D} = \left(\frac{3}{4\pi n} \right)^{1/3} \quad (35c)$$

The spin-polarized case in 3D yields

$$r_{s\sigma}^{3D} = \left(\frac{3}{4\pi n_{\sigma}} \right)^{1/3} \quad (36)$$

and

$$r_{s\uparrow}^{3D} = r_{s\downarrow}^{3D} = 2^{1/3} r_s^{3D} \quad (37)$$

when there is no spin-polarization. As the 3D case is the most common one, for the rest of this work we will denote $r_s = r_s^{3D}$ and $r_{s\sigma} = r_{s\sigma}^{3D}$ for ease of notation. It is also useful to define the following scaled Wigner–Seitz radius \tilde{r}_s (3D spin-unpolarized case):

$$\tilde{r}_s = \left(\frac{1}{n} \right)^{1/3} = \left(\frac{4\pi}{3} \right)^{1/3} r_s \quad (38)$$

The density-dependent variable \tilde{v}_{σ} is given in the spin-polarized case as¹⁵³

$$\tilde{v}_{\sigma} = \frac{\omega_{\sigma} n_{\sigma}^{1/3}}{1 + \omega_{\sigma} n_{\sigma}^{1/3}} \quad (39)$$

The spin-scaling function ϕ_p is given by¹⁵⁴

$$\begin{aligned} \phi_p(\zeta) &= \frac{1}{2} [(1 + \zeta)^p + (1 - \zeta)^p] \\ &= 2^{p-1} \frac{n_{\uparrow}^p + n_{\downarrow}^p}{n^p} \end{aligned} \quad (40)$$

The dimensionless reduced density gradient x in the spin-unpolarized case in $m = 1, 2$, and 3 dimensions is given by^{155–157}

$$x^{mD} = \frac{|\nabla n|}{n^{\frac{m+1}{m}}} \quad (41)$$

while in the spin-polarized case, it is given by

$$x_{\sigma}^{mD} = \frac{|\nabla n_{\sigma}|}{n_{\sigma}^{\frac{m+1}{m}}} \quad (42)$$

and

$$x_{\uparrow}^{mD} = x_{\downarrow}^{mD} = 2^{1/m} x^{mD} \quad (43)$$

when there is no spin-polarization. We again drop the dimensional superscripts in the 3D case, $x = x^{3D}$ and $x_{\sigma} = x_{\sigma}^{3D}$ for ease of notation.

The following total and spin-averaged quantities can be defined from x_{σ} :

$$\begin{aligned} x_{\text{tot},p}^2 &= \frac{x_{\uparrow}^2(1 + \zeta)^p + x_{\downarrow}^2(1 - \zeta)^p}{2^{5/3}} \\ &= 2^{p-5/3} \frac{x_{\uparrow}^2 n_{\uparrow}^p + x_{\downarrow}^2 n_{\downarrow}^p}{n^p} \end{aligned} \quad (44)$$

$$x_{\text{avg}}^2 = \frac{1}{2} (x_{\uparrow}^2 + x_{\downarrow}^2) \quad (45)$$

In the 3D case $p = 5/3$, and once again $x_{\text{tot}} = x_{\text{tot},5/3}$ for ease of notation.

The dimensionless reduced density gradient s in 3D reads in the spin-unpolarized case as^{158,159}

$$s = \frac{|\nabla n|}{2nk_F} = 2^{1/3} C_s x = \left(\frac{3}{2\pi} \right)^{1/3} |\nabla r_s| \quad (46)$$

where the Fermi wave vector k_F is given by

$$k_F = (3\pi^2 n)^{1/3} \quad (47)$$

The spin-polarized case in 3D yields

$$s_\sigma = \frac{|\nabla n_\sigma|}{2n_\sigma k_{F\sigma}} = C_s x_\sigma \quad (48)$$

where

$$k_{F\sigma} = (6\pi^2 n_\sigma)^{1/3} \quad (49)$$

When there is no spin-polarization, the expressions reduce to

$$s_\uparrow = s_\downarrow = s \quad (50)$$

where

$$k_{F\uparrow} = k_{F\downarrow} = k_F \quad (51)$$

The spin-polarized case in 2D reads

$$s_\sigma^{2D} = C_s^{2D} x_\sigma^{2D} \quad (52)$$

The dimensionless reduced density gradient p is given in the spin-unpolarized case as

$$p = s^2 \quad (53)$$

and in the spin-polarized case as

$$p_\sigma = s_\sigma^2 \quad (54)$$

When there is no spin polarization,

$$p_\uparrow = p_\downarrow = p \quad (55)$$

The spin-polarized case in 2D is analogous

$$p_\sigma^{2D} = (s_\sigma^{2D})^2 \quad (56)$$

The dimensionless reduced density gradient t reads in the spin-polarized case as^{148,149}

$$\begin{aligned} t &= \frac{|\nabla n|}{2\phi_{2/3}(\zeta) k_s n} \\ &= \frac{x}{4 \times 2^{1/3} \phi_{2/3}(\zeta) \sqrt{r_s}} \end{aligned} \quad (57)$$

where $k_s = \sqrt{4k_F/\pi}$ is the Thomas–Fermi screening length.

The dimensionless reduced Laplacian of the density u reads in the spin-unpolarized case in $m = 1, 2$, and 3 dimensions as^{160,161}

$$u^{mD} = \frac{\nabla^2 n}{n^{\frac{m+2}{m}}} \quad (58)$$

while the spin-polarized case is

$$u_\sigma^{mD} = \frac{\nabla^2 n_\sigma}{n_\sigma^{\frac{m+2}{m}}} \quad (59)$$

and once again if there is no spin-polarization then

$$u_\uparrow^{mD} = u_\downarrow^{mD} = 2^{2/m} u^{mD} \quad (60)$$

We again drop the superscripts in the 3D case, $u = u^{3D}$ and $u_\sigma = u_\sigma^{3D}$, for ease of notation.

The dimensionless reduced Laplacian of the density q is given in the spin-unpolarized case as¹⁶²

$$q = \frac{\nabla^2 n}{4n k_F^2} = 2^{2/3} C_s^2 u \quad (61)$$

and in the spin-polarized case as

$$q_\sigma = \frac{\nabla^2 n_\sigma}{4n_\sigma k_{F\sigma}^2} = C_s^2 u_\sigma \quad (62)$$

while

$$q_\uparrow = q_\downarrow = q \quad (63)$$

when there is no spin-polarization.

The KS noninteracting kinetic-energy density τ^2 is given in the spin-unpolarized case as

$$\tau = \frac{1}{2} \sum_i \underline{f_i} \nabla \psi_i^* \cdot \nabla \psi_i \quad (64)$$

where we underline that the factor 1/2 is included in our definition, which is not always the case in the literature, many authors defining τ without this factor. The spin-polarized case reads analogously as

$$\tau = \tau_\uparrow + \tau_\downarrow \quad (65)$$

where

$$\tau_\sigma = \frac{1}{2} \sum_i \underline{f_{i\sigma}} \nabla \psi_{i\sigma}^* \cdot \nabla \psi_{i\sigma} \quad (66)$$

and when there is no spin-polarization the expressions reduce to

$$\tau_\uparrow = \tau_\downarrow = \frac{\tau}{2} \quad (67)$$

The Thomas–Fermi kinetic-energy density τ^{TF} is given in the spin-unpolarized case as^{40,41}

$$\tau^{\text{TF}}[n] = 2^{-2/3} C_F n^{5/3} \quad (68)$$

and in the spin-polarized case as

$$\begin{aligned}\tau^{\text{TF}}[n_{\uparrow}, n_{\downarrow}] &= \tau_{\uparrow}^{\text{TF}} + \tau_{\downarrow}^{\text{TF}} \\ &= \tau^{\text{TF}}[n] \phi_{5/3}(\zeta)\end{aligned}\quad (69)$$

where

$$\tau_{\sigma}^{\text{TF}} = C_{\text{F}} n_{\sigma}^{5/3} \quad (70)$$

When there is no spin-polarization, we have that

$$\tau_{\uparrow}^{\text{TF}} = \tau_{\downarrow}^{\text{TF}} = \frac{\tau^{\text{TF}}}{2} \quad (71)$$

The von Weizsäcker kinetic-energy density τ^{W} is given in the spin-unpolarized case as¹⁶³

$$\tau^{\text{W}}[n] = \frac{1}{8} \frac{|\nabla n|^2}{n} \quad (72)$$

and in the spin-polarized case as

$$\tau^{\text{W}}[n_{\uparrow}, n_{\downarrow}] = \tau_{\uparrow}^{\text{W}} + \tau_{\downarrow}^{\text{W}} \neq \tau^{\text{W}}[n] \quad (73)$$

where

$$\tau_{\sigma}^{\text{W}} = \frac{1}{8} \frac{|\nabla n_{\sigma}|^2}{n_{\sigma}} \quad (74)$$

When there is no spin-polarization, the expressions are

$$\tau_{\uparrow}^{\text{W}} = \tau_{\downarrow}^{\text{W}} = \frac{\tau^{\text{W}}}{2} \quad (75)$$

The dimensionless kinetic-energy variable \tilde{t} is given in the spin-unpolarized case in $m = 1, 2,$ and 3 dimensions by

$$\tilde{t}^{m\text{D}} = \frac{\tau}{n^{\frac{m+2}{m}}} \quad (76)$$

and in the spin-polarized case as

$$\tilde{t}_{\sigma}^{m\text{D}} = \frac{\tau_{\sigma}}{n_{\sigma}^{\frac{m+2}{m}}} \quad (77)$$

When there is no spin-polarization, the expressions are

$$\tilde{t}_{\uparrow}^{m\text{D}} = \tilde{t}_{\downarrow}^{m\text{D}} = 2^{2/m} \tilde{t}^{m\text{D}} \quad (78)$$

Once again, we drop the superscripts in the 3D case, $\tilde{t} = \tilde{t}^{3\text{D}}$ and $\tilde{t}_{\sigma} = \tilde{t}_{\sigma}^{3\text{D}}$ for ease of notation. Note that the above definitions of \tilde{t} and \tilde{t}_{σ} may differ from similar definitions used in other works, such as eq. (23) in ref. 164.

The dimensionless iso-orbital indicator α is

given in the spin-unpolarized case by^{165,166}

$$\alpha = \frac{\tau - \tau^{\text{W}}[n]}{\tau^{\text{TF}}[n]} \quad (79)$$

and in the spin-polarized case by

$$\alpha_{\sigma} = \frac{\tau_{\sigma} - \tau_{\sigma}^{\text{W}}}{\tau_{\sigma}^{\text{TF}}} \quad (80)$$

When there is no spin polarization we recover

$$\alpha_{\uparrow} = \alpha_{\downarrow} = \alpha_{\text{c}} = \alpha \quad (81)$$

Note that several variants of α that are not equivalent in the presence of spin-polarization may be used in correlation functionals. Besides the total density formulation (which is thus spin-unpolarized) of eq. (79) relying on eqs. (68) and (72), an alternative is for instance (the subscript "c" in α_{c} stands for correlation)

$$\alpha_{\text{c}} = \frac{\tau - \tau^{\text{W}}[n]}{\tau^{\text{TF}}[n_{\uparrow}, n_{\downarrow}]} \quad (82)$$

where $\tau^{\text{W}}[n]$ is still calculated from the spin-unpolarized formula (eq. (72)), but $\tau^{\text{TF}}[n_{\uparrow}, n_{\downarrow}]$ is instead calculated from the spin-polarized formula (eq. (69)).

The dimensionless iso-orbital indicator z is given in the spin-unpolarized case as^{13,14}

$$z = \frac{\tau^{\text{W}}}{\tau} \quad (83)$$

and in the spin-polarized case as

$$z_{\sigma} = \frac{\tau_{\sigma}^{\text{W}}}{\tau_{\sigma}} \quad (84)$$

When there is no spin-polarization, the expressions are

$$z_{\uparrow} = z_{\downarrow} = z \quad (85)$$

The dimensionless kinetic-energy variable \tilde{z} is given in the spin-unpolarized case as^{167,168}

$$\tilde{z} = 2 (\tilde{t} - 2^{-2/3} C_{\text{F}}) \quad (86)$$

and in the spin-polarized case as

$$\tilde{z}_{\sigma} = 2 (\tilde{t}_{\sigma} - C_{\text{F}}) \quad (87)$$

When there is no spin-polarization, we have that

$$\tilde{z}_\uparrow = \tilde{z}_\downarrow = 2^{2/3}\tilde{z} \quad (88)$$

A total quantity can also be defined from \tilde{z}_σ

$$\tilde{z}_{\text{tot}} = \tilde{z}_\uparrow + \tilde{z}_\downarrow \quad (89)$$

The dimensionless kinetic-energy variable w reads in the spin-unpolarized case as¹⁶⁴

$$w = \frac{\tau^{\text{TF}} - \tau}{\tau^{\text{TF}} + \tau} = \frac{C_F - 2^{2/3}\tilde{t}}{C_F + 2^{2/3}\tilde{t}} \quad (90)$$

and in the spin-polarized case as

$$w_\sigma = \frac{\tau_\sigma^{\text{TF}} - \tau_\sigma}{\tau_\sigma^{\text{TF}} + \tau_\sigma} = \frac{C_F - \tilde{t}_\sigma}{C_F + \tilde{t}_\sigma} \quad (91)$$

When there is no spin-polarization,

$$w_\uparrow = w_\downarrow = w \quad (92)$$

The relations between α , z and \tilde{t} can be written in the spin-unpolarized case as

$$\alpha = \frac{5}{3} \frac{1-z}{z} p = \frac{2^{2/3}}{C_F} \left(\tilde{t} - \frac{1}{8} x^2 \right) \quad (93a)$$

$$z = \frac{5p}{3\alpha + 5p} = \frac{1}{8} \frac{x^2}{\tilde{t}} \quad (93b)$$

$$\tilde{t} = \frac{C_F}{2^{2/3}} \alpha + \frac{1}{8} x^2 = \frac{1}{8} \frac{x^2}{z} \quad (93c)$$

and in the spin-polarized case as

$$\alpha_\sigma = \frac{5}{3} \frac{1-z_\sigma}{z_\sigma} p_\sigma = \frac{1}{C_F} \left(\tilde{t}_\sigma - \frac{1}{8} x_\sigma^2 \right) \quad (94a)$$

$$z_\sigma = \frac{5p_\sigma}{3\alpha_\sigma + 5p_\sigma} = \frac{1}{8} \frac{x_\sigma^2}{\tilde{t}_\sigma} \quad (94b)$$

$$\tilde{t}_\sigma = C_F \alpha_\sigma + \frac{1}{8} x_\sigma^2 = \frac{1}{8} \frac{x_\sigma^2}{z_\sigma} \quad (94c)$$

The paramagnetic spin-current density \mathbf{j}_σ is given by

$$\mathbf{j}_\sigma = \text{Im} \left[\sum_i f_{i\sigma} \psi_{i\sigma}^* \nabla \psi_{i\sigma} \right] \quad (95)$$

2.2 Density functionals via constrained search

According to the variational principle, the ground-state energy of a many-electron system can be computed as

$$E_0 = \min_{\Psi \rightarrow N} \langle \Psi | \hat{T} + \hat{W} + \hat{V}_{\text{ext}} | \Psi \rangle \quad (96)$$

where $\hat{T} = -(1/2) \sum_{i=1}^N \nabla_i^2$ is the many-electron kinetic-energy operator, \hat{W} is the Coulomb interaction

$$\hat{W} = \frac{1}{2} \sum_{i \neq j}^N \frac{1}{|\mathbf{r}_i - \mathbf{r}_j|} \quad (97)$$

and

$$\hat{V}_{\text{ext}} = \sum_{i=1}^N v_{\text{ext}}(\mathbf{r}_i) \quad (98)$$

represents the scalar external potential.

The search of the minimum (or an infimum) in eq. (96) is carried over the admissible N -representable wavefunctions, *i.e.*, normalizable many-electron wavefunctions that are antisymmetric under exchange of particles, since electrons are fermions. It is also understood that these wavefunctions fulfill the boundary conditions of the problem at hand.

First, note that for all admissible fermionic wavefunctions with particle density n (in brief, $\Psi \rightarrow n$), we can write

$$\langle \Psi | \hat{V}_{\text{ext}} | \Psi \rangle = \int d^3r n(\mathbf{r}) v_{\text{ext}}(\mathbf{r}) \quad (99)$$

since the scalar external potential is diagonal in position space as per eq. (98). Next, following Levy¹⁶⁹ and Lieb¹⁷⁰, eq. (96) can be split as:

$$\begin{aligned} E_0 &= \min_{n \rightarrow N} \left\{ \min_{\Psi \rightarrow n} \langle \Psi | \hat{T} + \hat{W} | \Psi \rangle \right. \\ &\quad \left. + \int d^3r n(\mathbf{r}) v_{\text{ext}}(\mathbf{r}) \right\} \\ &= \min_{n \rightarrow N} \left\{ F[n] + \int d^3r n(\mathbf{r}) v_{\text{ext}}(\mathbf{r}) \right\} \end{aligned} \quad (100)$$

where, in the first line, the external minimization is carried out over particle density for N

fermions (i.e., N -representable n). In the second line of eq. (100), the functional of the particle density

$$F[n] = \langle \Psi[n] | \hat{T} + \hat{W} | \Psi[n] \rangle \quad (101)$$

is employed, where $\Psi[n]$ minimizes $\langle \Psi | \hat{T} + \hat{W} | \Psi \rangle$ for a given density n . $F[n]$ is often referred to as the *universal* functional, in a sense that it does not depend explicitly on the external potential and is, thus, not specific to a particular system. The Hohenberg–Kohn functional is obtained by restricting $F[n]$ to v -representable ground-state densities, i.e., densities obtained from the ground state of a potential.

Approaching practical applications, it is crucial to decompose $F[n]$ as

$$F[n] = T_s[n] + E_{\text{Hxc}}[n] \quad (102)$$

where

$$\begin{aligned} T_s[n] &\equiv \min_{\Psi \rightarrow n} \langle \Psi | \hat{T} | \Psi \rangle \\ &= \min_{\Psi_s \rightarrow n} \langle \Psi_s | \hat{T} | \Psi_s \rangle \\ &= \langle \Psi_s[n] | \hat{T} | \Psi_s[n] \rangle \end{aligned} \quad (103)$$

is the kinetic energy of the non-interacting KS wavefunction $\Psi_s[n]$, while the remainder is by definition the Hartree-exchange-correlation energy functional $E_{\text{Hxc}}[n]$ ⁵.

The Hartree-exchange component estimates the electron-electron interaction using the KS single Slater determinant state $|\Psi_s\rangle$ formed from orthonormal single-particle states

$$E_{\text{Hx}}[n] = \langle \Psi_s[n] | \hat{W} | \Psi_s[n] \rangle \quad (104)$$

It is simple to verify that

$$\langle \Psi_s[n] | \hat{W} | \Psi_s[n] \rangle = E_{\text{H}}[n] + E_{\text{x}}[n] \quad (105)$$

where $E_{\text{H}}[n]$ and $E_{\text{x}}[n]$ are given by eqs. (7) and (8), respectively. Hence, the correlation

⁵Notice that the step from the first to the second line in eq. (103) stresses the fact that the search can be restricted to non-interacting wave-functions as the interaction is not involved in the prescribed minimization.

component is given by

$$\begin{aligned} E_c[n] &= \langle \Psi[n] | \hat{T} + \hat{W} | \Psi[n] \rangle - E_{\text{Hx}}[n] - T_s[n] \\ &= \left(\langle \Psi[n] | \hat{W} | \Psi[n] \rangle - E_{\text{Hx}}[n] \right) \\ &\quad + \left(\langle \Psi[n] | \hat{T} | \Psi[n] \rangle - T_s[n] \right) \\ &= W_c[n] + T_c[n] \end{aligned} \quad (106)$$

Equations (104) and (106) show that the correlation energy functional of KS-DFT has not only an interaction component $W_c[n]$, but also a kinetic component $T_c[n]$.

2.3 Bounds

Via the constrained search one can readily verify that

$$T_c[n] \geq 0 \quad \text{and} \quad E_c[n] \leq 0 \quad (107)$$

and trivially, $E_{\text{H}}[n] > 0$ and $E_{\text{x}}[n] < 0$. Thus, also the sum of exchange and correlation energies must be negative

$$E_{\text{xc}}[n] < 0 \quad (108)$$

In view of eqs. (106) and (107), $W_c[n]$ must be non-positive, $W_c[n] \leq 0$. It then trivially also follows that

$$E_{\text{x}}[n] \geq E_{\text{xc}}[n] \quad (109)$$

A less trivial bound was derived by Lieb and Oxford.^{150,171} The LO bound states that the so-called indirect electron-electron interaction $\widetilde{W}[\Psi] = \langle \Psi | \hat{W} | \Psi \rangle - E_{\text{H}}[n_{\Psi}]$ (where n_{Ψ} denotes the density of Ψ) has a lower bound that can be expressed as

$$\widetilde{W}[\Psi] \geq -C_{\text{LO}} \int d^3r n_{\Psi}^{4/3}(\mathbf{r}) \quad (110)$$

In the original derivation of Lieb¹⁷¹ $C_{\text{LO}} \approx 8.52$, which was then lowered by Lieb and Oxford¹⁵⁰ to $C_{\text{LO}} \approx 1.6787$ and by Chan and Handy¹⁷² to $C_{\text{LO}} \approx 1.6358$. The bound is approached in the low-density limit.^{173–176} Seidl et al.¹⁷⁷ suggested a possible range of values as $1.4119 \leq C_{\text{LO}} \leq 1.6358$. Lewin et al.¹⁷⁸ have recently reported the value of $C_{\text{LO}} \approx 1.58$.

The latter work also established that the constant can be reduced to 1.25 for HF states. For one-electron densities there is a specific bound with $C_{\text{LO}}^{(1e)} \approx 1.092$,¹⁷⁹ and for opposite-spin two-electron densities $C_{\text{LO}}^{(2e)} \approx 1.234$.¹⁵⁰

Equation (110) implies a bound for the xc-energies.¹⁸⁰ To see this, first express the right-hand side via the exchange LDA,

$$\widetilde{W}[\Psi] \geq \lambda_{\text{LO}} E_{\text{x}}^{\text{LDA}}[n_{\Psi}] \quad (111)$$

where $\lambda_{\text{LO}} = (4/3)(\pi/3)^{1/3} C_{\text{LO}}$. The left-hand side can be restated in terms of density functionals as

$$E_{\text{x}}[n] + W_{\text{c}}[n] \geq \lambda_{\text{LO}} E_{\text{x}}^{\text{LDA}}[n] \quad (112)$$

Since $T_{\text{c}}[n]$ is non-negative,

$$E_{\text{xc}}[n] \geq E_{\text{x}}[n] + W_{\text{c}}[n] \geq \lambda_{\text{LO}} E_{\text{x}}^{\text{LDA}}[n] \quad (113)$$

In view of eq. (113), numerical analyses have highlighted the usefulness of considering tighter bounds for the xc energies of many-electron systems of common chemical interest.^{175,181,182}

Although the LO bound is valid for *integrated* energies, it has been often used locally at the level of xc-energy *densities*. This is clearly a sufficient but not a necessary condition to fulfill the correct bound. In fact, the condition is violated, e.g., in the asymptotic region of any finite system.^{29,183–186}

Equation (110) can be extended to lower spatial dimensions^{176,187,187–189} D . Based on scaling considerations, one must replace $n^{4/3}$ with $n^{1+1/D}$. However, note that the 1D case requires extra care.¹⁸⁹

2.4 Adiabatic connection formula

To design approximations for the xc energy, it is important to derive formal representations of the exact functional that can reveal useful information on the structure and behavior of the exact functional.

The so-called adiabatic connection expresses the possibility to smoothly link the KS system to the real interacting system.^{65,190–192} The strength of the interaction is varied between

$\lambda = 0$ and $\lambda = 1$ and, correspondingly, the one-body potential $\hat{V}(\lambda)$ is varied in such a way to keep the ground-state particle density unchanged and equal to n . Assuming that the ground state varies smoothly and preserves its symmetry, it is clear that $\hat{V}(\lambda = 0) = \hat{V}_{\text{s}} = \sum_{i=1}^N v_{\text{s}}(\mathbf{r}_i)$ and $\hat{V}(\lambda = 1) = \hat{V}_{\text{ext}}$. Next, writing the trivial identity

$$E_{\text{Hxc}}[n] = \int_0^1 d\lambda \frac{d}{d\lambda} \langle \Psi^\lambda[n] | \lambda \hat{W} | \Psi^\lambda[n] \rangle \quad (114)$$

one arrives at the expression

$$E_{\text{Hxc}}[n] = \int_0^1 d\lambda W^\lambda[n] \quad (115)$$

with the Hellmann–Feynman theorem.^{193,194} Equation (115) is the adiabatic connection formula: it captures both kinetic and interaction contributions (see remark below eq. (106)) via λ -dependent interactions $W^\lambda[n]$.

Notice that

$$\begin{aligned} W^\lambda[n] &= \langle \Psi^\lambda[n] | \hat{W} | \Psi^\lambda[n] \rangle \\ &= \frac{1}{2} \int d^3 r \int d^3 r' \frac{\rho_2^\lambda(\mathbf{r}, \mathbf{r}')}{|\mathbf{r} - \mathbf{r}'|} \end{aligned} \quad (116)$$

where

$$\begin{aligned} \rho_2^\lambda(\mathbf{r}, \mathbf{r}') &= N(N-1) \sum_{\sigma, \sigma'} \prod_{i=3}^N \int d^3 \mathbf{x}_i \\ &\times |\Psi^\lambda(\mathbf{r}\sigma, \mathbf{r}'\sigma', \mathbf{x}_3, \dots, \mathbf{x}_N)|^2 \end{aligned} \quad (117)$$

represents the distribution of the electron pairs in the system with coupling strength λ . Here, normalization is such that $\rho_2^\lambda(\mathbf{r}, \mathbf{r}')$ yields *twice* the number of electron pairs.

Importantly, eq. (116) shows that an approximation for $E_{\text{Hxc}}[n]$ does not necessarily require a model for the *full* Ψ^λ —it *only* requires a model for the λ -dependent pair correlation function $\rho_2^\lambda(\mathbf{r}, \mathbf{r}')$.

2.5 Hole functions

Hole functions are ingenious mathematical tools^{195,196} for setting up useful models of the

pair correlation function $\rho_2^\lambda(\mathbf{r}, \mathbf{r}')$ to be used in eqs. (115) and (116). One starts with the expression

$$\rho_2^\lambda(\mathbf{r}, \mathbf{r}') = n(\mathbf{r})n(\mathbf{r}') + n(\mathbf{r})h^\lambda(\mathbf{r}, \mathbf{r}') \quad (118)$$

The first term leads to $E_H[n]$, but alone it miscounts the number of electron pairs. The second term in eq. (118) enforces the correct counting of the pairs, thus

$$\int d^3r' h^\lambda(\mathbf{r}, \mathbf{r}') = -1 \quad (119)$$

Equation (119) can be interpreted by saying that $h^\lambda(\mathbf{r}, \mathbf{r}')$ describes how one particle is depleted around each reference position \mathbf{r} , leading to the name of *hole* function.

At $\lambda = 0$ we obtain for the KS determinant

$$\rho_{2,s}(\mathbf{r}, \mathbf{r}') = n(\mathbf{r})n(\mathbf{r}') + n(\mathbf{r})h_x(\mathbf{r}, \mathbf{r}') \quad (120)$$

where

$$h_x(\mathbf{r}, \mathbf{r}') = -\frac{\sum_\sigma |\gamma_\sigma(\mathbf{r}, \mathbf{r}')|^2}{n(\mathbf{r})} \leq 0 \quad (121)$$

is the exchange-hole function. Readily, $h_x(\mathbf{r}, \mathbf{r}) = -n(\mathbf{r})$. Thus, the exchange energy is obtained as

$$E_x[n] = \frac{1}{2} \int d^3r \int d^3r' \frac{n(\mathbf{r})h_x(\mathbf{r}, \mathbf{r}')}{|\mathbf{r} - \mathbf{r}'|} \quad (122)$$

(see also eq. (8)). Any accurate model for $h_x(\mathbf{r}, \mathbf{r}')$ must fulfill eq. (119) and thus satisfy

$$\int d^3r' h_x(\mathbf{r}, \mathbf{r}') = -1 \quad (123)$$

as can be easily verified using eq. (121).

Similarly, the correlation energy can be expressed in terms of the correlation-hole function

$$E_c[n] = \frac{1}{2} \int d^3r \int d^3r' \frac{n(\mathbf{r})h_c(\mathbf{r}, \mathbf{r}')}{|\mathbf{r} - \mathbf{r}'|} \quad (124)$$

via the coupling constant integration

$$h_c(\mathbf{r}, \mathbf{r}') = \int_0^1 d\lambda [h^\lambda(\mathbf{r}, \mathbf{r}') - h_x(\mathbf{r}, \mathbf{r}')] \quad (125)$$

(see eqs. (115) and (116)). Since $h_x(\mathbf{r}, \mathbf{r}')$ al-

ready fulfills eq. (119), it readily follows that

$$\int d^3r' h_c(\mathbf{r}, \mathbf{r}') = 0 \quad (126)$$

The exchange-only approximation trivially satisfies eq. (126) by setting the correlation hole identically to zero.

Approximations of xc-energies obtained through hole functions only require modeling a function of the interparticle distance u ($\mathbf{u} = \mathbf{r}' - \mathbf{r}$) at each reference point \mathbf{r} . Specifically,

$$E_{xc} = 4\pi \int d^3r n(\mathbf{r}) \int du u h_{xc}(\mathbf{r}, u) \quad (127)$$

where

$$h_{xc}(\mathbf{r}, u) = \int \frac{d\Omega_{\mathbf{u}}}{4\pi} h_{xc}(\mathbf{r}, \mathbf{r} + \mathbf{u}) \quad (128)$$

is the spherical average of $h_{xc}(\mathbf{r}, \mathbf{r}')$ around \mathbf{r} , obtained by integration over all possible interparticular solid angles $\Omega_{\mathbf{u}}$.

A further reduction in the model can be introduced by working at the level of the system average

$$h_{xc}(u) = \frac{1}{N} \int d^3r \int \frac{d\Omega_{\mathbf{u}}}{4\pi} n(\mathbf{r})h_{xc}(\mathbf{r}, \mathbf{r} + \mathbf{u}) \quad (129)$$

from which

$$E_{xc} = 4\pi N \int du u h_{xc}(u) \quad (130)$$

Accurate approximations of the xc-hole functions should reproduce not only the exchange and correlation sum rules discussed above (eqs. (123) and (126)), but also the correct behavior at small u . Due to the singular behavior of the Coulomb interaction in this limit, the hole function develops a cusp at $u = 0$ such that^{197–200}

$$\left. \frac{\partial h(\mathbf{r}, u)}{\partial u} \right|_{u=0} = \lambda [n(\mathbf{r}) + h^\lambda(\mathbf{r}, u = 0)] \quad (131)$$

while the non-interacting component ($\lambda = 0$) yields no contribution.

Finally, also notice that in the conventional gauge,^{201,202} the xc-energy density per particle

of eq. (13) is related to the xc-hole as follows

$$e_{\text{xc}}(\mathbf{r}) = \frac{1}{2} \int d^3r' \frac{h_{\text{xc}}(\mathbf{r}, \mathbf{r}')}{|\mathbf{r} - \mathbf{r}'|} \quad (132)$$

Far away from the center of a finite system, $e_{\text{xc}}(\mathbf{r})$ exhibits a $-1/(2r)$ behavior; a property that is already captured at the level of exact exchange.^{157,203}

2.6 Correlation energy via response functions

Correlation energies can be defined by exploiting the theory of linear response of a system, initially at equilibrium, to a time-dependent perturbation. The approach can provide accurate correlation energies, potentials, and ionization potentials^{69,204–207}. It can also capture van der Waals interaction from first principles.^{208–212} The essential facts go as follows.

Time-dependent DFT (TDDFT) determines the time-dependent particle density of an interacting system, $n(\mathbf{r}, t)$, via solution of a time-dependent KS equation^{213,214}

$$i \frac{\partial}{\partial t} \psi_i(\mathbf{r}, t) = \left[-\frac{1}{2} \nabla^2 + v_s(\mathbf{r}, t) \right] \psi_i(\mathbf{r}, t) \quad (133)$$

where t denotes the time variable, and spin indices are implicit. The time-dependent effective KS potential in eq. (133) is $v_s(\mathbf{r}, t) = v_{\text{ext}}(\mathbf{r}, t) + v_{\text{H}}(\mathbf{r}, t) + v_{\text{xc}}(\mathbf{r}, t)$, where $v_{\text{ext}}(\mathbf{r}, t)$ is the external time-dependent potential, which is usually the static external potential of the ground state problem (see section 1.2) plus an extra time-dependent external scalar field; $v_{\text{H}}(\mathbf{r}, t)$ is the Hartree potential evaluated on the instantaneous particle density; and $v_{\text{xc}}(\mathbf{r}, t)$ is the time-dependent xc-potential.

Notice that eq. (133) must be solved for the time-evolved KS orbitals that are occupied initially, *i.e.*, at $t = 0$. Also, it should be stressed that $v_{\text{xc}}(\mathbf{r}, t)$ depends on the *history* of the evolution of the particle density besides depending on the initial many-body states; this is to say that *it has a memory*.^{215,216} The adiabatic approximation of TDDFT employs ground-state xc potentials, and thus neglects this memory. If the initial conditions refer to a ground state,

the dependence on the initial states can be expressed via a functional dependence on the ground-state particle density.²¹⁷

In particular, TDDFT can be used to compute the response of the particle density $n \rightarrow n + \delta n$ to a perturbation $v \rightarrow v + \delta v$. The linear response function χ of the interacting system can be expressed in terms of the linear response function of the KS system χ_s . We thus obtain the Dyson-like equation:^{218,219}

$$\chi(\mathbf{r}, \mathbf{r}'; \omega) = \chi_s(\mathbf{r}, \mathbf{r}'; \omega) + \int d^3r_1 \int d^3r_2 \times \chi_s(\mathbf{r}, \mathbf{r}_1; \omega) f_{\text{Hxc}}(\mathbf{r}_1, \mathbf{r}_2; \omega) \chi(\mathbf{r}_2, \mathbf{r}'; \omega) \quad (134)$$

where

$$f_{\text{Hxc}}(\mathbf{r}, \mathbf{r}'; \omega) = \int d(t - t') e^{i\omega(t-t')} \times \frac{\delta v_{\text{Hxc}}[n](\mathbf{r}, t)}{\delta n(\mathbf{r}', t')} \Big|_{n(\mathbf{r})} \quad (135)$$

is the Fourier transformed Hartree-xc kernel⁶ and ω is the frequency. The functional dependence on the *memory* is reflected in a non-trivial frequency dependence of the kernel.

Aiming to compute the correlation energy, eq. (135) is evaluated on an initial ground-state density $n(\mathbf{r})$. The next crucial step is to realize that the pair function

$$\rho_2^\lambda(\mathbf{r}, \mathbf{r}') = \langle \Psi^\lambda | \hat{n}(\mathbf{r}) \hat{n}(\mathbf{r}') | \Psi^\lambda \rangle - \delta(\mathbf{r}' - \mathbf{r}) \langle \Psi^\lambda | \hat{n}(\mathbf{r}) | \Psi^\lambda \rangle \quad (136)$$

(see also eq. (117)) is closely related to the (time-ordered) density-density response function

$$i\chi^\lambda(\mathbf{r}, t; \mathbf{r}', t') = \langle \Psi^\lambda | T [\hat{n}(\mathbf{r}, t) \hat{n}(\mathbf{r}', t')] | \Psi^\lambda \rangle - \langle \Psi^\lambda | \hat{n}(\mathbf{r}) | \Psi^\lambda \rangle \langle \Psi^\lambda | \hat{n}(\mathbf{r}') | \Psi^\lambda \rangle \quad (137)$$

where $\hat{n}(\mathbf{r}) = \sum_{i=1}^N \delta(\mathbf{r} - \hat{\mathbf{r}}_i)$ is the particle density operator, T is the Wick time-ordering operator that orders the operators with larger time to the right, and λ is the strength of the interaction for a system along the adiabatic coupling

⁶We follow the common convention to use the same symbol for a time-dependent quantity and its Fourier transform.

path introduced in section 2.4. Eventually, one arrives at the expression of the fluctuation-dissipation theorem

$$\begin{aligned}\rho_{2,c}^\lambda(\mathbf{r}, \mathbf{r}') &= \rho_2^\lambda(\mathbf{r}, \mathbf{r}') - \rho_{2,s}(\mathbf{r}, \mathbf{r}') \\ &= - \int_{-\infty}^{+\infty} \frac{d\omega}{2\pi i} \Delta\chi^\lambda(\mathbf{r}, \mathbf{r}'; \omega)\end{aligned}\quad (138)$$

where $\rho_2^{\lambda=0} = \rho_{2,s}$ and $\Delta\chi^\lambda(\mathbf{r}, \mathbf{r}'; \omega) \equiv \chi^\lambda(\mathbf{r}, \mathbf{r}'; \omega) - \chi_s(\mathbf{r}, \mathbf{r}'; \omega)$. Substituting eq. (138) in eq. (124) (see also eq. (118)), one obtains the adiabatic-connection fluctuation-dissipation (ACFD) formula:^{65,191}

$$E_c = - \int d^3r \int d^3r' \int_0^1 d\lambda \int_0^{+\infty} \frac{d\omega}{2\pi} \frac{\Delta\chi^\lambda(\mathbf{r}, \mathbf{r}'; i\omega)}{|\mathbf{r} - \mathbf{r}'|}\quad (139)$$

where we have taken into account that the response functions are even in ω and, because they do not have poles in the upper half of the ω -plane for $\text{Re}(\omega) \geq 0$, the integral can be performed over imaginary frequencies. In this way, poles need no further consideration and integration become numerically easier.⁷

Equation (139) is an exact expression for the correlation energy. Approximations can be devised by using the Dyson-like equation

$$\begin{aligned}\chi^\lambda(\mathbf{r}, \mathbf{r}'; \omega) &= \chi_s(\mathbf{r}, \mathbf{r}'; \omega) + \int d^3r_1 \int d^3r_2 \\ &\times \chi_s(\mathbf{r}, \mathbf{r}_1; \omega) f_{\text{Hxc}}^\lambda(\mathbf{r}_1, \mathbf{r}_2; \omega) \chi^\lambda(\mathbf{r}_2, \mathbf{r}'; \omega)\end{aligned}\quad (140)$$

which, essentially, defines f_{Hxc}^λ . For consistency, $f_{\text{xc}}^{\lambda=0} = 0$, $f_{\text{xc}}^{\lambda=1} = f_{\text{xc}}$, and $f_{\text{H}}^\lambda \equiv \lambda/|\mathbf{r} - \mathbf{r}'|$. The simplest approximation is already of great importance. This is the *direct* random-phase approximation (dRPA),^{65,191,220} also denoted as RPA when confusion may not arise, in which $f_{\text{Hxc}}^\lambda(\mathbf{r}_1, \mathbf{r}_2; \omega) \approx f_{\text{H}}^\lambda$, i.e. both exchange and correlation contributions (and, thus, also the ω -dependence) are neglected. dRPA is not free from self-interaction and does not account for the fermionic anti-symmetry. The next logical step is to add exchange by switching from a time-dependent Hartree to the time-dependent

⁷Along the imaginary axis the response functions are real valued.

Hartree *plus* exchange formalism.²⁰⁶ Progress along these lines has been reviewed in refs. 69, 204, and 205.

2.7 Short-range behavior of the exchange-hole function and related quantities

Features of the exchange-hole function provide us with important information on the electronic structure of a system. First, notice that the exchange energy (see eqs. (122) and (243))

$$E_x[n] = \sum_\sigma \int d^3r n_\sigma(\mathbf{r}) e_{x\sigma}(\mathbf{r})\quad (141)$$

can be expressed in terms of spin-resolved exchange holes, $h_{x\sigma}(\mathbf{r}, \mathbf{r}')$, as follows

$$e_{x\sigma}(\mathbf{r}) = \frac{1}{2} \int d^3r' \frac{h_{x\sigma}(\mathbf{r}, \mathbf{r}')}{|\mathbf{r} - \mathbf{r}'|}\quad (142)$$

where, similarly to eqs. (121) and (123), $h_{x\sigma}(\mathbf{r}, \mathbf{r}') = -|\gamma_\sigma(\mathbf{r}, \mathbf{r}')|^2/n_\sigma(\mathbf{r})$ and

$$\int d^3r' h_{x\sigma}(\mathbf{r}, \mathbf{r}') = -1\quad (143)$$

Before proceeding further, also notice that the gauge chosen for the energy density in writing eq. (142) is such that $e_{x\sigma}(\mathbf{r})$ equals *half* of the potential generated by the exchange hole.⁸

$$U_{x\sigma}(\mathbf{r}) = \int d^3r' \frac{h_{x\sigma}(\mathbf{r}, \mathbf{r}')}{|\mathbf{r} - \mathbf{r}'|} = 2e_{x\sigma}(\mathbf{r})\quad (144)$$

In turn, it can be verified that $U_{x\sigma}(\mathbf{r})$ has the form of the Slater potential,⁴² which is an important component of $v_x(\mathbf{r})$.²²¹ Note that $U_{x\sigma}(\mathbf{r})$ will be noted as $v_{x\sigma}^{\text{Slater}}(\mathbf{r})$ in section 3.

Taylor expanding $h_{x\sigma}(\mathbf{r}, u)$ with respect to the interparticle distance u yields²²²

$$h_{x\sigma}(\mathbf{r}, u) = h_{x\sigma}(\mathbf{r}, \mathbf{r}) - C_{x\sigma}(\mathbf{r})u^2 + \dots\quad (145)$$

where

$$h_{x\sigma}(\mathbf{r}, \mathbf{r}) = -n_\sigma(\mathbf{r})\quad (146)$$

⁸To appreciate the interpretation, compare eq. (144) with eq. (11).

is the on-top exchange-hole function and

$$\begin{aligned} C_{x\sigma}(\mathbf{r}) &= \frac{1}{2} \frac{\partial^2 h_{x\sigma}(\mathbf{r}, u)}{\partial u^2} \Big|_{u=0} \\ &= \frac{1}{6} \nabla^2 n_\sigma(\mathbf{r}) - \frac{2}{3} D_\sigma(\mathbf{r}) \end{aligned} \quad (147)$$

is the curvature of the exchange-hole function and

$$D_\sigma(\mathbf{r}) = \tau_\sigma(\mathbf{r}) - \frac{1}{8} \frac{|\nabla n_\sigma(\mathbf{r})|^2}{n_\sigma(\mathbf{r})} \quad (148)$$

It is worth mentioning that $D_\sigma(\mathbf{r})$ enters the definition of the (spin-dependent) iso-orbital indicator

$$\alpha_\sigma(\mathbf{r}) = \frac{D_\sigma(\mathbf{r})}{D_\sigma^{\text{hom}}(\mathbf{r})} \quad (149)$$

where $D_\sigma^{\text{hom}} = \tau_\sigma^{\text{TF}}$ (see eq. (70)) is $D_\sigma(\mathbf{r})$ evaluated for a homogeneous electron gas with same density as the local density of the inhomogeneous systems of interest.

The iso-orbital indicator is an important building block of modern MGGAs. Its importance is due to the fact that it can be used to characterize distinct regions in a system with physical relevance. In fact, it vanishes for one-electron densities for each spin channel (thus the spin-unpolarized version also vanishes for two-electron systems), approaches one for slowly varying densities, and can be large in inter-shell regions.

Due to this, the iso-orbital indicator was first suggested as the essential ingredient of the electron localization function²²³

$$\text{ELF}_\sigma(\mathbf{r}) = \frac{1}{1 + \alpha_\sigma^2(\mathbf{r})} \quad (150)$$

which is a useful indicator of atomic shells and bonds in atoms, molecules, and solids. Interestingly, the properties of the ELF can be related to the ability of $\alpha_\sigma(\mathbf{r})$ to provide a measure of the local spin entanglement in inhomogeneous systems as relative to the homogeneous electron gas.²²⁴

Notice that the second term in eq. (148) is the kinetic-energy density of a *single-particle* orbital with same particle density as the N -

electron system (see eq. (72)), i.e., the kinetic-energy density of a non-interacting bosonic system with same density as the real system.⁹ Therefore, we may say that the ELF measures the excess in the (non-interacting) kinetic energy of a fermionic reference with respect to a bosonic reference—all normalized relative to the excess realized in a homogeneous reference system.²²⁶

The expression in eq. (148) (and thus in eq. (149) and related) is correct for real-valued orbitals. For complex-valued orbitals, which are necessary for degenerate ground states, time-dependent states, and to account for vector potentials of magnetic fields, extra terms must be included. The correct expression is obtained by replacing the kinetic-energy density τ_σ with $\tilde{\tau}_\sigma$ given by²²⁷

$$\tilde{\tau}_\sigma(\mathbf{r}) = \tau_\sigma(\mathbf{r}) - \frac{|\mathbf{j}_\sigma(\mathbf{r})|^2}{2n(\mathbf{r})} \quad (151)$$

where

$$\mathbf{j}_\sigma(\mathbf{r}) = \text{Im} \left[\sum_i f_{i\sigma} \psi_{i\sigma}^*(\mathbf{r}) \nabla \psi_{i\sigma}(\mathbf{r}) \right] \quad (152)$$

is the *paramagnetic* spin-resolved current density; Im stands, as usual, for the imaginary part. The expression of the curvature of the exchange hole accounting for $\mathbf{j}_\sigma(\mathbf{r})$ was originally given by Dobson²²⁸ and its importance to improve the description of degenerate ground states was stressed by Becke²²⁹. The time-dependent case was considered by Burnus et al.²³⁰ and the case of general non-collinear states was considered by Pittalis et al.²³¹ as well as by Desmarais et al.²³²

2.8 Self-interaction free conditions

From eq. (8), it is clear that for one-electron (1e) systems the Hartree and exchange contributions must cancel

$$E_{\text{H}}[n|_{1\text{e}}] + E_{\text{x}}[n|_{1\text{e}}] = 0 \quad (153)$$

⁹This system plays a central role in orbital-free DFT.²²⁵

and the correlation energy must vanish

$$E_c[n|_{1e}] = 0 \quad (154)$$

Approximations that obey these exact conditions are labeled (one-particle) *self-interaction* free.

Semi-local (sl) xc approximations can be corrected by using the self-interaction correction (SIC) by Perdew and Zunger²³³. This correction has the following form²³³

$$E_{xc}^{\text{SIC}}[n_{\uparrow}, n_{\downarrow}] = E_{xc}^{\text{sl}}[n_{\uparrow}, n_{\downarrow}] - \sum_{i\sigma} (E_{\text{H}}[n_{i\sigma}] + E_{xc}^{\text{sl}}[n_{i\sigma}, 0]) \quad (155)$$

where $n_{i\sigma} = f_{i\sigma} |\psi_{i\sigma}|^2$ are spin-orbital densities weighted by their occupations. Obviously, the SIC reduces to the semi-local approximation if this is already self-interaction free.

Resorting to this correction, size consistency can be preserved by using localized orbitals. Unfortunately, two sets of orbitals related by a unitary transformation yield different SICs, even though the transformation leaves the total density and the individual terms in the energy invariant. The recurring interest in this correction comes from the fact that it can improve the accuracy of semi-local approximations in some cases.²³⁴ However, it also exhibits some deficiencies like multiple local minima and symmetry breaking.^{235,236}

MGGAs offer other ways to enforce self-interactions-free conditions. At the level of exchange, this can be made by using eqs. (146) and (147). A discussion of more general spurious interactions that may occur in approximate ensemble-density functionals and their resolution can be found in refs. 237 and 47.

2.9 Scaling in DFT

Although the exact functional is not known, we can learn about its behavior in some relevant transformations and limits. This brings us to consider the coordinate scaled wavefunc-

tion^{238,239}

$$\Psi_{\gamma}(\mathbf{r}, \dots, \mathbf{r}_N) = \gamma^{3N/2} \Psi(\gamma\mathbf{r}, \dots, \gamma\mathbf{r}_N) \quad (156)$$

where γ is a real positive number. The scaling in eq. (156) does not change the normalization of the wave function, and thus the particle density scales as

$$n_{\gamma}(\mathbf{r}) = \gamma^3 n(\gamma\mathbf{r}) \quad (157)$$

When this coordinate scaling is applied to the HEG (more in section 2.10), the transformation is directly related to the high- ($\gamma \rightarrow +\infty$) and low-density ($\gamma \rightarrow 0$) limits, which, in turn, are directly related to the weakly and strongly correlated regimes.⁴ For finite systems, this connection is still valid but becomes more intricate.

For simplicity, we may consider finite systems without confining walls and with a single center (like an isolated atom). When $\gamma \rightarrow +\infty$, the scaled wavefunction is compressed, and the scaled density diverges to infinity at the center of the system. In the opposite limit, $\gamma \rightarrow 0$, the scaled wavefunction expands radially outward, leading the scaled density at the nuclear centers to vanish.

For the energy averages, it is simple to verify that $\langle \Psi_{\gamma} | \hat{T} | \Psi_{\gamma} \rangle = \gamma^2 \langle \Psi | \hat{T} | \Psi \rangle$, $\langle \Psi_{\gamma} | \hat{W} | \Psi_{\gamma} \rangle = \gamma \langle \Psi | \hat{W} | \Psi \rangle$, and $\langle \Psi_{\gamma} | \hat{V}_{\text{ext}} | \Psi_{\gamma} \rangle = \gamma^2 \langle \Psi | \hat{V}_{\text{ext}} | \Psi \rangle$. Notice that these scaling relations involve functionals of the wavefunction—not of the density. Homogeneous scaling relations are recovered only for the following functionals

$$T_s[n_{\gamma}] = \gamma^2 T_s[n] \quad (158a)$$

$$E_{\text{H}}[n_{\gamma}] = \gamma E_{\text{H}}[n] \quad (158b)$$

$$E_{\text{x}}[n_{\gamma}] = \gamma E_{\text{x}}[n] \quad (158c)$$

In general, density functionals do not scale homogeneously. For example, for the correlation energy functional, the following inequalities hold true: $E_c[n_{\gamma}] > \gamma E_c[n]$ for $\gamma > 1$ and $E_c[n_{\gamma}] < \gamma E_c[n]$ for $\gamma < 1$. Similar relations with inverted inequalities apply to the interacting kinetic energy $T[n]$, and consequently, to the kinetic contribution $T_c[n]$ to the correlation energy.

Since the scaled density can be associated

with a scaled interaction, one can verify that

$$F^\lambda[n_\gamma] = \gamma^2 F^{\lambda/\gamma}[n] \quad (159)$$

and

$$E_c^\lambda[n_\gamma] = \gamma^2 E_c^{\lambda/\gamma}[n] \quad (160)$$

For $\gamma \rightarrow +\infty$ ($\gamma \rightarrow +0$), the above relations connect the functional for the systems with $\lambda = 1$ evaluated on the *scaled* densities, with the functional of the systems with interaction $1/\gamma \rightarrow 0$ ($1/\gamma \rightarrow +\infty$) evaluated on the *unscaled* density.

More in detail, via Görling–Levy perturbation theory,^{66,240} one can verify that

$$\lim_{\gamma \rightarrow +\infty} \frac{E_{\text{xc}}[n_\gamma]}{\gamma} = E_{\text{x}}[n] \quad (161)$$

and

$$\lim_{\gamma \rightarrow +\infty} E_c[n_\gamma] = E_c^{(2)}[n] \quad (162)$$

where $E_c^{(2)}$ is the second-order contribution, specifically

$$E_c^{(2)} = - \sum_{\nu=1}^{+\infty} \frac{|\langle \Psi_s^0 | \hat{W} - \hat{V}_{\text{Hx}} | \Psi_s^\nu \rangle|^2}{E_0^\nu - E_0} \quad (163)$$

where $\hat{V}_{\text{Hx}} = \sum_{i=1}^N v_{\text{Hx}}(\mathbf{r}_i)$, Ψ_s^ν is the ν -th excited state (Slater determinant) of the KS N -particle Hamiltonian with ground state Ψ_s^0 .¹⁰ Notice that $E_c^{(2)}$ is scale invariant.

Combining these results we find that for $\gamma \gg 1$, $E_c[n_\gamma]$ contributes less than $E_{\text{x}}[n_\gamma]$ (which scales linearly) and far less than $T_s[n_\gamma]$ (which scales quadratically). For $\gamma \rightarrow 0$, one finds strictly correlated electrons (SCE), i.e. electrons for which the kinetic energy vanishes, leading to^{241,242}

$$\lim_{\gamma \rightarrow 0^+} \frac{E_{\text{Hxc}}[n_\gamma]}{\gamma} = W^{\text{SCE}}[n] \quad (164)$$

where $W^{\text{SCE}}[n] = \inf_{\Psi \rightarrow n} \langle \Psi | \hat{W} | \Psi \rangle$. The modeling of $W^{\text{SCE}}[n]$ is a fascinating topic that may lead to density functional approximations capable of modeling both weakly and strongly cor-

¹⁰Energy levels are assumed to be non-degenerate, possibly by the addition of small symmetry breaking perturbations.

related problems accurately.^{243–246}

2.10 High- and low-density limits of the homogeneous electron gas

The HEG (also commonly called uniform electron gas) is a system composed of electrons in a background of a uniformly smeared positive charge. This uniform background can be regarded as a jellium-like continuum. Hence, the system is also referred to as the jellium model.

Calculations of the properties of this system in the thermodynamic limit can be performed by considering $N \gg 1$ electrons in a box of volume $V \gg 1$. The limit of V and N going to infinity must be taken by keeping $n = N/V$ constant. Charge neutrality requires that the density of the positive background n_{b} and the density of the electrons are equal, $n_{\text{b}} = n$. Therefore, $E_{\text{H}}[n] + E_{\text{H}}[n_{\text{b}}] + \int d^3r v_{\text{ext}}(\mathbf{r})n(\mathbf{r}) = 0$, where $v_{\text{ext}}(\mathbf{r}) = -v_{\text{H}}[n_{\text{b}}](\mathbf{r})$.

The electron density of the 3D HEG can be given in terms of the Wigner–Seitz radius r_s

$$n = \frac{3}{4\pi} \frac{1}{r_s^3}, \quad (165)$$

and the spin polarization ζ written as

$$\zeta = \frac{n_{\uparrow} - n_{\downarrow}}{n} \quad (166)$$

The total energy *per particle* of the system is given by

$$e_{\text{tot}}(r_s, \zeta) = t_s(r_s, \zeta) + e_{\text{x}}(r_s, \zeta) + e_{\text{c}}(r_s, \zeta) \quad (167)$$

The first two terms are known exactly, namely the non-interacting kinetic energy

$$t_s(r_s, \zeta) = \frac{c_s(\zeta)}{r_s^2} = \frac{3}{10} \left(\frac{9\pi}{4} \right)^{2/3} \frac{\phi_{5/3}(\zeta)}{r_s^2} \quad (168)$$

and the exchange energy

$$e_{\text{x}}(r_s, \zeta) = \frac{c_{\text{x}}(\zeta)}{r_s} = -\frac{3}{4} \left(\frac{3}{2\pi} \right)^{2/3} \frac{\phi_{4/3}(\zeta)}{r_s} \quad (169)$$

where¹⁵⁴

$$\phi_p(\zeta) = \frac{1}{2} [(1 + \zeta)^p + (1 - \zeta)^p] \quad (170)$$

In the high-density limit ($r_s \rightarrow 0$) the correlation energy of the HEG has the asymptotic expansion²⁴⁷⁻²⁵³

$$e_c(r_s, \zeta) = \sum_{n=0}^{\infty} [a_n(\zeta) \ln(r_s) + b_n(\zeta)] r_s^n \quad (171)$$

The coefficients $a_0(\zeta)$, $b_0(\zeta)$, and $a_1(\zeta)$ arise from the summation of the ring diagrams in the RPA, and from second-order exchange. The first has the expression²⁵⁴

$$a_0(\zeta) = \frac{1}{4\pi^2} \left[2[1 - \ln(2)] + y_{\uparrow} y_{\downarrow} (y_{\uparrow} + y_{\downarrow}) - y_{\uparrow}^3 \ln \left(1 + \frac{y_{\downarrow}}{y_{\uparrow}} \right) - y_{\downarrow}^3 \ln \left(1 + \frac{y_{\uparrow}}{y_{\downarrow}} \right) \right] \quad (172)$$

in which

$$y_{\uparrow} = (1 + \zeta)^{1/3} \quad y_{\downarrow} = (1 - \zeta)^{1/3} \quad (173)$$

Notice that $a_0(\zeta = 0) = [1 - \ln(2)]/\pi^2$, recovers the RPA coefficient originally derived by Macke²⁴⁷. Sun, Perdew, and Seidl,^{252,253} furthermore found a practical approximation to eq. (172), given by

$$a_0(\zeta) = (-35.57\zeta^8 + 50.44\zeta^6 - 24.76\zeta^4 - 5.66\zeta^2 + 31.09) \times 10^{-3} \quad (174)$$

via a numerical fit.

The term $b_0(\zeta)$ was calculated by Hoffman²⁵⁵, unfortunately the exact formula is rather complicated and includes an integral that has to be evaluated numerically. A numerical approximation was given by Sun, Perdew, and Seidl:^{252,253}

$$b_0(\zeta) = (-21.36\zeta^8 + 36.43\zeta^6 - 13.58\zeta^4 + 19.69\zeta^2 - 46.92) \times 10^{-3} \quad (175)$$

The function $a_1(\zeta)$ of eq. (171) was calculated analytically by Loos and Gill²⁵⁶. A practical fit of $a_1(\zeta)$ was also given by Sun, Perdew, and

Seidl,^{252,253} (see `lda_c_dpi`) but it suffers from an order-of-limits problem.²⁵⁶ The correct expression was given later by Bhattarai et al.²⁵⁷

$$a_1(\zeta) = [9.22921 - 1.59532 \arcsin(\zeta^2) - 5.59489 \arcsin(\zeta^4) + 26.4127 \arcsin(\zeta^6) - 59.7952 \arcsin(\zeta^8) + 60.373 \arcsin(\zeta^{10}) - 22.6208 \arcsin(\zeta^{12})] \times 10^{-3} \quad (176)$$

where the arcsin expansion was chosen to recover the infinite slope of the exact $a_1(\zeta)$ at $|\zeta| = 1$.

In the opposite low-density limit ($r_s \rightarrow \infty$), the electronic behavior is similar to zero-point oscillations of the electrons about equilibrium positions. In this Wigner crystal^{243,244,258,259} the total energy becomes independent of ζ ^{260,261}

$$e_{\text{tot}}(r_s) = \frac{f_0}{r_s} + \frac{f_1}{r_s^{3/2}} + \frac{f_2}{r_s^2} + \dots \quad (177)$$

This leads to the following expansion for the correlation energy^{252,253}

$$e_c(r_s, \zeta) = \frac{f_0 - c_x(\zeta)}{r_s} + \frac{f_1}{r_s^{3/2}} + \frac{f_2 - c_s(\zeta)}{r_s^2} + \sum_{n=3}^{\infty} \frac{f_n}{r_s^{1+n/2}} + e_{\text{exp}}(r_s, \zeta) \quad (178)$$

where $f_0 = -0.9$, $f_1 = 1.5$, $f_2 = 0$, and $c_s(\zeta)$ and $c_x(\zeta)$ are defined implicitly by eqs. (168) and (169), respectively.

The contribution with $\phi_{2/3}(\zeta)$, given by eq. (170) (see also eq. (40)), arises from the exponential overlap of localized one-electron states.^{259,262}

For more insight on this important reference system, we recommend the excellent review of Loos and Gill⁵ and the book of Giuliani and Vignale⁴.

2.11 Gradient-expansion approximations

Approaching realistic inhomogeneous electron gases, it is useful to consider an electron gas in which the particle density varies slowly.^{1,4,263} These are weak inhomogeneities for which the

energy contributions can be expressed as expansions in terms of the particle density and its spatial derivatives.

The gradient expansions (GE) for the exchange and correlation energies read as follows

$$E_x[n] = -2^{-1/3} C_x \int d^3r n^{4/3} (1 + \mu s^2 + \dots) \quad (179a)$$

$$E_c[n] = \int d^3r n [e_c(n) + \beta(n)t^2 + \dots] \quad (179b)$$

where $C_x = (3/4)(6/\pi)^{1/3}$ and

$$s = \frac{|\nabla n|}{2nk_F} \quad (180a)$$

$$t = \frac{|\nabla n|}{2nk_s} \quad (180b)$$

The local Fermi wave vector in eq. (180a) is

$$k_F = (3\pi^2 n)^{1/3} \quad (181)$$

and the Thomas–Fermi screening length in eq. (180b) is

$$k_s = \sqrt{4k_F/\pi} \quad (182)$$

While k_F defines a length scale that measures the density inhomogeneities for $T_s[n]$ and $E_x[n]$, and k_s defines a length scale for the density inhomogeneities for $E_c[n]$.

Higher-order terms for eqs. (179a) and (179b) have also been derived and have sometimes been used in density functional approximations. Details can be found in section 3.

Notice that the reduced-density gradient s is dimensionless, and is a measure of the relative variation of the density n in space. The actual slowly-varying limit is one in which q/s is also small, where

$$q = \frac{\nabla^2 n}{4nk_F^2} \quad (183)$$

is a reduced Laplacian.

In the context of MGGAs and orbital-free DFT, the following expansion is also extremely

useful^{264–266}

$$\tau = \tau^{\text{TF}} \left[1 + \left(\frac{5}{27} \right) s^2 + \left(\frac{20}{9} \right) q + \dots \right] \quad (184)$$

where $\tau^{\text{TF}} = (3/10)(3\pi^2)^{2/3} n^{5/3}$ (see also eq. (68)).

Concerning the evaluation of the above coefficients, Sham¹⁴⁶ found $\mu^{\text{Sham}} = 7/81$ when resorting to a screened Coulomb interaction, while Antoniewicz and Kleinman¹⁴⁷ derived $\mu^{\text{GE}} = 10/81$ by considering the unscreened Coulomb interaction. The reason for this discrepancy is described by Svendsen and von Barth²⁶⁷ who showed that the Coulomb interaction is too singular to allow for the interchange of the operations of integration and expansion in wave vectors. Therefore, the procedures of expanding correlation functions in terms of density gradients followed by integrations may not yield the same result as directly expanding the integrated quantity in terms of density gradients.

For correlation, modulo an order of limit problem,¹⁵² Ma and Brueckner¹⁵¹ found $\beta^{\text{MB}} \equiv \beta(r_s \rightarrow 0) \approx 0.0667$.

It was quickly realized that gradient-expansion approximations failed to improve energies for inhomogeneous systems compared to the LDA. While one might attribute this failure to the significant inhomogeneity of real systems, such an argument would then question the surprising effectiveness of the LDA for real inhomogeneous systems.

One important aspect that explains the success of the LDA is the fact that it can be derived from the xc-hole of a quantum mechanical system: the HEG. Thus, it automatically satisfies many exact conditions that are relevant also for real systems. GE approximations do not stem from the xc-hole function of a real system. Instead, they emerge from perturbative and asymptotic expansions for the energy, and fail to satisfy important underlying exact conditions, such as the normalization of the hole functions. Promisingly, van Leeuwen²⁶⁸ has devised an approach to derive the gradient expansions directly for two-point correlation- and hole-functions.

2.12 Semiclassical expansion in the Lieb–Simon limit

Analyses of the Lieb–Simon²⁶⁹ limit (see section 2.12) have allowed to extract class-specific coefficients for the *gradients* in density functional approximations.^{270–276} This is a different mathematical limit that increases the nuclear Z and electron number N together to maintain the system electrically neutral. It has been shown that, in this limit, the ground-state density of atoms, molecules, and solids²⁶⁹ tends to the Thomas–Fermi density

$$n_{Z,N=Z}(\mathbf{r}) \xrightarrow{Z \rightarrow \infty} n_Z^{\text{TF}}(\mathbf{r}) = Z^2 n_{Z=1}^{\text{TF}}(Z^{1/3}\mathbf{r}) \quad (185)$$

and the total energy tends to the TF energy density

$$E_{Z,N=Z}(\mathbf{r}) \xrightarrow{Z \rightarrow \infty} E_{Z,N=Z}^{(\text{TF})} \sim Z^{7/3} \quad (186)$$

which is the leading term in the expansion of the energy in powers of $Z^{1/3}$.

For the exchange, it is expected that^{277–279}

$$E_x \xrightarrow{Z \rightarrow \infty} -A_x Z^{5/3} - B_x Z^{4/3} - C_x Z \ln Z - D_x Z + \dots \quad (187)$$

where $A_x \approx 0.220827$, while recent work²⁷⁹ has reported

$$E_x - E_x^{\text{LDA}} \approx -0.0254 Z \ln Z - 0.0560 Z \quad (188)$$

For the correlation energy, it is known that^{277,280}

$$E_c \approx -0.02727 Z \ln Z + 0.0372 Z \quad (189)$$

Note that the precise estimation of the above coefficients is still subject to active efforts.

2.13 From local to non-local xc potentials

Let us consider a general functional form that may depend on all the semi-local ingredients mentioned so far, i.e. a MGGA:

$$E_{\text{xc}}[n] = \int d^3r \epsilon_{\text{xc}}(n, \nabla n, \nabla^2 n, \tau) \quad (190)$$

where ϵ_{xc} is the xc-energy per unit *volume*. Using eq. (190) in eq. (12), we readily obtain

$$v_{\text{xc}} = \frac{\partial \epsilon_{\text{xc}}}{\partial n} - \nabla \cdot \left[\frac{\partial \epsilon_{\text{xc}}}{\partial \nabla n} \right] + \nabla^2 \left[\frac{\partial \epsilon_{\text{xc}}}{\partial \nabla^2 n} \right] + v_{\text{xc}}^{(\tau)} \quad (191)$$

where

$$v_{\text{xc}}^{(\tau)}(\mathbf{r}) = \int d^3r' \frac{\partial \epsilon_{\text{xc}}(\mathbf{r}')}{\partial \tau} \frac{\delta \tau(\mathbf{r}')}{\delta n(\mathbf{r})} \quad (192)$$

Two comments are in order: (i) Because the dependence of ϵ_{xc} on ∇n is via its modulus $|\nabla n|$, it is more convenient to express the second term via the symmetric quantity $|\nabla n|^2$ as follows

$$\nabla \cdot \left[\frac{\partial \epsilon_{\text{xc}}}{\partial \nabla n} \right] = 2 \nabla \cdot \left[\left(\frac{\partial \epsilon_{\text{xc}}}{\partial |\nabla n|^2} \right) \nabla n \right] \quad (193)$$

(ii) The integral in eq. (192) has a deceptively simple form: the dependence of $\tau(\mathbf{r})$ on the particle density n is not explicit (it is contained implicitly in the KS orbitals) and, thus, to evaluate the last term we must go through the chain of functional derivatives

$$\begin{aligned} \frac{\delta \tau(\mathbf{r}')}{\delta n(\mathbf{r})} &= \sum_i f_i \int d^3r'' \int d^3r''' \frac{\delta \tau(\mathbf{r}')}{\delta \psi_i^*(\mathbf{r}'')} \\ &\times \frac{\delta \psi_i^*(\mathbf{r}'')}{\delta v_s(\mathbf{r}''')} \frac{\delta v_s(\mathbf{r}''')}{\delta n(\mathbf{r})} + \text{c.c.} \end{aligned} \quad (194)$$

where the last two factors involve KS response functions. The calculation of the latter quantities is not trivial, making the implementation of eq. (192) rather complicated. In fact, if a functional E_{xc} depends implicitly on the density n , then the calculation of $\delta E_{\text{xc}}/\delta n$ is in general rather involved, but can be done with the optimized-effective potential (OEP).^{50,281} The OEP method has been applied to the HF exchange,^{50,263,281–283} to MGGA,^{284–287} to SIC functionals (see section 2.8),^{288,289} as well as to RPA methods (see section 2.6).^{69,204,205,290–292}

There is another way to obtain a single-particle equation in DFT that can greatly simplify the application of orbital dependent functionals. The constrained search formalism al-

lows us to write²⁹³

$$E_0 = \min_{\Phi_s \rightarrow N} \left\{ \langle \Phi_s | \hat{T} + \hat{V}_{\text{ext}} | \Phi_s \rangle + E_{\text{Hxc}}^{\text{GKS}}[\Phi_s] \right\} \quad (195)$$

where, through the assumption of a generalized non-interacting v -representability, one expresses all key quantities as functionals of a single determinant rather than of a single-particle density only.¹¹ The notation emphasizes that, in general, $\Phi_s \neq \Psi_s$ and $E_{\text{xc}}^{\text{GKS}}[\Phi_s] \neq E_{\text{xc}}[n]$. Performing the minimization yields

$$\left(-\frac{1}{2}\nabla^2 + v_{\text{ext}} + v_{\text{H}} \right) \psi_i + \frac{\delta E_{\text{xc}}^{\text{GKS}}[\Psi_s]}{\delta \psi_i^*} = \varepsilon_i \psi_i \quad (196)$$

This is the generalized KS equation (GKS), here written in a form especially suitable for τ -dependent MGGA. As shown below, this equation admits more general effective potentials than the regular KS equation, eq. (2). We note that the term GKS is sometimes used with a different meaning in quantum chemistry, where it is used to denote an extended HF/KS approaches with non-collinear spin^{294–297}.

Applying this scheme to the functional form defined in eq. (190) by inserting the definitions of the KS densities in terms of the spin-orbitals, we readily obtain

$$\frac{\delta E_{\text{xc}}^{\text{GKS}}[\Psi_s]}{\delta \psi_i^*(\mathbf{r})} = \hat{v}_{\text{xc}}^{\text{GKS}}(\mathbf{r}) \psi_i(\mathbf{r}) \quad (197)$$

where

$$\hat{v}_{\text{xc}}^{\text{GKS}} = \frac{\partial \epsilon_{\text{xc}}}{\partial n} - \nabla \cdot \left[\frac{\partial \epsilon_{\text{xc}}}{\partial \nabla n} \right] + \nabla^2 \left[\frac{\partial \epsilon_{\text{xc}}}{\partial \nabla^2 n} \right] + \hat{v}_{\text{xc}}^{(\tau)} \quad (198)$$

with

$$\hat{v}_{\text{xc}}^{(\tau)}(\mathbf{r}) \equiv -\frac{1}{2}\nabla \cdot \left(\frac{\partial \epsilon_{\text{xc}}}{\partial \tau} \nabla \right) \quad (199)$$

Comparing eq. (191) with eq. (198), we see that the first three terms are identical to each other, while $v_{\text{xc}}^{(\tau)}(\mathbf{r}) \neq \hat{v}_{\text{xc}}^{(\tau)}(\mathbf{r})$. Indeed, $v_{\text{xc}}^{(\tau)}(\mathbf{r})$ in eq. (192) is a position dependent *multiplicative* operator, while $\hat{v}_{\text{xc}}^{(\tau)}(\mathbf{r})$ in eq. (199) is a position dependent *differential* operator. The differential operator is usually chosen in the im-

¹¹The constraint of orthonormal single particle-orbitals is not stressed for brevity.

plementation of τ -dependent MGGA functionals.^{39,167,298–305} Note that, when using localized basis sets, one often uses integration by parts to avoid computing higher than first derivatives of the xc functional in eqs. (198) and (199).^{39,298}

Keeping in mind the crucial differences highlighted above, one can adopt a simplified notation by switching back to the usual symbols $\Phi_s \rightarrow \Psi_s$ and (as is often done in the literature) $E_{\text{xc}}^{\text{GKS}} \rightarrow E_{\text{xc}}$. While the total energies obtained from the KS and GKS scheme are usually similar, important differences can emerge in practice. The calculation of the fundamental gap via an orbital-dependent functional like a MGGA is an important example. Performing the KS (i.e., OEP) or a GKS calculation can make an important difference both in terms of the computational procedure and the physical picture.²⁸⁷ In the next section, the key differences involved in calculating the fundamental gap are illustrated.

2.14 Fundamental gaps

Charged excitations change the number of electrons in the system. A relevant property is given by the fundamental (band) gap

$$E_{\text{g}}(N) = I(N) - A(N) \quad (200)$$

where $I(N) = E(N-1) - E(N)$ is the ionization potential of the N -electron system and $A(N) = E(N) - E(N+1)$ is the negative of the electron affinity of the same system (i.e., the ionization potential of the $N+1$ -electron system). As the energy of the highest (H) occupied KS orbitals equals minus the ionization potential of the system^{48,49,306,307}

$$\varepsilon_{\text{H}}^{(N)} = -I(N) \quad (201)$$

it can be deduced that

$$E_{\text{g}}(N) = \varepsilon_{\text{H}}^{(N+1)} - \varepsilon_{\text{H}}^{(N)} \quad (202)$$

Equation (200), and thus, eq. (202) can be used directly for finite systems. Contrary to popular belief, eq. (200) can also be used for infinite solids,^{307–311} although some attention must be paid to periodicity.

An alternative approach emerges by extending DFT to fractional electron occupation numbers, i.e. ensemble DFT^{47,312}. Rather than restricting calculations to pure electronic ground states, this method employs ensemble states that represent statistical mixtures of systems with different total electron numbers. For example, $M = N + w$ electrons can be realized by mixing pure states with integer numbers of electrons as in $\Gamma_M = (1 - w)|\Psi^{(N)}\rangle\langle\Psi^{(N)}| + w|\Psi^{(N+1)}\rangle\langle\Psi^{(N+1)}|$. Importantly, Γ_M is an ensemble state with total energy

$$\mathcal{E} = (1 - w)E(N) + wE(N + 1) \quad (203)$$

and particle density

$$n = (1 - w)n_N + wn_{N+1} \quad (204)$$

Equations (203) and (204) show that the energy of a system as a function of a continuous number of electrons is a piecewise-linear interpolation of energy values at integer electron numbers.¹² We stress that piecewise linearity, freedom from self-interaction, and asymptotic correctness of the KS potential are three important related and yet nonequivalent properties of the exact density functional.¹³⁴

From now on, we shall use calligraphic letters to represent energies of ensembles. The dependence of ensemble-related quantities on the weights w , for brevity, is usually implied in the literature (unless otherwise necessary, for clarity). In view of the piecewise linearity of the ensemble energy \mathcal{E} as a function of the (fractional) electron number M , one can verify that

$$E_g(N) = \left. \frac{\partial \mathcal{E}}{\partial M} \right|_{M=N+\eta} - \left. \frac{\partial \mathcal{E}}{\partial M} \right|_{M=N-\eta} \quad (205)$$

where $\eta \rightarrow 0^+$ and $I(N) = -(\partial \mathcal{E} / \partial M)|_{N-1 < M < N}$ and $A(N) = -(\partial \mathcal{E} / \partial M)|_{N < M < N+1}$. As a result,

$$E_g(N) = \Delta_{\text{KS}} + \Delta_{\text{xc}} \quad (206)$$

¹²Interestingly, Yang et al.³¹³ have shown that this property can also be derived without explicitly invoking ensemble DFT.

where

$$\begin{aligned} \Delta_{\text{KS}} &= \varepsilon_{\text{L}}^{(N)} - \varepsilon_{\text{H}}^{(N)} \\ &= \left(\frac{\delta \mathcal{T}_s}{\delta n(\mathbf{r})} \right) \Big|_{N+\eta} - \left(\frac{\delta \mathcal{T}_s}{\delta n(\mathbf{r})} \right) \Big|_{N-\eta} \end{aligned} \quad (207)$$

and the famous derivative discontinuity term is

$$\begin{aligned} \Delta_{\text{xc}} &= \varepsilon_{\text{H}}^{(N+1)} - \varepsilon_{\text{L}}^{(N)} \\ &= \left(\frac{\delta \mathcal{E}_{\text{xc}}}{\delta n(\mathbf{r})} \right) \Big|_{N+\eta} - \left(\frac{\delta \mathcal{E}_{\text{xc}}}{\delta n(\mathbf{r})} \right) \Big|_{N-\eta} \end{aligned} \quad (208)$$

Notice that because the number of electrons can vary when referring to variations of the ensemble n , the functional derivatives of the ensemble functional with respect to n are fully determined: if the effective potential changes by a constant, this change will be captured.¹³

Importantly, it can be shown that in the generalized KS approach^{293,310}

$$E_g(N) \approx \Delta_{\text{GKS}} = \varepsilon_{\text{L,GKS}}^{(N)} - \varepsilon_{\text{H,GKS}}^{(N)} \quad (209)$$

avoiding the need for eq. (208), making the evaluation of the fundamental gap both intuitive and computationally straightforward. Clearly, the usefulness of eq. (209) is bound to the ability of the approximation employed to capture most of the discontinuity of the derivatives.^{310,314}

When standard LDA or GGA functionals are applied directly to ensemble densities in eq. (208), they yield a vanishing Δ_{xc} , leading to the well-known band gap problem of DFT. While these functional forms can be extended to ensemble DFT,³¹⁵ the fundamental issue persists: ensemble-LDA and ensemble-GGA still produce vanishing Δ_{xc} for infinite systems.³¹⁶ Orbital-dependent functionals—including exact exchange and τ -dependent MGGAs^{317,318}—can yield finite Δ_{xc} values even in extended systems.^{287,290,319} It is also worth mentioning that

¹³In regular KS-DFT, the variations of the density are constraint to a fixed particle number, $\int d^3r \delta n(\mathbf{r}) = 0$. It follows that v_{xc} can be determined only up to an arbitrary constant. The value of this constant does not affect the calculation of the total energy and of the density.

multiplicative potentials leading to finite Δ_{xc} in extended systems can be modeled. For example, the GLLB-SC functional³²⁰ leads to realistic values of Δ_{xc} both for materials^{320–322} and artificial low-dimensional systems,^{323,324} via adaptation of the model potential.

2.15 Electron-electron interaction in low-dimensional systems

Electrons can be confined to move in reduced dimensions. This can be achieved for example in semiconductor heterostructures, in which the formation of quantum wells can be modulated by putting in contact layers of different semiconductors and applying gating potentials.^{4,325} During the past decades, the ability to produce low-dimensional electron gases has led to the discovery of new physical phenomena and applications, including the integer and fractional quantum Hall effects, semiconductor nanodevices such as quantum dots, and a variety of topological quantum systems.

DFT can provide a practical yet sufficiently accurate approach to compute the electronic structure of confined low-dimensional quantum systems. Because the common 3D-LDA breaks down in the quasi-2D limit,^{326,327} and similarly, the 2D-LDA is expected to fail in quasi-1D limit,³²⁸ deriving novel approximations for low dimensions as well as dimensional crossovers³²⁹ is of great interest.

For many-electron systems *embedded* in crystals, the effective parameters can differ from their analogs in vacuum. For example, in a quantum dot the natural atomic unit of length is $a_* = \epsilon \hbar^2 / (m_* e^2)$, where ϵ is the dielectric constant of the material and m_* is the effective electron mass. Compared with the Bohr radius, $a_B = \hbar^2 / (m e^2)$, the length a_* is typically large, e.g., $a_* \approx 180 a_B$ in GaAs.^{4,187}

In 2D, the usual Coulomb interaction is still integrable, so it is used in most models. However, some of the semi-classical expansions that are used in the construction of a multitude of functionals become ill-defined, requiring alternative approaches for their determina-

tion.^{275,330,331}

The 1D case is particularly tricky. The Coulomb interaction is no longer integrable, and there is more than one choice to screen the interaction at short distances. When studying atoms and molecules in strong laser fields, one usually resorts to the so-called soft-Coulomb interaction^{332,333}

$$v^{\text{soft-Coulomb}}(x) = \frac{1}{\sqrt{x^2 + b^2}} \quad (210)$$

where b is a parameter. Another possibility is offered by an effective potential with an harmonic transversal confinement and long-range Coulomb tail,^{188,334} which is sometimes called the regularized Coulomb potential

$$v^{\text{reg-Coulomb}}(x) = \frac{\sqrt{\pi}}{2b} \exp\left(\frac{x^2}{4b^2}\right) \operatorname{erfc}\left(\frac{|x|}{2b}\right) \quad (211)$$

Equation (211) can be expanded around $x = \infty$ as $v^{\text{reg-Coulomb}}(x) \approx x^{-1} - 2b^2 x^{-3} + \dots$

We can also find in the literature the use of a contact interaction in 1D,^{176,188} given by

$$v^{\text{contact}}(x) = \eta \delta(x) \quad (212)$$

2.16 Thermal DFT

Thermodynamic equilibria of many-electron systems can be investigated by resorting to the KS-DFT formulation given by Mermin³³⁵. The starting point of the approach is the *grand canonical* Hamiltonian

$$\hat{\Omega} = \hat{H} - \mu \hat{N} - \tau_e \hat{S} \quad (213)$$

where \hat{H} is the Hamiltonian, \hat{N} is the particle-number operator, and \hat{S} is the entropy operator

$$\hat{S} = -k_B \ln \hat{\Gamma} \quad (214)$$

where

$$\hat{\Gamma} = \sum_{N,i} w_{N,i} |\Psi_{N,i}\rangle \langle \Psi_{N,i}| \quad (215)$$

is the ensemble operator. $\Psi_{N,i}$ are orthonormal N -particle states and $w_{N,i}$ are normalized statistical weights such that $\sum_{N,i} w_{N,i} = 1$.

Statistical properties of interest can be ob-

tained by averaging with respect to $\hat{\Gamma}$, namely,

$$O[\hat{\Gamma}] = \sum_{N,i} w_{N,i} \langle \Psi_{N,i} | \hat{O} | \Psi_{N,i} \rangle \quad (216)$$

The ensemble operator $\hat{\Gamma}$ to be used for computing thermal properties is found by minimizing $\Omega[\hat{\Gamma}]$, at a given temperature τ_e and chemical potential μ . The statistical weights are given by

$$w_{N,i}^0 = \frac{e^{-\beta(E_{N,i}^0 - \mu N)}}{\sum_{M,j} e^{-\beta(E_{M,j}^0 - \mu M)}} \quad (217)$$

where $E_{N,i}^0$ are the eigenvalues of the N -particle eigenstates. Correspondingly,

$$\begin{aligned} \Omega[\hat{\Gamma}] &= H[\hat{\Gamma}] - \tau_e S[\hat{\Gamma}] - \mu N[\hat{\Gamma}] \\ &= -k_B \tau_e \ln Z_G, \end{aligned} \quad (218)$$

where

$$Z_G = \sum_{N,i} e^{-\beta(E_{N,i}^0 - \mu N)} \quad (219)$$

is the grand canonical partition function.

Rephrasing Mermin's central result in the framework of the constrained search formulation, the grand potential is obtained by the minimization

$$\Omega = \min_n \left\{ F^{\tau_e}[n] + \int d^3r \, n(\mathbf{r})(v_{\text{ext}}(\mathbf{r}) - \mu) \right\} \quad (220)$$

where $n(\mathbf{r})$ is an ensemble N -representable density and

$$F^{\tau_e}[n] = \min_{\hat{\Gamma} \rightarrow n} \left\{ T[\hat{\Gamma}] + W[\hat{\Gamma}] - \tau_e S[\hat{\Gamma}] \right\} \quad (221)$$

Equation (221) defines the thermal universal functional. The universality of this quantity means that it doesn't depend explicitly *either* on the external potential *or* on μ . Denoting as $\Gamma^{\tau_e}[n]$ the minimizing statistical operator of eq. (221),

$$F^{\tau_e}[n] = T^{\tau_e}[n] + W^{\tau_e}[n] - \tau_e S^{\tau_e}[n] \quad (222)$$

where $T^{\tau_e}[n] = T[\hat{\Gamma}^{\tau_e}[n]]$, $W^{\tau_e}[n] = W[\hat{\Gamma}^{\tau_e}[n]]$, and $S^{\tau_e}[n] = S[\hat{\Gamma}^{\tau_e}[n]]$. Importantly, $F^{\tau_e}[n]$ differs from the $F[n]$ of ground-state DFT by the inclusion of the entropy.

In close analogy with KS-DFT, the interacting grand-canonical potential density functional can be decomposed as follows:

$$\begin{aligned} \Omega[n] &= F_s^{\tau_e}[n] + E_H[n] + \Omega_{\text{xc}}^{\tau_e}[n] \\ &+ \int d^3r \, n(\mathbf{r})(v_{\text{ext}}(\mathbf{r}) - \mu) \end{aligned} \quad (223)$$

The notation highlights that the temperature dependence of $E_H[n]$ enters only through the input equilibrium density. The xc *free-energy* density functional is given by

$$\Omega_{\text{xc}}^{\tau_e}[n] = F^{\tau_e}[n] - F_s^{\tau_e}[n] - E_H[n] \quad (224)$$

where $F_s^{\tau_e}[n] = T_s^{\tau_e}[n] - \tau_e S_s^{\tau_e}[n]$, $T_s^{\tau_e}[n] = T[\hat{\Gamma}_s^{\tau_e}[n]]$, and $S_s^{\tau_e}[n] = S[\hat{\Gamma}_s^{\tau_e}[n]]$.

The density matrix $\hat{\Gamma}_s^{\tau_e}[n]$ is obtained by solving the thermal KS equations. It is assumed that there exists an ensemble of a non-interacting system with the same average particle density *and* temperature as the interacting ensemble. The chemical potential of the KS system is determined consequently. The thermal counterpart of eq. (1) is of the form

$$\left[-\frac{1}{2} \nabla^2 + v_s^{\tau_e}(\mathbf{r}) \right] \psi_i^{\tau_e}(\mathbf{r}) = \varepsilon_i^{\tau_e} \psi_i^{\tau_e}(\mathbf{r}) \quad (225)$$

with

$$v_s^{\tau_e}(\mathbf{r}) = v_{\text{ext}}(\mathbf{r}) + v_H^{\tau_e}(\mathbf{r}) + v_{\text{xc}}^{\tau_e}(\mathbf{r}) \quad (226)$$

and accompanying density

$$n^{\tau_e}(\mathbf{r}) = \sum_i f_i^{\tau_e} |\psi_i^{\tau_e}(\mathbf{r})|^2 \quad (227)$$

where ¹⁴

$$f_i^{\tau_e} = \left[1 + e^{(\varepsilon_i^{\tau_e} - \mu)/\tau_e} \right]^{-1} \quad (228)$$

As for KS-DFT, it is also useful to split $\Omega_{\text{xc}}^{\tau_e}[n]$ into exchange and correlation components:

$$\Omega_{\text{xc}}^{\tau_e}[n] = \Omega_x^{\tau_e}[n] + \Omega_c^{\tau_e}[n] \quad (229)$$

¹⁴Although f_i resembles the Fermi function for non-interacting fermions, the subtle but important difference is that for the KS electrons, f_i depends also implicitly on the temperature through the KS eigenvalues.

where

$$\begin{aligned}\Omega_x^{\tau_e}[n] &= W[\Gamma_s^{\tau_e}[n]] - E_H[n] \\ &\equiv E_x[\gamma]\end{aligned}\quad (230)$$

where γ is the one-body reduced-density matrix of the thermal KS system. The notation in eq. (230) highlights that the dependence of $\Omega_x^{\tau_e}[n]$ on the temperature only comes implicitly through γ . An informative analysis and application of exact exchange in thermal DFT is given by Greiner et al.³³⁶ Notice the important fact that the kinetic *and* entropic contributions are *not* explicitly accounted for in the definition of the exchange free-energy functional, but through the correlation free-energy functional. Exact conditions useful to derive or test approximations are also known in this framework.^{337–340}

2.17 Non-collinear spin-DFT

The development of non-collinear spin-DFT has received multiple contributions in the last two decades, and is a topic that goes beyond the present review. For a review see, for example, refs. 341–355. It is, however, relevant to mention here how the widely spread (collinear) spin-resolved calculations are related to the more general non-collinear formalism. Let us consider spin-polarized states induced by external magnetic fields $\mathbf{B}_{\text{ext}}(\mathbf{r})$ via the coupling to the spin degrees of freedom $\mu_B \boldsymbol{\sigma} \cdot \mathbf{B}_{\text{ext}}(\mathbf{r})$, where $\boldsymbol{\sigma}$ stands for the vector of the 2×2 Pauli matrices and μ_B denotes the Bohr magneton.

Neglecting the effect of the vector potentials associated to the magnetic field and spin-orbit couplings, the (non-collinear) KS equations of spin-DFT³⁵⁶ have the form of single-particle Pauli equations:

$$\left[-\frac{1}{2} \nabla^2 + \mathbf{V}_s(\mathbf{r}) \right] \Phi_i(\mathbf{r}) = \epsilon_i \Phi_i(\mathbf{r}) \quad (231)$$

where $\Phi_i(\mathbf{r})$ are two-component Pauli spinors, and the KS (matrix) potential reads

$$\mathbf{V}_s(\mathbf{r}) = v_s(\mathbf{r}) + \mu_B \boldsymbol{\sigma} \cdot \mathbf{B}_s(\mathbf{r}) \quad (232)$$

The KS system of non-collinear spin-DFT re-

produces not only the particle density $n(\mathbf{r}) = \sum_i f_i \Phi_i^\dagger(\mathbf{r}) \Phi_i(\mathbf{r})$, but *also* the spin magnetization $\mathbf{m}(\mathbf{r}) = \sum_i f_i \Phi_i^\dagger(\mathbf{r}) \boldsymbol{\sigma} \Phi_i(\mathbf{r})$ of the interacting system. Notice that f_i are the occupation numbers of single-particle *spinors*, which thus have both a spin-up and a spin-down component.

The total energy is expressed as follows:

$$\begin{aligned}E &= T_s[n, \mathbf{m}] + E_H[n] + E_{\text{xc}}[n, \mathbf{m}] \\ &+ \int d^3r \, n v_{\text{ext}} + \mu_B \int d^3r \, \mathbf{m} \cdot \mathbf{B}_{\text{ext}}\end{aligned}\quad (233)$$

Notice that the KS kinetic energy and the xc energy are functionals of both $n(\mathbf{r})$ *and* $\mathbf{m}(\mathbf{r})$, which must be considered as independent variables. As usual, one can decompose the KS potential as $v_s(\mathbf{r}) = v_{\text{ext}}(\mathbf{r}) + v_H(\mathbf{r}) + v_{\text{xc}}(\mathbf{r})$ where $v_{\text{xc}}(\mathbf{r}) = \delta E_{\text{xc}}[n, \mathbf{m}] / \delta n|_{\mathbf{m}}$ and

$$\mathbf{B}_s(\mathbf{r}) = \mathbf{B}_{\text{ext}}(\mathbf{r}) + \mathbf{B}_{\text{xc}}(\mathbf{r}) \quad (234)$$

where

$$\mu_B \mathbf{B}_{\text{xc}}(\mathbf{r}) = \left. \frac{\delta E_{\text{xc}}[n, \mathbf{m}]}{\delta \mathbf{m}(\mathbf{r})} \right|_n \quad (235)$$

An important feature of $\mathbf{B}_{\text{xc}}(\mathbf{r})$ is its non-collinearity with respect to the magnetization $\mathbf{m}(\mathbf{r})$. As a result, $\mathbf{B}_{\text{xc}}(\mathbf{r})$ can exert a non-vanishing *local* torque. This property can be understood as necessary to the stationary non-collinear condition of the KS solution.³⁵⁷ However, because the electron-electron interaction cannot exert a net torque on the overall system, there can be no *global* torque:³⁵⁷

$$\int d^3r \, \mathbf{m}(\mathbf{r}) \times \mathbf{B}_{\text{xc}}(\mathbf{r}) = 0 \quad (236)$$

In many applications, however, the external magnetic field and the system's magnetization can be considered in a globally collinear configuration, for example along the z -axis. As a consequence, the KS equations become

$$\left[-\frac{1}{2} \nabla^2 + v_{s\sigma}(\mathbf{r}) \right] \psi_{i\sigma}(\mathbf{r}) = \epsilon_{i\sigma} \psi_{i\sigma}(\mathbf{r}) \quad (237)$$

where

$$v_{s\sigma}(\mathbf{r}) = v_{\text{ext}\sigma}(\mathbf{r}) + v_{\text{H}}(\mathbf{r}) + v_{\text{xc}\sigma}(\mathbf{r}) \quad (238\text{a})$$

$$v_{\text{xc}\sigma}(\mathbf{r}) = \left. \frac{\delta E_{\text{xc}}[n_{\uparrow}, n_{\downarrow}]}{\delta n_{\sigma}(\mathbf{r})} \right|_{n_{\bar{\sigma}}} \quad (238\text{b})$$

and

$$n_{\sigma}(\mathbf{r}) = \sum_i f_{i\sigma} |\psi_{i\sigma}(\mathbf{r})|^2 \quad (239)$$

yields the interacting spin densities, as well as the (total) interacting density $n = \sum_{\sigma} n_{\sigma}$.

Notice that the above notation stresses that when restricting the spin to be collinear, E_{xc} becomes a functional of both the spin densities n_{\uparrow} and n_{\downarrow} , i.e. $E_{\text{xc}}[n_{\uparrow}, n_{\downarrow}]$. Thus, even at vanishing external magnetic field, a system may develop a spontaneous magnetization that can be calculated in spin-polarized KS-DFT. This feature is of tremendous practical importance, since the ground states of most atoms, some molecules like O_2 , and many solids are indeed spin-polarized.

Spin-unrestricted calculations can be done for open-shell states also in vanishing magnetic fields by assigning different occupation numbers to the two spin channels and, thus, allowing for *spin-unrestricted* effective potential. Spin-unrestricted calculations can be exploited to obtain better energies for strongly correlated states, even for closed-shell states. The paradigmatic situation is the stretched H_2 molecule. The price to be paid for spuriously breaking the spin symmetry, however, is the incorrect symmetry of the spin densities and overstepping the realm of rigorous spin-DFT.³⁵⁸

Spin-unpolarized solutions at vanishing magnetization are such that $v_{s\uparrow}(\mathbf{r}) = v_{s\downarrow}(\mathbf{r}) = v_s(\mathbf{r})$ and, thus, $\varepsilon_{i\uparrow} = \varepsilon_{i\downarrow} = \varepsilon_i$ and $\psi_{i\uparrow}(\mathbf{r}) = \psi_{i\downarrow} = \psi_i(\mathbf{r})$. In this case, each single-particle state is doubly degenerate and can, therefore, be occupied by two electrons with opposite spins. We thus recover the description of closed-shell states of regular KS-DFT.

Finally, spin-current-DFT^{359–363} completes spin-DFT by accounting for both the vector potentials and spin-orbit coupling. Spin-current-DFT adds an explicit functional dependence on the paramagnetic-particle and the paramagnetic-spin currents. As a conse-

quence, the corresponding xc energy exhibits a $\text{U}(1) \times \text{SU}(2)$ gauge symmetry that can be usefully exploited for the construction of approximations. Long standing difficulties in spin-DFT can be resolved in spin-current-DFT at the MGGA level.^{231,232,364–366}

2.18 Enhancement factors and spin-resolved energies

2.18.1 Enhancement factors

Semi-local approximations can capture inhomogeneities and other non-local effects in xc energies beyond those that can be captured via a LDA. In order to stress this fact, they may be written—e.g. for a GGA—as follows

$$E_{\text{x}}^{\text{GGA}} = \int d^3r \epsilon_{\text{x}}^{\text{LDA}}(n(\mathbf{r})) F_{\text{x}}(n(\mathbf{r}), \nabla n(\mathbf{r})) \quad (240)$$

$$E_{\text{c}}^{\text{GGA}} = \int d^3r \epsilon_{\text{c}}^{\text{LDA}}(n(\mathbf{r})) F_{\text{c}}(n(\mathbf{r}), \nabla n(\mathbf{r})) \quad (241)$$

where $\epsilon_{\text{x}/\text{c}}$ denotes an x/c energy density per volume and $F_{\text{x}/\text{c}}$ an exchange/correlation *enhancement factor* that modifies the underlying LDA exchange/correlation. Note, however, that there is no unique definition of the enhancement factors in the literature.

Notice that while there is usually no ambiguity on the expression used for $\epsilon_{\text{x}}^{\text{LDA}}$, numerous analytical forms have been proposed for $\epsilon_{\text{c}}^{\text{LDA}}$ (see section 3.1.2), such that the used form should always be explicitly specified. Also notice that some enhancement factors do not reduce to one when $\nabla n(\mathbf{r}) \equiv 0$, such that in this limit $\epsilon_{\text{x}/\text{c}}^{\text{GGA}}$ does not recover $\epsilon_{\text{x}/\text{c}}^{\text{LDA}}$.

One of the purposes of using an enhancement factor is to interpret and analyze the effects of inhomogeneities on a calculated property. In this case, one may also find useful to define the total xc enhancement as follows

$$E_{\text{xc}}^{\text{GGA}} = \int d^3r \epsilon_{\text{x}}^{\text{LDA}}(n(\mathbf{r})) F_{\text{xc}}(n(\mathbf{r}), \nabla n(\mathbf{r})) \quad (242)$$

Here, only exchange $\epsilon_{\text{x}}^{\text{LDA}}$ is used as a common reference, such that correlation is regarded as an additional source of inhomogeneity beyond

LDA exchange.

2.18.2 Spin resolved exchange and kinetic energy

From eq. (8), one can readily verify that the exchange functional obeys the following spin decomposition:¹⁵⁴

$$E_x[n_\uparrow, n_\downarrow] = \frac{1}{2} (E_x[2n_\uparrow] + E_x[2n_\downarrow]), \quad (243)$$

where $E_x[2n_\sigma]$ is the exchange energy for a spin-restricted system of density (n_σ, n_σ) . Due to the way the factors of two enter into the expression, eq. (243) is also known as the spin-scaling relation for the exchange energy functional. An analogous relation also holds for the KS kinetic energy:

$$T_s[n_\uparrow, n_\downarrow] = \frac{1}{2} (T_s[2n_\uparrow] + T_s[2n_\downarrow]) \quad (244)$$

Collinear spin-DFT approximations can easily be obtained from a (closed-shell) DFT approximation using eqs. (243) and (244).

2.18.3 Spin-resolved correlation energy

The correlation energy functional does not obey a simple relation like eqs. (243) and (244). Therefore, knowing the closed-shell expression for the correlation energy is *not* sufficient to write its expression for spin-DFT.

Spin-resolved correlation functionals are usually reported in the form

$$E_{xc}^{GGA} = \int d^3r n(\mathbf{r}) \times e_{xc}^{GGA}(n_\uparrow(\mathbf{r}), n_\downarrow(\mathbf{r}), \nabla n_\uparrow(\mathbf{r}), \nabla n_\downarrow(\mathbf{r})) \quad (245)$$

where, for brevity, in this example we refer to a GGA, the LDA and MGGA cases being analogous, and the total density is $n = n_\uparrow + n_\downarrow$. Alternatively and fully equivalently to eq. (245), the expression can also be written in terms of

the spin-polarization $\zeta = (n_\uparrow - n_\downarrow) / n$ as

$$E_{xc}^{GGA} = \int d^3r n(\mathbf{r}) \times e_{xc}^{GGA}(n(\mathbf{r}), \zeta(\mathbf{r}), \nabla n(\mathbf{r}), \nabla \zeta(\mathbf{r})) \quad (246)$$

The exact spin-decomposition of the correlation functional has the following structure in terms of hole functions

$$E_c[n_\uparrow, n_\downarrow] = \sum_{\sigma\sigma'} \int d^3r \int d^3r' \frac{n_\sigma(\mathbf{r}) h_c^{\sigma\sigma'}(\mathbf{r}, \mathbf{r}')}{|\mathbf{r} - \mathbf{r}'|} \quad (247)$$

Equation (247) is a formal expression that does not tell much about the actual dependence on the spin densities, apart from revealing the presence of both parallel ($\sigma = \sigma'$) and antiparallel ($\sigma \neq \sigma'$) spin contributions.

A particularly useful decomposition into parallel and antiparallel components was proposed by Stoll et al.^{367, 368}. The parallel terms of the LDA correlation energy $e_c^{\text{LDA}}(n_\uparrow, n_\downarrow)$ —which are additive in spin—are defined as

$$e_{c\uparrow\uparrow}^{\text{LDA}}(n_\uparrow) = \frac{n_\uparrow}{n} e_c^{\text{LDA}}(n_\uparrow, 0) \quad (248a)$$

$$e_{c\downarrow\downarrow}^{\text{LDA}}(n_\downarrow) = \frac{n_\downarrow}{n} e_c^{\text{LDA}}(0, n_\downarrow) \quad (248b)$$

while the antiparallel term is obtained as the remainder of the correlation energy:

$$e_{c\uparrow\downarrow}^{\text{LDA}}(n_\uparrow, n_\downarrow) = e_c^{\text{LDA}}(n_\uparrow, n_\downarrow) - e_{c\uparrow\uparrow}^{\text{LDA}}(n_\uparrow) - e_{c\downarrow\downarrow}^{\text{LDA}}(n_\downarrow) \quad (249)$$

In spite of the usefulness of the the above expression, deficiencies of this decomposition have been pointed out by Gori-Giorgi and Perdew³⁶⁹.

Along the same lines, for GGA and MGGA functionals, one can thus consider

$$e_c[n_\uparrow, n_\downarrow] = \sum_{\sigma} e_{c\sigma\sigma}^{\text{LDA}}(n_\sigma) F_{c\sigma\sigma}[n_\sigma, 0] + e_{c\uparrow\downarrow}^{\text{LDA}}(n_\uparrow, n_\downarrow) F_{c\uparrow\downarrow}[n_\uparrow, n_\downarrow] \quad (250)$$

where $F_{c\sigma\sigma'}[n_\sigma, n_{\sigma'}]$ are appropriate spin-resolved enhancement factors, including the dependence on quantities beyond the spin-densities.

Finally, note that the correlation energy functional does not obey a simple spin-scaling relation like eq. (243) for exchange. Therefore, while the corresponding spin-unpolarized form of F_c defined by eq. (241) can trivially be recovered from a given spin-polarized form for $F_{c\sigma\sigma'}$, it may not be possible to deduce $F_{c\sigma\sigma'}$ from a given F_c .

2.18.4 Systematic fits of density functionals

Becke³⁷⁰ proposed a strategy for systematically fitting novel density functionals in 1997; the resulting form is commonly known as B97. The B97 functional form is extremely flexible, and it has been used by dozens of empirical GGA and hybrid-GGA functionals. It has also been extended to MGGA functionals. The critical innovation was to introduce a new normalized variable $0 \leq \tilde{u} \leq 1$

$$\tilde{u}(x) = \frac{\gamma x^2}{1 + \gamma x^2} \quad (251)$$

which can be used to systematically expand density functionals as power series. The definition of \tilde{u} depends on a (yet undetermined) nonlinear parameter γ . The variable x in eq. (251) can be any of the reduced density gradient x discussed in section 2.1.3 (spin-polarized, spin-unpolarized, or total).

The functional form for the exchange part

$$F_x^{\text{B97}} = \sum_{i=0}^m c_{i\sigma} [\tilde{u}(x_\sigma)]^i \quad (252)$$

where \tilde{u} is eq. (251) with $\gamma_x = 0.004$ that was directly adopted from earlier work of Becke¹⁵⁵. The functional form of the correlation part is given by eq. (250) with

$$F_{c\sigma\sigma}^{\text{B97}} = g_{c\sigma\sigma}^{\text{B97}}(x_\sigma) \quad (253a)$$

$$F_{c\uparrow\downarrow}^{\text{B97}} = g_{c\uparrow\downarrow}^{\text{B97}}(x_{\text{avg}}) \quad (253b)$$

where x_{avg} is defined by eq. (45) and the functions $g_{c\sigma\sigma'}^{\text{B97}}$ are simple polynomials of degree m :

$$g_{c\sigma\sigma'}^{\text{B97}}(x) = \sum_{i=0}^m c_{i\sigma\sigma'} [\tilde{u}(x)]^i \quad (254)$$

The parametrization of Perdew and Wang²⁶⁰ (see `lda_c_pw` below) was used to represent the energy density $e_{c\sigma\sigma'}^{\text{ref}}$ in eq. (250). The opposite-spin parameter $\gamma_{c\uparrow\downarrow} = 0.006$ was chosen to obtain the correct correlation energy for the He atom, and the same-spin parameter $\gamma_{c\sigma\sigma} = 0.2$ was then chosen to achieve the proper correlation energy for the Ne atom.³⁷⁰ Becke³⁷⁰ used the truncation $m = 2$ for the B97 hybrid functional, leading to 3 linear parameters each for exchange, opposite-spin correlation, and same-spin correlation.

3 Semi-local xc approximations

This section provides a comprehensive overview of semi-local functionals reported in the literature. Despite our systematic literature review, some functionals from less accessible or historical sources may not be included. However, we are confident that our review encompasses virtually all semi-local functionals of practical significance reported before 2026.

Semi-local functionals belong to the first three rungs of Jacob's ladder (see section 1.3): LDA (section 3.1), GGA (section 3.2), and MGGA (section 3.3). A further division is based on the type of the functional: exchange, correlation, or exchange-correlation, the latter essentially consisting of functionals that cannot be logically separated into exchange and correlation parts. The names of the functionals are those used in Libxc, however, note that some of the functionals described below are not yet implemented in the Libxc library.

3.1 Local-density approximation

The LDA is the simplest of all functional forms: the xc energy density per electron e_{xc} at every point in space \mathbf{r} depends solely on the spin densities $n_\sigma(\mathbf{r})$ of the system at that point:

$$\begin{aligned} E_{\text{xc}}^{\text{LDA}} &= \int d^3r n(\mathbf{r}) e_{\text{xc}}^{\text{LDA}}(n_\uparrow(\mathbf{r}), n_\downarrow(\mathbf{r})) \\ &= \int d^3r n(\mathbf{r}) e_{\text{xc}}^{\text{LDA}}(r_s(\mathbf{r}), \zeta(\mathbf{r})) \end{aligned} \quad (255)$$

In most LDA functionals, e_{xc}^{LDA} is the expression for the HEG, whose analytical form is known exactly for exchange, while fits to accurate data for correlation obtained from Monte Carlo (MC)^{371–373} or other methods³⁷⁴ are available.

In a non-relativistic framework, the exchange energy is given by a sum over the spin components¹⁵⁴ (see eq. (243)). This is obviously not the case for correlation, as discussed in section 2.18.3.

3.1.1 Exchange

`lda_x`^{142,143} (1929)

The exchange energy of the HEG is trivial to calculate, yielding the exchange LDA functional

$$e_x^{\text{LDA}}(n_\uparrow, n_\downarrow) = -C_x \frac{n_\uparrow^{4/3} + n_\downarrow^{4/3}}{n} \quad (256)$$

or, alternatively,

$$e_x^{\text{LDA}}(r_s, \zeta) = -A_x \frac{\phi_{4/3}(\zeta)}{r_s} \quad (257)$$

where A_x , C_x , and $\phi_{4/3}$ are given by eqs. (16), (17) and (40), respectively. With few exceptions, GGA and MGGA exchange functionals recover `lda_x` when evaluated for the HEG. Note that even though the LDA exchange has been surpassed by more modern functionals, it is still sometimes used in applications (combined with a LDA correlation functional) in modern literature.

Gáspar³⁷⁵, and later Kohn and Sham², derived the corresponding potential by minimizing the total energy:

$$v_{x\sigma}^{\text{LDA}} = - \left(\frac{6}{\pi} \right)^{1/3} n_\sigma^{1/3} \quad (258)$$

`lda_x_rae`³⁷⁶ (1973)

The `lda_x` functional contains a self-interaction error,²³³ which vanishes for the HEG, but may be significant in other systems. Rae³⁷⁶ proposed a form where this self-interaction error is explicitly removed from the functional by mul-

tiplying eq. (256) by a factor:

$$e_x^{\text{Rae}}(r_s, \zeta, N) = e_x^{\text{LDA}}(r_s, \zeta) \times \left(1 - \frac{8}{3} \delta_x + 2\delta_x^2 - \frac{1}{3} \delta_x^4 \right) \quad (259)$$

where the quantity δ_x is computed from the number of electrons N in the system as $\delta_x = (4N)^{-1/3}$. `lda_x_rae` was used to calculate the potential energy of rare-gas dimers with the additional inclusion of a dispersion energy term.

Note that as this functional depends on the total number of electrons obtained by an integral over all space

$$N = \int d^3r n(\mathbf{r}) \quad (260)$$

of the electron density $n(\mathbf{r})$ at each point, it is formally not an LDA, or even a semi-local functional. The functional `lda_x_rae` is implemented in Libxc with N handled as a user-defined parameter, that is set to $N = 1$ by default.

`lda_x_rel`^{34,35,377} (1978)

Relativistic corrections to `lda_x` can be included by multiplying each of the two terms in eq. (256) by the factor^{34,35,377}

$$\phi(n_\sigma) = 1 - \frac{3}{2} \left[\frac{\sqrt{1 + \beta^2}}{\beta} - \frac{\text{arcsinh}(\beta)}{\beta^2} \right]^2 \quad (261)$$

which is the sum of the longitudinal and transverse components (eqs. (4.3) and (4.7) in ref. 377). The retardation function β is defined as

$$\beta(n_\sigma) = \frac{(6\pi^2)^{1/3}}{c} n_\sigma^{1/3} \quad (262)$$

where c is the speed of light in vacuum. Note that $\lim_{c \rightarrow \infty} \phi = 1$ (non-relativistic limit).

`lda_x_2d`^{142,143,145} (2002)

The exchange energy of the HEG in 2D can be simply derived by changing the dimensionality of the integrals leading to `lda_x`. This yields

the energy density

$$e_x^{\text{LDA-2D}}(n_\uparrow, n_\downarrow) = -C_x^{2\text{D}} \frac{n_\uparrow^{3/2} + n_\downarrow^{3/2}}{n} \quad (263)$$

or, alternatively,

$$e_x^{\text{LDA-2D}}(r_s^{2\text{D}}, \zeta) = -A_x^{2\text{D}} \frac{\phi_{3/2}(\zeta)}{r_s^{2\text{D}}} \quad (264)$$

where $r_s^{2\text{D}}$ is given by eq. (35b), $\phi_{3/2}(\zeta)$ is given by eq. (40), $A_x^{2\text{D}}$ is given by eq. (18), and $C_x^{2\text{D}}$ is given by eq. (19).

[lda_x_1d_soft](#), [lda_x_1d_exponential](#)^{334,378} (2006)

The exchange energy in 1D cannot be expressed as a closed algebraic formula with most of the common interactions. However, it can be written in terms of the Fourier transform of the interaction potential:

$$e_x^{\text{LDA-1D}}(r_s^{1\text{D}}, \zeta) = -\frac{1}{4\pi b} \sum_{\sigma} [1 + \text{sgn}(\sigma)\zeta] \times \int_0^R dx F(x) \left(1 - \frac{x}{R}\right)$$

with

$$R = [1 + \text{sgn}(\sigma)\zeta] \frac{\pi b}{2r_s^{1\text{D}}} \quad (265)$$

and $r_s^{1\text{D}}$ is given by eq. (35a) and

$$F^{\text{soft-Coulomb}}(x) = 2K_0(x) \quad (266a)$$

$$F^{\text{exponential}}(x) = E_1(x^2)e^{x^2} \quad (266b)$$

where K_0 is the modified Bessel function and E_1 is the exponential integral.

These two functionals have never been published, but related work can be found in refs. [334](#) and [378](#).

[lda_x_sloc](#)³⁷⁹ (2017)

Finzel and Baranov³⁷⁹ proposed a simple local approximation for the Slater potential⁴² (eq. (144)) of the form

$$v_{x\sigma}^{\text{SLOC}} = -a(2n_\sigma)^b \quad (267)$$

which corresponds to an energy density given

by

$$e_x^{\text{SLOC}}(n, \zeta) = -\frac{a}{b+1} n^b \phi_{b+1}(\zeta) \quad (268)$$

where ϕ_{b+1} is given by eq. (40). The parameters $a = 1.67$ and $b = 0.3$ were determined by fitting eq. (267) to the Slater potential calculated using the HF wavefunctions of Clementi and Roetti³⁸⁰ for the Be, Ne, Mg, Ar, Ca, Zn, Kr, Sr, Pd and Xe atoms. Even though the exponent b is close to the 1/3 of the standard [lda_x](#), the prefactor a is considerably larger ($a = (3/\pi)^{1/3} \approx 0.984745$ for [lda_x](#)), leading to a much more negative potential. Band gaps calculated with this functional are considerably improved when compared to the original [lda_x](#).^{379,381,382} Note that no correlation was added to exchange in the calculations.

[lda_x_t_sloc](#)³⁸² (2020)

Borlido et al.³⁸² reparameterized [lda_x_sloc](#) in order to improve the accuracy of the band gap of solids. For a subset of 85 solids among the 473 solids considered in their work, the optimal parameters a and b in eq. (267) were determined to be $a = 1.775$ and $b = 0.260$. The mean absolute error for the band gap on the whole set of 473 solids is 0.61 eV, while it is 0.66 eV for [lda_x_sloc](#).

3.1.2 Correlation

[lda_c_wigner](#)³⁸³ (1938)

Wigner³⁸³ proposed an extremely simple parametrization for the correlation functional. It reads as

$$e_c^{\text{Wigner}}(r_s) = -\frac{a}{b+r_s} \quad (269)$$

with $a = 0.44$ and $b = 7.8$. It is noteworthy that this expression satisfies the uniform scaling requirements,³⁸⁴ and despite its simplicity, it gives fairly good values for the correlation energy. Wigner³⁸³ only considered the spin-unpolarized case, but a spin-polarized version ([lda_c_ow](#), [lda_c_ow_lyp](#)) was later developed by Stewart and Gill³⁸⁵. Note that the implementation of [lda_c_wigner](#) in Libxc is the spin-polarized version, i.e., eq. (291) with the

values of a and b mentioned above.

[lda_c_xalpha](#)⁴² (1951)

This is the famous X_α method of Slater⁴², which he proposed as a simplification of the HF method. In his theory, the exchange functional has the same form as [lda_x](#), but the functional is multiplied by $3\alpha/2$, where α is a parameter. The difference to [lda_x](#) is interpreted as correlation:

$$e_c^{X\alpha} = \left(\frac{3}{2}\alpha - 1\right) e_x^{\text{LDA}} \quad (270)$$

In Slater’s original work, $\alpha = 1$, but since then the $X\alpha$ form has been used in numerous applications using values for α fit in a variety of ways (see, e.g., refs. [386](#) and [387](#)).

[lda_c_rpa](#)^{250,388} (1957)

Another well-known approximation to the correlation energy of the HEG is the random phase approximation (RPA),²⁵⁰ which is based on the infinite resummation of the so-called bubble diagrams—the most highly divergent diagrams in each order of perturbation theory for the HEG. It reads as

$$e_c^{\text{RPA}}(r_s) = 0.0311 \ln(r_s) - 0.048 + 0.009r_s \ln(r_s) - 0.018r_s \quad (271)$$

Note that this is, in fact, the correct high-density limit, and it has therefore been commonly used in the construction of functionals.

[lda_c_gombas](#)^{389,390} (1965)

The [lda_c_wigner](#) functional was extended by Gombás who added the high-density limit to eq. (269), leading to

$$e_c^{\text{Gombás}}(r_s) = -\frac{\beta_1}{1 + \beta_2 \tilde{r}_s} - \gamma_1 \ln\left(1 + \frac{\gamma_2}{\tilde{r}_s}\right) \quad (272)$$

where \tilde{r}_s is eq. (38) and $\beta_1 = 0.0357$, $\beta_2 = 0.0562$, $\gamma_1 = 0.0311$, and $\gamma_2 = 2.39$.

[lda_c_hl](#)³⁹¹ (1971)

Hedin and Lundqvist³⁹¹ proposed the following parametrization to the correlation energy of the HEG as obtained previously by Singwi et al.³⁹²:

$$e_c^{\text{HL}}(r_s) = -c \left[(1 + y^3) \ln\left(1 + \frac{1}{y}\right) + \frac{y}{2} - y^2 - \frac{1}{3} \right] \quad (273)$$

where $y = r_s/r$ and the fitting parameters are $c = 0.0225$ and $r = 21$.

[lda_c_vbh](#)³⁵⁶ (1972)

von Barth and Hedin³⁵⁶ generalized the original DFT formulation of Hohenberg, Kohn, and Sham^{1,2} to the case of spin-polarized systems. Their spin-dependent correlation functional is based on a simple interpolation between the correlation energy of the ferromagnetic (F) and paramagnetic (P) phases of the HEG. It reads as

$$e_c^{\text{vBH}}(r_s, \zeta) = e_c^{\text{P}}(r_s) + [e_c^{\text{F}}(r_s) - e_c^{\text{P}}(r_s)] f_c(\zeta) \quad (274)$$

The ζ -dependence of the function $f_c(\zeta)$ is similar to the case of exchange (see eq. (257)):

$$f_c(\zeta) = \frac{\phi_{4/3}(\zeta) - 1}{2^{1/3} - 1} \quad (275)$$

where $\phi_{4/3}(\zeta)$ is given by eq. (40). The correlation energies of the ferromagnetic (e_c^{F}) and paramagnetic (e_c^{P}) HEG were individually parameterized using the Hedin and Lundqvist³⁹¹ form given by eq. (273) to the correlation energy of the HEG calculated using a “two-bubble” approximation to the irreducible polarization. The resulting parameters in eq. (273) are $c^{\text{F}} = 0.0127$ and $r^{\text{F}} = 75$ for e_c^{F} , and $c^{\text{P}} = 0.0252$ and $r^{\text{P}} = 30$ for e_c^{P} .

[lda_c_gk72](#)³⁹³ (1972)

Gordon and Kim³⁹³ interpolated between the high-density [lda_c_rpa](#) expansion (eq. (271) with a coefficient of -0.01 instead of -0.018 in the last term) and the low-density expansion²⁵⁹ given by

$$e_c^{\text{low}}(r_s) = -\frac{0.438}{r_s} + \frac{1.325}{r_s^{3/2}} - \frac{1.47}{r_s^2} - \frac{0.4}{r_s^{5/2}} \quad (276)$$

to arrive at the interpolation formula

$$e_c^{\text{middle}}(r_s) = -0.06156 + 0.01898 \ln(r_s) \quad (277)$$

for the mid-range density regime that they defined as $r_s \in [0.7, 10]$. The resulting functional, which consists of these three formulas corresponding to different density regimes, was used to study the interaction potential between two closed-shell atoms or ions. Note that eq. (22) in

ref. 393 appears to have a wrong overall sign, as shown by the attempted reproduction of Figure 1 in that paper. It also appears that the data in the figure was scaled by a factor of 10.

`lda_c_gl`¹⁹² (1976)

Gunnarsson and Lundqvist¹⁹² proposed another variant of the `lda_c_vbh` functional (eq. (274)). This time, the functional was fit to the correlation energy of the HEG calculated using a plasmon model and an approximation to the electronic self-energy that takes into account only the lowest order term in the dynamically screened interaction. The resulting parameters in eq. (273) are $c^F = 0.0203$ and $r^F = 15.9$ for e_c^F , and $c^P = 0.0333$ and $r^P = 11.4$ for e_c^P .

`lda_c_mcweeny`³⁹⁴ (1976)

McWeeny³⁹⁴ evaluated the `mgga_c_cs` functional for the HEG for the complete range of the density parameter r_s . It turns out that the results reproduce rather well both the low and high density limits, and that they can be fit with high accuracy over the whole range by a `lda_c_wigner` form, with $a = [3/(4\pi)]^{1/3}/2.946$ and $b = 9.652a$ in eq. (269).

`lda_c_br78`³⁹⁵ (1978)

In order to study the interaction between rare-gas atoms, Brual Jr. and Rothstein³⁹⁵ proposed to use the `lda_c_wigner` functional, but with the two parameters, $a = [3/(4\pi)]^{1/3}/21.437$ and $b = 9.810a$ in eq. (269), tuned in order to reproduce exactly the correlation energy of the He atom. With these parameters the correlation energies of the Ne and Ar atoms are also well reproduced.

`lda_c_vwn`, `lda_c_vwn_rpa`, `lda_c_vwn_1`, `lda_c_vwn_2`, `lda_c_vwn_3`, `lda_c_vwn_4`³⁹⁶ (1980)

The Vosko–Wilk–Nusair³⁹⁶ (VWN) correlation functional is one of the first *modern* LDAs, and is still commonly used nowadays. It is based on a Padé approximant technique to accurately interpolate the MC results of Ceperley and Alder³⁷¹. Furthermore, by combining these results with the spin-dependence of the RPA correlation energy, Vosko et al.³⁹⁶ were able to obtain an accurate parametrization of the HEG

for relevant ranges of r_s and ζ . The functional reads as

$$e_c^{\text{VWN}}(r_s, \zeta) = e_c^P(r_s) + [e_c^F(r_s) - e_c^P(r_s)] f_c(\zeta) \zeta^4 + \frac{f_c(\zeta)}{f_c''(0)} (1 - \zeta^4) \alpha_c(r_s) \quad (278)$$

where α_c is the spin-stiffness coefficient given by

$$\alpha_c(r_s) = \left. \frac{\partial^2 e_c(r_s, \zeta)}{\partial \zeta^2} \right|_{\zeta=0} \quad (279)$$

The function $f_c(\zeta)$ is the same as in the `lda_c_vbh` functional (see eq. (275)), but we can see that the spin interpolation is now considerably more complex. The second derivative of $f_c(\zeta)$ at $\zeta = 0$ gives $f_c''(0) = 4/[9(2^{1/3} - 1)]$, and the functions e_c^P , e_c^F , and α_c are parameterized using the form

$$G(y) = A \left\{ \ln \frac{y^2}{X(y)} + \frac{2b}{Q} \arctan \frac{Q}{2y+b} - \frac{by_0}{X(y_0)} \left[\ln \frac{(y-y_0)^2}{X(y)} + 2 \frac{b+2y_0}{Q} \arctan \frac{Q}{2y+b} \right] \right\} \quad (280)$$

with $Q = \sqrt{4c - b^2}$ and $X(y) = y^2 + by + c$. VWN provided a fit to both MC and RPA data, with the latter only given as a test of the adequacy of eq. (280) to interpolate over the relevant range of r_s .

Unfortunately, the several versions of the VWN functional given in the paper³⁹⁶ later led to confusion in the community,¹²⁸ in particular regarding the construction of the hybrid functional B3LYP.^{397,398} Various versions of the VWN functional are described below:

- `lda_c_vwn` uses eqs. (278) and (280) with the MC coefficients. This is the functional that was recommended by Vosko et al.³⁹⁶, which is sometimes referred to as VWN5 in the literature. This is the version used in `hyb_gga_xc_b3lyp5` as implemented in Libxc.
- `lda_c_vwn_rpa` uses eq. (280) with the RPA coefficients, but uses the older spin-interpolation formula of `lda_c_vbh` given by eq. (274). This is the version used

in `hyb_gga_xc_b3lyp` as implemented in Libxc.

- `lda_c_vwn_1` uses eq. (280) with the MC coefficients, but uses the older spin-interpolation formula of `lda_c_vbh` given by eq. (274).
- `lda_c_vwn_2` is given by

$$e_c^{\text{VWN2}}(r_s, \zeta) = e_c^{\text{P, MC}}(r_s) + [e_c^{\text{F, RPA}}(r_s) - e_c^{\text{P, RPA}}(r_s)] f_c(\zeta)(\zeta^4 - 1) + [e_c^{\text{F, MC}}(r_s) - e_c^{\text{P, MC}}(r_s)] f_c(\zeta) + \frac{f_c(\zeta)}{f_c''(0)} (1 - \zeta^4) \alpha_c^{\text{RPA}}(r_s)$$

which uses both MC and RPA coefficients in eq. (280).

- `lda_c_vwn_3` uses the spin interpolation given by eq. (278) with the MC coefficients, but with a spin-stiffness coefficient that is rescaled as follows:

$$\alpha_c^{\text{VWN3}}(r_s) = \alpha_c^{\text{RPA}}(r_s) \times \frac{e_c^{\text{F, MC}}(r_s) - e_c^{\text{P, MC}}(r_s)}{e_c^{\text{F, RPA}}(r_s) - e_c^{\text{P, RPA}}(r_s)} \quad (281)$$

This amounts to the assumption that the spin-dependence of the correlation energy is the same as for the RPA for fixed r_s . This is the version used in `hyb_gga_xc_b3lyp3` as implemented in Libxc.

- `lda_c_vwn_4` uses the spin interpolation of eq. (278) with the MC coefficients in eq. (280), with the exception of the spin stiffness α_c that is calculated at the RPA level.

`lda_c_pz`²³³ (1981)

In an appendix to their famous paper on the self-interaction correction to DFT, Perdew and Zunger²³³ presented a new fit to the Ceperley and Alder³⁷¹ MC results. The spin-dependence was modeled by the `lda_c_vbh` formula given by eq. (274), even if the more accurate `lda_c_vwn` form was already known at the time. To describe the density dependence,

they divided the r_s range in two intervals. For large r_s (low density n), the parametrization proposed by Ceperley³⁹⁹ for the correlation energy was used:

$$e_c^{\text{PZ}, r_s \geq 1}(r_s) = \frac{\gamma}{1 + \beta_1 \sqrt{r_s} + \beta_2 r_s} \quad (282)$$

where γ , β_1 , and β_2 are parameters fit to the MC results for the ferromagnetic and paramagnetic cases. For small r_s , the RPA form for the high-density limit (eq. (271)),

$$e_c^{\text{PZ}, r_s < 1}(r_s) = A \ln(r_s) + B + Cr_s \ln(r_s) + Dr_s \quad (283)$$

was used. For the paramagnetic case, A and B were taken from the RPA calculation of Gell-Mann and Brueckner²⁵⁰ while for the ferromagnetic case Perdew and Zunger²³³ used Misawa's scaling relation of RPA⁴⁰⁰

$$e_c^{\text{RPA, F}}(r_s) = \frac{1}{2} e_c^{\text{RPA, P}}(r_s/2^{4/3}) \quad (284)$$

Finally, C and D were obtained by requiring that both the correlation energy and the corresponding potential are continuous at $r_s = 1$, leading to

$$D = \frac{\gamma}{1 + \beta_1 + \beta_2} - B \quad (285a)$$

$$C = A - D + \gamma \frac{\frac{1}{2}\beta_1 + \beta_2}{(1 + \beta_1 + \beta_2)^2} \quad (285b)$$

respectively. Unfortunately, this functional suffers from two problems: (i) even if it is continuous and differentiable at $r_s = 1$, the second derivative is discontinuous and higher derivatives diverge. This unphysical behavior can be problematic in the calculation of second- and higher-order response properties. It also leads to slow convergence in numerical quadrature.⁴⁰¹ (ii) Truncated numerical values were given for both C and D ,⁴⁰⁰ that have found their way into several implementations of this functional. Unfortunately, these approximate values lead to some small artificial discontinuities in the functional. Although the functional still appears to be used, we recommend migrating to better-behaved functionals such as `lda_c_pw`, instead.

`lda_c_bj89`⁴⁰² (1989)

By considering a system of two electrons with opposite spins that interact only when their separation is smaller than a cutoff distance r_c , a non-local expression for the correlation potential v_c was obtained by Barbiellini and Jarlborg⁴⁰². Then, by making a correspondence between the HEG and such two-electron systems filling the whole space, numerical values obtained with the non-local potential were fit by using a local potential that has a form given by the functional derivative of the `lda_c_wigner` functional. For the corresponding correlation functional (eq. (269)) this led to the parameters $a = 0.18647$ and $b = 1.89173$.

`lda_c_pw`, `lda_c_pw_rpa`^{260,403} (1992)

Perdew and Wang²⁶⁰ proposed a new LDA correlation functional^{260,403} that tried to simplify and remove some of the deficiencies of the previous `lda_c_vwn` and `lda_c_pz` forms. This functional uses the more precise spin-interpolation given by eq. (278), but with a r_s -dependence of *minus* the spin-stiffness $-\alpha_c(r_s)$ and of the paramagnetic and ferromagnetic correlation energy densities that is given by

$$G(r_s) = -2A(1 + \alpha_1 r_s) \times \ln \left[1 + \frac{1}{2A \left(\beta_1 r_s^{1/2} + \beta_2 r_s + \beta_3 r_s^{3/2} + \beta_4 r_s^{p+1} \right)} \right] \quad (286)$$

Two sets of parameters were provided; one set determined from known exact results and accurate MC data^{371,396} (`lda_c_pw`), and the other from RPA³⁹⁶ (`lda_c_pw_rpa`). The parameters A , β_1 , and β_2 were chosen such that the high-density limit (same form as eq. (271)) is recovered, while p (1 and 3/4 for exact and RPA, respectively) was determined from the low-density expansion (same form as eq. (276)). Finally, α_1 , β_3 , and β_4 were fit to either MC or RPA data. The functional `lda_c_pw` (often referred to as PW92 in the literature) is the LDA component of numerous GGA and MGGA correlation functionals like `gga_c_pbe`.

`lda_c_ob_pz`, `lda_c_ob_pw`^{372,373} (1994)

Ortiz and Ballone³⁷² revisited the MC results of Ceperley and Alder³⁷¹ with variational and

fixed-node diffusion MC methods. They considered larger systems with better statistics and also partial spin polarization, the latter point being especially important. They provided two different parametrizations for their results, one using the `lda_c_pz` form and another using the `lda_c_pw` form. Note that the values of C given in Table VI of ref. 372 for `lda_c_ob_pz` have the wrong sign.

`lda_c_ml1`, `lda_c_ml2`^{404,405} (1994)

Proynov and Salahub⁴⁰⁴ derived a functional for the opposite-spin correlation from a model pair-correlation. The main difference to the standard LDA is that this functional does not diverge logarithmically at small r_s (high density n) and is constructed such that it has a small self-interaction error for the H atom. It is written as (note eq. (5) in the Erratum⁴⁰⁵)

$$e_{c\uparrow\downarrow}^{\text{ML}}(r_s, \zeta) = \frac{n(1 - \zeta^2)}{4} Q^{\uparrow\downarrow}(r_s, \zeta) \quad (287)$$

where the function $Q^{\uparrow\downarrow}$ is

$$Q^{\uparrow\downarrow}(r_s, \zeta) = -\frac{b_1}{1 + b_2 k_{\uparrow\downarrow}} + \frac{b_3}{k_{\uparrow\downarrow}} \ln \left(1 + \frac{b_4}{k_{\uparrow\downarrow}} \right) + \frac{b_5}{k_{\uparrow\downarrow}} - \frac{b_6}{k_{\uparrow\downarrow}^2} \quad (288)$$

with the parameters $b_1 = 2.763169$, $b_2 = 1.757515$, $b_3 = 1.741397$, $b_4 = 0.568985$, $b_5 = 1.572202$, and $b_6 = 1.885389$, and where the opposite-spin inverse correlation length $k_{\uparrow\downarrow}$ is given by

$$k_{\uparrow\downarrow}(r_s, \zeta) = \frac{C}{\tilde{r}_s} \alpha(\zeta) \frac{(1 + \zeta)^{1/3} (1 - \zeta)^{1/3}}{2\phi_{1/3}(\zeta)} \quad (289)$$

where \tilde{r}_s is given by eq. (38). The parameter $C = 6.187335$ and the correlation factor α , presumed to be independent of r_s , is given by

$$\alpha(\zeta) = 2f_c \phi_q(\zeta) \quad (290)$$

with q and f_c used as interpolation parameters. Proynov and Salahub⁴⁰⁴ claimed that since α is ζ dependent, parallel-spin correlation can also be accounted for. Two strategies to perform the fitting were used: (i) trying to reproduce the correlation energy of the HEG led to the values

$f_c = 0.2026$ and $q = 0.084$ (`lda_c_m11`); (ii) fitting to the experimental binding energy of a set of seven small molecules led to $f_c = 0.266$ and $q = 0.5$ (`lda_c_m12`). The latter choice, when combined with `lda_x` for exchange, turned out to yield good binding energies and equilibrium bond lengths for a larger set of small molecules.

`lda_c_ow`, `lda_c_ow_lyp`³⁸⁵ (1995)

Stewart and Gill³⁸⁵ tried to develop a functional that retains the accuracy of `gga_c_lyp` with a simpler analytical formula that is more physically transparent. With that in mind, they decided to retain the first term of the `gga_c_lyp` correlation energy, leading to

$$e_c^{\text{OW}}(r_s) = - (1 - \zeta^2) \frac{a}{b + r_s} \quad (291)$$

where a and b are parameters, and OW stands for optimized Wigner. This is thus a generalization of `lda_c_wigner` (eq. (269)) to the spin-polarized case. Two versions of this functional were given: (i) `lda_c_ow_lyp`, where $a = 0.04918b$ and $b = [3/(4\pi)]^{1/3}/0.349$ were fixed to their values in the `gga_c_lyp` functional, and (ii) `lda_c_ow`, with b unchanged, but $a = 0.0526b$ optimized to reproduce the correlation energy of the ten lightest atoms (H to Ne). Tests of their correlation functionals on the G2 dataset^{406,407} in combination with `gga_x_b88` led to the finding that `lda_c_ow_lyp` gives overall similar results to the more complicated `gga_c_lyp`.

`lda_c_lp96`, `lda_c_lp96_b`^{408,409} (1996)

By rescaling the interaction term by a coupling constant λ , one can decompose the correlation energy as²³⁸

$$\lambda E_c^\lambda[n] = T_c^\lambda[n] + \lambda V_c^\lambda[n] \quad (292)$$

where the first term is the contribution of the kinetic energy to the correlation energy of DFT and the second is the potential energy contribution. One can prove that these quantities obey a series of exact conditions, such as^{238,410}

$$T_c^\lambda[n] = -\lambda^2 \frac{dE_c^\lambda[n]}{d\lambda} \quad (293)$$

Starting from these identities, and from the as-

sumption that $E_c^\lambda[n]$ has a Taylor expansion as a function of λ , Liu and Parr arrived at the conclusion that E_c and T_c can be expressed as combinations of homogeneous functionals of different degrees in terms of coordinate scaling. Furthermore, they showed that when E_c and T_c are of the LDA type, they are linear combinations of homogeneous functionals of degree $(4 - i)/3$, where $i = 1, 2, 3, \dots$. Taking into account the first four terms in the expansion leads to the following functional form for the correlation:

$$e_c^{\text{LP96}}(n) = C_1 + C_2 n^{-1/3} + C_3 n^{-2/3} + C_4 n^{-1} \quad (294)$$

By first considering eq. (294) with $C_4 = 0$, Liu and Parr fit accurate correlation energies for the atoms He through Ar^{411,412} and obtained $C_1 = -0.0603$, $C_2 = 0.0175$, and $C_3 = -0.00053$ (`lda_c_lp96`). However, note that different values for C_2 and C_3 were given in ref. 409 ($C_1 = -0.0603$, $C_2 = 0.0715$, and $C_3 = -0.0053$), and that it is not clear which set is correct. The values from ref. 408 are used in the Libxc implementation of `lda_c_lp96`.

Finally, by taking into account also the term $C_4 n^{-1}$, and optimizing the coefficients for both the correlation and kinetic energies simultaneously, the values $C_1 = -0.0532$, $C_2 = 0.0121$, $C_3 = -0.0003$, and $C_4 = -0.0070$ were obtained (`lda_c_lp96_b`).

`lda_c_2d_amgb`^{413,414} (2002)

By fitting new data obtained from fixed-node diffusion MC simulation of the ground state of the 2D HEG, Attaccalite et al.⁴¹³ provided an analytic expression for the correlation energy as a function of the density parameter r_s^{2D} (eq. (35b)) and spin-polarization ζ^{2D} , defined analogously to the 3D case. For ease of notation, we imply $r_s = r_s^{2D}$ and $\zeta = \zeta^{2D}$ in the equations below. The basic idea is to interpolate between the low-density and high-density regimes. The ζ dependence of e_{xc} at low density is well described by $c_0 + c_1 \zeta^2 + c_2 \zeta^4$, whilst at high density the behavior is given by $e_c = a_0(\zeta) + a_1(\zeta) r_s \ln r_s + \mathcal{O}(r_s)$,⁴¹⁵ and from these known limits Attaccalite et al.⁴¹³ pro-

posed the following expression:

$$e_c^{\text{AMGB-2D}}(r_s, \zeta) = (e^{-\beta r_s} - 1) e_x^{(6)}(r_s, \zeta) + \alpha_0(r_s) + \alpha_1(r_s) \zeta^2 + \alpha_2(r_s) \zeta^4 \quad (295)$$

where

$$e_x^{(6)}(r_s, \zeta) = e_x(r_s, \zeta) - \left(1 + \frac{3}{8}\zeta^2 + \frac{3}{128}\zeta^4\right) e_x(r_s, 0) \quad (296)$$

is the Taylor expansion of the exchange functional with the terms up to the fourth order in ζ subtracted. A generalization of eq. (286) was chosen for the functions $\alpha_i(r_s)$:

$$\alpha_i(r_s) = A_i + (B_i r_s + C_i r_s^2 + D_i r_s^3) \times \ln \left(1 + \frac{1}{E_i r_s + F_i r_s^{3/2} + G_i r_s^2 + H_i r_s^3} \right) \quad (297)$$

whose parameters were obtained either from the known exact limits or from a fit of the MC data.

[lda_c_rc04](#)⁴¹⁶ (2004)

Ragot and Cortona⁴¹⁶ modified the procedure of Colle and Salvetti⁴¹⁷ in order to include explicitly the contribution of the kinetic energy to the correlation energy. This was done by deducing a Gaussian approximation to the one-particle density matrix that goes beyond HF. By applying this approximation to the HEG they arrived at an expression for the correlation kinetic energy τ_c . Finally, the correlation energy was obtained by standard integration of the following relation that is valid for the HEG:^{260,403,418}

$$\tau_c = -\frac{\partial(r_s e_c)}{\partial r_s} \quad (298)$$

After taking into account some asymptotic considerations, the final form of the functional reads

$$e_c^{\text{RC04}}(r_s) = \frac{A \arctan(B + C r_s) + D}{r_s} \quad (299)$$

with the parameters $A = -0.655868$, $B = 4.888270$, $C = 3.177037$, and $D = 0.897889$. Although the original work⁴¹⁶ only presented the spin-unpolarized form of the func-

tional, later works^{419,420} (see [gga_c_tca](#) and [gga_c_rev_tca](#)) suggested that the spin-dependent extension could be built by multiplying eq. (299) by $\phi_{2/3}^3(\zeta)$.

[lda_c_1d_css](#)³³⁴ (2006)

Casula et al.³³⁴ studied the ground state of a quasi 1D HEG, confined laterally by a harmonic potential of the type $V(r_\perp) = r_\perp^2 / (4b^4)$, where b is the confinement strength. They computed the exact correlation energy employing the lattice regularized diffusion MC method, and then used a function with seven parameters to fit the MC results (below, for ease of notation $r_s = r_s^{\text{1D}}$, eq. (35a)):

$$e_c^{\text{CSS}}(r_s) = -\frac{r_s}{A + B r_s^n + C r_s^2} \ln(1 + \alpha r_s + \beta r_s^m) \quad (300)$$

This expression has the correct behavior at the high-density limit, $e_c^{\text{CSS}}(r_s \rightarrow 0) \propto r_s^2$ (this result can be obtained analytically by using a wavefunction of the Slater-Jastrow type), and at the low-density limit, $e_c^{\text{CSS}}(r_s \rightarrow \infty) \propto \ln(r_s)/r_s$. A set of parameters (A , B , C , α , β , m , and n) was obtained for each value of the confinement strength b that they considered.

[lda_c_2d_prm](#), [lda_c_2d_prm_mod](#)⁴²¹ (2008)

Pittalis et al.⁴²¹ developed a functional for the 2D HEG, starting from an explicit derivation of the Colle-Salvetti formula⁴¹⁷ in 2D. They obtained an expression for the correlation energy similar to the original one of Colle and Salvetti⁴¹⁷. Then, to simplify the formula they used an additional *ad hoc* Gaussian approximation for the two-body density matrix $\rho_2(\mathbf{r}_1, \mathbf{r}_2)$ in terms of the center of mass $\mathbf{r} = (\mathbf{r}_1 + \mathbf{r}_2)/2$ and relative $\mathbf{r}_{12} = \mathbf{r}_2 - \mathbf{r}_1$ coordinates:

$$\rho_2(\mathbf{r}_1, \mathbf{r}_2) = \rho_2(\mathbf{r}, \mathbf{r}) e^{-c\beta^2(\mathbf{r})r_{12}^2} \quad (301)$$

where $c = \pi / [2(N-1)q^2]$, N is the number of electrons (eq. (260)), and $\beta = q\sqrt{n}$ with $q = 2.258$ is a fitting parameter that was determined from a reference correlation energy for the singlet state of a two-electron parabolic quantum dot. This led to the correlation energy

functional given by

$$e_c^{\text{PRM}} = c(N-1) \left[\frac{\sqrt{\pi}\beta}{2\sqrt{2+c}}(\Phi-1)^2 + \frac{\Phi(\Phi-1)}{2+c} \right. \\ \left. + \frac{\sqrt{\pi}\Phi^2}{4\beta(2+c)^{3/2}} + \frac{\sqrt{\pi}\beta}{\sqrt{1+c}}(\Phi-1) + \frac{\Phi}{1+c} \right] \quad (302)$$

where $\Phi = \beta / (\beta + \sqrt{\pi}/2)$.

Pittalis et al.⁴²¹ also considered a modification of eq. (302) (`lda_c_2d_prm_mod`). It consists of replacing $(\Phi - 1)^2$ by $\Phi - 1$ in the first term, and a refitting the value for q ($q^{\text{mod}} = 3.9274$). `lda_c_2d_prm_mod` clearly improves over `lda_c_2d_prm` for the correlation energy of parabolic and square quantum dots.

The explicit dependence on the number of electrons N makes these functionals formally not semi-local functionals (see discussion for `lda_x_rae`). The functional `lda_c_2d_prm` is implemented in Libxc with N handled as a user-defined parameter, that is set to $N = 2$ by default.

`lda_c_pk09`^{422,423} (2009)

This is an interpolation of the correlation energy of the HEG, whose expression was derived from the adiabatic connection formula^{65,190–192} It is accurate for densities in the range $0.1 \leq r_s \leq 30$ and for the full range of spin polarization. The opposite- and parallel-spin components, constructed separately, are given by

$$e_{c\uparrow\downarrow}^{\text{PK09}} = \frac{n_\uparrow n_\downarrow}{n} \left[Q_1^{\uparrow\downarrow}(k_{\uparrow\downarrow}) + Q_2^{\uparrow\downarrow}(k_{\uparrow\downarrow}) + Q_3^{\uparrow\downarrow}(k_{\uparrow\downarrow}) \right] \quad (303a)$$

$$e_{c\sigma\sigma}^{\text{PK09}} = \frac{n_\sigma^2}{2n} [Q_1^\sigma(k_\sigma) + Q_2^\sigma(k_\sigma) + Q_3^\sigma(k_\sigma)] \quad (303b)$$

respectively, where the functions $Q_i^{\uparrow\downarrow}(k_{\uparrow\downarrow})$ and $Q_i^\sigma(k_\sigma)$ have the same analytical form and

read⁴²⁴

$$Q_1(k) = \frac{1}{D_1(k)} \left\{ -\arctan(a_2 k + a_3) \frac{D_2(k)}{k} \right. \\ \left. - \frac{D_3(k)}{k} \ln[D_1(k)] + \frac{\ln(k)}{k} D_4(k) \right. \\ \left. - a_4 k + a_{12} + \frac{a_{14}}{k} + \frac{a_{18}}{k^2} \right\} \quad (304a)$$

$$Q_2(k) = -\frac{c_1}{k} - \frac{c_2}{k^2} - \frac{c_3}{k} \ln(k) + \frac{c_4}{k} \ln[D_5(k)] \\ + \frac{c_8}{k} \arctan(a_2 k + a_3) + \frac{c_9}{k} \ln(k + c_{10}) \\ - \frac{c_{11}}{k} \ln[D_6(k)] \quad (304b)$$

$$Q_3(k) = \frac{c_{19}}{k} \arctan\left(\frac{c_{20}}{c_{21}k + c_{22}}\right) \\ - \frac{c_{23}}{k} \operatorname{arctanh}\left[\frac{c_{24} + c_{25}k}{D_8(k)}\right] \\ - \frac{c_{15}}{k} \ln[D_7(k)] - \frac{c_{29}}{k^2} D_8(k) \quad (304c)$$

In the above expressions, the functions $D_i(k)$ are given by

$$D_i(k) = b_{i,2}k^2 + b_{i,1}k + b_{i,0} \quad (305)$$

for $i = 1, \dots, 7$ and

$$D_8(k) = (b_{8,2}k^2 + b_{8,1}k + b_{8,0})^{1/2} \quad (306)$$

The opposite-spin wave vector in eq. (303a) is given by

$$k_{\uparrow\downarrow} = \beta_{\text{eff}}(r_s) \frac{2k_{\text{F}\uparrow}k_{\text{F}\downarrow}}{k_{\text{F}\uparrow} + k_{\text{F}\downarrow}} \quad (307)$$

where $k_{\text{F}\sigma}$ is the Fermi wave vector (eq. (49)) and

$$\beta_{\text{eff}}(r_s) = \eta_1 + \eta_2 e^{-\eta_3 r_s^{1/3}} r_s^{1/4} + \eta_4 e^{-\eta_5 r_s^{1/3}} r_s^{1/3} \quad (308)$$

while the parallel-spin wave vector in eq. (303b) reads

$$k_\sigma = \alpha_{\text{eff}}(r_s, \zeta) k_{\text{F}\sigma} \quad (309)$$

where

$$\alpha_{\text{eff}}(r_s, \zeta) = \alpha_n(r_s)\alpha_\zeta(r_s, \zeta) \quad (310)$$

with

$$\alpha_n(r_s) = \eta_6 + \eta_7 e^{-\eta_8 r_s^{1/3}} r_s^{2/3} + \eta_9 e^{-\eta_{10} r_s^{1/3}} r_s^{1/3} \quad (311a)$$

$$\alpha_\zeta(r_s, \zeta) = \frac{2}{(1 + \zeta)^{s(r_s, \zeta)} + (1 - \zeta)^{s(r_s, \zeta)}} \quad (311b)$$

where $s(r_s, \zeta) = 1.28 f_r(r_s) f_s(\zeta)$ with $f_r(r_s) = P_1(r_s)/P_2(r_s)$ and $f_s(\zeta) = P_3(\zeta)/P_4(\zeta)$. The functions P_i are polynomials.^{422,423} The coefficients in the functions Q_i and D_i were determined from the derivation of the functional expression. The parameters in the screening functions β_{eff} and α_{eff} were fit with high accuracy to reference data.⁴²⁴ Note that the functional `lda_c_pk09` has numerical instabilities.

`lda_c_dpi`^{252,253} (2010)

From the known asymptotes of the correlation energy of the HEG at the high- and low-density limits, Sun et al.²⁵² constructed a functional, named density-parameter interpolation (DPI), that interpolates between these two limits. The functional reads

$$e_c^{\text{DPI}}(r_s, \zeta) = \frac{I_0(r_s, \zeta) + I_1(r_s) b_1(\zeta)}{J_0(r_s, \zeta) + J_1(r_s, \zeta) b_1(\zeta)} \quad (312)$$

where

$$I_0(r_s, \zeta) = [a_0(\zeta) + a_1(\zeta) r_s] \ln \left(\frac{r_s}{1 + r_s} \right) + b_0(\zeta) + 2a_0(\zeta) [1 - (1 + r_s)^{-1/2}] \quad (313a)$$

$$I_1(r_s) = \frac{r_s}{1 + r_s} \quad (313b)$$

and ($i = 0, 1$)

$$J_i(r_s, \zeta) = \frac{1}{2} [1 + (-1)^i] + D_i(\zeta) [1 - (1 + r_s^2)^{-1/4}] + E_i(\zeta) [(1 + r_s^2)^{1/4} - (1 + r_s^2)^{-1/2}] + F_i(\zeta) [(1 + r_s^2)^{1/2} - (1 + r_s^2)^{-1/2}] \quad (314)$$

with

$$F_0(\zeta) = \frac{b_0(\zeta) - a_1(\zeta) + 2a_0(\zeta)}{f_0 - c_x(\zeta)} \quad (315a)$$

$$E_0(\zeta) = -\frac{f_1 F_0(\zeta) + 2a_0(\zeta)}{f_0 - c_x(\zeta)} \quad (315b)$$

$$D_0(\zeta) = -\frac{f_1 E_0(\zeta) + [f_2 - c_s(\zeta)] F_0(\zeta)}{f_0 - c_x(\zeta)} + \frac{\frac{1}{2} a_1(\zeta) - a_0(\zeta)}{f_0 - c_x(\zeta)} - 1 \quad (315c)$$

$$F_1(\zeta) = \frac{1}{f_0 - c_x(\zeta)} \quad (315d)$$

$$E_1(\zeta) = -f_1 F_1^2(\zeta) \quad (315e)$$

$$D_1(\zeta) = f_1^2 F_1^3(\zeta) - [f_2 - c_s(\zeta)] F_1^2(\zeta) - F_1(\zeta) \quad (315f)$$

In the equations above, $c_s(\zeta) = A_k \phi_{5/3}(\zeta)$, $c_x(\zeta) = -A_x \phi_{4/3}(\zeta)$, $a_0(\zeta)$ is eq. (174), $b_0(\zeta)$ is eq. (175),

$$a_1(\zeta) = [9.229 + 0.2263 \arcsin(\zeta^2) - 17.61 \arcsin(\zeta^4) + 36.70 \arcsin(\zeta^6) - 23.20 \arcsin(\zeta^8)] \times 10^{-3} \quad (316)$$

and

$$b_1(\zeta) = \frac{I_0(r_s^t, \zeta) - e_c^{\text{DPI}}(r_s^t, \zeta) J_0(r_s^t, \zeta)}{e_c^{\text{DPI}}(r_s^t, \zeta) J_1(r_s^t, \zeta) - I_1(r_s^t)} \quad (317)$$

where $r_s^t = 75$ is the density at which the ferromagnetic phase transition of the HEG occurs according to MC results.³⁷¹ As underlined in this work, this is the only information from MC data that is used in the construction of the functional.

The `lda_c_dpi` correlation functional shows good agreement with MC results at $\zeta = 0$ and $\zeta = 1$. Also, by construction the functional has the proper analytical structure to all orders in the low- and high-density limits, which is not the case of `lda_c_vwn` and `lda_c_pw`. However, note that an error in eq. (316) has been later detected^{5,256,257} and then implemented in Libxc as `lda_c_corrmpi`.

`lda_c_1d_loos`⁴²⁵ (2013)

This is a functional for the correlation energy in the 1D HEG developed assuming full spin polarization. First, Loos⁴²⁵ derived the expansion for the high-density limit:

$$e_c^{\text{high}}(r_s^{\text{1D}}) = \epsilon_0 + \epsilon_1 r_s^{\text{1D}} + \dots \quad (318)$$

where $\epsilon_0 = -\pi^2/360$ and $\epsilon_1 = 0.00845$. Then, by considering the low-density expansion given by^{426,427}

$$e_c^{\text{low}}(r_s^{\text{1D}}) = \frac{\eta_0}{r_s^{\text{1D}}} + \frac{\eta_1}{(r_s^{\text{1D}})^{3/2}} + \dots \quad (319)$$

where $\eta_0 = -\ln(\sqrt{2\pi}) + 3/4$ and $\eta_1 = 0.359933$, he proposed the following interpolation (see ref. 428) between eqs. (318) and (319):

$$e_c^{\text{Loos-1D}}(r_s^{\text{1D}}) = \gamma^2 \sum_{i=0}^3 c_i \gamma^i (1-\gamma)^{3-i} \quad (320)$$

where

$$\gamma(r_s^{\text{1D}}) = \frac{\sqrt{1 + 4kr_s^{\text{1D}}} - 1}{2kr_s^{\text{1D}}} \quad (321)$$

and $c_0 = k\eta_0$, $c_1 = 4k\eta_0 + k^{3/2}\eta_1$, $c_2 = 5\epsilon_0 + \epsilon_1/k$, $c_3 = \epsilon_1$, and $k = 0.414254$. The value of k was determined from MC data.^{426,429} Loos⁴²⁵ reports an agreement between eq. (320) and the MC data within 0.1 mE_h.

[lda_c_1d_glda1](#)⁴³⁰ (2014)

Loos et al.⁴³⁰ considered the behavior of a HEG confined to a D -sphere, i.e. the surface of a $(D+1)$ -dimensional sphere. The system is supposed to be fully spin polarized as for [lda_c_1d_loos](#). Using Rayleigh–Schrödinger perturbation theory, the ground-state energy of the 1D version of the model (N electrons are confined to a ring of radius R) can be expanded in terms of the Wigner–Seitz radius r_s^{1D} (eq. (35a)), that is here given by $r_s^{\text{1D}} = \pi R/N$.⁴²⁶ They used the dimensionless exchange hole curvature, given by $\eta = 1 - 1/N^2$, as intermediate variable that depends on N . Notice that Loos et al.⁴³⁰ define the curvature of the relevant pair function in their eq. (6). This definition is then applied at the HF level (see eq. (7)) on the single-particle orbitals in eq. (8).

In the high-density regime, the correlation

kernel of the reduced correlation energy admits the following expression:⁴³⁰

$$e_c^{\text{high}}(r_s^{\text{1D}}, \eta) = \sum_{l=0}^{\infty} \alpha_l(\eta) (r_s^{\text{1D}})^l \quad (322)$$

Considering only the first term in eq. (322) and modifying it such that it vanishes when $N = 1$ gives

$$\tilde{\alpha}_0(\eta) = -\frac{\pi^2}{360}\eta + (1-\eta) \frac{\ln^2(1-\eta) - 6\ln(1-\eta)}{348} \quad (323)$$

with $0 \leq \eta \leq 1$. A similar expression to eq. (322) can also be found for low densities ($r_s^{\text{1D}} \gg 1$), namely

$$e_c^{\text{low}}(r_s^{\text{1D}}, \eta) = \sum_{l=0}^{\infty} \beta_l(\eta) (r_s^{\text{1D}})^{-1-l/2} \quad (324)$$

As done above for the high-density regime, considering only the first term in eq. (324) and modifying it such that it is zero for $N = 1$ leads to

$$\tilde{\beta}_0(\eta) = \left[\frac{3}{4} - \frac{\ln(2\pi)}{2} \right] \eta - \frac{(1-\eta)\ln(1-\eta)}{16} \quad (325)$$

with $0 \leq \eta \leq 1$.

Then, the two limits derived above are interpolated in order to get an expression that can be used at all density regimes. This leads to a generalization of the traditional LDA (gLDA):

$$\begin{aligned} \tilde{e}_c(r_s^{\text{1D}}, \eta) &= \tilde{\alpha}_0(\eta) \\ &\times F\left(1, \frac{3}{2}, \tilde{\gamma}(\eta), \frac{2\tilde{\alpha}_0(\eta)[1-\tilde{\gamma}(\eta)]}{\tilde{\beta}_0(\eta)} r_s^{\text{1D}}\right) \end{aligned} \quad (326)$$

where F is the hypergeometric function and

$$\tilde{\gamma}(\eta) = \frac{19}{16} \frac{4 - 3\sqrt{1-\eta}}{2 - \sqrt{1-\eta}} \quad (327)$$

for $0 \leq \eta \leq 1$. Loos et al.⁴³⁰ proposed to use eq. (326) for $\eta \geq 1$ with $\tilde{\alpha}_0(\eta)$, $\tilde{\beta}_0(\eta)$, and $\tilde{\gamma}(\eta)$ replaced by $\alpha = -\pi^2/360$, $\beta = 3/4 - \ln(2\pi)/2$, and $\gamma = 19/8$, respectively. Equation (326) for $0 \leq \eta < 1$ and its modification for $\eta \geq 1$ thus constitute the [lda_c_1d_glda1](#) functional.

The explicit dependence on the number of electrons N through η makes this formally not a semi-local functional (see discussion for `lda_x_rae`).

`lda_c_chachiyo`⁴³¹ (2016)

The starting point of this functional is the second-order Møller–Plesset perturbative expansion of the correlation energy for the HEG as a power series in r_s^{-1} at the low-density limit. Of course, the resulting expression does not reproduce the correct divergence at high density, where `lda_c_rpa` is exact. The workaround of Chachiyo⁴³¹ workaround to this problem was to include the r_s^{-1} -expansion inside a logarithm:

$$e_c^{\text{Cha-LDA}} = a \ln \left(1 + \frac{b}{r_s} + \frac{c}{r_s^2} \right) \quad (328)$$

where a , b , and c are to be determined. He set $b = c$ based on arguments about the connection between the low- and high-density regimes. Dependence on spin is included with eq. (274), and the following values for a and b are deduced from the RPA high-density limit:^{250,256} $a^{\text{P}} = [\ln(2) - 1] / (2\pi^2)$, $b^{\text{P}} = 20.4562557$, $a^{\text{F}} = a^{\text{P}}/2$, and $b^{\text{F}} = 27.4203609$.

`lda_c_karasiev`⁴³² (2016)

Karasiev⁴³² noted that the simple `lda_c_chachiyo` functional form starts to deviate considerably from the MC data³⁷¹ for large values of r_s . He proposed solving this problem by fitting the parameter b in eq. (328) to the MC data, while keeping the value of c at its original value $c = b$, with b from `lda_c_chachiyo`. The new values are $b^{\text{P}} = 21.7392245$ and $b^{\text{F}} = 28.3559732$. This new parametrization leads to a much better agreement with accurate correlation energy in the low-density region, without deteriorating the quality of the functional in the mid- and high-density regions.

`lda_c_corrmpi`²⁵⁷ (2018)

This functional is the same as `lda_c_dpi`, except for the ζ -dependent function $a_1(\zeta)$ (eq. (316)) that is replaced by eq. (176). As detected by Loos and Gill,^{5,256} the value $a_1(\zeta = 1)$ used for constructing `lda_c_dpi` was not correct due to an order-of-limits problem. Then, based on the work of Loos and Gill, Bhattarai

et al.²⁵⁷ proposed this new parametrization for $a_1(\zeta)$.

`lda_c_upw92`, `lda_c_rpw92`⁴³³ (2018)

The work of Ruggeri et al.⁴³³ presented an evaluation of the correlation energy of the fully spin-polarized HEG at densities corresponding to $r_s = 0.5$ and 1 at a meV accuracy. This was achieved with a combination of full configuration-interaction MC and fixed-node diffusion MC methods with a finite-size extrapolation. It was shown that the PW92 (`lda_c_pw`) functional underestimates the energy of the spin-polarized HEG by 3–6 meV. To resolve this issue, two reparametrizations of PW92 that are less biased towards low densities were done. The first one is an unweighted fit (`lda_c_upw92`) to the original MC data of Ceperley and Alder³⁷¹ and the second one is a revised unweighted fit to the Ceperley–Alder and new MC results (`lda_c_rpw92`).

`lda_c_chachiyo_mod`^{431,434} (2020)

This functional has essentially the same form as `lda_c_chachiyo` with, however, a single change: the spin-interpolation function $f_c(\zeta)$ in eq. (274) is replaced by

$$f_c(\zeta) = 2 [1 - \phi_{2/3}^3(\zeta)] \quad (329)$$

`lda_c_karasiev_mod`^{432,434} (2020)

This functional differs from `lda_c_chachiyo_mod` in the values of the paramagnetic b^{P} and ferromagnetic b^{F} parameters in eq. (328) that come from `lda_c_karasiev`. Note that this functional has not been published, but is available in Libxc.

`lda_c_w20`⁴³⁵ (2020)

Xie et al.⁴³⁵ constructed an accurate correlation functional (W20, where “W” stands for Wuhan) by interpolating between the high- and low-density limits of the HEG correlation energy (see section 2.10). No reference MC data was used, as commonly done (e.g., `lda_c_vwn`), therefore their functional contains no fitting parameter. The functional uses eq. (274) for the spin interpolation, where the individual paramagnetic and ferromagnetic energies are de-

scribed by the *ansatz*

$$e_c^{\text{W20}}(r_s) = G(r_s) - \frac{a_0}{2} \times \ln \left[1 + \frac{D(r_s)}{r_s} + \frac{E(r_s)}{r_s^{3/2}} + \frac{F(r_s)}{r_s^2} \right] \quad (330)$$

where

$$D(r_s) = e^{-2b_0/a_0} - 2 \left[1 - e^{-(r_s/100)^2} \right] \times \left[\frac{f_0 - c_x}{a_0} + \frac{1}{2} e^{-2b_0/a_0} \right] \quad (331a)$$

$$E(r_s) = - \frac{2 \left[1 - e^{-(r_s/100)^2} \right] f_1}{a_0} \quad (331b)$$

$$F(r_s) = e^{-2b_0/a_0} - 2 \left[1 - e^{-(r_s/100)^2} \right] \times \left[\frac{f_2 - c_s}{a_0} + \frac{1}{2} e^{-2b_0/a_0} \right] \quad (331c)$$

$$G(r_s) = \frac{r_s}{1 + 10e^{(r_s/100)^2} r_s^{5/4}} \times \left[-a_1 \ln \left(1 + \frac{1}{r_s} \right) + b_1 \right] \quad (331d)$$

This interpolation *ansatz* was inspired by [lda_c_chachiy](#) and [lda_c_dpi](#), while the Gaussian exponential term was used to control the asymptotic behavior of the functional similarly to [gga_x_pw91](#). The values of the coefficients a_0 , a_1 , b_0 , b_1 , c_x , and c_s (for $\zeta = 0$ and 1) and of f_0 , f_1 , and f_2 (ζ -independent) were fully determined by the high- and low-density expansions of the correlation energy of the HEG (see section 2.10 and refs. 5, 252, and 253). As the value of b_1 has only been determined for the paramagnetic term, it was set to zero in the ferromagnetic term.

This formula shows better accuracy in the low-density region than the popular PW92 ([lda_c_pw](#)) correlation functional that was fit to MC data.

[lda_c_adv](#)^{436,437} (2023)

The correlation energy of the HEG in the paramagnetic⁴³⁶ and ferromagnetic phases⁴³⁷ was calculated using accurate variational and diffusion quantum MC methods. The ranges of densities that were considered correspond to $0.5 \leq r_s \leq 100$ and $0.5 \leq r_s \leq 20$ for the para-

magnetic and ferromagnetic cases, respectively. Then, these MC data were fit as functions of r_s . For the paramagnetic case, the function reads

$$e_c^{\text{P,ADV}}(r_s) = A^{\text{P}} \ln(r_s) + C^{\text{P}} + B^{\text{P}} r_s \ln(r_s) + \frac{D^{\text{P}}}{r_s^{3/4}} + \frac{\gamma^{\text{P}}}{1 + \beta_1^{\text{P}} r_s^{1/2} + \beta_2^{\text{P}} r_s} \quad (332)$$

where $A^{\text{P}} = 0.000435098$, $B^{\text{P}} = -3.02312 \times 10^{-7}$, $C^{\text{P}} = -0.00221852$, $D^{\text{P}} = -0.0134875$, $\gamma^{\text{P}} = -0.077337$, $\beta_1^{\text{P}} = 0.470881$, and $\beta_2^{\text{P}} = 0.262613$. The function for the ferromagnetic case is given by

$$e_c^{\text{F,ADV}}(r_s) = \frac{A^{\text{F}} \ln(r_s) + B^{\text{F}} + \gamma^{\text{F}} r_s}{1 + \beta_1^{\text{F}} r_s^{3/2} + \beta_2^{\text{F}} r_s^2} \quad (333)$$

where $A^{\text{F}} = 0.0169245$, $B^{\text{F}} = -0.0250295$, $\gamma^{\text{F}} = -0.0174433$, $\beta_1^{\text{F}} = 0.283806$, and $\beta_2^{\text{F}} = 0.0520433$.

Note that Azadi et al.⁴³⁷ did not specify any interpolation scheme, like for instance eqs. (274) and (275), for calculating the correlation energy at intermediate values of the spin-polarization ζ .

[lda_c_rpf](#)³⁷⁴ (2024)

Benites et al.³⁷⁴ calculated the correlation energy of the HEG using an approach based on a perturbative expansion with an interaction vertex that is renormalized by the RPA method. They argued that this method should lead to results that are more accurate than those obtained from quantum MC calculations.³⁷¹ These data for the correlation energy were then fitted, taking into account the small- and large- r_s behaviors. The functional form for the fit reads

$$e_c^{\text{RPAF}}(r_s, \zeta) = [a_0(\zeta) + a_1(\zeta)r_s] \ln \left[1 + \frac{a_2(\zeta)}{r_s^2} \right] + [b_0(\zeta) + b_1(\zeta)r_s] \ln \left[1 + \frac{b_2(\zeta)}{r_s^{7/4}} \right] \quad (334)$$

where the ζ -dependent functions a_i and b_i are given by

$$a_0(\zeta) = -\frac{1}{2} \left[c_L(\zeta) + \frac{7}{4} b_0(\zeta) \right] \quad (335a)$$

$$b_0(\zeta) = \frac{2c_0(\zeta) + c_L(\zeta) \ln[a_2(\zeta)]}{2 \ln[b_2(\zeta)] - \frac{7}{4} \ln[a_2(\zeta)]} \quad (335b)$$

$$a_1(\zeta) = \frac{e_1(\zeta)}{a_2(\zeta)} \quad (335c)$$

$$b_1(\zeta) = \frac{e_0}{b_2(\zeta)} \quad (335d)$$

$$a_2(\zeta) = a_{20} + a_{21}(\chi - 2) + a_{22} \left[\frac{\ln(\chi)}{\chi} - \frac{\ln(2)}{2} \right] \quad (335e)$$

$$b_2(\zeta) = b_{20} + b_{21}(\chi - 2) + b_{22} \left[\frac{\ln(\chi)}{\chi} - \frac{\ln(2)}{2} \right] \quad (335f)$$

In these equations, $\chi = \lambda_\uparrow + \lambda_\downarrow$ with $\lambda_\sigma = [1 + \text{sgn}(\sigma)\zeta]^{1/3}$, and the ζ -dependent functions read

$$e_1(\zeta) = \sum_{n=0}^2 e_{1n} \zeta^{2n} \quad (336a)$$

$$c_0(\zeta) = \sum_{n=0}^1 c_{0n} \zeta^{2n} + \sum_{n=1}^3 \bar{c}_{0n} (\chi^n - 2^n) \quad (336b)$$

$$c_L(\zeta) = \frac{1}{\pi^2} \left\{ [1 - \ln(2)] + \frac{1}{2} \lambda_\uparrow \lambda_\downarrow \chi - \ln(\chi) + \frac{1}{2} \sum_{\sigma} \lambda_{\sigma}^3 \ln(\lambda_{\sigma}) \right\} \quad (336c)$$

Calculations of the lattice constants and bulk moduli of solids show that the results differ slightly depending on the LDA correlation functional, the standard `lda_c_pw` or `lda_c_rpaf`, that is used.

3.1.3 Exchange and correlation

`lda_xc_lp_a`, `lda_xc_lp_b`, `lda_xc_lp_a_n`, `lda_xc_lp_b_n`⁴³⁸ (1990)

The exact xc energy E_{xc} can be calculated from the diagonal of the two-particle density matrix $\rho_2(\mathbf{r}_1, \mathbf{r}_2)$ (see section 2.4). Consequently, Lee and Parr⁴³⁸ addressed the xc problem by pro-

viding a formal ansatz for $\rho_2(\mathbf{r}_1, \mathbf{r}_2)$:

$$\rho_2(\mathbf{r}_1, \mathbf{r}_2) = n(\mathbf{r}_1)n(\mathbf{r}_2) \times \left[1 - \frac{1 + F(\mathbf{r}, r_{12})}{1 + \alpha(\mathbf{r})} e^{-\alpha(\mathbf{r})r_{12}} \right] \quad (337)$$

where $\mathbf{r} = (\mathbf{r}_1 + \mathbf{r}_2)/2$ and $r_{12} = r_2 - r_1$. In passing we stress that while in the original article the normalization of $\rho_2(\mathbf{r}_1, \mathbf{r}_2)$ equals the number of electron pairs, here the normalization of $\rho_2(\mathbf{r}_1, \mathbf{r}_2)$ equals the *double* of the electron pairs. Thus, an explicit factor of 1/2 is explicitly retained in our expression of the electron-electron interaction. The functions $\alpha(\mathbf{r})$ and $F(\mathbf{r}, r_{12})$ are assumed to be well behaved, and are expanded in powers of r_{12} . Note here that $\alpha(\mathbf{r})$ is not the MGGGA ingredient of eq. (79). The Coulomb part of the density matrix, $n(\mathbf{r}_1)n(\mathbf{r}_2)$, can also be Taylor expanded in powers of r_{12} . Its average over $\Omega_{r_{12}}$ gives rise to

$$n^2(\mathbf{r}) - \frac{2}{3} \left(\tau^W(\mathbf{r}) - \frac{1}{8} \nabla^2 n(\mathbf{r}) \right) n(\mathbf{r}) r_{12}^2 + \mathcal{O}(r_{12}^3) \quad (338)$$

So far, E_{xc} can be formally computed. At this point, Lee and Parr⁴³⁸ proposed $\alpha(\mathbf{r})$ to be considered as the reciprocal of a screening length and chose $\alpha(\mathbf{r}) = \kappa n^{1/3}(\mathbf{r})$, for some constant κ . Furthermore, the product of two infinite series that appear in the formula can be written in different ways, leading to two alternative expressions for E_{xc} . By approximating the unknown functions that enter these expressions as functions of the density, they arrived at a functional form and proposed several variants based on this form. Considering here the LDA-type variants, the general expression is given by (only the spin-unpolarized version was developed)

$$e_{xc}^{\text{LP-LDA}} = -a \frac{1 + \frac{b}{N}}{1 + \frac{c}{N}} \frac{1}{\left(\frac{4}{3}\pi\right)^{1/3} r_s + k} \quad (339)$$

which is an extension of the `lda_c_wigner` form, with N being the number of electrons in the system. Four different optimizations of eq. (339) were proposed. The parameters were

determined from a fit to the xc energies of a series of 10 closed-shell neutral and ionized atoms, from He to Ar. The functionals are

- **lda_xc_lp_a**: b , c , and k are set to zero, leading to $a = 0.8626$. This functional is equivalent to the simple **lda_c_xalpha** form, see eq. (257).
- **lda_xc_lp_b**: b and c are set to zero, leading to $a = 0.906$ and $k = 0.021987$. This functional is equivalent to the **lda_c_wigner** form, see eq. (269).
- **lda_xc_lp_a_n**: only k is set to zero, which leads to $a = 0.7475$, $b = 17.1903$, and $c = 14.1936$.
- **lda_xc_lp_b_n**: all parameters are optimized, yielding $a = 0.76799$, $b = 17.5943$, $c = 14.8893$, and $k = 4.115 \times 10^{-3}$.

The other functionals proposed by Lee and Parr⁴³⁸ involve a correction to eq. (339) that depends on the gradient and Laplacian of n (see **mgga_xc_lp90**).

The explicit dependence on the number of electrons N makes these functionals not semi-local functionals (see discussion for **lda_x_rae**).

lda_xc_f92⁴³⁹ (1992)

Fuentealba⁴³⁹ derived this functional by using a simple Gaussian approximation for the correlation-factor model in the second-order density matrix. The form is of the $X\alpha$ type (see **lda_c_xalpha**):

$$e_{\text{xc}}^{\text{F92}}(n) = -Cn^{1/3} \quad (340)$$

where

$$C = \pi \frac{k_1 k_2}{k_1 + k_2} (1 + A) \quad (341)$$

with $A = -0.4144$ and $k_1 k_2 / (k_1 + k_2) = 0.4548$, which were determined by a fit to accurate xc energy of the Ne atom. Compared to **lda_x**, the factor C has a slightly larger magnitude, $C / (2^{-1/3} C_x) \approx 1.132886$. This ratio is clearly smaller than the ratio of 3/2 for **lda_c_xalpha**.

lda_xc_teter93⁴⁴⁰ (1993)

The most popular functionals at the time of the

work of Goedecker et al.⁴⁴⁰ suffered from various problems: (i) analytical expressions that were complicated and often involved logarithms or exponentials that are expensive to evaluate, and (ii) functional derivatives that had discontinuities. To resolve these issues, Teter proposed a simple Padé approximation for the total xc energy density:

$$e_{\text{xc}}^{\text{Teter93}}(r_s, \zeta) = \frac{a_0(\zeta) + a_1(\zeta)r_s + a_2(\zeta)r_s^2 + a_3(\zeta)r_s^3}{b_1(\zeta)r_s + b_2(\zeta)r_s^2 + b_3(\zeta)r_s^3 + b_4(\zeta)r_s^4} \quad (342)$$

where $a_i(\zeta)$ and $b_i(\zeta)$ are spin-interpolated with

$$a_i(\zeta) = a_i + a'_i f_c(\zeta) \quad (343a)$$

$$b_i(\zeta) = b_i + b'_i f_c(\zeta) \quad (343b)$$

where $f_c(\zeta)$ is defined by eq. (275). It was shown that eq. (342) reproduces accurately the results from **lda_c_pw**.

Note that this functional was originally developed and implemented in ABINIT⁷⁹ by Teter in 1993, which explains its name (**lda_xc_teter93**). The functional was then published only a couple of years later.⁴⁴⁰

lda_xc_zlp⁴⁴¹ (1993)

The functional proposed by Zhao et al.⁴⁴¹ was derived with the help of the relationship between the universal kinetic-energy and electron-electron repulsion functionals,²³⁹ from which it can be deduced that

$$e_{\text{xc}}[n] = \int_0^1 d\lambda \lambda \tilde{e}_{\text{xc}}[n_{1/\lambda}] \quad (344)$$

where $n_\lambda(\mathbf{r}) = \lambda^3 n(\lambda \mathbf{r})$ and λ is the coupling constant. With eq. (344) a new functional e_{xc} can be obtained from an existing \tilde{e}_{xc} . Choosing **lda_xc_lp_b** for \tilde{e}_{xc} (i.e., Wigner-type form, eq. (269)), the following analytical form is obtained:

$$e_{\text{xc}}^{\text{ZLP-LDA}}(n) = -a_0 n^{1/3} \times \left[1 - \kappa n^{1/3} \ln \left(1 + \frac{1}{\kappa n^{1/3}} \right) \right] \quad (345)$$

where the parameters were determined the same way as in ref. 438 (`lda_xc_lp_a`, etc.), leading to $a_0 = 0.93222$ and $\kappa = 9.47362 \times 10^{-3}$. Note that no spin-polarized formulation of this functional was provided by Zhao et al. 441. Also note that the functional `mgga_xc_zlp` was constructed using the same procedure.

`lda_xc_tih`²⁰ (1996)

Tozer et al.²⁰ implemented the method of Zhao et al.⁴⁴² (ZMP) to invert the KS equations, and therefore to obtain an accurate xc potential from high-level ab-initio densities. Then, they applied the method to Ne, HF, N₂, H₂O, and N₂ at 1.5 times the equilibrium distance. In the next step, this data was used to train a neural network that is of the LDA type: the (single) input feature is the density n at some point in space, and the output is the xc potential v_{xc} at the same point. Their network contained a single hidden layer with 8 neurons, and used the tanh function as the activation function. This led to a simple model with 25 parameters, which that can be written explicitly as

$$z_j = \tanh(w_{2j-1} + w_{2j}n) \quad (346)$$

for the output of the j th hidden node ($j = 1 \dots 8$) and

$$v_{\text{xc}} = w_{17} + \sum_{i=18}^{25} w_i z_{i-17} \quad (347)$$

for the xc potential.

Although this is a functional for the potential, not the energy, Tozer et al.²⁰ also noted that since the potential depends only on the density n , the corresponding xc energy could be obtained from⁴⁴³

$$E_{\text{xc}}[n] = -\frac{1}{3} \int d^3r v_{\text{xc}}[n(\mathbf{r})] \mathbf{r} \cdot \nabla n(\mathbf{r}) \quad (348)$$

which also enabled the calculation of forces acting on the nuclei. The calculated geometries of molecules that were reasonably represented in the training set are similar to the LDA values, while eigenvalues were improved. However, the bond lengths of LiH and Li₂ (not covered by the training set) were largely overestimated.

`lda_xc_th_fl`⁴⁴⁴ (1997)

The form of this functional is based on eq. (533), which is also the expression for the GGA functionals `gga_xc_th_fc`, `gga_xc_th_fcfo`, and `gga_xc_th_fco` developed in the same work.⁴⁴⁴ However, in the case of `lda_xc_th_fl` $b = c = d = 0$, turning this functional into a LDA since R_a in eq. (534) depends only on the density. The four coefficients ω_{a000} in eq. (533), with $a = 7/6, 8/6, 9/6,$ and $10/6$, were determined from a fit to the exact xc potentials of 10 closed-shell atoms (H₂, H₂O, N₂, HF, CO, LiH, BH, Ne, F₂, and CH₄) calculated from the inversion scheme of Zhao et al.⁴⁴²

`lda_xc_j99`⁴⁴⁵ (1999)

The model of two electrons used in ref. 402 to derive an opposite-spin correlation functional (`lda_c_bj89`) was extended by Jarlborg⁴⁴⁵ to also include parallel-spin correlation as well as exchange. Considering only the spin-unpolarized case leads to the following local potential:

$$v_{\text{xc}}(n) = \alpha n^{1/3} + \beta n^{1/6} \quad (349)$$

where $\alpha = -1.05$ and $\beta = -0.035$. The corresponding xc energy density is given by

$$e_{\text{xc}}(n) = \alpha \frac{3}{4} n^{1/3} + \beta \frac{6}{7} n^{1/6} \quad (350)$$

Note that the signs of α and β in eq. (10) of ref. 445 are wrong.

`lda_xc_ksdt`, `lda_xc_corrksdt`^{446,447} (2014, 2018)

Karasiev et al.⁴⁴⁶ proposed an analytical parametrization for the xc free energy of the HEG, with full dependence on the temperature τ_e . It uses an explicit dependence on the reduced temperature $\theta = \tau_e/\tau_e^{\text{F}}$, where

$$\tau_e^{\text{F}} = \frac{k_{\text{F}}^2}{2k_{\text{B}}} = \frac{\left(\frac{9\pi}{4}\right)^{2/3}}{2k_{\text{B}}r_s^2} \quad (351)$$

is the Fermi temperature, and an interpolation for the spin-polarization ζ . They used a Padé form for both the paramagnetic and ferromag-

netic cases:

$$\tilde{f}_{xc}^{\text{KSDF}}(r_s, \theta) = -\frac{1}{r_s} \frac{\omega a(\theta) + b(\theta)r_s^{1/2} + c(\theta)r_s}{1 + d(\theta)r_s^{1/2} + e(\theta)r_s} \quad (352)$$

where $\omega_0 = 1$ and $\omega_1 = 2^{1/3}$ for the paramagnetic and ferromagnetic case, respectively. The functions in eq. (352) are given by

$$a(\theta) = a_0 \tanh\left(\frac{1}{\theta}\right) \frac{a_1 + a_2\theta^2 + a_3\theta^3 + a_4\theta^4}{1 + a_5\theta^2 + a_6\theta^4} \quad (353a)$$

$$b(\theta) = \tanh\left(\frac{1}{\sqrt{\theta}}\right) \frac{b_1 + b_2\theta^2 + b_3\theta^4}{1 + b_4\theta^2 + b_5\theta^4} \quad (353b)$$

$$c(\theta) = (c_1 + c_2 e^{-c_3/\theta}) e(\theta) \quad (353c)$$

$$d(\theta) = \tanh\left(\frac{1}{\sqrt{\theta}}\right) \frac{d_1 + d_2\theta^2 + d_3\theta^4}{1 + d_4\theta^2 + d_5\theta^4} \quad (353d)$$

$$e(\theta) = \tanh\left(\frac{1}{\theta}\right) \frac{e_1 + e_2\theta^2 + e_3\theta^4}{1 + e_4\theta^2 + e_5\theta^4} \quad (353e)$$

In the above functions, $a_0 = 1/(\pi\lambda)$ with $\lambda = [4/(9\pi)]^{1/3}$, while b_1 , c_1 , d_1 , and e_1 were fit to $\tau_e = 0$ MC data⁴⁴⁸ and the remaining parameters were fit to finite- τ_e MC data,⁴⁴⁹ keeping the ratio b_3/b_5 fixed.

Finally, the ζ -dependent xc free-energy functional is written as

$$f_{xc}^{\text{KSDF}}(r_s, \zeta, \theta) = \tilde{f}_{xcF}^{\text{KSDF}}(r_s, \theta/2^{2/3})\Phi(r_s, \zeta, \theta) + \tilde{f}_{xcP}^{\text{KSDF}}(r_s, \theta)[1 - \Phi(r_s, \zeta, \theta)] \quad (354)$$

The interpolating function Φ , previously developed by Perrot and Dharma-wardana,^{450,451} is defined as

$$\Phi(r_s, \zeta, \theta) = \frac{(1 + \zeta)^{\alpha(r_s, \theta)} + (1 - \zeta)^{\alpha(r_s, \theta)} - 2}{2^{\alpha(r_s, \theta)} - 2} \quad (355)$$

with

$$\alpha(r_s, \theta) = 2 - \frac{g_1 + g_2 r_s}{1 + g_3 r_s} e^{-\theta(l_1 + l_2 \theta \sqrt{r_s})} \quad (356)$$

In ref. 447, it was reported that an error was made during the parametrization of `lda_xc_ksdt`, and corrected values of the parameters b_i , c_i , d_i , and e_i in eq. (353) for the paramagnetic case were given

(`lda_xc_corrksdt`).

`lda_xc_1d_ehwlrgrg_1`, `lda_xc_1d_ehwlrgrg_2`, `lda_xc_1d_ehwlrgrg_3`⁴⁵² (2016)

LDA functionals are usually derived from the HEG as the reference system. Entwistle et al.⁴⁵² used alternative systems, namely few-electron slabs that resemble the HEG in a finite region of space. To illustrate this concept they decided to work in 1D, using a soft-Coulomb interaction of the form $v(x) = 1/(|x| + 1)$ (compare to eq. (210)). The exact xc energy was then calculated for slabs containing one, two, and three electrons, and fit to the form

$$e_{xc}^{\text{EHWLRG}}(n) = (a_1 + a_2 n + a_3 n^2) n^\alpha \quad (357)$$

The fit parameters turn out to be $\alpha = 0.638$, $a_1 = -0.803$, $a_2 = 0.82$, and $a_3 = -0.47$ for one-electron slabs (`lda_xc_1d_ehwlrgrg_1`), $\alpha = 0.604$, $a_1 = -0.74$, $a_2 = 0.68$, and $a_3 = -0.38$ for two-electron slabs (`lda_xc_1d_ehwlrgrg_2`), and $\alpha = 0.61$, $a_1 = -0.77$, $a_2 = 0.79$, and $a_3 = -0.48$ for three-electron slabs (`lda_xc_1d_ehwlrgrg_3`). The application of these functionals on various model systems (e.g., harmonic well) shows that they have a reduced amount of self-interaction error.

`lda_xc_gdsmfb`⁴⁵³ (2017)

The free-energy functional `lda_xc_ksdt` suffers from two shortcomings: (i) there was a lack of accurate MC data for low temperatures (corresponding to a reduced temperature $\theta < 0.5$), and (ii) there were only MC results for the paramagnetic case. This was solved by Groth et al.⁴⁵³ who performed these calculations and reparameterized the functional `lda_xc_ksdt`. Furthermore, they introduced an extra modification to `lda_xc_ksdt`, namely θ in eq. (354) is replaced by $\theta_0 = \theta(1 + \zeta)^{2/3}$. The final form of this functional can reproduce the temperature-dependent MC data to an unequaled accuracy of $\sim 0.3\%$.

3.2 Generalized-gradient approximation

In the GGA, the xc energy may be written as

$$E_{xc}^{\text{GGA}} = \int d^3r n(\mathbf{r}) \times e_{xc}^{\text{GGA}}(n_{\uparrow}(\mathbf{r}), n_{\downarrow}(\mathbf{r}), \nabla n_{\uparrow}(\mathbf{r}), \nabla n_{\downarrow}(\mathbf{r})) \quad (358)$$

Thus, GGA functionals include semi-local information through the local dependence of e_{xc}^{GGA} on the gradient of the spin density ∇n_{σ} . In practice, the exchange and the correlation energies are usually described separately.

The exchange energy is obtained as the sum of spin-resolved exchange energies

$$E_x = \sum_{\sigma} E_{x\sigma} \quad (359)$$

where the GGA exchange functional E_x is typically written in terms of an enhancement F_x of the expression for exact exchange for the HEG

$$E_{x\sigma} = \int d^3r \epsilon_x^{\text{LDA}}(n_{\sigma}(\mathbf{r})) F_x(x_{\sigma}(\mathbf{r})) \quad (360)$$

which can also be written in the form of eq. (240). The LDA expression (`lda_x`) is

$$\epsilon_x^{\text{LDA}}(n_{\sigma}) = -C_x n_{\sigma}^{4/3} \quad (361)$$

In this work, we shall use the (natural) LDA as the baseline to report $F_x(x_{\sigma}(\mathbf{r}))$ (or $F_x(s_{\sigma}(\mathbf{r}))$). Often, the enhancement factors are chosen such that $F_x \rightarrow 1$ in the HEG limit, maintaining exactness for the HEG; however, enhancement factors that use a different reference than the HEG may not reproduce this limit.

Given the DFT expression for the exchange functional E_x in the form of eq. (240), we can get the spin-resolved version by applying the spin-scaling relation, eq. (243). Below we report the enhancement factors F_x directly as functions of the spin-resolved reduced-density gradients (either x_{σ} or s_{σ} , usually following the original works). We use a compact notation that does not attach a spin index to F_x , as this function has the same form for the up and down

variables.

For obtaining the spin-unpolarized expression from a spin-resolved expression as the above, refer to the correct definitions of the various constants (section 2.1.2) and variables (section 2.1.3), as the same symbols can have different definitions depending on the author.

The forms of GGA correlation functionals E_c are usually more complicated, and most of them depend on two types of variables: ones that involve the density of only one spin, like x_{σ} , and ones that involve both spin channels, like $x_{\text{tot},p}$ (eq. (44)). A separation between the parallel- and opposite-spin correlation components using eq. (250) is sometimes used to construct functionals, and can also be useful for physical interpretation.

Note that a few among the GGA functionals described below are not GGA functionals by the strict definition of eq. (358). This is the case, for instance, if there is an additional dependence on the number of electrons N (e.g., `gga_x_lambda_lo_n`, see also `lda_x_rae`) or if the xc potential was directly modeled with no associated energy functional (e.g., `gga_x_lb`).

3.2.1 Exchange

`gga_x_herman`⁴⁵⁴ (1969)

Using dimensionality arguments, Herman et al.⁴⁵⁴ proposed the so-called $X\alpha\beta$ gradient correction to the `lda_x` (or `lda_c_xalpha`) functional:

$$F_x^{\text{Herman}} = \alpha \frac{3}{2} + \frac{\beta}{C_x} x_{\sigma}^2 \quad (362)$$

With $\alpha = 2/3$, the correct exchange energy of the HEG (i.e., `lda_x`) is recovered. The value of β was empirically determined for a few atoms, and is typically in the range 0.004–0.005 for atomic systems. Unfortunately, this functional leads to an exchange potential $v_{x\sigma}$ that diverges in the asymptotic region of atoms and molecules. Furthermore, as noted by Becke¹⁵⁵, this functional lacks universality as the value of β necessary to reproduce the exact exchange energy varies considerably.

We note that in the work of Herman et al.⁴⁵⁴

there is an ambiguity regarding the precise definition of β . Therefore, we chose eq. (19) in ref. 155 as the correct definition of β .

[gga_x_b86](#)¹⁵⁵ (1986)

In order to resolve the divergence problem in the vacuum caused by a term proportional to x_σ^2 in the enhancement factor F_x ,⁴⁵⁴ Becke¹⁵⁵ proposed

$$F_x^{\text{B86}} = \alpha \frac{3}{2} + \frac{\beta}{C_x} \frac{x_\sigma^2}{1 + \gamma x_\sigma^2} \quad (363)$$

This form conveniently cuts off the exchange energy-density in the regions where the reduced-density gradient x_σ becomes too large. The value $\alpha = 2/3$ was chosen to recover [lda_x](#) for constant densities, while $\beta = 0.0036$ and $\gamma = 0.004$ were fit to the HF exchange energy of 20 atoms from H to Xe. Becke¹⁵⁵ also noted that the optimal value of β is virtually independent of the atom.

Note that eq. (363) has in fact the same analytical form given by eq. (378) of [gga_x_pbe](#), and the corresponding parameters for [gga_x_b86](#) are $\mu^{\text{B86}} = \beta / (C_s^2 C_x) = 0.235$ and $\kappa^{\text{B86}} = \mu^{\text{B86}} C_s^2 / \gamma = 0.967$.

[gga_x_pw86](#)^{158,159} (1986)

Perdew and Wang proposed an exchange functional derived from the gradient expansion of the exchange hole suitably cut off in order to fulfill two exact properties: negativity and an integration that gives minus one (i.e., deficiency of one electron). In order to fit the functional numerically obtained from their constructed exchange hole, they used the following form:

$$F_x^{\text{PW86}} = \left(1 + \frac{a}{m} s_\sigma^2 + b s_\sigma^4 + c s_\sigma^6 \right)^m \quad (364)$$

The value $a = 0.0864$ was chosen so that the functional fulfills what was at that time wrongly considered as the correct low- s_σ expansion of the exchange energy density (μ^{Sham} , see section 2.11), while the other parameters ($b = 14$, $c = 0.2$, and $m = 1/15$) were determined from the fitting procedure. This functional was quite popular in the past and has been used as the basis for more recent functionals, e.g., [gga_x_rpw86](#).

[gga_x_b86_mgc](#)¹⁵⁶ (1986)

Becke¹⁵⁶ proposed a slightly modified version of his functional [gga_x_b86](#). By looking at the limit of strongly inhomogeneous systems, i.e., systems having regions with large gradient x_σ , he concluded that the enhancement factor F_x should go as $x_\sigma^{2/5}$. His final form smoothly interpolates between the low- and high-density limits (MGC stands for modified gradient correction):

$$F_x^{\text{B86-MGC}} = 1 + \frac{\beta}{C_x} \frac{x_\sigma^2}{(1 + \gamma x_\sigma^2)^{4/5}} \quad (365)$$

where the two parameters β and γ were fit to the exchange energies of five rare-gas atoms, yielding $\beta = 0.00375$ and $\gamma = 0.007$.

[gga_x_vmd86](#)⁴⁵⁵ (1986)

Motivated by the development of [gga_x_b86](#) and [gga_x_pw86](#), Vosko and Macdonald⁴⁵⁵ chose a Padé form for F_x :

$$F_x^{\text{VMD86}} = \frac{1 + \left(b_1 + \frac{\beta}{2^{1/3} C_x} \right) x_\sigma^2 + a_2 x_\sigma^4}{1 + b_1 x_\sigma^2 + b_2 x_\sigma^4} \quad (366)$$

where $\beta = 7 / [432\pi (3\pi^2)^{1/3}]$ was calculated by Sham¹⁴⁶ (see section 2.11), while $a_2 = 0.001064/2^{4/3}$, $b_1 = 0.0641/2^{2/3}$, and $b_2 = 0.000459/2^{4/3}$ were obtained by fitting to HF exchange energy densities of atoms. Despite an improved description for the density n , the functional leads to large errors for the integrated exchange energy.

[gga_x_dk87_r1](#), [gga_x_dk87_r2](#)⁴⁵⁶ (1987)

Inspired by the [gga_x_b86](#) functional, DePristo and Kress⁴⁵⁶ proposed the use of a rational expression for the enhancement factor:

$$F_x^{\text{DK87}} = 1 + \frac{\beta_g}{C_x} x_\sigma^2 \frac{1 + a_1 x_\sigma^\alpha}{1 + b_1 x_\sigma^2} \quad (367)$$

where $\beta_g = 7/[432\pi(6\pi^2)^{1/3}]$ was chosen to ensure the low density-gradient limit derived by Sham¹⁴⁶ (i.e., μ^{Sham} , see section 2.11, which was later recognized as incorrect). Furthermore, this form is proportional to $|\nabla n_\sigma|$ for large gradient ($x_\sigma \rightarrow \infty$), which DePristo and Kress⁴⁵⁶ considered as appropriate. The pa-

rameters in eq. (367) were fit to the HF exchange energies of the atoms He, Ne, Ar, and Kr. There are two versions of this functional, defined by $(a_1, b_1, \alpha) = (0.861504, 0.044286, 1)$ for `gga_x_dk87_r1`, where $\alpha = 1$ was fixed, and $(0.861213, 0.042076, 0.98)$ for `gga_x_dk87_r2`.

Note that the spin index σ is probably missing in the definition of y given by eq. (4) in ref. 456, since this should be x_σ as defined in our work.

`gga_x_b88`¹⁵⁷ (1988)

This functional by Becke¹⁵⁷ is widely considered as the most famous and most widely used GGA exchange functional in the chemistry community, such that ref. 157 has been cited more than 50000 times. It has been particularly successful when combined with `gga_c_lyp` for correlation (BLYP), but also as the GGA component in the hybrid functional B3LYP (`hyb_gga_xc_b3lyp`).³⁹⁷ Two main ingredients were used for its construction: (i) the correct behavior at the low-density gradient x_σ limit should be obeyed (as in most exchange functionals developed so far), and (ii) the exchange energy density for neutral finite systems should have the exact asymptotic decay $-1/(2r)$ when $r \rightarrow \infty$. To obtain a functional form obeying condition (ii), Becke¹⁵⁷ noted that the density n decays asymptotically as $e^{-\alpha r}$, where α is related to the ionization potential of the system. With this in mind, he proposed the following form:

$$F_x^{\text{B88}} = 1 + \frac{\beta}{C_x} \frac{x_\sigma^2}{1 + \gamma \beta x_\sigma \operatorname{arcsinh}(x_\sigma)} \quad (368)$$

As $\gamma = 6$ was fixed by the asymptotics, this functional has only one free parameter, $\beta = 0.0042$, which was optimized to reproduce the exchange energy of the six rare-gas atoms from He to Rn.

`gga_x_llp1`, `gga_x_llp2`⁴⁵⁷ (1991)

Lee et al.⁴⁵⁷ suggested to use the enhancement factor of an exchange functional as the enhancement factor of a kinetic-energy functional, and vice versa. To illustrate this *conjointness conjecture*, they chose the `gga_x_b88` enhancement factor and performed reparametrizations by fits to the HF exchange and kinetic energies of the rare-gas atoms He, Ne, Ar, Kr, and Xe. With

the product $\gamma\beta$ in eq. (368) fixed to 0.0253, β was determined to be either $\beta = 0.0045135$ (`gga_x_llp1`) if the exchange energy is fitted, or $\beta = 0.0043952$ (`gga_x_llp2`) if the difference between the kinetic and exchange energies is fitted. This value of β also used in the kinetic-energy functional.

`gga_x_pw91`^{458–460} (1991)

The basic idea behind the construction of the PW91 functional (`gga_x_pw91` + `gga_c_pw91`) is to use a real-space cutoff to remove the spurious long-range contributions to the second-order density-gradient expansion of the xc hole. The exchange part of PW91 is based on the `gga_x_b88` functional, but it further includes a Gaussian term to enforce the correct small-gradient limit, as well as a x_σ^4 term that ensures Levy’s scaling inequality²³⁹ and the LO bound (eq. (113)). The enhancement factor reads

$$F_x^{\text{PW91}} = 1 + \frac{(c + de^{-\gamma s_\sigma^2}) s_\sigma^2 - f s_\sigma^\alpha}{1 + a s_\sigma \operatorname{arcsinh}(b s_\sigma) + f s_\sigma^\alpha} \quad (369)$$

The constants appeared in refs. 459 and 460 with the values $a = 0.19645$, $b = 7.7956$, $c = 0.2743$, $d = -0.1508$, and $f = 0.004$. (The parameters $\alpha = 4$ and $\gamma = 100$ are included here for reasons that will become clear when discussing `gga_x_mpw91` and `gga_xc_opwlyp_d`). However, it should be underlined that these are not free parameters, and that they are related to $\beta^{\text{B88}} = 0.0042$ in eq. (368) of `gga_x_b88` and to other fundamental constants:⁴⁶¹

$$\begin{aligned} a &= \frac{6\beta^{\text{B88}}}{C_s}, & b &= \frac{1}{C_s}, & c &= \frac{\beta^{\text{B88}}}{C_x C_s^2}, \\ d &= \frac{\delta - \beta^{\text{B88}}}{C_x C_s^2}, & f &= \frac{10^{-6}}{C_x C_s^\alpha} \end{aligned} \quad (370)$$

where $\delta = 5(36\pi)^{-5/3}$. Note that the definition in eq. (370) leads to $f \approx 0.003969$, which differs slightly from the value 0.004 mentioned above.

PW91 was the most commonly used functional in the solid-state community until the mid-1990s when its simplified successor PBE (`gga_x_pbe` + `gga_c_pbe`) arrived.

`gga_x_ecmv92`⁴⁶² (1992)

Engel et al.⁴⁶² first showed that a GGA ex-

change functional *cannot* reproduce the asymptotics of both the exchange energy density $e_x \rightarrow -1/(2r)$ and the exchange potential $v_{x\sigma} \rightarrow -1/r$ for finite systems simultaneously. They also demonstrated that the satisfaction of the correct asymptotic behavior of e_x (the most important condition for the `gga_x_b88` functional, for example) is not required to obtain an accurate exchange energy, and for this they used an enhancement factor in the form of a Padé function that violates this requirement:

$$F_x^{\text{ECMV92}} = \frac{1 + a_1 p_\sigma + a_2 p_\sigma^2 + a_3 p_\sigma^3}{1 + b_1 p_\sigma + b_2 p_\sigma^2 + b_3 p_\sigma^3} \quad (371)$$

where $a_3 = b_3 = 0$ (see `gga_x_ev93`). By fitting to the exact exchange energy of 15 atoms, they obtained the values $a_1 = 27.8428$, $a_2 = 11.7683$, $b_1 = 27.5026$, and $b_2 = 5.7728$. It turns out that this form does reproduce the exchange energy of those 15 atoms even better than `gga_x_b88`, thus showing that having $e_x \rightarrow -1/(2r)$ is not required.

`gga_x_lg93`¹⁸⁴ (1993)

Lacks and Gordon¹⁸⁴ observed existing GGA functionals to lead to an inaccurate contribution from exchange to the interaction energy in the van der Waals dimers He_2 and Ne_2 . This prompted them to construct a new GGA functional, choosing a form similar to `gga_x_pw86` that recovers the gradient expansion at small s_σ and satisfies known scaling inequalities²³⁹ at large s_σ :

$$F_x^{\text{LG93}} = \frac{\left(1 + \sum_{i=1}^6 a_{2i} s_\sigma^{2i}\right)^b}{1 + a_d s_\sigma^2} \quad (372)$$

The value $a_2 = (a_d + 0.1234)/b$ was obtained from the small gradient limit, while the other coefficients (with the exception of a_d) were fit to total energies of He, Ne, and C^{4+} , to atomization energies (calculated with HF exchange) of He_2 and Ne_2 separated by 4, 5, and 6 bohr, and to the first-principle value for the exchange energy at $s_\sigma = 0.5$ calculated by Perdew. They obtained $a_4 = 29.790$, $a_6 = 22.417$, $a_8 = 12.119$, $a_{10} = 1570.1$, $a_{12} = 55.944$, and $b = 0.024974$. The value of a_d turned out to be small and to not influence the results much, leading to the

choice $a_d = 10^{-8}$.

Curiously, Lacks and Gordon¹⁸⁴ also stressed that the LO bound (eq. (113)), an exact inequality of the total exchange energy, is strongly violated *locally* at large density gradients and should therefore not be used as a constraint in the construction of functionals. However, note that this condition is actually built into some of the most used exchange functionals in solid-state physics, like `gga_x_pw91` or `gga_x_pbe`.

`gga_x_ev93`⁴⁶³ (1993)

Following the observation that `gga_x_pw91` leads to a potential $v_{x\sigma}$ that is not particularly accurate, even though it yields considerably better exchange energies than `lda_x`, Engel and Vosko⁴⁶³ constructed a functional designed to reproduce more accurately the EXX-OEP of atoms. The enhancement factor they used is the Padé approximant given by eq. (371). As a training set to determine the parameters a_i and b_i they used the EXX-OEPs^{50,281} of 20 atoms ranging from Kr to Rn. It was argued that this choice of rather heavy atoms was an attempt to better describe solids. Finally, the objective function to be minimized by the fit involved the difference between the exact and approximate exchange potentials, weighted by the function $[3n_\sigma(\mathbf{r}) + \mathbf{r} \cdot \nabla n_\sigma(\mathbf{r})]/E_{x\sigma}[n_\sigma]$, where $E_{x\sigma}[n_\sigma] = (1/2)E_{x\sigma}[2n_\sigma]$. This choice was motivated by the virial relation

$$E_{x\sigma}[n_\sigma] = \int d^3r v_{x\sigma}(\mathbf{r}) [3n_\sigma(\mathbf{r}) + \mathbf{r} \cdot \nabla n_\sigma(\mathbf{r})] \quad (373)$$

In this way, Engel and Vosko ensured that their functional yields not only accurate potentials, but also accurate exchange energies. With $a_1 - b_1 = \mu^{\text{GE}}$ fixed by the density-gradient expansion coefficient (see section 2.11), the obtained parameters are $a_1 = 1.647127$, $a_2 = 0.980118$, $a_3 = 0.017399$, $b_1 = 1.523671$, $b_2 = 0.367229$, and $b_3 = 0.011282$. Compared to `gga_x_pw91`, `gga_x_ev93` provides more accurate exchange potentials, but exchange energies of lower quality.

`gga_x_lb`⁴⁶⁴ (1994)

A well known failure of most GGA exchange

potentials $v_{x\sigma}$ is to decay exponentially, instead of having the proper $-1/r$ behavior in the vacuum far from the nuclei.^{462,465} To resolve this problem, van Leeuwen and Baerends⁴⁶⁴ proposed to model the xc potential directly using the same form as the one used by Becke for the `gga_x_b88` energy density:

$$v_{x\sigma}^{\text{LB}} = v_{x\sigma}^{\text{LDA}} - n_{\sigma}^{1/3} \frac{\beta x_{\sigma}^2}{1 + \gamma \beta x_{\sigma} \operatorname{arcsinh}(x_{\sigma})} \quad (374)$$

where $v_{x\sigma}^{\text{LDA}}$ is the `lda_x` potential (eq. (258)) and $\gamma = 3$ was chosen instead of $\gamma = 6$ in eq. (368) of `gga_x_b88` to ensure a $-1/r$ asymptotic behavior of the potential. The value $\beta = 0.05$ was fit to the Be atom.

The `gga_x_lb` potential (usually combined with a LDA correlation functional like `lda_c_vwn`) is especially adapted for time-dependent simulations, where ionization, which is extremely sensitive to the decay of the potential, plays an important role. However, one has to keep in mind that modeling directly the potential leads to a series of problems. In particular, it can be proven that such potentials are in general not functional derivatives of any energy functional (see `gga_x_fd_lb94`), and therefore violate serious constraints like the zero-force theorem.^{466,467} As a consequence, such potentials do not allow, for example, the calculation of structural properties.

`gga_x_b88_6311g`⁴⁶⁸ (1994)

Ugalde et al.⁴⁶⁸ reoptimized the value of β of the `gga_x_b88` enhancement factor (eq. (368)) using the popular 6-311G** Gaussian-type basis set. By performing a least-square fit to the HF exchange energies of the three rare-gas atoms He, Ne, and Ar, they found a single minimum at $\beta = 0.0051$, which is larger than the value $\beta = 0.0042$ found by Becke for `gga_x_b88` who used the six rare-gas atoms He through Rn.

`gga_x_fr_ge2`, `gga_x_ol1`⁴⁶⁹ (1995)

In order to provide further support in favor of the conjointness conjecture between the exchange and kinetic-energy functionals,⁴⁵⁷ Fuentealba and Reyes⁴⁶⁹ chose to convert two kinetic-energy functionals, the gradient expansion at second order and one of the two func-

tionals in the work of Ou-Yang and Levy⁴⁷⁰ into exchange functionals, leading to

$$F_x^{\text{GE2}} = 2^{1/3} \frac{c_1}{C_x} (1 + c_2 x_{\sigma}^2) \quad (375)$$

and

$$F_x^{\text{OL1}} = 2^{1/3} \frac{c_1}{C_x} \left(1 + \frac{1}{72} x_{\sigma}^2 + \frac{c_2 x_{\sigma}}{1 + 2^{5/3} x_{\sigma}} \right) \quad (376)$$

respectively. The parameters c_1 and c_2 were adjusted to reproduce the HF exchange energies of the He and Ne atoms, leading to $c_1 = 0.7670$ and $c_2 = 0.00172$ for `gga_x_fr_ge2`, and $c_1 = 0.07064$ and $c_2 = 34.0135$ for `gga_x_ol1`. `gga_x_ol1` is more accurate than `gga_x_fr_ge2` for the atomic exchange energies of light atoms, while the opposite is true for heavier atoms. Note that these two functionals do not recover the `lda_x` limit for the HEG.

`gga_x_lrc_b88`, `gga_x_lrc_pw91`⁴⁷¹ (1995)

The idea behind the construction of these two potentials is to recover the asymptotic $-1/r$ behavior of the exact exchange potential in the vacuum. Alike for `gga_x_lb` the easier way to satisfy this requirement is to model directly the potential. Lembarki et al.⁴⁷¹ chose the mathematical forms of the `gga_x_b88` and `gga_x_pw91` functionals for `gga_x_lrc_b88` and `gga_x_lrc_pw91`, respectively:

$$v_x^{\text{LRC}} = v_x^{\text{LDA}} - 2C_x \sum_{\sigma} n_{\sigma}^{1/3} (F_x^{\text{GGA}} - 1) \quad (377)$$

where $v_x^{\text{LDA}} = -(3n/\pi)^{1/3}$ (spin-unpolarized form of `lda_x`) and F_x^{GGA} is either eq. (368) or eq. (369) with, however new values for some of the parameters entering into the enhancement factors.

The modified parameter in eq. (368) is β , whose new value ($\beta = 0.323$) was obtained by fitting to the highest occupied molecular orbital energies of the He, Ne, and Ar atoms. In eq. (369), $a = a_2 b_2$, $b = a_1$, $c = a_2$, and $f = 0$ are the modified parameters, where $a_1 = 0.8074$, $a_2 = 0.5627$, and $b_2 = 3/(3\pi^2)^{1/3}$, while d and γ are unchanged. b_2 and f were chosen such that the proper decay $-1/r$ of the

potential is recovered, while a_1 and a_2 were obtained from a fit to the highest occupied molecular orbital energies of the He, Ne, and Ar atoms.

Note that these two potentials are formulated such that $v_{x\uparrow} = v_{x\downarrow}$, which is not in accordance with the spin-scaling relation for exchange (eq. (243)).

`gga_x_pbe`, `gga_x_pbe_mod`, `gga_x_pbe_gaussian`^{148,149} (1996)

The main objective of Perdew et al.¹⁴⁸ when proposing this functional was to simplify the PW91 (`gga_x_pw91` + `gga_c_pw91`) functional that is overly complicated and has some deficiencies, such as an unsatisfactory description of the linear response of the HEG or a potential that has wiggles. The PBE (`gga_x_pbe` + `gga_c_pbe`) functional is certainly the most famous and used GGA functional in solid-state physics, with ref. 148 cited more than 200000 times. It is in any case a good functional that does not suffer from overfitting, analytic problems, or numerical instabilities, and which yields reasonable results in a wide variety of physical circumstances.

The construction of the exchange part `gga_x_pbe` was based on the following four conditions. (i) The functional must scale correctly under uniform density scaling, and must recover `lda_x` for the HEG. (ii) It must obey the exact spin-scaling relationship given by eq. (243). (iii) For small gradients, it should recover the linear response of `lda_x`. (iv) The LO bound (eq. (113)) must be satisfied for all possible densities and gradients. They proposed the following, rather simple enhancement factor that obeys all these conditions:

$$F_x^{\text{PBE}} = 1 + \kappa \left[1 - \frac{\kappa}{\kappa + f_0(s_\sigma)} \right] \quad (378)$$

where the function $f_0(s_\sigma) = \mu^{\text{PBE}} s_\sigma^2$. The parameter $\kappa = \kappa^{\text{PBE}}$ is determined by condition (iv), while $\mu^{\text{PBE}} = \beta^{\text{MB}} \pi^2/3$ comes from condition (iii). Finally, β^{MB} comes from the high-density limit¹⁵¹ of the weakly r_s -dependent gradient coefficient of the correlation energy. Note that eq. (378) has the same analytical form as the enhancement factor of `gga_x_b86`,

eq. (363).

Finally, we mention that three implementations of PBE exchange, which differ in the values of κ^{PBE} and μ^{PBE} , are available in Libxc:

- `gga_x_pbe`: $\kappa^{\text{PBE}} = 0.804$ and $\mu^{\text{PBE}} = 0.2195149727645171$. μ^{PBE} is related to $\beta^{\text{MB}} = 0.06672455060314922$ (used in `gga_c_pbe`) via $\mu^{\text{PBE}} = \beta^{\text{MB}} \pi^2/3$.
- `gga_x_pbe_mod`: $\kappa^{\text{PBE}} = 0.804$ and $\mu^{\text{PBE}} = \beta^{\text{MB}} \pi^2/3 \approx 0.219516$,⁴⁷² where $\beta^{\text{MB}} = 0.066725$ is a less precise value.
- `gga_x_pbe_gaussian`: $\kappa^{\text{PBE}} = 0.804000423825475$ and $\mu^{\text{PBE}} = 0.219510240580611$. Along with β^{MB} used in `gga_c_pbe_gaussian`, these are the values used in the GAUSSIAN program.⁹

See Lehtola and Marques¹²⁸ for further discussion on these various choices for the parameters.

`gga_x_g96`⁴⁷³ (1996)

To construct this intriguing functional, Gill⁴⁷³ wondered if the *baroque* tendency to construct complicated functionals is really necessary to obtain accurate results. This prompted him to propose one of the simplest possible forms for the exchange functional:

$$F_x^{\text{G96}} = 1 + \frac{\beta}{C_x} x_\sigma^{3/2} \quad (379)$$

where the constant $\beta = 1/137$ was chosen to reproduce the HF exchange energy of the Ar atom. This functional is not analytic at $x_\sigma = 0$ and diverges for $x_\sigma \rightarrow \infty$, which was considered by Gill⁴⁷³ as not problematic and even necessary to obtain accurate results. Surprisingly, when combined with `gga_c_lyp` for correlation, this functional yields similar results for the G2 set⁴⁰⁶ as the canonical BLYP functional (`gga_x_b88` + `gga_c_lyp`) in the 6-311+(2df,p) and 6-31G(d) basis sets. This led Gill⁴⁷³ to conclude that the accuracy of a functional does not depend critically on its asymptotic behaviour, which may be true depending on the property. However, due to the divergence for $x_\sigma \rightarrow \infty$, the functional likely will encounter convergence

issues when employed with a numerically robust solution method.

`gga_x_ft97_a`, `gga_x_ft97_b`⁴⁷⁴ (1997)

There is an infinite number of possible functionals that fulfill the asymptotic requirement that went into the construction of `gga_x_b88`. Filatov and Thiel⁴⁷⁴ proposed a whole family of such functionals (labeled by the integer m), given by the enhancement factor

$$F_x^{\text{FT97}} = 1 + \frac{\beta}{C_x} \frac{x_\sigma^2}{\left\{1 + \left(\frac{6\beta}{m}\right)^m x_\sigma^m [\text{arcsinh}(x_\sigma^m)]^m\right\}^{1/m}} \quad (380)$$

where m and β are parameters. This family includes `gga_x_b88` for $m = 1$. By fitting to exact exchange energies of light atoms, $m = 2$ and $\beta = 0.00293$ were obtained as the optimal values. It should be noted that this value of β is not empirical, but has been determined from a model of the exchange hole in inhomogeneous systems.²²² The thus defined `gga_x_ft97_a` functional reproduces the exact exchange energies of light atoms from H to Ne more accurately than `gga_x_b88` and `gga_x_pw91`, but the functional is less accurate for heavier atoms. To resolve this problem, Filatov and Thiel⁴⁷⁴ proposed an improved functional, `gga_x_ft97_b`, where the constant β is replaced by the function

$$\beta_\sigma = \beta_0 + \frac{\beta_1 |\nabla n_\sigma|^2}{\beta_2^2 + |\nabla n_\sigma|^2} \quad (381)$$

The values of the three parameters (β_0 , β_1 , and β_2) were then fit to the exact exchange energies of the atoms H, He, Li, Be, Ne, Mg, Ar, Kr, and Xe, yielding $\beta_0 = 0.002913644$, $\beta_1 = 0.0009474169$, and $\beta_2 = 2501.149$ (beware of the missing power 2 for β_2 in eq. (16a) of ref. 474).

These two functionals, combined with `gga_c_ft97` for correlation, give results for the G2 dataset of molecules⁴⁰⁶ that are comparable to the hybrid functional B3LYP.³⁹⁷

`gga_x_pbe_r`^{183,475} (1998)

Zhang and Yang¹⁸³ argued that although the `gga_x_pbe` functional was built using solely theoretical arguments, without resort to any fit-

ting procedure, there is still some flexibility in the choice of κ . In fact, κ is fixed by the *local* LO bound, which is a sufficient but not a necessary criterion to satisfy the integrated LO bound, eq. (113). This led them to propose a new revised value of $\kappa = 1.245$ in eq. (378), obtained by fitting to exact exchange energies of atoms from He to Ar. This choice improves significantly over the original `gga_x_pbe` for atomic total energies and molecular atomization energies. This reparametrization of `gga_x_pbe` is commonly known as revPBE in the literature. Also note that `gga_x_pbe_r` was used as the GGA exchange component of the first non-local van der Waals functional vdW-DF.^{476,477}

`gga_x_mpw91`⁴⁶¹ (1998)

This is a modification of the original `gga_x_pw91` functional, motivated by earlier work by Lacks and Gordon¹⁸⁴, who noted that although the coefficient and exponent of the s_σ^α term in eq. (369) do not affect significantly atomic exchange energies, they are important in the asymptotic low-density and large-gradient regions that may be relevant for noncovalently bound systems. In order to obtain correct long-range behavior of the exchange energy, and essential characteristics to describe noncovalent bonds, Adamo and Barone⁴⁶¹ modified the α and β^{B88} parameters of `gga_x_pw91` (see eqs. (369) and (370)) by fitting to the exact exchange energies of atoms on the first and second rows of the periodic table and rare-gas dimers (He_2 and Ne_2) close to their van der Waals equilibrium bond length. They obtained $\alpha = 3.72$ and $\beta = 0.00426$. Note that the values of α and β given in ref. 461 are incorrect.

`gga_x_hcth_a`⁴⁷⁸ (1998)

This is one of the three functionals proposed in ref. 478; the others are `gga_xc_hcth_93` and the hybrid B97-1. This functional was used to study the stability of the fit to the analytical form chosen as

$$F_x^{\text{HCTH-A}} = a_0 - a_1 (F_x^{\text{B88}} - 1) - a_2 \frac{dF_x^{\text{B88}}}{d\beta} \quad (382)$$

The last two terms involve the `gga_x_b88` enhancement factor (eq. (368)) and its derivative with respect to the parameter β , and they were

evaluated at the unmodified value $\beta = 0.0042$. The remaining parameters a_i were fit using the same procedure as that for `gga_xc_hcth_93`, leading to $a_0 = 1.09878$, $a_1 = -2.51173$, and $a_2 = 0.0156233$. This functional was fit jointly with `gga_c_hcth_a`, and should therefore be used only in combination with it. Note that since a_0 is not equal to one, this functional does not reduce to `lda_x` for the HEG.

`gga_x_rpbe`⁴⁷⁹ (1999) Hammer et al.⁴⁷⁹ showed that `gga_x_pbe_r` improves over `gga_x_pbe` for the chemisorption energy of atoms and molecules on transition-metal surfaces. However, they also discussed about the possible violation of the local form of the LO bound (eq. (113)) by `gga_x_pbe_r`. To solve this problem, they developed an alternative revision of `gga_x_pbe`, which gives the same improvement for the chemisorption energies as `gga_x_pbe_r` and at the same time fulfills the LO criterion locally. The enhancement factor of their functional is given by

$$F_x^{\text{RPBE}} = 1 + \kappa \left(1 - e^{-\mu s_\sigma^2/\kappa}\right) \quad (383)$$

where μ and κ have the same values as in the original `gga_x_pbe`. This functional is commonly known as RPBE in the literature.

`gga_x_gg99`, `gga_x_kgg99`⁴⁸⁰ (1999) Gilbert and Gill⁴⁸⁰ discussed a way to decompose a local xc energy into contributions from each value of the reduced-density gradient x_σ . They then proposed a reference system given by one electron feeling an effective-core potential of the form

$$V(r) = - \left[\text{sech}^2(r) + \frac{\tanh(r)}{r} \right] \quad (384)$$

By demanding that the decomposition of the exchange-energy reproduces exactly its HF counterpart for this system (which only includes the cancellation of the self-energy for the one electron), they then arrived at the enhancement factor

$$F_x^{\text{GG99}} = \frac{1}{C_x} \frac{\pi^2 - 12r \ln(1 + e^{-2r}) + 12 L_2(-e^{-2r})}{2 \times 3^{1/3} \pi r \text{sech}^{2/3}(r)} \quad (385)$$

where L_2 is the dilogarithm function. The reduced-density gradient is given by

$$x_\sigma(r) = 2\pi \sinh(r) \left[\frac{\text{sech}(r)}{3} \right]^{1/3} \quad (386)$$

which is an equation that has to be inverted to obtain r , either analytically (see eq. (22) in ref. 480) or numerically, so that it can be used in an implementation of eq. (385).

From the small-gradient expansion of this functional given by

$$\lim_{x_\sigma \rightarrow 0} F_x^{\text{GG99}} \approx 0.9864 + 0.004827 x_\sigma^2 - 0.00002194 x_\sigma^4 \quad (387)$$

it is interesting to observe that the functional reduces to $F_x \approx 0.9864$ for the HEG, which is quite close to `lda_x` ($F_x = 1$), even if the `lda_x` limit was not used in the construction of `gga_x_gg99`. Furthermore, the quadratic term in eq. (387) is remarkably close to the corresponding value $\beta/C_x = 0.0042/C_x \approx 0.004514$ obtained by Becke in `gga_x_b88` by fitting to HF exchange energies of rare-gas atoms.

The `gga_x_gg99` functional was found to consistently underestimate the absolute value of the exchange energy in the bonding regions of molecules. To correct for this behavior, Gilbert and Gill⁴⁸⁰ proposed adding a constant to eq. (385):

$$F_x^{\kappa\text{GG99}} = F_x^{\text{GG99}} - \frac{\kappa}{C_x} \quad (388)$$

By a simple minimization procedure they obtained the value $\kappa = -0.047$, thus defining the `gga_x_kgg99` functional. By adding this term, the atomization energy of molecules is clearly improved. At $x_\sigma = 0$, $F_x^{\kappa\text{GG99}} \approx 1.0369$, which is also close to `lda_x`.

`gga_x_lbm`⁴⁸¹ (2000)

This is a generalization of the original `gga_x_lb` potential, with two empirical parameters in eq. (374). The new parameter $\alpha = 1.19$, which multiplies $v_{x\sigma}^{\text{LDA}}$, and $\beta = 0.01$ were fit to reproduce the excitation energies and the dipole polarizabilities of small molecules. It turns out that besides improving static hyperpolarizabil-

ities, the `gga_x_lbm` potential also modifies the relative frequency dependence with respect to `lda_x` and `gga_x_lb`. Note that `gga_x_lbm` was proposed in particular to be used as a part of the SAOP (statistical averaging of orbital potentials) potential.

`gga_x_b88m`⁴⁸² (2000)

As shown in ref. 483, the original value of the parameter β in the enhancement factor of `gga_x_b88` (eq. (368)) might not be the optimal choice for molecular properties that may of course strongly depend on the associated correlation functional. Therefore, Proynov et al.⁴⁸² reoptimized β together with the parameters in `mgga_c_tau1` using the molecules N_2 , F_2 , O_2 , HF , CN , H_2O , CH_4 , C_2H_4 , NH_3 , C_6H_6 , and the hydrogen-bonded water dimer.⁴⁸⁴ They obtained the value $\beta = 0.0045$.

`gga_x_lag`⁴⁸⁵ (2000)

In most cases, GGA functionals have been constructed using the HEG and/or atoms or molecules as reference systems in order to fix the asymptotics or to fit coefficients. These are not, however, the only possible reference systems. Vitos et al.⁴⁸⁵ used the Airy gas as a reference in their local Airy gas (LAG) functional. This is a model of an edge electron gas, previously studied by Kohn and Mattsson⁴⁸⁶, where the external potential is given as

$$v(z) = \begin{cases} \infty, & z \leq -L \\ Fz, & z > -L \end{cases} \quad (389)$$

where $-L$ is the position of the edge and F defines a length scale. Vitos et al.⁴⁸⁵ chose the exchange energy of this Airy gas model to construct and parameterize a GGA exchange functional. For this purpose, they used a generalized form based on `gga_x_b86_mgc`

$$F_x^{\text{LAG}} = 1 + \frac{a_1 s_\sigma^{a_2}}{(1 + a_3 s_\sigma^{a_2})^{a_4}} \quad (390)$$

with the parameters $a_1 = 0.041106$, $a_2 = 2.626712$, $a_3 = 0.092070$, and $a_4 = 0.657946$. Calculations on finite and extended systems⁴⁸⁵ showed that `gga_x_lag` combined with `lda_c_pw` is in general more accurate than LDA (`lda_x` + `lda_c_pw`). Compared to PBE

(`gga_x_pbe` + `gga_c_pbe`), it is worse for atoms, better for solids, and of similar accuracy for diatomic molecules.

`gga_x_optx`⁴⁸⁷ (2001)

In their study of the left-right (static) correlation, Handy and Cohen⁴⁸⁷ experimented with various parameterized forms for the exchange functional in order to optimize the HF energies of first- and second-row atoms. The considered forms included one similar to a previous proposal of Becke in `gga_x_b86`:

$$F_x^{\text{OPTX}} = a + b \frac{\gamma^2 x_\sigma^4}{(1 + \gamma x_\sigma^2)^2} \quad (391)$$

with $a = 1.05151$, $b = 1.43169/C_x$, and $\gamma = 0.006$. Note that since a is not equal to 1, `gga_x_optx` does not reduce to `lda_x` for the HEG.

Handy and Cohen⁴⁸⁷ then combined `gga_x_optx` with several correlation functionals (`gga_c_lyp`, `gga_c_p86`, or `lda_c_pw`) and reported improved geometries and atomization energies for molecular systems compared to `gga_x_b88` combined with the same correlation functionals. In their work, they also mentioned that no improvement was obtained by including dependence either on the Laplacian of the density or on the kinetic-energy density.

`gga_x_mpbe`⁴⁸⁸ (2002)

This functional uses a series expansion in $s_\sigma^2/(1 + a s_\sigma^2)$, equivalent to the B97 form of eq. (251).³⁷⁰ Here, the parameters are determined in order to fulfill the same mathematical constraints used in the construction of `gga_x_pbe`. As no improvement was found in going beyond second order in the expansion, the functional reads

$$F_x^{\text{mPBE}} = 1 + C_1 \frac{s_\sigma^2}{1 + a s_\sigma^2} + C_2 \left(\frac{s_\sigma^2}{1 + a s_\sigma^2} \right)^2 \quad (392)$$

The parameter C_1 is set as $C_1 = \mu^{\text{PBE}}$ in order to obey the density gradient-expansion and recover the `lda_x` linear response, while the LO bound gives another condition. The final degree of freedom is used to minimize the error in atomic exchange energies for the H–Ar atoms. This yields $C_2 = -0.015$ and $a = 0.157$. The

results obtained with this functional are quite accurate for a variety of structural, thermodynamic, kinetic, and spectroscopic properties.

[gga_x_hs_mb88](#), [gga_x_hs_mpw91](#)⁴⁸⁹ (2002) Following the strategy used for the design of [gga_x_lrc_b88](#) and [gga_x_lrc_pw91](#), Harbola and Sen⁴⁸⁹ modeled directly the exchange potential by using the exchange-energy density e_x of a GGA functional:

$$v_x^{\text{HS}} = 2e_x^{\text{GGA}} + \frac{k_{\text{F}}}{\beta\pi} \quad (393)$$

where k_{F} is the Fermi wave vector (eq. (47)) and β an empirical parameter. The first term in eq. (393) is interpreted as an approximation to the Slater potential (see eq. (144)). The [gga_x_b88](#) and [gga_x_pw91](#) functionals were used for e_x^{GGA} , leading to [gga_x_hs_mb88](#) and [gga_x_hs_mpw91](#), respectively. $\beta = 2.25$ was determined as the average of β values that minimize the total energies of the Ne, Ar, and Xe atoms. However, note that eq. (393) reduces to the [lda_x](#) expression for the HEG only with $\beta = 2$.

The two proposed potentials improve for the highest occupied molecular orbital energies of closed-shell atoms (He, Be, Ne, Mg, Ar, and Ca) compared to the [gga_x_b88](#) and [gga_x_pw91](#) functionals, respectively. Note that these potentials were apparently formulated only for spin-unpolarized calculations.

[gga_x_kt1](#)⁴⁹⁰ (2003)

Keal and Tozer⁴⁹⁰ proposed a simple gradient correction, which improves the structure of the xc potential $v_{\text{xc}\sigma}$. They realized that the shape of the shell structure could be improved by using functionals leading to a vanishing Hessian term in $v_{\text{xc}\sigma}$. This led them to propose the form

$$F_x^{\text{KT1}} = 1 - \frac{\gamma}{C_x} \frac{n_\sigma^{4/3}}{n_\sigma^{4/3} + \delta} x_\sigma^2 \quad (394)$$

By using [lda_c_vwn](#) for correlation, and empirically adjusting the two parameters to get accurate isotropic magnetic resonance chemical shielding of small molecules they obtained $\gamma = -0.006$ and $\delta = 0.1$. Note that in addition to the reduced-density gradient x_σ , eq. (394)

also depends on n_σ . This means that the functional does not satisfy the uniform density scaling condition for exchange. This suggests that this gradient correction may be considered as a combined xc term, instead of modeling only exchange. The [gga_x_kt1](#) functional is used in the xc functionals [gga_xc_kt1](#), [gga_xc_kt2](#), and [gga_xc_kt3](#).

[gga_x_xpbe](#)⁴⁹¹ (2004)

In spite of the popularity of the PBE ([gga_x_pbe](#) + [gga_c_pbe](#)) functional, it leads to unacceptable errors in thermochemical data (heats of formation). Therefore, Xu and Goddard⁴⁹¹ decided to refit all parameters of PBE against accurate data of the H–Ar atoms and the van der Waals interaction properties of Ne₂. The exchange part of this extended xPBE functional has parameters $\mu = 0.23214$ and $\kappa = 0.91954$ (see [gga_c_xpbe](#) for the correlation part). The xPBE functional leads not only to a clear improvement in thermochemistry, but also in geometries, ionization potentials, electron affinities, and proton affinities, as well as in the description of van der Waals and hydrogen interactions.

[gga_x_bayesian](#)⁴⁹² (2005)

In their work on performing Bayesian error estimation in DFT, Mortensen et al.⁴⁹² developed an exchange functional with the form

$$F_x^{\text{Bayesian}} = \sum_{i=1}^{N_p} \theta_i \left(\frac{s_\sigma}{1 + s_\sigma} \right)^{2i-2} \quad (395)$$

With $N_p = 3$ that suffices for an optimal fit without over-fitting, the parameters θ_i were obtained by fitting experimental data for the atomization energies of 20 small molecules and for the cohesive energies of 11 solids. Although not explicitly specified in the paper, the correlation energy was probably represented by [gga_c_pbe](#). Mortensen et al.⁴⁹² obtained $\theta_1 = 1.0008$, $\theta_2 = 0.1926$, and $\theta_3 = 1.8962$. The resulting enhancement factor follows quite closely [gga_x_pbe](#) at low values of the reduced-density gradient s_σ , but for s_σ values greater than 1.5 it rises more steeply to finally become more similar to the [gga_x_rpbe](#) enhancement factor. The functional is a good compromise between PBE

and RPBE for the simultaneous description of atomization energies of molecules and the cohesive energies of solids.

`gga_x_am05`^{493,494} (2005)

Akin to `gga_x_lag`, this exchange functional uses the Airy gas as a reference system. It intends to solve a problem with `gga_x_lag` that does not reproduce the right limiting behavior far outside the electronic surface. The construction of the functional consists of two steps. In the first step, a local Airy approximation (LAA) is proposed. It is based on (i) the leading behavior of the exchange energy far outside the surface, (ii) the asymptotic expansions of the Airy functions, and (iii) the `lda_x` limit. It reads

$$F_x^{\text{LAA}}(s_\sigma) = \frac{1 + cs_\sigma^2}{1 + \frac{cs_\sigma^2}{F_x^{\text{b}}(s_\sigma)}} \quad (396)$$

where the function $F_x^{\text{b}}(s_\sigma)$ is given by

$$F_x^{\text{b}}(s_\sigma) = \frac{\pi}{3} \frac{s_\sigma}{\xi_t(s_\sigma) [d + \xi_t(s_\sigma)^2]^{1/4}} \quad (397)$$

with

$$\xi_t(s_\sigma) = \left[\frac{3}{2} W \left(\frac{s_\sigma^{3/2}}{2\sqrt{6}} \right) \right]^{2/3} \quad (398)$$

where W is the Lambert function, $d = [(4/3)^{1/3} 2\pi/3]^4$, and $c = 0.7168$ comes from a least-squares fit to the exact Airy gas exchange. Finally, as Airy exchange parametrizations are designed to accurately model the electron gas at a surface and are not expected to yield good results in the interior regions, Armiento and Mattsson⁴⁹³ proposed the following interpolation as the second step in the construction of the functional:

$$F_x^{\text{AM05}} = X(s_\sigma) + [1 - X(s_\sigma)] F_x^{\text{LAA}}(s_\sigma) \quad (399)$$

with the function $X(s_\sigma)$ given by

$$X(s_\sigma) = \frac{1}{1 + \alpha s_\sigma^2} \quad (400)$$

The parameter $\alpha = 2.804$ was determined by a fit to jellium xc surface energies. Actually, this

interpolation does not appear entirely necessary, as F_x^{LAA} already approaches the `lda_x` in the limit of small s_σ , and only changes slightly the results with respect to F_x^{LAA} .

Combined with its correlation counterpart `gga_c_am05`, the functional gives results that are similar to those from PBEsol (`gga_x_pbe_sol` + `gga_c_pbe_sol`)⁴⁹⁵ and far better⁴⁹⁶ than the LDA and PBE (`gga_x_pbe` + `gga_c_pbe`) results for the lattice constant and bulk modulus.

`gga_x_wc`⁴⁹⁷ (2006)

Wu and Cohen⁴⁹⁷ presented an exchange functional based on a diffuse radial cutoff for the exchange hole in the real space, and the gradient expansion of the exchange energy at small gradients s_σ . It retains the behavior of `gga_x_pbe` at small values of s_σ , but consists of the following modification in the analytical form: In the original `gga_x_pbe` exchange functional, given by eq. (378), the function $f_0(s_\sigma)$ is simply proportional to s_σ^2 , but here it is given by

$$f_0(s_\sigma) = \frac{10}{81} s_\sigma^2 + \left(\mu - \frac{10}{81} \right) s_\sigma^2 e^{-s_\sigma^2} + \ln(1 + cs_\sigma^4) \quad (401)$$

The parameters κ and μ in eq. (378) have the same values as in the original `gga_x_pbe`, while c is set to recover the fourth order gradient expansion at small values of s_σ , and is given by

$$c = \frac{146}{2025} \left(\frac{2}{3} \right)^2 - \frac{73}{405} \frac{2}{3} + \left(\mu - \frac{10}{81} \right) \quad (402)$$

This functional, combined with `gga_c_pbe`, is more accurate than PBE (`gga_x_pbe` + `gga_c_pbe`) for the geometry of solids, but has a lower accuracy for the cohesive energy.

`gga_x_pbea`⁴⁹⁸ (2007)

Madsen⁴⁹⁸ constructed an exchange functional that obeys the same conditions as `gga_x_pbe`, but which contains an additional parameter (α):

$$F_x^{\text{PBE}\alpha} = 1 + \kappa \left[1 - \frac{1}{\left(1 + \frac{\mu}{\alpha\kappa} s_\sigma^2 \right)^2} \right] \quad (403)$$

where κ and μ have the same values as in `gga_x_pbe`, while $\alpha = 0.52$ was obtained to reproduce the second-order term of the gradient expansion of exchange for the slowly varying electron gas. This functional is free of empirical parameters and gives good geometries for densely packed solids when used with `gga_c_pbe`.

`gga_x_pbe_sol`^{271,272} (2008)

Numerical results and analyses of enhancement factors suggest that functionals like `gga_x_b88` that exhibit an enhanced dependence on the density gradient s_σ yield accurate atomization energies and total energies of finite systems, but are not so good for the geometry of solids. The opposite trends can also be observed with functionals that have a weaker dependence on s_σ and obey more closely the density-gradient expansion of the slowly varying electron gas; note, however, that this argument has been under debate.^{495,499}

Based on these observations, Perdew et al.²⁷¹ proposed PBEsol (`gga_x_pbe_sol` + `gga_c_pbe_sol`) that obeys the density-gradient expansion (thus, μ^{GE} is chosen in eq. (378) and is the only difference with respect to `gga_x_pbe`) and that was specifically designed for properties of solids. PBEsol particularly improves over PBE (`gga_x_pbe` + `gga_c_pbe`) on the geometry and the surface energy similarly as `gga_x_wc`, `gga_x_am05`, and `gga_x_sogga` do. PBEsol has been used quite extensively by the solid-state community.

`gga_x_sogga`⁵⁰⁰ (2008)

It is true that PBEsol (`gga_x_pbe_sol` + `gga_c_pbe_sol`) improves on the original PBE (`gga_x_pbe` + `gga_c_pbe`) in several aspects, notably the geometry of solids. However, the choice of β for `gga_c_pbe_sol` violates the gradient expansion of correlation. Zhao and Truhlar⁵⁰⁰ built a functional that restores the gradient expansions for both exchange and correlation, and that enforces a tighter LO bound, namely the most stringent value determined by Odashima and Capelle¹⁷⁵. The `gga_x_sogga` functional is written as a half-and-half mixture of `gga_x_pbe` (eq. (378)) and `gga_x_rpbe`

(eq. (383)):

$$F_x^{\text{SOGGA}} = \frac{1}{2} (F_x^{\text{PBE}} + F_x^{\text{RPBE}}) \quad (404)$$

The value $\mu = \mu^{\text{GE}}$ in eqs. (378) and (383) is chosen to fulfill the exchange gradient expansion, while the aforementioned LO bound leads to $\kappa = 0.552$. Combined with `gga_c_pbe` (which respects the gradient expansion for correlation) it performs slightly better than PBEsol for lattice constants, and performs similarly for molecular atomization energies.

`gga_x_pbe_tca`⁴²⁰ (2008)

This is another revision of the parameters of `gga_x_pbe`. Tognetti et al.⁴²⁰ decided to keep the original value μ^{PBE} in eq. (378), but required that the LO bound is locally respected only in the interval that Perdew et al.^{501,502} called the *physical interval*, i.e., $0 < s_\sigma < 3$. Furthermore, they used the improved LO bound by Chan and Handy¹⁷². This led to $\kappa = 1.227$, a value that is close to the empirical value $\kappa = 1.245$ of `gga_x_pbe_r`.

When combined with `gga_c_revtpca` for correlation, `gga_x_pbe_tca` leads to significant improvements for molecular atomization energies and activation barriers with respect to PBE (`gga_x_pbe` + `gga_c_pbe`).

`gga_x_2d_b86_mgc`⁵⁰³ (2009)

This 2D counterpart of `gga_x_b86_mgc` reads

$$F_x^{\text{B86-MGC-2D}} = 1 + \frac{\beta}{C_x^{2\text{D}}} \frac{(x_\sigma^{2\text{D}})^2}{[1 + \gamma (x_\sigma^{2\text{D}})^2]^{3/4}} \quad (405)$$

where $x_\sigma^{2\text{D}}$ is eq. (42) with $m = 2$, and $C_x^{2\text{D}}$ is eq. (19). The $3/4$ exponent in the denominator was chosen such that the functional has the correct large-gradient limit in 2D. The values $\beta = 0.003317$ and $\gamma = 0.008323$ were obtained by fitting to exchange energies of parabolic quantum dots. Note that these values are close to the ones obtained by Becke in the 3D case (`gga_x_b86_mgc`). The functional improves considerably over `lda_x_2d` for the exchange energy of parabolic and square quantum dots.

`gga_x_mb88`⁵⁰⁴ (2009)

This functional is a reparametrization of the popular `gga_x_b88` for activation barriers of proton transfer reactions. Using a training set of 55 small molecules from the G2 set,^{406,505} Tognetti and Adamo⁵⁰⁴ obtained a value of $\beta = 0.0011$ in eq. (368). Besides the improvement obtained with this functional (when combined with `gga_c_p86`) over BP86 (`gga_x_b88 + gga_c_p86`) and BLYP (`gga_x_b88 + gga_c_lyp`) for proton transfer reactions, it also appears to improve atomization energies and geometries of molecules.

`gga_x_rpw86`⁵⁰⁶ (2009)

Murray et al.⁵⁰⁶ showed that `gga_x_pw86` has the correct $s_\sigma^{2/5}$ behavior in the limit of large values of s_σ . However, the fit version given by eq. (364) gives a slightly different coefficient than the one implied by the original analytical expression. They decided therefore to reparameterize the functional in order to recover the analytical coefficient, and at the same time to fulfill the correct low-density gradient limit (μ^{GE}). The revised parameters read $a = 0.1234$, $b = 17.33$, and $c = 0.163$. Compared to most other GGA functionals, an important advantage of `gga_x_pw86` and its revised version `gga_x_rpw86` is to agree well with the HF exchange. Therefore, they should not lead to spurious exchange binding, and be a suitable exchange component of functionals that explicitly include van der Waals interactions, such as vdW-DF2.⁵⁰⁷

`gga_x_pbe_jsjr`⁵⁰⁸ (2009)

Pedroza et al.⁵⁰⁸ looked at two important parameters of the PBE functional: the μ parameter of `gga_x_pbe` and the β parameter of `gga_c_pbe`. They considered three new combinations of β and μ . Among them (J_s, J_r) corresponds to $\beta = 0.046$ (the value in `gga_c_pbe_sol`, which was obtained by fitting to jellium (J) surface (s) energies, abbreviated as J_s) and μ calculated from $\mu = \pi^2\beta/3 \approx 0.151334$ ⁴⁷², which is the relation between μ and β to get the correct xc linear response (r) of bulk jellium, abbreviated as J_r . It turns out that among the tested PBE-type functionals, the combination (J_s, J_r) predicts the most accurate interatomic distances in small molecules.

`gga_x_rge2`⁵⁰⁹ (2009)

The form of this exchange functional is inspired by `gga_x_pbe` (eq. (378)), but it employs a different function $f_0(s_\sigma)$:

$$f_0(s_\sigma) = \mu^{\text{GE}} s_\sigma^2 + \frac{(\mu^{\text{GE}})^2}{\kappa} s_\sigma^4 \quad (406)$$

The resulting functional not only recovers the slowly varying density limit (since μ^{GE} in eq. (406) is chosen), but it also leads to a vanishing s_σ^4 term in the expansion. Therefore, the functional recovers the second-order gradient expansion for exchange over a wide range of values of s_σ . Combined with `gga_c_pbe` or `gga_c_rge2` for correlation, it leads to results for molecules and solids that indicate that the accuracy of this functional is rather similar to that of PBE (`gga_x_pbe + gga_c_pbe`).

`gga_x_airy`⁵¹⁰ (2009)

This is a new fit for the exchange energy per particle of the Airy-gas model (see `gga_x_lag`), which was obtained by a nonlinear least-square method. Its expression reads

$$F_x^{\text{Airy}} = \frac{a_1 s_\sigma^{a_2}}{(1 + a_3 s_\sigma^{a_2})^{a_4}} + \frac{1 - a_5 s_\sigma^{a_6} + a_7 s_\sigma^{a_8}}{1 + a_9 s_\sigma^{a_{10}}} \quad (407)$$

The parameters a_1, a_2, a_3 , and a_4 are the same as in `gga_x_lag`, while $a_5 = 133.983631$, $a_6 = 3.217063$, $a_7 = 136.707378$, $a_8 = 3.223476$, $a_9 = 2.675484$, and $a_{10} = 3.473804$.

This functional was combined with `gga_c_airy_rpa` correlation, leading to the ARPA functional. Further improvement can be obtained by adding a short-range correction to the RPA correlation energy (ARPA+):

$$e_{\text{xc}}^{\text{ARPA+}} = e_{\text{xc}}^{\text{ARPA}} + (e_c^{\text{PBE}} - e_c^{\text{PBE-RPA}}) \quad (408)$$

where e_c^{PBE} is `gga_c_pbe` and $e_c^{\text{PBE-RPA}}$ is `gga_c_pbe_rpa`. While accurate for surface xc energies, ARPA+ has no advantage over PBE (`gga_x_pbe + gga_c_pbe`) or PBEsol (`gga_x_pbe_sol + gga_c_pbe_sol`) for molecules and solids.

`gga_x_vmt_ge, gga_x_vmt_pbe`⁵¹¹ (2009)

To build this functional, Vela et al.⁵¹¹ chose an enhancement factor that recovers the correct

behavior for the electron gas at small and large values of s_σ , obeys the density-gradient expansion at small s_σ , and satisfies the LO bound for all values of s_σ . The form of F_x was furthermore chosen such that it relates to `gga_x_pbe`:

$$F_x^{\text{VMT}} = 1 + \mu s_\sigma^2 \frac{e^{-\alpha s_\sigma^2}}{1 + \mu s_\sigma^2} \quad (409)$$

Two possibilities for μ were proposed, either the value μ^{GE} coming from the density gradient-expansion (`gga_x_vmt_ge`), or the value μ^{PBE} used in `gga_x_pbe` (`gga_x_vmt_pbe`). The value of α was chosen with the LO bound, leading to $\alpha^{\text{GE}} = 0.001553$ and $\alpha^{\text{PBE}} = 0.002762$ for μ^{GE} and μ^{PBE} , respectively. The two functionals were combined with `gga_c_pbe` for correlation, and `gga_x_vmt_pbe` appears to be more accurate at reproducing the atomization energies of a set of small molecules than PBE (`gga_x_pbe` + `gga_c_pbe`), while `gga_x_vmt_ge` is much less accurate.

`gga_x_ssb_sw`⁵¹² (2009)

From studies of spin states, hydrogen bonding, π - π stacking, geometries, and $S_{\text{N}}2$ reaction barriers, it emerged that `gga_x_optx` shows a good performance for spin states and reaction barriers, while `gga_x_pbe` works well for weak interactions. This functional is an attempt of getting the best of both worlds by switching between `gga_x_optx` and `gga_x_pbe` in the appropriate range of s_σ . This is achieved by the following modification of `gga_x_pbe`:

$$F_x^{\text{SSB-sw}} = a + \frac{bs_\sigma^2}{1 + cs_\sigma^2} - \frac{ds_\sigma^2}{1 + es_\sigma^4} \quad (410)$$

The parameter $a = 1.05151$ is the same as in eq. (391) of `gga_x_optx`, while c is determined by the LO bound ($a + b/c = 1 + \kappa^{\text{PBE}}$). The remaining three parameters are fit to reproduce `gga_x_optx` for $s_\sigma \leq 0.7$ and `gga_x_pbe` for $s_\sigma \geq 0.9$, leading to $b = 0.191458$, $c = 0.254433$, $d = 0.180708$, and $e = 4.036674$. Note that it is not mentioned in ref. 512 which correlation functional was used.

`gga_x_ssb`, `gga_x_ssb_d`⁵¹³ (2009)

In an attempt to get a balanced exchange functional capable of yielding good results for

a number of different properties such as π - π stacking, hydrogen bonding, $S_{\text{N}}2$ barriers, and geometries of organic and organometallic systems, Swart et al.⁵¹³ proposed to mix their `gga_x_ssb_sw` functional with `gga_x_kt1`:

$$F_x^{\text{SSB}} = F_x^{\text{SSB-sw}} + (F_x^{\text{KT1}} - 1) \quad (411)$$

The parameters in eqs. (394) and (410) were redefined and reoptimized using a mixture of various properties and databases. This was done in combination with the correlation functional `gga_c_spbe` and either including or excluding Grimme’s D2 dispersion correction,^{514,515} leading to `gga_x_ssb_d` and `gga_x_ssb`, respectively. In eq. (394) δ is unchanged ($\delta = 0.1$), while γ is defined as $\gamma = ufbC_xC_s^2$. In eq. (410), d is defined as $d = b(1 - u)$. The values of the parameters that were obtained after reoptimization with the constraint $a + b/c = 1.804$ as in `gga_x_ssb_sw` are as follows. For `gga_x_ssb` $a = 1.071769$, $b = 0.137574$, $c = 0.187883$, $e = 6.635315$, $u = -1.205643$, and $f = 0.995010$. For `gga_x_ssb_d` $a = 1.079966$, $b = 0.197465$, $c = 0.272729$, $e = 5.873645$, $u = -0.749940$, $f = 0.949488$, and $s_6 = 0.847455$, where s_6 is the parameter in Grimme’s D2 correction.

This functional corrects only a small region in the reduced-density gradient s_σ space when compared to `gga_x_pbe`, but this leads to a large influence on the performance of the functional and several properties appear to be described quite well. This is true even for some systems put forward by Grimme as difficult cases.

`gga_x_eb88`²⁷³ (2009)

Elliott and Burke²⁷³ revisited `gga_x_b88` by providing a non-empirical derivation of the parameter β in eq. (368). For that they used the expansion of the energy of a neutral atom in the limit of large nuclear charge Z . It is known^{516,517} that the leading term in the total energy in this limit is given correctly by the Thomas–Fermi model, and that the first term in the exchange energy is given by the LDA. The subsequent terms in the expansions can be used to construct functionals beyond the LDA. By calculating the exchange energy of atoms with Z up to 88 they obtained the coefficient

$\beta = 0.0050/2^{1/3} \approx 0.003969$,⁴⁷² a value that is close to $\beta = 0.0042$ derived by Becke¹⁵⁷ by fitting to the HF exchange energies of the rare-gas atoms He to Rn.

`gga_x_lambda_ch`, `gga_x_lambda_oc2`, `gga_x_lambda_lo_n`, `gga_x_lambda_ch_n`, `gga_x_lambda_oc2_n`⁵¹⁸ (2009)

These five functionals, based on the `gga_x_pbe` form, were obtained by revisiting the LO bound. Known properties about the bound for systems with various numbers of electrons N are the following:

$$\lambda(N = 1) = 1.48 \quad (412a)$$

$$\lambda(N = 2) > 1.67 \quad (412b)$$

$$\lambda(N + 1) \geq \lambda(N) \quad (412c)$$

$$\lambda(N \rightarrow \infty) \leq \lambda_\infty \quad (412d)$$

with λ_∞ a constant for which several values have been proposed: $\lambda_{\text{LO}} = 2.273$,¹⁵⁰ $\lambda_{\text{CH}} = 2.215$,¹⁷² and $\lambda_{\text{OC}_2} = 2.00$.^{175,181} Odashima et al.⁵¹⁸ used these known properties to propose a N -dependent tight bound:

$$\lambda(N, \lambda_\infty) = \left(1 - \frac{1}{N}\right) \lambda_\infty + \frac{\lambda(N = 1)}{N} \quad (413)$$

which can be easily used in eq. (378) by noticing that the κ parameter is simply related to λ by

$$\kappa = \frac{\lambda}{2^{1/3}} - 1 \quad (414)$$

By using the above choices, five new variants of `gga_x_pbe` were proposed:

- PBE(λ_{CH}): eq. (414) with $\lambda = \lambda_{\text{CH}}$.
- PBE(λ_{OC_2}): eq. (414) with $\lambda = \lambda_{\text{OC}_2}$.
- PBE($\lambda_{\text{LO}}(N)$): eqs. (413) and (414) with $\lambda_\infty = \lambda_{\text{LO}}$.
- PBE($\lambda_{\text{CH}}(N)$): eqs. (413) and (414) with $\lambda_\infty = \lambda_{\text{CH}}$.
- PBE($\lambda_{\text{OC}_2}(N)$): eqs. (413) and (414) with $\lambda_\infty = \lambda_{\text{OC}_2}$.

Let us recall that the original `gga_x_pbe` corresponds to eq. (414) with $\lambda = \lambda_{\text{LO}}$. It was found that atomization energies and bond lengths of

molecules are rather insensitive to the choice of the LO bound.

The `gga_x_lambda_lo_n`, `gga_x_lambda_ch_n`, and `gga_x_lambda_oc2_n` functionals are implemented in Libxc with N in eq. (413) handled as a user-defined parameter, that is set to $N = \infty$ by default. The explicit dependence on the number of electrons N makes these functionals formally not semi-local functionals (see discussion for `lda_x_rae`).

`gga_x_c09x`⁵¹⁹ (2010)

This functional was developed with the goal of being compatible with a non-local correlation functional for van der Waals interactions.^{476,477,520} The chosen form is given by

$$F_x^{\text{C09x}} = 1 + \mu s_\sigma^2 e^{-\alpha s_\sigma^2} + \kappa \left(1 - e^{-\alpha s_\sigma^2/2}\right) \quad (415)$$

with the parameters $\mu = 0.0617$, $\kappa = 1.245$, and $\alpha = 0.0483$ determined by trying to reproduce (i) the gradient expansion approximation (with the gradient coefficient determined by Sham¹⁴⁶, see section 2.11) for $s_\sigma < 1.5$ and (ii) `gga_x_pbe_r` for $8 < s_\sigma < 10$. Constraint (i) was chosen such that the functional is more adapted for solids than for finite systems, while constraint (ii) ensures that exchange does not contribute much to van der Waals bonding, as it shouldn't.

Using `gga_x_c09x` instead of `gga_x_pbe_r` as the exchange part of the vdW-DF functional^{476,477} (C09-vdW) leads to significant improvements in the intermolecular interaction energies of the molecular dimers in the S22 dataset.⁵²¹

`gga_x_pbek1_vdw`, `gga_x_optpbe_vdw`, `gga_x_optb88_vdw`⁵²² (2010)

These three functionals were proposed as alternatives to `gga_x_pbe_r` for the exchange part of the vdW-DF functional for van der Waals interactions.^{476,477} All three contain empirical parameters that were tuned in order to minimize the mean absolute error on the intermolecular interaction energies of the S22 dataset of molecular dimers.⁵²¹

The `gga_x_pbek1_vdw` functional has the same form as `gga_x_pbe` and the optimization led to $\kappa = 1.00$ ($\mu = \mu^{\text{PBE}}$ was kept fixed).

Note that this value of κ does not ensure the fulfillment of the LO bound.

Next, `gga_x_optpbe_vdw` consists of a mixture of `gga_x_pbe` and `gga_x_rpbe`:

$$F_x^{\text{optPBE-vdW}} = aF_x^{\text{PBE}} + (1 - a)F_x^{\text{RPBE}} \quad (416)$$

where the mixing fraction a , as well as κ and μ in eqs. (378) and (383), were optimized, leading to $a = 0.945268$, $\kappa = 1.04804$, and $\mu = 0.175519$.

Finally, `gga_x_optb88_vdw` has the same form as `gga_x_b88`, and the optimization led to $\beta = 0.22C_xC_s^2 \approx 0.003369$ ⁴⁷² and $\gamma = 1/(1.2C_xC_s) \approx 6.981317$ ⁴⁷² for the parameters in eq. (368). Note that this value of γ is incompatible with the exact asymptotic behavior of the exchange energy density that was used in constructing `gga_x_b88`.

The vdW-DF variant using `gga_x_optb88_vdw` for exchange is clearly more accurate than `gga_x_pbek1_vdw` or `gga_x_optpbe_vdw` for the S22 dataset.

`gga_x_pbeint`⁵²³ (2010)

This functional was developed with the goal of being accurate for hybrid interfaces, such as molecules adsorbed on surfaces. It consists of a simple approximation based on the `gga_x_pbe` form, where μ^{PBE} in eq. (378) is replaced by the function

$$\mu^{\text{PBEint}}(s_\sigma) = \mu^{\text{GE}} + (\mu^{\text{PBE}} - \mu^{\text{GE}}) \frac{\alpha s_\sigma^2}{1 + \alpha s_\sigma^2} \quad (417)$$

where μ^{GE} is the value that comes from the density-gradient expansion. In the rapidly varying density regime (large s_σ) this functional approaches `gga_x_pbe`, while in the slowly varying density regime (small s_σ) it recovers `gga_x_pbe_sol`. The value of $\alpha = 0.197$ was fixed in order to ensure smooth derivatives of the functional. The functional was designed to be combined with `gga_c_pbeint`, and as expected, this combination yields results that are intermediate between PBE (`gga_x_pbe` + `gga_c_pbe`) and PBEsol (`gga_x_pbe_sol` + `gga_c_pbe_sol`), with improvements in the geometry and interaction energy of molecules adsorbed on Cu clusters.

`gga_x_revssb_d`^{524,525} (2011)

This is a revised version of `gga_x_ssb_d` where the parameters in eqs. (394) and (410) were re-optimized. Following the suggestion^{526,527} to set $s_6 = 1$ in Grimme’s D2 dispersion correction^{514,515} for a balanced description of dispersion forces, the other parameters were readjusted. The new values are $a = 1.082138$, $b = 0.177998$, $c = 0.246582$, $e = 6.284673$, $u = -0.618168$, $f = 1.0$, and $r_0 = 1.3$ (a parameter in the D2 correction that was 1.0 in `gga_x_ssb_d`). As for `gga_x_ssb_d`, $d = b(1 - u)$ and the constraint $a + b/c = 1.804$ was applied.

`gga_x_fd_lb94`, `gga_x_fd_rev1b94`⁵²⁸ (2011)

`gga_x_lb` was introduced by direct modeling of the potential $v_{x\sigma}^{\text{LB}}$ itself, bypassing the usual derivation from an energy functional. It has since been demonstrated that no energy functional whose functional derivative yields this potential exists.^{466,467} Gaiduk and Staroverov⁵²⁸ showed how to complement such “stray” potential by additional terms so that it becomes a proper functional derivative. By applying their method to `gga_x_lb`, they obtained the following functional:

$$F_x^{\text{fd-LB94}} = 1 - \frac{1}{C_x} x_\sigma [J_0(\xi^{-1} x_\sigma) \ln(\xi^{-1} x_\sigma) - J_1(\xi^{-1} x_\sigma)] \quad (418)$$

where $\xi = 2^{1/3}$ and

$$J_n(x) = -\frac{3}{4} \int_0^x dt \frac{\beta \xi \ln^n t}{1 + 3\beta \xi t \ln \left[\xi t + \sqrt{(\xi t)^2 + 1} \right]} \quad (419)$$

with $\beta = 0.05$. However, eq. (418) leads to a functional derivative that has no resemblance to the original potential `gga_x_lb`. Furthermore, the exchange energies of atoms are unrealistically too large by roughly 50%. Nevertheless, by choosing a much smaller value of $\beta = 0.004$, leading to `gga_x_fd_rev1b94`, much more reasonable exchange energies are obtained.

`gga_x_apbe`²⁷⁴ (2011)

This is yet another version of the `gga_x_pbe` functional. In this case, the parameter $\mu =$

0.260 in eq. (378) was determined from the density-gradient expansion of the semiclassical neutral atom,^{273,529} which is used here as the reference system (see `gga_x_eb88`). Combined with its correlation counterpart `gga_c_apbe`, this asymptotic PBE-like functional (APBE) provides accurate results for atomization energies and geometries of various types of molecules (organic, metal complexes, and transition-metal dimers). However, APBE is less accurate than PBE (`gga_x_pbe` + `gga_c_pbe`) for solid-state properties.

`gga_x_htbs`⁵³⁰ (2011)

The idea for this functional comes from the analysis of GGA functionals that have markedly different analytical forms and accuracy. In particular, exchange functionals that yield good results for the geometry of solids, such as `gga_x_wc` or `gga_x_pbe_sol` have an enhancement factor F_x that increases with s_σ slower than that of `gga_x_pbe`. Unfortunately, these *soft* GGAs overestimate atomization energies much more than `gga_x_pbe` does. However, for GGAs that lead to accurate atomization energies of molecules, such as `gga_x_b88` or `gga_x_rpbe`, F_x grows faster than that of `gga_x_pbe`. Not surprisingly, perhaps, these *strong* GGAs largely overestimate lattice constants.

In order to try to get the best of both worlds, Haas et al.⁵³⁰ suggested to interpolate between the enhancement factors of `gga_x_wc` and `gga_x_rpbe`:

$$F_x^{\text{HTBS}} = \begin{cases} F_x^{\text{WC}}(s_\sigma), & s_\sigma \leq s_1 \\ F_x^{\text{G}}(s_\sigma), & s_1 < s_\sigma \leq s_2 \\ F_x^{\text{RPBE}}(s_\sigma), & s_\sigma > s_2 \end{cases} \quad (420)$$

where

$$F_x^{\text{G}}(s_\sigma) = G(s_\sigma)F_x^{\text{RPBE}}(s_\sigma) + [1 - G(s_\sigma)]F_x^{\text{WC}}(s_\sigma) \quad (421)$$

and the function $G(s_\sigma)$ is a smooth interpolating function:

$$G(s_\sigma) = \sum_{i=1}^6 c_i(s_1, s_2) s_\sigma^{i-1} \quad (422)$$

The six coefficients c_i are determined by requir-

ing that F_x^{HTBS} and its two first derivatives are continuous at s_1 and s_2 . The switching points s_1 and s_2 were chosen such that the atomization energies of 20 molecules and the lattice constants of 60 solids are optimal, leading to $s_1 = 0.6$ and $s_2 = 2.6$.

The `gga_x_htbs` functional with `gga_c_pbe` for correlation appears to compete in accuracy with the best specialized GGA functionals for molecules and solids. However, this gain in accuracy comes at the price that it excessively overestimates the lattice constants of solids containing alkali atoms.

`gga_x_sogga11`⁵³¹ (2011)

This functional is an attempt to obey the density-gradient expansion at small values of s_σ and at the same time exhibit reasonable accuracy for the geometry and energetics of molecules. It uses a flexible form:

$$F_x^{\text{SOGGA11}} = g_1(s_\sigma) + g_2(s_\sigma) \quad (423)$$

where the functions g_1 and g_2 are given by

$$g_1(s_\sigma) = \sum_{i=0}^m a_i \left(1 - \frac{1}{1 + \frac{\mu}{\kappa} s_\sigma^2} \right)^i \quad (424a)$$

$$g_2(s_\sigma) = \sum_{i=0}^m b_i \left(1 - e^{-\mu s_\sigma^2 / \kappa} \right)^i \quad (424b)$$

are power expansions of the enhancement factors of `gga_x_pbe` (eq. (378)) and `gga_x_rpbe` (eq. (383)), respectively. The HEG limit given by `lda_x` is guaranteed by the condition $a_0 + b_0 = 1$, and, making the same choices as for `gga_x_sogga`, the density-gradient expansion implies that $\mu = \mu^{\text{GE}}$, while $\kappa = 0.552$ (coupled with the constraint $a_1 + b_1 = \kappa$) is imposed by the tighter LO bound.¹⁷⁵ Together with the parameters of the correlation counterpart `gga_c_sogga11`, the parameters a_i and b_i ($m = 5$ was chosen as a good choice) were fit to training data, involving main-group and transition-metal thermochemistry, kinetics, π interactions, and noncovalent interactions. This functional is accurate for bond lengths in molecules, and is more accurate than numerous other GGA functionals tested in ref. 531 for the energetics of finite systems. Note that the sign

in front of $(\mu/\kappa)s^2$ in eq. (3) of ref. 531 is wrong.

`gga_x_optb86b_vdw`⁵³² (2011)

Akin to `gga_x_pbek1_vdw`, `gga_x_optpbe_vdw`, and `gga_x_optb88_vdw`, proposed previously by Klimeš et al.⁵²², this functional was designed to be used as the exchange part of the vdW-DF functional.^{476,477} It is a reparametrization of `gga_x_b86_mgc`, where the parameters $\beta = \mu^{\text{GE}}C_xC_s^2$ and $\gamma = \mu^{\text{GE}}C_s^2$ in eq. (365) were chosen such that the density-gradient expansion of the exchange is recovered. The resulting functional has an accuracy similar to `gga_x_optb88_vdw` on the S22 reference set of molecular dimers,⁵²¹ and is quite accurate for the lattice constant and atomization energy of normal bulk solids. Furthermore, it has an improved asymptotic behavior by construction.

`gga_x_bpccac`⁵³³ (2012)

This functional uses an approach that was developed by Grüning et al.⁵³⁴ to correct the asymptotic behavior of an exchange potential. It is designed to switch between two functionals, one that describes accurately the bulk density region, and another that has a correct behavior in the asymptotic tail. Brémond et al.⁵³³ applied this procedure to the exchange energy density, and used the following switching function:

$$f(x_\sigma) = \frac{1}{1 + e^{-\alpha(2^{-1/3}x_\sigma - \beta)}} \quad (425)$$

where α and β are parameters that determine the transition between the two types of regions. As limiting enhancement factors, they chose `gga_x_pbe_tca` (appropriate for the bulk region) and `gga_x_pw91` (appropriate for the asymptotic region), leading to

$$F_x^{\text{BPCCAC}} = [1 - f(x_\sigma)]F_x^{\text{PBE-TCA}} + f(x_\sigma)F_x^{\text{PW91}} \quad (426)$$

The values of $\alpha = 1$ and $\beta = 19$ were chosen based on atomization energy errors in the G2 test set,^{406,505} and by seeking a compromise to describe correctly weakly interacting systems. This functional, combined with `gga_c_revtpca` for correlation, leads to a balanced description of both strongly and weakly interacting sys-

tems.

`gga_x_vmt84_ge`, `gga_x_vmt84_pbe`⁵³⁵ (2012)

These functionals are evolutions of their predecessors `gga_x_vmt_ge` and `gga_x_vmt_pbe`. While `gga_x_vmt_ge` and `gga_x_vmt_pbe` do not satisfy the asymptotic condition^{173,174}

$$\lim_{s_\sigma \rightarrow \infty} s_\sigma^{1/2} F_x(s_\sigma) < \infty \quad (427)$$

these functionals proposed by Vela et al.⁵³⁵ are constructed such that eq. (427) is obeyed. The form is given by

$$F_x^{\text{VMT}\{m,n\}} = F_x^{\text{VMT}} + \left(1 - e^{-\alpha s_\sigma^{m/2}}\right) (s_\sigma^{-n/2} - 1) \quad (428)$$

where F_x^{VMT} is eq. (409). According to Vela et al.⁵³⁵, `gga_x_pw91` and `gga_x_lg93` are the only previously existing GGA exchange functionals that satisfy eq. (427). The values $m = 8$ and $n = 4$ were chosen from a series of exact requirements and by requiring that the enhancement factor is smooth over the relevant range of s_σ . Two values for μ in the F_x^{VMT} component were considered, $\mu = \mu^{\text{GE}}$ leading to `gga_x_vmt84_ge`, and $\mu = \mu^{\text{PBE}}$ to `gga_x_vmt84_pbe`. The corresponding values of α in eq. (428) were fixed by the LO bound, leading to $\alpha^{\text{GE}} = 0.000023$ and $\alpha^{\text{PBE}} = 0.000074$, respectively.

The `gga_x_vmt84_ge` functional was combined with the correlation functionals `gga_c_lyp` and `gga_c_pbe_jrgx`, while `gga_x_vmt84_pbe` was combined with `gga_c_lyp` and `gga_c_pbe`. Overall, `gga_x_vmt84_ge` and `gga_x_vmt84_pbe` yielded results similar to `gga_x_vmt_ge` and `gga_x_vmt_pbe`, respectively.

`gga_x_n12`¹⁵³ (2012)

The enhancement factor of this functional is defined by a power series

$$F_{xc}^{\text{N12}} = \sum_{i=0}^m \sum_{j=0}^{m'} a_{ij} \tilde{u}_\sigma^i v_\sigma^j \quad (429)$$

where $\tilde{u}_\sigma = \tilde{u}(x_\sigma)$ given by eq. (251) that was originally used by Becke¹⁵⁵ in his functional `gga_x_b86`, and \tilde{v}_σ is eq. (39). This form was

inspired by the expansions proposed in earlier works.^{370,536} It is important to note that F_{xc}^{N12} not only depends on the reduced-density gradient x_σ (or s_σ) as a GGA exchange functional usually does, but it also depends on the density n_σ (i.e., $F_{xc}^{N12} = F_{xc}^{N12}(n_\sigma, x_\sigma)$).

The expansion was truncated at $m = m' = 3$ (16 linear parameters), which was concluded as large enough for good accuracy without leading to numerical instability. The value $\gamma_\sigma = 0.004$ for the parameter in eq. (251) is originally from `gga_x_b86`, while $\omega_\sigma = 2.5$ in eq. (39) was determined in ref. 153. The coefficients a_{00} , a_{10} , a_{20} , and a_{30} were obtained analytically from the expansion to third order in \tilde{u}_σ of `gga_x_pbe_sol`. As such, in the low-density limit eq. (429) reduces to `gga_x_pbe_sol` and to `lda_x` if $x_\sigma = 0$. The remaining parameters were fit together with the parameters of the correlation part `gga_c_n12` to a series of databases including both energetic and structural data of molecules and solids.

N12 (`gga_x_n12` + `gga_c_n12`) was then tested on a few properties or types of systems (e.g., semiconductors band gaps or cohesive energies of solids) that were not used in the training set. The results were quite accurate except for the band gaps.

`gga_x_pbe_mol`⁵³⁷ (2012)

For the hydrogen atom (or any other one-electron system system for that matter) it is well known that the exact exchange energy exactly cancels out the Hartree energy, while approximate xc functionals lead to an amount of self-interaction error.²³³ del Campo et al.⁵³⁷ used this exact condition to fix the μ parameter in eq. (378) of the `gga_x_pbe` functional (the original value $\kappa = \kappa^{\text{PBE}}$ is kept), leading to $\mu = 0.27583$. When combined with `gga_c_pbe_mol`, this functional gives substantial improvement over the original PBE (`gga_x_pbe` + `gga_c_pbe`) in the prediction of the heats of formation of molecules, while retaining the PBE quality for the description of other molecular properties.

`gga_x_q2d`⁵³⁸ (2012)

Chiodo et al.⁵³⁸ proposed a functional that obeys nonuniform scaling in 1D and that is ac-

curate in the whole quasi 2D (Q2D) regime. They chose an infinite-barrier quantum well as reference system, while still requiring the functional to fulfill several conditions of the 3D case, like recovering `lda_x` and satisfying the LO bound. The exchange functional is then constructed by interpolating between the `gga_x_pbe_sol` functional and the 2D limit.⁵³⁹ The enhancement factor reads

$$F_x^{\text{Q2D}} = \frac{F_x^{\text{PBEsol}}(s_\sigma)(c - s_\sigma^4) + 0.5217s_\sigma^{7/2}(1 + s_\sigma^2)}{c + s_\sigma^6} \quad (430)$$

where the coefficient $c = 100$ was obtained by fitting to the reference system.

When combined with its correlation counterpart `gga_c_q2d`, this functional predicts accurate results for the surface energy and bulk lattice constant of transition metals.

`gga_x_2d_b88`, `gga_x_2d_b86`, `gga_x_2d_pbe`^{275,331} (2014)

These three functionals are the 2D counterparts of `gga_x_b88`, `gga_x_b86`, and `gga_x_pbe`, respectively. (Note that only `gga_x_2d_b88` was published in ref. 275, while the two others are unpublished.)

The famous `gga_x_b88` functional of Becke¹⁵⁷ can be generalized to finite 2D systems. The counterpart of eq. (368) reads

$$F_x^{\text{B88-2D}} = 1 + \frac{\beta}{C_x^{2D}} \frac{(x_\sigma^{2D})^2}{1 + \gamma\beta x_\sigma^{2D} \operatorname{arcsinh}(x_\sigma^{2D})} \quad (431)$$

where x_σ^{2D} is given by eq. (42) with $m = 2$, and C_x^{2D} is eq. (19). In this case, the coefficients γ and β cannot be determined by dimensional analysis. However, one can use the requirement that the 2D exchange-hole potential behaves as $1/r$ for densities that behave as $e^{-a_0 r^2}$ at large r ,⁵⁴⁰ which implies $\gamma = 8$. The coefficient $\beta = 0.007$ was obtained by fitting to the exact-exchange energy of a set of parabolic quantum dots.

Next, `gga_x_2d_b86` is expressed in a different, yet totally equivalent way to the 3D version (eq. (363) with $\alpha = 2/3$):

$$F_x^{\text{B86-2D}} = \frac{1 + \beta (x_\sigma^{2D})^2}{1 + \gamma (x_\sigma^{2D})^2} \quad (432)$$

where the parameters $\beta = 0.002105$ and $\gamma = 0.000119$ were fit to exact-exchange results for parabolic quantum dots.

Finally, `gga_x_2d_pbe` has the same form as its 3D counterpart, eq. (378), but with the obvious substitution of s_σ by its 2D version s_σ^{2D} given by eq. (52). The parameters $\kappa = 0.4604$ and $\mu = 0.354546875$ were in this case fit to exact-exchange results for parabolic quantum dots.

`gga_x_ak13`⁵⁴¹ (2013)

Armiento and Kümmel⁵⁴¹ tried to construct an exchange energy functional whose potential $v_{x\sigma}$ retains an interesting property of the `mgga_x_bj06` potential, namely the asymptotic limit $v_{x\sigma} \rightarrow \sim \sqrt{-\varepsilon_I^0}$, where $\varepsilon_I^0 = \varepsilon_H - \lim_{r \rightarrow \infty} v_{x\sigma}$, and ε_H is the eigenvalue of the highest occupied molecular orbital. This feature is important, as it is strongly related to the xc derivative discontinuity.³¹² Noticing that the product $n_\sigma^{1/3} s_\sigma$ leads to this asymptotic limit, they could derive a differential equation (eq. (14) in the supplemental material of ref. 541) for the enhancement factor that yields a potential satisfying this limit. Solving this equation yields

$$F(s_\sigma) = B_1 s_\sigma \ln(s_\sigma) \quad (433)$$

As this form is somewhat too limited to be useful in practice, the analysis was repeated for the case of the asymptotic limit far outside the surface of a half-infinite solid. In this case, the enhancement factor that yields the correct asymptotic limit is

$$F(s_\sigma) = B_2 s_\sigma \ln[\ln(s_\sigma)] \quad (434)$$

By combining eqs. (433) and (434) and regularizing the expression for small s_σ , the final expression for the enhancement factor is given by

$$F_x^{\text{AK13}} = 1 + B_1 s_\sigma \ln(1 + s_\sigma) + B_2 s_\sigma \ln[1 + \ln(1 + s_\sigma)] \quad (435)$$

with the choice $B_2 = \mu^{\text{GE}} - B_1$ in order to ensure the recovery of the second-order density-gradient expansion (see section 2.11). The re-

maining constant $B_1 = (3/5)\mu^{\text{GE}} + 8\pi/15$ sets the strength of the xc derivative discontinuity, and it was determined by demanding that the system-independent term in the asymptotic expansion of $v_{x\sigma}$ yields $-1/r$.

Compared to `lda_x` (or `gga_x_pbe`), `gga_x_ak13` significantly opens the band gap in the semiconductors Si and Ge in a similar way to exact-exchange calculations, and correctly moves down the d bands in Cu bulk metal.

`gga_x_s12g`⁵⁴² (2013)

This functional builds upon its predecessors `gga_x_ssb_sw`, `gga_x_ssb`, and `gga_x_ssb_d`. Here, a similar expression for the enhancement factor is chosen with the difference that a fourth-order term in x_σ is present in the numerator. The form of the enhancement function was chosen to be more flat in the low x_σ regime, and it is given by

$$F_x^{\text{S12g}} = A + B \left(1 - \frac{1}{1 + Cx_\sigma^2 + Dx_\sigma^4} \right) \times \left(1 - \frac{1}{1 + Ex_\sigma^2} \right) \quad (436)$$

B is fixed by imposing the tight LO bound from Chan and Handy¹⁷², leading to $B = 1.757 - A$. This exchange functional was then combined with `gga_c_pbe` for correlation and Grimme's D3 dispersion correction,⁵⁴³ and the remaining parameters (A , C , D , and E in eq. (436) and $s_{r,6}$ and s_8 in the D3 correction) were obtained from a fit to a series of databases for small molecules. The resulting values are $A = 1.03842032$, $C = 0.00403198$, $D = 0.00104596$, $E = 0.00594635$, $s_{r,6} = 1.17755954$, and $s_8 = 0.84432515$.

The functional was shown to work well for a series of molecular properties, including weakly and strongly bound systems, as well as spin-state energies.

`gga_x_lv_rpw86`⁵⁴⁴ (2014)

This is an exchange functional based on the plasmon description within the non-local correlation functionals for van der Waals interactions.^{476,477} In the regime with reduced-density gradient $s_\sigma \lesssim 2.5$ which dominates the non-local correlation component of the bind-

ing energy, the functional is made close to the Langreth–Vosko (LV) screened exchange⁵⁴⁵ (defined below). For larger values of s_σ , dominated by exchange, the functional becomes similar to `gga_x_rpw86` that includes the proper large- s_σ behavior of exchange discussed in ref. 506. This leads to the following enhancement factor:

$$F_x^{\text{LV-rPW86}} = \frac{1}{1 + \alpha s_\sigma^6} F_x^{\text{LV}}(s_\sigma) + \frac{\alpha s_\sigma^6}{\beta + \alpha s_\sigma^6} F_x^{\text{rPW86}}(s_\sigma) \quad (437)$$

where $F_x^{\text{LV}} = 1 + \mu_{\text{LV}} s^2$ with $\mu_{\text{LV}} = -Z_{\text{ab}}/9$ where $Z_{\text{ab}} = -0.8491$,⁵⁴⁵ while F_x^{rPW86} is given by eq. (364) with the coefficients of `gga_x_rpw86`. The parameters $\alpha = 0.02178$ and $\beta = 1.15$ were determined such that $F_x^{\text{LV-rPW86}}$ reproduces at best F_x^{LV} in the $0 < s_\sigma < 2$ interval and F_x^{rPW86} in the $4 < s_\sigma < 10$ interval.

`gga_x_lv_rpw86` is used as the exchange component of the non-local van der Waals functional vdW-DF-cx,⁵⁴⁴ which appears to perform well for the intermolecular distance and binding energy of weakly bound dimers (the S22 set was used⁵²¹) as well as for the lattice constants of layered materials and strongly-bound solids.

`gga_x_bcgp`⁵⁴⁶ (2014)

This functional, which has the same form as `gga_x_pbe`, is similar in spirit to `gga_x_eb88`, as both use the large nuclear charge Z limit of atoms in order to fix parameters in the functional. Actually, it turned out that the two most used exchange GGA functionals (`gga_x_b88` and `gga_x_pbe`) yield exchange energies that are already relatively accurate in this limit.²⁷³ The functional `gga_x_eb88` is the modified version of `gga_x_b88` that leads to the correct value at the large Z limit. In the case of `gga_x_pbe`, the necessary modification is an increase in the value of μ in eq. (378) by 13%, leading to `gga_x_bcgp` with $\mu = 0.249$. This functional was combined with `gga_c_acgga` for correlation.

`gga_x_b86_r`^{547,548} (2014)

This is a reparametrization from Hamada⁵⁴⁷ of the `gga_x_b86_mgc` functional, designed to be an improvement over `gga_x_rpw86` that is the exchange part of the second version of the non-local van der Waals functional vdW-DF2.⁵⁰⁷ In eq. (365), the parameter β is determined by the correct small density-gradient limit, while γ is arbitrarily determined by a least square fit to the original `gga_x_b86_mgc` for $8 < s_\sigma < 10$. The resulting parameters are $\beta = \mu^{\text{GE}} C_x C_s^2$ and $\gamma = \mu^{\text{GE}} C_s^2 / \kappa$, where $\kappa = 0.7114$. The revised van der Waals functional, rev-vdW-DF2, appears to lead to significantly improved results compared to vdW-DF2.

`gga_x_cap`⁵⁴⁹ (2015)

Carmona-Espíndola et al.⁵⁴⁹ developed an exchange functional whose potential has the right asymptotic behavior for finite systems. Furthermore, they also required it to have the correct behavior at the small density-gradient limit ($\lim_{s_\sigma \rightarrow 0} F_x = 1 + \mu s_\sigma^2$), and it to be similar to other accurate GGA exchange functionals in the interval $0 \leq s_\sigma \leq 3$ that is relevant for the total energy. With these requirements, they arrived at the following form:

$$F_x^{\text{CAP}} = 1 + 2^{1/3} \frac{\alpha}{C_x} \frac{s_\sigma \ln(1 + s_\sigma)}{1 + c \ln(1 + s_\sigma)} \quad (438)$$

The constant $c = \alpha / (3\pi^2)^{1/3}$ in this *correct asymptotic potential* (CAP) functional is obtained from the asymptotic expansion, while $\alpha = C_x \mu / 2^{1/3}$ is chosen from the small density gradient limit.

Combined with `gga_c_lyp` or `gga_c_pbe` for the correlation, several values for μ were tested (e.g., μ^{PBE} from `gga_x_pbe` or μ^{GE}). The one leading to the most accurate heats of formation of molecules is μ^{PBE} .

This non-empirical functional yields a competitive description of various molecular properties. Furthermore, thanks to its well-behaved exchange potential in the asymptotic region, the description of properties that depend on response functions calculated from time-dependent DFT are improved compared to standard GGA functionals.

`gga_x_gam`⁵⁵⁰ (2015)

This gradient approximation for molecules (GAM) has the same non-separable xc form as `gga_x_n12`, and therefore should not be considered a pure exchange functional. As in `gga_x_n12`, $m = m' = 3$ in eq. (429), $\gamma_\sigma = 0.004$ in eq. (251), and $\omega_\sigma = 2.5$ in eq. (39). The 16 linear parameters of the functional, together with the 10 parameters of the associated pure correlation functional `gga_c_gam`, were optimized with a particular emphasis for quantities relevant for homogeneous catalysis (main-group and transition-metal bond energies, reaction-barrier heights, and geometry). Also included in the training set are databases for the ionization potentials, electron affinities, interaction energies of weakly-bound systems, lattice constants of solids, etc. During the optimization, a smoothness constraint was applied in order to get a functional that has a reasonable shape without large unphysical variations. Unlike `gga_x_n12`, the functional was not constrained to reduce to `lda_x` for the HEG.

Among the numerous GGA functionals tested in ref. 550, the GAM functional (`gga_x_gam` + `gga_c_gam`) lead to the most accurate results for most of the considered 30 properties, and could also sometimes compete with MGGA and hybrid functionals.

`gga_x_pbefe`⁵⁵¹ (2015)

Standard LDA and GGA functionals, such as PBE (`gga_x_pbe` + `gga_c_pbe`) or PBEsol (`gga_x_pbe_sol` + `gga_c_pbe_sol`) yield large errors for the formation energies of solids. For example, PBE gives errors of the order of 0.25 eV/atom for a set of 252 solids.⁵⁵² The PBEfe functional is an attempt at improving the accuracy at the GGA level. It is an empirical functional with the same mathematical form as PBE, whose parameters in the exchange (`gga_x_pbefe`) and correlation (`gga_c_pbefe`) parts were optimized for a set of 94 formation energies of binary compounds. The new values of the exchange parameters in eq. (378) are $\mu = 0.346$ and $\kappa = 0.437$.

When tested on a set of 104 binary and 33 ternary compounds, PBEfe leads to an average absolute error for the formation energy of

0.125 eV/atom (compared to 0.178 eV/atom for LDA and 0.248 eV/atom for PBE), a value that could be further reduced by introducing a Hubbard U interaction. Such an improvement could be obtained without deteriorating the accuracy for the geometries.

`gga_x_pbetrans`⁵⁵³ (2016)

This is an attempt from Brémond et al.⁵⁵³ at providing a functional that is more similar to `gga_x_pbe_r` in the bulk regions (where strong bonds are present) and to `gga_x_pbe` in the asymptotic regions (relevant to weak interactions), in order to keep the best of both approaches. This is achieved by using the `gga_x_pbe` form, eq. (378), and interpolating the value of κ as follows:

$$\kappa(s_\sigma) = [1 - f(s_\sigma)] \kappa^{\text{revPBE}} + f(s_\sigma) \kappa^{\text{PBE}} \quad (439)$$

where $\kappa^{\text{revPBE}} = 1.245$ and the interpolating function is chosen to have the form of a Fermi distribution:

$$f(s_\sigma) = \frac{1}{1 + e^{-\alpha(s_\sigma - \beta)}} \quad (440)$$

In this way, the functional reduces to `gga_x_pbe` for small values of s_σ , and to `gga_x_pbe_r` for large values of s_σ . Note that this functional is constructed using a similar strategy as for `gga_x_bpccac`. It was found that large values of α lead to better results but also to issues in the self-consistent field procedure. As in `gga_x_bpccac` (which uses x_σ instead of s_σ) the value $\alpha = 2(3\pi^2)^{1/3}$ is chosen as a good compromise. The chosen value $\beta = 3$ represents the upper bound of the physical range of values for s_σ in bulk solids.

Combined with `gga_c_pbe` or `gga_c_revtca`, the functional is quite accurate for both strongly-bound and weakly-bound systems.

`gga_x_pbepow`⁵⁵⁴ (2016)

This functional takes further the ideas of power series used in previous functionals.³⁷⁰ Here, a power series truncated at order m of the `gga_x_pbe` exchange enhancement factor is

used:

$$F_x^{\text{PBEpow}} = 1 + \sum_{i=1}^m c_{xi} \left(\frac{\gamma_x s_\sigma^2}{1 + \gamma_x s_\sigma^2} \right)^i \quad (441)$$

In order for this expression to satisfy the small density-gradient behavior and the LO bound, the parameters are set to $\gamma_x = m\mu^{\text{PBE}}/\kappa^{\text{PBE}}$ and $c_{xi} = \kappa^{\text{PBE}}/m$. With these requirements, the functional has the same slowly (small s_σ) and rapidly (large s_σ) varying limits as `gga_x_pbe`. Furthermore, it is bounded for $m \rightarrow \infty$, with high-order terms ($m > 10$) not affecting significantly the results. Br mond⁵⁵⁴ recommends, however, that in practice m should be chosen as large as possible, keeping in mind the computational cost. Note that the value $m = 100$ is chosen in Libxc.

When combined with `gga_c_pbe`, `gga_x_pbepow` improves results for molecular covalent interactions, while keeping a performance similar to PBE (`gga_x_pbe` + `gga_c_pbe`) for noncovalent interactions.

`gga_x_sg4`⁵⁵⁵ (2016)

One of the most important exact conditions for the development of GGA or MGGA exchange functionals is the small density-gradient expansion. Many functionals are built in order to reproduce this expansion up to quadratic order. The `gga_x_sg4` goes one step beyond, and introduces an extension of the modified gradient expansion²⁷³ to fourth order:

$$\lim_{s_\sigma \rightarrow 0} F_x(s_\sigma) = 1 + \mu s_\sigma^2 + \nu s_\sigma^4 + O(s_\sigma^6) \quad (442)$$

By looking at the slowly varying density region of nonrelativistic large neutral atoms (i.e., when $Z \rightarrow \infty$, see discussion for `gga_x_eb88`), one obtains $\mu^{\text{MGE2}} = 0.260$ (close to the value from ref. 273) and $\nu^{\text{MGE4}} = -0.195$.

The proposed semiclassical GGA at fourth order (SG4), which obeys the expansion eq. (442) and the LO bound, is given by

$$F_x^{\text{SG4}} = 1 + \kappa_1 + \kappa_2 - \frac{\kappa_1 \left(1 - \frac{\mu_1}{\kappa_1} s_\sigma^2 \right)}{1 - \left(\frac{\mu_1}{\kappa_1} s_\sigma^2 \right)^5} - \frac{\kappa_2}{1 + \frac{\mu_2}{\kappa_2} s_\sigma^2} \quad (443)$$

where $\kappa_1 + \kappa_2 = \kappa^{\text{PBE}}$ comes from the LO bound, while $\mu_1 + \mu_2 = \mu^{\text{MGE2}}$ and $\kappa_2 = -\mu_2^2/\nu^{\text{MGE4}}$. The remaining parameter $\mu_1 = 0.042$ was obtained by fitting to the exchange ionization potential in the semiclassical neutral atom limit.

Together with its correlation counterpart `gga_c_sg4`, this functional performs quite well in a broad range of problems for both molecules and solid-state systems.

`gga_x_lspbe`, `gga_x_lsrpbe`⁵⁵⁶ (2016)

Pacheco-Kato et al.⁵⁵⁶ proposed two functionals that aim at simplifying the `gga_x_pw91` enhancement factor, while maintaining or improving its performance. These functionals are based on `gga_x_pbe` and `gga_x_rpbbe` while adding a Gaussian tail to satisfy the asymptotic reduced-density gradient constraint, eq. (427). The functionals read

$$F_x^{\text{ls(R)PBE}} = F_x^{(\text{R})\text{PBE}} - (\kappa + 1) \left(1 - e^{-\alpha s_\sigma^2} \right) \quad (444)$$

There are three parameters defining the functionals, specifically μ in eqs. (378) and (383), κ , and α . Pacheco-Kato et al.⁵⁵⁶ chose the value of $\kappa = \kappa^{\text{PBE}}$ as used in both `gga_x_pbe` and `gga_x_rpbbe`. The small- s_σ expansion of the functional shows that

$$\mu_x = \mu - \alpha - \alpha\kappa \quad (445)$$

is the second-order coefficient. Several non-empirical values for μ_x were considered: μ^{GE} of the exact density-gradient expansion, μ^{PBE} from `gga_x_pbe`, $\mu^{\text{APBE}} = 0.260$ from the asymptotic expansion of the semi-classical approximation used in `gga_x_apbe`, and $\mu^{\text{PBEmol}} = 0.27583$ from `gga_x_pbe_mol`, which was deduced from atomic hydrogen. This leads to four versions for each of these two functionals (thus, eight exchange functionals). Finally, α is chosen such that the maximum of eq. (444) (related to the local LO bound) is equal to the maximum value of `gga_x_pw91` (1.641).

These eight exchange functionals were combined with three correlation functionals (`gga_c_lyp`, `gga_c_pw91`, and `gga_c_pbe` with $\beta = 3\mu_x/\pi^2$), leading to 24 functionals in to-

tal, which were tested on various molecular properties.

Among these eight exchange functionals, the ones available in Libxc are the two using $\mu_x = \mu^{\text{PBE}}$, `gga_x_lspbe` and `gga_x_lsrpbe`.

`gga_x_kdt16`⁴⁴⁷ (2016)

Karasiev et al.⁴⁴⁷ proposed this exchange free-energy functional as an improvement of `lda_xc_ksdt` for applications at nonzero temperature τ_e . The expression for the free-energy per particle (given in the supplemental material of ref. 557) is given by

$$f_x^{\text{KDT16}} = f_x^{\text{LDA}}(n, \tau_e) F_x^{\text{KDT16}}(s_{2x}) \quad (446)$$

where

$$f_x^{\text{LDA}}(n, \tau_e) = e_x^{\text{LDA}}(n) \tilde{A}_x(\theta) \quad (447)$$

with $\theta = \tau_e/\tau_e^{\text{F}}$ and τ_e^{F} being the Fermi temperature (eq. (351)), e_x^{LDA} given by eq. (256) and

$$y = \frac{2}{3}\theta^{3/2} \quad (448)$$

$$u = y^{2/3} \quad (449)$$

$$v = y^{4/3} \quad (450)$$

$$\tilde{A}_x(y) = \frac{a_{\ln} y^4 \ln(y) + a_{2.5} u^{5/2} + \sum_{i=1}^8 a_i u^i}{1 + \sum_{i=1}^4 b_i v^i} \quad (451)$$

and

$$F_x^{\text{KDT16}}(s_{2x}) = 1 + \frac{\nu_x s_{2x}}{1 + \alpha |s_{2x}|} \quad (452)$$

where s_{2x} is a τ_e -dependent reduced-density gradient:

$$s_{2x}(n, \nabla n, \tau_e) = s^2 \frac{\tilde{B}_x(\theta)}{\tilde{A}_x(\theta)} \quad (453)$$

with

$$\tilde{B}_x(y) = \frac{\sum_{i=2}^{10} a_i u^i}{1 + \sum_{i=1}^{10} b_i u^i} \quad (454)$$

The parameters in eq. (452) were chosen to have the `gga_x_pbe` values, $\nu_x = \mu^{\text{PBE}}$ and $\alpha = \nu_x/\kappa = \nu_x/\kappa^{\text{PBE}} = 0.27302$, so that eq. (378) is recovered at $\tau_e = 0$ K (note that $\lim_{\tau_e \rightarrow 0} s_{2x} = s^2$). Furthermore, since $\lim_{\tau_e \rightarrow 0} \tilde{A}_x(y) = 1$, eq. (446) recovers the energy per particle of `gga_x_pbe` at $\tau_e = 0$ K.

Combined with the `gga_c_kdt16` correlation free-energy functional, applications on deuterium and aluminium show that KDT16 improves over PBE (`gga_x_pbe` + `gga_c_pbe`).

`gga_x_ncap`⁵⁵⁸ (2019)

This functional was developed by taking into account the correct $-1/r$ asymptotic behavior of the exchange potential $v_{x\sigma}$ for finite systems. Furthermore, it preserves the correct density-gradient expansion behavior at small s_σ . The functional form is given by

$$F_x^{\text{NCAP}} = 1 + \mu \tanh(s_\sigma) \operatorname{arcsinh}(s_\sigma) \times \frac{1 + \alpha [(1 - \delta)s_\sigma \ln(1 + s_\sigma) + \delta s_\sigma]}{1 + \beta \tanh(s_\sigma) \operatorname{arcsinh}(s_\sigma)} \quad (455)$$

where μ , α , β , and δ are parameters. The density-gradient expansion fixes the value of $\alpha = 4\pi\beta/(3\mu)$. Furthermore, $\mu = \mu^{\text{PBE}}$ is fixed at the `gga_x_pbe` value. The values $\beta \approx 0.018086$ ⁵⁵⁹ and $\delta \approx 0.304121$ ⁵⁵⁹ were by demanding that the exact exchange energy and the exact highest occupied orbital of the H atom are reproduced. Note that alike any GGA exchange functional with a corresponding potential that reproduces the asymptotic behavior $-1/r$, `gga_x_ncap` does not obey the local version of the LO bound (see section 2.3).

When combined with `gga_c_p86` for correlation, this exchange functional is able to compete with more advanced functionals, such as the τ -MGGA SCAN (`mgga_x_scan` + `mgga_c_scan`) or the hybrid B3LYP,³⁹⁷ in the reproduction of several properties. It also yields KS eigenvalues of the highest occupied orbitals that are use-

ful approximations to the ionization potential thanks to the inclusion of a systematic derivative discontinuity shift in v_x .

[gga_x_df3_opt1](#), [gga_x_df3_opt2](#)²¹² (2020)
The [gga_x_df3_opt1](#) and [gga_x_df3_opt2](#) functionals have the same mathematical forms as [gga_x_b88](#) and [gga_x_b86_mgc](#), respectively. They were designed to be compatible with a novel form of the non-local van der Waals functional.²¹² Both GGA functionals contain two parameters, β and γ , see eqs. (365) and (368). The β parameter was fixed by requiring the density-gradient expansion at second order to be obeyed with the correct coefficient μ^{GE} (see section 2.11), leading to $\beta = \mu^{\text{GE}} C_x C_s^2$ in both functionals. The second parameter was optimized on the S22 \times 5 set of molecular dimers,⁵⁶⁰ leading to $\gamma = 1/(\kappa C_x C_s)$ with $\kappa = 1.10$ in eq. (368) for [gga_x_df3_opt1](#), and $\gamma = \mu^{\text{GE}} C_s^2/\kappa$ with $\kappa = 0.58$ in eq. (365) for [gga_x_df3_opt2](#). Note that two parameters in the non-local correlation functional were also optimized.

The non-local van der Waals functionals vdW-DF3-opt1 and vdW-DF3-opt2 were shown to be overall accurate for both weakly and strongly bound systems.

[gga_x_chachiyo](#)⁵⁶¹ (2020)

This functional was constructed such that the exchange-energy density has the proper decay $-1/(2r)$ in the asymptotic region of finite systems, and the functional recovers the correct second-order term in the expansion in the limit of a slowly varying density. For the latter condition, the considered model system is an HEG that is perturbed by an external potential which induces Bragg diffraction of the Fermi electrons. The enhancement factor of the functional is given by

$$F_x^{\text{Cha}} = \frac{3a^2 x_\sigma^2 + \pi^2 \ln(ax_\sigma + 1)}{(3ax_\sigma + \pi^2) \ln(ax_\sigma + 1)} \quad (456)$$

where $a = (2/9)(\pi/6)^{1/3}$ as determined from the second condition mentioned above. When combined with [gga_c_chachiyo](#) for correlation, the functional appears to be quite accurate for

total and binding energies of molecules.

[gga_x_t_pbe1](#), [gga_x_t_pbe2](#)³⁸² (2020)

The PBE functional ([gga_x_pbe](#) + [gga_c_pbe](#)) is known to severely underestimate the band gap of solids. Two reparametrizations of the exchange component were made by Borlido et al.³⁸² by fitting to the experimental band gap of a set of 85 solids, leading to new values for μ and κ in eq. (378). The obtained values are $(\mu, \kappa) = (2/3, 3 + 1/6) \approx (0.666667, 3.166667)$ for [gga_x_t_pbe1](#) and $(\mu, \kappa) = (1/3, 12 + 5/6) \approx (0.333333, 12.833333)$ for [gga_x_t_pbe2](#). The mean absolute error obtained for the whole set of 473 solids considered in ref. 382 is 0.59 eV for both reparametrizations, which is lower than the 1.1 eV obtained with the original PBE functional.³⁸¹

[gga_x_lppbe](#), [gga_x_lplsrpbe](#), [gga_x_lpcap](#), [gga_x_lpnncap](#)⁵⁶² (2020)

Albavera-Mata et al.⁵⁶² constructed 20 exchange functionals in total, all based on the relationship $\mu = \pi^2 \beta/3$ between the second-order coefficients μ and β in the density-gradient expansions of exchange and correlation, respectively. First, they considered four different forms for the exchange enhancement factor F_x :

- [gga_x_lppbe](#): Equation (378) of [gga_x_pbe](#).
- [gga_x_lplsrpbe](#): Equation (444) of [gga_x_lsrpbe](#) with $e^{-\alpha s_\sigma^2}$ replaced by $e^{-\alpha \mu s_\sigma^2/\kappa}$, where $\alpha = 0.023534$ while $\kappa = \kappa^{\text{PBE}}$ is unchanged.
- [gga_x_lpcap](#): Equation (438) of [gga_x_cap](#).
- [gga_x_lpnncap](#): Equation (455) of [gga_x_nncap](#).

Then, in each of these four functionals, μ is calculated with $\mu = \pi^2 \beta/3$, where five different choices for β were considered:

- β^{MB} , which is the high-density limit.¹⁵¹
- $\beta(r_s) = 16(3/\pi)^{1/3} C_c(r_s)$, where $C_c(r_s)$ is given by eq. (460).⁵⁶³

- $\beta(r_s)$ given by eq. (502) that was derived at the beyond-RPA level.¹⁵¹
- $\beta(r_s)$ given by eq. (525) with two different sets for the coefficients:⁵⁶⁴ the one used in `gga_c_acggap`, and $a = 3.0$, $b = 1.046$, $c = 0.100$, and $d = 0.1778$.

Albavera-Mata et al.⁵⁶² noted that the use of a r_s -dependent function for μ leads to a functional that does not satisfy the uniform density scaling, as required for exchange. Therefore, they argued that such functionals are not pure exchange, but also include a correlation component.

These 20 functionals were combined with `gga_c_p86` or `gga_c_pbe` and their performance was evaluated for various molecular and solid-state properties. Among them, there is for instance `gga_x_lpcap`, with β calculated from eq. (525) with the second set of coefficients, and combined with `gga_c_pbe`, that has a good accuracy for both molecular and solid-state systems.

`gga_x_ncapr`⁵⁶⁵ (2022)

Noting that `gga_x_ncapr` tends to overestimate the ionization potential and electron affinity of molecules, a revised version (`gga_x_ncapr`) that mitigates this problem was proposed. `gga_x_ncapr` has the same mathematical form as eq. (455), but with modified values for most parameters. The parameter δ , which influences the behavior at $s_\sigma \rightarrow \infty$ (i.e., in the asymptotic region of finite systems), is changed to $\delta = 0.5$. Consequently, β , that is determined so that the exchange and Hartree energies cancel for the hydrogen atom, is now $\beta \approx 0.017983$,⁵⁵⁹ while α is also modified through the relation $\alpha = 4\pi\beta/(3\mu)$ with $\mu = \mu^{\text{PBE}}$ unchanged.

It has to be noted that the ionization potentials, electron affinities, and band gaps calculated with `gga_x_ncapr` + `gga_c_p86` for correlation were obtained from orbital energies that were shifted by quantities related to the xc derivative discontinuity.

`gga_x_ktbm_a`, `gga_x_ktbm_b`⁵⁶⁶ (2022)

In addition to the set of 25 trained `mgga_x_ktbm` functionals that they proposed, Kovács et al.⁵⁶⁶ also applied the same train-

ing procedure at the simpler GGA level. The enhancement factor is given by eq. (679) with $N = 3$ for the summations over i , while restricting the second summation to $j = 0$ in order to eliminate the dependence on the kinetic-energy density. The functional `gga_c_pbe` is used for correlation. As explained in more detail for `mgga_x_ktbm`, 25 parametrizations of eq. (679), resulting from different choices for the weights of the properties in the training set, were obtained, leading to the `gga_x_ktbm_a` functionals. In addition, another set of 25 functionals (`gga_x_ktbm_b`) was obtained by releasing the `lda_x` limit of the HEG during the training, leading to a total of 50 functionals.

As expected, these GGA functionals are overall less accurate than their τ -MGGA counterparts `mgga_x_ktbm`.

`gga_x_bkl1`, `gga_x_bkl2`⁵⁶⁷ (2024)

These functionals were presented as improvements over PBE (`gga_x_pbe` + `gga_c_pbe`) for the band gap of solids. The mathematical form is given by

$$F_x^{\text{BKL}} = 1 + \gamma\kappa \left(e^{-\alpha\mu s_\sigma^2/\kappa} - e^{-\beta\mu s_\sigma^2/\kappa} \right) \quad (457)$$

where the values of μ and κ are the same as in `gga_x_pbe`, while α , β , and γ are new parameters. Two sets of parameters were proposed: $(\alpha, \beta, \gamma) = (0.01, 2.5, 0.98)$ and $(0.01, 0.5, 0.96)$, which correspond to `gga_x_bkl1` and `gga_x_bkl2`, respectively. These choices for the parameters, β in particular, were made in conjunction with the choice for a parameter in the correlation counterparts `gga_c_bkl1` and `gga_c_bkl2`, such that the second-order terms in the density gradient expansions of exchange and correlation cancel each other. These two functionals, BKL1 (`gga_x_bkl1` + `gga_c_bkl1`) and BKL2 (`gga_x_bkl2` + `gga_c_bkl2`), lead to band gaps that are larger than the PBE values, however, quite erratically. The functionals also appear unreliable for geometries.

3.2.2 Correlation

[gga_c_lm](#)^{6,568–570} (1985)

This is perhaps the first modern GGA correlation functional. It is based on a simple approximation to the leading term in the gradient expansion of the correlation energy. It was originally developed for spin-compensated systems,^{6,568,569} but was later generalized to the spin-polarized case:⁵⁷⁰

$$e_c^{\text{LM}} = e_c^{\text{vBH}}(r_s, \zeta) + \frac{J}{\alpha^2 r_s} \times \left[2 \frac{x^2}{\sqrt{\phi_{5/3}(\zeta)}} e^{-F} - \frac{7}{9} x_{\text{tot},4/3}^2 \right] \quad (458)$$

where e_c^{vBH} is the LDA component represented by [lda_c_vbh](#), $x_{\text{tot},4/3}^2$ is given by eq. (44), $J = \pi / \left[16 (3\pi^2)^{4/3} \right]$, $\alpha = (4\pi/3)^{1/6}$, and

$$F = \frac{\sqrt{3}f}{\left(\frac{3}{\pi}\right)^{1/6}} \frac{x}{\alpha\sqrt{r_s}} \quad (459)$$

where f was proposed to be 0.15 (the value used in Libxc) or 0.17. Note that this functional should not be considered a pure correlation functional, as discussed for [gga_c_p86](#) below.

[gga_c_p86](#), [gga_c_p86_ft](#)^{571,572} (1986)

For this functional, Perdew⁵⁷¹ tried to go beyond the [gga_c_lm](#) functional by proposing two modifications: (i) removing the last term in eq. (458), which is actually a piece of the density-gradient expansion for the exchange energy, and (ii) going beyond the RPA for the correlation energy of the HEG and inhomogeneity effects on which the functional is based. These effects are included through the coefficient of the density-gradient expansion of the correlation energy, calculated beyond the RPA,^{573,574} as parameterized by Rasolt and Geldart⁵⁶³:

$$C_c(r_s) = a^{\text{RG}} + \frac{b^{\text{RG}} + \alpha^{\text{RG}} r_s + \beta^{\text{RG}} r_s^2}{1 + \gamma^{\text{RG}} r_s + \delta^{\text{RG}} r_s^2 + 10^4 \beta^{\text{RG}} r_s^3} \quad (460)$$

where $a^{\text{RG}} = 0.001667$, $b^{\text{RG}} = 0.002568$, $\alpha^{\text{RG}} = 0.023266$, $\beta^{\text{RG}} = 7.389 \times 10^{-6}$, $\gamma^{\text{RG}} = 8.723$, and $\delta^{\text{RG}} = 0.472$. The actual form of the functional

is

$$e_c^{\text{P86}} = e_c^{\text{PZ}}(r_s, \zeta) + \frac{C_c(r_s)}{\alpha^2 r_s} \frac{x^2}{\sqrt{\phi_{5/3}(\zeta)}} e^{-F} \quad (461)$$

where e_c^{PZ} is [lda_c_pz](#), $\alpha = (4\pi/3)^{1/6}$, and

$$F = \tilde{f} \frac{C_c(0)}{C_c(r_s)} \frac{x}{\alpha\sqrt{r_s}} \quad (462)$$

with $C_c(0) = a^{\text{RG}} + b^{\text{RG}}$ and $\tilde{f} = (9\pi)^{1/6} f$, where the cutoff parameter $f = 0.11$ was chosen such that the exact correlation energy of the Ne atom is reproduced. Note that [gga_c_p86](#) has been frequently combined with [gga_x_b88](#) for exchange, leading to the BP86 functional.

Note that there are two implementations of this functional in Libxc: [gga_c_p86](#) where $(9\pi)^{1/6}$ in \tilde{f} is approximated as 1.745 (as in ref. 571), and [gga_c_p86_ft](#) where $(9\pi)^{1/6}$ is accurate to machine precision.¹²⁸

[gga_c_lyp](#)^{575,576} (1989)

This is probably the most famous GGA correlation functional in the quantum chemistry community. It was derived from the $(\nabla^2 n, \tau)$ -MGGA functional [mgga_c_cs](#) of Colle and Salvetti⁴¹⁷ by using a second-order density-gradient expansion for the kinetic-energy density τ .⁵⁷⁵ The resulting functional has a dependence on $\nabla^2 n$ that is then eliminated by a suitable partial integration.⁵⁷⁶ The functional form

reads

$$e_c^{\text{LYP}} = a \left\{ \begin{aligned} & -\frac{1 - \zeta^2}{1 + \bar{d}r_s} \\ & -\omega x^2 \left[\frac{1}{72} (1 - \zeta^2) (47 - 7\delta) - \frac{2}{3} \right] \\ & -\omega 2^{-2/3} C_F (1 - \zeta^2) \phi_{8/3}(\zeta) \\ & + \frac{\omega}{8} (1 - \zeta^2) \left(\frac{5}{2} - \frac{\delta}{18} \right) x_{\text{tot},8/3}^2(\zeta) \\ & + \frac{\omega}{144} (1 - \zeta^2) (\delta - 11) x_{\text{tot},11/3}^2(\zeta) \\ & - \frac{\omega}{2^{8/3}} \left[\frac{2^{8/3}}{3} x_{\text{tot},8/3}^2(\zeta) \right. \\ & - \frac{1}{4} x_{\downarrow}^2 (1 + \zeta)^2 (1 - \zeta)^{8/3} \\ & \left. - \frac{1}{4} x_{\uparrow}^2 (1 - \zeta)^2 (1 + \zeta)^{8/3} \right] \end{aligned} \right\} \quad (463)$$

where $x_{\text{tot},p}$ is given by eq. (44) and

$$\omega = \frac{be^{-\bar{c}r_s}}{1 + \bar{d}r_s} \quad (464a)$$

$$\delta = \bar{c}r_s + \frac{\bar{d}r_s}{1 + \bar{d}r_s} \quad (464b)$$

The parameters are the same as in the `mgga_c_cs` functional, namely $a = 0.04918$, $b = 0.132$, $\bar{c} = 0.2533(4\pi/3)^{1/3}$, $\bar{d} = 0.349(4\pi/3)^{1/3}$, and C_F is eq. (22).

BLYP (`gga_x_b88` + `gga_c_lyp`) and the hybrid B3LYP³⁹⁷ functionals have been among the most popular GGA functionals for calculations of finite systems.

`gga_c_wl`⁵⁷⁷ (1990)

This functional from Wilson and Levy⁵⁷⁷ can be seen as a GGA extension of the `lda_c_wigner` functional, where the extra freedom given by the inclusion of the density gradient ∇n_{σ} is used such that some coordinate scaling requirements are satisfied. It has the following analytical form:

$$e_c^{\text{WL}} = \sqrt{1 - \zeta^2} \frac{a + bx}{c + d(x_{\uparrow} + x_{\downarrow}) + r_s} \quad (465)$$

The values of the constants, which were obtained by fitting accurate reference correlation energies of eight atomic systems (He, Li⁺,

Be²⁺, Be, B⁺, Ne, Mg, and Ar) are $a = -0.74860$, $b = 0.06001$, $c = 3.60073$, and $d = 0.90000$. `gga_c_wl` is an extremely simple functional that leads to accurate atomic correlation energies. Furthermore, this functional provides accurate ionization potentials and atomization energies when combined with HF exchange, while other correlation functionals, such as `gga_c_lyp` or `gga_c_pw91`, are usually not compatible with HF exchange.⁵⁷⁸ However, the price to pay is that the combination of `gga_c_wl` with common GGA exchange functionals may yield quite inaccurate results, due to the lack of error cancellation between exchange and correlation that is common at the GGA and MGGA levels.

`gga_c_pw91`^{458–460,579} (1991)

Alike several of its predecessors, e.g. `gga_c_lm` or `gga_c_p86`, the correlation component of the famous PW91 (`gga_x_pw91` + `gga_c_pw91`) functional has no empirical parameters. For small density gradients, it reduces to the second-order density-gradient expansion with coefficients from Rasolt and Geldart⁵⁶³ (see eq. (460)). The functional form reads

$$e_c^{\text{PW91}} = e_c^{\text{PW-LDA}}(r_s, \zeta) + H_0(\phi_{2/3}, t, A) + H_1(r_s, \phi_{2/3}, t) \quad (466)$$

As we can see, there are two correcting terms to the `lda_c_pw` term. The first one is

$$H_0(\phi_{2/3}, t, A) = \gamma \phi_{2/3}^3 \ln \left[1 + \frac{\beta}{\gamma} \frac{t^2 + At^4}{1 + A(t^2 + At^4)} \right] \quad (467)$$

where A is defined as

$$A(r_s, \zeta, \phi_{2/3}) = \frac{\beta}{\gamma w_1} \quad (468)$$

with

$$w_1 = e^{-e_c^{\text{PW-LDA}}(r_s, \zeta)/(\gamma \phi_{2/3}^3)} - 1 \quad (469)$$

The parameters entering into eqs. (467) and (468) are $\beta = \beta^{\text{MB}}$ and $\gamma = \beta^2/(2\alpha)$, with $\alpha = 0.09$, $\nu = (16/\pi)(3\pi^2)^{1/3}$, and $C_c(0) = a^{\text{RG}} + b^{\text{RG}}$, which is the value of the Rasolt and Geldart⁵⁶³ second-order density-gradient expansion at $r_s = 0$ (see eq. (460)).

The second term, H_1 , reads

$$H_1(r_s, \phi_{2/3}, t) = \nu \left[C_c(r_s) - C_c(0) - \frac{3}{7}c_x \right] \times \phi_{2/3}^3 t^2 e^{-a_1 r_s \phi_{2/3}^4 t^2} \quad (470)$$

where $C_c(r_s)$ is eq. (460), $a_1 = 400 [4 / (9\pi)]^{1/3} / \pi$, and $c_x = -a^{\text{RG}}$ is the coefficient of the density-gradient correction for exchange (see eq. (460)).

[gga_c_f94](#)⁵⁸⁰ (1994)

This functional was derived starting from a Gaussian approximation for the correlation-factor model in the second-order density matrix (see e.g. discussion for [lda_xc_lp_a](#)). By using known mathematical conditions and by fitting to accurate correlation energies for the closed-shell atoms He, Be, Ne, and Mg, Fuentealba⁵⁸⁰ arrived at a Wigner-type expression for the correlation-energy density:

$$e_c^{\text{F94}} = -\frac{\pi}{2\sqrt{k}} (1 - \zeta^2) \frac{c_1 + c_2 x^2}{c_3 + c_4 x^2 + c_5 r_s} \quad (471)$$

where $c_1 = 0.2146a_0$, $c_2 = 0.1781a_2/k$, $c_3 = 0.8862a_0k$, $c_4 = 1.3293a_2$, and $c_5 = (4\pi/3)^{1/3} a_0 \sqrt{k}$, with $a_0 = 5.00703$, $a_2 = 0.01193$, and $k = 0.40283$.

Tests showed that the [gga_c_f94](#) functional is less accurate than [gga_c_w1](#) and [gga_c_lyp](#) for correlation energies of light neutral and cationic atoms.

[gga_c_w94](#)⁵⁸¹ (1994)

Coordinate-scaling relations are often used in functional development, and Wilson⁵⁸¹ wondered if their obedience is actually useful for accuracy. To answer this question, he tested various existing and newly proposed functionals that obey coordinate-scaling relations to various degrees. Several new functional forms were constructed using [lda_c_wigner](#) as starting point. It turned out that no functional of the considered forms could obey all constraints. The form that fulfills all conditions except one due to Levy and Perdew^{173,174} (that was only approximately obeyed) is

$$e_c^{\text{W94}} = \frac{a\sqrt{1 - \zeta^{5/3}}}{b + cx^{51/16} + dx^2 r_s + r_s} \quad (472)$$

where the coefficients $a = -1$, $b = 11.8$, $c = 0.150670$, and $d = 0.01102 (4\pi/3)^{1/3}$ were obtained by otherwise the same parametrization procedure as for [gga_c_w1](#), with the exception that the parametrization was constrained such that the correlation energy is always negative. We note that $\zeta^{5/3}$ in eq. (472) gives a complex value when $\zeta < 0$, which can be overcome by taking the absolute value of ζ , at the price of making it non-differentiable at $\zeta = 0$.

The results suggest that adhering to the constraints is beneficial for accuracy.

[gga_c_pbe](#), [gga_c_pbe_gaussian](#)^{148,149} (1996)

The correlation component of the famous PBE ([gga_x_pbe](#) + [gga_c_pbe](#)) functional was designed to obey three exact mathematical conditions. (i) Recovery of the exact second-order density-gradient expansion in the slowly varying density limit ($t \rightarrow 0$). (ii) Vanishing correlation energy in the rapidly varying density limit ($t \rightarrow \infty$). (iii) Correct scaling (as a constant) under a uniform scaling in the high-density limit ($r_s \rightarrow 0$). Based on these conditions, the following ansatz for the correlation energy was proposed:

$$e_c^{\text{PBE}} = e_c^{\text{PW-LDA}}(r_s, \zeta) + H_0(\phi_{2/3}, t, A) \quad (473)$$

where $e_c^{\text{PW-LDA}}$ is [lda_c_pw](#) and H_0 is eq. (467), wherein $\beta = \beta^{\text{MB}}$, which is the high-density limit of the coefficient of the density-gradient expansion, condition (i), and $\gamma = [1 - \ln(2)]/\pi^2$, leading to the canceling of the logarithmic divergence of [lda_c_pw](#), as implied by condition (iii). Besides the use of a different value for γ , the main difference compared to eq. (466) of the [gga_c_pw91](#) functional concerns the term H_1 that is not present in eq. (473), leading to a simpler correlation functional.

Note that two implementations of PBE correlation are available in Libxc. They differ in the value of β^{PBE} :

- [gga_c_pbe](#): $\beta^{\text{MB}} = 0.06672455060314922$, which is related to $\mu^{\text{PBE}} = 0.2195149727645171$ (used in [gga_x_pbe](#)) via $\mu^{\text{PBE}} = \beta^{\text{MB}} \pi^2 / 3$.
- [gga_c_pbe_gaussian](#): $\beta^{\text{MB}} = 15.75592 \times 0.004235 = 0.0667263212$. Along with

κ^{PBE} and μ^{PBE} used in `gga_x_pbe_gaussian`, these are the values used in the GAUSSIAN program.^{9,128}

`gga_c_ft97`^{474,582} (1997)

This correlation energy functional, which has often been combined with `gga_x_ft97_a` or `gga_x_ft97_b`, is based on a short-range approximation for the Coulomb hole function which describes electron pairs with same spins and with opposite spins separately. This generalizes earlier works by Gritsenko et al.^{583,584} to inhomogeneous systems by assuming a model dependence of the effective correlation radius on the density gradient.

The functional has a rather complicated mathematical form and, as mentioned above, it consists of separate parallel (\parallel) and perpendicular (\perp) spin components that have different expressions. The functional reads

$$e_c^{\text{FT97}} = \frac{1 + \zeta}{2} [e_c^\perp(r_{s\downarrow}, \nabla r_{s\downarrow}) + e_c^\parallel(r_{s\uparrow}, \nabla r_{s\uparrow})] + \frac{1 - \zeta}{2} [e_c^\perp(r_{s\uparrow}, \nabla r_{s\uparrow}) + e_c^\parallel(r_{s\downarrow}, \nabla r_{s\downarrow})] \quad (474)$$

where $r_{s\sigma}$ is given by eq. (36) (note that $\nabla r_{s\sigma} = -(36\pi)^{-1/3} (\nabla n_\sigma) / n_\sigma^{4/3}$) and e_c^\perp and e_c^\parallel are defined below.

The opposite-spin term is given by

$$e_c^\perp(r_{s\sigma}, \nabla r_{s\sigma}) = \frac{C_0(0)}{2} \left\{ e^{\mu^\perp} \text{Ei}(-\mu^\perp) + (a^\perp)^2 \left[\mu^\perp e^{\mu^\perp} \text{Ei}(-\mu^\perp) + 1 \right] \right\} \quad (475)$$

where $C_0(0) = [1 - \ln(2)] / \pi^2$, $\text{Ei}(x)$ denotes the exponential integral, and the $(r_{s\sigma}, \nabla r_{s\sigma})$ -dependent functions a^\perp and μ^\perp are defined as follows.

First, a^\perp is given by

$$a^\perp(r_{s\sigma}, \nabla r_{s\sigma}) = (k^\perp r_{s\sigma})^{-2} \frac{6 + 4\sqrt{\mu^\perp} + 4\mu^\perp}{3 + 6\sqrt{\mu^\perp} + 6\mu^\perp} \quad (476)$$

where $k^\perp r_{s\sigma}$ (k^\perp will be defined below) is an effective correlation length, which is assumed to be directly related to the corresponding Wigner–Seitz radius $r_{s\sigma}$. The main advantage

of this choice is that the final form of the functional is able to reproduce the leading terms of the exact high-density and low-density expansions for the HEG.

Second, μ^\perp is defined as

$$\mu^\perp(r_{s\sigma}, \nabla r_{s\sigma}) = \frac{2C_0(0)}{3} \frac{r_{s\sigma}}{(k^\perp)^2} \quad (477)$$

The function k^\perp that relates the effective correlation length to $r_{s\sigma}$ reads

$$k^\perp(r_{s\sigma}, \nabla r_{s\sigma}) = \left\{ k_0^\perp - k_1^\perp \left[1 - e^{-r_1^\perp (r_{s\sigma})^{4/5}} \right] \right\} F^\perp \quad (478)$$

where $k_0^\perp = 1.291551074$, $k_1^\perp = 0.349064173$, $r_1^\perp = 0.083275880$, and the inhomogeneity factor F^\perp reads

$$F^\perp(r_{s\sigma}, \nabla r_{s\sigma}) = \frac{1 + a_1 |\nabla r_{s\sigma}|^2 + a_2^2 |\nabla r_{s\sigma}|^4}{\sqrt{1 + a_3 \frac{|\nabla r_{s\sigma}|^2}{r_{s\sigma}}}} \times e^{-a_2^2 |\nabla r_{s\sigma}|^4} \quad (479)$$

with $a_1 = 1.622118767$, $a_2 = 0.489958076$, and $a_3 = 1.379021941$.

The parallel-spin term is given by

$$e_c^\parallel(r_{s\sigma}, \nabla r_{s\sigma}) = e^{-(r_{s\sigma})^2 / (e_1 \sqrt{r_{s\sigma}} + e_2 r_{s\sigma})^2} \times \tilde{e}_c^\perp(r_{s\sigma}, \nabla r_{s\sigma}) \quad (480)$$

where $e_1 = 0.939016$, $e_2 = 1.733170$, and \tilde{e}_c^\perp has the same form as eq. (475), but with k^\perp replaced by

$$k^\parallel(r_{s\sigma}, \nabla r_{s\sigma}) = \left\{ k_0^\parallel + k_1^\parallel \left[1 - e^{-r_1^\parallel (r_{s\sigma})^{1/2}} \right] - k_2^\parallel \left[1 - e^{-r_2^\parallel (r_{s\sigma})^{2/5}} \right] \right\} F^\parallel \quad (481)$$

where $k_0^\parallel = 1.200801774$, $k_1^\parallel = 0.859614445$, $k_2^\parallel = 0.812904345$, $r_1^\parallel = 1.089338848$, $r_2^\parallel = 0.655638823$, and the inhomogeneity factor F^\parallel is given by

$$F^\parallel(r_{s\sigma}, \nabla r_{s\sigma}) = \frac{1 + a_4^2 |\nabla r_{s\sigma}|^4}{\sqrt{1 + a_5 \frac{|\nabla r_{s\sigma}|^2}{r_{s\sigma}}}} e^{-a_4^2 |\nabla r_{s\sigma}|^4} \quad (482)$$

where $a_4 = 4.946281353$ and $a_5 = 3.600612059$,

which was chosen to reproduce the correct density-gradient expansion for the correlation energy of an electron gas with a high and slowly varying density, as well as several coordinate-scaling constraints.

Note that e_1 , e_2 , k_0^\perp , k_1^\perp , r_1^\perp , k_0^\parallel , k_1^\parallel , k_2^\parallel , r_1^\parallel , and r_2^\parallel were determined by a fitting against exact results for the HEG. In contrast, a_1 , a_2 , a_3 , and a_4 are empirical parameters obtained through fitting calculated correlation energies to experimental values for a set of atoms. Finally, a_5 was fixed by an exact constraint.

[gga_c_hcth_a](#)⁴⁷⁸ (1998)

This is the correlation functional that was fit together with [gga_x_hcth_a](#). Its mathematical form is given by eqs. (253) and (254) alike the correlation component of the B97 hybrid functional³⁷⁰ (see section 2.18.4). In contrast to B97, the [lda_c_vwn](#) functional was used to represent the energy density $e_{c\sigma\sigma}^{\text{ref}}$, in eq. (250), and $m = 3$ was chosen for the sum in eq. (254).

[gga_c_wi0](#), [gga_c_wi](#)³⁸⁴ (1998)

This is another functional based on the [lda_c_wigner](#) form, similar in spirit to the [gga_c_wl](#) functional. Although this form is much less complicated than most other GGA approximations for the correlation energy, it is flexible enough such that most of the mathematical constraints, 24(!), can be satisfied. Only the spin-unpolarized case was considered, and the expression is given by

$$e_c^{\text{WI}} = \frac{a + bx^2 e^{-kx^2}}{c + r_s(1 + \bar{d}x^{7/2})} \quad (483)$$

In the first version of this functional, [gga_c_wi0](#), the values $a = -0.44$ and $c = 7.8$ were chosen such that this functional correctly reduces to the [lda_c_wigner](#) form in the low-density limit for the HEG. The other parameters (together with the exponent 7/2) were obtained by fitting to exact values of model two-electron densities and of the He atom.⁵⁸⁵ The values are $b = 0.0032407$, $k = 0.000311$, and $\bar{d} = 0.0073(4\pi/3)^{1/3}$. The second version, [gga_c_wi](#), sacrificed some theoretical elegance for a better numerical accuracy, and included reference values for He, Li⁺, Ne, and Ar in the

fit of the coefficients, leading to $a = -0.0652$, $b = 0.0007$, $c = 0.21$, $\bar{d} = 0.001(4\pi/3)^{1/3}$, and $k = 0.001$.

[gga_c_op_b88](#), [gga_c_op_xalpha](#), [gga_c_op_pw91](#), [gga_c_op_g96](#), [gga_c_op_pbe](#)^{586,587} (1999)

Tsuneda et al.⁵⁸⁶ proposed a one-parameter progressive (OP) correlation functional through re-examination of the Colle–Salvetti functional [mgga_c_cs](#). In particular, they noticed that in the final [mgga_c_cs](#) fit, the sign of the term containing the function W is not the same as in the expression derived from the many-body ansatz for the wavefunction. A further analysis led to the conclusion that this term has no clear physical meaning, and that it should not be incorporated in the correlation functional, unless the corresponding exchange functional (see below) depends on the second derivative of the density.

From these considerations the following form for the correlation functional was proposed:

$$e_c^{\text{OP}} = -\frac{4n_\uparrow n_\downarrow}{n} \frac{a_1 \beta_{\uparrow\downarrow} + a_2}{\beta_{\uparrow\downarrow}^4 + b_1 \beta_{\uparrow\downarrow}^3 + b_2 \beta_{\uparrow\downarrow}^2} \quad (484)$$

This form is directly related to the one derived by Colle and Salvetti⁴¹⁷ (see eqs. (15) and (16) of ref. 417), if the terms containing W are neglected and the substitutions $q = \beta_{\uparrow\downarrow}/n^{1/3}$ and $n^2 \rightarrow 4n_\uparrow n_\downarrow$ are made. The coefficients $a_1 = 1.5214/4$, $a_2 = 0.5764/4$, $b_1 = 1.1284$, and $b_2 = 0.3183$ were derived by Colle and Salvetti⁴¹⁷. The correlation length defined by Becke¹⁹⁶ was used to propose the following expression for $\beta_{\uparrow\downarrow}$:

$$\beta_{\uparrow\downarrow} = 2C_x q_{\uparrow\downarrow}^{\text{OP}} \frac{n_\uparrow^{1/3} n_\downarrow^{1/3} F_x(x_\uparrow) F_x(x_\downarrow)}{n_\uparrow^{1/3} F_x(x_\uparrow) + n_\downarrow^{1/3} F_x(x_\downarrow)} \quad (485)$$

where C_x is given by eq. (17) and F_x can be any GGA exchange enhancement factor. The OP functional contains only the parameter $q_{\uparrow\downarrow}^{\text{OP}}$, which is a measure of the size of the correlation hole. Its value was obtained by fitting to the exact correlation energy of the C atom, leading to $q_{\uparrow\downarrow}^{\text{OP-B88}} = 2.3670$ when F_x is chosen as the enhancement factor of the [gga_x_b88](#) functional.

As claimed and underlined in refs. 586 and 587, the OP functional was constructed such that it obeys all conditions of the exact correlation functional, provided that the chosen F_x corresponds to an exchange functional that obeys all conditions of the exact exchange functional.

In ref. 587, other exchange enhancement factors were considered, and $q_{\uparrow\downarrow}^{\text{OP}}$ was determined by fitting to the exact correlation energy of the Ar atom. The values are $q_{\uparrow\downarrow}^{\text{OP-X}\alpha} = 2.5654$ for `lda_x`, $q_{\uparrow\downarrow}^{\text{OP-PW91}} = 2.3706$ for `gga_x_pw91`, $q_{\uparrow\downarrow}^{\text{OP-G96}} = 2.3638$ for `gga_x_g96`, and $q_{\uparrow\downarrow}^{\text{OP-PBE}} = 2.3789$ for `gga_x_pbe`.

`gga_c_pbe_rpa`^{588,589} (2000)

This functional was constructed by Yan et al. 588 aiming at providing a correction to the RPA correlation energy at short range. First, they calculated a numerical correction to `lda_c_pw_rpa` at the RPA level. Then, a GGA analytical expression was used to fit these numerical values, or more precisely, the difference between `gga_c_pbe` and these RPA numerical values. The chosen expression for the fit is similar to the expression of the `gga_c_pbe` functional:

$$e_c^{\text{PBE-RPA}} = e_c^{\text{PW-RPA}}(r_s, \zeta) + H^{\text{PBE-RPA}}(\phi_{2/3}, t, A_{\text{RPA}}) \quad (486)$$

where $e_c^{\text{PW-RPA}}$ is `lda_c_pw_rpa` and

$$H^{\text{PBE-RPA}}(\phi_{2/3}, t, A_{\text{RPA}}) = \gamma \phi_{2/3}^3 \times \ln \left[1 + \frac{\beta}{\gamma} t^2 \frac{1 + \xi_1 A_{\text{RPA}} t^2 + A_{\text{RPA}}^2 t^4}{1 + \xi_1 A_{\text{RPA}} t^2 + \xi_2 A_{\text{RPA}}^2 t^4 + A_{\text{RPA}}^3 t^6} \right] \quad (487)$$

where $\xi_1 = 3.8 + 2.0(s - 2.17)\zeta^4$ with s given by eq. (46), $\xi_2 = 6.2 + 9.0\zeta^4$, and

$$A_{\text{RPA}}(r_s, \zeta, \phi_{2/3}) = \frac{\beta}{\gamma} \frac{1}{e^{-e_c^{\text{PW-RPA}}(r_s, \zeta)/(\gamma \phi_{2/3}^3)} - 1} \quad (488)$$

Although not specified in ref. 588, the values of β and γ should be the same as for `gga_c_pbe`.

The difference between `gga_c_pbe` and `gga_c_pbe_rpa` is used as a short-range correction to the RPA energy, leading to the RPA+

correlation energy:

$$e_c^{\text{RPA+}} = e_c^{\text{RPA}} + (e_c^{\text{PBE}} - e_c^{\text{PBE-RPA}}) \quad (489)$$

`gga_c_pbe_rpa` is also used in the ARPA+ functional (see eq. (408)).

`gga_c_optc`⁵⁹⁰ (2001)

The starting point for the development of this functional were Møller–Plesset calculations for atoms at the second-order (MP2) level, leading to correlation energies decomposed into parallel and perpendicular contributions. As the MP2 total correlation energy represents only about 80% of the exact total correlation energy, the MP2 contributions were scaled with the same coefficient. The next step was to construct a functional based on the Stoll decomposition (see section 2.18.3), for which the `gga_c_pw91` functional was chosen:

$$e_c^{\text{OPTC}} = c_1 e_c^{\text{PW91}}[n_{\uparrow}, n_{\downarrow}] + c_2 \sum_{\sigma} e_{c\sigma\sigma}^{\text{PW91}}[n_{\sigma}] \quad (490)$$

where the coefficients $c_1 = 1.1015$ and $c_2 = 0.6625$ were obtained by separately fitting to the perpendicular and parallel contributions to the scaled MP2 correlation energy, respectively. From these values for c_1 and c_2 , it is quite clear that `gga_c_pw91` underestimates (overestimates) the magnitude of the perpendicular (parallel) components. Note also that since c_1 and c_2 are not equal to one, eq. (490) does not reduce to the correlation energy of the HEG (`lda_c_pw`) for vanishing density gradients. Even if binding energies of small molecules calculated with `gga_x_optx` plus `gga_c_optc` are quite accurate in many cases, large errors were also obtained. Unfortunately, neither refitting `gga_x_optx` nor refining `gga_c_optc` was sufficient to resolve the problem.

`gga_c_cs1`⁵⁹¹ (2002)

In this functional, correlation is split into opposite-spin and parallel-spin contributions according to the Stoll decomposition (see section 2.18.3). For the opposite-spin component, Handy and Cohen⁵⁹¹ chose the Colle–Salvetti expression (see `mgga_c_cs`), however they considered only the first term of `gga_c_lyp`, while the rest was regarded as unimportant. They

wrote therefore the opposite-spin contribution as a simplification of `gga_c_lyp`, including a truncation factor obtained from the correlation hole size. The expression reads

$$e_{c\uparrow\downarrow}^{\text{CS1}} = \frac{1}{n^2} \frac{n_\uparrow n_\downarrow}{1 + dn^{-1/3}} \left[C_3 + C_4 \frac{\gamma^2 x^4}{(1 + \gamma x^2)^2} \right] \quad (491)$$

where $\gamma = 0.006$ as in `gga_x_optx`, $d = 0.349$ comes from `mgga_c_cs`, and $C_3 = -0.159068$ and $C_4 = 0.007953$ were fit to exact opposite-spin correlation energies for 18 first and second row atoms.

Next, Handy and Cohen⁵⁹¹ tested several forms for the parallel contribution to the correlation energy, while maintaining the similarity to eq. (491). This part of the functional reads

$$e_{c\sigma\sigma}^{\text{CS1}} = \frac{1}{n} \frac{n_\sigma}{1 + dn_\sigma^{-1/3}} \left[C_1 + C_2 \frac{\gamma^2 x_\sigma^4}{(1 + \gamma x_\sigma^2)^2} \right] \quad (492)$$

where $C_1 = -0.018897$ and $C_2 = 0.155240$ were also determined by first fitting to the correlation energies of the 18 atoms, and then refining the values using 93 atomic and molecular systems. Note that in eqs. (24) and (25) of the original paper,⁵⁹¹ the γ^2 factor in the numerator of the second term is missing, and that a minus sign multiplying eqs. (24) is also missing. The corrected expressions, reproduced here, correspond to eqs. (8) and (6) in ref. 592.

When combined with the `gga_x_optx` functional, `gga_c_cs1` appears to yield high-quality correlation energies of atoms and atomization energies of small and medium-size molecules. However, it systematically overestimates bond lengths and is not very accurate for hydrogen bonded systems.⁵⁹²

`gga_c_tau_hcth`⁵⁹³ (2002)

This functional has the same form as the B97 correlation functional, given by eq. (250) with `lda_c_pw` for the reference LDA component and eqs. (253) and (254) as described for `gga_c_hcth_a`. The truncation $m = 3$ in eq. (254) was used, and the $2 \times 4 = 8$ parameters were optimized together with the 8 parameters of the exchange counterpart `mgga_x_tau_hcth`.

`gga_c_xpbe`⁴⁹¹ (2004)

The two parameters of `gga_c_pbe` were optimized as described for `gga_x_xpbe`, leading to $\beta = 0.089809$ and $\alpha = 0.197363$ (then $\gamma = \beta^2 / (2\alpha) \approx 0.020434$ ⁴⁷²).

`gga_c_am05`^{493,494} (2005)

This is the correlation counterpart to `gga_x_am05`. In contrast with the MC results for the HEG,^{371–373} no exact reference correlation energy has been calculated for electrons in a linear potential (Airy gas model). To obtain a correlation functional, Armiento and Mattsson⁴⁹³ used `lda_c_pw` multiplied by a function that contains two parameters, which were fit to jellium surface xc energies obtained from an improved RPA scheme.^{588,589} The resulting spin-dependent functional reads⁴⁹⁴

$$e_c^{\text{AM05}} = e_c^{\text{PW-LDA}}(r_s, \zeta) \times \sum_{\sigma} \frac{1 + \text{sgn}(\sigma)\zeta}{2} \{X(s_\sigma) + [1 - X(s_\sigma)]\gamma\} \quad (493)$$

where $X(s_\sigma)$ is the same function as in `gga_x_am05` (eq. (400)), while the value of $\gamma = 0.8098$ was fit at the same time as α in eq. (400) to the jellium surface xc energies mentioned above.

`gga_c_pbe_sol`^{271,272} (2008)

This is a refitting of the `gga_c_pbe` functional to surface xc energies calculated with the TPSS (`mgga_x_tpss` + `mgga_c_tpss`) τ -MGGGA functional. This procedure led to $\beta = 0.046$ in eqs. (467) and (468), which is relatively close to $\beta = 3\mu^{\text{GE}}/\pi^2 \approx 0.037526$ from the linear response requirement (see `gga_c_pbe_jrgx`). In contrast, to satisfy the density-gradient expansion would require the much larger value $\beta = \beta^{\text{MB}}$. The combination of `gga_x_pbe_sol` and `gga_c_pbe_sol` leads to the PBEsol functional that is popular in the solid-state community.

`gga_c_tca`⁴¹⁹ (2008)

This GGA functional is built upon `lda_c_rc04`, and rests on a simple ansatz for the enhancement factor. It has the form

$$e_c^{\text{TCA}} = e_c^{\text{RC04}}(r_s) \phi_{2/3}^3(\zeta) F_c(s) \quad (494)$$

where e_c^{RC04} is given by eq. (299), which is then

multiplied by $\phi_{2/3}^3$ for a generalization to spin-polarized systems. For the enhancement factor $F_c(s)$, Tognetti et al.⁴¹⁹ chose

$$F_c(s) = \frac{1}{1 + \sigma s^\alpha} \quad (495)$$

which reduces to one for the HEG, and which vanishes in the rapidly varying limit ($s \rightarrow \infty$). These two conditions are also used in the construction of the `gga_c_pbe` functional. To determine the numerical values of the parameters σ and α , Tognetti et al.⁴¹⁹ used an approach developed by Zupan et al.^{501,502} who used averages of quantities like r_s , ζ , and s . A similar scheme is used here and applied to the He, Be, and Ar atoms. The resulting values are $\sigma = 1.43$ and $\alpha = 2.30$. When combined with `gga_x_pbe`, this functional appears to outperform considerably the standard PBE (`gga_x_pbe` + `gga_c_pbe`) for atomic and molecular systems.⁴¹⁹

`gga_c_revTCA`⁴²⁰ (2008)

This is an improved version of `gga_c_tca` that attempts to eliminate the self-interaction error while still staying at the GGA level. This is achieved by adding a function D to the `gga_c_tca` expression (see eq. (494)):

$$e_c^{\text{revTCA}} = e_c^{\text{TCA}}(r_s, \zeta, s) [1 - D(r_s, \zeta, s)] \quad (496)$$

The function D is chosen such that the following four constraints are satisfied: (i) e_c^{RC04} is recovered for the HEG, (ii) $e_c^{\text{revTCA}} \leq 0$, (iii) $D(r_s^{\text{H}}, \zeta = 1, s^{\text{H}}) = 1$ for any hydrogenoid atom (i.e., no self-interaction error), where $r_s^{\text{H}}(r) = n e_c^{\text{RC04}} e^{(2/3)Zr}$ (e_c^{RC04} is eq. (299)), $s^{\text{H}}(r) = aZr_s^{\text{H}}(r)$, and $a = [4/(9\pi)]^{1/3}$, and (iv) e_c^{TCA} is recovered for spin-unpolarized systems. These four conditions are fulfilled with the following form:

$$D(r_s, \zeta, s) = \zeta^4 \left\{ 1 - \left[\frac{\sin\left(\frac{\pi s}{ar_s}\right)}{\frac{\pi s}{ar_s}} \right]^2 \right\} \quad (497)$$

Note that, contrary to some self-interaction corrected MGGA functionals, `gga_c_revTCA` is

zero only for hydrogenoid atoms, but not for all other one-electron systems. The `gga_c_revTCA` functional was combined with `gga_x_pbe_tca` for exchange.

`gga_c_rge2`⁵⁰⁹ (2009)

This functional, designed to be combined with `gga_x_rge2`, uses the popular `gga_c_pbe` form. However, in this case, the coefficient β of the density-gradient expansion for correlation eqs. (467) and (468) was set to $\beta = 0.053$ in order to reproduce TPSS (`mgga_x_tpss` + `mgga_c_tpss`) jellium surface xc energies, similarly as done for `gga_c_pbe_sol`.

`gga_c_airy_rpa`⁵¹⁰ (2009)

This is a fit of the RPA correlation energy of the Airy-gas model valid at any spin-polarization ζ . The analytical form is given by

$$e_c^{\text{Airy-RPA}} = e_c^{\text{PW-RPA}}(r_s, \zeta) F_c(s_c) \quad (498)$$

where $e_c^{\text{PW-RPA}}$ is `lda_c_pw_rpa` and the correlation enhancement factor F_c is given by

$$F_c(s_c) = \frac{1 + b_1 s_c^3 + b_2 s_c^4}{1 + b_3 s_c^3 + b_4 s_c^4} \quad (499)$$

where

$$s_c = \phi_{2/3}(\zeta) \frac{|\nabla n|}{2(3\pi^2)^{1/3} n^{7.9/6}} \quad (500)$$

is a reduced-density gradient. The fitting coefficients b_i in eq. (499) are $b_1 = 1.01453936$, $b_2 = 0.3255243$, $b_3 = 0.941597104$, and $b_4 = 0.587664306$. This correlation functional was combined with the corresponding `gga_x_airy` functional for exchange.

`gga_c_spbe`⁵¹³ (2009)

This is the correlation part of the functional developed by Swart et al.⁵¹³ that should be combined with `gga_x_ssb`. It is based on the `gga_c_pbe` functional, but with a function H_0 (defined by eq. (467)) that is slightly modified by removing the quartic terms in t :

$$H_0(\phi_{2/3}, t, A) = \gamma \phi_{2/3}^3 \ln \left(1 + \frac{\beta}{\gamma} \frac{t^2}{1 + At^2} \right) \quad (501)$$

The parameters β and γ were not modified.

`gga_c_pbe_jrgx`⁵⁰⁸ (2009)

This is another variation of the `gga_c_pbe` functional, where β in eqs. (467) and (468) is obtained from $\beta = 3\mu^{\text{GE}}/\pi^2 \approx 0.037526$ ⁴⁷² (relation to recover the LDA linear response¹⁴⁸) using the value of the density-gradient expansion for exchange μ^{GE} in eq. (378).

`gga_c_regtpss`^{594,595} (2009)

This variant of the `gga_c_pbe` functional, also called vPBEc in the literature, was proposed by Perdew et al.⁵⁹⁴ as a building block of their `mgga_c_revtpss` functional. It incorporates the density dependence of the parameter β of Ma and Brueckner¹⁵¹ that was later derived by Hu and Langreth⁵⁷⁴ at the beyond-RPA level. The fit to the Hu and Langreth⁵⁷⁴ result reads

$$\beta(r_s) = \beta_0 \frac{1 + ar_s}{1 + br_s} \quad (502)$$

where $\beta_0 = \beta^{\text{MB}}$, $a = 0.1$, and $b = 0.1778$. Equation (502) replaces the constant $\beta = \beta^{\text{MB}}$ in eqs. (467) and (468) of `gga_c_pbe`, and was chosen such that the second-order density-gradient terms for exchange and correlation cancel in the low-density limit ($r_s \rightarrow \infty$). The use of eq. (502) leads to slightly larger atomization energies and smaller surface energies than with the standard `gga_c_pbe` functional. The functional `gga_c_regtpss` is used as the correlation component in the τ -MGGA functionals MS0, MS1, and MS2,^{596,597} as well as MVS,⁵⁹⁸ whose exchange components are `mgga_x_ms0`, `mgga_x_ms1`, `mgga_x_ms2`, and `mgga_x_mvs`, respectively.

`gga_c_tm_w1`, `gga_c_tm_w1`, `gga_c_tm_w2`, `gga_c_tm_wi`⁵⁹⁹ (2009)

Several correlation functionals originally developed by Wilson and co-workers were reoptimized using reference correlation energies of the He–Ar atoms.⁶⁰⁰

The functional `gga_c_tm_w1` has the same form as `gga_c_w1`, where the newly optimized parameters in eq. (465) are $a = -0.190969$, $b = 0.01527752$, $c = 0.2809$, and $d = 0.222$.

The analytical form of `gga_c_tm_w1` is similar to eq. (472) of `gga_c_w94` with $x^{51/16}$ in the denominator replaced by x^6 . The optimized parameters are $a = -0.0676$, $b = 0.1849$,

$c = 0.000104$, and $d = -0.011$.

In the case of `gga_c_tm_w2` the functional form is exactly the same as that of `gga_c_w94`, and the newly optimized parameters are $a = -0.076176$, $b = 0.00000529$, $c = 0.0086$, and $d = 0.02$.

Finally, `gga_c_tm_wi` has the same form as `gga_c_wi0` and `gga_c_wi`, but with the newly optimized parameters in eq. (483) $a = -1.20077764$, $b = -0.45989783612$, $c = 0.127449$, $\bar{d} = 0.078$, and $k = 71.2336$.

`gga_c_tm_lyp`, `gga_c_tm_pbe`, `gga_c_tm_wpbe`, `gga_c_tm_cs1`⁵⁹⁹ (2009)

Using reference correlation energies of the He–Ar atoms,⁶⁰⁰ existing correlation functionals were reoptimized.

`gga_c_tm_lyp` is a reoptimization of `gga_c_lyp`. The new values of the parameters in eqs. (463) and (464) are $a = 0.0393$, $b = 0.21$, $\bar{c} = 0.41(4\pi/3)^{1/3}$, and $\bar{d} = 0.15(4\pi/3)^{1/3}$.

`gga_c_tm_pbe` is a reoptimization of `gga_c_pbe`. The new values of β and γ in eqs. (467) and (468) are $\gamma = -0.0156$ and $\beta = 3.38\gamma = -0.052728$.

`gga_c_tm_wpbe` is a reparametrization of the correlation part of `gga_xc_pbe1w`, where the parameter a_c in eq. (540) was reoptimized to 0.955. Note that `lda_c_pw` is here used as the LDA component, while it appears that `lda_c_vwn` was used in the original `gga_xc_pbe1w` functional.

`gga_c_tm_cs1` is a reparametrization of `gga_c_cs1`, and the new values of the parameters in eqs. (491) and (492) are $C_1 = -0.0398$, $C_2 = 6.5$, $C_3 = -0.0747$, $C_4 = -19$, $d = 0.514$ and $\gamma = 0.00062$.

Compared to their respective original functional, all reoptimized versions improve the correlation energy of the neutral atoms He–Ar and cations Li^+ – K^+ . However, all reoptimized functionals except `gga_c_tm_cs1` lead to an increase of the average error for the heavier closed-shell atoms from Ca to Rn.

`gga_c_tm_bpbe`, `gga_c_tm_qpbe`, `gga_c_tm_rpbe`⁵⁹⁹ (2009)

In addition to the functionals discussed above, Thakkar and McCarthy⁵⁹⁹ also proposed three modifications of `gga_c_pbe`, each containing

a parameter that was optimized for the correlation energy of atoms. `gga_c_tm_bpbe` differs from `gga_c_pbe` only in the parameter β (in eqs. (467) and (468)) that was optimized to $\beta = 0.06$. The `gga_c_tm_qpbe` and `gga_c_tm_rpbe` functionals have the same form as `gga_c_regtpss`, and differ from it in the value of only one parameter in eq. (502). The parameter that was varied is β_0 and b for `gga_c_tm_qpbe` and `gga_c_tm_rpbe`, respectively, and the new values are $\beta_0 = 0.063$ and $b = 0.25$.

`gga_c_tm_a1`, `gga_c_tm_a2`, `gga_c_tm_a3`, `gga_c_tm_wlv`⁵⁹⁹ (2009)

In the search for an accurate correlation functional, Thakkar and McCarthy⁵⁹⁹ proposed four novel forms. Their constructions start with rather simple functional forms of the LDA type (mostly `lda_c_wigner`), to which a dependence on the density gradient is added. The parameters p_i appearing in the functionals were also fit to accurate reference atomic correlation energies.⁶⁰⁰ The first functional, `gga_c_tm_a1` is given by

$$e_c^{A1} = -p_1^2 \frac{\phi_{2/3}^3(\zeta) (1 - e^{-p_2^2 r_s})}{r_s [1 + p_3 (x_\uparrow + x_\downarrow)]} \quad (503)$$

where $p_1 = 167$, $p_2 = 0.695$, and $p_3 = 3.31 \times 10^4$. The second functional, `gga_c_tm_a2`, reads

$$e_c^{A2} = -p_1^2 \frac{\phi_{2/3}^3(\zeta)}{(1 + p_2^2 r_s) [1 + p_3 (x_\uparrow + x_\downarrow)]} \quad (504)$$

where $p_1 = 7.95$, $p_2 = 0.53$, and $p_3 = 153$. Inspired by `lda_c_rc04` and `gga_c_tca`, the third functional has the following expression:

$$e_c^{A3} = \frac{S_V(\zeta) [1 - p_1^2 \arctan(p_3 r_s + 1)]}{p_2 r_s + p_4 (x_\uparrow + x_\downarrow)^2} \quad (505)$$

where $p_1 = 1.272$, $p_2 = 9.1$, $p_3 = 1.236$, and $p_4 = 0.135$. Finally, `gga_c_tm_wlv` consists of `gga_c_wl`, but with a dependence on ζ that is modified so that the correlation energy does not vanish in the case of maximal multiplicity in

systems for more than one electron:

$$e_c^{\text{WLV}} = -p_1^2 \frac{S_V(\zeta) (1 + p_3 x)}{r_s + p_2^2 + p_4 (x_\uparrow + x_\downarrow)} \quad (506)$$

where $p_1 = 12$, $p_2 = -20$, $p_3 = -0.048$, and $p_4 = 310$. The function $S_V(\zeta)$ in eqs. (505) and (506) is given by

$$S_V(\zeta) = 1 - c (1 + \delta \zeta^4) [2\phi_{4/3}(\zeta) - 2] \quad (507)$$

with $c = 0.611042$ and $\delta = 0.574082$.

The correlation energies obtained with the four functionals are quite accurate for the light He–Ne atoms, but not so for heavier atoms.

`gga_c_pbeint`⁵²³ (2010)

This is the correlation functional that should be combined with `gga_x_pbeint`. It has the same form as the `gga_c_pbe` functional, but with the parameter $\beta = 0.052$ in eqs. (467) and (468), which was obtained by a refit to jellium surface energies.

`gga_c_apbe`²⁷⁴ (2011)

This is the counterpart of `gga_x_apbe` for correlation. It uses the `gga_c_pbe` form, but the parameter β in eqs. (467) and (468) is calculated from the linear-response relation $\beta = 3\mu/\pi^2 \approx 0.079031$,⁴⁷² with $\mu = 0.260$ that is the value used in `gga_x_apbe`.

`gga_c_sogga11`⁵³¹ (2011)

Peperati et al.⁵³¹ chose for this correlation functional a mathematical expression that is rather similar to the associated exchange part `gga_x_sogga11`:

$$e_c^{\text{SOGGA11}} = e_c^{\text{PW-LDA}}(r_s, \zeta) \times [g_1(r_s, \zeta, t) + g_2(r_s, \zeta, t)] \quad (508)$$

where $e_c^{\text{PW-LDA}}$ is `lda_c_pw` and (compare to eq. (424))

$$g_1(r_s, \zeta, t) = \sum_{i=0}^m a_i \left[1 - \frac{1}{1 + y(r_s, \zeta, t)} \right]^i \quad (509a)$$

$$g_2(r_s, \zeta, t) = \sum_{i=0}^m b_i [1 - e^{-y(r_s, \zeta, t)}]^i \quad (509b)$$

with the function $y(r_s, \zeta, t)$ defined as

$$y(r_s, \zeta, t) = -\frac{\beta\phi_{2/3}^3 t^2}{e_c^{\text{PW-LDA}}(r_s, \zeta)} \quad (510)$$

The HEG limit imposes the constraint $a_0 + b_0 = 1$, while the density-gradient expansion to second order implies $\beta = \beta^{\text{MB}}$, coupled with $a_1 + b_1 = -1$. With these constraints imposed, the parameters a_i and b_i in eq. (509) (with $m = 5$) were optimized together with `gga_x_sogga11`. It is relatively easy to see that eq. (510) is dimensionless, and that it is the leading order term in the expansion of H_0 (eq. (467)) in powers of t .

`gga_c_zpbeint`, `gga_c_zpbesol`⁶⁰¹ (2011)

Constantin et al.⁶⁰¹ tried to improve calculated atomization energies of molecules and solids by introducing a simple spin-dependent correction to existing functionals for the rapidly varying density regime. The general form of these new functionals is given by

$$e_c^{\text{zPBE-type}} = e_c^{\text{LDA}}(r_s, \zeta) + f(t, \zeta)H_0(\phi_{2/3}, t, A) \quad (511)$$

where e_c^{LDA} is a LDA correlation functional (which might be `lda_c_pw` although it is not specified) and H_0 is the gradient correction of the `gga_c_pbe` functional given by eq. (467). The function f was chosen such that it reduces to unity for spin-unpolarized systems, as well as for spin-polarized densities that are slowly varying ($t \rightarrow 0$). Its form reads

$$f(t, \zeta) = \phi_{2/3}^{\alpha t^3}(\zeta) \quad (512)$$

Several underlying PBE-type functionals were used in ref. 601. However, only two showed improved results for finite values of α , namely `gga_c_pbeint` and `gga_c_pbe_sol` (combined with `gga_x_pbeint` and `gga_x_pbe_sol`, respectively). The resulting corrected functionals, `gga_c_zpbeint` and `gga_c_zpbesol`, use $\alpha = 2.4$ and $\alpha = 4.8$, respectively, which were obtained through minimization of the error in the atomization energies of the AE6 test set.^{602,603}

Tests on molecules and solids for various properties showed that zPBEint is overall

more accurate than zPBEsol, PBE (`gga_x_pbe` + `gga_c_pbe`), PBEsol (`gga_x_pbe_sol` + `gga_c_pbe_sol`), and PBEint (`gga_x_pbeint` + `gga_c_pbeint`).

`gga_c_n12`¹⁵³ (2012)

This is the correlation part of N12 (a member of the Minnesota family of functionals) to be used together with the non-separable functional `gga_x_n12`. It employs the B97 form³⁷⁰ for correlation (see section 2.18.4). This functional reduces to `lda_c_pw` for the HEG, as $c_{0\sigma\sigma'} = 1$ is chosen for the two zeroth-order coefficients in eq. (254). The other coefficients $c_{i\sigma\sigma'}$ ($m = 4$ in eq. (254) is chosen) were fit together with the ones for `gga_x_n12`, therefore `gga_c_n12` should not be combined with any other exchange functional.

Note that the parallel- and opposite-spin parameters $c_{i\sigma\sigma'}$ appear to be inverted in the original paper of Peverati and Truhlar¹⁵³.

`gga_c_pbe_mol`⁵³⁷ (2012)

This is the correlation counterpart of `gga_x_pbe_mol`. It has the same form as `gga_c_pbe`, but with the parameter $\beta = 3\mu/\pi^2 \approx 0.08384$ ⁶⁰⁴ (linear-response requirement^{148,149}) with $\mu = 0.27583$ as used in `gga_x_pbe_mol`.

`gga_c_pbeloc`⁶⁰⁵ (2012)

It is known that a GGA correlation functional should tend to zero in the rapidly varying density limit ($t \rightarrow \infty$). Constantin et al.⁶⁰⁵ found that the correlation energy density of `gga_c_pbe`, which depends on the parameter β (in eq. (467)), exhibits a too slowly decaying Taylor expansion at $t = \infty$. To correct this behavior, thus making the correlation energy density more *localized*, they proposed to replace the constant $\beta = \beta^{\text{MB}}$ of `gga_c_pbe` by the function

$$\beta(r_s, t) = \beta_0 + at^2 f(r_s) \quad (513)$$

where β_0 and a are constants. The function $f(r_s)$ determines the correction in the high- and low-density limits, and is chosen to fulfill two constraints: (i) Under uniform scaling, $\beta(r_s, t)$ should reduce to β_0 at the high- and low-density limits; (ii) $\beta_0 < \beta^{\text{MB}}$, which is deduced from

the fact that `gga_c_pbeloc` is constructed to be more localized than the original `gga_c_pbe`. The proposed function that satisfies these two requirements is given by

$$f(r_s) = 1 - e^{-r_s^2} \quad (514)$$

while $\beta_0 = 3\mu^{\text{GE}}/\pi^2 \approx 0.0375$,⁶⁰⁴ the same choice as in `gga_c_pbe_jrgx`. The parameter $a = 0.08$ was obtained by fitting to jellium surface correlation energies obtained with `mgga_c_revtpss`, which are considered accurate.^{606,607}

Test calculations for molecular properties (atomization energies, barrier heights, kinetics, and binding energies of hydrogen-bonded dimers) show that the localization procedure improves the compatibility of the correlation functional with the HF exchange, significantly reducing the errors compared to using the standard `gga_c_pbe` or `gga_c_lyp` functional. Note that `mgga_c_tpssloc` is based on `gga_c_pbeloc`.

`gga_c_zvpbeint`, `gga_c_zvpbesol`⁶⁰⁸ (2012) The `gga_c_zpbeint` and `gga_c_zpbesol` functionals have a couple of pitfalls. First, the correction for spin dependence, eq. (512), should have an effect only in the valence regions, as these functionals were proposed to improve the description of bonds. Second, they may yield spuriously large contributions in atomic inter-shell regions. In order to solve these problems, Constantin et al.⁶⁰⁸ proposed a more flexible alternative to eq. (512):

$$f(\nu, \zeta) = e^{-\alpha\nu^3(r_s, \zeta, t)|\zeta|^\omega} \quad (515)$$

where α and ω are parameters, and ν is given by

$$\nu(r_s, \zeta, t) = t\phi_{2/3}(\zeta) \left(\frac{3}{r_s}\right)^x \quad (516)$$

where x is another parameter. α and x were determined by minimizing the information-entropy-like function for the one-electron densities' statistical ensemble. This led to $x = 1/6$, and $\alpha = 1.0$ and 1.8 when using the `gga_c_pbeint` and `gga_c_pbe_sol` values for the other parameters, respectively. In contrast, the parameter $\omega = 9/2$ (the optimal value for

both functionals) was fixed by introducing additional constraints based on partially polarized model systems.

Tests on molecular systems for various properties showed that `zvPBEint` (`gga_x_pbeint` + `gga_c_zvpbeint`), and the original `zPBEint` (`gga_x_pbeint` + `gga_c_zpbeint`) and `zPBEsol` (`gga_x_pbe_sol` + `gga_c_zpbesol`) are overall the most accurate PBE-type functionals.

`gga_c_q2d`⁵³⁸ (2012)

This functional is the correlation counterpart of `gga_x_q2d`, and it was constructed following the same ideas; both functionals are designed for the quasi-2D regime. It consists of an interpolation between the `gga_c_pbe` functional and the 2D limit given by `lda_c_2d_amgb`:

$$e_c^{\text{Q2D}} = e_c^{\text{PBE}}(r_s, \zeta, t) + \frac{t^4(1+t^2)}{d+t^6} \times [-e_c^{\text{PBE}}(r_s, \zeta, t) + e_c^{\text{AMGB-2D}}(r_s^{2\text{D}}, \zeta)] \quad (517)$$

where $r_s^{2\text{D}}$ is given by eq. (35b) which is connected to the common 3D variables n and s through the following relation:⁵³⁹

$$r_s^{2\text{D}} = 1.704n^{-1/3}\sqrt{s} \quad (518)$$

The coefficient $d = 10^6$ in eq. (517) was fit to a reference system, namely an infinite-barrier quantum well.

`gga_c_gapc`, `gga_c_gaploc`⁶⁰⁹ (2014)

Following the idea behind the construction of `mgga_c_kcis`, which is based on the HEG with a gap,⁶¹⁰⁻⁶¹³ Fabiano et al.⁶⁰⁹ proposed two GGA functionals. In this model, the general form has the same spin-dependence as eq. (274), where e_c^{P} and e_c^{F} are given by

$$e_c(r_s, G) = \frac{e_c^{\text{rPW-LDA}}(r_s) + c_1(r_s)G}{1 + c_2(r_s)G + c_3(r_s)G^2} \quad (519)$$

and $e_c^{\text{rPW-LDA}}$ is a reparametrization of `lda_c_pw` at $\zeta = 0$ (P) or $\zeta = 1$ (F), and the functions c_i are given by eq. (721) with reparameterized a_i , b_i , and f_c and with $e_c^{\text{PW-LDA}}$ replaced by $e_c^{\text{rPW-LDA}}$.⁶⁰⁹

The first proposed local gap function G reads

$$G^{\text{GAPc}}(r_s, \zeta, t) = \phi_{2/3}^3 \frac{\beta(r_s)t^2}{c_1(r_s) - c_2(r_s)e_c^{\text{rPW-LDA}}(r_s)} \times H(r_s, t) \quad (520)$$

where β is defined by eq. (502) and H reads

$$H(r_s, t) = \frac{a + Ar_s \ln(r_s)\beta^{-1}(r_s)t^2}{a + t^2} \quad (521)$$

with $a = 30$, which was determined by fitting to the exact correlation energies of the He, Ne, and Ar atoms. Note that A in eq. (521) is the same parameter as in the reparameterized $e_c^{\text{rPW-LDA}}$ (see eq. (286)). All mathematical constraints satisfied by `gga_c_pbe` are also satisfied by `gga_c_gapc`. In addition the second-order density-gradient expansion is recovered at any density regime, while that is only the case for the high-density regime for `gga_c_pbe`.

The second local gap function G is given by

$$G^{\text{GAPloc}}(r_s, s, t) = f_G \frac{s^{\alpha(t)+2}}{r_s^2} \frac{b + s^2}{1 + s^{\alpha(t)+2}} \quad (522)$$

where s is the reduced-density gradient given by eq. (46), $f_G = (9\pi/4)^{2/3}/2$ (note that the expression for f_G given in ref. 609 is wrong), and

$$\alpha(t) = \frac{\alpha_1 + t^3}{1 + t^3} \quad (523)$$

The parameters $b = 14.709046$ (in eq. (522)) and $\alpha_1 = 6.54613$ (in eq. (523)) were determined from a fit to the exact correlation energy density of the He atom. `gga_c_gaploc` satisfies all constraints satisfied by `gga_c_pbe` except the second-order density-gradient expansion that was not considered.

`gga_c_gapc` competes with the standard `gga_c_pbe` and `gga_c_lyp` for correlation energies of atoms and ions, but is clearly more accurate for the jellium surface correlation energy. The combination of `gga_x_pbe_r` and `gga_c_gapc` leads to good results for various molecular properties. `gga_c_gaploc` is more accurate than `gga_c_gapc` for correlation energies of atoms and ions, but is less accurate for

the jellium surface correlation energy.

`gga_c_acgga`, `gga_c_acggap`^{546,564} (2014)

High-level quantum results were used to study the behavior of the correlation energy of neutral atoms in the limit of large nuclear charge, $Z \rightarrow \infty$. The LDA (e.g., `lda_c_pw`) gives correctly the leading contribution. For the following term Burke et al.⁵⁴⁶ found that `gga_c_pbe` yields already a relatively accurate value, which is considerably better than the one predicted by `gga_c_lyp`. They then devised a new asymptotically corrected GGA (acGGA) functional that takes into account exactly this $Z \rightarrow \infty$ limit. The functional is obtained from `gga_c_pbe` by replacing t in eq. (467) by

$$t' = t \sqrt{\frac{\eta + t}{\eta + \tilde{c}t}} \quad (524)$$

with $\eta = 4.5$ chosen to reproduce the real-space cutoff curve for the xc hole, and $\tilde{c} = 1.467$ is chosen to reproduce the $Z \rightarrow \infty$ value for the correlation energy. The resulting functional, `gga_c_acgga`, satisfies all the conditions of `gga_c_pbe`, but, unlike `gga_c_pbe`, contains the leading real-space cutoff correction to $\ln t$.

In order to improve the dependence on r_s , the parameter β in eq. (467) is made r_s -dependent:

$$\beta(r_s) = \beta_0 \frac{1 + ar_s(b + cr_s)}{1 + ar_s(1 + dr_s)} \quad (525)$$

leading to the `gga_c_acggap` (acGGA+) functional. The parameters $\beta_0 = \beta^{\text{MB}}$, $a = 0.5$, $b = 1$, $c = 0.16667$, and $d = 0.29633$ were chosen so that $d\beta/dr_s = 0$ at $r_s = 0$.⁵⁶³

The atomization energies of molecules were calculated by combining `gga_c_acgga` with `gga_x_b88` or `gga_x_bcgp`, and `gga_c_acggap` with `gga_x_b88`. Using `gga_c_acggap` leads to slight improvement compared to `gga_c_acgga`.

`gga_c_gam`⁵⁵⁰ (2015)

This functional is the correlation companion of `gga_x_gam`. It has the same analytical form as `gga_c_n12`, which is based on the B97 functional form³⁷⁰ (section 2.18.4). The truncation $m = 4$ was chosen in eq. (254), and the 10 linear coefficients of the functional were fit together with those in `gga_x_gam`. However, contrary to

gga_c_n12, the functional was not constrained to recover the LDA for the HEG.

gga_c_zvpbeloc⁶¹⁴ (2015)

The construction of this functional follows the same strategy as for **mgga_c_zvtpss** and **mgga_c_zvtpssloc**, which consists of multiplying the correlation energy density of an existing functional, here **gga_c_pbeloc**, by the function $f(\nu, \zeta)$ given by eq. (515). The goal is to improve compatibility with HF. The function ν in eq. (515) is here given by

$$\nu(r_s, |\nabla n|) = A^{-1} |\nabla n| r_s^{10/3} \quad (526)$$

where $A = 4 [3/(4\pi^4)]^{1/18} [3/(4\pi)]^{10/9}$. The parameters $\omega = 2.0$ and $\alpha = 0.5$ in eq. (515) were determined by requiring an accurate ζ -dependence of the functional for $\zeta \gtrsim 0.3$.

Results for the atomization energies, barrier heights, and kinetic properties^{602,603,615} demonstrate that **gga_c_zvpbeloc** is more compatible with HF exchange than the other GGA correlation functionals **gga_c_lyp**, **gga_c_pbe**, and **gga_c_pbeloc**. Ref. 614 also considered a hybrid functional that mixes **gga_c_zvpbeloc** with the APBE (**gga_x_apbe** + **gga_c_apbe**) functional and HF exchange.

gga_c_pbefe⁵⁵¹ (2015)

This functional is the correlation counterpart of **gga_x_pbefe**. The two were optimized together for the formation energies of solids. The analytical form is the same as **gga_c_pbe**, but with a different value for the parameter β (0.043) in eqs. (467) and (468). The original **gga_c_pbe** value for the γ parameter was kept, since varying it failed to considerably improve the results.

gga_c_sg4⁵⁵⁵ (2016)

This is the correlation companion of **gga_x_sg4**. There are two main ideas behind the construction of this functional. The first is to require the functional to closely reproduce the semi-classical correlation energy expansion of neutral atoms at large nuclear charge Z .⁵⁴⁶ The second is that the functional should recover **gga_c_apbe** in the core region of heavy atoms, where $r_s \rightarrow 0$ and $s \rightarrow 0$. The functional is thus written as eqs. (511) and (512), with H_0

having the **gga_c_pbe** form (eq. (467)), but with β that is here the function:

$$\beta(r_s, t) = \beta_0 + \sigma t \left(1 - e^{-r_s^2}\right) \quad (527)$$

(note the similarity with eq. (513) of the **gga_c_pbeloc** functional). The values of the parameters are $\beta_0 = 3\mu^{\text{MGE2}}/\pi^2$ ($\mu^{\text{MGE2}} = 0.260$, see **gga_x_sg4**) in order to recover the LDA linear response and $\sigma = 0.07$, that was fitted to accurate jellium xc surface energies.⁶⁰⁷ In eq. (512), α was reoptimized by minimizing the information entropy function,⁶⁰¹ leading to $\alpha = 0.8$.

gga_c_kdt16⁴⁴⁷ (2016)

This functional was designed to represent the correlation free energy and is the counterpart of the **gga_x_kdt16** exchange free energy. The correlation free energy per particle, only available for the spin-unpolarized case, reads

$$f_c^{\text{KDT16}} = f_c^{\text{LDA}} + H_0(f_c^{\text{LDA}}, \zeta = 0, q_c) \quad (528)$$

where $f_c^{\text{LDA}} = f_{\text{xc}}^{\text{corrKSDT}}(\zeta = 0) - f_x^{\text{LDA}}(\zeta = 0)$, with $f_{\text{xc}}^{\text{corrKSDT}}$ corresponding to **lda_xc_corrksdt**, f_x^{LDA} is given by eq. (447), H_0 is the gradient correction term of **gga_c_pbe** (eq. (467)) evaluated with f_c^{LDA} instead of $e_c^{\text{PW-LDA}}$, and with the τ_e -dependent reduced-density gradient

$$q_c(n, \nabla n, \tau_e) = t_0 \sqrt{\tilde{B}_c(r_s, \theta)} \quad (529)$$

instead of t (eq. (57)). In eq. (529), $t_0 = t(\zeta = 0)$ and

$$\tilde{B}_c(r_s, \theta) = \frac{1 + \sum_{i=1}^4 (a_i + b_i r_s^{1/2} + c_i r_s) u^i}{1 + \sum_{i=1}^5 (d_i + e_i r_s^{3/2} + f_i r_s^3) u^i} \quad (530)$$

with $u = \theta^{13/4}$, where $\theta = \tau_e/\tau_e^{\text{F}}$ and τ_e^{F} is the Fermi temperature (eq. (351)).

gga_c_mggac⁶¹⁶ (2019)

This functional has the same form as **gga_c_pbe**, but with $\beta = 0.030$ in eqs. (467) and (468) that was optimized in combination

with `mgga_x_mggac` for exchange for the lattice constant of a set of bulk solids.

`gga_c_ccdf`⁶¹⁷ (2019)

Coupled-cluster methods^{618,619} are able to provide highly accurate correlation energies. Therefore, results or quantities obtained from coupled-cluster calculations can be used for the development of density functionals. Following this strategy, Margraf et al.⁶¹⁷ calculated the coupled-cluster with singles and doubles correlation energy density e_c^{cc} for the He isoelectronic series from H^- to Ne^{8+} . Then, using a simple function of the `lda_c_wigner` type (eq. (291) for the spin-polarized version), they performed a fit to the data points (n, e_c^{cc}) and obtained $a = (c_1/c_2)/(4\pi/3)^{1/3}$ and $b = a/c_1$, with $c_1 = 0.0468$ and $c_2 = 0.023$ for the parameters in eq. (291). In a second step, this Wigner-type function is multiplied by another function depending on the reduced-density gradient s :

$$e_c^{ccDF} = -\frac{a}{b+r_s} \left[1 - \frac{c_3}{1 + e^{-c_4(s-c_5)}} \right] \quad (531)$$

where the parameters $c_3 = 0.544$, $c_4 = 23.401$, and $c_5 = 0.479$ were obtained by fitting to the coupled-cluster correlation energies of the atoms of the He isoelectronic series. Note that only the spin-unpolarized form of the functional was presented in ref. 617.

The functional `gga_c_ccdf` is more accurate than `gga_c_pbe` for the correlation energy of the light He and Be atoms. However, for heavier atoms it significantly underestimates the magnitude of the correlation energy and is less accurate than `gga_c_pbe`. This is explained by the fact that `gga_c_ccdf` is based on `lda_c_wigner` that in principle does not account for parallel-spin correlation, which is more important in heavier atoms.

`gga_c_chachiyo`⁴³⁴ (2020)

Chachiyo and Chachiyo⁴³⁴ proposed the following simple formula for the correlation energy:

$$e_c^{\text{Cha-GGA}} = e_c^{\text{Cha-LDA-mod}} (1 + t_0^2)^{h/e_c^{\text{Cha-LDA-mod}}} \quad (532)$$

where $e_c^{\text{Cha-LDA-mod}}$ is `lda_c_chachiyo_mod` (developed by one of the authors), t_0 corresponds

to eq. (57) evaluated at $\zeta = 0$, and $h = \beta^{\text{MB}}$ that was determined such that eq. (532) recovers the expression of Ma and Brueckner¹⁵¹ in the limit of a slowly varying density (i.e. when $t \rightarrow 0$). Combined with `gga_x_chachiyo`, this correlation functional leads to quite accurate atomization energies of molecules and competes with the popular BLYP (`gga_x_b88 + gga_c_lyp`).

`gga_c_bkl1`, `gga_c_bkl2`⁵⁶⁷ (2024)

The `gga_c_bkl1` and `gga_c_bkl2` functionals were designed to be used with their exchange companions `gga_x_bkl1` and `gga_x_bkl2`, respectively. They have the same form as `gga_c_pbe`, but with a rescaling of the variable t in eq. (467) by 2.5 (`gga_c_bkl1`) and 0.5 (`gga_c_bkl2`).

3.2.3 Exchange and correlation

`gga_xc_th_fc`, `gga_xc_th_fcfo`, `gga_xc_th_fcfo`⁴⁴⁴ (1997)

Zhao et al.⁴⁴² showed how to obtain the xc potential $v_{xc\sigma}$ corresponding to a given electron density n . When a density is calculated using a high-level, high-accuracy wavefunction method, one can argue that the ZMP *inversion* method should lead to a xc potential that is close to exact. The idea of Tozer et al.⁴⁴⁴ is to fit a fairly flexible GGA form for the xc functional to accurate potentials obtained from the ZMP method. The chosen form for the expansion is given by

$$e_{xc}^{\text{TH}} = \frac{1}{n} \sum_{abcd} \omega_{abcd} R_a S_b X_c Y_d \quad (533)$$

where ω_{abcd} are the empirical coefficients and

$$R_a = n_{\uparrow}^a + n_{\downarrow}^a \quad (534a)$$

$$S_b = \zeta^{2b} \quad (534b)$$

$$X_c = \frac{|\nabla n_{\uparrow}|^c + |\nabla n_{\downarrow}|^c}{2n^{4c/3}} \quad (534c)$$

$$Y_d = \left(\frac{2|\nabla n_{\uparrow}|^2 + 2|\nabla n_{\downarrow}|^2 - |\nabla n|^2}{n^{8/3}} \right)^d \quad (534d)$$

The values of the powers in eq. (534) that were considered are $a = 7/6$, $8/6$, $9/6$, and $10/6$,

$b = 0$ and 1 , $c = 0$, 1 , and 2 , and $d = 0$ and 1 . Note that eq. (533) was proposed without taking into account the known exact conditions that a functional should satisfy. Therefore, one should not expect a large degree of transferability with such a functional form.

Four functionals based on eq. (533) were proposed.⁴⁴⁴ The first two were obtained by fitting the weights ω_{abcd} to the exact xc potentials of 10 closed-shell systems, namely H_2 , H_2O , N_2 , HF , CO , LiH , BH , Ne , F_2 , and CH_4 . One of them is `lda_xc_th_fl`, which is a LDA since $b = c = d = 0$. For the other functional, `gga_xc_th_fc`, Tozer et al.⁴⁴⁴ set $b = d = 0$. Note that, even if these functionals were fit only to spin-unpolarized potentials, they still retain a (non-linear) dependence on ζ .

For the two other functionals, they added the xc potentials of the open-shell systems Li , C , N , O , F , CH , CH_2 , NH_2 , and O_2 to the training set. In the first case (`gga_xc_th_fcfo`), the difference to the `gga_xc_th_fc` potentials was fitted with 8 extra parameters, while the `gga_xc_th_fco` functional was fitted directly to a combination to all closed- and open-shell potentials available.

These functionals are found to yield reasonably accurate optimized geometries, and significantly more accurate asymptotic density than conventional functionals like BLYP (`gga_x_b88` + `gga_c_lyp`). However, the xc energies (and therefore the total energies) turn out to be significantly too negative, with an error that increases linearly with the number of electrons.⁶²⁰

`gga_xc_th1`⁶²⁰ (1998)

From the work of Perdew et al.³¹² on the derivative discontinuity of the energy at integer electron numbers, Tozer and Handy⁶²⁰ found an ambiguity in the determination of the xc potential $v_{xc\sigma}$ obtained through the ZMP inversion procedure.⁴⁴² While in the development of their previous functionals (`gga_xc_th_fco`, etc.) the inverted xc potentials were assumed to vanish asymptotically, they should, in fact, go to a finite constant related to the chemical hardness of the system. This was assumed to be the reason for the too negative xc energies obtained with the functionals developed in ref. 444.

In order to circumvent this problem, Tozer and Handy⁶²⁰ used the same functional form as for `gga_xc_th_fco`, namely eqs. (533) and (534), but changed their optimization procedure by: (i) allowing for a finite asymptotic value of the potential, where this value is obtained self-consistently during the fitting; (ii) fitting not only the near-exact (shifted) xc potentials but also xc energies computed from atomic energies and experimental atomization and zero-point energies.^{406,621,622} The training set for determining the coefficients ω_{abcd} in eq. (533) was composed of the same systems as for `gga_xc_th_fco` plus the H atom. Compared to BLYP (`gga_x_b88` + `gga_c_lyp`), the `gga_xc_th1` functional leads to improved total energies and geometries that are of similar accuracy. Nevertheless, Tozer and Handy⁶²⁰ also mentioned that atomization energies should not be as accurate as BLYP, since energy differences were not really used in the fitting procedure of `gga_xc_th1`.

`gga_xc_th2`⁶²³ (1998)

The development of this functional follows the same steps as for `gga_xc_th1`, but with atomization energies used in the fitting procedure. The coefficients in eq. (533) were fitted to (i) near-exact (shifted) xc ZMP⁴⁴² potentials, (ii) experimental atomization energies of the 13 molecules in the training set, and (iii) the xc energies of the atoms in the training set. The resulting functional retains the good performance of `gga_xc_th1` for total energies, but improves significantly the evaluation of atomization energies, as expected.

`gga_xc_th3`, `gga_xc_th4`⁶²⁴ (1998)

The `gga_xc_th3` functional, whose expression is given by eq. (533), was designed using the same procedure as for `gga_xc_th2`, i.e. by fitting near-exact (shifted) ZMP⁴⁴² xc potentials, atomization energies of molecules, and xc energies of atoms, but with an extended training set, which includes 68 systems (53 molecules and 15 atoms) taken from the G1 set.^{622,625} The `gga_xc_th3` functional outperforms `gga_xc_th2`, especially for systems including second-row atoms. Geometries are of a similar quality as with BLYP (`gga_x_b88` +

`gga_c_lyp`).

Handy and Tozer⁶²⁴ decided to propose yet another version of their functional, `gga_xc_th4`, by adding the error in the forces to the fitting procedure. Their objective was to improve the usual overestimation of bond lengths by most GGA functionals. The resulting `gga_xc_th4` yields energetics similar to `gga_xc_th3`, but now yields geometries that are more accurate, and as good as the results obtained with the hybrid functional B3LYP.³⁹⁷

`gga_xc_edf1`⁴⁸³ (1998)

This functional was constructed with three goals in mind: (i) to increase the degree of *empiricism* of the functional (hence the name empirical density functional 1, EDF1), (ii) to provide a functional that is accurate for small Gaussian basis sets (indeed nothing guarantees that the best functionals in the large basis-set limit perform well for small basis sets), and (iii) to evaluate the effect of using HF exchange on the accuracy of the functional, in spite of the additional computational effort. The chosen Gaussian basis set is 6-31+G*, and the functional uses the popular `gga_x_b88` and `gga_c_lyp` approximations:

$$e_{xc}^{\text{EDF1}} = a_1 e_x^{\text{LDA}} + a_2 e_x^{\text{B88}}(\beta_1) + a_3 e_x^{\text{B88}}(\beta_2) + e_c^{\text{LYP}}(a, b, \bar{c}, \bar{d}) \quad (535)$$

The coefficients $a_1 = 1.030952 - a_2 - a_3$, $a_2 = 10.4017$, and $a_3 = -8.44793$, and the parameters in eq. (368) ($\beta_1 = 0.0035$ and $\beta_2 = 0.0042$) and in eqs. (463) and (464) ($a = 0.055$, $b = 0.158$, $\bar{c} = 0.25(4\pi/3)^{1/3}$, and $\bar{d} = 0.3505(4\pi/3)^{1/3}$) were adjusted to a series of experimental data similar to the original G2 set.⁴⁰⁶ The functional `gga_xc_edf1` was, at that time, claimed as the best functional for the study of molecules with the small 6-31+G* basis set.

`gga_xc_hcth_93`⁴⁷⁸ (1998)

Hamprecht et al.⁴⁷⁸ fitted the flexible B97 form³⁷⁰ (see section 2.18.4) self-consistently to a large molecular database. They used energetics data (total energies for first-row atoms and cations, ionization potentials for second-row atoms, and atomization energies of molecules

involving first- and second-row atoms), equilibrium geometries of molecules, and numerical xc potentials $v_{xc\sigma}$ from densities calculated with accurate wavefunction methods by using the ZMP inversion method⁴⁴² in their fitting set. As the training set included data for 93 molecular systems, this functional became later known as `gga_xc_hcth_93`. Due to the large training data set, there were fewer problems of overfitting than Becke³⁷⁰ encountered with the original B97 functional, which allowed Hamprecht et al.⁴⁷⁸ to use $m = 4$ in the expansions for exchange (eq. (252)) and correlation (eq. (254)), while Becke³⁷⁰ had used $m = 2$. The functional `gga_xc_hcth_93` improves over BLYP (`gga_x_b88` + `gga_c_lyp`) and the hybrid B3LYP³⁹⁷ for the energetics of molecules.

`gga_xc_hcth_120`, `gga_xc_hcth_147`⁶²⁶ (2000)

To obtain these two functionals, Boese et al.⁶²⁶ also used the B97 form (section 2.18.4). As in `gga_xc_hcth_93`, $m = 4$ was used in the expansions for exchange and correlation (eqs. (252) and (254)), however they increased the number of molecular systems in the training set to 120 (`gga_xc_hcth_120`) and 147 (`gga_xc_hcth_147`). The systems that were added consist mainly of cationic molecules, anionic atoms and molecules, and a few hydrogen bonded dimers.

Note that in ref. 626 the sign of the $c_{1\sigma\sigma}$ parameter (in eq. (254) for parallel-spin correlation) of `gga_xc_hcth_147` is wrong, but was later given correctly in ref. 627. Ref. 627 also reports more decimals for the coefficients than ref. 626 does.

`gga_xc_b97_gga1`⁶²⁸ (2000)

This functional uses the B97 form (section 2.18.4). Furthermore, $m = 2$ is used for the series eqs. (252) and (254) as in B97 (a larger value of m had been used in `gga_xc_hcth_93`, for instance). The nine empirical parameters were reoptimized to the same 93 molecular systems used for `gga_xc_hcth_93`, but without the xc potentials obtained from the ZMP inversion scheme.⁴⁴² The functional appears to be the most accurate among the numerous other GGA functionals tested by Cohen and Handy⁶²⁸.

`gga_xc_hcth_407`⁶²⁹ (2001)

This is the fourth member of the HCTH family of functionals, which already included `gga_xc_hcth_93`, `gga_xc_hcth_120`, and `gga_xc_hcth_147`. The functional form of `gga_xc_hcth_407` is the one used originally for B97³⁷⁰ (section 2.18.4), but with $m = 4$ in eqs. (252) and (254). For this functional, Boese and Handy⁶²⁹ used a considerably larger training set of 407 molecular systems, including most of the G2-2 set,^{505,630} to which two hydrogen-bonded dimers and eight transition-metal complexes were added. Even though `gga_xc_hcth_407` was trained on many more systems, it does not systematically lead to a better accuracy compared to its predecessors.

`gga_xc_hcth_p14`, `gga_xc_hcth_p76`⁶³¹ (2001)

This is yet another functional using the flexible B97 form³⁷⁰ (section 2.18.4). In contrast to the first HCTH functional, `gga_xc_hcth_93`, Menconi et al.⁶³¹ decided not to use energetics data, but to fit only to near-exact xc potentials (of 93 molecules⁴⁷⁸) obtained from the ZMP inversion procedure.⁴⁴² As for `gga_xc_hcth_93`, $m = 4$ was used in eqs. (252) and (254). These new functionals are therefore expected to yield worse energetics, but to give better quantities related to the derivatives of the energy such as the geometry or nuclear shielding constants.

For `gga_xc_hcth_93`, the fit to the xc potentials was weighted by the function n_{σ}^p with $p = 2/3$ in order to give more weight in the fitting to the regions of space with more density. Various values of p were tried, two of which yielded interesting results. The functional `gga_xc_hcth_p14`, corresponding to $p = 1/4$, was found to simultaneously yield optimal molecular structures, thermochemistry, and static polarizabilities, while `gga_xc_hcth_p76` ($p = 7/6$) is extremely inaccurate for these properties, but is the most recommended functional for the calculation of NMR isotropic shielding constants.

`gga_xc_kt1`, `gga_xc_kt2`⁴⁹⁰ (2003)

`gga_xc_kt1` consists of `gga_x_kt1` plus `lda_c_vwn` for correlation. Since `gga_x_kt1` was constructed to yield accurate potentials $v_{xc\sigma}$ without constraint on total energies,

`gga_xc_kt1` leads to inaccurate molecular structures and atomization energies. To circumvent this issue, and to improve these properties, a more flexible form was proposed:

$$e_{xc}^{KT2} = \alpha e_x^{LDA} + \beta e_c^{VWN} + \Delta e_x^{KT1} \quad (536)$$

where e_x^{LDA} is eq. (256) (`lda_x`), e_c^{VWN} is eq. (278) (`lda_c_vwn`), and $\Delta e_x^{KT1} = e_x^{KT1} - e_x^{LDA}$ is the gradient-correction term of `gga_x_kt1` (see eq. (394)). The parameters $\alpha = 1.07173$ and $\beta = 0.576727$ were fit to atomization energies and ionization potentials. It turns out that `gga_xc_kt2` improves molecular structures and atomization energies, while still maintaining the excellent accuracy observed with `gga_xc_kt1` for the shielding constants.

`gga_xc_hcth_407p`⁶³² (2003)

The dataset used to optimize the parameters of the `gga_xc_hcth_407` functional included two hydrogen bonded systems, namely $(H_2O)_2$ and $(HF)_2$. However, it was shown that this functional could not reliably describe systems with bent hydrogen bonds, such as the ammonia dimer $(NH_3)_2$. In order to improve performance in such cases, Boese et al.⁶³² decided to add the ammonia dimer to the training set. The reparametrization of `gga_xc_hcth_407`, named HCTH407+ (`gga_xc_hcth_407p`), was then used to perform molecular dynamics of liquid ammonia.

`gga_xc_xlyp`⁶³³ (2004)

The motivation behind the design of this GGA functional (and its hybrid version X3LYP) is to properly describe weakly-bound systems, while still providing accurate results for thermochemistry. As noncovalent interactions involve large interatomic distances, and therefore regions of space with large values of the reduced gradient s , Xu and Goddard⁶³³ tried to construct an exchange enhancement factor F_x that is appropriate in such regions with large values of s . By evaluating F_x for a Gaussian density distribution they observed that it is overestimated by `gga_x_b88` and underestimated by `gga_x_pw91`. They proposed, therefore, to combine these two functionals together with

`gga_c_lyp` for correlation as

$$e_{xc}^{XLYP} = a_1 e_x^{LDA} + a_2 e_x^{B88} + a_3 e_x^{PW91} + e_c^{LYP} \quad (537)$$

The parameters $a_1 = 1 - a_2 - a_3$, $a_2 = 0.722$, and $a_3 = 0.347$ were determined with the constraint that `lda_x` is recovered for the HEG by fitting to the total energies of 10 atoms, the ionization potentials of 16 atoms, the electron affinities of 10 atoms, and the atomization energies of 38 molecules. In particular, He_2 and Ne_2 were included as representative van der Waals systems. The resulting functional `gga_xc_xlyp`, as well as X3LYP, show good and balanced accuracy for both covalent and noncovalent systems.

`gga_xc_kt3`⁶³⁴ (2004)

This functional clearly improves over its predecessors `gga_xc_kt1` and `gga_xc_kt2` for various molecular properties (atomization energies, bond lengths, ionization potentials, etc.), while still being as accurate for the shielding constants. This was achieved by the introduction of further gradient-dependent terms:

$$e_{xc}^{KT3} = \alpha e_x^{LDA} + \beta e_c^{LYP} + \Delta e_x^{KT1} + \epsilon \Delta e_x^{OPTX} \quad (538)$$

where e_x^{LDA} is eq. (256) (`lda_x`), e_c^{LYP} is eq. (463) (`gga_c_lyp`), $\Delta e_x^{KT1} = e_x^{KT1} - e_x^{LDA}$ is the gradient-correction term of `gga_x_kt1` (see eq. (394)), and

$$\Delta e_x^{OPTX} = \frac{1}{n} \sum_{\sigma} n_{\sigma}^{4/3} \left(\frac{0.006 x_{\sigma}^2}{1 + 0.006 x_{\sigma}^2} \right)^2 \quad (539)$$

which has the same form as the gradient-correction term of `gga_x_optx` (see eq. (391)). Equation (538) has five parameters that were determined empirically: $\gamma = -0.004$ and $\delta = 0.1$ in eq. (394) were determined from shielding constants, $\alpha = 1.092$ was adjusted for bond lengths, while $\beta = 0.864409$ and $\epsilon = -0.925452$ were fit to atomization energies.

`gga_xc_mpwlyp1w`, `gga_xc_pbe1w`, `gga_xc_pbelyp1w`⁶³⁵ (2005)

These three functionals were constructed specifically for simulations of water by tuning the parameter a_c that determines the relative weights

of LDA and GGA in correlation:

$$e_{xc} = e_x^{GGA} + (1 - a_c) e_c^{LDA} + a_c e_c^{GGA} \quad (540)$$

where e_c^{LDA} corresponds to `lda_c_vwn` in all three functionals, while e_x^{GGA} and e_c^{GGA} are

- `gga_x_mpw91` and `gga_c_lyp` in `gga_xc_mpwlyp1w`
- `gga_x_pbe` and `gga_c_pbe` in `gga_xc_pbe1w`
- `gga_x_pbe` and `gga_c_lyp` in `gga_xc_pbelyp1w`

a_c was obtained by minimizing the average error on the noncovalent interaction energies of 36 water clusters (28 dimers and 8 trimers) and its values are 0.88, 0.74, and 0.54 for `gga_xc_mpwlyp1w`, `gga_xc_pbe1w`, and `gga_xc_pbelyp1w`, respectively.

The three functionals are as accurate as more expensive hybrid functionals for the 36 water clusters. However, they are clearly worse for AE6 atomization energies and BH6 barrier heights.^{602,603}

`gga_xc_b97_d`⁵¹⁵ (2006)

This GGA functional again has the flexible B97 mathematical form³⁷⁰ (section 2.18.4). It was designed to be combined with Grimme's D2 empirical dispersion correction for noncovalent interactions.⁵¹⁵ The truncation in eqs. (252) and (254) was chosen as $m = 2$ as in B97 to avoid overfitting. The parameters $c_{i\sigma\sigma'}$ and $c_{i\sigma}$ were fit together with the parameters of the D2 correction to a training set composed of 30 atomization energies of molecules, 8 ionization energies of atoms, 3 proton affinities, 15 chemical reactions, and 21 noncovalently bound complexes. This functional, combined with the D2 dispersion correction, leads to high-quality structures and interaction energies of van der Waals complexes, as well as various properties of covalently bound systems.

`gga_xc_srp`⁶³⁶ (2009)

This functional is a mixture of the RPBE (`gga_x_rpbe` + `gga_c_pbe`) and PW91 (`gga_x_pw91` + `gga_c_pw91`) functionals:

$$E_{xc}^{SRP} = a E_{xc}^{RPBE} + (1 - a) E_{xc}^{PW91} \quad (541)$$

where $a = 0.43$ is a specific reaction parameter (SRP)⁶³⁷ that was determined to best reproduce experimental D₂ dissociation probabilities on the Cu(111) surface. Díaz et al.⁶³⁶ used `gga_xc_srp` to explore in more detail the potential energy surface of H₂/D₂ + Cu(111).

`gga_xc_oblyp_d`, `gga_xc_opwlyp_d`, `gga_xc_opbe_d`⁶³⁸ (2010)

Together with `mgga_xc_otpss_d`, these are reparameterizations of relatively popular functionals obtained by fitting to a set of 143 reference values. The set consists of 49 atomization energies (mostly from the G2/97 test set⁵⁰⁵), 15 atomic total energies, 8 ionization potentials and 7 electron affinities of atoms from the G2-1 test set,⁴⁰⁶ the isomerization reaction from isoctane to *n*-octane, the binding energy of the 5 smallest molecular dimers from the S22 database,⁵²¹ and 58 decomposition energies from the MB08-165 set.⁶³⁹ Moreover, these functionals were optimized with the D2 dispersion correction of Grimme.⁵¹⁵

`gga_xc_oblyp_d` is a combination of `gga_x_b88` with the new parameter $\beta = 0.00401$ in eq. (368) and `gga_c_lyp` with the new parameters $a = 0.05047$, $b = 0.140$, $\bar{c} = 0.2196(4\pi/3)^{1/3}$, and $\bar{d} = 0.363(4\pi/3)^{1/3}$ in eqs. (463) and (464).

`gga_xc_opwlyp_d` is a combination of reoptimized versions of `gga_x_pw91` and `gga_c_lyp`. The reoptimized parameters of the exchange functional are $\alpha = 0.79$, $\beta = 0.00402$, and $\gamma = 0.8894/C_s^2$ in eqs. (369) and (370). Interestingly, the value of β is remarkably close to $\beta^{\text{B88}} = 0.0042$ used in the original `gga_x_b88` and `gga_x_pw91` functionals. The reoptimized parameters for the correlation functional are $a = 0.04960$, $b = 0.144$, $\bar{c} = 0.2262(4\pi/3)^{1/3}$, and $\bar{d} = 0.346(4\pi/3)^{1/3}$ in eqs. (463) and (464).

`gga_xc_opbe_d` is a reoptimized version of PBE, with new parameters $\kappa = 1.2010$ and $\mu = 0.21198$ in eq. (378) for `gga_x_pbe` and $\beta = 0.04636$ in eqs. (467) and (468) for `gga_c_pbe`.

It turns out that both `gga_xc_oblyp_d` and `gga_xc_opwlyp_d` only yield small differences with respect to the original functionals (note that `gga_xc_opwlyp_d` was actually compared to mPWLYP (`gga_x_mpw91` +

`gga_c_lyp`)). The effect of the reoptimization on `gga_xc_opbe_d` is larger and the description of some properties is indeed improved.

`gga_xc_srp48`⁶⁴⁰ (2012)

This functional differs from `gga_xc_srp` in two respects. In eq. (541), PW91 is replaced by PBE (`gga_x_pbe` + `gga_c_pbe`) and the empirical parameter a was reparameterized ($a = 0.48$) to take into account differences in the settings used in the calculations. As in ref. 636, the functional was applied to the dissociation of H₂/D₂ on the Cu(111) surface.

`gga_xc_beefvdw`⁶⁴¹ (2012)

A common problem with functionals that have many empirical parameters, such as `gga_xc_hcth_93`, is overfitting. For this functional, Wellendorff et al.⁶⁴¹ tried to mitigate this problem by using techniques that are standard in machine learning. This was achieved by adding a regularization term to the cost function that is minimized during the fitting of the parameters. A standard Tikhonov regularization method⁶⁴² was used, leading to solution vectors with small coefficients for higher-order polynomials, and therefore rather smooth functional forms that show no strong unphysical variations.

The GGA component of the chosen functional reads (BEEF stands for Bayesian error estimation functional)

$$e_{xc}^{\text{BEEF-vdW}} = e_x^{\text{BEEF-vdW}} + \alpha_c e_c^{\text{PW-LDA}} + (1 - \alpha_c) e_c^{\text{PBE}} \quad (542)$$

where the enhancement factor of the exchange part is expanded in Legendre polynomials B_m :

$$F_x^{\text{BEEF-vdW}} = \sum_{m=0}^M a_m B_m[r(s_\sigma)] \quad (543)$$

where a_m are the expansion coefficients and

$$r(s_\sigma) = \frac{2s_\sigma^2}{q + s_\sigma^2} - 1 \quad (544)$$

with $q = 4$, which transforms $r(s_\sigma)$ into the interval $[-1, 1]$. The parameter $M = 29$ was chosen in eq. (543), leading to a total of 31 parameters (including α_c). As shown in

eq. (542), this exchange functional is mixed with the `lda_c_pw` and `gga_c_pbe` correlation functionals. Furthermore, the non-local correlation functional vdW-DF2⁵⁰⁷ was added to `gga_xc_beefvdw` for the training procedure.

The 31 parameters were fit to a large training set of reference values that consists of the following subsets: CE17 (17 chemisorption energies), RE42 (42 reaction energies), DBH24/08 (24 reaction barriers⁶⁴³), G2/97 (148 formation energies⁵⁰⁵), Sol34Ec (cohesive energies of 34 solids), and S22×5 (intermolecular interaction energies of 22 molecular dimers at five different intermolecular separations⁵⁶⁰).

Benchmarking against numerous other GGA and GGA-vdW functionals revealed that `gga_xc_beefvdw`+vdW-DF2 appears to be a rather general purpose xc functional, leading to small errors across a large range of properties.

`gga_xc_hle16`⁶⁴⁴ (2016)

This functional consists of a simple rescaling of `gga_xc_hcth_407`, where the exchange and correlation components are multiplied by 1.25 and 0.5, respectively. These scaling parameters were empirically determined so that the band gap of semiconductors and excitation energy of molecules are enlarged, leading to better agreement with experiment. However, results for ground-state properties can be inaccurate, which is particularly the case for geometries, since bond lengths in molecules and solids are in most cases strongly underestimated.

`gga_xc_b97_3c`⁶⁴⁵ (2018)

This functional of Brandenburg et al.⁶⁴⁵, B97-3c, is a revised version of B97-D⁵¹⁵ (`gga_xc_b97_d`). It is composed of three parts: the GGA part `gga_xc_b97_3c`, a D3 dispersion correction,⁶⁴⁶ and a term that corrects for basis-set incompleteness.⁶⁴⁷ `gga_xc_b97_3c` is a reparametrization of the GGA part of the B97 hybrid functional³⁷⁰ (section 2.18.4). The coefficients $c_{i\sigma}$ in eq. (252) and $c_{i\sigma\sigma'}$ in eq. (254) were optimized by fitting to a training set that includes various properties: 20 atomization energies, 43 chemical reactions, 27 non-covalent interaction energies, 4 total atomic energies, and 17 geometries of small molecules. It is re-

ported that B97-3c is more accurate than the more expensive hybrid B3LYP-D3.

`gga_xc_dlb97`⁶⁴⁸ (2025)

This is the GGA component of the dispersion-corrected dlB97+D_{as}²⁰ functional. It is a reparametrization of the B97 form³⁷⁰ (section 2.18.4). The value $m = 3$ was used in eqs. (252) and (254), and the coefficients $c_{0\sigma}$ and $c_{0\sigma\sigma'}$ were set to 1 such that the correct LDA limit of the HEG is recovered. The remaining nine empirical parameters $c_{i\sigma}$ and $c_{i\sigma\sigma'}$ ($i = 1, 2$ and 3) were optimized on a set of 589 reference interaction energies. The D_{as}²⁰ dispersion term⁶⁴⁹ was included during the training procedure.

The functional dlB97+D_{as}²⁰ competes in accuracy with more expensive dispersion-corrected functionals based on a MGGA or hybrid functional.

3.3 Meta-generalized gradient approximation

MGGAs introduce an additional dependence on the kinetic-energy density τ_σ and/or density Laplacian $\nabla^2 n_\sigma$ to the GGA form. The most general MGGA form for spin-polarized states is given by

$$E_{xc}^{MGGA} = \int d^3r n(\mathbf{r}) \times e_{xc}^{MGGA}(n_\uparrow(\mathbf{r}), n_\downarrow(\mathbf{r}), \nabla n_\uparrow(\mathbf{r}), \nabla n_\downarrow(\mathbf{r}), \nabla^2 n_\uparrow(\mathbf{r}), \nabla^2 n_\downarrow(\mathbf{r}), \tau_\uparrow(\mathbf{r}), \tau_\downarrow(\mathbf{r})) \quad (545)$$

Figure 2 shows the possible dependencies of the various subcategories of MGGA functionals. It also illustrates the terminology in use, which can be confusing at first. Going upward, we find the meta-LDAs (MLDAs); the $\nabla^2 n$ -MGGAs, which are usually referred to as deorbitalized or Laplacian-level MGGAs; τ -MGGAs, which presently represent the most popular type of MGGA; and finally, the $(\nabla^2 n, \tau)$ -MGGAs, which depend on all variables. τ -MGGAs have been reviewed a decade ago by Della Sala et al.¹³³

Although the name and performance of the MLDA tend to place this functional below the

GGA,⁶⁵⁰ the form may be regarded as the simplest MGGA (the idea stems from the fact that the gradient expansion of τ contains both ∇n and $\nabla^2 n$, see eq. (184)). Interestingly, the MLDA may also be regarded as the base of a *meta-ladder*, i.e., a ladder of approximations stemming from the MLDA rather than from the LDA.⁶⁵⁰ The MLDA, however, remains largely unexplored: there are only a few examples of MLDA,^{286,650,651} like the hLTA (`mgga_x_hlta` + `mgga_c_hltapw`) for instance.

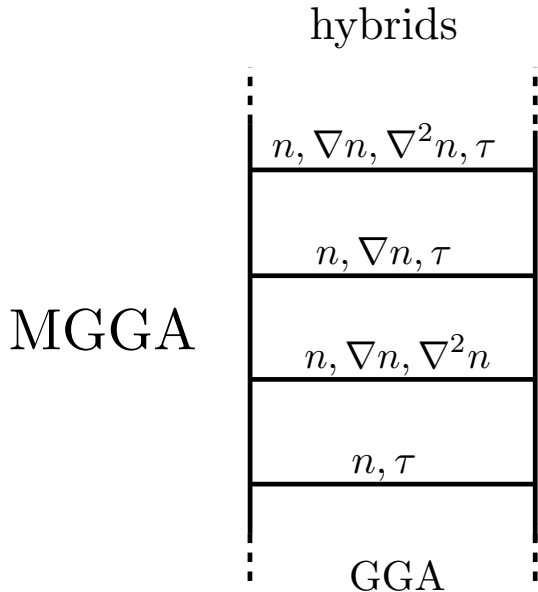


Figure 2: Categorization of semi-local approximations above GGAs and below hybrids: they all belong to the MGGA category.

As for the GGAs (section 3.2), the exchange enhancement factors F_x of MGGA are defined according to eqs. (360) and (361), but with additional dependence on variables like α_σ or z_σ . MGGA correlation functionals E_c are usually also more complicated, and sometimes based on eq. (250). As usual, caution must be exerted by referring to the correct definitions of constants (section 2.1.2) and variables (section 2.1.3): authors have different definitions for the same symbols.

It should also be mentioned that a couple of the functionals presented below do not strictly belong to the MGGA defined by eq. (545). This is the case when the potential is directly modeled (e.g., `mgga_x_bj06`) or with `mgga_x_theta_mgga` and `mgga_c_theta_mgga`

that have a dependence on the second derivative of n_σ through $\nabla |\nabla n_\sigma|$ instead of $\nabla^2 n_\sigma$.

3.3.1 Exchange

`mgga_x_gdme_nv`⁶⁵² (1972)

Negele and Vautherin⁶⁵² derived an expansion for the density matrix in the context of nuclear matter. The expression they obtained depends on the density, the Laplacian of the density and the kinetic-energy density, and using this generalized density matrix expansion (GDME) in the exchange energy expression leads to the following enhancement factor:

$$F_x^{\text{GDME}} = \frac{(A + \frac{3}{5}B) 2^{1/3}}{C_x (3\pi^2)^{2/3}} + \frac{B}{C_x 2^{1/3} (3\pi^2)^{4/3}} \times \left[\left(a^2 - a + \frac{1}{2} \right) u_\sigma - 2\tilde{t}_\sigma \right] \quad (546)$$

where $A = 9\pi/4$, $B = 35\pi/12$, and $a = 1/2$. Note that the parameter a comes from the definition of the relative ($\mathbf{r}_{12} = \mathbf{r}_2 - \mathbf{r}_1$) and center of mass ($\mathbf{R} = a\mathbf{r}_1 + (1-a)\mathbf{r}_2$) coordinates of the two interacting particles, which were used to expand the density matrix.

Calculations on molecules⁶⁵³ showed that this $(\nabla^2 n, \tau)$ -MGGA functional leads to exchange energies that differ substantially from the reference HF results, so that the mean error is even worse (about twice larger) than with `lda_x`.

`mgga_x_rllda`^{653,654} (1978)

By noting that there is some arbitrariness in the choice of the momentum k in the density matrix expansion of Negele and Vautherin⁶⁵², Campi and Bouyssy⁶⁵⁴ proposed to use $k_\sigma = \sqrt{[2\tau_\sigma - (1/4)\nabla^2 n_\sigma] / [(3/5)n_\sigma]}$ instead of eq. (49) in order to cancel the second term in eq. (546), leading to

$$F_x^{\text{RLDA}} = f \frac{3\pi}{C_x} \frac{1}{2\tilde{t}_\sigma - \frac{1}{4}u_\sigma} \quad (547)$$

Different values for the parameter f can be found in the literature^{653–656} (see also `mgga_x_gp86` discussed below). We note that, with $f = 9/10$, the `lda_x` result is recovered for the HEG. The functional `mgga_x_rllda` implemented in Libxc corresponds to $f = 5/4$, which

according to ref. 656 is the value from Campi and Bouyssy⁶⁵⁴.

`mgga_x_gp86`⁶⁵⁵ (1986)

Ghosh and Parr⁶⁵⁵ derived an expression for the first-order density matrix from the phase-space distribution function proposed in ref. 657. Using this density matrix leads to an approximate expression for the exchange energy that depends on the kinetic-energy density, eq. (547) with $f = 1$. Noteworthy, the enhancement factor reduces to 10/9 for the HEG, i.e. the correct `lda_x` limit, $F_x^{\text{LDA}} = 1$, is not recovered. Note that this functional was later re-derived by Manby and Knowles⁶⁵⁶.

`mgga_x_br89`, `mgga_x_br89_1`⁶⁵⁸ (1989)

Becke and Roussel⁶⁵⁸ proposed the following model for the spherically averaged exchange hole:

$$h_{x\sigma}^{\text{BR89}}(r_{12}) = -\frac{a_\sigma}{16\pi b_\sigma r_{12}} \left[\begin{aligned} & \times (a_\sigma |b_\sigma - r_{12}| + 1) e^{-a_\sigma |b_\sigma - r_{12}|} \\ & - (a_\sigma |b_\sigma + r_{12}| + 1) e^{-a_\sigma |b_\sigma + r_{12}|} \end{aligned} \right] \quad (548)$$

where $r_{12} = |\mathbf{r}_2 - \mathbf{r}_1|$ denotes the distance from the reference position (see section 2.5). This form is based on the exchange hole of the hydrogenic atom, and the positive parameters a_σ and b_σ are determined by requiring $h_{x\sigma}^{\text{BR89}}$ to reproduce the second-order Taylor expansion of the exact exchange hole at any reference position in space for any inhomogeneous system. This condition leads to the following equation for a_σ and b_σ :

$$\frac{c_\sigma e^{-2c_\sigma/3}}{c_\sigma - 2} = \frac{2}{3} \pi^{2/3} \frac{1}{\tilde{C}_{x\sigma}} \quad (549)$$

where

$$\tilde{C}_{x\sigma} = \frac{1}{6} \left[u_\sigma - 2\gamma \left(2\tilde{t}_\sigma - \frac{1}{4} x_\sigma^2 \right) \right] \quad (550)$$

is the exchange-hole curvature (for $\gamma = 1$, $\tilde{C}_{x\sigma} = C_{x\sigma}/n_\sigma^{5/3}$, where $C_{x\sigma}$ is eq. (147)) and $c_\sigma = a_\sigma b_\sigma$. Note that although a unique and positive root exists for c_σ , there is no closed-form solution, so that eq. (549)

has to be solved numerically (e.g., with the Newton–Raphson method) at each point of space. Once c_σ is calculated, b_σ can be obtained with $b_\sigma = [c_\sigma^3 e^{-c_\sigma} / (8\pi n_\sigma)]^{1/3}$, which is used for evaluating the energy (eq. (551)). Note that the numerical solution of eq. (549) can be avoided; see the `mgga_x_br89_explicit` and `mgga_x_br89_explicit_1` functionals discussed later, which offer a robust alternative.

The expression for the functional is obtained by using eq. (548) in the definition of the exchange energy in terms of the exchange hole (see eqs. (141) and (142)), which yields

$$e_{x\sigma}^{\text{BR89}} = -\frac{1}{2b_\sigma} \left[1 - e^{-c_\sigma} \left(1 + \frac{c_\sigma}{2} \right) \right] \quad (551)$$

Two values for the parameter γ in eq. (550) were considered in ref. 658: $\gamma = 1$ (`mgga_x_br89_1`) and 0.8 (`mgga_x_br89`), with the later recovering `lda_x` in the HEG limit.

`mgga_x_br89` and `mgga_x_br89_1` were combined with the `gga_c_p86` correlation functional in refs. 298 and 659, and tested for the geometries and atomization energies of molecules. It turns out that the functional is superior to LDA, and can sometimes compete with BP86 (`gga_x_b88` + `gga_c_p86`). Note that `mgga_x_br89` and `mgga_x_br89_1` are $(\nabla^2 n, \tau)$ -MGGAs.

A quantity that will be used later in the definition of other functionals is the Coulomb potential created by the exchange hole $h_{x\sigma}^{\text{BR89}}$:

$$v_{x\sigma}^{\text{BR89,hole}} = 2e_{x\sigma}^{\text{BR89}} \quad (552)$$

It has been shown^{660,661} to be an accurate approximation to the Slater potential⁴² (eq. (144)), which is the main reason why it has been used as a component in semi-local potentials like `mgga_x_bj06` or `mgga_x_tb09`. Note that eq. (552) should not be confused with $v_{x\sigma}^{\text{BR89}}$, the functional derivative of eq. (551).

`mgga_x_jk`¹⁶⁰ (1995)

The functional of Jemmer and Knowles¹⁶⁰ depends on the Laplacian of the density, but not on the kinetic-energy density, therefore it is a

pure density functional. Its form is given by

$$F_x^{\text{JK}} = 1 + \frac{F_x^{\text{B88}}(x_\sigma) - 1}{1 + 2 \frac{x_\sigma^2 - u_\sigma}{x_\sigma^2}} \quad (553)$$

where F_x^{B88} is the `gga_x_b88` enhancement factor (eq. (368)). The functional was constructed such that both the energy density and potential $v_{\text{xc},\sigma}$ have the correct behavior in the asymptotic regions far into the vacuum. Numerical instabilities were reported for this functional and attributed to the dependence of the potential on the high-order derivatives (up to the fourth order) of the density. Lehtola and Marques⁴⁰¹ pointed out that the denominator in eq. (553) can become arbitrarily small or vanish.

`mgga_x_gdme_0`, `mgga_x_gdme_kos`, `mgga_x_gdme_vt`⁶⁵³ (1996)

These functionals from Koehl et al.⁶⁵³ are generalizations of `mgga_x_gdme_nv`, where the density matrix is expanded using a more general definition for the coordinate system of the two electrons at \mathbf{r}_1 and \mathbf{r}_2 . Koehl et al.⁶⁵³ considered values other than $a = 1/2$ in eq. (546). Furthermore, other values for A and B in eq. (546) were also considered. Thus, several variants of `mgga_x_gdme_nv`, which differ in the values of a , A , and B , were proposed. The values of the parameters (a, A, B) are $(0, 9\pi/4, 35\pi/12)$ for `mgga_x_gdme_0`, $(0.00638, 9\pi/4, 35\pi/12)$ for `mgga_x_gdme_kos`, and $(0, 7.31275, 5.43182)$ for `mgga_x_gdme_vt`. The coefficient a for `mgga_x_gdme_kos` was obtained by minimizing the average error in the exchange energy with respect to the HF reference for the molecules in the test set. The same procedure was used to determine A and B when $a = 0$ (`mgga_x_gdme_vt`). The average error obtained with `mgga_x_gdme_vt` is the smallest, and it is actually smaller than that of `gga_x_b88`.

`mgga_x_ft98`¹⁶¹ (1998)

This is a $\nabla^2 n$ -MGGA functional. Its enhance-

ment factor is given by

$$F_x^{\text{FT98}} = \left[\frac{1 + a f_1(x_\sigma) x_\sigma^2 + b f_2(x_\sigma, u_\sigma) (x_\sigma^2 - u_\sigma)^2}{1 + 36 C_x^2 b x_\sigma^2} \right]^{1/2} \quad (554)$$

where

$$f_1(x_\sigma) = \frac{(1 + a_1 x_\sigma^2)^{1/2}}{(1 + b_1 x_\sigma^2)^{3/4}} \quad (555)$$

and

$$f_2(x_\sigma, u_\sigma) = \frac{[1 + a_2 q_1(x_\sigma, u_\sigma)] [1 + q_2(x_\sigma, u_\sigma)]}{[1 + (2^{1/3} - 1) q_2(x_\sigma, u_\sigma)]^3} \quad (556)$$

with

$$q_1(x_\sigma, u_\sigma) = \frac{(x_\sigma^2 - u_\sigma)^2}{(1 + x_\sigma^2)^2} \quad (557)$$

and

$$q_2(x_\sigma, u_\sigma) = \frac{(b_2^2 + 1)^{1/2} - b_2}{x_\sigma^4 - u_\sigma^2 - b_2 + [(x_\sigma^4 - u_\sigma^2 - b_2)^2 + 1]^{1/2}} \quad (558)$$

The functions f_1 and f_2 were chosen such that

$$\lim_{x_\sigma \rightarrow 0} f_1(x_\sigma) = 1 \quad (559a)$$

$$\lim_{x_\sigma \rightarrow 0} \lim_{u_\sigma \rightarrow 0} f_2(x_\sigma, u_\sigma) = 1 \quad (559b)$$

$$\lim_{x_\sigma \rightarrow \infty} \lim_{u_\sigma \rightarrow \infty} f_2(x_\sigma, u_\sigma) = 1 \quad (559c)$$

$$\lim_{x_\sigma \rightarrow \text{const}} \lim_{u_\sigma \rightarrow -\infty} f_2(x_\sigma, u_\sigma) \propto r \quad (559d)$$

where r is the distance into the vacuum far from the finite system. These conditions guarantee (i) the recovery of the small density-gradient expansion at fourth order²⁶⁷ (eqs. (559a) and (559b)), (ii) a $-1/r$ -type asymptotic behavior for the exchange energy density and potential (eq. (559c)), and (iii) a finite value of the exchange energy density close to the nuclei (eq. (559d)).

In eq. (554), $a \approx 0.00528014$ ⁶⁰⁴ and $b \approx 0.00003904539$ ⁶⁰⁴ were determined such that the coefficients in the small density-gradient expansion at fourth order of eq. (554) have the correct values.²⁶⁷ The a_i and b_i parameters in

eqs. (555), (556) and (558) were obtained by fitting to the exact exchange energy of a set of atoms (H, He, Be, Ne, Mg, Ar, Ca, Kr, Sr, and Xe), leading to $a_1 = 2.816049$, $a_2 = 0.879058$, $b_1 = 0.398773$, and $b_2 = 66.364138$.

When combined with `mgga_c_ft98` for correlation, the functional has an accuracy similar to that of the B3LYP hybrid functional³⁹⁷ for atomization energies, geometries, and dipole moments of molecules.

`mgga_x_gvt4`^{167,168} (1998)

The construction of this functional starts with a second-order expansion of the density matrix in the relative coordinate $s = |\mathbf{r}_1 - \mathbf{r}_2|$. The derivation continues by inserting this expression into the exchange functional, performing the integral in s analytically, and finally eliminating the dependence on the Laplacian of the density by integrating by parts. The resulting form is then generalized, leading to

$$F_x^{\text{GVT4}} = -\frac{1}{C_x} f^{\text{GVT4}}(x_\sigma, \tilde{z}_\sigma) \quad (560)$$

where

$$f^{\text{GVT4}}(x_\sigma, \tilde{z}_\sigma) = \frac{a}{\gamma_\sigma} + \frac{bx_\sigma^2 + c\tilde{z}_\sigma}{\gamma_\sigma^2} + \frac{dx_\sigma^4 + ex_\sigma^2\tilde{z}_\sigma + f\tilde{z}_\sigma^2}{\gamma_\sigma^3} \quad (561)$$

with \tilde{z}_σ given by eq. (87) and

$$\gamma_\sigma = 1 + \alpha(x_\sigma^2 + \tilde{z}_\sigma) \quad (562)$$

The seven parameters (a , b , c , d , e , f , and α), given in ref. 168, were adjusted to minimize the error with respect to the experimental values of atomization energies and ionization potentials of an extended G2 set.⁴⁰⁶ Note that the parameters were fit together with those of the `mgga_c_vsxc` correlation functional. Also note that the $f\tilde{z}_\sigma^2$ term in eq. (561) leads to numerical problems,⁶⁶² so more recent functionals based on this form tend to have $f = 0$.

The VSXC (`mgga_x_gvt4` + `mgga_c_vsxc`) functional is superior in accuracy to the B3LYP hybrid functional³⁹⁷ for some of the considered properties.

`mgga_x_lta`⁶⁵¹ (1999)

The idea of Ernzerhof and Scuseria⁶⁵¹ was to write a τ -MGGA functional in the spirit of the `lda_x` functional, but using as basic variable the kinetic-energy density τ_σ instead of the electron density n_σ . To achieve this, they inverted the Thomas–Fermi expression for the kinetic energy density of the HEG (eq. (70)) to obtain

$$\tilde{n}_\sigma = \left(\frac{\tau_\sigma}{C_F} \right)^{3/5} \quad (563)$$

This expression can then be inserted in `lda_x`, therefore transforming it into a τ -MGGA functional, the so-called local- τ approximation. The enhancement factor reads

$$F_x^{\text{LTA}} = \left(\frac{\tilde{t}_\sigma}{C_F} \right)^{4/5} \quad (564)$$

Note that this procedure can be obviously generalized, and used to transform any LDA into a τ -MGGA. An example is given by `mgga_x_hlta`. The `mgga_x_lta` functional respects the homogeneous scaling condition and the normalization of the exchange hole. Furthermore, it recovers `lda_x` for the HEG. When applied to a series of atomization processes, it yields results that are somewhat complementary to `lda_x`, and thus overall not accurate. Lehtola and Marques⁶⁵⁰ showed that eq. (564) leads to divergences in the exponentially decaying asymptotic region.

`mgga_x_pkzb`^{13,14} (1999)

Perdew et al.¹³ constructed an enhancement factor that recovers the fourth-order gradient expansion²⁶⁷ in the limit of a slowly varying density. It has the same form as the enhancement factor of `gga_x_pbe` (see eq. (378)), but with the function f_0 replaced by

$$f_0^{\text{PKZB}} = \mu^{\text{GE}} p_\sigma + \frac{146}{2025} \tilde{q}_\sigma^2 - \frac{73}{405} \tilde{q}_\sigma p_\sigma + \left[D + \frac{(\mu^{\text{GE}})^2}{\kappa} \right] p_\sigma^2 \quad (565)$$

where \tilde{q}_σ is defined as

$$\tilde{q}_\sigma = 6C_s^2 \tilde{t}_\sigma - \frac{9}{20} - \frac{p_\sigma}{12} \quad (566)$$

The constant D is not known from the density-gradient expansion, and was therefore fit in order to minimize the error in the atomization energies of 20 molecules,^{148,149} leading to $D = 0.113$. Finally, $\kappa = \kappa^{\text{PBE}}$ in eqs. (378) and (565) is the same value as in `gga_x_pbe`.

When combined with `mgga_c_pkzb`, this functional yields molecular atomization energies and metal surface energies that are significantly improved over those of PBE (`gga_x_pbe` + `gga_c_pbe`), while lattice constants are slightly improved (see the Erratum¹⁴).

`mgga_x_th`⁶⁶³ (2000)

Starting from the density-matrix expansion, Tsuneda and Hirao⁶⁶³ derived a functional that has a rather simple analytical form and has no adjustable parameter. The enhancement factor is given by

$$F_x^{\text{TH}} = \frac{1}{C_x} \frac{27\pi}{10\tilde{t}_\sigma} \left(1 + \frac{7x_\sigma^2}{108\tilde{t}_\sigma} \right) \quad (567)$$

They showed that this functional satisfies several conditions obeyed by the exact functional, like the LO bound, eq. (113), or possibly the coefficient in the density-gradient expansion in the limit of a slowly varying density. The functional, that was named HF- τ_σ in ref. 663, leads to exchange energies for the atoms H to Ar that are too large (i.e., too negative) by 10–20%.

`mgga_x_b00`¹⁶⁴ (2000)

Becke¹⁶⁴ arrived at the conclusion that the quantity $C_F/\tilde{t}_\sigma = \tau_\sigma^{\text{TF}}/\tau_\sigma$ is a useful measure of the delocalization of the exchange hole in a system by analyzing a simple model composed of a hydrogen atom with arbitrary fractional occupation. This led him to suggest that the exchange hole should be strongly delocalized in regions with values of C_F/\tilde{t}_σ much smaller than one, $C_F/\tilde{t}_\sigma \ll 1$. Then, starting from `mgga_x_br89_1` (i.e., with the parameter γ set to 1.0), he proposed a functional with the following enhancement factor:

$$F_x^{\text{B00}} = F_x^{\text{BR89},\gamma=1} [1 + a_t f_x(w_\sigma)] \quad (568)$$

where the variable C_F/\tilde{t}_σ has been conveniently transformed to w_σ (eq. (91)) that lies in the interval $[-1, 1]$. To construct the function $f_x(w_\sigma)$,

Becke¹⁶⁴ noticed that his delocalization model does not apply for the limiting values of w_σ . He therefore chose a function that vanishes at $w_\sigma = -1$ and $w_\sigma = 1$, and whose first derivative also does the same. This led to the choice

$$f_x(w_\sigma) = w_\sigma - 2w_\sigma^3 + w_\sigma^5 \quad (569)$$

Finally, the constant $a_t = 0.928$ was adjusted to optimize the results for the G2 atomization-energy test set⁴⁰⁶ without an additional correlation functional.

`mgga_x_mk00b`⁶⁵⁶ (2000)

Manby and Knowles⁶⁵⁶ re-derived the `mgga_x_gp86` functional by using a simple Gaussian ansatz for the one-particle density matrix, which was chosen such that it fulfills four exact conditions. Tests on atoms and molecules showed that while `mgga_x_gp86` is more accurate than `lda_x` for total energies, it is still much less accurate than `gga_x_b88`. However, the gap between the highest occupied and lowest unoccupied orbitals is described much more accurately with `mgga_x_gp86` compared to `lda_x` and `gga_x_b88`.

Since the errors for total energies closely parallel those of `lda_x`, Manby and Knowles⁶⁵⁶ argued that they can be corrected with the mixture

$$F_x^{\text{MK00B}} = F_x^{\text{GP86}} + (F_x^{\text{B88}} - 1) \quad (570)$$

where F_x^{B88} is the `gga_x_b88` enhancement factor, eq. (368). To finalize the construction of `mgga_x_mk00b`, the value of β in eq. (368) was reoptimized to minimize the error in the total exchange energies of the He, Ne, and Ar atoms, leading to $\beta = 0.0016$. The functional `mgga_x_mk00b` appears to lead to much improved total energies, similar in quality to `gga_x_b88`, while still maintaining the accuracy of `mgga_x_gp86` for the gap.

`mgga_x_edmgga`⁶⁶⁴ (2001)

This functional depends on both the kinetic-energy density and the Laplacian of the density. It was constructed such that the enhancement factor is correct at the nuclear cusp, in the slowly varying density limit, in the regions far from nuclei, and such that it is always positive.

The enhancement factor of EDMGGA (energy density MGGA) reads

$$F_x^{\text{EDMGGA}} = c_1 + \frac{c_2 q_\sigma^{\text{B}}}{1 + c_3 \sqrt{q_\sigma^{\text{B}}} \operatorname{arcsinh}[c_4 (q_\sigma^{\text{B}} - 1)]} \quad (571)$$

where

$$q_\sigma^{\text{B}} = a Q_\sigma^{\text{B}} + \sqrt{1 + (a Q_\sigma^{\text{B}})^2} \quad (572)$$

with

$$Q_\sigma^{\text{B}} = 1 - \frac{1}{C_{\text{F}}} \left(\tilde{t}_\sigma - \frac{x_\sigma^2}{8} - \frac{u_\sigma}{4} \right) \quad (573)$$

The parameters c_1 , c_2 , c_3 , and c_4 in eq. (571), which were chosen such that the four aforementioned conditions are satisfied, are given by

$$c_1 = \frac{1}{3} \left(\frac{4\pi^2}{3} \right)^{1/3} \quad (574a)$$

$$c_2 = 1 - c_1 \quad (574b)$$

$$c_3 = \frac{c_2 \sqrt{2a}}{2b} \quad (574c)$$

$$c_4 = \frac{c_3^2 - 0.09834\mu}{c_3^3} \quad (574d)$$

where $b = (2\pi/9)\sqrt{6/5}$. The values $a = 0.704$ and $\mu = 0.21$ were obtained from a fit to the HF exchange energies of 18 spherical atoms and ions. Note that the two expressions for c_4 given by eq. (50) in ref. 664 do not agree, leading to markedly different values. As the second expression, eq. (574d), leads to positive values it was chosen for the implementation of the functional in Libxc. The accuracy of this functional for the exchange energy of atoms and molecules is similar to that of `gga_x_b88`.

`mgga_x_tau_hcth`⁵⁹³ (2002)

Boese and Handy⁵⁹³ introduced this functional as the τ -MGGA successor of the HCTH GGA functionals (e.g., `gga_xc_hcth_407`). It combines the flexible form used originally for the semi-local exchange component of the B97 hybrid functional,³⁷⁰ with the idea of Becke¹⁶⁴ for the description of delocalized exchange (see `mgga_x_b00`). The functional consists of two parts. The local (L) GGA part is modeled exactly in the same way as in B97, while the non-

local (NL) MGGA part also uses this form, but it is multiplied by the function $f_x(w_\sigma)$ defined by eq. (569):

$$F_x^{\tau\text{-HCTH}} = F_{\text{xL}}(x_\sigma) + F_{\text{xNL}}(x_\sigma) f_x(w_\sigma) \quad (575)$$

where F_{xL} and F_{xNL} are both given by eq. (252) with $m = 3$, leading to $2 \times 4 = 8$ parameters. These parameters, together with the 8 parameters of the correlation companion `gga_c_tau_hcth`, were optimized using the set of 407 atomic and molecular systems.⁶²⁹

Tests on various molecular properties show that τ -HCTH improves over `gga_xc_hcth_407` and competes with the B3LYP³⁹⁷ and B97-1⁴⁷⁸ hybrid functionals.

`mgga_x_tpss`¹⁶⁶ (2003)

This functional was developed to correct some deficiencies of PKZB (`mgga_x_pkzb` + `mgga_c_pkzb`), namely the poor description of equilibrium bond lengths⁶⁶⁵ and hydrogen-bonded complexes.⁶⁶⁶ It is still constructed based on the `gga_x_pbe` enhancement factor and the fourth-order density-gradient expansion from ref. 267, adding a few more constraints.

The function f_0 (see eqs. (378) and (565)) is now generalized to

$$f_0^{\text{TPSS}} = \frac{1}{(1 + \sqrt{e} p_\sigma)^2} \left\{ \left[\mu^{\text{GE}} + c \frac{z_\sigma^f}{(1 + z_\sigma^2)^2} \right] p_\sigma + \frac{146}{2025} \tilde{q}_\sigma^2 - \frac{73}{405\sqrt{2}} \tilde{q}_\sigma \sqrt{\frac{9}{25} z_\sigma^2 + p_\sigma^2} + \frac{(\mu^{\text{GE}})^2}{\kappa} p_\sigma^2 + 2\sqrt{e} \mu^{\text{GE}} \frac{9}{25} z_\sigma^2 + e \mu^{\text{PBE}} p_\sigma^3 \right\} \quad (576)$$

with $f = 2$. Compared to eq. (565) a few differences can be observed. First, there is the dependence on the variable z_σ (eq. (84)). Then, the constant D in `mgga_x_pkzb` is set to zero, which is consistent with the best numerical estimate for this coefficient.²⁶⁷ Finally, the function \tilde{q}_σ is replaced by

$$\tilde{q}_\sigma = \frac{9}{20} \frac{\alpha_\sigma - 1}{\sqrt{1 + b\alpha_\sigma(\alpha_\sigma - 1)}} + \frac{2}{3} p_\sigma \quad (577)$$

This function employs the iso-orbital indicator α_σ that, as noted in section 2.5, is related to the the curvature of the exchange hole and (even more directly) to the electron-localization function of Becke and Edgecombe.^{224,230,232,667,668}

Besides the usual constants μ^{GE} and μ^{PBE} , the parameters $c = 1.59096$ and $e = 1.537$ were chosen to eliminate the divergence of the functional at the nucleus for a two-electron density and to yield the exact exchange energy of the H atom. Finally, the parameter $b = 0.40$ was chosen as the smallest value such that the enhancement factor increases monotonically as a function of p_σ .

TPSS (`mgga_x_tpss` + `mgga_c_tpss`), which was quite popular, gives generally good results for a wide range of systems and properties, correcting the overestimated PKZB bond lengths in molecules, hydrogen-bonded complexes, and ionic solids.

`mgga_x_bj06`⁶⁶⁰ (2006)

Becke and Johnson⁶⁶⁰ noted that the difference between the EXX-OEP and Slater⁴² potentials $\Delta v_{x\sigma} = v_{x\sigma}^{\text{EXX-OEP}} - v_{x\sigma}^{\text{Slater}}$ (where $v_{x\sigma}^{\text{Slater}}$ is given by eq. (144)) is characterized by a step-like structure in multi-shell atoms, and that this structure can be modeled by the ratio τ_σ/n_σ . They thus proposed this simple approximation to the EXX-OEP potential

$$v_{x\sigma}^{\text{BJ06}} = v_{x\sigma}^{\text{Slater}} + \frac{1}{\pi} \sqrt{\frac{5}{6}} \sqrt{\frac{\tau_\sigma}{n_\sigma}} \quad (578)$$

that fulfills the following conditions: (i) it is invariant to any unitary transformation of the orbitals, (ii) it shows the step-like structure characteristic of $\Delta v_{x\sigma}$ in atoms, (iii) it recovers the exact (i.e. `lda_x`) HEG limit (eq. (258)), and (iv) it is exact for any hydrogenic atom. As this potential was directly modeled, it suffers from the same drawbacks as `gga_x_lb`. In particular, it has no associated energy functional. Moreover, asymptotically it approaches a constant whose value depends on the eigenvalue of the highest occupied orbital (see also ref. 669) and it is not gauge invariant (see `mgga_x_rpp09` for a gauge-invariant modification).

As suggested by Becke and Johnson⁶⁶⁰, the Slater potential, which is computationally

expensive, can be accurately replaced by eq. (552):

$$v_{x\sigma}^{\text{BJ06}} = v_{x\sigma}^{\text{BR89,hole}} + \frac{1}{\pi} \sqrt{\frac{5}{6}} \sqrt{\frac{\tau_\sigma}{n_\sigma}} \quad (579)$$

which is the version available in Libxc (`mgga_x_bj06`). Note that `mgga_x_bj06` is a component of the `mgga_x_tb09` potential.

`mgga_x_m06_l`⁶⁷⁰ (2006)

Benchmark calculations revealed that the hybrid M05⁶⁷¹ and `mgga_x_gvt4` functionals give complementary results for a series of properties. While the former is rather accurate for noncovalent interactions and barrier heights, the latter is excellent for thermochemistry. These observations suggested Zhao and Truhlar⁶⁷⁰ to propose a functional form that can be seen as a mixture between the semi-local part of M05 and `mgga_x_gvt4`:

$$F_x^{\text{M06-L}} = F_x^{\text{PBE}}(s_\sigma) f(w_\sigma) + f^{\text{GVT4}}(x_\sigma, \tilde{z}_\sigma) \quad (580)$$

where F_x^{PBE} is the `gga_x_pbe` enhancement factor (eq. (378)), f^{GVT4} is defined by eq. (561), and

$$f(w_\sigma) = \sum_{i=0}^m a_i w_\sigma^i \quad (581)$$

The variables \tilde{z}_σ and w_σ are given by eqs. (87) and (91), respectively. The parameters a_i in eq. (581) ($m = 11$ was chosen) and the ones in eq. (561) were determined, along with those of the correlation counterpart `mgga_c_m06_l`, self-consistently by minimizing the error for a series of databases including thermochemistry, thermochemical kinetics, and noncovalent interactions. Note that the constraint $a_0 + a = 1$ was applied such that `mgga_x_m06_l` reduces to `lda_x` for the HEG. The M06-L functional (`mgga_x_m06_l` + `mgga_c_m06_l`) was then tested using 22 energetic databases, a set of bond lengths, and a set of 36 harmonic vibrational frequencies, yielding an excellent overall performance. The same functional form was refit in 2017 as revM06-L (`mgga_x_revM06_l` + `mgga_c_revM06_l`) by Wang et al.⁶⁷² Lehtola⁶⁷³ found M06-L to yield a nonphysical solution for the hydrogen atom,

suggesting issues with overfitting.

`mgga_x_modtpss`⁶⁷⁴ (2007)

This is a one-parameter empirical reoptimization of the `mgga_x_tpss` functional. The parameter chosen to be optimized was μ^{PBE} in eq. (576), which determines the large s_σ limit of the functional. As eq. (576) was built to reproduce the fourth-order gradient expansion of ref. 267, changing μ^{PBE} should not influence the small s_σ limit. The values of c and e were also adjusted such that the constraints obeyed by `mgga_x_tpss` are also fulfilled by the reoptimized version. As training sets, Perdew et al.⁶⁷⁴ used AE6 (atomization energies of six molecules) and BH6 (six reaction-barrier heights).^{602,603}

The optimized parameters are $\mu^{\text{modTPSS}} = 0.252$, $c = 1.38496$, and $e = 1.37$. The value of μ^{modTPSS} is slightly larger than original μ^{PBE} , but the modification yields considerably improved atomization energies and slightly improved reaction barriers.

`mgga_x_2d_prhg07`⁶⁷⁵ (2007)

Equations (141) and (142) can be readily adapted to 2D artificial systems. Essentially, the form of the Coulomb interaction is unchanged but position vectors are restricted to depend only on two spatial variables. Thus, the spherical average must be replaced by a cylindrical average. The cylindrical average of the x-hole and, consequently, the energy density have simple analytical expressions for the ground state of one-particle systems in a harmonic confinement. Following a strategy similar to the one used by Becke and Roussel⁶⁵⁸ for `mgga_x_br89`, Pittalis et al.⁶⁷⁵ derived a functional for 2D systems.

The exchange energy density is given by

$$e_{x\sigma}^{\text{PRHG07-2D}} = -\frac{1}{2}\sqrt{|a_\sigma|\pi}e^{-a_\sigma b_\sigma/2}I_0(a_\sigma b_\sigma/2) \quad (582)$$

where $I_0(x)$ (with $I_0(0) = 1$) is the zeroth-order modified Bessel function of the first kind, and a_σ and b_σ are position-dependent functions. From the second-order Taylor expansion of the exact exchange hole, the following rela-

tions were derived ($c_\sigma = a_\sigma b_\sigma$):

$$(c_\sigma - 1)e^{c_\sigma} = \frac{\tilde{C}_{x\sigma}^{2D}}{\pi} \quad (583)$$

$$a_\sigma = \pi n_\sigma e^{c_\sigma} \quad (584)$$

where

$$\tilde{C}_{x\sigma}^{2D} = \frac{1}{4} \left[u_\sigma^{2D} - 4\tilde{t}_\sigma^{2D} + \frac{1}{2} (x_\sigma^{2D})^2 + 2\frac{|\mathbf{j}_\sigma|^2}{n_\sigma^3} \right] \quad (585)$$

is the exchange-hole curvature, i.e. the 3D version of eq. (550). In eq. (585), x_σ^{2D} , u_σ^{2D} , and \tilde{t}_σ^{2D} are given by eqs. (42), (59) and (77), respectively, with $m = 2$. As eq. (549) for `mgga_x_br89`, eq. (583) is an implicit function of c_σ , and therefore of the density.

The exchange energy and shape of the exchange-hole potential obtained with this functional show good agreement with the data obtained from the EXX Krieger–Li–Iafrate (EXX-KLI) method.^{465,676,677} Pittalis et al.⁶⁷⁵ also showed that in the limit of the 2D HEG the functional reduces to $(3/16)\pi^{3/2}e_x^{\text{LDA-2D}}$, where $e_x^{\text{LDA-2D}}$ is given by eq. (263). The multiplication of `lda_x_2d` by $(3/16)\pi^{3/2} \approx 1.044061$ improves the agreement with the EXX results for quantum dots.

`mgga_x_br89_explicit`, `mgga_x_br89_explicit_1`⁶⁷⁸ (2008)

In the evaluation of `mgga_x_br89`, the parameter c_σ is obtained by solving a nonlinear implicit equation, eq. (549), at each point in space. This can only be done numerically, by using Newton–Raphson method for instance. As a more convenient way to calculate c_σ , Proynov et al.⁶⁷⁸ proposed the following analytical and explicit expression for c_σ as a function of $y_\sigma = (2/3)\pi^{2/3}/\tilde{C}_{x\sigma}$ (the right-hand side of eq. (549)):

$$c_\sigma(y_\sigma) = g(y_\sigma) \frac{P_1(y_\sigma)}{P_2(y_\sigma)} \quad (586)$$

where

$$g(y_\sigma) = \begin{cases} -\arctan(a_1 y_\sigma + a_2) + a_3, & -\infty \leq y_\sigma \leq 0 \\ \operatorname{arccsch}(B y_\sigma) + 2, & 0 < y_\sigma \leq \infty \end{cases} \quad (587a)$$

$$P_1(y_\sigma) = \begin{cases} \sum_{i=0}^5 c_i y_\sigma^i, & -\infty \leq y_\sigma \leq 0 \\ \sum_{i=0}^5 d_i y_\sigma^i, & 0 < y_\sigma \leq \infty \end{cases} \quad (587b)$$

$$P_2(y_\sigma) = \begin{cases} \sum_{i=0}^5 b_i y_\sigma^i, & -\infty \leq y_\sigma \leq 0 \\ \sum_{i=0}^5 e_i y_\sigma^i, & 0 < y_\sigma \leq \infty \end{cases} \quad (587c)$$

The coefficients B , a_i , b_i , c_i , d_i , and e_i were optimized so that the original function c_σ calculated numerically is accurately reproduced and the results obtained for properties are virtually identical to `mgga_x_br89`.

The difference between `mgga_x_br89_explicit` and `mgga_x_br89_explicit_1` lies in the parameter γ in eq. (550), which is 0.8 and 1, respectively.

`mgga_x_revtpss`^{594,595} (2009)

The objective of this revised version of `mgga_x_tpss` was to reproduce the excellent results for the lattice constants of solids of `gga_x_pbe_sol` without compromising the good results for the atomization energies of molecules. To achieve this goal, the `mgga_x_tpss` form (eq. (576)) was slightly altered by (i) using $f = 3$, thereby shifting that term from 6th order to 8th order in the density-gradient expansion, and (ii) changing μ^{PBE} to a value closer to μ^{GE} used in `gga_x_pbe_sol`, and adjusting the values of c and e to respect the conditions originally obeyed by `mgga_x_tpss`. It turns out that with $\mu^{\text{revTPSS}} = 0.14$, $c = 2.35203946$, and $e = 2.16769874$ the enhancement factor is close to `gga_x_pbe_sol` for the range $s_\sigma < 3$, and especially for $s_\sigma < 1$ that is more relevant for the second-order density-gradient expansion for exchange. However, note that `mgga_x_tpss`

and `mgga_x_revtpss` have an order-of-limits problem,⁶⁷⁹ as the enhancement factor yields different values depending on how the limits $s_\sigma \rightarrow 0$ and $\alpha_\sigma \rightarrow 0$ are taken, as discussed in more detail for `mgga_x_regtpss`.

This functional, when combined with the companion `mgga_c_revtpss`, yields quite accurate results for the lattice constants and cohesive energies of solids, surface energies, and molecular atomization energies.

`mgga_x_tb09`⁶⁸⁰ (2009)

Inspired by the improved description of the band gap of insulators and semiconductors by `mgga_x_bj06` over the standard LDA and PBE (`gga_x_pbe` + `gga_c_pbe`) functionals,⁶⁸¹ Tran and Blaha⁶⁸⁰ suggested the following modification of `mgga_x_bj06` as a further improvement:

$$v_{x\sigma}^{\text{TB09}} = c v_{x\sigma}^{\text{BR89,hole}} + (3c - 2) \frac{1}{\pi} \sqrt{\frac{5}{6}} \sqrt{\frac{\tau_\sigma}{n_\sigma}} \quad (588)$$

where $v_{x\sigma}^{\text{BR89,hole}}$ is eq. (552) with $\gamma = 0.8$. For the parameter c , a system-dependent expression is chosen:

$$c = \alpha + \beta \left[\frac{1}{V_{\text{cell}}} \int_{\text{cell}} d\mathbf{r}' \frac{|\nabla n(\mathbf{r}')|}{n(\mathbf{r}')} \right]^e \quad (589)$$

where V_{cell} is the volume of the unit cell and $e = 1/2$. Associated with the LDA correlation potential from `lda_c_pw`, $\alpha = -0.012$ and $\beta = 1.023$ were obtained by fitting to the experimental band gaps of a set of 23 solids.

`mgga_x_tb09` is to date the most accurate semi-local method for the calculation of band gaps of semiconductors and insulators.^{381,382,682} Note that the TB09 potential (`mgga_x_tb09` + `lda_c_pw`) is also commonly called the modified Becke-Johnson (mBJ) potential.

As is obvious from eq. (589), this functional is not formally a semi-local functional. It is also important to note that because of this, eq. (589) is not implemented in Libxc. Instead, c in eq. (588) is handled as a parameter that has to be provided by the DFT code calling Libxc.

As is also seen from the definition of c , this potential is meant to be used only for bulk periodic systems, since for systems with vacuum or an interface, the average of $|\nabla n|/n$ in the unit

cell has no meaning and eq. (589) cannot be used. For such systems, a solution is either to fix c to a suitable value or to use `mgga_x_lmbj` that depends on a local average of $|\nabla n|/n$.

`mgga_x_rpp09`⁶⁸³ (2009)

This exchange potential was designed to correct deficiencies of `mgga_x_bj06`. Its mathematical form reads

$$v_{x\sigma}^{\text{RPP09}} = v_{x\sigma}^{\text{Slater}} + \frac{1}{\pi} \sqrt{\frac{5}{6}} \sqrt{\frac{D_\sigma}{n_\sigma}} \quad (590)$$

where $v_{x\sigma}^{\text{Slater}}$ is the Slater potential⁴² given by eq. (144) and

$$D_\sigma = \tau_\sigma - \tau_\sigma^{\text{W}} - \frac{|\mathbf{j}_\sigma|^2}{2n_\sigma} \quad (591)$$

Thus, the difference from `mgga_x_bj06` is the function D_σ that is given by $D_\sigma = \tau_\sigma$ in the case of `mgga_x_bj06`, see eq. (578). Thanks to this new form for D_σ , the `mgga_x_rpp09` potential is gauge invariant, exact for any single-orbital system, and approaches zero asymptotically at $r \rightarrow \infty$, which was not the case of `mgga_x_bj06`.

In ref. 684 it was shown that `mgga_x_rpp09` is more accurate than `mgga_x_bj06` for ionization potentials and electron affinities of atoms and molecules. However, the relative accuracy of the two potentials for polarizabilities depends on the type of systems.

Note that the Slater potential in eq. (590) is replaced by eq. (552) for the implementation of `mgga_x_rpp09` in Libxc.

`mgga_x_2d_prhg07_prp10`⁵⁴⁰ (2010)

This potential can be considered as the 2D version of `mgga_x_rpp09`, since it is also based on `mgga_x_bj06` and the arguments invoked for its derivation are basically the same. Therefore, its mathematical form is similar to eq. (590):

$$v_{x\sigma}^{\text{PRP10-2D}} = v_{x\sigma}^{\text{Slater-2D}} + \frac{4}{3\pi} \sqrt{\frac{D_\sigma}{n_\sigma}} \quad (592)$$

where D_σ is also given by eq. (591). Calculations on quasi-2D quantum dots showed that the shape of the `mgga_x_2d_prhg07_prp10` potential is similar to that of the EXX-KLI.

Since the non-local Slater potential^{4,42,675} is expensive to evaluate, Pittalis et al.⁵⁴⁰ suggested to replace it with the approximation given by $v_{x\sigma}^{\text{PRHG07-2D,hole}} = 2e_{x\sigma}^{\text{PRHG07-2D}}$ from the `mgga_x_2d_prhg07` functional. This leads to the semi-local `mgga_x_2d_prhg07_prp10` potential, as implemented in Libxc.

`mgga_x_m11_1`⁶⁸⁵ (2011)

This empirical functional from Peverati and Truhlar⁶⁸⁵ is based on a splitting of the Coulomb operator, leading to an enhancement factor that consists of short- and long-range parts:

$$F_x^{\text{M11-L}} = F_x^{\text{SR-M11-L}} + F_x^{\text{LR-M11-L}} \quad (593)$$

that were chosen as combinations of the enhancement factors of the `gga_x_pbe` (eq. (378)) and `gga_x_rpbe` (eq. (383)) functionals:

$$F_x^{\text{SR-M11-L}} = G(a_\sigma) [f_1^{\text{SR}}(w_\sigma) F_x^{\text{PBE}}(s_\sigma) + f_2^{\text{SR}}(w_\sigma) F_x^{\text{RPBE}}(s_\sigma)] \quad (594a)$$

$$F_x^{\text{LR-M11-L}} = [1 - G(a_\sigma)] [f_1^{\text{LR}}(w_\sigma) F_x^{\text{PBE}}(s_\sigma) + f_2^{\text{LR}}(w_\sigma) F_x^{\text{RPBE}}(s_\sigma)] \quad (594b)$$

The functions $f_i^{\text{SR/LR}}$ are given by eq. (581) with w_σ defined as eq. (91), and $m = 8$ was found sufficiently large for a converged accuracy. The splitting of the Coulomb operator is based on the error function $\text{erf}[\omega(\mathbf{r}_1 - \mathbf{r}_2)]$, therefore the function G is given by

$$G(a_\sigma) = 1 - \frac{8}{3} a_\sigma \left[\sqrt{\pi} \text{erf} \left(\frac{1}{2a_\sigma} \right) - 3a_\sigma + 4a_\sigma^3 + (2a_\sigma - 4a_\sigma^3) e^{-1/(4a_\sigma^2)} \right] \quad (595)$$

with

$$a_\sigma = \frac{\omega}{2(12\pi^2 n_\sigma)^{1/3}} \quad (596)$$

Although the coefficients in the functions $f_i^{\text{SR/LR}}$, as well as the range-separation parameter ω (0.25) in eq. (596) were empirically tuned together with the parameters of `mgga_c_m11_1` correlation, several relations between them were imposed so that the following physical conditions are satisfied: the HEG limit, the second-

order term in the density-gradient expansion, and no contribution from the τ -dependent terms at the end points $w_\sigma = -1$ (exponential tails) and $w_\sigma = 1$ (bond saddle points).

A particular emphasis was put on systems with multiconfigurational character for the development of the M11-L functional, which is claimed accurate for a variety of molecular properties and to compete with hybrid functionals. Regarding solid-state properties, M11-L yields lattice constants with an accuracy that is intermediate between PBE (`gga_x_pbe` + `gga_c_pbe`) and PBEsol (`gga_x_pbe_sol` + `gga_c_pbe_sol`).

Like M06-L (`mgga_x_m06_1` + `mgga_c_m06_1`), also M11-L has been found to lead to unphysical solutions for the hydrogen atom,⁶⁷³ suggesting issues with overfitting.

`mgga_x_mn12_1`⁶⁸⁶ (2012)

Peverati and Truhlar⁶⁸⁶ proposed to extend `gga_x_n12` by adding a dependence on the kinetic-energy density via w_σ (eq. (91)):

$$F_{xc}^{\text{MN12-L}} = \sum_{i=0}^3 \sum_{j=0}^{3-i} \sum_{k=0}^{5-i-j} a_{ijk} \tilde{v}_\sigma^i \tilde{u}_\sigma^j w_\sigma^k \quad (597)$$

where \tilde{v}_σ and $\tilde{u}_\sigma = \tilde{u}(x_\sigma)$ are given by eq. (39) with $\omega_\sigma = 2.5$, and eq. (251) with $\gamma_\sigma = 0.004$, respectively. Alike `gga_x_n12`, this functional is not a pure exchange functional, but rather a nonseparable xc functional. The parameters a_{ijk} in eq. (597) were optimized together with those of `mgga_c_mn12_1` using molecular and solid-state databases. The only constraint that was applied during the optimization was an upper bound of 25 for the absolute values of a_{ijk} . Compared to N12 (`gga_x_n12` + `gga_c_n12`), MN12-L improves the results for most of the tested molecular and solid-state properties.

`mgga_x_revtpss`⁶⁸⁷ (2012)

Since the `mgga_x_tb09` potential has the tendency to underestimate small and medium band gaps of solids, two reparametrizations of eq. (589) were proposed to address this issue. The first reparametrization, `mgga_x_revtpss`, corresponds to $\alpha = 0.488$, $\beta = 0.5$, and $e = 1$, and leads to more

balanced results for band gaps smaller than ~ 7 eV. However, `mgga_x_revtpss` still underestimates band gaps that are smaller than ~ 3 eV, such as those in *sp*-semiconductors, and targeting these systems in particular motivated the `mgga_x_revtpss` reparametrization ($\alpha = 0.267$, $\beta = 0.656$, and $e = 1$) that is more accurate on average for these systems. Note that $e = 1$ for both reparametrizations, while $e = 1/2$ in the original `mgga_x_tb09`. Alike the original `mgga_x_tb09` potential, these two reparametrizations should be combined with a LDA correlation potential like `lda_c_pw`.

`mgga_x_regtpss`⁶⁷⁹ (2012)

The iso-orbital indicators z_σ and α_σ are related by eq. (94b), which suffers from the following order-of-limits anomaly:

$$\lim_{p_\sigma \rightarrow 0} \lim_{\alpha_\sigma \rightarrow 0} z_\sigma = 1 \quad (598a)$$

$$\lim_{\alpha_\sigma \rightarrow 0} \lim_{p_\sigma \rightarrow 0} z_\sigma = 0 \quad (598b)$$

that spreads to the enhancement factor of `mgga_x_revtpss` (and `mgga_x_tpss`) and may be a source of problems. A regularization of the enhancement factor that eliminates this order-of-limits problem can be achieved as follows:

$$F_x^{\text{regTPSS}} = F_x^{\text{revTPSS}}(s_\sigma, \alpha_\sigma) + f(\alpha_\sigma) e^{-cp_\sigma} \times [F_x^{\text{revTPSS}}(s_\sigma, \alpha_\sigma = 0) - F_x^{\text{revTPSS}}(s_\sigma, \alpha_\sigma)] \quad (599)$$

where

$$f(\alpha_\sigma) = \frac{(1 - \alpha_\sigma)^3}{[1 + (d\alpha_\sigma)^2]^{3/2}} \quad (600)$$

with $c = 3$ and $d = 1.475$.

A combination of `mgga_x_regtpss` with `mgga_c_revtpss` for correlation does not provide good results. Therefore, a compatible correlation functional, the GGA `gga_c_regtpss`, was proposed so that the accuracy is qualitatively similar to the parent revTPSS (`mgga_x_revtpss` + `mgga_c_revtpss`) functional.

`mgga_x_vt84`⁶⁸⁸ (2012)

Based on `gga_x_vmt84_ge` and `gga_x_vmt84_pbe`, the enhancement factor of the `mgga_x_vt84`

functional of del Campo et al.⁶⁸⁸ is given by

$$F_x^{\text{meta-VT84}} = 1 + \frac{f_0^{\text{meta-VT84}} e^{-(\gamma/\mu^{\text{GE}})f_0^{\text{meta-VT84}}}}{1 + f_0^{\text{meta-VT84}}} + \left[1 - e^{-\gamma(f_0^{\text{meta-VT84}}/\mu^{\text{GE}})^2} \right] \left(\frac{\mu^{\text{GE}}}{f_0^{\text{meta-VT84}}} - 1 \right) \quad (601)$$

where

$$f_0^{\text{meta-VT84}} = \frac{1}{(1 + \sqrt{e}p_\sigma)^2} \left\{ \left[\mu^{\text{GE}} + c \frac{z_\sigma^3}{(1 + z_\sigma^2)^2} \right] p_\sigma + \frac{146}{2025} \tilde{q}_\sigma^2 - \frac{73}{405\sqrt{2}} \tilde{q}_\sigma \sqrt{\frac{9}{25} z_\sigma^2 + p_\sigma^2} + \left[\frac{\gamma}{(\mu^{\text{GE}})^2} + \frac{\gamma}{\mu^{\text{GE}}} + 1 \right] (\mu^{\text{GE}})^2 p_\sigma^2 + 2\sqrt{e}\mu^{\text{GE}} \frac{9}{25} z_\sigma^2 + e\mu^{\text{GE}} p_\sigma^3 \right\} \quad (602)$$

which shows some differences compared to eq. (576) of `mgga_x_tpss`. The values of the parameters in eqs. (601) and (602) are $\gamma = 0.000023$, $c = 2.14951$, and $e = 1.987$, while \tilde{q}_σ is given by eq. (577) with $b = 0.40$. All these parameters were determined from mathematical constraints: the LO bound, the second-order density-gradient expansion at small p_σ , and the behavior at the limit of large p_σ .

When combined with `mgga_c_revtpss` correlation, the accuracy for molecular properties appears similar to that of revTPSS (`mgga_x_revtpss` + `mgga_c_revtpss`).

`mgga_x_ms0`⁵⁹⁶ (2012)

Sun et al.⁵⁹⁶ constructed a rather simple τ -MGGA functional with a uncoupled dependence on the variables s_σ and α_σ :

$$F_x^{\text{MS0}} = F_x^1(s_\sigma) + f(\alpha_\sigma) [F_x^0(s_\sigma) - F_x^1(s_\sigma)] \quad (603)$$

where F_x^0 and F_x^1 are both given by eq. (378), but with different functions f_0 :

$$f_0(s_\sigma) = \mu^{\text{GE}} s_\sigma^2 + c \quad (604)$$

for F_x^0 and

$$f_0(s_\sigma) = \mu^{\text{GE}} s_\sigma^2 \quad (605)$$

for F_x^1 . The function

$$f(\alpha_\sigma) = \frac{(1 - \alpha_\sigma^2)^3}{1 + \alpha_\sigma^3 + b\alpha_\sigma^6} \quad (606)$$

with $b = 1$ (this parameter is introduced later in `mgga_x_ms2`) interpolates between F_x^0 at $\alpha_\sigma = 0$ and F_x^1 at $\alpha_\sigma = 1$. This form was chosen such that the functional (i) obeys the second-order density-gradient expansion thanks to $\mu = \mu^{\text{GE}}$ in the functions f_0 , (ii) gives accurate exchange jellium surface energies, and (iii) reproduces the HF exchange energies of the H atom and 12-noninteracting electron hydrogenic anion with nuclear charge $Z = 1$ (H^{11-}).⁶⁸⁹ Condition (iii) was used to fix the parameters $c = 0.28771$ in eq. (604) and $\kappa = 0.29$ in eq. (378).

When combined with `gga_c_revtpss` for correlation, `mgga_x_ms0` is somehow less accurate than revTPSS (`mgga_x_revtpss` + `mgga_c_revtpss`) for enthalpies of formation,^{596,597} but more accurate for lattice constants of solids. Considering all results for atoms, molecules, surfaces, and solids, this functional has a well-balanced accuracy.

`mgga_x_ms1`, `mgga_x_ms2`⁵⁹⁷ (2013)

These two functionals have the same form as `mgga_x_ms0`, but with one or two parameters empirically determined using various training sets: AE6 and BH6,^{602,603,690} G2/97,^{505,630} and BH42/03.⁶⁹¹ In the one-parameter functional `mgga_x_ms1`, only $\kappa = 0.404$ (in eq. (378)) was optimized, while $c = 0.18150$ (in eq. (604)) was still chosen such that the functional reproduces the exact exchange energy of the H atom. For the two-parameter `mgga_x_ms2`, both $\kappa = 0.504$ and $b = 4.0$ (in eq. (606)) were optimized, leading to $c = 0.14601$ (again from the H atom). Note that b has a strong influence on the behavior of the enhancement factor for $\alpha_\sigma > 1$.

Compared to `mgga_x_ms0`, these two functionals lead to improved results for heats of formation, while being of similar (good) accuracy for barrier heights and noncovalent interactions.

`mgga_x_bloc`⁶⁹² (2013)

This functional was constructed with a balanced nonlocality, such that it is compatible with `mgga_c_tpssloc`. To achieve this, Con-

stantin et al.⁶⁹² generalized the power f in eq. (576) of the `mgga_x_tpss` functional by making it z_σ -dependent:

$$f(z_\sigma) = a + bz_\sigma \quad (607)$$

This function f , which controls the behavior of the functional at small s_σ , should obey the following constraints: (i) $f(z_\sigma) \geq 3$ for $z_\sigma \leq 0.3$, so that the fourth-order density-gradient expansion is recovered for a large range of s_σ , (ii) $f(z_\sigma) \leq 2$ for $z_\sigma \geq 0.6$, so that the enhancement factor of `mgga_x_bloc` is larger than the one of `mgga_x_tpss` in the rapidly varying density region, and (iii) the functional reproduces the xc jellium surface energies obtained with the accurate diffusion MC method when combined with `mgga_c_tpssloc`.^{606,693} With the values $a = 4.0$ and $b = -3.3$, these three conditions are satisfied.

The BLOC functional, `mgga_x_bloc` plus `mgga_c_tpssloc`, appears to improve over the standard TPSS (`mgga_x_tpss` + `mgga_c_tpss`) and revTPSS (`mgga_x_revtpss` + `mgga_c_revtpss`) for a series of molecular and solid-state properties.

`mgga_x_mbeef`⁶⁹⁴ (2014)

This τ -MGGA functional is built in a similar way as the exchange part of `gga_xc_beefvdw` (see eq. (543)) which is further augmented by a dependence on the kinetic-energy density:

$$F_x^{\text{mBEEF}} = \sum_{m=0}^M \sum_{n=0}^N a_{mn} B_m[r(s_\sigma)] B_n[f(\alpha_\sigma)] \quad (608)$$

The variable transformation $r(s_\sigma)$ is given by eq. (544) with the value of $q = \kappa^{\text{PBE}}/\mu^{\text{GE}} = 6.5124$ obtained through a Padé approximant to the `gga_x_pbe_sol` enhancement factor, while $f(\alpha_\sigma)$ is eq. (606) with $b = 1$, the same function as in `mgga_x_ms0`.

To optimize the 64 parameters of the functional ($M = N = 7$ in eq. (608)), Wellendorff et al.⁶⁹⁴ followed a similar protocol as for `gga_xc_beefvdw`, but with slightly updated training datasets. They used G3/99⁶⁹⁵ (formation energies of molecules), RE42⁶⁴¹ (reaction energies), CE27a (chemisorption energies, ref-

erenced to free atoms rather than gas-phase adsorbates as in the original CE27 set⁶⁴¹), Sol54Ec (cohesive energies), and Sol58LC (lattice constants). The two latter sets^{641,696} expand the original Sol27Ec and Sol27LC sets by including diatomic rocksalt, cesium chloride, and zincblende crystals. Note that the S22⁵²¹ and S22 \times 5⁵⁶⁰ datasets of weak intermolecular interaction energies of molecular complexes were this time not included in the training set.

The mBEEF functional (`mgga_x_mbeef` combined with `gga_c_pbe_sol`) yields more accurate cohesive energies and lattice constants than `gga_xc_beefvdw`+vdW-DF2, while retaining the high accuracy for molecular and surface properties. Slightly improved results are also obtained for the S22 dataset, even though no van der Waals dispersion term being included in the functional, but mBEEF is still clearly less accurate than other van der Waals functionals like C09-vdW (see `gga_x_c09x`) or optPBE-vdW (see `gga_x_optpbe_vdw`).

`mgga_x_tlda`²⁸⁶ (2014)

Following the strategy used for the construction of `mgga_x_lta`, eq. (563) is used in `lda_x` to obtain a τ -MGGA. However, while this was done for the full dependence on n_σ in the case of `mgga_x_lta`, here the substitution is done partially, only in the exchange energy per particle (instead of per volume). The motivation for this choice is the possibility to interpret the functional as an approximation for the averaged exchange hole using the hole of the HEG. This leads to the following enhancement factor:

$$F_x^{\text{tLDA}} = \left(\frac{\tilde{t}_\sigma}{C_F} \right)^{1/5} \quad (609)$$

Calculations on light spherical atoms (He, Be, Ne, Mg, and Ar) lead to rather reasonable total energies (more accurate than `lda_x`, but less accurate than `gga_x_pbe`), however negative values are obtained for derivative discontinuities, in contrast to the positive values obtained with EXX-KLI. The functional `mgga_x_hlta`, which is discussed later, is a generalization of `mgga_x_lta` and `mgga_x_tlda`.

`mgga_x_revtpb09_lhp`⁶⁹⁷ (2014)

Jishi et al.⁶⁹⁷ reported that the original `mgga_x_tb09` potential, as well as its reparameterized version `mgga_x_revttb09_ktb_2`, may lead to band gaps of lead halide perovskites (LHP) that are underestimated by more than 1 eV. This prompted them to propose a new reparametrization that is much more accurate for these compounds. The new values of the parameters in eq. (589) were obtained with spin-orbit coupling included in the calculations, and they are $\alpha = 0.4$, $\beta = 1.0$, and $e = 1/2$.

`mgga_x_mvs`⁵⁹⁸ (2015)

This *made very simple* (MVS) τ -MGGA functional was constructed in order to obey a tight LO bound,⁶⁹⁸ together with other constraints, including the second-order density-gradient expansion for the slowly varying density and the asymptotic expansion of the exchange energy at large nuclear charge Z of neutral atoms (see ref. 273 and `gga_x_eb88`). The enhancement factor is written as

$$F_x^{\text{MVS}} = \frac{1 + k_0 f_x(\alpha_\sigma)}{(1 + b s_\sigma^4)^{1/8}} \quad (610)$$

In F_x^{MVS} , $k_0 = 0.174$ was determined from the tight LO bound at $\alpha_\sigma = 0$. The denominator was designed such that eq. (427) is obeyed, a required condition to get a finite exchange-energy density for the nonuniform scaling limit of a density.^{538,698} The parameter $b = 0.0233$ was fixed such that the exact exchange energy of the H atom is reproduced. Finally,

$$f_x(\alpha_\sigma) = \frac{1 - \alpha_\sigma}{[(1 + e_1 \alpha_\sigma^2)^2 + c_1 \alpha_\sigma^4]^{1/4}} \quad (611)$$

interpolates between the two regimes $\alpha_\sigma = 0$ (one or two-electron systems) and $\alpha_\sigma = 1$ (HEG), and tends to a constant at $\alpha_\sigma \rightarrow \infty$. The parameter $e_1 = -1.6665$ is fixed by the large- Z asymptotic expansion mentioned above, and $c_1 = 0.7438$ so that the second-order density-gradient expansion is recovered.

Note that the enhancement factor given by eq. (610) is rather different from most other GGA and MGGA functionals, as it decreases monotonically with increasing s_σ or α_σ . Other functionals that show a similar behavior are

`mgga_x_mbeef` and `mgga_x_scan`.

Combined with `gga_c_regtpss`, this functional is accurate for intermolecular interaction energies (even though no dispersion van der Waals term is included) and lattice constants of solids, quite accurate for barrier heights, but rather poor for the heats of formation of molecules, similarly to PBE (`gga_x_pbe` + `gga_c_pbe`).

`mgga_x_scan`²⁷⁶ (2015)

The *strongly constrained and appropriately normed* (SCAN) exchange functional, together with its correlation companion `mgga_c_scan`, was built in order to obey a large number of exact conditions (17 in total!). The price to pay for this is, of course, complexity, and this is indeed one of the most complex functionals ever proposed.

The idea is to use the iso-orbital indicator α_σ to interpolate between the various regimes, each one being well-described by a different form. Due to its connection to the electron-localization function,^{230,667,668} α_σ can be used to measure the localization of the electrons and to discern between different kinds of bonds. In regions of space dominated by a single covalent bond $\alpha_\sigma \approx 0$, while in the case of a metallic bond $\alpha_\sigma \approx 1$, and for a weak bond $\alpha_\sigma \gg 1$. In practice, the interpolation is performed between $\alpha_\sigma = 0$ and $\alpha_\sigma = 1$, while the region relevant for weak bonds (large α_σ) is obtained through an extrapolation. Based on these arguments, Sun et al.²⁷⁶ proposed the following enhancement factor:

$$F_x^{\text{SCAN}} = \{h_x^1(s_\sigma, \alpha_\sigma) + f(\alpha_\sigma) \times [h_x^0 - h_x^1(s_\sigma, \alpha_\sigma)]\} g(s_\sigma) \quad (612)$$

The interpolating function f is chosen as

$$f(\alpha) = e^{-c_1 \alpha / (1-\alpha)} \theta(1-\alpha) - d e^{c_2 / (1-\alpha)} \theta(\alpha-1) \quad (613)$$

where c_1 , c_2 , and d are parameters and θ is the step function. As eq. (613) is also used by `mgga_c_scan`, the spin σ and exchange (x) or correlation (c) indices are not shown.

To construct the function h_x^1 , which describes the $\alpha \approx 1$ regime, Sun et al.²⁷⁶ used a `gga_x_pbe` form, eq. (378), where f_0 is con-

structed by using the fourth-order density-gradient expansion for exchange,²⁶⁷ which is valid for small s_σ and $\alpha_\sigma \approx 1$:

$$f_0^{\text{SCAN}}(s_\sigma, \alpha_\sigma) = \mu^{\text{GE}} s_\sigma^2 + b_4 s_\sigma^4 e^{-(|b_4|/\mu^{\text{GE}})s_\sigma^2} + \left[b_1 s_\sigma^2 + b_2 (1 - \alpha_\sigma) e^{-b_3(1-\alpha_\sigma)^2} \right]^2 \quad (614)$$

with $b_1 = 511/(27000b_2)$, $b_2 = \sqrt{5913/405000}$, $b_3 = 1/2$, and $b_4 = (\mu^{\text{GE}})^2/\kappa - 1606/18225 - b_1^2$.

The constant $h_x^0 = 1.174$ was fixed by imposing the strict LO bound for two-electron densities.⁶⁹⁸ Finally, the function g is defined by

$$g(s_\sigma) = 1 - e^{-a_1/\sqrt{s_\sigma}} \quad (615)$$

with the parameter $a_1 = 4.9479$ chosen such that the functional reproduces the exact exchange energy of the H atom.

The four remaining parameters, namely $c_{1x} = 0.667$, $c_{2x} = 0.8$, and $d_x = 1.24$ in eq. (613), and $\kappa = 0.065$ in eq. (378) and in the definition of b_4 , were fit together with the three parameters of `mgga_c_scan` (c_{1c} , c_{2c} , and d_c) by requiring that SCAN reproduce accurately the following quantities: (i) the large nuclear charge Z asymptotic coefficients of the xc energy of rare-gas atoms,^{273,274,546} (ii) the binding energy curve of Ar₂,⁶⁹⁹ and (iii) jellium surface xc energies calculated from a MC method.^{606,700}

SCAN is a popular functional, especially in the solid-state community. However, it is also known to lead to numerical instabilities, which prompted the development of more stable versions of SCAN, namely rSCAN (`mgga_x_rscan` + `mgga_c_rscan`), r²SCAN (`mgga_x_r2scan` + `mgga_c_r2scan`), and r⁴SCAN exchange (`mgga_x_r4scan`).

`mgga_x_theta_mgga`⁷⁰¹ (2015)

The enhancement factor of this functional is given by eq. (378) with $\kappa = \kappa^{\text{PBE}}$ and a function f_0 that reads

$$f_0(s_\sigma, \theta_\sigma) = \{ \tilde{g}(\theta_\sigma) \mu^{\text{H}} + [1 - \tilde{g}(\theta_\sigma)] \mu^{\text{GE}} \} s_\sigma^2 \quad (616)$$

where

$$\tilde{g}(\theta_\sigma) = \frac{1}{1 + \theta_\sigma^2} \quad (617)$$

with

$$\theta_\sigma = \frac{\left| \nabla \left(\frac{|\nabla n_\sigma|^2}{n_\sigma^2} \right) \right|^2}{\frac{|\nabla n_\sigma|^6}{n_\sigma^6}} \quad (618)$$

Equation (616) is an interpolation between μ^{GE} of the second-order density-gradient expansion at small s_σ and $\mu^{\text{H}} = 0.27583$, which was determined such that `gga_x_pbe_mol` recovers the exact exchange energy of the H atom. The functional `mgga_x_theta_mgga` does not depend on the kinetic-energy density and is thus an orbital-free functional. However, compared to all other orbital-free $\nabla^2 n$ -MGGA functionals, the notable difference is that the dependence on the second derivatives of the density n_σ is not via $\nabla^2 n_\sigma$, but via $\nabla |\nabla n_\sigma|$ in the numerator of the density overlap regions indicator θ_σ . This can be seen from

$$\begin{aligned} \nabla \left(\frac{|\nabla n_\sigma|^2}{n_\sigma^2} \right) &= 2 \frac{|\nabla n_\sigma|}{n_\sigma^3} \\ &\quad \times (n_\sigma \nabla |\nabla n_\sigma| - |\nabla n_\sigma| \nabla n_\sigma) \end{aligned} \quad (619)$$

When combined with its correlation counterpart `mgga_c_theta_mgga`, the accuracy for various molecular properties is overall good and sometimes quite similar to TPSS (`mgga_x_tpss` + `mgga_c_tpss`) or revTPSS (`mgga_x_revtpss` + `mgga_c_revtpss`).

`mgga_x_mn15_1`⁷⁰² (2015)

This nonseparable xc functional has the same form as `mgga_x_mn12_1`, the only difference concerns the linear coefficients a_{ijk} in eq. (597) that were reoptimized together with the associated pure correlation `mgga_c_mn15_1`. Compared to MN12-L (`mgga_x_mn12_1` + `mgga_c_mn12_1`), the reference database for the optimization was enlarged such that MN15-L has a broader accuracy for molecular and solid-state properties.

`mgga_x_tm`⁷⁰³ (2016)

Starting from the construction of an exchange hole, Tao and Mo⁷⁰³ arrived at the following

expression for the enhancement factor:

$$F_x^{\text{TM}} = \tilde{w}_\sigma F_x^{\text{DME}} + (1 - \tilde{w}_\sigma) F_x^{\text{SC}} \quad (620)$$

which is a linear combination of two enhancement factors weighted by the function

$$\tilde{w}_\sigma = \frac{z_\sigma^2 + 3z_\sigma^3}{(1 + z_\sigma^3)^2} \quad (621)$$

The DME (density matrix expansion) and SC (slowly varying correction) enhancement factors are given by

$$F_x^{\text{DME}} = \frac{1}{f_\sigma^2} + \frac{7}{9} \frac{R_\sigma}{f_\sigma^4} \quad (622)$$

and

$$F_x^{\text{SC}} = \left\{ 1 + 10 \left[\left(\mu^{\text{GE}} + \frac{50}{729} p_\sigma \right) p_\sigma + \frac{146}{2025} \tilde{q}_\sigma^2 - \frac{73}{405} \tilde{q}_\sigma \frac{3}{5} z_\sigma (1 - z_\sigma) \right] \right\}^{1/10} \quad (623)$$

respectively. In eq. (622)

$$f_\sigma = \left(1 + 10 \frac{70}{27} y_\sigma + \beta y_\sigma^2 \right)^{1/10} \quad (624)$$

and

$$R_\sigma = 1 + \frac{595}{54} (2\lambda - 1)^2 p_\sigma - \frac{1}{C_F} \left[\tilde{t}_\sigma - 3 \left(\lambda^2 - \lambda + \frac{1}{2} \right) \left(\tilde{t}_\sigma - C_F - \frac{1}{72} x_\sigma^2 \right) \right] \quad (625)$$

where $y_\sigma = (2\lambda - 1)^2 p_\sigma$ and \tilde{q}_σ is eq. (577) with $b = 0$. The two parameters $\beta = 79.873$ (in eq. (624)) and $\lambda = 0.6866$ (in eq. (625)) were determined from the exact exchange energy of the H atom and the requirement of a smooth and monotonically increasing behavior of F_x^{DME} .

Combined with the associated correlation `mgga_c_tm`, the functional appears to be fairly accurate for various molecular and solid-state properties. Tao and Mo⁷⁰³ also combined `mgga_x_tm` with `mgga_c_tpss`, which leads to substantial improvement for the jellium surface xc energies.

`mgga_x_sa_tpss`⁷⁰⁴ (2016)

Constantin et al.⁷⁰⁴ modified `mgga_x_tpss` in order to achieve the correct $\propto -1/z$ decay of the xc energy per particle and xc potential with the distance z from the surface in the vacuum. The modification consists of replacing the constant $\kappa = \kappa^{\text{PBE}}$ in eqs. (378) and (576) by the function

$$\kappa_\sigma = \frac{2\pi}{3\sqrt{5}} \frac{\sqrt{\alpha_\sigma + 1}}{\sqrt{a + \ln(\alpha_\sigma + b)}} \quad (626)$$

where $a = 2.413$ and $b = 0.348$ were chosen such that $\kappa = \kappa^{\text{PBE}}$ (i.e., `mgga_x_tpss`) is recovered when $\alpha = 1$ and $\alpha = 0$. The resulting functional still obeys the exact mathematical constraints satisfied by `mgga_x_tpss`. However, an exception is the LO bound that is satisfied only globally, while it is also satisfied locally by `mgga_x_tpss`. Yet, Constantin et al.⁷⁰⁴ mentioned that a simplified version of the Lewin-Lieb bound^{705,706} is locally satisfied.

The accuracy of the functional is similar to that of `mgga_x_tpss` for systems with covalent bonds, but it should improve the description of surface-related properties.

`mgga_x_mbeefvdw`⁷⁰⁷ (2016)

The empirical mBEEF-vdW functional was developed for accuracy for a wide range of systems and properties. Its construction follows the strategy used for its predecessors, `gga_xc_beefvdw` and `mgga_x_mbeef`. The exchange part of mBEEF-vdW, `mgga_x_mbeefvdw`, is given by eq. (608) with $M = N = 4$, while $M = N = 7$ was used for `mgga_x_mbeef`. The training sets used for the optimization of the 25 coefficients a_{mn} in eq. (608) are essentially the same as the ones used for `gga_xc_beefvdw` and `mgga_x_mbeef`. The training was carried out in conjunction with a correlation functional that consists of a combination of `lda_c_pw`, `gga_c_pbe_sol`, and the non-local vdW-DF2 term,⁵⁰⁷ whose mixing coefficients were also optimized, leading to the values 0.41, 0.36, and 0.89, respectively. As for its predecessors, a regularization was applied to obtain a smooth exchange functional. It should be noted that neither `mgga_x_mbeefvdw` nor the correlation part reduce to the correct LDA limit for the HEG.

A comparison with numerous other GGA and MGGA functionals shows that mBEEF-vdW is among the most accurate functionals for many of the considered properties.

[mgga_x_gx](#), [mgga_x_pbe_gx](#)⁷⁰⁸ (2017)

By considering the finite HEG, Loos⁷⁰⁸ derived a functional that is given by

$$F_x^{\text{GX}} = \begin{cases} F_x^{\text{gX}}(\alpha_\sigma), & 0 \leq \alpha_\sigma \leq 1 \\ 1 + (1 - \alpha_\infty) \frac{1 - \alpha_\sigma}{1 + \alpha_\sigma}, & \alpha_\sigma > 1 \end{cases} \quad (627)$$

where $\alpha_\infty = 0.852$ and

$$F_x^{\text{gX}} = \frac{C_x^{\text{GLDA}}(0)}{C_x^{\text{GLDA}}(1)} + \alpha_\sigma \frac{c_0 + c_1 \alpha_\sigma}{1 + (c_0 + c_1 - 1) \alpha_\sigma} \times \left[1 - \frac{C_x^{\text{GLDA}}(0)}{C_x^{\text{GLDA}}(1)} \right] \quad (628)$$

with $C_x^{\text{GLDA}}(1) = -C_x$, $C_x^{\text{GLDA}}(0) = -(4/3)(2/\pi)^{1/3}$, $c_0 = 0.827411$, and $c_1 = -0.643560$. The latter two parameters were obtained by fitting to the exact exchange energy of the finite HEG for occupations of orbitals corresponding to an angular momentum ranging from 1 to 10. The particularity of this τ -MGGA functional is to depend on the electron density n_σ and iso-orbital indicator α_σ , but not on a reduced-density gradient like x_σ or s_σ . As it should, eq. (628) reduces to [lda_x](#) for the HEG, i.e. when $\alpha_\sigma = 1$. MGGA functionals of this type are termed as generalized LDA by Loos⁷⁰⁸. The [mgga_x_gx](#) functional provides inaccurate exchange energies of neutral atoms and ions and is numerically unstable.

Loos⁷⁰⁸ noted that a problem of [mgga_x_gx](#) is its inability to distinguish between homogeneous and inhomogeneous one-electron systems. That is due to the aforementioned missing dependence on a reduced-density gradient. To remedy this, [mgga_x_gx](#) is multiplied by a simplified PBE-like enhancement factor:

$$F_x^{\text{PBE-GX}} = \frac{1}{1 + \mu x_\sigma^2} F_x^{\text{GX}} \quad (629)$$

where $\mu = 0.001015549$ was chosen so that the exact exchange energy of the H atom is obtained. The exchange energies of neutral atoms and ions obtained with [mgga_x_pbe_gx](#)

are accurate and compete with standard GGA and MGGA functionals. The functional [mgga_x_pbe_gx](#) was also combined with various GGA and MGGA correlation functionals, and the combination [mgga_x_pbe_gx](#) + [mgga_c_scan](#) appears quite accurate for atomization energies of diatomic molecules.

[mgga_x_2d_js17](#)⁷⁰⁹ (2017)

The construction of this functional for 2D systems starts with a density matrix expansion for the exchange hole that is required to satisfy the HEG limit ([lda_x_2d](#)) and two other conditions for the behavior with respect to the distance $\mathbf{r}_{12} = \mathbf{r}_2 - \mathbf{r}_1$ from the reference electron (second-order term in the expansion in $|\mathbf{r}_{12}|$ and large $|\mathbf{r}_{12}|$ limit). The resulting enhancement factor is given by

$$F_x^{\text{JS17-2D}} = \frac{1}{f_\sigma} + \frac{2}{5} \frac{R_\sigma}{f_\sigma^3} \quad (630)$$

where we have neglected the dependence on the paramagnetic current density \mathbf{j}_σ (eq. (95)) that was introduced for gauge invariance. Furthermore

$$f_\sigma = \left[1 + 90(2\lambda - 1)^2 p_\sigma^{2D} + \beta(2\lambda - 1)^4 (p_\sigma^{2D})^2 \right]^{1/15} \quad (631)$$

and

$$R_\sigma = 1 + \frac{128}{21} (2\lambda - 1)^2 p_\sigma^{2D} + \frac{1}{4\pi} \left[3 \left(\lambda^2 - \lambda + \frac{1}{2} \right) (\tilde{t}_\sigma^{2D} - 4\pi) - \tilde{t}_\sigma^{2D} \right] \quad (632)$$

with $\lambda = 0.74$ (fit to EXX-KLI results) and $\beta = 30$ such that $F_x^{\text{JS17-2D}}$ is smooth at $p_\sigma^{2D} \approx 0$. In these equations, p_σ^{2D} is given by eq. (56) and \tilde{t}_σ^{2D} is given by eq. (77) with $m = 2$.

Calculations on 2D systems (parabolically confined quantum dots and Gaussian quantum dots) show an agreement with EXX-KLI that is improved compared to the other 2D functionals [gga_x_2d_b86_mgc](#), [gga_x_2d_b88](#), and [mgga_x_2d_prhg07](#).

[mgga_x_rev06_1](#)⁶⁷² (2017)

This functional has the same form as `mgga_x_m06_1` and was combined with the corresponding correlation `mgga_c_revM06_1` for a reoptimization of the parameters. Compared to M06-L (`mgga_x_m06_1` + `mgga_c_m06_1`), the functional is made less prone to numerical problems by imposing some degree of smoothness and removing large terms in eq. (561), which is the second term in eq. (580) (M06-L and revM06-L have overall 34 and 31 parameters, respectively). With respect to M06-L, the results are improved for both molecular and solid-state properties.

`mgga_x_scan1`, `mgga_x_revscan1`, `mgga_x_mvsl`⁷¹⁰⁻⁷¹² (2017)

Mejia-Rodriguez and Trickey proposed and tested various deorbitalized versions of the τ -MGGA functionals TPSS (`mgga_x_tpss` + `mgga_c_tpss`), SCAN (`mgga_x_scan` + `mgga_c_scan`), and MVS (`mgga_x_mvs` + `mgga_c_regtpss`). The replacement of the kinetic-energy density τ_σ by an orbital-free expression depending on n_σ , ∇n_σ , and $\nabla^2 n_\sigma$ was achieved using six different approximations, leading overall to 18 deorbitalized functionals. Among them, `mgga_x_scan1` and `mgga_x_mvsl` are the most interesting for accuracy, and they are described below.

`mgga_x_scan1` uses PC07opt,⁷¹⁰ a reoptimized version of the PC07 expression,⁷¹³ for τ_σ . Its expression is given by

$$\tau_\sigma^{\text{PC07}} = \tau_\sigma^{\text{TF}} F_t^{\text{PC07}}(p_\sigma, q_\sigma) \quad (633)$$

where τ_σ^{TF} is given by eq. (70) and

$$F_t^{\text{PC07}} = F_t^{\text{W}} + z_\sigma^{\text{PC07}} \theta^{\text{PC07}}(z_\sigma^{\text{PC07}}) \quad (634)$$

with $F_t^{\text{W}} = (5/3) p_\sigma$, $z_\sigma^{\text{PC07}} = F_t^{\text{MGE4}} - F_t^{\text{W}}$,

$$\theta^{\text{PC07}}(z) = \begin{cases} 0, & z \leq 0 \\ \left[\frac{1 + e^{a/(a-z)}}{e^{a/z} + e^{a/(a-z)}} \right]^b, & 0 < z < a \\ 1, & z \geq a \end{cases} \quad (635)$$

and

$$F_t^{\text{MGE4}} = \frac{F_t^{(0)} + F_t^{(2)} + F_t^{(4)}}{\sqrt{1 + \left[\frac{F_t^{(4)}}{1 + F_t^{\text{W}}} \right]^2}} \quad (636)$$

where $F_t^{(0)} = 1$, $F_t^{(2)} = (1/9) F_t^{\text{W}} + (20/9) q_\sigma$, and $F_t^{(4)} = (8/81) q_\sigma^2 - (1/9) p_\sigma q_\sigma + (8/243) p_\sigma^2$. Perdew and Constantin⁷¹³ fit the kinetic energy of atomic and jellium systems to find the parameters $a = 0.5389$ and $b = 3$ in eq. (635) (PC07). Mejía-Rodríguez and Trickey⁷¹⁰ proposed the new values $a = 1.784720$ and $b = 0.258304$, leading to PC07opt.

The orbital-free kinetic-energy density used in `mgga_x_mvsl`, which is based on the form developed in ref. 714, is given by

$$\tau_\sigma^{\text{CRopt}} = \tau_\sigma^{\text{TF}} F_t^{\text{CRopt}}(p_\sigma, q_\sigma) \quad (637)$$

where

$$F_t^{\text{CRopt}} = 1 + F_t^{\text{W}} + z_\sigma^{\text{CRopt}} \theta^{\text{CR}}(z_\sigma^{\text{CRopt}}) \quad (638)$$

with $z_\sigma^{\text{CRopt}} = a p_\sigma + b q_\sigma - F_t^{\text{W}}$, where $a = -0.295491$ and $b = 2.615740$,⁷¹⁰ and

$$\theta^{\text{CR}}(z) = \left\{ 1 - e^{-1/|z|^4} [1 - H(z)] \right\}^{1/4} \quad (639)$$

where $H(z)$ is the Heaviside step function.

SCAN-L (`mgga_x_scan1` + `mgga_c_scan1`) leads to an accuracy that is quite close to that of the parent SCAN functional for molecular and solid-state properties. However, the band gaps of solids are exceptions: they are smaller with SCAN-L, which can be explained by the xc derivative discontinuity.³¹² Note that `mgga_x_revscan1`, a deorbitalized version of `mgga_x_revscan` also using $\tau_\sigma^{\text{PC07}}$, has not been discussed in the literature, but is available in Libxc. The `mgga_x_mvsl` functional was tested more extensively in ref. 715, where it was shown that it is more accurate than the parent `mgga_x_mvs` functional for various molecular and solid-state properties (excluding band gaps).

`mgga_x_lltpss`⁷¹⁶ (2018)

With the goal of accelerating calculations at

the MGGA level using the density fitting technique, Bienvenu and Knizia⁷¹⁶ replaced the kinetic-energy density τ_σ in `mgga_x_tpss` by the orbital-free $\nabla^2 n_\sigma$ -dependent approximation $\tau_\sigma^{\text{PC07}}$ given by eq. (633).⁷¹³ Calculations on a set of 28 reaction energies showed that the deorbitalized LL-TPSS, the combination of `mgga_x_lltpss` and `mgga_c_lltpss`, only slightly degrades the results compared to the original TPSS (`mgga_x_tpss` + `mgga_c_tpss`) functional.

`mgga_x_rtpss`⁷¹⁷ (2018)

The motivation for proposing this functional was to improve results for the chemisorption of atoms and molecules on surfaces over those obtained with popular GGA and MGGA functionals. Since `gga_x_rpbe` improves over `gga_x_pbe` for such systems, eq. (383) is chosen and turned into a τ -MGGA by replacing μs_σ^2 by the function f_0^{TPSS} (eq. (576)) used in `mgga_x_tpss`:

$$F_x^{\text{RTPSS}} = 1 + \kappa \left(1 - e^{-f_0^{\text{TPSS}}/\kappa} \right) \quad (640)$$

Among the constraints satisfied by `mgga_x_tpss`, the exact exchange energy of the H atom is the only one that is not satisfied by eq. (640). RTPSS (`mgga_x_rtpss` + `mgga_c_tpss`) has an accuracy similar to RPBE (`gga_x_rpbe` + `gga_c_pbe`) for chemisorption properties, and improves over popular functionals like PBE (`gga_x_pbe` + `gga_c_pbe`), TPSS (`mgga_x_tpss` + `mgga_c_tpss`), and SCAN (`mgga_x_scan` + `mgga_c_scan`). However, it does not appear particularly accurate in the case of the weaker physisorption of molecules on surfaces.

`mgga_x_revscan`⁷¹⁸ (2018)

This functional has the same form as `mgga_x_scan`, but the parameters in eq. (613) were reoptimized together with the parameters in `mgga_c_revscan` to give accurate atomization energies for the molecules in the AE6 test set.^{602,603} The new values of the exchange parameters are $c_{1x} = 0.607$, $c_{2x} = 0.7$, and $d_x = 1.37$.

`mgga_x_ms2b`⁷¹⁹ (2019)

The functional MS2 β (`mgga_x_ms2b`) is a modified version of `mgga_x_ms2`, where the iso-orbital indicator α_σ (eq. (80)) is replaced by $2\beta_\sigma$, where β_σ is defined by

$$\beta_\sigma = \frac{\alpha_\sigma}{\alpha_\sigma + \frac{5}{3}s_\sigma^2 + 1} \quad (641)$$

The motivation for this modification is that derivatives of α_σ vary rapidly in space and lead to numerical instabilities, while β_σ largely alleviates such problems. The parameters in MS2 β are as follows. $\kappa = 0.504$ has the same value as in `mgga_x_ms2`. To recover the same behavior for noncovalent bonds as that for `mgga_x_ms2`, the parameter $b^{\text{MS2}} = 4.0$ in `mgga_x_ms2` is adjusted to $b = (27b^{\text{MS2}} - 9)/64 = 1.546875$. As discussed for `mgga_x_ms2_rev`, the parameter c was slightly modified to $c = 0.14607$. As for `mgga_x_ms2`, the associated correlation is `gga_c_regtpps`.

`mgga_x_ms2_rev`⁷¹⁹ (2019)

This functional is the same as `mgga_x_ms2`, but with a slight change of the value of the parameter c (0.14607 here, while it is 0.14601 in `mgga_x_ms2`).

`mgga_x_revtb09_hop`⁷²⁰ (2019)

For the same reason that led to the development of `mgga_x_revtb09_lhp`, Traoré et al.⁷²⁰ reparameterized `mgga_x_tb09` for improving the results for 3D and layered hybrid organic-inorganic perovskites (HOP), whose band gaps are clearly underestimated by `mgga_x_tb09`. It was found that tuning α in eq. (589) is sufficient. This led to $\alpha = 0.65$, while $\beta = 1.023$ and $e = 1/2$ remain unchanged. Note that the calculations were done in a pseudopotential framework and with spin-orbit coupling included. `mgga_x_revtb09_hop` leads to band gaps for these perovskites that agree well with the experimental values.

`mgga_x_revtm`⁷²¹ (2019)

This functional has the same analytical form as `mgga_x_tm`, but uses $b = 0.40$ in the definition of \tilde{q}_σ (see eq. (577)), as in `mgga_x_tpss`. The motivation behind this modification is to improve the behavior of the functional in the bond region, where the density varies slowly,

and in the region of overlapping closed shells, where the iso-orbital indicator α_σ is large. When used in combination with `mgga_c_revtm`, the functional improves over the original TM (`mgga_x_tm` + `mgga_c_tm`) for many of the considered molecular and solid-state properties, as well as jellium surface energies.

`mgga_x_mbrxh_bg`, `mgga_x_mbrxc_bg`⁷²² (2019) Aiming at removing the dependence on $\nabla^2 n_\sigma$ present in `mgga_x_br89`, Patra et al.⁷²² used the second-order density-gradient expansion of τ_σ ,

$$\tau_\sigma = \tau_\sigma^{\text{TF}} + \frac{1}{9}\tau_\sigma^{\text{W}} + \frac{1}{6}\nabla^2 n_\sigma \quad (642)$$

to approximate $\nabla^2 n_\sigma$ by

$$\nabla^2 n_\sigma \approx 6 \left(\tau_\sigma - \tau_\sigma^{\text{TF}} - \frac{1}{9}\tau_\sigma^{\text{W}} \right) \quad (643)$$

and substituted this expression in the expression for the exchange-hole curvature given by eq. (550). This leads to

$$\tilde{C}_{x\sigma} = \left(1 - \frac{2}{3}\gamma \right) \tilde{t}_\sigma - C_{\text{F}} + \frac{1}{12} \left(\gamma - \frac{1}{6} \right) x_\sigma^2 \quad (644)$$

Note that the corresponding eq. (10) in ref. 722 contains errors. This led Patra et al.⁷²² to propose a more general form:

$$\tilde{C}_{x\sigma} = a_1 2\tilde{t}_\sigma - C_{\text{F}} + a_2 x_\sigma^2 + a_3 x_\sigma^4 \quad (645)$$

where a_1 , a_2 , and a_3 are parameters.

Two sets of values for (a_1, a_2, a_3) were proposed. The first set, $(0.23432, 0.089, 0.0053)$ (`mgga_x_mbrxh_bg`), was obtained by using the electron density and exchange hole of the H atom as originally for `mgga_x_br89`, leading to the nonlinear equation of the Becke–Roussel scheme (eq. (549)). For the second set, $(0.074746, 0.147, 0.0032)$ (`mgga_x_mbrxc_bg`), a cuspless H atom was used, which results in a nonlinear equation that differs from eq. (549):

$$\frac{(1 + c_\sigma)^{5/3} e^{-2c_\sigma/3}}{c_\sigma - 3} = (32\pi)^{2/3} \frac{1}{6\tilde{C}_{x\sigma}} \quad (646)$$

In both cases, a_1 was determined by requiring that the correct HEG limit, `lda_x`, is recovered for a constant electron density, while a_2

was fixed from a modified second-order density-gradient expansion.⁵⁵⁵ Then, a_3 was empirically determined by a fit to the band gap of a set of solids (C, Si, Ge, InAs, AgBr, and Ne).

The functional `mgga_x_mbrxc_bg` is particularly interesting for band gap calculations, since it is clearly more accurate than standard functionals like PBE (`gga_x_pbe` + `gga_c_pbe`) or SCAN (`mgga_x_scan` + `mgga_c_scan`).

`mgga_x_mggac`⁶¹⁶ (2019)

The construction of this functional is based on `mgga_x_br89` or, more particularly, on `mgga_x_mbrxc_bg`. The objective is to obtain a functional that has a more appropriate analytical form, and which may therefore be more accurate than its predecessors. `mgga_x_mggac` still uses the exchange-hole curvature $\tilde{C}_{x\sigma}$ in eq. (646), like `mgga_x_mbrxc_bg`. However, instead of eq. (645), the functional employs an alternate formulation that is expressed solely as a function of the iso-orbital indicator α_σ :

$$\tilde{C}_{x\sigma} = (32\pi)^{2/3} \frac{1}{6\Lambda(\alpha_\sigma)} \quad (647)$$

where

$$\Lambda(\alpha_\sigma) = \frac{\beta_1 + \beta_2 \alpha_\sigma + \beta_3 \alpha_\sigma^2}{1 + \beta_4 \alpha_\sigma + \beta_5 \alpha_\sigma^2} \quad (648)$$

The values of the parameters β_i in eq. (648), which were determined from known exact conditions, are the following: $\beta_1 = 3.712$ (LO bound), $\beta_2 = 2.0$ and $\beta_4 = 0.1$ (exchange energies of rare-gas atoms and tight LO bound $F_x \leq 1.174$), $\beta_3 = 2.595 + 0.5197\beta_4 + 0.559\beta_2$ (HEG limit), and $\beta_5 = -3\beta_3$ (minimum value of F_x reached when $\alpha_\sigma \rightarrow \infty$).

Coupled with `gga_c_mggac` for correlation, the functional leads to results that are more accurate than the standard PBE (`gga_x_pbe` + `gga_c_pbe`) and SCAN (`mgga_x_scan` + `mgga_c_scan`) for some molecular properties (e.g. barrier heights), as well as for the band gap of solids. However, hydrogen-bond dissociation energies appear to be badly described. The more recent correlation functional `mgga_c_rmggac` shows improved compatibility with `mgga_x_mggac`.

[mgga_x_rscan](#)⁷²³ (2019)

To alleviate the numerical problems encountered with the SCAN ([mgga_x_scan](#) + [mgga_c_scan](#)) functional, Bartók and Yates⁷²³ proposed to substitute the iso-orbital indicator α_σ (eq. (80)) in [mgga_x_scan](#) by the regularized α'_σ , defined as

$$\alpha'_\sigma = \frac{\tilde{\alpha}_\sigma^3}{\tilde{\alpha}_\sigma^2 + \alpha_r} \quad (649)$$

where

$$\tilde{\alpha}_\sigma = \frac{\tau_\sigma - \tau_\sigma^W}{\tau_\sigma^{\text{TF}} + \frac{1}{2}\tau_r} \quad (650)$$

and $\alpha_r = 10^{-3}$ and $\tau_r = 10^{-4}$ are small regularization constants. The introduction of τ_r cures the divergence in α_σ occurring in low-density regions dominated by a single orbital. Furthermore, thanks to α_r , the derivatives of α'_σ with respect to n_σ , ∇n_σ , and τ_σ vanish, reducing numerical noise.

Another reason for the numerical instability of SCAN is that the switching function given by eq. (613) has highly oscillatory derivatives around $\alpha_\sigma \approx 1$. To remedy this problem, eq. (613) is replaced by the following function in the interval $\alpha'_\sigma \in (0, 2.5)$:

$$f(\alpha'_\sigma) = \sum_{n=0}^7 c_n (\alpha'_\sigma)^n \quad (651)$$

When used with the corresponding correlation functional [mgga_c_rscan](#), the accuracy of rSCAN is usually quite similar to the native SCAN, although an increase of the error is observed for formation enthalpies of molecules.^{724,725} It was also noted^{723,726,727} that rSCAN does not satisfy some exact constraints that were originally obeyed by SCAN (see discussion for [mgga_x_r2scan](#) and [mgga_c_r2scan](#)).

[mgga_x_mbr](#), [mgga_x_revttb09_mbr](#)⁷²⁸ (2019)

From an expansion of the exchange hole with a generalized coordinate transformation with the parameter $\lambda \in [1/2, 1]$, which depends on the reduced-density gradient x_σ but not on $\nabla^2 n_\sigma$ (removed with the help of eq. (643)), the following function for the exchange-hole curvature

$\tilde{C}_{x\sigma}$ in the nonlinear equation eq. (549) is obtained:

$$\tilde{C}_{x\sigma} = \frac{1}{6} \left[6 \left(\lambda^2 - \lambda + \frac{1}{2} \right) \left(2\tilde{t}_\sigma - 2C_F - \frac{1}{36}x_\sigma^2 \right) + \frac{6}{5} (6\pi^2)^{2/3} (f_\sigma^2 - 1) - 4\gamma\tilde{D}_\sigma \right] \quad (652)$$

where

$$f_\sigma = \left[1 + 10 \left(\frac{70}{27} \right) \frac{1}{4(6\pi^2)^{2/3}} (2\lambda - 1)^2 x_\sigma^2 + \frac{\beta}{16(6\pi^2)^{4/3}} (2\lambda - 1)^4 x_\sigma^4 \right]^{1/10} \quad (653)$$

and

$$\tilde{D}_\sigma = \tilde{t}_\sigma - \frac{1}{8}(2\lambda - 1)^2 x_\sigma^2 \quad (654)$$

With the choice $\gamma = 1$, the values $\lambda = 0.877$ and $\beta = 20.00$ were determined such that the exact exchange energies of the H and He atoms are recovered.

The exchange energies obtained for rare-gas atoms are close to exact and more accurate than with [mgga_x_br89](#) and [mgga_x_br89_1](#). Furthermore, eq. (652) has also been used in the context of band gap calculations of bulk solids with a [mgga_x_tb09](#) potential modified as follows. The potential $v_{x\sigma}^{\text{BR89,hole}}$ in eq. (588) is calculated using eq. (652) instead of eq. (550). Then $\alpha = -0.030$ and $\beta = 1.0$ in eq. (589) (not to be confused with β in eq. (653)) with $e = 1/2$ were refitted. As with the original [mgga_x_tb09](#) potential, the accuracy of [mgga_x_revttb09_mbr](#) for the band gap is good and clearly superior to that of standard functionals.

[mgga_x_msb86bl](#), [mgga_x_mspbel](#), [mgga_x_msrpbel](#)⁷²⁹ (2019)

These three functionals have the same construction as [mgga_x_ms0](#): the global τ -MGGA enhancement factor is given by eq. (603), where $F_x^1(s_\sigma)$ and $F_x^0(s_\sigma)$ are GGA-type enhancement factors, while $f(\alpha_\sigma)$ (eq. (606) with $b = 1$) is the τ -MGGA component of the functional. After choosing a form for $F_x^1(s_\sigma)$, $F_x^0(s_\sigma)$ is then obtained by just replacing μs_σ^2 by $\mu s_\sigma^2 + c$, where c is a parameter to be determined.

The functions $F_x^1(s_\sigma)$ used in [mgga_x_msb86bl](#),

`mgga_x_mspbel`, and `mgga_x_msrbel` are eq. (365) of `gga_x_b86_mgc` with redefined constants,

$$F_x^{\text{B86-MGC}} = 1 + \frac{\mu s_\sigma^2}{\left(1 + \frac{\mu}{\kappa} s_\sigma^2\right)^{4/5}} \quad (655)$$

eq. (378) of `gga_x_pbe`, and eq. (383) of `gga_x_rpbe`, respectively. The values of μ in these enhancement factors differ from the original values and are here chosen to be $\mu = \mu^{\text{GE}}$ (more appropriate for metals), while $\kappa = \kappa^{\text{PBE}}$ was deduced from the LO bound. The parameter c in the corresponding $F_x^0(s_\sigma)$ was determined such that the exact exchange energy of the H atom is reproduced, and the obtained values are $c = 0.08809161$ (`mgga_x_msb86b1`), $c = 0.1036199$ (`mgga_x_mspbel`), and $c = 0.0767086$ (`mgga_x_msrbel`). `gga_c_regtpss` has been used for correlation.

By construction, these functionals should describe both metals (when $\alpha_\sigma \approx 1$) and single-orbital regions (when $\alpha_\sigma \approx 0$) well, which is argued to be the reason for their accurate description of the dissociative chemisorption of H_2 on metals, as well as of the lattice constants of bulk metals.

`mgga_x_task`⁷³⁰ (2019)

Aschebrock and Kümmel⁷³⁰ recognized that a positive and large derivative discontinuity can be obtained from a MGGA functional if the enhancement factor satisfies

$$\frac{\partial F_x}{\partial \alpha_\sigma} < 0 \quad (656)$$

As a function F_x that fulfills this condition they proposed

$$F_x^{\text{TASK}} = h_x^0 g(s_\sigma) + [1 - f(\alpha_\sigma)] \times [h_x^1(s_\sigma) - h_x^0] g^d(s_\sigma) \quad (657)$$

that has the same form as eq. (612) of `mgga_x_scan` if the power $d = 1$. The definitions of the various quantities in eq. (657) are as follows. $h_x^0 = 1.174$, such that the strongly tightened LO bound, $F_x \leq 1.174$,⁶⁹⁸ as well as $F_x(s_\sigma, \alpha_\sigma) \leq F_x(s_\sigma, \alpha_\sigma = 0) \leq 1.174$ are

obeyed. The function g is given by

$$g(s_\sigma) = 1 - e^{-c s_\sigma^{-1/2}} \quad (658)$$

where $c = 4.9479$ so that the correct energy of the H atom is obtained. The functions h_x^1 and f are given by

$$h_x^1(s_\sigma) = \sum_{i=0}^2 a_i R_i(s_\sigma^2) \quad (659)$$

where R_i are Chebyshev rational functions, $a_0 = 0.938719$, $a_1 = -0.076371$, and $a_2 = -0.0150899$, and

$$f(\alpha_\sigma) = \sum_{i=0}^4 b_i R_i(\alpha_\sigma) \quad (660)$$

where $b_0 = -0.628591$, $b_1 = -2.10315$, $b_2 = -0.5$, $b_3 = 0.103153$, and $b_4 = 0.128591$. The coefficients a_i and b_i were determined such that (i) the fourth-order density-gradient expansion of exchange²⁶⁷ in the limit of a slowly varying density with $\alpha_\sigma \approx 1$ is recovered and (ii) $f(\alpha_\sigma \rightarrow \infty) = -3$, which ensures that $\partial F_x / \partial \alpha_\sigma$ satisfies eq. (656) and that it has a sizable value at small α_σ . Finally, the power $d = 10$ in eq. (657) was chosen for a fast decay of F_x^{TASK} in the asymptotic region, where s_σ is large, and to ensure a negative exchange-energy density.

By requiring a large derivative discontinuity, which is equivalent to incorporating a strong amount of nonlocality (termed as ultranonlocality), and gaps are much larger than those obtained with standard functionals, like PBE (`gga_x_pbe` + `gga_c_pbe`) or SCAN (`mgga_x_scan` + `mgga_c_scan`), and in good agreement with experiment. Combined with `mgga_c_ccalda` for the correlation, the functional leads to atomization energies of molecules that are quite accurate and competes with PBE or SCAN.⁷³¹ However, the functional does not work for hydrogen bonds.⁷³²

`mgga_x_lmbj`⁷³³⁻⁷³⁵ (2020)

Because of its dependence on the average of $|\nabla n|/n$ in the unit cell (see eq. (589)), the `mgga_x_tb09` potential cannot be applied to systems with vacuum or an interface. To rem-

edy this, Rauch et al.⁷³³ proposed replacing eq. (589) by the position-dependent function

$$c(\mathbf{r}) = \alpha + \beta \bar{g}(\mathbf{r}) \quad (661)$$

where

$$\bar{g}(\mathbf{r}) = \frac{1}{(2\pi\sigma^2)^{3/2}} \int d^3r' g(\mathbf{r}') \exp\left(-\frac{|\mathbf{r} - \mathbf{r}'|^2}{2\sigma^2}\right) \quad (662)$$

with

$$g(\mathbf{r}) = \frac{1 - \alpha}{\beta} \left[1 - \operatorname{erf}\left(\frac{n(\mathbf{r})}{n_{\text{th}}}\right) \right] + \frac{|\nabla n(\mathbf{r})|}{n(\mathbf{r})} \operatorname{erf}\left(\frac{n(\mathbf{r})}{n_{\text{th}}}\right) \quad (663)$$

As we can see, the average of $|\nabla n|/n$ in the unit cell is replaced by a local average (eq. (662)) around \mathbf{r} within a region whose spatial extent is determined by the Gaussian smearing σ . Note that eq. (663) is used instead of $|\nabla n|/n$ in order to avoid numerical problems and to have a potential that has the correct asymptotic limit. In eqs. (661) to (663), $\alpha = 0.488$ and $\beta = 0.5$ are from the `mgga_x_revttb09_ktb_1` reparametrization, while $\sigma = 3.78$ and the density threshold $n_{\text{th}} = 6.96 \times 10^{-4}$ were determined in ref. 735 from a fit to *GW* band gaps of 2D materials from the C2DB database.⁷³⁶ `mgga_x_lmbj` should be used together with a LDA correlation potential, e.g. that of `lda_c_pz` or `lda_c_pw`. As discussed later, `mgga_x_revlmbj` is a revised version of `mgga_x_lmbj` that improves the results for the band gap of 2D materials.

`mgga_x_t_mbj`, `mgga_x_t_rpp`³⁸² (2020)

`mgga_x_t_mbj` is a reparameterized version of the `mgga_x_ttb09` potential. The two parameters α and β in eq. (589) (with $e = 1/2$) were reoptimized for the band gaps of 85 solids, leading to the optimal values $\alpha = -0.125$ and $\beta = 1.100$. For the full set of 473 solids, the mean absolute error on the band gap, 0.5 eV, is similar to what is obtained with the original `mgga_x_ttb09`.³⁸¹

Following the idea of `mgga_x_ttb09`, the `mgga_x_t_rpp` potential is a modification of `mgga_x_rpp09`, where a parameter c is intro-

duced as a weighting factor for the two terms in eq. (590):

$$v_{x\sigma}^{\text{t-RPP}} = cv_{x\sigma}^{\text{BR89,hole}} + (3c - 2) \frac{1}{\pi} \sqrt{\frac{5}{6}} \sqrt{\frac{D_\sigma}{n_\sigma}} \quad (664)$$

where $v_{x\sigma}^{\text{BR89,hole}}$ is eq. (552) and c is given by eq. (589) with $e = 1/2$. Equation (664) differs from eq. (588) in the second term, where τ_σ is replaced by D_σ (eq. (591) with \mathbf{j}_σ ignored). $\alpha = 0.225$ and $\beta = 0.825$ were optimized for the band gaps of the 85 solids mentioned above. With a mean absolute error of 0.63 eV for the band gaps of the set of 473 solids, the performance of `mgga_x_t_rpp` is inferior to that of `mgga_x_ttb09` and `mgga_x_t_mbj`.

`mgga_x_r2scan`^{726,727} (2020)

Furness et al.⁷²⁶ pointed out that the regularized rSCAN functional (`mgga_x_rscan` + `mgga_c_rscan`) does not satisfy several of the mathematical constraints that are satisfied by the original SCAN (`mgga_x_scan` + `mgga_c_scan`) functional. This led them to propose another regularized version of SCAN that restores most of these constraints. For exchange, the first change made in `mgga_x_scan` concerns the iso-orbital indicator α_σ , that is replaced by

$$\tilde{\alpha}_\sigma = \frac{\tau_\sigma - \tau_\sigma^{\text{W}}}{\tau_\sigma^{\text{TF}} + \eta \tau_\sigma^{\text{W}}} \quad (665)$$

where $\eta = 10^{-3}$ is a regularization parameter. The second modification consists of replacing eq. (614) by

$$f_0^{\text{r}^2\text{SCAN}}(p_\sigma) = \left(C_\eta C_{2x} e^{-p_\sigma^2/d_{\text{p}2}^4} + \mu^{\text{GE}} \right) p_\sigma \quad (666)$$

where $C_\eta = 20/27 + 5\eta/3$, $C_{2x} \approx -0.162742$ ⁵⁵⁹ (see ref. 726 for the accurate expression), and $d_{\text{p}2} = 0.361$ (see ref. 727). Note that eq. (666) depends only on p_σ , while eq. (614) depends on both p_σ and α_σ . Finally, the last modification concerns the switching function $f(\alpha_\sigma)$ in eq. (612) that is chosen as eq. (651) from `mgga_x_rscan`, but which is evaluated with eq. (665). The correct HEG limit of `lda_x`, the second-order term in the density-gradient expansion, and the correct scaling properties are now recovered by the functional, while this

was not the case with `mgga_x_rscan`. However, the correct fourth-order term in the density-gradient expansion is not recovered. `r2SCAN` (`mgga_x_r2scan` + `mgga_c_r2scan`) retains the accuracy of `SCAN`.

`mgga_x_r2scanl`⁷³⁷ (2020)

This is a deorbitalized version of `mgga_x_r2scan`, obtained by following the same strategy as for `mgga_x_scanl`, namely replacing the kinetic-energy density τ_σ by the orbital-free (and $\nabla_\sigma^2 n$ -dependent) approximation $\tau_\sigma^{\text{PC07opt}}$ ^{710,711} (see eq. (633)). A combination of the functional with the corresponding `mgga_c_r2scanl` for correlation leads to results that are rather similar to those of the parent functional `r2SCAN` (`mgga_x_r2scan` + `mgga_c_r2scan`). However, a notable difference is the clear reduction of the magnetic moment in the ferromagnetic metals Fe, Co, and Ni. While `r2SCAN` and `SCAN` strongly overestimate the magnetic moment, `SCAN-L` (`mgga_x_scanl` + `mgga_c_scanl`) and `r2SCAN-L` lead to better agreement with experiment.

`mgga_x_regtm`⁷³⁸ (2020)

Furness et al.⁷³⁹ noticed that the enhancement factor of `mgga_x_tm`, eq. (620), suffers from the following order-of-limits problem:

$$\lim_{\alpha_\sigma \rightarrow 0} \lim_{p_\sigma \rightarrow 0} F_x^{\text{TM}}(p_\sigma, \alpha_\sigma) \approx 1.0137 \quad (667a)$$

$$\lim_{p_\sigma \rightarrow 0} \lim_{\alpha_\sigma \rightarrow 0} F_x^{\text{TM}}(p_\sigma, \alpha_\sigma) \approx 1.1132 \quad (667b)$$

that has its roots in the weight function \tilde{w}_σ (eq. (621)) when z_σ is calculated from eq. (94b). To solve this problem, Patra et al.⁷³⁸ proposed to evaluate \tilde{w}_σ with a modified variable z'_σ :

$$z'_\sigma = \frac{1}{1 + \frac{3}{5} \frac{\alpha_\sigma}{p_\sigma + f(\alpha_\sigma)e^{-cp_\sigma}}} \quad (668)$$

where $c = 3$ and $f(\alpha_\sigma)$ is given by eq. (600) with $d = 1.475$. Note that z'_σ is used only in \tilde{w}_σ , while F_x^{DME} and F_x^{SC} use the original variable z_σ . This modification leads to the same value (≈ 1.1132) for both eqs. (667a) and (667b).

When used with `gga_c_regtpss` for correlation, results can be more accurate than those of `TM` (`mgga_x_tm` + `mgga_c_tm`) for some

properties, like the phase transition pressure in solids or the band gap. A more recent functional, `mgga_c_rregtm`, shows better compatibility with `mgga_x_regtm`.

`mgga_x_hlta`⁶⁵⁰ (2021)

The functionals `mgga_x_lta` and `mgga_x_tlda` were derived by converting (with the help of eq. (563)) the dependence on n_σ in `lda_x` into a dependence on τ_σ . The difference between the two functionals is that the $n_\sigma \rightarrow \tau_\sigma$ conversion is done in the exchange-energy per volume in the case of `mgga_x_lta`, and only in the exchange-energy per particle for `mgga_x_tlda`. A more general approach is to replace n_σ by

$$n_\sigma^{\text{eff}} = \tilde{n}_\sigma^x n_\sigma^{1-x} \quad (669)$$

where \tilde{n}_σ is eq. (563) and x a parameter. `mgga_x_lta` and `mgga_x_tlda` correspond to $x = 1$ and $1/4$, respectively. This leads to an enhancement factor given by

$$F_x^{\text{xLTA}} = \left(\frac{\tilde{t}_\sigma}{C_F} \right)^{4x/5} \quad (670)$$

This defines a new type of functionals that was termed as meta-LDA (MLDA), which recover the HEG limit `lda_x`. Equation (670) has been tested on atoms (total and exchange energy) and molecules (atomization energy) for various values of the parameter x , and with or without correlation (e.g., `mgga_c_hlta` that also uses eq. (669)). It was shown that choosing $x = 1/2$ (`mgga_x_hlta`) and adding `mgga_c_hlta` for correlation leads to a mean error for the atomization energy of molecules that is one third of the mean error obtained with LDA, which is however still much larger than the errors from standard GGA functionals like BLYP (`gga_x_b88` + `gga_c_lyp`) or PBE (`gga_x_pbe` + `gga_c_pbe`).

`mgga_x_mtask`⁷⁴⁰ (2021)

`mgga_x_task` has been shown to be accurate for the band gap of bulk solids, however further improvement for 1D and 2D systems is needed, since band gaps for these systems are still too small when compared to reference results. To achieve this goal, two modifications in

`mgga_x_task` were made to enhance the non-locality. The first one consists of choosing an upper bound for F_x that is less tight: $h_x^0 = 1.29$ (1.174 in `mgga_x_task`) in eq. (657). The second modification is an adjustment of the large- α_σ limit of $f(\alpha_\sigma)$ (eq. (660)): $f(\alpha_\sigma \rightarrow \infty) = -3.5$ (-3 in `mgga_x_task`). Because of these changes, the coefficients a_i and b_i in eqs. (659) and (660) had to be recalculated, and the new values are given by $a_0 = 0.924374$, $a_1 = -0.09276847$, $a_2 = -0.017143$, $b_0 = -0.639572$, $b_1 = -2.087488$, $b_2 = -0.625$, $b_3 = -0.162512$, and $b_4 = 0.014572$. The functional `mgga_x_mtask` provides band gaps of low-dimensional systems that are slightly larger compared to those of `mgga_x_task` and closer to reference results.⁷⁴¹

`mgga_x_mcml`⁷⁴² (2021)

The analytical form chosen by Brown et al.⁷⁴² for this functional is given by eq. (608) of `mgga_x_mbeef`. As in `mgga_x_mbeef`, $q = \kappa^{\text{PBE}}/\mu^{\text{GE}} = 6.5124$ in eq. (544), so that the enhancement factor of `gga_x_pbe_sol` is recovered. However, $b = 4.0$ in eq. (606), as in `mgga_x_ms2`. Finally, the 64 linear parameters a_{mn} ($M = N = 7$ in eq. (608)) were determined from a fit to reference data of various molecular and solid-state properties, while constraining three conditions: the HEG limit of `lda_x`, the second-order density-gradient expansion, and the correct exchange energy of the H atom.

Combined with `gga_c_regtpss` for correlation, the functional shows good performance for surface reaction energies (chemisorption and physisorption), weak intermolecular interaction energies, and bulk properties (lattice constants and bulk moduli).

`mgga_x_revlmbj`⁷⁴¹ (2021)

This is a revised version of the `mgga_x_lmbj` potential. The new value of $\beta = 0.6$ in eq. (661) was reoptimized against the GW band gaps of 298 2D systems from the C2DB database.⁷³⁶ Along with `mgga_x_mtask`, GLLB-SC,³²⁰ and HSE06,^{743–745} the `mgga_x_revlmbj` potential (combined with `lda_c_pw` for correlation) belongs to the group of the most accurate xc methods for the band gap of 2D systems.

`mgga_x_r2scan01`⁷⁴⁶ (2022)

`mgga_x_r2scan01` differs from `mgga_x_r2scan` only by the value of the regularization parameter η in eq. (665) that is larger ($\eta = 10^{-2}$) to avoid rapid oscillations in atomic potentials.

`mgga_x_tscanl`⁵⁵⁷ (2022)

This is an exchange free-energy functional that is useful for modeling matter at elevated temperature τ_e . It is based on the deorbitalized `mgga_x_scanl`, and the τ_e -dependent free-energy correction is calculated at the GGA level as the difference between the free-energy functional `gga_x_kdt16` and the standard functional `gga_x_pbe`:

$$f_x^{\text{T-SCAN-L}} = e_x^{\text{SCAN-L}} + f_x^{\text{KDT16}} - e_x^{\text{PBE}} \quad (671)$$

Combined with its counterpart `mgga_c_tscanl`, the functional yields pressures and direct current conductivities of warm dense He and Al that are improved compared to PBE (`gga_x_pbe` + `gga_c_pbe`), SCAN-L (`mgga_x_scanl` + `mgga_c_scanl`), and KDT16 (`gga_x_kdt16` + `gga_c_kdt16`).

`mgga_x_rppscan`⁷⁴⁷ (2022)

The functional `mgga_x_rscan`, a regularized version of `mgga_x_scan`, does not obey several mathematical constraints that are obeyed by `mgga_x_scan`. Two of these constraints, the HEG limit and the behavior under coordinate scaling, can be restored by replacing the `mgga_x_rscan` expression for the iso-orbital indicator (eqs. (649) and (650)) with the variant used in `mgga_x_r2scan`, eq. (665). This substitution, done together with the corresponding one in correlation (`mgga_c_rppscan`), leads to the r++SCAN functional, whose accuracy remains essentially unchanged compared to rSCAN (`mgga_x_rscan` + `mgga_c_rscan`).

`mgga_x_r4scan`⁷⁴⁷ (2022)

`mgga_x_r2scan` was constructed to be smoother than `mgga_x_scan`, however the price to pay was to sacrifice the constraint of the fourth-order term in the density-gradient expansion.²⁶⁷ In order to remedy this, Furness et al.⁷⁴⁷ proposed to add a term, ΔF_{4g} , to the

`mgga_x_r2scan` enhancement factor:

$$F_x^{\text{r}^4\text{SCAN}} = \{h_x^1(p_\sigma) + f(\tilde{\alpha}_\sigma) [h_x^0 - h_x^1(p_\sigma)] + \Delta F_4(p_\sigma, \tilde{\alpha}_\sigma)\} g(p_\sigma) \quad (672)$$

where

$$\Delta F_4(p_\sigma, \tilde{\alpha}_\sigma) = \{C_{2x} [(1 - \tilde{\alpha}_\sigma) - C_\eta p_\sigma] + C_{\tilde{\alpha}\tilde{\alpha}}(1 - \tilde{\alpha}_\sigma)^2 + C_{p\tilde{\alpha}} p_\sigma(1 - \tilde{\alpha}_\sigma) + C_{pp} p_\sigma^2\} \Delta F_4^{\text{damp}}(p_\sigma, \tilde{\alpha}_\sigma) \quad (673)$$

with

$$\Delta F_4^{\text{damp}}(p_\sigma, \tilde{\alpha}_\sigma) = \frac{2\tilde{\alpha}_\sigma^2}{1 + \tilde{\alpha}_\sigma^4} \times e^{-(1 - \tilde{\alpha}_\sigma)^2/d_{\tilde{\alpha}^4}^2 - p_\sigma^2/d_{p^4}^4} \quad (674)$$

The constants in eqs. (673) and (674) are given by (see ref. 747 for their relations to other constants) $C_{\tilde{\alpha}\tilde{\alpha}} \approx -0.059353$,⁴⁷² $C_{p\tilde{\alpha}} \approx 0.040268$,⁴⁷² $C_{pp} \approx -0.088077$,⁴⁷² $d_{\tilde{\alpha}^4} = 0.178$, and $d_{p^4} = 0.802$. The two latter parameters were determined by minimizing the error for the xc energy of rare-gas atoms and jellium surface. The other parameters and functions are the same as in `mgga_x_r2scan`.

The functional `mgga_x_r4scan` is not as smooth as `mgga_x_r2scan`, but still numerically more stable than the original `mgga_x_scan`. Using `mgga_c_r2scan` for correlation, the overall accuracy of `mgga_x_r4scan` is similar to `mgga_x_r2scan`, with however a slight increase of the error for the atomization energies of molecules. Furness et al.⁷⁴⁷ recommend the use of r²SCAN over r⁴SCAN.

`mgga_x_vcml`⁷⁴⁸ (2022)

This empirical functional has the same analytical form as `mgga_x_mcml`, which is in turn based on `mgga_x_mbeef`. As for `mgga_x_mcml`, an optimization of the 64 parameters a_{mn} in eq. (608), where $M = N = 7$, was done with `gga_c_regtpss` for the correlation. However, a non-local correlation functional for van der Waals interaction, rVV10,⁷⁴⁹ was here also added (and the parameter b in rVV10 optimized together with the a_{mn}) in order to account more

accurately of the dispersion interaction. The functional shows good performance for a variety of properties involving finite and extended systems, as well as noncovalent systems.

`mgga_x_ofr2`⁷⁵⁰ (2022)

With the aim of proposing a functional that is particularly accurate for metallic systems and computationally efficient, Kaplan and Perdew⁷⁵⁰ chose to deorbitalize the `mgga_x_r2scan` functional by substituting τ_σ in eq. (665) by (RPP stands for r²SCAN piecewise-polynomial)

$$\tau_\sigma^{\text{RPP}} = \tau_\sigma^{\text{TF}} \left[\alpha^{\text{RPP}}(p_\sigma, q_\sigma) + \frac{5}{3} p_\sigma \right] \quad (675)$$

where τ_σ^{TF} is given by eq. (70) and

$$\alpha^{\text{RPP}}(x) = \begin{cases} 0, & x < 0 \\ x^4 (A + Bx + Cx^2 + Dx^3), & 0 \leq x \leq x_0 \\ x, & x > x_0 \end{cases} \quad (676)$$

with

$$x(p_\sigma, q_\sigma) = 1 - \frac{40}{27} p_\sigma + \frac{20}{9} q_\sigma + c_3 p_\sigma^2 e^{-|c_3| p_\sigma} + x_4(p_\sigma, q_\sigma) e^{-(p_\sigma/c_1)^2 - (q_\sigma/c_2)^2} \quad (677)$$

where

$$x_4(p_\sigma, q_\sigma) = b_{qq} q_\sigma^2 + b_{pq} p_\sigma q_\sigma + (b_{pp} - c_3) p_\sigma^2 \quad (678)$$

The choice $A = 20/x_0^3$, $B = -45/x_0^4$, $C = 36/x_0^5$, and $D = -10/x_0^6$ was made such that $\alpha^{\text{RPP}}(x)$ is continuous at $x = x_0$ up to the third derivative. The parameters $x_0 = 0.819411$, $c_1 = 0.201352$, $c_2 = 0.185020$, and $c_3 = 1.53804$ were determined by minimizing the error of the xc energy of rare-gas atoms (Ne, Ar, Kr, and Xe), and jellium surfaces and clusters at selected densities, while $b_{qq} \approx 1.801019$, $b_{pq} \approx -1.850497$, and $b_{pp} \approx 0.974002$ (see ref. 750 for their relations to other constants) enforce the fourth-order density-gradient expansion. Importantly, the correct density-gradient expansion up to the fourth order is recovered, while it is only obeyed to the second order in

`mgga_x_r2scan`.

Compared to `r2SCAN`, the OFR2 (`mgga_x_ofr2` + `mgga_c_ofr2`) functional has a better accuracy for lattice constant of solids and for formation enthalpies of intermetallic elements, but is less accurate for band gaps of solids and atomization energies of molecules and solids.

`mgga_x_ktbn`⁵⁶⁶ (2022)

25 functionals were trained with the goal of exploring the limit of the MGGA approximation for exchange and proposing a functional that shows a good and well-balanced accuracy for three selected properties of bulk solids (lattice constant, cohesive energy, and band gap). The form chosen for the enhancement factor is the Padé type:

$$F_x^{\text{KTBM}} = \frac{\sum_{i=0}^N \sum_{j=0}^{N-i} c_{ij} p_\sigma^i \left(\frac{\tilde{t}_\sigma}{C_F} \right)^j}{\sum_{i=0}^N \sum_{j=0}^{N-i} d_{ij} p_\sigma^i \left(\frac{\tilde{t}_\sigma}{C_F} \right)^j} \quad (679)$$

where c_{ij} and d_{ij} are parameters that were determined by fitting experimental data for the three aforementioned properties. The training sets consists of 44 solids for the lattice constant and cohesive energy,⁷⁵¹ and 440 solids for the band gap.³⁸² $N = 2$ in eq. (679) was used and the correct HEG limit (`lda_x`) was enforced with

$$d_{00} + d_{01} + d_{02} = c_{00} + c_{01} + c_{02} \quad (680)$$

leading to 11 independent parameters. Using a larger value for N or releasing the HEG-limit condition led to no significant improvement in the accuracy of the functional. The training of eq. (679), combined with `mgga_c_scan` for correlation, was carried out by minimizing a loss function that consists of a linear combination of the mean absolute relative error of the three properties. In total, 25 choices for the relative weights of the mean absolute relative error of the three properties were considered, resulting in 25 different parametrizations of eq. (679), all available in Libxc. Among them, mGGA23 (`mgga_x_ktbn_23` in Libxc) has a quite good accuracy for all three prop-

erties. mGGA23' (`mgga_x_ktbn_gap` in Libxc), a variation of mGGA23, that was trained by using the mean absolute error instead of the mean absolute relative error, is accurate for the band gap, but not for the two other properties.

Restricting the summations over j in eq. (679) to $j = 0$ leads to GGA functionals (see `gga_x_ktbn_a` and `gga_x_ktbn_b`).

`mgga_x_sregtm_1`, `mgga_x_sregtm_2`, `mgga_x_sregtm_3`⁷⁵² (2023)

Francisco et al.⁷⁵² noticed that the variable z'_σ (eq. (668)) used in `mgga_x_regtm` can be negative, in particular when p_σ is small and α_σ is larger than 1 (see eq. (600)). This is an unwanted feature since the original function z_σ is by definition always positive. To alleviate this problem, they proposed a positive-definite alternative to z'_σ :

$$z_\sigma^{\text{rev}} = \frac{5p_\sigma + \epsilon_p}{5p_\sigma + 3\alpha_\sigma + \epsilon_p} \quad (681)$$

where ϵ_p is a parameter. The functional `mgga_x_sregtm_1` is obtained by replacing z_σ by z_σ^{rev} only in \tilde{w}_σ of the `mgga_x_tm` enhancement factor (eq. (620)), while `mgga_x_sregtm_2` corresponds to a replacement in \tilde{w}_σ and F_x^{SC} . With `mgga_c_rregtm` for correlation, $\epsilon_p = 0.5$ was determined for `mgga_x_sregtm_1` and `mgga_x_sregtm_2` as a good compromise between accuracy for molecular properties (heats of formation, bond lengths, and vibrational frequencies) and an approximate satisfaction of the second-order density-gradient expansion. Using $\epsilon_p = 0.58568$ (note that there is a typo in ref. 752) in `mgga_x_sregtm_2` to satisfy exactly the second-order density-gradient expansion leads to `mgga_x_sregtm_3`. Similarly to `mgga_x_regtm`, these functionals lead to a value of ≈ 1.1132 for both eqs. (667a) and (667b).

Calculations for molecular and solid-state properties show that `mgga_x_sregtm_2` has a better overall accuracy than `mgga_x_sregtm_2` and `mgga_x_sregtm_3`, and is competitive with `r2SCAN` (`mgga_x_r2scan` + `mgga_c_r2scan`).

`mgga_x_sregtml_2`⁷⁵³ (2023)

This functional is a deorbitalized version of

`mgga_x_sregtm_2`, where the kinetic-energy density τ_σ is replaced by the orbital-free approximation $\tau_\sigma^{\text{PCrep}}$ ⁷⁵³ that is a reoptimization of $\tau_\sigma^{\text{PC07}}$ (see eq. (633)) with $a \approx 1.504402$ and $b \approx 0.615645$ in eq. (635). Compared to `mgga_x_sregtm_2`, the results for molecular and solid-state properties are in general somewhat deteriorated (`mgga_c_rregtm` is used for correlation).

`mgga_x_stmlq`⁷⁵⁴ (2024)

Francisco et al.⁷⁵⁴ proposed another deorbitalized version of the `mgga_x_sregtm_2` functional, by replacing the reduced Laplacian q_σ (eq. (62)) by a smoother version ($\tilde{q}_\sigma^{\text{L}}$). The functional is constructed from the following steps that correspond to *Scheme 1* in ref. 754.

1. The orbital-free $\tau_\sigma^{\text{PC07opt}}$ ^{710,711} (eq. (633)) is used to calculate $\alpha_\sigma^{\text{L0}}$ with eq. (94a).
2. $\alpha_\sigma^{\text{L0}}$ is used to calculate $\tilde{q}_\sigma^{\text{L0}}$ with eq. (577) ($b = 0$).
3. $\tilde{q}_\sigma^{\text{L0}}$ replaces q_σ in $\tau_\sigma^{\text{PC07opt}}$ to calculate α_σ^{L} with eq. (94a).
4. α_σ^{L} is used to calculate $\tilde{q}_\sigma^{\text{L}}$ with eq. (577) ($b = 0$).
5. Finally, the components of the functional are evaluated as follows:
 - (a) F_x^{SC} , given by eq. (623), is calculated with the following two changes: (i) \tilde{q}_σ is replaced by $\tilde{q}_\sigma^{\text{L}}$ and (ii) z_σ is replaced by z_σ^{rev} (eq. (681)) with α_σ replaced by α_σ^{L} .
 - (b) F_x^{DME} , given by eq. (622), is calculated with α_σ replaced by α_σ^{L} .
 - (c) \tilde{w}_σ , given by eq. (621), is calculated with z_σ replaced by z_σ^{rev} (eq. (681)), where α_σ is replaced by α_σ^{L} .

It is argued that this replacement leads to results that are closer to those of the parent functional `mgga_x_sregtm_2` than with `mgga_x_sregtml_2`. This is specifically the case for molecular properties (heats of formation, bond lengths, and vibrational frequencies).

`mgga_x_eel`⁷⁵⁵ (2023)

In the same spirit as `mgga_x_task`, this functional was developed with an emphasis on ultranonlocality in order to obtain a potential that mimics the EXX-KLI potential. Requirements for the HEG limit and the H atom are used for constructing the functional with the aim to obtain a response to a static electric field similar to that of EXX-KLI. The enhancement factor reads

$$F_x^{\text{EEL}} = k \left\{ G \left(s_\sigma^2 + \frac{3}{5} \alpha_0 \tanh \left(\frac{\alpha_\sigma}{\alpha_0} \right) \right) - G(s_\sigma^2) \right\} + G(s_\sigma^2) \quad (682)$$

where

$$G(x) = h_x^0 \left[1 - e^{-c(x-s_0^2)^{-1/4}} \Theta(x - s_0^2) \right] \quad (683)$$

In eq. (683), $h_x^0 = 1.174$ (strongly tightened bound requirement⁶⁹⁸), $c = 4.759279$ (exact energy of the H atom), and $s_0 = (6\pi)^{-1/3}$ (the smallest value of s_σ for a doubly occupied $1s$ -orbital-like exponential density). In eq. (682), $\alpha_0 = 3$ was found to be a good choice such that $\alpha_0 \tanh(\alpha_\sigma/\alpha_0)$ is similar to α_σ and remains positive. With this choice for α_0 ,

$$k = \frac{1 - h_x^0}{G \left[\frac{3}{5} \alpha_0 \tanh(\alpha_0^{-1}) \right] - h_x^0} \approx 51.555804^{472} \quad (684)$$

is obtained by requiring that $F_x^{\text{EEL}}(s_\sigma = 0, \alpha_\sigma = 1) = 1$ (HEG limit).

The functional shows a good ability to reproduce EXX-KLI results for the static electric longitudinal polarizability of hydrogen chains and of $\text{C}_{2N}\text{H}_{2N+2}$ oligomers of polyacetylene.

`mgga_x_rmsb86bl`, `mgga_x_rmspbel`, `mgga_x_rmsrpbel`⁷⁵⁶ (2024)

These functionals have the same mathematical form as `mgga_x_msb86bl`, `mgga_x_mspb`, and `mgga_x_msrbel`, but use the regularized iso-orbital indicator $\tilde{\alpha}_\sigma$ proposed for `mgga_x_r2scan`, given by eq. (665) with $\eta = 10^{-3}$, for evaluating the switching function from eq. (606) that is used in the enhancement factor (eq. (603)).

Calculations of adsorption energies and dis-

sociation barriers of molecules on Cu(111) surfaces show that `mgga_x_rmsrpbel` can compete with `gga_xc_beefvdw`, when combined with the `gga_c_regtpss` and rVV10⁷⁴⁹ correlation functionals.

`mgga_x_lak`³¹⁸ (2024)

Lebeda et al.³¹⁸ constructed a functional that is based on a careful examination of the relative weight of the contributions from the density gradient and kinetic-energy density to the density-gradient expansions of exchange and correlation. Their goal was to demonstrate that it is possible to get accurate results at the MGGA level for standard molecular properties (atomization energies and bond lengths), like SCAN (`mgga_x_scan` + `mgga_c_scan`) does, and the band gaps of solids, with `mgga_x_task` being a good example.

The enhancement factor of the exchange component of the nonempirical LAK functional has a form similar to eq. (612) of `mgga_x_scan` or eq. (657) of `mgga_x_task`:

$$F_x^{\text{LAK}} = h_x^0 g(s_\sigma) + [1 - f(\alpha_\sigma)] \times [h_x^1(s_\sigma) - h_x^0] g_{\text{num}}(s_\sigma) \quad (685)$$

with the various quantities described as follows. The parameter $h_x^0 = 1.174$ is fixed by the strongly tightened LO bound,⁶⁹⁸ while $g(s_\sigma)$ is given by eq. (658) that was parameterized to yield the correct energy of the H atom. The functions

$$h_x^1(s_\sigma) = h_x^{\text{GEA4}}(s_\sigma) + k_x(s_\sigma) [a_x - h_x^{\text{GEA4}}(s_\sigma)] \quad (686a)$$

$$f(\alpha_\sigma) = \frac{2}{\pi} \arctan \left\{ \frac{\pi}{2} \left[c_1 \frac{\alpha_\sigma - 1}{\alpha_\sigma} + c_2 (\alpha_\sigma - 1)^2 \right] \right\} \quad (686b)$$

have mathematical forms that were guided by the fourth-order density-gradient expansion.^{267,730} In $h_x^1(s_\sigma)$,

$$h_x^{\text{GEA4}}(s_\sigma) = 1 + \mu_{s,x} s_\sigma^2 + \nu_s s_\sigma^4 + h_x^0 [1 - g(s_\sigma)] \quad (687a)$$

$$k_x(s_\sigma) = e^{-1/[(s_\sigma/a_x)^2(1+s_\sigma^2)]} \quad (687b)$$

with $a_x = 1.1$. In $f(\alpha_\sigma)$, $c_1 = \mu_{\alpha,x}/(h_x^0 - 1)$

and $c_2 = (\mu_{\alpha,x} + \nu_\alpha)/(h_x^0 - 1)$. The constants

$$\mu_{\alpha,x} = -\frac{97 + 3h_x^0 + \sqrt{(3h_x^0)^2 + 74166h_x^0 - 64175}}{1200} \quad (688)$$

$\mu_{s,x} = (10 + 60\mu_{\alpha,x})/81$, $\nu_\alpha = (73 - 50\mu_{\alpha,x})/5000$, and $\nu_s = -(1606 - 50\mu_{\alpha,x})/18825$ control the relative importance of α_σ (i.e., τ_σ) and s_σ in the density-gradient expansion. Besides the fourth-order density-gradient expansion, other requirements that were involved to derive the functional form are, for instance, eq. (656) or a smooth enhancement factor.

Furthermore, $k_x(s_\sigma)$ was determined from the requirement that $\partial F_x/\partial s_\sigma|_{\alpha_\sigma=1}$ should be positive for $0.5 \lesssim s_\sigma \lesssim 1.2$ and negative for $s_\sigma \gtrsim 1.2$. The function $g_{\text{num}}(s_\sigma)$ in eq. (685) reads

$$g_{\text{num}}(s_\sigma) = 1 - e^{-(a_{\text{num}}/s_\sigma)^2} \quad (689)$$

attenuates the dependence on α_σ at large values of s_σ in order to reduce numerical instabilities. The value $a_{\text{num}} = 5$ was chosen.

The LAK functional, `mgga_x_lak` combined with `mgga_c_lak`, is as accurate as SCAN (`mgga_x_scan` + `mgga_c_scan`) for atomization energies and bond lengths of molecules, and as accurate as the HSE06⁷⁴³⁻⁷⁴⁵ range-separated hybrid for band gaps smaller than 4 eV.

`mgga_x_mscan`³⁶⁵ (2025)

Desmarais et al.³⁶⁵ proposed ncSCAN, an extension of SCAN (`mgga_x_scan` + `mgga_c_scan`) to the more general noncollinear spin-current DFT framework. They also derived the collinear limit of ncSCAN, which they termed modified SCAN (mSCAN) that is discussed here.

The energy density of the exchange component `mgga_x_mscan` is given by

$$e_x^{\text{mSCAN}} = e_x^{\text{LDA}}(n_\uparrow, n_\downarrow) F_x^{\text{SCAN}}(s, \tilde{\alpha}) \quad (690)$$

where

$$\tilde{\alpha} = \frac{n_\uparrow \tau_\uparrow + n_\downarrow \tau_\downarrow - \frac{1}{4} \nabla n_\uparrow \cdot \nabla n_\downarrow}{n_\uparrow \tau_\uparrow^{\text{TF}} + n_\downarrow \tau_\downarrow^{\text{TF}}} \quad (691)$$

Importantly, `mgga_x_mscan` recovers the orig-

inal `mgga_x_scan` only in the non-magnetic case. In the magnetic case, `mgga_x_mscan` differs from `mgga_x_scan`, since the enhancement factor F_x^{SCAN} (eq. (612)) is here evaluated with n and s , while the iso-orbital indicator $\tilde{\alpha}$ has a different construction. As a consequence, `mgga_x_mscan` does not obey the spin decomposition given by eq. (243), but its parent form is properly $U(1) \times SU(2)$ gauge invariant.

It was shown³⁶⁵ that mSCAN (`mgga_x_mscan` + `mgga_c_mscan`) fixes the reported failures of SCAN for magnetism.

`mgga_x_rs`⁷⁵⁷ (2025)

This functional was devised with the goal of reducing the one-electron self-interaction error in exchange at the MGGA level. Ramasamy et al.⁷⁵⁷ pointed out that `mgga_x_scan` reduces to a GGA functional,

$$F_x^{\text{SCAN-i}} = 1.174 \left(1 - e^{-as_\sigma^{-1/2}} \right) \quad (692)$$

for one-electron systems (“i” stands for iso-orbital). This is a disadvantage since the flexibility of MGGAs, i.e. the dependence on τ_σ , is lost and the one-electron self-interaction error cannot be efficiently reduced. This led them to propose an enhancement factor based on eq. (692), which also depends on the Laplacian of the density:

$$F_x^{\text{RS}} = 1.174 \left(1 - e^{-as_\sigma^{-1/2}} \right) g(s_\sigma, q_\sigma) \quad (693)$$

where

$$g(s_\sigma, q_\sigma) = \frac{1}{1 + \ln \{ 1 + e^{b[q_\sigma - q_0(s_\sigma)]} \}} \quad (694)$$

with

$$q_0(s_\sigma) = s_\sigma^2 \left\{ 1 - \frac{2}{3 \ln \left[(6\pi)^{1/3} (1 + s_\sigma^2)^{1/2} \right]} \right\} \quad (695)$$

The function g was chosen in order to have an appropriate behavior with respect to q_σ (e.g., under coordinate scaling), while the form of q_0 is based on an analysis of the hydrogen atom. The parameters $a = 5.93$ and $b = 36.29$ in eqs. (693) and (694) were determined by a fit to

the exact exchange energies of two one-electron systems: the hydrogen atom and the Gaussian density.

The orbital-free `mgga_x_rs` functional shows improvement for the binding energy curve of H_2^+ over `gga_x_pbe`, `mgga_x_scan`, and `mgga_x_scanl`.

3.3.2 Correlation

`mgga_c_cs`^{417,575} (1988)

Colle and Salvetti⁴¹⁷ proposed a correlation functional that depends on the electron density and the second-order reduced-density matrix. Then, Lee et al.⁵⁷⁵ re-expressed the functional in terms of the kinetic-energy density instead of the second-order density matrix, and generalized it to spin-polarized systems. The resulting functional reads

$$e_c^{\text{CS}} = -\frac{a}{n} \frac{\gamma(\zeta)}{1 + dn^{-1/3}} \left\{ n + 2bn^{-5/3} e^{-cn^{-1/3}} \times \left[n_\uparrow \left(\tau_\uparrow - \frac{1}{8} \nabla^2 n_\uparrow \right) + n_\downarrow \left(\tau_\downarrow - \frac{1}{8} \nabla^2 n_\downarrow \right) - n \left(\tau^{\text{W}} - \frac{1}{8} \nabla^2 n \right) \right] \right\} \quad (696)$$

where

$$\gamma(\zeta) = 2 - \phi_2(\zeta) \quad (697)$$

The parameters $a = 0.04918$, $b = 0.132$, $c = 0.2533$, and $d = 0.349$ were fit to data for the He atom. Tested on neutral and positively charged atoms, as well as on simple molecules, the functional leads to correlation energies that differ from reference data by at most a few mE_h in most cases.

Note that the functional was later on modified to eliminate the dependence on τ_σ and $\nabla^2 n_\sigma$,^{575,576} leading to the famous `gga_c_lyp` correlation functional.

`mgga_c_b88`¹⁹⁶ (1988)

Becke¹⁹⁶ constructed this functional using known conditions for the correlation hole: the zero-charge sum rule and the cusp behavior at short interelectronic distances. Based on the Stoll decomposition, see section 2.18.3, the

functional reads

$$e_{c_{\uparrow\downarrow}}^{\text{B88}} = -0.8 \frac{n_{\uparrow} n_{\downarrow}}{n} z_{\uparrow\downarrow}^2 \left[1 - \frac{\ln(1 + z_{\uparrow\downarrow})}{z_{\uparrow\downarrow}} \right] \quad (698)$$

$$e_{c_{\sigma\sigma}}^{\text{B88}} = -0.01 \frac{n_{\sigma}}{n} 2D_{\sigma} z_{\sigma\sigma}^4 \left[1 - 2 \frac{\ln(1 + \frac{1}{2} z_{\sigma\sigma})}{z_{\sigma\sigma}} \right] \quad (699)$$

where

$$z_{\sigma\sigma'} = c_{\sigma\sigma'} \left(R_{\text{F}}^{\sigma} + R_{\text{F}}^{\sigma'} \right) \quad (700a)$$

$$D_{\sigma} = \tau_{\sigma} - \tau_{\sigma}^{\text{W}} \quad (700b)$$

The quantity $z_{\sigma\sigma'}$ is the correlation length, with $R_{\text{F}}^{\sigma} = -1/v_{\text{x},\sigma}^{\text{hole}}$ that is identified as the inverse of the Coulomb potential $v_{\text{x},\sigma}^{\text{hole}}$ created by the exchange hole, for which an exchange functional has to be chosen. Becke¹⁹⁶ chose `gga_x_b86_mgc`, leading to

$$R_{\text{F}}^{\sigma} = \frac{1}{2C_{\text{x}} n_{\sigma}^{1/3} F_{\text{x}}^{\text{B86-MGC}}(x_{\sigma})} \quad (701)$$

where $F_{\text{x}}^{\text{B86-MGC}}$ is eq. (365). The parameter $c_{\uparrow\downarrow} = 0.63$ in eq. (700a) was chosen for the opposite-spin correlation such that the exact correlation energy of the He atom is reproduced. Similarly, $c_{\sigma\sigma} = 0.96$ for the same-spin correlation was determined from the Ne atom. The functional is more accurate than `gga_c_p86` for atomic correlation energies.

`mgga_c_b94`⁷⁵⁸ (1994)

The analytical form of this functional differs from `mgga_c_b88` in the exchange hole Coulomb potential $v_{\text{x},\sigma}^{\text{hole}}$, that is here chosen as the expression from `mgga_x_br89_1`, i.e. eq. (552). Compared to `mgga_c_b88`, the expression chosen here for $v_{\text{x},\sigma}^{\text{hole}}$ depends additionally on $\nabla^2 n_{\sigma}$ and τ_{σ} . Also, the parameter $c_{\sigma\sigma}$ in eq. (700a) for same-spin correlation was reoptimized ($c_{\sigma\sigma} = 0.88$) by fitting to reference correlation energies of the atoms in the first and second rows of the periodic table. This functional was combined with `mgga_x_br89_1` for exchange to calculate the atomization energies, ionization potentials, and proton affinities of molecules.

`mgga_c_lap1`, `mgga_c_lap2`^{759,760} (1994)

These functionals are extensions of `lda_c_m11`

and `lda_c_m12`. The expression for the correlation energy density is also given by eqs. (287) and (288) with

$$k_{\uparrow\downarrow} = \alpha \frac{2k_{\uparrow}k_{\downarrow}}{k_{\uparrow} + k_{\downarrow}} \quad (702)$$

for the opposite-spin inverse correlation length. However, instead of using eq. (49) for k_{σ} in eq. (702) as in the case of `lda_c_m11` and `lda_c_m12` (which leads to eq. (289)), the following expression is here used (note that eq. (11) in ref. 759 has a typo):

$$k_{\sigma}^2 = \frac{1}{\beta_{\sigma}} = \frac{2}{3} \frac{1}{n_{\sigma}} \left(\tau_{\sigma} - \frac{1}{8} \nabla^2 n_{\sigma} \right) \quad (703)$$

which introduces the dependence on $\nabla^2 n_{\sigma}$ and τ_{σ} . Equation (703) was introduced in the context of the local thermodynamic approach in DFT, where β_{σ} is defined as a local temperature parameter.⁶⁵⁷

The correlation functional was then combined with `gga_x_b88` for exchange to determine the optimal values of α in eq. (702) and b_3 in eq. (288) for the binding energies of 19 molecules (the other parameters b_i were kept unchanged). However, the correlation functional was implemented only for the energy, while the corresponding potential was replaced by its LDA limit (i.e., when k_{σ} given by eq. (49) is used in eq. (702)). In order to compensate for this inconsistency, two values of α were considered: α_{e} in the energy functional and α_{p} in the potential. The optimized values of the functional `mgga_c_lap1` are $\alpha_{\text{e}} = 1.29$, $\alpha_{\text{p}} = 0.2$, and $b_3 = 1.45$. In another procedure, `mgga_c_lap2`, where the beyond-LDA corrections in both exchange and correlation are accounted for only in the energy functional (i.e., the xc potential is entirely of LDA type), $\alpha_{\text{e}} = 1.27$, $\alpha_{\text{p}} = 0.196$, and $b_3 = 1.48$ were obtained.

Results for geometries and binding energies of molecules show that the functionals can be more accurate than standard GGA functionals, such as BP86 (`gga_x_b88` + `gga_c_p86`) or PW91 (`gga_x_pw91` + `gga_c_pw91`). It was also noted that the values of the parameters α_{e} , α_{p} , and b_3 listed above are still valid when

`gga_x_b88` is replaced by `gga_x_pw86` for the exchange.

`mgga_c_lap1_b`, `mgga_c_lap2_b`⁷⁶¹ (1995)

These are reparametrizations of `mgga_c_lap1` and `mgga_c_lap2`. The parameters α_e , α_p , and b_3 were reoptimized using a larger training set. The new values are $\alpha_e = 1.255$, $\alpha_p = 0.394$, and $b_3 = 1.48$ for `mgga_c_lap1_b`, and $\alpha_e = 1.27$, $\alpha_p = 0.392$, and $b_3 = 1.48$ for `mgga_c_lap2_b`.

`mgga_c_bc95`¹⁶⁵ (1995)

Becke¹⁶⁵ developed a correlation functional based on four minimal requirements: (i) correct HEG limit, (ii) separate handling of the parallel- and opposite-spin correlations (see section 2.18.3), (iii) vanishing correlation energy for one-electron systems, and (iv) accurate fit to exact correlation energies of atoms. Requirement (iii) can be satisfied with the iso-orbital indicator α_σ that vanishes for any one-electron system and can therefore remove a part of the self-interaction error. However, Becke¹⁶⁵ observed that using in eq. (250) the simple form $F_{c\sigma\sigma} = \alpha_\sigma$ for the parallel-spin correlation (with $F_{c\uparrow\downarrow} = 1$) leads to a considerable overestimation of the correlation energy. Therefore, inspired by the construction of his previous correlation functional `mgga_c_b88`, he introduced density-gradient dependent cutoffs:

$$F_{c\uparrow\downarrow}^{\text{BC95}} = \frac{1}{1 + c_{\uparrow\downarrow} 2x_{\text{avg}}^2} \quad (704a)$$

$$F_{c\sigma\sigma}^{\text{BC95}} = \frac{\alpha_\sigma}{(1 + c_{\sigma\sigma} x_\sigma^2)^2} \quad (704b)$$

where x_{avg}^2 is given by eq. (45). The parameters $c_{\uparrow\downarrow} = 0.0031$ and $c_{\sigma\sigma} = 0.038$ were fit to the correlation energies of the He and Ne atoms, respectively. `lda_c_pw` is used as the LDA component in eq. (250).

The functional `mgga_c_bc95` was combined with `gga_x_b88` as well as HF exchange for calculations of the thermochemical properties of the molecules of the G2 dataset^{406,622}.

`mgga_c_blap3`, `mgga_c_plap3`, `mgga_c_-blapt`⁴⁸⁴ (1997)

These are successors of the correlation functionals `lda_c_ml1` and `mgga_c_lap1` proposed previously by the same authors. The novelty

here is that parallel-spin correlation is also accounted for. In the Stoll decomposition (see section 2.18.3), the parallel-spin term is given by

$$e_{c\sigma\sigma} = \left(1 - \frac{1}{N_\sigma}\right) \frac{1}{2} \frac{n_\sigma^2}{n} Q^{\sigma\sigma}(k_\sigma) \quad (705)$$

where N_σ is the number of spin- σ electrons in the system. Based on similarities between opposite- and parallel-spin correlations it is assumed that (C_p is a reduction factor)

$$Q^{\sigma\sigma}(k_\sigma) = C_p Q^{\uparrow\downarrow}(k_\sigma) \quad (706)$$

with $Q^{\uparrow\downarrow}$ given by eq. (288) and k_σ by eq. (703) multiplied by a factor α_e^2 :

$$k_\sigma^2 = \alpha_e^2 \frac{2}{3} \frac{1}{n_\sigma} \left(\tau_\sigma - \frac{1}{8} \nabla^2 n_\sigma \right) \quad (707)$$

Opposite-spin correlation is then obtained from eqs. (287) and (288) with a opposite-spin inverse correlation length given by

$$k_{\uparrow\downarrow} = \frac{2k_\uparrow k_\downarrow}{k_\uparrow + k_\downarrow} \quad (708)$$

where k_σ is defined by eq. (707).

Using an optimization procedure for the parameters α_e , α_p , b_3 (in eq. (288)), and C_p similar to `mgga_c_lap1`, the values obtained are $\alpha_e = 1.276$, $\alpha_p = 0.394$, $b_3 = 1.477$, and $C_p = 0.04$ for `mgga_c_blap3` (when `gga_x_b88` is used for exchange) or $\alpha_e = 1.26$, $\alpha_p = 0.394$, $b_3 = 1.48$, and $C_p = 0.01$ for `mgga_c_plap3` (when `gga_x_pw86` is used for exchange). Another set of parameters (`mgga_c_blapt`), $\alpha_e = 1.235$, $\alpha_p = 0.495$, $b_3 = 1.7414$, and $C_p = 0.54$, was obtained by fitting to accurate correlation energies of the atoms He to Ar (in combination with `gga_x_b88`).

Compared to `mgga_c_lap1`, which does not include parallel-spin correlation, a modest improvement is obtained with `mgga_c_blap3` and `mgga_c_plap3` for the binding energy of molecules.

Note that the explicit dependence on N_σ in eq. (705) makes these functionals formally not semi-local functionals (see discussion for

`lda_x_rae`).

`mgga_c_th`^{133,762} (1997)

This functional of Tsuneda and Hirao⁷⁶², which is based on `mgga_c_cs` and uses the Stoll decomposition (see section 2.18.3), reads

$$e_{c\uparrow\downarrow}^{\text{TH}} = -\frac{1}{n} \left(\frac{n_{\uparrow}^{1/3}}{K_{\downarrow}} + \frac{n_{\downarrow}^{1/3}}{K_{\uparrow}} \right)^3 \frac{0.04488}{1 + \frac{0.7826}{\beta_{\uparrow\downarrow}}} \quad (709a)$$

$$e_{c\sigma\sigma}^{\text{TH}} = -0.07614 \frac{n_{\sigma} W_{\sigma\sigma}}{n K_{\sigma}^3} \quad (709b)$$

In the above equations, $K_{\sigma} = 2C_x F_x^{\text{B88}}$, where F_x^{B88} is the enhancement factor of `gga_x_b88` given by eq. (368), and

$$W_{\sigma\sigma} = \frac{2n_{\sigma} A_{\sigma}}{n_{\sigma}^2 \beta_{\sigma\sigma}^2} \quad (710)$$

with

$$A_{\sigma} = \tau_{\sigma} - \tau_{\sigma}^{\text{W}} \quad (711)$$

The numerator of eq. (710) is derived from the diagonal element of the second-order HF reduced-density matrix. In eqs. (709a) and (710),

$$\beta_{\sigma\sigma'} = q_{\sigma\sigma'} \frac{n_{\sigma}^{1/3} n_{\sigma'}^{1/3} K_{\sigma} K_{\sigma'}}{n_{\sigma}^{1/3} K_{\sigma} + n_{\sigma'}^{1/3} K_{\sigma'}} \quad (712)$$

where the parameters $q_{\uparrow\downarrow} = 2.68$ and $q_{\sigma\sigma} = 2.60$ were determined by fitting to the exact correlation energies of the He and Be atoms, respectively. Then, with these values for $q_{\sigma\sigma'}$, the various coefficients in eqs. (709a) and (709b) were determined by a least-square fit of a more accurate expression for the correlation energy.

The correlation energies of atoms from He to Ar obtained with this functional are overall close to those obtained with `mgga_c_cs`.

`mgga_c_ft98`¹⁶¹ (1998)

Alike its exchange counterpart `mgga_x_ft98`, this functional depends on the Laplacian of the density $\nabla^2 n_{\sigma}$. The analytical form is the same as that of `gga_c_ft97` with the following differences. First, $|\nabla r_{s\sigma}|^2$ is replaced by

$$y_{\sigma} = |\nabla r_{s\sigma}|^2 + c_1 (|\nabla r_{s\sigma}|^2 - \nabla^2 r_{s\sigma})^2 \quad (713)$$

which introduces the dependence on $\nabla^2 n_{\sigma}$. Then, eqs. (479) and (482) are substituted by the similar functions

$$F^{\perp}(r_{s\sigma}, y_{\sigma}) = (1 + c_2^2 y_{\sigma}^2) \frac{e^{-c_2^2 y_{\sigma}^2}}{\sqrt{1 + c_3 \frac{y_{\sigma}}{r_{s\sigma}}}} \quad (714)$$

and

$$F^{\parallel}(r_{s\sigma}, y_{\sigma}) = \frac{1 + c_4^2 y_{\sigma}^2}{\sqrt{1 + (4.979634 - c_3) \frac{y_{\sigma}}{r_{s\sigma}}}} e^{-c_4^2 y_{\sigma}^2} \quad (715)$$

respectively, where $c_1 = 0.099635$, $c_2 = 0.083726$, $c_3 = 0.064988$, and $c_4 = 2.807834$ were obtained by fitting to reference correlation energies of atoms.⁶⁰⁰

`mgga_c_vsxc`^{167,168} (1998)

Van Voorhis and Scuseria¹⁶⁷ proposed to parameterize this correlation functional using the same function f^{GVT4} (eq. (561)) as the one used in the exchange companion `mgga_x_gvt4`. Based on the Stoll decomposition, eq. (250) with `lda_c_pw`, the functional reads

$$F_{c\sigma\sigma}^{\text{VSXC}} = (1 - z_{\sigma}) f_{c\sigma\sigma}^{\text{GVT4}}(x_{\sigma}, \tilde{z}_{\sigma}) \quad (716a)$$

$$F_{c\uparrow\downarrow}^{\text{VSXC}} = f_{c\uparrow\downarrow}^{\text{GVT4}}\left(\sqrt{2}x_{\text{avg}}, \tilde{z}_{\text{tot}}\right) \quad (716b)$$

where x_{avg} is eq. (45) and \tilde{z}_{tot} is eq. (89). The two sets of parameters in eq. (561) (14 in total), given in ref. 168 with full accuracy, were optimized together with the seven parameters for exchange.

`mgga_c_kcis`⁶¹⁰⁻⁶¹³ (1999)

The energy spectrum of the HEG is continuous, while that of finite systems consists of discrete states up to the ionization threshold. The idea from Krieger et al.⁶¹⁰ for constructing the functional `mgga_c_kcis` is to include the discrete character of the spectrum of finite systems by considering the HEG with a gap in the excitation spectrum (measured locally by G , defined below). This is a way to include a feature of inhomogeneous systems into the theoretical model to go beyond the HEG. Based on this,

the expression for the functional is given by

$$e_c^{\text{KCIS}} = e_c^{\text{GGA-GAP}}(n_\uparrow, n_\downarrow, \nabla n) - \frac{1}{n} \sum_\sigma z_\sigma n_\sigma e_c^{\text{GGA-GAP}}(n_\sigma, 0, \nabla n_\sigma) \quad (717)$$

where

$$e_c^{\text{GGA-GAP}}(n_\uparrow, n_\downarrow, g) = e_c^{\text{GAP,P}}(r_s, g, G) + f_c(\zeta) \times [e_c^{\text{GAP,F}}(r_s, g, G) - e_c^{\text{GAP,P}}(r_s, g, G)] \quad (718)$$

with $f_c(\zeta)$ given by eq. (275), $g = |\nabla n_\sigma|$, $G = g^2/(8n_\sigma^2)$, and

$$e_c^{\text{GAP,P}}(r_s, g, G) = \frac{e_c^{\text{GGA,P}}(r_s, g) + c_1(r_s)G}{1 + c_2(r_s)G + c_3(r_s)G^2} \quad (719a)$$

$$e_c^{\text{GAP,F}}(r_s, g, G) = \frac{e_c^{\text{GGA,F}}(r_s, g) + 0.7c_1(r_s)G}{1 + 1.5c_2(r_s)G + 2.59c_3(r_s)G^2} \quad (719b)$$

where

$$e_c^{\text{GGA,P}}(r_s, g) = \frac{e_c^{\text{PW-LDA}}(\zeta = 0)}{1 + \beta \ln \left(1 + \frac{t_0^2}{|e_c^{\text{PW-LDA}}(\zeta = 0)|} \right)} \quad (720a)$$

$$e_c^{\text{GGA,F}}(r_s, g) = \frac{e_c^{\text{PW-LDA}}(\zeta = 1)}{1 + \beta \ln \left(1 + \frac{2^{-1/3}t_0^2}{|e_c^{\text{PW-LDA}}(\zeta = 1)|} \right)} \quad (720b)$$

with $t_0 = t(\zeta = 0)$ given by eq. (57), $\beta = \beta^{\text{MB}}$, and $e_c^{\text{PW-LDA}}$ is `lda_c_pw` correlation-energy density. The functions $c_i(r_s)$ in eqs. (719a) and (719b) are given by

$$c_1(r_s) = C \frac{2(e'_c)^2 - e_c^{\text{PW-LDA}}(\zeta = 0)e''_c}{2\{Ce'_c - [e_c^{\text{PW-LDA}}(\zeta = 0)]^2\}} \quad (721a)$$

$$c_2(r_s) = \frac{2e_c^{\text{PW-LDA}}(\zeta = 0)e'_c - Ce''_c}{2\{Ce'_c - [e_c^{\text{PW-LDA}}(\zeta = 0)]^2\}} \quad (721b)$$

$$c_3(r_s) = -\frac{2(e'_c)^2 - e_c^{\text{PW-LDA}}(\zeta = 0)e''_c}{2\{Ce'_c - [e_c^{\text{PW-LDA}}(\zeta = 0)]^2\}} \quad (721c)$$

where

$$e'_c(r_s) = \frac{a_1 r_s^{3/2}}{1 + a_2 r_s^{1/2} + a_3 r_s + a_1 r_s^{3/2}} \quad (722a)$$

$$e''_c(r_s) = \sum_{i=3}^7 b_i r_s^i \quad (722b)$$

$$C(r_s) = f_c r_s^{-2} \quad (722c)$$

with $f_c = 0.06483(9\pi/4)^{2/3}$.

Besides recovering the correct limit of the HEG and having the proper scaling behavior in the high-density limit, the functional is also free of one-electron self-interaction error, since $z_\sigma = 1$ for one-electron systems, leading to a cancellation of the two terms in eq. (717).

`mgga_c_pkzb`^{13,14} (1999)

For the companion functional of `mgga_x_pkzb`, Perdew et al.¹³ decided to use the kinetic-energy density to remove the self-interaction error in the correlation functional for one-particle densities. Their functional can be written in the Stoll form eq. (250), using `gga_c_pbe` as the reference functional $e_{c\sigma\sigma'}^{\text{ref}}$ and

$$F_{c\uparrow\downarrow}^{\text{PKZB}} = 1 + C \left(\frac{x_{\text{tot},5/3}^2}{8\tilde{t}} \right)^2 \quad (723a)$$

$$F_{c\sigma\sigma}^{\text{PKZB}} = F_{c\uparrow\downarrow}^{\text{PKZB}} - (1 + C)z_\sigma^2 \quad (723b)$$

with $x_{\text{tot},5/3}^2$ given by eq. (44). It is rather simple to see that since for one-electron densities $F_{c\uparrow\downarrow}^{\text{PKZB}} \rightarrow 1 + C$, $F_{c\sigma\sigma}^{\text{PKZB}} \rightarrow 0$, and $e_{c\uparrow\downarrow}^{\text{PBE}} \rightarrow 0$, the total `mgga_c_pkzb` correlation energy vanishes. The constant $C = 0.53$ was fitted such that surface correlation energies for jellium (with $2 \leq r_s \leq 6$) agree well with the values from `gga_c_pbe`.

`mgga_c_tau1`⁴⁸² (2000)

This functional belongs to the family of functionals `lda_c_ml1`, `mgga_c_lap1`, and `mgga_c_blap3` previously developed by Proynov et al.⁴⁸². It was derived by using different forms (eqs. (726) and (729)) for the second-order term in the expansion of the opposite-

and parallel-spin Hartree-like pair density in the adiabatic connection formula. Within the Stoll decomposition (see section 2.18.3), the opposite-spin term reads

$$e_{c\uparrow\downarrow}^{\tau 1} = \frac{n_{\uparrow}n_{\downarrow}}{n}Q^{\uparrow\downarrow}(k_{\uparrow\downarrow}) + \frac{B_{\uparrow\downarrow}^2}{n}Q_2^{\uparrow\downarrow}(k_{\uparrow\downarrow}) \quad (724)$$

where $Q^{\uparrow\downarrow}$ is given by eq. (288),

$$Q_2^{\uparrow\downarrow}(k) = -\frac{c_1}{k^2(1+c_2k)} - \frac{c_3}{k^3}\ln\left(1+\frac{c_4}{k}\right) + \frac{c_5}{k^3} + \frac{c_6}{k^4} \quad (725)$$

and

$$B_{\uparrow\downarrow}^2 = \beta_2 \left[\frac{1}{12} (n_{\uparrow}\nabla^2 n_{\downarrow} + n_{\downarrow}\nabla^2 n_{\uparrow}) - \frac{1}{6} \nabla n_{\uparrow} \cdot \nabla n_{\downarrow} \right] e^{-c/n^{1/3}} \quad (726)$$

with $c = 0.253$.^{417,763} The coefficients c_i in eq. (725) are $c_1 = 0.583090$, $c_2 = 1.757515$, $c_3 = 4.377624$, $c_4 = 0.568985$, $c_5 = 0.331770$, and $c_6 = 2.302031$. For the parallel-spin correlation, the energy density is given by

$$e_{c\sigma\sigma}^{\tau 1} = \left(1 - \frac{1}{N_{\sigma}}\right) \frac{1}{2} \frac{n_{\sigma}^2}{n} [Q^{\sigma\sigma}(k_{\sigma}) + B_{\sigma\sigma}^2 Q_2^{\sigma\sigma}(k_{\sigma})] \quad (727)$$

where N_{σ} is the number of spin- σ electrons in the system, $Q^{\sigma\sigma}$ is calculated with eq. (706), similarly

$$Q_2^{\sigma\sigma}(k_{\sigma}) = C_p Q_2^{\uparrow\downarrow}(k_{\sigma}) \quad (728)$$

and

$$B_{\sigma\sigma}^2 = \frac{\gamma_2}{n_{\sigma}} (\tau_{\sigma} - 2\tau_{\sigma}^W) e^{-c/n^{1/3}} \quad (729)$$

In the equations above, k_{σ} and $k_{\uparrow\downarrow}$ are given by eqs. (707) and (708), respectively.

The parameters were optimized for the binding energies of a small set of molecules, and the obtained values are $\alpha_e = 1.299$ (in eq. (707)), $b_3 = 1.47$ (in eq. (288)), $C_p = 0.045$ (in eq. (728)), and $\gamma_2 = 0.175$ (in eq. (729)). The functional was combined with `gga_x_b88m` for exchange that was optimized together with the parameters of `mgga_c_tau1`. Note that the

value of the parameter β_2 in eq. (726) was set to zero since the second term in eq. (724) did not lead to any improvement in the results.

The functional improves over the standard GGA functional BP86 (`gga_x_b88` combined with `gga_c_p86`) for the binding energy and geometry of molecules, but is not as accurate as the B3LYP hybrid.³⁹⁷

Note that the explicit dependence on N_{σ} in eq. (727) makes the `mgga_c_tau1` functional formally not a semi-local functional (see discussion for `lda_x_rae`).

`mgga_c_kcisk`⁷⁶⁴ (2001)

This functional is an alternative version of `mgga_c_kcis` that is based on the HEG with a gap in the excitation spectrum. The differences with respect to `mgga_c_kcis` concern eqs. (720a) and (720b) that are now given by

$$e_c^{\text{GGA,P}}(r_s, g) = \frac{e_c^{\text{PW-LDA}}(r_s, \zeta = 0)}{1 + p \ln \left[1 + \frac{\gamma_0(r_s)t_0^2}{p |e_c^{\text{PW-LDA}}(r_s, \zeta = 0)|} \right]} \quad (730a)$$

$$e_c^{\text{GGA,F}}(r_s, g) = \frac{e_c^{\text{PW-LDA}}(r_s, \zeta = 1)}{1 + p \ln \left[1 + \frac{2^{-1/3}\gamma_1(r_s)t_0^2}{p |e_c^{\text{PW-LDA}}(r_s, \zeta = 1)|} \right]} \quad (730b)$$

where $t_0 = t(\zeta = 0)$ (see eq. (57)), $e_c^{\text{PW-LDA}}$ is `lda_c_pw`, $p = 0.193$ (fit to reference atomic correlation energies), and

$$\gamma_0(r_s) = \beta + \frac{20}{3\pi(3\pi^2n)^{1/3}} e_c(2^{1/3}r_s, \zeta = 0) \quad (731a)$$

$$\gamma_1(r_s) = \beta + \frac{20}{3\pi(6\pi^2n)^{1/3}} e_c^{\text{PW-LDA}}(r_s, \zeta = 0) \quad (731b)$$

with $\beta = \beta^{\text{MB}}$. Note that $2^{1/3}r_s$ in eq. (731a) corresponds to $n/2$. Also note that eq. (22) in ref. 764 is incorrect. The functional was combined with `mgga_x_pkzsb` for the calculation of the atomization energies of molecules.

`mgga_c_tpss`¹⁶⁶ (2003)

The correlation companion of `mgga_x_tpss` was developed as a (small) correction to

mgga_c_pkzb. To start with, the functional is written as

$$e_c^{\text{TPSS}} = e_c^{\text{revPKZB}} (1 + dz^3 e_c^{\text{revPKZB}}) \quad (732)$$

where e_c^{revPKZB} is a revised version of **mgga_c_pkzb**. Unfortunately, there is a small change to this functional that makes impossible to write it as eq. (250) for the Stoll decomposition. The quantity e_c^{revPKZB} reads

$$e_c^{\text{revPKZB}} = [1 + C(\zeta, \xi)z^2] e_c^{\text{PBE}}[n_\uparrow, n_\downarrow] - [1 + C(\zeta, \xi)] z^2 \sum_{\sigma} \frac{1 + \text{sgn}(\sigma)\zeta}{2} \tilde{e}_c \quad (733)$$

where e_c^{PBE} is the **gga_c_pbe** correlation-energy density and

$$\tilde{e}_c = \max(e_c^{\text{PBE}}[n_\uparrow, 0], e_c^{\text{PBE}}[n_\uparrow, n_\downarrow]) \quad (734)$$

The main differences with respect to **mgga_c_pkzb** are (i) the replacement of z_σ (eq. (84)) by the non-spin resolved z (eq. (83)) in eq. (723b), (ii) the max function in eq. (734) that ensures that the correlation energy is negative for all densities, (iii) the second-order d -term in eq. (732), and (iv) the constant C that is replaced by a function $C(\zeta, \xi)$, where $\xi = |\nabla\zeta|/[2(3\pi^2n)^{1/3}]$. To determine $C(\zeta, \xi)$, Tao et al.¹⁶⁶ used the fact that in the strong-interaction limit e_{xc} should become independent of the spin-polarization ζ . To achieve this independence in the range $0 \leq |\zeta| \leq 0.7$ it is required that

$$C(\zeta, 0) = c_0 + c_1\zeta^2 + c_2\zeta^4 + c_3\zeta^6 \quad (735)$$

with $c_0 = 0.53$, $c_1 = 0.87$, $c_2 = 0.50$, and $c_3 = 2.26$. The dependence on ξ is designed in order to remove the self-interaction error for monovalent atoms (like Li):

$$C(\zeta, \xi) = \frac{C(\zeta, 0)}{[1 + \xi^2\phi_{-4/3}(\zeta)]^4} \quad (736)$$

Finally, the remaining constant $d = 2.8$ (in eq. (732)) was chosen such that **mgga_c_tpss** reproduces the **gga_c_pbe** surface correlation energy of jellium over the range of valence-electron bulk densities.

mgga_c_m06_l⁶⁷⁰ (2006)

As for its exchange counterpart **mgga_x_m06_l**, this functional can be seen as a mixture between **mgga_c_vsxc** and the correlation component of the M05 hybrid functional.⁶⁷¹ Using the Stoll decomposition given by eq. (250), with **lda_c_pw** for the reference LDA functional, the functions $F_{c\sigma\sigma'}$ are given by

$$F_{c\sigma\sigma}^{\text{M06-L}} = (1 - z_\sigma) [g_{c\sigma\sigma}^{\text{B97}}(x_\sigma) + f_{c\sigma\sigma}^{\text{GVt4}}(x_\sigma, \tilde{z}_\sigma)] \quad (737a)$$

$$F_{c\uparrow\downarrow}^{\text{M06-L}} = g_{c\uparrow\downarrow}^{\text{B97}}(\sqrt{2}x_{\text{avg}}) + f_{c\uparrow\downarrow}^{\text{GVt4}}(\sqrt{2}x_{\text{avg}}, \tilde{z}_{\text{tot}}) \quad (737b)$$

where $g_{c\sigma\sigma'}^{\text{B97}}$ is given by eq. (254) with $m = 4$, $f_{c\sigma\sigma'}^{\text{GVt4}}$ is the function defined in eq. (561) with $f = 0$, x_{avg} is eq. (45), and \tilde{z}_{tot} is eq. (89). The parameters in eqs. (254) and (561) were optimized together with those of **mgga_x_m06_l**. The requirement that the functional should reduce to **lda_c_pw** for the HEG was imposed, leading to the constraints

$$c_{0\sigma\sigma} + a_{\sigma\sigma} = 1 \quad (738a)$$

$$c_{0\uparrow\downarrow} + a_{\uparrow\downarrow} = 1 \quad (738b)$$

where $c_{0\sigma\sigma'}$ are the $i = 0$ coefficients in eq. (254) and $a_{\sigma\sigma'}$ are the coefficients in the first term of eq. (561).

mgga_c_tlap1, **mgga_c_tlap2**^{765,766} (2007)

This functional is based on the previous functionals developed by Proynov et al. (**lda_c_ml1**, **mgga_c_lap1**, and **mgga_c_blap3**). The expression is the same as for **mgga_c_blap3** with the difference that the expressions for k_σ (eq. (707)) and $k_{\uparrow\downarrow}$ (eq. (708)) are replaced by

$$k_\sigma^2 = \alpha_e^2 \alpha_{\text{eff}}^2 \frac{10}{3} \frac{1}{n_\sigma} \left(\tau_\sigma - \frac{1}{8} \nabla^2 n_\sigma \right) \quad (739)$$

and

$$k_{\uparrow\downarrow} = \beta_e \beta_{\text{eff}} \frac{2b_{s\uparrow}b_{s\downarrow}}{\sqrt{n_\uparrow}b_{s\downarrow} + \sqrt{n_\downarrow}b_{s\uparrow}} \quad (740)$$

respectively. In eq. (740)

$$b_{s\sigma} = \sqrt{\frac{10}{3} \left(\tau_\sigma - \frac{1}{8} \nabla^2 n_\sigma \right)} \quad (741)$$

and β_{eff} is given by eq. (308), while in eq. (739) $\alpha_{\text{eff}} = \alpha_n$ that is given by eq. (311a). The coefficients η_i in α_{eff} and β_{eff} were obtained from data for the HEG.⁴²⁴ Other differences with respect to `mgga_c_blap3` concern the values of the parameters. $b_3 = 1.741397$ in eq. (288) is chosen to be the original value from `lda_c_m11`, while $C_p = 1$ in eq. (706). Using `gga_x_b88` for exchange, α_e in eq. (739) and β_e in eq. (740) were optimized for the binding energies and geometries of a set of molecules, leading to $\alpha_e = 2.53$ and $\beta_e = 1.087$ (`mgga_c_tlap1`). In another optimization scheme (`mgga_c_tlap2`), where the potential is the LDA-type limit (as done for `mgga_c_lap2`), the value of the additional parameters in the potential, $\alpha_p = \beta_p = 0.786$, were obtained by fitting the geometries of the molecules. The functional has a good accuracy for the binding energy of molecules and improves over its predecessors.

`mgga_c_revtpss`^{594,595} (2009)

For this revised version of `mgga_c_tpss`, Perdew et al.⁵⁹⁴ decided to use `gga_c_regtpss` instead of `gga_c_pbe` in eqs. (733) and (734). The coefficients in the function $C(\zeta, 0)$ (eq. (735)) were then readjusted in order to fulfill the original conditions entering into the construction of `mgga_c_tpss`, leading to $c_0 = 0.59$, $c_1 = 0.9269$, $c_2 = 0.6225$, and $c_3 = 2.1540$. The functional `mgga_x_revtpss` is the exchange counterpart.

`mgga_c_tpssloc`⁶⁰⁵ (2012)

This functional was derived by first substituting `gga_c_pbe` for `gga_c_pbeloc` in eqs. (733) and (734) of `mgga_c_tpss`. The new values $d = 4.5$ in eq. (732) and $c_0 = 0.35$ in eq. (735) were obtained from a fit to data of jellium surfaces⁶⁰⁷ and the Hooke atom.⁷⁶⁷

Similarly to what was observed with `gga_c_pbeloc`, `mgga_c_tpssloc` exhibits a better compatibility with HF/EXX, compared

to `mgga_c_tpss` or `mgga_c_revtpss`.

`mgga_c_zvtpss`, `mgga_c_zvtpssloc`⁶⁰⁸ (2012)

The idea behind the construction of these functionals was to improve the compatibility of a MGGA correlation functional with HF/EXX. For this purpose, Constantin et al.⁶⁰⁸ found useful to multiply the energy density e_c of e.g. `mgga_c_tpss` or `mgga_c_tpssloc` by the function $f(\nu, \zeta)$ given by eq. (515), with $x = 1/6$ in eq. (516). The parameters ω and α in eq. (515) were determined by imposing two conditions: (i) the parent functional should be closely recovered for $\zeta \lesssim 0.3$, which concerns mainly the unpolarized core regions, and (ii) the exact ζ -dependence (invariance for one-electron systems) should be reproduced as much as possible for $\zeta \gtrsim 0.7$. These two conditions led to $\omega = 9/2$, for both `mgga_c_zvtpss` and `mgga_c_zvtpssloc`, and $\alpha = 6$ and 8 for `mgga_c_zvtpss` and `mgga_c_zvtpssloc`, respectively.

Results for atomization energies, barrier heights, and kinetic properties^{602,603,615} show that `mgga_c_zvtpss` and `mgga_c_zvtpssloc` are indeed more compatible with HF exchange than their parent functionals. Note that the same idea was also applied for constructing `gga_c_zvpbeloc`.

`mgga_c_m11_1`⁶⁸⁵ (2011)

This functional has the same analytical form as the correlation component of the M08-HX and M08-SO hybrid functionals.⁷⁶⁸ The tradition of using the Stoll ansatz (see section 2.18.3) to describe separately the opposite- and parallel-spin contributions to the correlation energy is here not followed, as this had been shown to be inaccurate for the HEG.³⁶⁹ Consequently, the self-interaction correction factor $1 - z_\sigma$ (used in `mgga_c_m06_1` for instance) is also not used, since it can lead to convergence problems.⁷⁶⁹ Instead, an interpolation between the `lda_c_pw` and `gga_c_pbe` functionals is used:

$$e_c^{\text{M08}} = \sum_{i=0}^m c_i w^i e_c^{\text{PW-LDA}} + \sum_{i=0}^m d_i w^i H_0 \quad (742)$$

where H_0 is the gradient correction of `gga_c_pbe` (see eq. (473)). The variable w

is defined by eq. (90) and $m = 8$ is chosen for the sums in the case of `mgga_c_m11_1`, while $m = 11$ was chosen for M08-HX and M08-SO.⁷⁶⁸ The parameters c_i and d_i were fit together with the parameters in the associated exchange functional, `mgga_x_m11_1`. The correct HEG limit (LDA, represented by `lda_c_pw`) and the second-order term in the density-gradient expansion were used as constraints for the parameters.

`mgga_c_mn12_1`⁶⁸⁶ (2012)

This functional has the same form as the correlation component of the M08-HX and M08-SO hybrid functionals⁷⁶⁸ with $m = 8$ for the sums in eq. (742). The parameters c_i and d_i were re-fit together with the associated exchange functional, `mgga_x_mn12_1`. Note that the correct HEG limit (LDA) was not enforced.

`mgga_c_cc`⁷⁷⁰ (2014)

Schmidt et al.⁷⁷⁰ constructed a correlation functional based on the following requirements: it should (i) be compatible with HF and (ii) be free from one-electron self-interaction error, (iii) have an energy density that has the correct asymptotic behavior in the vacuum, and (iv) have the correct HEG limit. The functional form satisfying these requirements that they proposed depends on the HF exchange-energy density e_x^{HF} :

$$e_c = \frac{1 - z\zeta^2}{1 + c\zeta^2} (e_x^{\text{LDA}} - e_x^{\text{HF}}) + e_c^{\text{CC}} \quad (743)$$

where e_x^{LDA} is `lda_x` and e_c^{CC} is the following τ -MGGA component (`mgga_c_cc`):

$$e_c^{\text{CC}} = (1 - z\zeta^2) e_c^{\text{PW-LDA}} \quad (744)$$

where $e_c^{\text{PW-LDA}}$ is `lda_c_pw`. Thanks to the dependence on $1 - z\zeta^2$ in eqs. (743) and (744), the functional gives zero correlation energy in the case of one-electron systems, i.e. when $\zeta = 1$ and $z = 1$. Equation (743) contains an empirical parameter (c) whose suggested value is 0.5. Note that `mgga_c_cc` is a component of the `mgga_c_ccalda` functional.

`mgga_c_scan`²⁷⁶ (2015)

The correlation component of the popular

SCAN functional is written as an interpolation in the variable α_c (eq. (82)), similarly to its exchange counterpart `mgga_x_scan`:

$$e_c^{\text{SCAN}} = e_c^1 + f(\alpha_c) (e_c^0 - e_c^1) \quad (745)$$

The interpolation function f is the same as in `mgga_x_scan`, eq. (613). The three parameters ($c_{1c} = 0.64$, $c_{2c} = 1.5$, and $d_c = 0.7$) entering f were fit together with the four parameters of the exchange part, as explained for `mgga_x_scan`.

The function $e_c^1 = e_c^{\text{SCAN}}(\alpha_c = 1)$ was taken as a variant of `gga_c_pbe` altered to improve the 2D limit under nonuniform scaling. The differences to `gga_c_pbe` (eqs. (467) and (473)) are the replacements of the constant β by eq. (502) and of the function H_0 by

$$H_1^{\text{SCAN}} = \gamma\phi_{2/3}^3 \ln \left\{ 1 + \frac{\beta}{\gamma A} [1 - g(At^2)] \right\} \quad (746)$$

with

$$g(At^2) = \frac{1}{(1 + 4At^2)^{1/4}} \quad (747)$$

The function $e_c^0 = e_c^{\text{SCAN}}(\alpha_c = 0)$ was modeled in analogy with e_c^1 , and realizing that this function could only depend on s (eq. (46)) and not on t (eq. (57)). It reads

$$e_c^0 = [e_{c,\text{LDA}}^{\text{SCAN}}(r_s) + H_0^{\text{SCAN}}(r_s, s)] G_c(\zeta) \quad (748)$$

The ζ -dependent function

$$G_c(\zeta) = \{1 - 2.3631 [\phi_{4/3}(\zeta) - 1]\} (1 - \zeta^{12}) \quad (749)$$

was chosen such that (i) the correlation energy is zero for any one-electron systems, and (ii) $e_{xc}^{\text{SCAN}}/e_x^{\text{LDA}}$ (e_x^{LDA} is eq. (256)) is independent of ζ in the interval $0 \leq |\zeta| < 0.7$ when $r_s \rightarrow \infty$, $s = 0$, and $\alpha_c = 0$.⁷⁷¹

The LDA-type component $e_{c,\text{LDA}}^{\text{SCAN}}$ reads

$$e_{c,\text{LDA}}^{\text{SCAN}}(r_s) = -\frac{b_{1c}}{1 + b_{2c}\sqrt{r_s} + b_{3c}r_s} \quad (750)$$

The parameters b_{ic} were determined as follows: $b_{1c} = 0.0285764$ was fit to reproduce the high-density limit of the two-electron ion with nuclear charge $Z \rightarrow \infty$;⁷⁷² $b_{2c} = 0.0889$ was adjusted to reproduce the xc energy of the He

atom;¹⁵⁷ finally, $b_{3c} = 0.125541$ was obtained from the lower bound on the xc energies of two-electron systems.¹⁵⁰

The remaining quantity, H_0^{SCAN} , is given by

$$H_0^{\text{SCAN}}(r_s, s) = b_{1c} \ln \{1 + w_0(r_s) \times [1 - g_\infty(\zeta = 0, s)]\} \quad (751)$$

where

$$w_0(r_s) = e^{-e_{c,\text{LDA}}^{\text{SCAN}}(r_s)/b_{1c}} - 1 \quad (752)$$

with $g_\infty(\zeta = 0, s)$ being the $r_s \rightarrow \infty$ limit of eq. (747):

$$g_\infty(\zeta = 0, s) = \frac{1}{(1 + 4\chi_\infty s^2)^{1/4}} \quad (753)$$

with $\chi_\infty \approx 0.128026$.⁵⁵⁹

[mgga_c_theta_mgga](#)⁷⁰¹ (2015)

This correlation functional is orbital-free alike its exchange counterpart [mgga_x_theta_mgga](#), and depends on the variable $\tilde{g}(\theta)$ given by eqs. (617) and (618), which are now defined in terms of the total density n instead of n_σ . The functional form is given by eq. (732) of [mgga_c_tpss](#), but with two modifications: z is replaced by $\tilde{g}(\theta)$ and $\beta = \beta^{\text{MB}}$ in e_c^{PBE} ([gga_c_pbe](#)) is replaced by

$$\beta(\theta) = \tilde{g}(\theta) \beta^{\text{H}} + [1 - \tilde{g}(\theta)] \beta^{\text{GE}} \quad (754)$$

where $\beta^{\text{H}} = 0.08384$ and $\beta^{\text{GE}} = 0.0375$ are calculated from μ^{H} and μ^{GE} (used in [mgga_x_theta_mgga](#)), respectively, using the relation $\beta = 3\mu/\pi^2$ in order to recover the LDA linear response.

[mgga_c_mn15_1](#)⁷⁰² (2015)

This functional has the same analytical form as the correlation component of the M08-HX and M08-SO hybrid functionals,⁷⁶⁸ with $m = 8$ for the sums in eq. (742). The parameters c_i and d_i were refit together with those in the associated exchange functional, [mgga_x_mn15_1](#). Note that this functional does not reduce to the correct LDA limit of the HEG.

[mgga_c_tm](#)⁷⁰³ (2016)

This functional has the same form as [mgga_c_tpss](#), but uses a simpler expression

for $C(\zeta, 0)$ in eq. (736):

$$C(\zeta, 0) = c_1 \zeta^2 + c_2 \zeta^4 \quad (755)$$

where the coefficients $c_1 = 0.1$ and $c_2 = 0.32$ were determined to improve the low-density (i.e., strong-interaction) limit.

[mgga_c_scanl](#)⁷¹⁰⁻⁷¹² (2017)

This is a deorbitalized version of [mgga_c_scan](#), where the kinetic-energy density τ is replaced by the orbital-free approximation $\tau^{\text{PC07opt}}[n_\uparrow, n_\downarrow] = \tau_\uparrow^{\text{PC07opt}} + \tau_\downarrow^{\text{PC07opt}}$ (see eq. (633)), which depends on the Laplacian of the density.^{710,711} It is the correlation counterpart of the deorbitalized exchange [mgga_x_scanl](#).

[mgga_c_rev06_1](#)⁶⁷² (2017)

This functional has the same analytical form as [mgga_c_m06_1](#), but with a different choice for the parameters in eq. (561) that are set to zero and therefore not optimized: $f = 0$ in the case of [mgga_c_m06_1](#), while $d = e = 0$ for [mgga_c_rev06_1](#). The parameters were reoptimized together with the associated exchange functional, [mgga_x_rev06_1](#). Unlike [mgga_c_m06_1](#), the correct HEG limit was not imposed.

[mgga_c_revscan](#)⁷¹⁸ (2018)

Since the Taylor gradient expansion of the function g in [mgga_c_scan](#) (eqs. (747) and (753)) has a nonzero fourth-order term, a deviation from the second-order expansion is more pronounced than in the case of [gga_c_pbe](#). This led Mezei et al.⁷¹⁸ to propose the following alternative:

$$g(At^2) = \frac{1}{2(1 + 8At^2)^{1/4}} + \frac{1}{2(1 + 80A^2t^4)^{1/8}} \quad (756a)$$

$$g_\infty(\zeta = 0, s) = \frac{1}{2(1 + 8\chi_\infty s^2)^{1/4}} + \frac{1}{2(1 + 80\chi_\infty^2 s^4)^{1/8}} \quad (756b)$$

that has no fourth-order term in the expansion. With this revised function g , the parameters in eq. (750) were redetermined from the following

conditions (with the original `mgga_x_scan` for exchange): (i) high-density limit of the correlation energy of the two-electron ions ($b_{1c} = 0.030197$), (ii) correlation energy of the He atom ($b_{2c} = 0.06623$), and (iii) single-orbital lower bound $e_{xc}^{\text{revSCAN}}/e_x^{\text{LDA}} \leq 1.67082$ (e_x^{LDA} is eq. (256)) for the low-density limit of the HEG ($b_{3c} = 0.16672$).

Finally, the values $c_{1c} = 1.131$, $c_{2c} = 1.7$, and $d_c = 1.37$ for the parameters in eq. (613) were obtained empirically by a fit to the atomization energy of the AE6 test set.^{602,603} This was done conjointly with a refitting of parameters in `mgga_x_revscan`.

`mgga_c_lltpss`⁷¹⁶ (2018)

Similarly to the corresponding exchange `mgga_x_lltpss`, this functional was obtained from `mgga_c_tpss` by replacing the kinetic-energy density τ by the orbital-free Laplacian-dependent approximation $\tau^{\text{PC07}}[n]$ from Perdew and Constantin⁷¹³, see eq. (633).

`mgga_c_rscan`⁷²³ (2019)

This functional was derived the same way as its exchange counterpart `mgga_x_rscan`, that is, by using regularized versions of the iso-orbital indicator and switching function in `mgga_c_scan`. More precisely, the switching function $f(\alpha_c)$ in eq. (745) is replaced by a function $f(\alpha'_c)$ having the same form as eq. (651) (with different coefficients c_n), with α'_c given by

$$\alpha'_c = \frac{\tilde{\alpha}_c^3}{\tilde{\alpha}_c^2 + \alpha_r} \quad (757)$$

where

$$\tilde{\alpha}_c = \frac{\tau - \tau^{\text{W}}[n]}{(\tau^{\text{TF}}[n] + \tau_r) \phi_{5/3}(\zeta)} \quad (758)$$

while $\alpha_r = 10^{-3}$ and $\tau_r = 10^{-4}$ have the same values as in `mgga_x_rscan`.

`mgga_c_revtm`⁷²¹ (2019)

This functional is a revised version of `mgga_c_tm`. It is obtained from `mgga_c_tm` similarly as `mgga_c_revtpss` is derived from `mgga_c_tpss`, namely by replacing $\beta = \beta^{\text{MB}}$ (in eqs. (467) and (468) of `gga_c_pbe` that is a component of `mgga_c_tm`) by eq. (502). The corresponding exchange functional is `mgga_x_revtm`.

`mgga_c_r2scan`^{726,727} (2020)

This functional is a numerically more stable variant of `mgga_c_scan` that satisfies the same exact constraints. It is the correlation counterpart of `mgga_x_r2scan`. The modifications with respect to `mgga_c_scan` are the following. The first one is the substitution of α_c (eq. (82)) by

$$\tilde{\alpha}_c = \frac{\tau - \tau^{\text{W}}[n]}{\tau^{\text{TF}}[n] \phi_{5/3}(\zeta) + \eta \tau^{\text{W}}[n]} \quad (759)$$

and using the switching function $f(\tilde{\alpha}_c)$ of `mgga_c_rscan`, but with eq. (759) as variable. The other modification concerns the function $g(At^2)$ (eq. (747)) that is replaced by

$$g(At^2, \Delta y) = \frac{1}{[1 + 4(At^2 - \Delta y)]^{1/4}} \quad (760)$$

where

$$\begin{aligned} \Delta y = & \frac{\Delta f_{c2}}{27\gamma \phi_{5/3} \phi_{2/3}^3 w_1} \left\{ 20r_s \right. \\ & \times \left[\frac{\partial (e_{c,\text{LDA}}^{\text{SCAN}} G_c)}{\partial r_s} - \frac{\partial e_c^{\text{PW-LDA}}}{\partial r_s} \right] \\ & \left. - 45\eta (e_{c,\text{LDA}}^{\text{SCAN}} G_c - e_c^{\text{PW-LDA}}) \right\} p e^{-p^2/d_{p2}^4} \end{aligned} \quad (761)$$

with $\eta = 10^{-3}$, $\Delta f_{c2} \approx -0.711402$ ⁵⁵⁹ (see ref. 726 for the accurate expression), $d_{p2} = 0.361$, $\gamma = [1 - \ln(2)]/\pi^2$, and w_1 given by eq. (469). The other quantities are the same as in `mgga_c_scan`: $e_{c,\text{LDA}}^{\text{SCAN}}$ is eq. (750), $e_c^{\text{PW-LDA}}$ is the energy density of `lda_c_pw`, G_c is eq. (749), and A is eq. (468) with β given by eq. (502).

`mgga_c_r2scanl`⁷³⁷ (2020)

This functional is derived from `mgga_c_r2scan` by replacing the kinetic-energy density τ by the orbital-free approximation $\tau^{\text{PC07opt}}[n_\uparrow, n_\downarrow] = \tau_\uparrow^{\text{PC07opt}} + \tau_\downarrow^{\text{PC07opt}}$, see eq. (633), which depends on the density Laplacian.^{710,711} `mgga_x_r2scanl` is the corresponding exchange functional.

`mgga_c_hltapw`⁶⁵⁰ (2021)

This functional has the same mathematical

form as `lda_c_pw`, but with the density n_σ replaced by n_σ^{eff} , given by eq. (669) with $x = 1/2$, and n replaced by $n^{\text{eff}} = n_\uparrow^{\text{eff}} + n_\downarrow^{\text{eff}}$. This substitution of the density was proposed as a way to turn a LDA functional into a MLDA functional. This was used as the correlation counterpart of `mgga_x_hlta`.

`mgga_c_rmggac`⁷⁷³ (2021)

The `mgga_x_mggac` exchange functional was originally combined with `gga_c_mggac` for correlation. Aiming at improving the accuracy, a correlation functional that is more suited for use with `mgga_x_mggac` was proposed. Its mathematical form differs from `mgga_c_scan` in two places. First, $\beta = \beta^{\text{MB}}$ is used instead of eq. (502). Second, the switching function f (see eqs. (613) and (745)) is replaced by

$$f(s, \alpha) = 1 - \frac{3g^3(s, \alpha)}{1 + g^3(s, \alpha) + g^6(s, \alpha)} \quad (762)$$

where

$$g(s, \alpha) = \frac{(1 + \gamma_1)\alpha}{\gamma_1 + \alpha + \gamma_2 s^2} \quad (763)$$

with $\gamma_1 = 0.08$ and $\gamma_2 = 0.3$ that were obtained by a fit to the atomization energies of the molecules in the AE6 test set.^{602,603} Note that eq. (762) depends on s (eq. (46)) and α (eq. (79)), while the function f of `mgga_c_scan` depends on α_c (eq. (82)).

`mgga_c_rregtm`⁷⁷⁴ (2021)

The `mgga_x_regtm` exchange functional was originally combined with `gga_c_regtpss` for correlation. A correlation functional that is more compatible with `mgga_x_regtm` was constructed to obtain improved results. It is based on `mgga_c_scan`, the only difference being that the switching function f (eqs. (613) and (745)) is replaced by eq. (762) with a function g that depends on α (eq. (79)) and has no dependence on s :

$$g(\alpha) = \frac{(1 + \gamma_1)\alpha}{\gamma_1 + \alpha} \quad (764)$$

The empirical parameter $\gamma_1 = 0.2$ was tuned for accurate atomization energies for the AE6 set of molecules.^{602,603}

`mgga_c_r2scan01`⁷⁴⁶ (2022)

Alike `mgga_x_r2scan01`, `mgga_c_r2scan01` dif-

fers from `mgga_c_r2scan` only by the value of η that is larger ($\eta = 10^{-2}$).

`mgga_c_tscanl`⁵⁵⁷ (2022)

This correlation free-energy functional is the counterpart of `mgga_x_tscanl`. Similarly, the τ_e -dependent free-energy correction to `mgga_c_scanl` is calculated at the GGA level as the difference between the free energy from `gga_c_kdt16` and the standard `gga_c_pbe` functional:

$$f_c^{\text{T-SCAN-L}} = e_c^{\text{SCAN-L}} + f_c^{\text{KDT16}} - e_c^{\text{PBE}} \quad (765)$$

`mgga_c_rppscan`⁷⁴⁷ (2022)

The functional `mgga_c_rscan`, a regularized version of `mgga_c_scan`, does not recover the correct HEG limit, LDA (`lda_c_pw`). As for the associated exchange `mgga_x_rppscan`, this limit can be recovered by using the iso-orbital indicator given by eq. (759) in `mgga_c_rscan`, instead of eqs. (757) and (758).

`mgga_c_ofr2`⁷⁵⁰ (2022)

This functional is a deorbitalized version of `mgga_c_r2scan`, where the kinetic-energy density τ in eq. (759) is replaced by an orbital-free approximation, $\tau^{\text{RPP}}[n_\uparrow, n_\downarrow] = \tau_\uparrow^{\text{RPP}} + \tau_\downarrow^{\text{RPP}}$, where τ_σ^{RPP} is defined by eq. (675). `mgga_x_ofr2` is the associated exchange.

`mgga_c_ccalda`⁷³¹ (2022)

This correlation functional was designed with the goal of providing a good accuracy for the atomization energies of molecules when combined `mgga_x_task`. The functional `mgga_x_task` has a reduced self-interaction error and provides the exact energy of the H atom, which suggested Lebeda et al.⁷³¹ to combine it with `mgga_c_cc` that shares similar features. This combination leads to atomization energies that are in most cases improved compared to those obtained with `mgga_x_task` + `lda_c_pw`. Also, the good accuracy of `mgga_x_task` for the band gap of solids is not altered by the addition of `mgga_c_cc`.

However, results for molecules containing the light H or Li atoms are extremely inaccurate. A remedy is to combine eq. (744) and `lda_c_pw`:

$$e_c^{\text{CCaLDA}} = f(\alpha)e_c^{\text{CC}} + [1 - f(\alpha)]e_c^{\text{PW-LDA}} \quad (766)$$

where

$$f(\alpha) = (1 + c) \frac{\alpha}{1 + c\alpha} \quad (767)$$

with α given by eq. (79), which is the spin-unpolarized version of the iso-orbital indicator, and $c = 10000$ that was chosen such that the numerical differences with respect to eq. (744) occur only for $\alpha \approx 0$, and should therefore affect only systems containing H and Li atoms.

mgga_c_ldag⁷⁷⁵ (2023)

This functional was constructed by following the same route as for **mgga_c_kcis**, **gga_c_gapc**, and **gga_c_gaploc** that are based on the HEG with a gap. The correlation-energy density is given by eq. (274), where e_c^P and e_c^F are given by eqs. (719a) and (719b) with two substitutions. First, $e_c^{\text{GGA,P}}$ and $e_c^{\text{GGA,F}}$ are replaced by the spin-unpolarized $e_c^{\text{PW-LDA}}(\zeta = 0)$ and spin-polarized $e_c^{\text{PW-LDA}}(\zeta = 1)$ limits of the **lda_c_pw** correlation-energy density, respectively. The second substitution consists of replacing the local gap $G = \tau^W/n$ by

$$G = \frac{\tau^W}{n} \frac{\tilde{x}}{1 + z + \tilde{x}} \quad (768)$$

where z is given by eq. (83) and

$$\tilde{x} = \frac{\tau_c}{\tau} \frac{1}{1 - z + \delta} \quad (769)$$

with $\tau_c = 1$ (chosen arbitrarily) and $\delta = 10^{-10}$ that was introduced to prevent the denominator of eq. (769) from becoming zero when $z = 1$. Combined with **lda_x** exchange, the functional is more accurate than LDA for the ionization potentials of atoms and molecules, as well as the surface energies of metallic surfaces.

mgga_c_lak³¹⁸ (2024)

Following the same idea as for the associated exchange functional, **mgga_x_lak**, this nonempirical functional from Lebeda et al.³¹⁸ is written as an interpolation between the $\alpha_c = 0$ and $\alpha_c = 1$ limits:

$$e_c^{\text{LAK}} = e_c^0(r_s, \zeta, s) + [1 - f(r_s, \alpha_c)] \times [e_c^1(r_s, \zeta, s) - e_c^0(r_s, \zeta, s)] g_{\text{num}}(s) \quad (770)$$

The interpolation function f reads

$$f(r_s, \alpha_c) = \frac{2}{\pi} \arctan \left[\frac{\pi}{2} f^{\text{GEA2}}(r_s) \hat{\alpha}(r_s, \alpha_c) \right] \quad (771)$$

where $\hat{\alpha} = (\alpha_c - 1) / (r_s \alpha_c)$ and

$$f^{\text{GEA2}}(r_s) = \frac{\beta_{\hat{\alpha}}(r_s)}{e_c^1(r_s, \zeta = 0, s = 0) - e_c^0(r_s, \zeta = 0, s = 0)} \quad (772)$$

with $\beta_{\hat{\alpha}} = C_x (8\pi/3)^{-1/3} \mu_{\alpha,c}$, where $\mu_{\alpha,c} = C_{\mu_\alpha} \mu_\alpha - \mu_{\alpha,x}$, with $\mu_{\alpha,x}$ given by eq. (688) and $\mu_\alpha = -\mu_{\alpha,x}/2$. The final lengthy expression for C_{μ_α} can be found in the supplemental material of ref. 318.

The functions $e_c^0 = e_c^{\text{LAK}}(\alpha_c = 0)$ and $e_c^1 = e_c^{\text{LAK}}(\alpha_c = 1)$ are defined as follows.

The expression for e_c^0 is basically the same as eq. (748) of **mgga_c_scan** with, however, eq. (750) that is replaced by $e_{c,\text{LDA}}^{\text{LAK}} = -b_{1c}/(1 + b_{2c}r_s)$, with $b_{1c} = 0.0468$ (He iso-electronic series⁶¹⁷) and $b_{2c} = 0.205601$ (single-orbital lower bound $e_{xc}^{\text{LAK}}/e_x^{\text{LDA}} \leq 1.67082$). Note that this value of b_{1c} is then also used in eqs. (751) and (752). The other difference is χ_∞ in eq. (753) that is here given by 1.55344, which was determined to reproduce the correlation energy of the two-electron ion at the limit $Z \rightarrow \infty$ of the nuclear charge Z .

The term e_c^1 has the form given by eq. (473) of **gga_c_pbe**, with H_0 replaced by

$$H_1^{\text{LAK}}(r_s, \zeta, t) = \begin{cases} H_1^+(r_s, \zeta, t), & \beta_t(r_s) \geq 0 \\ H_1^-(r_s, \zeta, t), & \beta_t(r_s) < 0 \end{cases} \quad (773)$$

where

$$H_1^\pm(r_s, \zeta, t) = \gamma \phi_{2/3}^3 \ln [1 + w_1 (1 - g_1^\pm) \times (1 - g_2 \pm g_3^\pm)] \quad (774)$$

with $\gamma = [1 - \ln(2)]/\pi^2$, w_1 given by eq. (469),

and

$$g_1^\pm(r_s, t) = \frac{1}{[1 \pm 4A(r_s, \zeta)t^2]^{1/4}} \quad (775a)$$

$$g_2(r_s, t) = \frac{1}{1 + [A(r_s, \zeta)t^2]^2} \quad (775b)$$

$$g_3^+(r_s, t) = \frac{1}{1 + a_c A(r_s, \zeta)t^2} \quad (775c)$$

$$g_3^-(r_s, t) = \frac{1}{1 - [w_1(r_s, \zeta) + b_{3c}] A(r_s, \zeta)t^2} \quad (775d)$$

In the above equations, the functions are given by $A = \beta_t / (\gamma w_1)$, $\beta_t = -C_x (8\pi/3)^{-1/3} \mu_{s,c} / c_t$, $c_t = (3\pi^2/16)^{2/3} / \phi_{2/3}^2$, and

$$\mu_{s,c}(r_s) = \mu^{\text{GE}} [C_{\mu_\alpha}(r_s)(1 + 6\mu_\alpha) - (1 + 6\mu_{\alpha,x})] \quad (776)$$

while the parameters are $a_c = 10$ and $b_{3c} = 2.85$.

Finally, g_{num} is defined by eq. (689), which is also used in `mgga_x_lak`.

Some of the exact constraints that were invoked in the development of `mgga_c_lak` are negativity of the correlation energy, uniform density scaling to the high- and low-density limits, nonuniform density scaling, and vanishing correlation energy for one-electron spin-polarized systems.

`mgga_c_mscan`³⁶⁵ (2025)

This is the correlation counterpart of `mgga_x_mscan` in the mSCAN functional, which is the collinear limit of ncSCAN for noncollinear spin-current DFT calculations.³⁶⁵ The correlation energy density is given by

$$e_c^{\text{mSCAN}} = e_c^{\text{PW-LDA}}(r_s, \zeta) F_c^{\text{SCAN}}(n, \zeta, s, \tilde{\alpha}) \quad (777)$$

where $e_c^{\text{PW-LDA}}$ is `lda_c_pw` and F_c^{SCAN} is defined as $e_c^{\text{SCAN}} / e_c^{\text{PW-LDA}}$ (see eq. (745)), but it is evaluated with a different iso-orbital indicator ($\tilde{\alpha}$, defined by eq. (691)). The functional `mgga_c_mscan` recovers `mgga_c_scan` in the non-magnetic case, but not in the polarized case.

3.3.3 Exchange and correlation

`mgga_xc_lp90`, `mgga_xc_lp90_a`, `mgga_xc_lp90_n`⁴³⁸ (1990)

These functionals arise from the way to rewrite the product of two infinite series described in `lda_xc_lp_a`. This leads to a functional form that is more flexible than eq. (339) and that depends on the gradient and Laplacian of the density (only the spin-unpolarized version was developed):

$$e_{\text{xc}}^{\text{LP-MGGA}} = - \left[a \frac{1 + \frac{b}{N}}{1 + \frac{c}{N}} + \frac{d}{8} (x^2 - u) \right] \times \frac{1}{\left(\frac{4}{3}\pi\right)^{1/3} r_s + k} \quad (778)$$

where N is the number of electrons. The coefficients were fit the same way as for the more simple LDA variants (e.g. `lda_xc_lp_a`), leading to three functionals:

- `mgga_xc_lp90`: $a = 0.80569$, $d = 2.4271 \times 10^{-2}$, and $k = 4.0743 \times 10^{-3}$, while b and c are set to zero. Note that this value of d is the corrected one mentioned in ref. 441.
- `mgga_xc_lp90_a`: $a = 0.7874$ and $d = 2.801 \times 10^{-2}$, while b , c , and k are set to zero.
- `mgga_xc_lp90_n`: $a = 0.7615$, $b = 1.6034$, $c = 2.1437$, and $d = 6.151 \times 10^{-2}$, with k set to zero.

As expected, these functionals improve over their LDA counterparts, like `lda_xc_lp_a`, for the xc energies of atoms.

The explicit dependence on the number of electrons N in eq. (778) makes the `mgga_xc_lp90_n` functional not a semi-local functional (see discussion for `lda_x_rae`). As $b = c = 0$ for `mgga_xc_lp90` and `mgga_xc_lp90_a`, these functionals are not affected by this issue.

`mgga_xc_zlp`⁴⁴¹ (1993)

This functional is a more flexible variant

of `lda_xc_zlp`. It is similarly derived from eq. (344), by choosing the functional `mgga_xc_lp90` for \tilde{e}_{xc} . This leads to

$$e_{xc}^{\text{ZLP-MGGA}} = - \left[cn^{1/3} + dn^{-4/3} \left(\tau^W - \frac{1}{8} \nabla^2 n \right) \right] \times \left[1 - \kappa n^{1/3} \ln \left(1 + \frac{1}{\kappa n^{1/3}} \right) \right] \quad (779)$$

where $c = 0.828432$, $d = 2.15509 \times 10^{-2}$, and $\kappa = 2.047107 \times 10^{-3}$ were obtained from a least-squares fit to reference xc energies of closed-shell atoms and ions.

`mgga_xc_b00_local`¹⁶⁴ (2000)

Becke¹⁶⁴ constructed an empirical hybrid functional that uses the `mgga_x_br89_1` and `mgga_c_b88` functionals for the semi-local part. His idea was to transform this hybrid functional into a pure semi-local form by replacing the HF exchange by the `mgga_x_b00` functional, itself based on `mgga_x_br89_1` (eqs. (568) and (569) with $a_t = 1$), leading to

$$e_{xc}^{\text{B00-local}} = \sum_{\sigma} \left\{ [1 + a_x f_x(w_{\sigma})] e_{x\sigma}^{\text{BR89}, \gamma=1} + a_{c\sigma\sigma} e_{c\sigma\sigma}^{\text{B88}} \right\} + a_{c\uparrow\downarrow} e_{c\uparrow\downarrow}^{\text{B88}} \quad (780)$$

The parameters were reoptimized by a fit to the experimental atomization energies of the G2 set,⁴⁰⁶ yielding $a_x = 0.135$, $a_{c\sigma\sigma} = 0.95$, and $a_{c\uparrow\downarrow} = 1.14$.

While the parent hybrid functional leads to a 1.73 kcal/mol mean absolute error of the atomization energies of the G2 set, the semi-local variant `mgga_xc_b00_local` achieves a slightly larger error of 1.87 kcal/mol at a much reduced computational cost.

`mgga_xc_tpsslyp1w`⁶³⁵ (2005)

This functional was constructed using the same strategy as for `gga_xc_mpwlyp1w`, `gga_xc_pbe1w`, and `gga_xc_pbelyp1w`, the only difference being that a τ -MGGA (`mgga_x_tpss`) was used for exchange in eq. (540) instead of a GGA. The correlation was chosen as `gga_c_lyp` and the value of a_c that was optimized for water clusters is 0.74. The functional `mgga_xc_tpsslyp1w` performs similarly as the three other functionals.

`mgga_xc_cc06`⁷⁷⁶ (2006)

By comparing the xc-energy density for bulk silicon calculated with variational MC^{777,778} with the LDA approximation, Cancio and Chou⁷⁷⁶ remarked that the difference between these two quantities can be modeled by a simple function of the Laplacian of the density. They therefore proposed the following form:

$$e_{xc}^{\text{CC06}} = (e_x^{\text{LDA}} + e_c^{\text{PW-LDA}}) F_{xc}^{\text{CC06}}(u) \quad (781)$$

where e_x^{LDA} is `lda_x`, $e_c^{\text{PW-LDA}}$ is `lda_c_pw`, and the enhancement factor reads

$$F_{xc}^{\text{CC06}}(u) = 1 + \frac{\alpha + \beta [3/(4\pi)]^{2/3} u}{1 + \gamma [3/(4\pi)]^{2/3} u} \quad (782)$$

The three parameters were fit to reproduce the variational MC xc-energy density for bulk silicon, yielding $\alpha = -0.0007$, $\beta = 0.0080$, and $\gamma = 0.026$. Note that since α is nonzero, the functional does not recover the correct HEG limit (LDA), i.e. $F_{xc}^{\text{CC06}}(u = 0) = 1 + \alpha = 0.9993$ instead of 1, albeit the deviation is small. Note that u in eq. (782) is given by eq. (58) with $n = n_{\uparrow} + n_{\downarrow}$ also in the spin-polarized case.

`mgga_xc_otpss_d`⁶³⁸ (2010)

This is a reparametrization of the TPSS functional (`mgga_x_tpss` + `mgga_c_tpss`), performed in the same way as for `gga_xc_oblyp_d`, `gga_xc_opwlyp_d`, and `gga_xc_opbe_d`. In particular, the D2 dispersion correction of Grimme⁵¹⁵ was included. The new parameters in `mgga_x_tpss` exchange are $b = 3.43$, $c = 0.75896$, $e = 0.165$, $\mu = 0.41567$, and $\kappa = 0.778$ (the last two are parameters of `gga_x_pbe` entering the definition of `mgga_x_tpss`). The parameters in the correlation part `mgga_c_tpss` are $d = 0.7$ and $\beta = 0.08861$ (the last one is in the `gga_c_pbe` part of `mgga_c_tpss`). In their study, Goerigk and Grimme⁶³⁸ found that `mgga_xc_otpss_d` outperforms all other considered GGA functionals, with errors comparable to the computationally more expensive hybrid functional B3LYP³⁹⁷ combined with the D2 dispersion term⁵¹⁵ (B3LYP-D⁷⁷⁹).

`mgga_xc_b97m_v`⁷⁸⁰ (2015)

B97M-V is an empirical functional with a highly flexible mathematical form for exchange

and correlation, which also includes a non-local term (VV10⁷⁸¹) to account for noncovalent interactions. The semi-local part of B97M-V, `mgga_xc_b97m_v`, reads

$$e_{xc}^{\text{B97M-V}} = \sum_{\sigma} (e_{x\sigma}^{\text{B97M-V}} + e_{c\sigma\sigma}^{\text{B97M-V}}) + e_{c\uparrow\downarrow}^{\text{B97M-V}} \quad (783)$$

where $e_{c\sigma\sigma}^{\text{B97M-V}}$ and $e_{c\uparrow\downarrow}^{\text{B97M-V}}$ represent parallel-spin and opposite-spin correlations, respectively, as defined by the Stoll decomposition (see section 2.18.3). All terms in eq. (783) have the form

$$e^{\text{B97M-V}} = e^{\text{LDA}} g(w, \tilde{u}) \quad (784)$$

with e^{LDA} corresponding to `lda_x` for exchange and `lda_c_pw` for correlation, and

$$g(w, \tilde{u}) = \sum_i \sum_j c_{ij} w^i \tilde{u}^j \quad (785)$$

In eq. (785), $w = w_{\sigma}$ and $\tilde{u} = \tilde{u}_{x\sigma} = \tilde{u}(x_{\sigma})$ for exchange, $w = w_{\sigma}$ and $\tilde{u} = \tilde{u}_{c\sigma\sigma} = \tilde{u}(x_{\sigma})$ for parallel-spin correlation, or $w = w_{\uparrow\downarrow} = (\tilde{t}_{\uparrow}^{-1} + \tilde{t}_{\downarrow}^{-1} - 2C_{\text{F}}^{-1}) / (\tilde{t}_{\uparrow}^{-1} + \tilde{t}_{\downarrow}^{-1} + 2C_{\text{F}}^{-1})$ and $\tilde{u} = \tilde{u}_{c\uparrow\downarrow} = \tilde{u}(x_{\text{avg}})$ for opposite-spin correlation. The values from `gga_x_b86` ($\gamma_x = 0.004$) and the B97 hybrid functional³⁷⁰ ($\gamma_{c\sigma\sigma} = 0.2$ and $\gamma_{c\uparrow\downarrow} = 0.006$) were used for the parameter γ in \tilde{u} (eq. (251)).

The coefficients c_{ij} in eq. (785) were obtained from a training procedure using a molecular set of 1095 data points (787 for thermochemistry and 308 for noncovalent interactions). Billions of functional fits were considered, imposing the correct HEG limit. Additional datasets were employed for validating and testing the obtained functional fits, paying careful attention to the number of parameters and the numerical behavior of the fit. The final functional form contains twelve optimized parameters, four for each of the terms in eq. (783):

$$g_x(w_{\sigma}, \tilde{u}_{x\sigma}) = 1 + 0.416w_{\sigma} + 1.308\tilde{u}_{x\sigma} + 3.07w_{\sigma}\tilde{u}_{x\sigma} + 1.901\tilde{u}_{x\sigma}^2 \quad (786a)$$

$$g_{c\sigma\sigma}(w_{\sigma}, \tilde{u}_{c\sigma\sigma}) = 1 - 5.668w_{\sigma} - 1.855\tilde{u}_{c\sigma\sigma}^2 - 20.497w_{\sigma}^3\tilde{u}_{c\sigma\sigma}^2 - 20.364w_{\sigma}^4\tilde{u}_{c\sigma\sigma}^2 \quad (786b)$$

$$g_{c\uparrow\downarrow}(w_{\uparrow\downarrow}, \tilde{u}_{c\uparrow\downarrow}) = 1 + 2.535w_{\uparrow\downarrow} + 1.573\tilde{u}_{c\uparrow\downarrow} - 6.427w_{\uparrow\downarrow}^3\tilde{u}_{c\uparrow\downarrow}^2 - 6.298\tilde{u}_{c\uparrow\downarrow}^3 \quad (786c)$$

The functional exhibits excellent accuracy for a broad range of molecular systems and properties, including noncovalent bonds, and is one of the most accurate MGGA functionals for molecular calculations.

`mgga_xc_hle17`⁷⁸² (2017)

This functional is similar to `gga_xc_hle16`, since it also consists of a simple rescaling of an existing functional (TPSS with `mgga_x_tpss` and `mgga_c_tpss` are multiplied by 1.25 and 0.5, respectively) that was proposed to get accurate band gaps of semiconductors and excitation energies of molecules. Compared to `gga_xc_hle16`, the results are improved for many properties, however the geometries are still extremely inaccurate for some classes of systems.

`mgga_xc_t_hle17`, `mgga_xc_t_rscan`³⁸² (2020)

Similarly to `mgga_xc_hle17`, `mgga_xc_t_hle17` is a rescaling of TPSS. The functional `mgga_x_tpss` and `mgga_c_tpss` are multiplied by the factors 1.35 and 1.00, respectively; these factors were obtained by fitting to the experimental band gaps of 85 solids. The accuracy for the band gap of solids is similar to that of `mgga_xc_hle17`, whose coefficients were also tuned for this property.

In the same way, `mgga_xc_t_rscan` consists of `mgga_x_rscan` and `mgga_c_rscan` multiplied by factors (1.30 and 1.40, respectively) that are optimal for the band gap of solids, and is therefore superior to rSCAN for this property.

4 Conclusions and Outlook

Over the past six decades, exchange-correlation functionals have evolved from the conceptually simple local density approximation to increas-

ingly sophisticated semi-local approximations and other families of functionals like the hybrids or non-local van der Waals functionals. This review has systematically documented this progression through the first three rungs of Jacob’s ladder: LDA, GGA, and MGGA functionals.

The historical developments involve several distinct paradigms in functional construction. Early functionals, beginning with the LDA in the 1960s, relied heavily on exact properties of the homogeneous electron gas. The introduction of GGAs in the 1980s and the 1990s marked a shift toward incorporating gradient corrections to better describe inhomogeneous systems, like real molecules, solids, surfaces, etc. Functionals like PBE established principles of systematic construction from exact constraints. The 1990s and 2000s saw the establishment of MGGA, which added a dependence on the kinetic-energy density and enabled the fulfillment of additional exact conditions, particularly regarding one-electron self-interaction and the description of various bonding regimes.

More recent developments have combined different design philosophies. Some functionals incorporate extensive empirical parameterization to achieve high accuracy for specific classes of systems and properties, while others maintain strict adherence to exact constraints with minimal empiricism. The contrast between these approaches, formal rigor versus pragmatic accuracy, remains a defining characteristic in the development of exchange-correlation functionals.

Despite the proliferation of hundreds of functionals, a relatively small subset dominates for practical applications. For extended systems, PBE and its variants remain workhorses due to their balance of accuracy, computational efficiency, and theoretical soundness, as well as the extensive experience practitioners have accumulated with these functionals over the years. For molecular systems, B3LYP (not included in this review) retains widespread use, partly due to extensive benchmarking and familiarity. More recent functionals like SCAN have gained traction by demonstrating improved accuracy while maintaining computational tractability and satisfying important exact constraints. The

choice of functional remains highly system- and property-dependent. No single functional performs optimally across all systems or applications, and the “best” functional often depends on whether one prioritizes energetic properties, geometries, response properties, or other observables. This reality underscores that the quest for a truly universal functional remains unfulfilled.

Several fundamental challenges persist. The derivative discontinuity of the exact exchange-correlation potential, which is crucial for accurate band gap predictions, remains difficult to capture with semi-local approximations despite recent advances. The self-interaction problem has not yet been fully resolved and semi-local functionals are also unable to correctly describe charge-transfer states, although range-separated functionals have provided some relief. Strong correlation effects continue to challenge even sophisticated MGGA, and their practical treatment may require going beyond semi-local functionals. The development of functionals that perform uniformly well across different length scales, from molecules to solids, remains an open problem.

Future progress may come from several directions. This can be achieved by moving beyond the limitations of semi-local approximations and enlarging the space of functional forms to include hybrid functionals, from global to local variants. More recently, machine learning approaches offer the promise of discovering functional forms that would be difficult to construct through traditional means, though ensuring transferability and physical interpretability remains challenging. Deeper understanding of the mathematical structure of density functionals, such as the analysis of the strictly-correlated electron limit and dimensional scaling, may reveal new avenues for systematic improvements. The development of functionals specifically designed for ensemble DFT and thermal DFT applications represents another frontier with growing practical importance.

The emergence of comprehensive libraries like Libxc has profoundly impacted the field by enabling consistent implementation and comparison of functionals across different codes. This

standardization has enhanced reproducibility and facilitated rigorous benchmarking, allowing the community to more objectively assess functional performance. Continued efforts in this direction, including careful documentation and validation, remain essential for the progress of the field.

Semi-local functionals continue to play an indispensable role in computational chemistry and materials science. While hybrid functionals, range-separated methods, and other beyond-semi-local approaches offer improved accuracy for many applications, the computational efficiency and reliability of semi-local functionals ensure their continued relevance, particularly for large-scale simulations. The rich interplay between formal theory, physical insight, and empirical validation that has characterized functional development over the past decades shows no signs of exhaustion. As our understanding deepens and computational capabilities expand, semi-local functionals will undoubtedly continue to evolve, remaining essential tools for understanding the electronic structure of matter.

CRedit statement

FT Conceptualization, Data curation, Formal analysis, Investigation, Methodology, Writing - original draft, Writing - review & editing

SL Conceptualization, Funding acquisition, Investigation, Software, Validation, Writing - original draft, Writing - review & editing

SP Conceptualization, Formal analysis, Investigation, Methodology, Writing - original draft, Writing - review & editing

MALM Conceptualization, Formal analysis, Investigation, Methodology, Project administration, Software, Writing - original draft, Writing - review & editing

Acknowledgement SL thanks the Academy of Finland for financial support under project numbers 350282 and 353749.

References

- (1) Hohenberg, P.; Kohn, W. Inhomogeneous Electron Gas. *Phys. Rev.* **1964**, *136*, B864–B871, DOI: doi:10.1103/PhysRev.136.B864.
- (2) Kohn, W.; Sham, L. J. Self-Consistent Equations Including Exchange and Correlation Effects. *Phys. Rev.* **1965**, *140*, A1133–A1138, DOI: doi:10.1103/PhysRev.140.A1133.
- (3) Perdew, J. P.; Schmidt, K. Jacob’s ladder of density functional approximations for the exchange-correlation energy. *AIP Conf. Proc.* **2001**, *577*, 1–20, DOI: doi:10.1063/1.1390175.
- (4) Giuliani, G.; Vignale, G. *Quantum Theory of the Electron Liquid*; Cambridge University Press, 2005; DOI: doi:10.1017/cbo9780511619915.
- (5) Loos, P.-F.; Gill, P. M. W. The uniform electron gas. *WIREs Comput. Mol. Sci.* **2016**, *6*, 410–429, DOI: doi:10.1002/wcms.1257.
- (6) Langreth, D. C.; Mehl, M. J. Easily Implementable Nonlocal Exchange-Correlation Energy Functional. *Phys. Rev. Lett.* **1981**, *47*, 446, DOI: doi:10.1103/PhysRevLett.47.446.
- (7) Johnson, B. G.; Gill, P. M. W.; Pople, J. A. The performance of a family of density functional methods. *J. Chem. Phys.* **1993**, *98*, 5612, DOI: doi:10.1063/1.464906.
- (8) Johnson, B. G. Erratum: The performance of a family of density functional methods [J. Chem. Phys. 98, 5612 (1993)]. *J. Chem. Phys.* **1994**, *101*, 9202–9202, DOI: doi:10.1063/1.468507.
- (9) Frisch, M. J. et al. Gaussian 16 Revision B.01. 2016.
- (10) Pople, J. A.; Gill, P. M. W.; Johnson, B. G. Kohn–Sham density-functional theory within a finite

- basis set. *Chem. Phys. Lett.* **1992**, *199*, 557–560, DOI: doi:[10.1016/0009-2614\(92\)85009-Y](https://doi.org/10.1016/0009-2614(92)85009-Y).
- (11) Becke, A. D. A new mixing of Hartree–Fock and local density-functional theories. *J. Chem. Phys.* **1993**, *98*, 1372, DOI: doi:[10.1063/1.464304](https://doi.org/10.1063/1.464304).
- (12) Becke, A. D. Density-functional thermochemistry. III. The role of exact exchange. *J. Chem. Phys.* **1993**, *98*, 5648, DOI: doi:[10.1063/1.464913](https://doi.org/10.1063/1.464913).
- (13) Perdew, J.; Kurth, S.; Zupan, A.; Blaha, P. Accurate Density Functional with Correct Formal Properties: A Step Beyond the Generalized Gradient Approximation. *Phys. Rev. Lett.* **1999**, *82*, 2544–2547, DOI: doi:[10.1103/PhysRevLett.82.2544](https://doi.org/10.1103/PhysRevLett.82.2544).
- (14) Perdew, J. P.; Kurth, S.; Zupan, A.; Blaha, P. Erratum: Accurate Density Functional with Correct Formal Properties: A Step Beyond the Generalized Gradient Approximation [Phys. Rev. Lett. 82, 2544 (1999)]. *Phys. Rev. Lett.* **1999**, *82*, 5179–5179, DOI: doi:[10.1103/PhysRevLett.82.5179](https://doi.org/10.1103/PhysRevLett.82.5179).
- (15) Toulouse, J.; Colonna, F. m. c.; Savin, A. Long-range–short-range separation of the electron–electron interaction in density-functional theory. *Phys. Rev. A* **2004**, *70*, 062505, DOI: doi:[10.1103/PhysRevA.70.062505](https://doi.org/10.1103/PhysRevA.70.062505).
- (16) Jaramillo, J.; Scuseria, G. E.; Ernzerhof, M. Local hybrid functionals. *J. Chem. Phys.* **2003**, *118*, 1068–1073, DOI: doi:[10.1063/1.1528936](https://doi.org/10.1063/1.1528936).
- (17) Maier, T. M.; Arbuznikov, A. V.; Kaupp, M. Local hybrid functionals: Theory, implementation, and performance of an emerging new tool in quantum chemistry and beyond. *Wiley Interdiscip. Rev. Comput. Mol. Sci.* **2019**, *9*, e1378, DOI: doi:[10.1002/wcms.1378](https://doi.org/10.1002/wcms.1378).
- (18) Zhao, Y.; Lynch, B. J.; Truhlar, D. G. Doubly Hybrid Meta DFT: New Multi-Coefficient Correlation and Density Functional Methods for Thermochemistry and Thermochemical Kinetics. *J. Phys. Chem. A* **2004**, *108*, 4786–4791, DOI: doi:[10.1021/jp049253v](https://doi.org/10.1021/jp049253v).
- (19) Grimme, S. Semiempirical hybrid density functional with perturbative second-order correlation. *J. Chem. Phys.* **2006**, *124*, 034108, DOI: doi:[10.1063/1.2148954](https://doi.org/10.1063/1.2148954).
- (20) Tozer, D. J.; Ingamells, V. E.; Handy, N. C. Exchange–correlation potentials. *J. Chem. Phys.* **1996**, *105*, 9200–9213, DOI: doi:[10.1063/1.472753](https://doi.org/10.1063/1.472753).
- (21) Zheng, X.; Hu, L.; Wang, X.; Chen, G. A generalized exchange–correlation functional: the Neural-Networks approach. *Chem. Phys. Lett.* **2004**, *390*, 186–192, DOI: doi:[10.1016/j.cplett.2004.04.020](https://doi.org/10.1016/j.cplett.2004.04.020).
- (22) Kirkpatrick, J. et al. Pushing the frontiers of density functionals by solving the fractional electron problem. *Science* **2021**, *374*, 1385–1389, DOI: doi:[10.1126/science.abj6511](https://doi.org/10.1126/science.abj6511).
- (23) Voss, J. Machine learning for accuracy in density functional approximations. *J. Comput. Chem.* **2024**, *45*, 1829–1845, DOI: doi:[10.1002/jcc.27366](https://doi.org/10.1002/jcc.27366).
- (24) Luise, G. et al. Accurate and scalable exchange–correlation with deep learning. *arXiv* **2025**, 2506.14665, DOI: doi:[10.48550/arXiv.2506.14665](https://doi.org/10.48550/arXiv.2506.14665).
- (25) Toulouse, J. In *Density Functional Theory: Modeling, Mathematical Analysis, Computational Methods, and Applications*; Cancès, E., Friesecke, G., Eds.; Springer International Publishing: Cham, 2023; pp 1–90.
- (26) Mardirossian, N.; Head-Gordon, M. Thirty years of density functional theory in computational chemistry:

- an overview and extensive assessment of 200 density functionals. *Mol. Phys.* **2017**, *115*, 2315–2372, DOI: doi:[10.1080/00268976.2017.1333644](https://doi.org/10.1080/00268976.2017.1333644).
- (27) Yu, H. S.; Li, S. L.; Truhlar, D. G. Perspective: Kohn–Sham density functional theory descending a staircase. *J. Chem. Phys.* **2016**, *145*, 130901, DOI: doi:[10.1063/1.4963168](https://doi.org/10.1063/1.4963168).
- (28) Jones, R. O. Density functional theory: Its origins, rise to prominence, and future. *Rev. Mod. Phys.* **2015**, *87*, 897–923, DOI: doi:[10.1103/RevModPhys.87.897](https://doi.org/10.1103/RevModPhys.87.897).
- (29) Becke, A. D. Perspective: Fifty years of density-functional theory in chemical physics. *J. Chem. Phys.* **2014**, *140*, 18A301, DOI: doi:[10.1063/1.4869598](https://doi.org/10.1063/1.4869598).
- (30) Burke, K. Perspective on density functional theory. *J. Chem. Phys.* **2012**, *136*, 150901, DOI: doi:[10.1063/1.4704546](https://doi.org/10.1063/1.4704546).
- (31) Scuseria, G. E.; Staroverov, V. N. In *Theory and Applications of Computational Chemistry*; Dykstra, C. E., Frenking, G., Kim, K. S., Scuseria, G. E., Eds.; Elsevier: Amsterdam, 2005; pp 669–724, DOI: doi:[10.1016/B978-044451719-7/50067-6](https://doi.org/10.1016/B978-044451719-7/50067-6).
- (32) Weymuth, T.; Reiher, M. The transferability limits of static benchmarks. *Phys. Chem. Chem. Phys.* **2022**, *24*, 14692–14698, DOI: doi:[10.1039/d2cp01725c](https://doi.org/10.1039/d2cp01725c).
- (33) Rajagopal, A. K.; Callaway, J. Inhomogeneous Electron Gas. *Phys. Rev. B* **1973**, *7*, 1912–1919, DOI: doi:[10.1103/PhysRevB.7.1912](https://doi.org/10.1103/PhysRevB.7.1912).
- (34) Rajagopal, A. K. Inhomogeneous relativistic electron gas. *J. Phys. C: Solid State Phys.* **1978**, *11*, L943, DOI: doi:[10.1088/0022-3719/11/24/002](https://doi.org/10.1088/0022-3719/11/24/002).
- (35) MacDonald, A. H.; Vosko, S. H. A relativistic density functional formalism. *J. Phys. C: Solid State Phys.* **1979**, *12*, 2977, DOI: doi:[10.1088/0022-3719/12/15/007](https://doi.org/10.1088/0022-3719/12/15/007).
- (36) Hasnip, P. J.; Refson, K.; Probert, M. I. J.; Yates, J. R.; Clark, S. J.; Pickard, C. J. Density functional theory in the solid state. *Philos. Trans. R. Soc. A Math. Phys. Eng. Sci.* **2014**, *372*, 20130270–20130270, DOI: doi:[10.1098/rsta.2013.0270](https://doi.org/10.1098/rsta.2013.0270).
- (37) Lejaeghere, K. et al. Reproducibility in density functional theory calculations of solids. *Science* **2016**, *351*, aad3000, DOI: doi:[10.1126/science.aad3000](https://doi.org/10.1126/science.aad3000).
- (38) Lehtola, S. A review on non-relativistic, fully numerical electronic structure calculations on atoms and diatomic molecules. *Int. J. Quantum Chem.* **2019**, *119*, e25968, DOI: doi:[10.1002/qua.25968](https://doi.org/10.1002/qua.25968).
- (39) Lehtola, S.; Blockhuys, F.; Van Alsenoy, C. An Overview of Self-Consistent Field Calculations Within Finite Basis Sets. *Molecules* **2020**, *25*, 1218, DOI: doi:[10.3390/molecules25051218](https://doi.org/10.3390/molecules25051218).
- (40) Thomas, L. H. The calculation of atomic fields. *Math. Proc. Cambridge Philos. Soc.* **1927**, *23*, 542, DOI: doi:[10.1017/S0305004100011683](https://doi.org/10.1017/S0305004100011683).
- (41) Fermi, E. Un metodo statistico per la determinazione di alcune proprietà dell’atomo. (Italian) [A Statistical Method for the Determination of Some Atomic Properties]. *Rend. Accad. Naz. Lincei* **1927**, *6*, 602.
- (42) Slater, J. C. A Simplification of the Hartree–Fock Method. *Phys. Rev.* **1951**, *81*, 385, DOI: doi:[10.1103/PhysRev.81.385](https://doi.org/10.1103/PhysRev.81.385).
- (43) Kohn, W. In *Highlights of Condensed Matter Theory*; Fumi, B. A., Tosi, M. P., Eds.; North-Holland, 1985; Chapter Density Functional Theory: Fundamentals and Applications, pp 1–15.
- (44) Görling, A. Symmetry in density-functional theory. *Phys. Rev.*

- A **1993**, *47*, 2783–2799, DOI: doi:10.1103/PhysRevA.47.2783.
- (45) Ullrich, C. A.; Kohn, W. Kohn-Sham Theory for Ground-State Ensembles. *Phys. Rev. Lett.* **2001**, *87*, 093001, DOI: doi:10.1103/PhysRevLett.87.093001.
- (46) Capelle, K.; Ullrich, C. A.; Vignale, G. Degenerate ground states and nonunique potentials: Breakdown and restoration of density functionals. *Phys. Rev. A* **2007**, *76*, 012508, DOI: doi:10.1103/physreva.76.012508.
- (47) Gould, T.; Kronik, L.; Pittalis, S. “Ensemble-ization” of density functional theory. *J. Chem. Phys.* **2026**, *164*, 040901, DOI: doi:10.1063/5.0274509.
- (48) Levy, M.; Perdew, J. P.; Sahni, V. Exact differential equation for the density and ionization energy of a many-particle system. *Phys. Rev. A* **1984**, *30*, 2745–2748, DOI: doi:10.1103/PhysRevA.30.2745.
- (49) Almbladh, C.-O.; von Barth, U. Exact results for the charge and spin densities, exchange-correlation potentials, and density-functional eigenvalues. *Phys. Rev. B* **1985**, *31*, 3231–3244, DOI: doi:10.1103/PhysRevB.31.3231.
- (50) Talman, J.; Shadwick, W. Optimized effective atomic central potential. *Phys. Rev. A* **1976**, *14*, 36–40, DOI: doi:10.1103/PhysRevA.14.36.
- (51) Kreibich, T.; Kurth, S.; Grabo, T.; Gross, E. In *Density Functional Theory*; Löwdin, P.-O., Ed.; Advances in Quantum Chemistry; Academic Press, 1998; Vol. 33; pp 31–48, DOI: doi:10.1016/S0065-3276(08)60428-1.
- (52) Della Sala, F.; Görling, A. Asymptotic Behavior of the Kohn–Sham Exchange Potential. *Phys. Rev. Lett.* **2002**, *89*, 033003, DOI: doi:10.1103/PhysRevLett.89.033003.
- (53) Gori-Giorgi, P.; Gál, T.; Baerends, E. J. Asymptotic behaviour of the electron density and the Kohn–Sham potential in case of a Kohn–Sham HOMO nodal plane. *Mol. Phys.* **2016**, *114*, 1086–1097, DOI: doi:10.1080/00268976.2015.1137643.
- (54) Born, M.; Oppenheimer, R. Zur Quantentheorie der Molekeln. *Ann. Phys. (Berlin)* **1927**, *389*, 457–484, DOI: doi:10.1002/andp.19273892002.
- (55) Capitani, J. F.; Nalewajski, R. F.; Parr, R. G. Non-Born–Oppenheimer density functional theory of molecular systems. *J. Chem. Phys.* **1982**, *76*, 568, DOI: doi:10.1063/1.442703.
- (56) Witt, W. C.; del Rio, B. G.; Dieterich, J. M.; Carter, E. A. Orbital-free density functional theory for materials research. *J. Mater. Res.* **2018**, *33*, 777–795, DOI: doi:10.1557/jmr.2017.462.
- (57) Mi, W.; Luo, K.; Trickey, S. B.; Pavanello, M. Orbital-Free Density Functional Theory: An Attractive Electronic Structure Method for Large-Scale First-Principles Simulations. *Chem. Rev.* **2023**, *123*, 12039–12104, DOI: doi:10.1021/acs.chemrev.2c00758.
- (58) Xu, Q.; Ma, C.; Mi, W.; Wang, Y.; Ma, Y. Recent advancements and challenges in orbital-free density functional theory. *WIREs Comput. Mol. Sci.* **2024**, *14*, e1724, DOI: doi:10.1002/wcms.1724.
- (59) Wagner, L. O.; Baker, T. E.; Stoudenmire, E. M.; Burke, K.; White, S. R. Kohn–Sham calculations with the exact functional. *Phys. Rev. B* **2014**, *90*, 045109, DOI: doi:10.1103/PhysRevB.90.045109.
- (60) Rohr, D. R.; Savin, A. Full configuration interaction wave function as a formal solution to the optimized effective potential and Kohn–Sham models in finite basis sets. *J. Mol. Struct.:*

- THEOCHEM* **2010**, *943*, 90–93, DOI: doi:[10.1016/j.theochem.2009.10.037](https://doi.org/10.1016/j.theochem.2009.10.037).
- (61) Wagner, L. O.; Baker, T. E.; Stoudenmire, E. M.; Burke, K.; White, S. R. Kohn–Sham calculations with the exact functional. *Phys. Rev. B* **2014**, *90*, 045109, DOI: doi:[10.1103/PhysRevB.90.045109](https://doi.org/10.1103/PhysRevB.90.045109).
- (62) Goerigk, L.; Hansen, A.; Bauer, C.; Ehrlich, S.; Najibi, A.; Grimme, S. A look at the density functional theory zoo with the advanced GMTKN55 database for general main group thermochemistry, kinetics and noncovalent interactions. *Phys. Chem. Chem. Phys.* **2017**, *19*, 32184–32215, DOI: doi:[10.1039/C7CP04913G](https://doi.org/10.1039/C7CP04913G).
- (63) Goerigk, L.; Mehta, N. A Trip to the Density Functional Theory Zoo: Warnings and Recommendations for the User. *Aust. J. Chem.* **2019**, *72*, 563, DOI: doi:[10.1071/ch19023](https://doi.org/10.1071/ch19023).
- (64) Pople, J. A. Nobel Lecture: Quantum chemical models. *Rev. Mod. Phys.* **1999**, *71*, 1267–1274, DOI: doi:[10.1103/RevModPhys.71.1267](https://doi.org/10.1103/RevModPhys.71.1267).
- (65) Langreth, D. C.; Perdew, J. P. The exchange-correlation energy of a metallic surface. *Solid State Commun.* **1975**, *17*, 1425–1429, DOI: doi:[10.1016/0038-1098\(75\)90618-3](https://doi.org/10.1016/0038-1098(75)90618-3).
- (66) Görling, A.; Levy, M. Exact Kohn–Sham scheme based on perturbation theory. *Phys. Rev. A* **1994**, *50*, 196–204, DOI: doi:[10.1103/PhysRevA.50.196](https://doi.org/10.1103/PhysRevA.50.196).
- (67) Furche, F. Developing the random phase approximation into a practical post-Kohn–Sham correlation model. *J. Chem. Phys.* **2008**, *129*, 114105, DOI: doi:[10.1063/1.2977789](https://doi.org/10.1063/1.2977789).
- (68) Hellgren, M.; Rohr, D. R.; Gross, E. K. U. Correlation potentials for molecular bond dissociation within the self-consistent random phase approximation. *J. Chem. Phys.* **2012**, *136*, 034106, DOI: doi:[10.1063/1.3676174](https://doi.org/10.1063/1.3676174).
- (69) Ren, X.; Rinke, P.; Joas, C.; Scheffler, M. Random-phase approximation and its applications in computational chemistry and materials science. *47*, 7447–7471, DOI: doi:[10.1007/s10853-012-6570-4](https://doi.org/10.1007/s10853-012-6570-4).
- (70) Chen, G. P.; Voora, V. K.; Agee, M. M.; Balasubramani, S. G.; Furche, F. Random-Phase Approximation Methods. *Annu. Rev. Phys. Chem.* **2017**, *68*, 421–445, DOI: doi:[10.1146/annurev-physchem-040215-112308](https://doi.org/10.1146/annurev-physchem-040215-112308).
- (71) Trushin, E.; Fauser, S.; Mölkner, A.; Erhard, J.; Görling, A. Accurate Correlation Potentials from the Self-Consistent Random Phase Approximation. *Phys. Rev. Lett.* **2025**, *134*, 016402, DOI: doi:[10.1103/PhysRevLett.134.016402](https://doi.org/10.1103/PhysRevLett.134.016402).
- (72) Lehtola, S. A call to arms: Making the case for more reusable libraries. *J. Chem. Phys.* **2023**, *159*, 180901, DOI: doi:[10.1063/5.0175165](https://doi.org/10.1063/5.0175165).
- (73) Strange, R.; Manby, F. R.; Knowles, P. J. Automatic code generation in density functional theory. *Comput. Phys. Commun.* **2001**, *136*, 310–318, DOI: doi:[10.1016/S0010-4655\(01\)00148-5](https://doi.org/10.1016/S0010-4655(01)00148-5).
- (74) Sałek, P.; Hesselmann, A. A self-contained and portable density functional theory library for use in ab initio quantum chemistry programs. *J. Comput. Chem.* **2007**, *28*, 2569–2575, DOI: doi:[10.1002/jcc.20758](https://doi.org/10.1002/jcc.20758).
- (75) Ekström, U.; Visscher, L.; Bast, R.; Thorvaldsen, A. J.; Ruud, K. Arbitrary-Order Density Functional Response Theory from Automatic Differentiation. *J. Chem. Theory Comput.* **2010**, *6*, 1971–1980, DOI: doi:[10.1021/ct100117s](https://doi.org/10.1021/ct100117s).
- (76) Lehtola, S.; Steigemann, C.; Oliveira, M. J.; Marques, M. A. Recent developments in libxc — A comprehensive library of functionals for density

- functional theory. *SoftwareX* **2018**, *7*, 1–5, DOI: doi:[10.1016/j.softx.2017.11.002](https://doi.org/10.1016/j.softx.2017.11.002).
- (77) Marques, M. A. L.; Oliveira, M. J. T.; Burnus, T. LIBXC: A library of exchange and correlation functionals for density functional theory. *Comput. Phys. Commun.* **2012**, *183*, 2272–2281, DOI: doi:[10.1016/j.cpc.2012.05.007](https://doi.org/10.1016/j.cpc.2012.05.007).
- (78) Lin, P.; Ren, X.; Liu, X.; He, L. Ab initio electronic structure calculations based on numerical atomic orbitals: Basic formalisms and recent progresses. *Wiley Interdiscip. Rev. Comput. Mol. Sci.* **2024**, *14*, e1687, DOI: doi:[10.1002/wcms.1687](https://doi.org/10.1002/wcms.1687).
- (79) Gonze, X. et al. The ABINIT project: Impact, environment and recent developments. *Comput. Phys. Commun.* **2020**, *248*, 107042, DOI: doi:[10.1016/j.cpc.2019.107042](https://doi.org/10.1016/j.cpc.2019.107042).
- (80) Kang, S.; Woo, J.; Kim, J.; Kim, H.; Kim, Y.; Lim, J.; Choi, S.; Kim, W. Y. ACE-Molecule: An open-source real-space quantum chemistry package. *J. Chem. Phys.* **2020**, *152*, 124110, DOI: doi:[10.1063/5.0002959](https://doi.org/10.1063/5.0002959).
- (81) Baerends, E. J. et al. The Amsterdam Modeling Suite. *J. Chem. Phys.* **2025**, *162*, 162501, DOI: doi:[10.1063/5.0258496](https://doi.org/10.1063/5.0258496).
- (82) Oliveira, M. J. T.; Nogueira, F. Generating relativistic pseudo-potentials with explicit incorporation of semi-core states using APE, the Atomic Pseudo-potentials Engine. *Comput. Phys. Commun.* **2008**, *178*, 524–534, DOI: doi:[10.1016/j.cpc.2007.11.003](https://doi.org/10.1016/j.cpc.2007.11.003).
- (83) Holzwarth, N. A. W.; Tackett, A. R.; Matthews, G. E. A Projector Augmented Wave (PAW) code for electronic structure calculations, Part I: atom-paw for generating atom-centered functions. *Comput. Phys. Commun.* **2001**, *135*, 329–347, DOI: doi:[10.1016/S0010-4655\(00\)00244-7](https://doi.org/10.1016/S0010-4655(00)00244-7).
- (84) Shiozaki, T. BAGEL: Brilliantly Advanced General Electronic-structure Library. *Wiley Interdiscip. Rev. Comput. Mol. Sci.* **2018**, *8*, e1331, DOI: doi:[10.1002/wcms.1331](https://doi.org/10.1002/wcms.1331).
- (85) Ratcliff, L. E.; Dawson, W.; Fisicaro, G.; Caliste, D.; Mohr, S.; Degomme, A.; Videau, B.; Cristiglio, V.; Stella, M.; D’Alessandro, M.; Goedecker, S.; Nakajima, T.; Deutsch, T.; Genovese, L. Flexibilities of wavelets as a computational basis set for large-scale electronic structure calculations. *J. Chem. Phys.* **2020**, *152*, 194110, DOI: doi:[10.1063/5.0004792](https://doi.org/10.1063/5.0004792).
- (86) Clark, S. J.; Segall, M. D.; Pickard, C. J.; Hasnip, P. J.; Probert, M. I. J.; Refson, K.; Payne, M. C. First principles methods using CASTEP. *Z. Kristallogr. Cryst. Mater.* **2005**, *220*, 567–570, DOI: doi:[10.1524/zkri.220.5.567.65075](https://doi.org/10.1524/zkri.220.5.567.65075).
- (87) Williams-Young, D. B.; Petrone, A.; Sun, S.; Stetina, T. F.; Lestranger, P.; Hoyer, C. E.; Nascimento, D. R.; Koulias, L.; Wildman, A.; Kasper, J.; Goings, J. J.; Ding, F.; DePrince, A. E.; Valeev, E. F.; Li, X. The Chronus Quantum software package. *Wiley Interdiscip. Rev. Comput. Mol. Sci.* **2020**, *10*, e1436, DOI: doi:[10.1002/wcms.1436](https://doi.org/10.1002/wcms.1436).
- (88) Nakata, A.; Baker, J. S.; Mujahed, S. Y.; Poulton, J. T. L.; Arapan, S.; Lin, J.; Raza, Z.; Yadav, S.; Truflandier, L.; Miyazaki, T.; Bowler, D. R. Large scale and linear scaling DFT with the CONQUEST code. *J. Chem. Phys.* **2020**, *152*, 164112, DOI: doi:[10.1063/5.0005074](https://doi.org/10.1063/5.0005074).
- (89) Kühne, T. D. et al. CP2K: An electronic structure and molecular dynamics software package - Quickstep: Efficient and accurate electronic structure calculations. *J. Chem. Phys.* **2020**, *152*, 194103, DOI: doi:[10.1063/5.0007045](https://doi.org/10.1063/5.0007045).
- (90) Hutter, J.; Iannuzzi, M. CPMD: Car-Parrinello molecular dy-

- namics. *Z. Kristallogr. Cryst. Mater.* **2005**, *220*, 549–551, DOI: doi:[10.1524/zkri.220.5.549.65080](https://doi.org/10.1524/zkri.220.5.549.65080).
- (91) Geudtner, G.; Calaminici, P.; Carmona-Espíndola, J.; del Campo, J. M.; Domínguez-Soria, V. D.; Moreno, R. F.; Gamboa, G. U.; Goursot, A.; Köster, A. M.; Reveles, J. U.; Mineva, T.; Vásquez-Pérez, J. M.; Vela, A.; Zúñiga-Gutierrez, B.; Salahub, D. R. de Mon2k. *Wiley Interdiscip. Rev. Comput. Mol. Sci.* **2012**, *2*, 548–555, DOI: doi:[10.1002/wcms.98](https://doi.org/10.1002/wcms.98).
- (92) Motamarri, P.; Das, S.; Rudraraju, S.; Ghosh, K.; Davydov, D.; Gavini, V. DFT-FE – A massively parallel adaptive finite-element code for large-scale density functional theory calculations. *Comput. Phys. Commun.* **2020**, *246*, 106853, DOI: doi:[10.1016/j.cpc.2019.07.016](https://doi.org/10.1016/j.cpc.2019.07.016).
- (93) Herbst, M. F.; Levitt, A.; Cancès, E. DFTK: A Julian approach for simulating electrons in solids. *Julia-Con Proceedings* **2021**, *3*, 69, DOI: doi:[10.21105/jcon.00069](https://doi.org/10.21105/jcon.00069).
- (94) The Elk Code. <http://elk.sourceforge.net/>.
- (95) Lehtola, J.; Hakala, M.; Sakko, A.; Hämmäläinen, K. ERKALE – A flexible program package for X-ray properties of atoms and molecules. *J. Comput. Chem.* **2012**, *33*, 1572–1585, DOI: doi:[10.1002/jcc.22987](https://doi.org/10.1002/jcc.22987).
- (96) Gulans, A.; Kontur, S.; Meisenbichler, C.; Nabok, D.; Pavone, P.; Rigamonti, S.; Sagmeister, S.; Werner, U.; Draxl, C. exciting: a full-potential all-electron package implementing density-functional theory and many-body perturbation theory. *J. Phys. Condens. Matter* **2014**, *26*, 363202, DOI: doi:[10.1088/0953-8984/26/36/363202](https://doi.org/10.1088/0953-8984/26/36/363202).
- (97) Blum, V.; Gehrke, R.; Hanke, F.; Havu, P.; Havu, V.; Ren, X.; Reuter, K.; Scheffler, M. Ab initio molecular simulations with numeric atom-centered orbitals. *Comput. Phys. Commun.* **2009**, *180*, 2175–2196, DOI: doi:[10.1016/j.cpc.2009.06.022](https://doi.org/10.1016/j.cpc.2009.06.022).
- (98) The FLEUR project. <https://www.flapw.de/>.
- (99) Barca, G. M. J. et al. Recent developments in the general atomic and molecular electronic structure system. *J. Chem. Phys.* **2020**, *152*, 154102, DOI: doi:[10.1063/5.0005188](https://doi.org/10.1063/5.0005188).
- (100) Mortensen, J. J. et al. GPAW: An open Python package for electronic structure calculations. *J. Chem. Phys.* **2024**, *160*, 092503, DOI: doi:[10.1063/5.0182685](https://doi.org/10.1063/5.0182685).
- (101) Lehtola, S. Fully numerical Hartree–Fock and density functional calculations. I. Atoms. *Int. J. Quantum Chem.* **2019**, *119*, e25945, DOI: doi:[10.1002/qua.25945](https://doi.org/10.1002/qua.25945).
- (102) Chan, M.; Verstraelen, T.; Tehrani, A.; Richer, M.; Yang, X. D.; Kim, T. D.; Vöhringer-Martinez, E.; Heidar-Zadeh, F.; Ayers, P. W. The tale of HORTON: Lessons learned in a decade of scientific software development. *J. Chem. Phys.* **2024**, *160*, 162501, DOI: doi:[10.1063/5.0196638](https://doi.org/10.1063/5.0196638).
- (103) Andrade, X.; Pemmaraju, C. D.; Kartsev, A.; Xiao, J.; Lindenberg, A.; Rajpurohit, S.; Tan, L. Z.; Ogitsu, T.; Correa, A. A. Inq, a Modern GPU-Accelerated Computational Framework for (Time-Dependent) Density Functional Theory. *J. Chem. Theory Comput.* **2021**, *17*, 7447–7467, DOI: doi:[10.1021/acs.jctc.1c00562](https://doi.org/10.1021/acs.jctc.1c00562).
- (104) Sundararaman, R.; Letchworth-Weaver, K.; Schwarz, K. A.; Gunceler, D.; Ozhables, Y.; Arias, T. A. JDFTx: Software for joint density-functional theory. *SoftwareX* **2017**, *6*, 278–284, DOI: doi:[10.1016/j.softx.2017.10.006](https://doi.org/10.1016/j.softx.2017.10.006).

- (105) Harrison, R. J. et al. MADNESS: A Multiresolution, Adaptive Numerical Environment for Scientific Simulation. *SIAM J. Sci. Comput.* **2016**, *38*, S123–S142, DOI: doi:10.1137/15m1026171.
- (106) Bruneval, F.; Rangel, T.; Hamed, S. M.; Shao, M.; Yang, C.; Neaton, J. B. MOLGW 1: Many-body perturbation theory software for atoms, molecules, and clusters. *Comput. Phys. Commun.* **2016**, *208*, 149–161, DOI: doi:10.1016/j.cpc.2016.06.019.
- (107) Werner, H.-J. et al. The Molpro quantum chemistry package. *J. Chem. Phys.* **2020**, *152*, 144107, DOI: doi:10.1063/5.0005081.
- (108) Mester, D.; Nagy, P. R.; Csóka, J.; Gyevi-Nagy, L.; Szabó, P. B.; Horváth, R. A.; Petrov, K.; Hégyel, B.; Ladóczki, B.; Samu, G.; Lórinicz, B. D.; Kállay, M. Overview of Developments in the MRCC Program System. *J. Phys. Chem. A* **2025**, *129*, 2086–2107, DOI: doi:10.1021/acs.jpca.4c07807.
- (109) Aprà, E. et al. NWChem: Past, present, and future. *J. Chem. Phys.* **2020**, *152*, 184102, DOI: doi:10.1063/5.0004997.
- (110) Tancogne-Dejean, N. et al. Octopus, a computational framework for exploring light-driven phenomena and quantum dynamics in extended and finite systems. *J. Chem. Phys.* **2020**, *152*, 124119, DOI: doi:10.1063/1.5142502.
- (111) Manni, G. L. et al. The OpenMolcas Web: A Community-Driven Approach to Advancing Computational Chemistry. *J. Chem. Theory Comput.* **2023**, *19*, 6933–6991, DOI: doi:10.1021/acs.jctc.3c00182.
- (112) Neese, F.; Wennmohs, F.; Becker, U.; Riplinger, C. The ORCA quantum chemistry program package. *J. Chem. Phys.* **2020**, *152*, 224108, DOI: doi:10.1063/5.0004608.
- (113) Chen, M.; Xia, J.; Huang, C.; Dieterich, J. M.; Hung, L.; Shin, I.; Carter, E. A. Introducing PROFESS 3.0: An advanced program for orbital-free density functional theory molecular dynamics simulations. *Comput. Phys. Commun.* **2015**, *190*, 228–230, DOI: doi:10.1016/j.cpc.2014.12.021.
- (114) Smith, D. G. A. et al. Psi4 1.4: Open-source software for high-throughput quantum chemistry. *J. Chem. Phys.* **2020**, *152*, 184108, DOI: doi:10.1063/5.0006002.
- (115) Sun, Q. et al. Recent developments in the PYSCF program package. *J. Chem. Phys.* **2020**, *153*, 024109, DOI: doi:10.1063/5.0006074.
- (116) Smidstrup, S. et al. QuantumATK: an integrated platform of electronic and atomic-scale modelling tools. *J. Phys.: Condens. Matter* **2020**, *32*, 015901, DOI: doi:10.1088/1361-648x/ab4007.
- (117) Giannozzi, P. et al. Advanced capabilities for materials modelling with Quantum ESPRESSO. *J. Phys.: Condens. Matter* **2017**, *29*, 465901, DOI: doi:10.1088/1361-648x/aa8f79.
- (118) RMG. <https://github.com/RMGDFT/rmgdft/>.
- (119) Niemeyer, N.; Eschenbach, P.; Bensberg, M.; Tölle, J.; Hellmann, L.; Lampe, L.; Massolle, A.; Rikus, A.; Schnieders, D.; Unsleber, J. P.; Neugebauer, J. The subsystem quantum chemistry program Serenity. *Wiley Interdiscip. Rev. Comput. Mol. Sci.* **2022**, *13*, e1647, DOI: doi:10.1002/wcms.1647.
- (120) Chachiyo, T.; Chachiyo, H. Siam Quantum 2: An open-source C toolbox for quantum modeling and electronic structure development. *J. Chem. Phys.* **2026**, *164*, 052501, DOI: doi:10.1063/5.0310183.

- (121) García, A. et al. SIESTA: Recent developments and applications. *J. Chem. Phys.* **2020**, *152*, 204108, DOI: doi:[10.1063/5.0005077](https://doi.org/10.1063/5.0005077).
- (122) The SIRIUS domain-specific library for electronic-structure calculations. <https://github.com/electronic-structure/SIRIUS>.
- (123) Franzke, Y. J. et al. TURBOMOLE: Today and Tomorrow. *J. Chem. Theory Comput.* **2023**, *19*, 6859–6890, DOI: doi:[10.1021/acs.jctc.3c00347](https://doi.org/10.1021/acs.jctc.3c00347).
- (124) Kresse, G.; Joubert, D. From ultrasoft pseudopotentials to the projector augmented-wave method. *Phys. Rev. B* **1999**, *59*, 1758–1775, DOI: doi:[10.1103/PhysRevB.59.1758](https://doi.org/10.1103/PhysRevB.59.1758).
- (125) Rinkevicius, Z.; Li, X.; Vahtras, O.; Ahmadzadeh, K.; Brand, M.; Ringholm, M.; List, N. H.; Scheurer, M.; Scott, M.; Dreuw, A.; Norman, P. VeloxChem: A Python-driven density-functional theory program for spectroscopy simulations in high-performance computing environments. *Wiley Interdiscip. Rev. Comput. Mol. Sci.* **2019**, *10*, e1457, DOI: doi:[10.1002/wcms.1457](https://doi.org/10.1002/wcms.1457).
- (126) Blaha, P.; Schwarz, K.; Tran, F.; Laskowski, R.; Madsen, G. K. H.; Marks, L. D. WIEN2k: An APW+lo program for calculating the properties of solids. *J. Chem. Phys.* **2020**, *152*, 074101, DOI: doi:[10.1063/1.5143061](https://doi.org/10.1063/1.5143061).
- (127) Sangalli, D. et al. Many-body perturbation theory calculations using the yambo code. *J. Phys.: Condens. Matter* **2019**, *31*, 325902, DOI: doi:[10.1088/1361-648X/ab15d0](https://doi.org/10.1088/1361-648X/ab15d0).
- (128) Lehtola, S.; Marques, M. A. L. Reproducibility of density functional approximations: How new functionals should be reported. *J. Chem. Phys.* **2023**, *159*, 114116, DOI: doi:[10.1063/5.0167763](https://doi.org/10.1063/5.0167763).
- (129) Ernzerhof, M.; Perdew, J. P.; Burke, K. In *Density Functional Theory I: Functionals and Effective Potentials*; Nalewajski, R. F., Ed.; Springer Berlin Heidelberg, pp 1–30, DOI: doi:[10.1007/3-540-61091-X_1](https://doi.org/10.1007/3-540-61091-X_1).
- (130) Fiolhais, C.; Nogueira, F.; Marques, M. *A Primer in density functional theory*; Springer: Berlin [etc.], 2003.
- (131) Burke, K. In *Lecture Notes in Physics*; Marques, M. A. L., Ullrich, C. A., Nogueira, F., Rubio, A., Burke, K., Gross, E. K. U., Eds.; Springer, 2006; Vol. 706; Chapter 11, p 181, DOI: doi:[10.1007/b11767107](https://doi.org/10.1007/b11767107).
- (132) Cohen, A. J.; Mori-Sánchez, P.; Yang, W. Challenges for density functional theory. *Chem. Rev.* **2012**, *112*, 289–320, DOI: doi:[10.1021/cr200107z](https://doi.org/10.1021/cr200107z).
- (133) Della Sala, F.; Fabiano, E.; Constantin, L. A. Kinetic-energy-density dependent semilocal exchange-correlation functionals. *Int. J. Quantum Chem.* **2016**, *116*, 1641–1694, DOI: doi:[10.1002/qua.25224](https://doi.org/10.1002/qua.25224).
- (134) Kronik, L.; Kümmel, S. Piecewise linearity, freedom from self-interaction, and a Coulomb asymptotic potential: three related yet inequivalent properties of the exact density functional. *Phys. Chem. Chem. Phys.* **2020**, *22*, 16467–16481, DOI: doi:[10.1039/D0CP02564J](https://doi.org/10.1039/D0CP02564J).
- (135) Kaplan, A. D.; Levy, M.; Perdew, J. P. The Predictive Power of Exact Constraints and Appropriate Norms in Density Functional Theory. *Annu. Rev. Phys. Chem.* **2023**, *74*, 193–218, DOI: doi:[10.1146/annurev-physchem-062422-013259](https://doi.org/10.1146/annurev-physchem-062422-013259).
- (136) van Leeuwen, R. *Density Functional Approach to the Many-Body Problem: Key Concepts and Exact Functionals*; Advances in Quantum Chemistry; Academic Press, 2003; Vol. 43; pp 25–94,

- DOI: doi:[10.1016/S0065-3276\(03\)43002-5](https://doi.org/10.1016/S0065-3276(03)43002-5).
- (137) Eschrig, H. *The Fundamentals of Density Functional Theory*; Edition am Gutenbergplatz, 2003.
- (138) Kvaal, S. In *Density Functional Theory: Modeling, Mathematical Analysis, Computational Methods, and Applications*; Cancès, E., Friesecke, G., Eds.; Springer International Publishing, pp 267–306, DOI: doi:[10.1007/978-3-031-22340-2_5](https://doi.org/10.1007/978-3-031-22340-2_5).
- (139) Sutter, S. M.; Penz, M.; Ruggenthaler, M.; Leeuwen, R. v.; Giesbertz, K. J. H. Solution of the v-representability problem on a one-dimensional torus. *J. Phys. A* **2024**, *57*, 475202, DOI: doi:[10.1088/1751-8121/ad8a2a](https://doi.org/10.1088/1751-8121/ad8a2a).
- (140) Teale, A. M.; Helgaker, T. *Lieb variation principle in density-functional theory*; EMS Press, 2022; p 527–559.
- (141) Mohr, P. J.; Newell, D. B.; Taylor, B. N.; Tiesinga, E. CODATA recommended values of the fundamental physical constants: 2022. *Rev. Mod. Phys.* **2025**, *97*, 025002, DOI: doi:[10.1103/RevModPhys.97.025002](https://doi.org/10.1103/RevModPhys.97.025002).
- (142) Dirac, P. A. M. Note on Exchange Phenomena in the Thomas Atom. *Math. Proc. Cambridge Philos. Soc.* **1930**, *26*, 376–385, DOI: doi:[10.1017/S0305004100016108](https://doi.org/10.1017/S0305004100016108).
- (143) Bloch, F. Bemerkung zur Elektronentheorie des Ferromagnetismus und der elektrischen Leitfähigkeit. *Z. Phys.* **1929**, *57*, 545–555, DOI: doi:[10.1007/BF01340281](https://doi.org/10.1007/BF01340281).
- (144) Wigner, E.; Seitz, F. On the Constitution of Metallic Sodium. II. *Phys. Rev.* **1934**, *46*, 509–524, DOI: doi:[10.1103/PhysRev.46.509](https://doi.org/10.1103/PhysRev.46.509).
- (145) Tanatar, B.; Ceperley, D. M. Ground state of the two-dimensional electron gas. *Phys. Rev. B* **1989**, *39*, 5005–5016, DOI: doi:[10.1103/PhysRevB.39.5005](https://doi.org/10.1103/PhysRevB.39.5005).
- (146) Sham, L. In *Computational Methods in Band Theory*; Marcus, P., Janak, J., Williams, A., Eds.; The IBM Research Symposia Series; Springer US, 1971; pp 458–468, DOI: doi:[10.1007/978-1-4684-1890-3_36](https://doi.org/10.1007/978-1-4684-1890-3_36).
- (147) Antoniewicz, P. R.; Kleinman, L. Kohn–Sham exchange potential exact to first order in $\rho(K \rightarrow)/\rho_0$. *Phys. Rev. B* **1985**, *31*, 6779–6781, DOI: doi:[10.1103/PhysRevB.31.6779](https://doi.org/10.1103/PhysRevB.31.6779).
- (148) Perdew, J. P.; Burke, K.; Ernzerhof, M. Generalized Gradient Approximation Made Simple. *Phys. Rev. Lett.* **1996**, *77*, 3865, DOI: doi:[10.1103/PhysRevLett.77.3865](https://doi.org/10.1103/PhysRevLett.77.3865).
- (149) Perdew, J. P.; Burke, K.; Ernzerhof, M. Errata: Generalized Gradient Approximation Made Simple [Phys. Rev. Lett. 77, 3865 (1996)]. *Phys. Rev. Lett.* **1997**, *78*, 1396, DOI: doi:[10.1103/PhysRevLett.78.1396](https://doi.org/10.1103/PhysRevLett.78.1396).
- (150) Lieb, E. H.; Oxford, S. Improved lower bound on the indirect Coulomb energy. *Int. J. Quantum Chem.* **1981**, *19*, 427–439, DOI: doi:[10.1002/qua.560190306](https://doi.org/10.1002/qua.560190306).
- (151) Ma, S.-k.; Brueckner, K. A. Correlation Energy of an Electron Gas with a Slowly Varying High Density. *Phys. Rev.* **1968**, *165*, 18–31, DOI: doi:[10.1103/PhysRev.165.18](https://doi.org/10.1103/PhysRev.165.18).
- (152) Langreth, D. C.; Vosko, S. H. Exact electron-gas response functions at high density. *Phys. Rev. Lett.* **1987**, *59*, 497–500, DOI: doi:[10.1103/PhysRevLett.59.497](https://doi.org/10.1103/PhysRevLett.59.497).
- (153) Peverati, R.; Truhlar, D. G. Exchange-Correlation Functional with Good Accuracy for Both Structural and Energetic Properties while Depending Only on the Density and Its Gradient. *J. Chem. Theory Comput.* **2012**, *8*, 2310, DOI: doi:[10.1021/ct3002656](https://doi.org/10.1021/ct3002656).

- (154) Oliver, G. L.; Perdew, J. P. Spin-density gradient expansion for the kinetic energy. *Phys. Rev. A* **1979**, *20*, 397–403, DOI: doi:[10.1103/PhysRevA.20.397](https://doi.org/10.1103/PhysRevA.20.397).
- (155) Becke, A. D. Density functional calculations of molecular bond energies. *J. Chem. Phys.* **1986**, *84*, 4524, DOI: doi:[10.1063/1.450025](https://doi.org/10.1063/1.450025).
- (156) Becke, A. D. On the large-gradient behavior of the density functional exchange energy. *J. Chem. Phys.* **1986**, *85*, 7184, DOI: doi:[10.1063/1.451353](https://doi.org/10.1063/1.451353).
- (157) Becke, A. D. Density-functional exchange-energy approximation with correct asymptotic behavior. *Phys. Rev. A* **1988**, *38*, 3098, DOI: doi:[10.1103/PhysRevA.38.3098](https://doi.org/10.1103/PhysRevA.38.3098).
- (158) Perdew, J. P.; Yue, W. Accurate and simple density functional for the electronic exchange energy: Generalized gradient approximation. *Phys. Rev. B* **1986**, *33*, 8800, DOI: doi:[10.1103/PhysRevB.33.8800](https://doi.org/10.1103/PhysRevB.33.8800).
- (159) Perdew, J. P.; Yue, W. Erratum: Accurate and simple density functional for the electronic exchange energy: Generalized gradient approximation. *Phys. Rev. B* **1989**, *40*, 3399, DOI: doi:[10.1103/PhysRevB.40.3399](https://doi.org/10.1103/PhysRevB.40.3399).
- (160) Jemmer, P.; Knowles, P. J. Exchange energy in Kohn–Sham density-functional theory. *Phys. Rev. A* **1995**, *51*, 3571–3575, DOI: doi:[10.1103/PhysRevA.51.3571](https://doi.org/10.1103/PhysRevA.51.3571).
- (161) Filatov, M.; Thiel, W. Exchange-correlation density functional beyond the gradient approximation. *Phys. Rev. A* **1998**, *57*, 189–199, DOI: doi:[10.1103/PhysRevA.57.189](https://doi.org/10.1103/PhysRevA.57.189).
- (162) Engel, E.; Vosko, S. H. Fourth-order gradient corrections to the exchange-only energy functional: Importance of $\nabla^2 n$ contributions. *Phys. Rev. B* **1994**, *50*, 10498–10505, DOI: doi:[10.1103/PhysRevB.50.10498](https://doi.org/10.1103/PhysRevB.50.10498).
- (163) von Weizsäcker, C. F. Zur Theorie der Kernmassen. *Z. Phys.* **1935**, *96*, 431, DOI: doi:[10.1007/BF01337700](https://doi.org/10.1007/BF01337700).
- (164) Becke, A. D. Simulation of delocalized exchange by local density functionals. *J. Chem. Phys.* **2000**, *112*, 4020–4026, DOI: doi:[10.1063/1.480951](https://doi.org/10.1063/1.480951).
- (165) Becke, A. D. Density-functional thermochemistry. IV. A new dynamical correlation functional and implications for exact-exchange mixing. *J. Chem. Phys.* **1996**, *104*, 1040, DOI: doi:[10.1063/1.470829](https://doi.org/10.1063/1.470829).
- (166) Tao, J.; Perdew, J. P.; Staroverov, V. N.; Scuseria, G. E. Climbing the Density Functional Ladder: Nonempirical Meta-Generalized Gradient Approximation Designed for Molecules and Solids. *Phys. Rev. Lett.* **2003**, *91*, 146401, DOI: doi:[10.1103/PhysRevLett.91.146401](https://doi.org/10.1103/PhysRevLett.91.146401).
- (167) Van Voorhis, T.; Scuseria, G. E. A novel form for the exchange-correlation energy functional. *J. Chem. Phys.* **1998**, *109*, 400, DOI: doi:[10.1063/1.476577](https://doi.org/10.1063/1.476577).
- (168) Van Voorhis, T.; Scuseria, G. E. Erratum: "A novel form for the exchange-correlation energy functional" [J. Chem. Phys. 109, 400 (1998)]. *J. Chem. Phys.* **2008**, *129*, 219901, DOI: doi:[10.1063/1.3005348](https://doi.org/10.1063/1.3005348).
- (169) Levy, M. Universal variational functionals of electron densities, first-order density matrices, and natural spin-orbitals and solution of the v -representability problem. *Proc. Natl. Acad. Sci. U. S. A.* **1979**, *76*, 6062–6065, DOI: doi:[10.1073/pnas.76.12.6062](https://doi.org/10.1073/pnas.76.12.6062).
- (170) Lieb, E. H. Density functionals for coulomb systems. *Int. J. Quantum Chem.* **1983**, *24*, 243–277, DOI: doi:[10.1002/qua.560240302](https://doi.org/10.1002/qua.560240302).

- (171) Lieb, E. H. A lower bound for Coulomb energies. *Phys. Lett. A* **1979**, *70*, 444–446, DOI: doi:[10.1016/0375-9601\(79\)90358-X](https://doi.org/10.1016/0375-9601(79)90358-X).
- (172) Chan, G. K.-L.; Handy, N. C. Optimized Lieb-Oxford bound for the exchange-correlation energy. *Phys. Rev. A* **1999**, *59*, 3075–3077, DOI: doi:[10.1103/PhysRevA.59.3075](https://doi.org/10.1103/PhysRevA.59.3075).
- (173) Levy, M.; Perdew, J. P. Tight bound and convexity constraint on the exchange-correlation-energy functional in the low-density limit, and other formal tests of generalized-gradient approximations. *Phys. Rev. B* **1993**, *48*, 11638–11645, DOI: doi:[10.1103/PhysRevB.48.11638](https://doi.org/10.1103/PhysRevB.48.11638).
- (174) Levy, M.; Perdew, J. P. Erratum: Tight bound and convexity constraint on the exchange-correlation-energy functional in the low-density limit, and other formal tests of generalized-gradient approximations [Phys. Rev. B 48, 11638 (1993)]. *Phys. Rev. B* **1997**, *55*, 13321–13321, DOI: doi:[10.1103/PhysRevB.55.13321](https://doi.org/10.1103/PhysRevB.55.13321).
- (175) Odashima, M. M.; Capelle, K. How tight is the Lieb-Oxford bound? *J. Chem. Phys.* **2007**, *127*, 054106, DOI: doi:[10.1063/1.2759202](https://doi.org/10.1063/1.2759202).
- (176) Räsänen, E.; Pittalis, S.; Capelle, K.; Proetto, C. R. Lower Bounds on the Exchange-Correlation Energy in Reduced Dimensions. *Phys. Rev. Lett.* **2009**, *102*, 206406, DOI: doi:[10.1103/PhysRevLett.102.206406](https://doi.org/10.1103/PhysRevLett.102.206406).
- (177) Seidl, M.; Vuckovic, S.; Gori-Giorgi, P. Challenging the Lieb–Oxford bound in a systematic way. *Mol. Phys.* **2016**, *114*, 1076–1085, DOI: doi:[10.1080/00268976.2015.1136440](https://doi.org/10.1080/00268976.2015.1136440).
- (178) Lewin, M.; Lieb, E. H.; Seiringer, R. Improved Lieb–Oxford bound on the indirect and exchange energies. *Lett. Math. Phys.* **112**, 92, DOI: doi:[10.1007/s11005-022-01584-5](https://doi.org/10.1007/s11005-022-01584-5).
- (179) Gadre, S. R.; Bartolotti, L. J.; Handy, N. C. Bounds for Coulomb energies. *J. Chem. Phys.* **1980**, *72*, 1034–1038, DOI: doi:[10.1063/1.439270](https://doi.org/10.1063/1.439270).
- (180) Perdew, J. P.; Ziesche, P.; Eschrig, H. Electronic structure of solids’ 91. 1991.
- (181) Odashima, M. M.; Capelle, K. Empirical analysis of the Lieb-Oxford bound in ions and molecules. *Int. J. Quantum Chem.* **2008**, *108*, 2428–2432, DOI: doi:[10.1002/qua.21677](https://doi.org/10.1002/qua.21677).
- (182) Fauser, S.; Trushin, E.; Görling, A. Highly precise values for the energy ratios underlying the Lieb–Oxford bound and the convexity conjecture for the adiabatic connection. *J. Chem. Phys.* **2025**, *162*, 164108, DOI: doi:[10.1063/5.0263582](https://doi.org/10.1063/5.0263582).
- (183) Zhang, Y.; Yang, W. Comment on “Generalized Gradient Approximation Made Simple”. *Phys. Rev. Lett.* **1998**, *80*, 890, DOI: doi:[10.1103/PhysRevLett.80.890](https://doi.org/10.1103/PhysRevLett.80.890).
- (184) Lacks, D. J.; Gordon, R. G. Pair interactions of rare-gas atoms as a test of exchange-energy-density functionals in regions of large density gradients. *Phys. Rev. A* **1993**, *47*, 4681, DOI: doi:[10.1103/PhysRevA.47.4681](https://doi.org/10.1103/PhysRevA.47.4681).
- (185) Vilhena, J. G.; Räsänen, E.; Lehto-vaara, L.; Marques, M. A. L. Violation of a local form of the Lieb-Oxford bound. *Phys. Rev. A* **2012**, *85*, 052514, DOI: doi:[10.1103/physreva.85.052514](https://doi.org/10.1103/physreva.85.052514).
- (186) Mirschink, A.; Seidl, M.; Gori-Giorgi, P. Energy Densities in the Strong-Interaction Limit of Density Functional Theory. *J. Chem. Theory Comput.* **2012**, *8*, 3097–3107, DOI: doi:[10.1021/ct3003892](https://doi.org/10.1021/ct3003892).
- (187) Lieb, E. H.; Solovej, J. P.; Yngvason, J. Ground states of large quantum dots in magnetic fields. *Phys. Rev. B* **1995**, *51*, 10646–10665, DOI: doi:[10.1103/PhysRevB.51.10646](https://doi.org/10.1103/PhysRevB.51.10646).

- (188) Räsänen, E.; Seidl, M.; Gori-Giorgi, P. Strictly correlated uniform electron droplets. *Phys. Rev. B* **2011**, *83*, 195111, DOI: doi:[10.1103/PhysRevB.83.195111](https://doi.org/10.1103/PhysRevB.83.195111).
- (189) Laestadius, A.; Faulstich, F. M. One-dimensional Lieb-Oxford bounds. *J. Chem. Phys.* **2020**, *152*, 234112, DOI: doi:[10.1063/5.0009419](https://doi.org/10.1063/5.0009419).
- (190) Harris, J.; Jones, R. O. The surface energy of a bounded electron gas. *J. Phys. F: Met. Phys.* **1974**, *4*, 1170–1186, DOI: doi:[10.1088/0305-4608/4/8/013](https://doi.org/10.1088/0305-4608/4/8/013).
- (191) Langreth, D. C.; Perdew, J. P. Exchange-correlation energy of a metallic surface: Wave-vector analysis. *Phys. Rev. B* **1977**, *15*, 2884–2901, DOI: doi:[10.1103/PhysRevB.15.2884](https://doi.org/10.1103/PhysRevB.15.2884).
- (192) Gunnarsson, O.; Lundqvist, B. I. Exchange and correlation in atoms, molecules, and solids by the spin-density-functional formalism. *Phys. Rev. B* **1976**, *13*, 4274, DOI: doi:[10.1103/PhysRevB.13.4274](https://doi.org/10.1103/PhysRevB.13.4274).
- (193) Hellmann, H. A New Approximation Method in the Problem of Many Electrons. *J. Chem. Phys.* **1935**, *3*, 61, DOI: doi:[10.1063/1.1749559](https://doi.org/10.1063/1.1749559).
- (194) Feynman, R. P. Forces in Molecules. *Phys. Rev.* **1939**, *56*, 340–343, DOI: doi:[10.1103/PhysRev.56.340](https://doi.org/10.1103/PhysRev.56.340).
- (195) McWeeny, R. Some Recent Advances in Density Matrix Theory. *Rev. Mod. Phys.* **1960**, *32*, 335–369, DOI: doi:[10.1103/RevModPhys.32.335](https://doi.org/10.1103/RevModPhys.32.335).
- (196) Becke, A. D. Correlation energy of an inhomogeneous electron gas: A coordinate-space model. *J. Chem. Phys.* **1988**, *88*, 1053–1062, DOI: doi:[10.1063/1.454274](https://doi.org/10.1063/1.454274).
- (197) Kato, T. On the eigenfunctions of many-particle systems in quantum mechanics. *Commun. Pure Appl. Math.* **1957**, *10*, 151–177, DOI: doi:[10.1002/cpa.3160100201](https://doi.org/10.1002/cpa.3160100201).
- (198) Kimball, J. C. Short-Range Correlations and Electron-Gas Response Functions. *Phys. Rev. A* **1973**, *7*, 1648–1652, DOI: doi:[10.1103/PhysRevA.7.1648](https://doi.org/10.1103/PhysRevA.7.1648).
- (199) Kutzelnigg, W.; Klopper, W. Wave functions with terms linear in the interelectronic coordinates to take care of the correlation cusp. I. General theory. *J. Chem. Phys.* **1991**, *94*, 1985–2001, DOI: doi:[10.1063/1.459921](https://doi.org/10.1063/1.459921).
- (200) Burke, K.; Perdew, J. P.; Ernzerhof, M. Why semilocal functionals work: Accuracy of the on-top pair density and importance of system averaging. *J. Chem. Phys.* **1998**, *109*, 3760–3771, DOI: doi:[10.1063/1.476976](https://doi.org/10.1063/1.476976).
- (201) Tao, J.; Staroverov, V. N.; Scuseria, G. E.; Perdew, J. P. Exact-exchange energy density in the gauge of a semilocal density-functional approximation. *Phys. Rev. A* **2008**, *77*, 012509, DOI: doi:[10.1103/PhysRevA.77.012509](https://doi.org/10.1103/PhysRevA.77.012509).
- (202) Perdew, J. P.; Staroverov, V. N.; Tao, J.; Scuseria, G. E. Density functional with full exact exchange, balanced nonlocality of correlation, and constraint satisfaction. *Phys. Rev. A* **2008**, *78*, 052513, DOI: doi:[10.1103/PhysRevA.78.052513](https://doi.org/10.1103/PhysRevA.78.052513).
- (203) March, N. H. Asymptotic formula far from nucleus for exchange energy density in Hartree-Fock theory of closed-shell atoms. *Phys. Rev. A* **1987**, *36*, 5077–5078, DOI: doi:[10.1103/PhysRevA.36.5077](https://doi.org/10.1103/PhysRevA.36.5077).
- (204) Heßelmann, A.; Görling, A. Random-phase approximation correlation methods for molecules and solids. *Mol. Phys.* **2011**, *109*, 2473–2500, DOI: doi:[10.1080/00268976.2011.614282](https://doi.org/10.1080/00268976.2011.614282).
- (205) Chen, G. P.; Voora, V. K.; Agee, M. M.; Balasubramani, S. G.; Furche, F. Random-Phase Approximation Methods. *Annu. Rev. Phys. Chem.* **2017**, *68*, 421–445, DOI: doi:[10.1146/annurev-physchem-040215-112308](https://doi.org/10.1146/annurev-physchem-040215-112308).

- (206) Hellgren, M.; Baguet, L. Random phase approximation with exchange for an accurate description of crystalline polymorphism. *Phys. Rev. Res.* **2021**, *3*, 033263, DOI: doi:10.1103/PhysRevResearch.3.033263.
- (207) Trushin, E.; Fauser, S.; Molkner, A.; Erhard, J.; Gorling, A. Accurate Correlation Potentials from the Self-Consistent Random Phase Approximation. *Phys. Rev. Lett.* **2025**, *134*, 016402, DOI: doi:10.1103/PhysRevLett.134.016402.
- (208) Kohn, W.; Meir, Y.; Makarov, D. E. van der Waals Energies in Density Functional Theory. *Phys. Rev. Lett.* **1998**, *80*, 4153–4156, DOI: doi:10.1103/PhysRevLett.80.4153.
- (209) Dobson, J. F.; Gould, T. Calculation of dispersion energies. *J. Phys.: Condens. Matter* **2012**, *24*, 073201, DOI: doi:10.1088/0953-8984/24/7/073201.
- (210) Dobson, J. F.; Gould, T.; Vignale, G. How Many-Body Effects Modify the van der Waals Interaction between Graphene Sheets. *Phys. Rev. X* **2014**, *4*, 021040, DOI: doi:10.1103/PhysRevX.4.021040.
- (211) Colonna, N.; Hellgren, M.; de Gironcoli, S. Molecular bonding with the RPax: From weak dispersion forces to strong correlation. *Phys. Rev. B* **2016**, *93*, 195108, DOI: doi:10.1103/PhysRevB.93.195108.
- (212) Chakraborty, D.; Berland, K.; Thonhauser, T. Next-Generation Nonlocal van der Waals Density Functional. *J. Chem. Theory Comput.* **2020**, *16*, 5893–5911, DOI: doi:10.1021/acs.jctc.0c00471.
- (213) Runge, E.; Gross, E. K. U. Density-Functional Theory for Time-Dependent Systems. *Phys. Rev. Lett.* **1984**, *52*, 997–1000, DOI: doi:10.1103/PhysRevLett.52.997.
- (214) Vignale, G. Real-time resolution of the causality paradox of time-dependent density-functional theory. *Phys. Rev. A* **2008**, *77*, 062511, DOI: doi:10.1103/PhysRevA.77.062511.
- (215) Dobson, J. F. Harmonic-Potential Theorem: Implications for Approximate Many-Body Theories. *Phys. Rev. Lett.* **1994**, *73*, 2244–2247, DOI: doi:10.1103/PhysRevLett.73.2244.
- (216) Vignale, G.; Ullrich, C. A.; Conti, S. Time-Dependent Density Functional Theory Beyond the Adiabatic Local Density Approximation. *Phys. Rev. Lett.* **1997**, *79*, 4878–4881, DOI: doi:10.1103/PhysRevLett.79.4878.
- (217) Maitra, N. T.; Burke, K.; Woodward, C. Memory in Time-Dependent Density Functional Theory. *Phys. Rev. Lett.* **2002**, *89*, 023002, DOI: doi:10.1103/PhysRevLett.89.023002.
- (218) Gross, E. K. U.; Kohn, W. Local density-functional theory of frequency-dependent linear response. *Phys. Rev. Lett.* **1985**, *55*, 2850–2852, DOI: doi:10.1103/PhysRevLett.55.2850.
- (219) Petersilka, M.; Gossmann, U. J.; Gross, E. K. U. Excitation Energies from Time-Dependent Density-Functional Theory. *Phys. Rev. Lett.* **1996**, *76*, 1212–1215, DOI: doi:10.1103/PhysRevLett.76.1212.
- (220) Bohm, D.; Pines, D. A Collective Description of Electron Interactions. I. Magnetic Interactions. *Phys. Rev.* **1951**, *82*, 625–634, DOI: doi:10.1103/PhysRev.82.625.
- (221) Gritsenko, O.; van Leeuwen, R.; van Lenthe, E.; Baerends, E. J. Self-consistent approximation to the Kohn–Sham exchange potential. *Phys. Rev. A* **1995**, *51*, 1944–1954, DOI: doi:10.1103/PhysRevA.51.1944.

- (222) Becke, A. D. Hartree–Fock exchange energy of an inhomogeneous electron gas. *Int. J. Quantum Chem.* **1983**, *23*, 1915–1922, DOI: doi:[10.1002/qua.560230605](https://doi.org/10.1002/qua.560230605).
- (223) Becke, A. D.; Edgecombe, K. E. A simple measure of electron localization in atomic and molecular systems. *J. Chem. Phys.* **1990**, *92*, 5397, DOI: doi:[10.1063/1.458517](https://doi.org/10.1063/1.458517).
- (224) Pittalis, S.; Troiani, F.; Rozzi, C. A.; Vignale, G. Ab initio theory of spin entanglement in atoms and molecules. *Phys. Rev. B* **2015**, *91*, 075109, DOI: doi:[10.1103/PhysRevB.91.075109](https://doi.org/10.1103/PhysRevB.91.075109).
- (225) Mi, W.; Luo, K.; Trickey, S. B.; Pavanello, M. Orbital-Free Density Functional Theory: An Attractive Electronic Structure Method for Large-Scale First-Principles Simulations. *Chem. Rev.* **2023**, *123*, 12039–12104, DOI: doi:[10.1021/acs.chemrev.2c00758](https://doi.org/10.1021/acs.chemrev.2c00758).
- (226) Savin, A.; Jepsen, O.; Flad, J.; Andersen, O. K.; Preuss, H.; von Schnering, H. G. Electron Localization in Solid-State Structures of the Elements: the Diamond Structure. *Angew. Chem., Int. Ed.* **1992**, *31*, 187–188, DOI: doi:[10.1002/anie.199201871](https://doi.org/10.1002/anie.199201871).
- (227) Tao, J. Explicit inclusion of paramagnetic current density in the exchange-correlation functionals of current-density functional theory. *Phys. Rev. B* **2005**, *71*, 205107, DOI: doi:[10.1103/PhysRevB.71.205107](https://doi.org/10.1103/PhysRevB.71.205107).
- (228) Dobson, J. F. Interpretation of the Fermi hole curvature. *J. Chem. Phys.* **1991**, *94*, 4328–4333, DOI: doi:[10.1063/1.460619](https://doi.org/10.1063/1.460619).
- (229) Becke, A. D. Current density in exchange-correlation functionals: Application to atomic states. *J. Chem. Phys.* **2002**, *117*, 6935–6938, DOI: doi:[10.1063/1.1503772](https://doi.org/10.1063/1.1503772).
- (230) Burnus, T.; Marques, M. A. L.; Gross, E. K. U. Time-dependent electron localization function. *Phys. Rev. A* **2005**, *71*, 010501, DOI: doi:[10.1103/PhysRevA.71.010501](https://doi.org/10.1103/PhysRevA.71.010501).
- (231) Pittalis, S.; Vignale, G.; Eich, F. G. $U(1) \times SU(2)$ gauge invariance made simple for density functional approximations. *Phys. Rev. B* **2017**, *96*, 035141, DOI: doi:[10.1103/PhysRevB.96.035141](https://doi.org/10.1103/PhysRevB.96.035141).
- (232) Desmarais, J. K.; Vignale, G.; Bencheikh, K.; Erba, A.; Pittalis, S. Electron Localization Function for Noncollinear Spins. *Phys. Rev. Lett.* **2024**, *133*, 136401, DOI: doi:[10.1103/PhysRevLett.133.136401](https://doi.org/10.1103/PhysRevLett.133.136401).
- (233) Perdew, J. P.; Zunger, A. Self-interaction correction to density-functional approximations for many-electron systems. *Phys. Rev. B* **1981**, *23*, 5048, DOI: doi:[10.1103/PhysRevB.23.5048](https://doi.org/10.1103/PhysRevB.23.5048).
- (234) Perdew, J. P.; Ruzsinszky, A.; Sun, J.; Pederson, M. R. Paradox of Self-Interaction Correction: How Can Anything So Right Be So Wrong? *Adv. At. Mol. Opt. Phys.* **2015**, *64*, 1–14, DOI: doi:[10.1016/bs.aamop.2015.06.004](https://doi.org/10.1016/bs.aamop.2015.06.004).
- (235) Lehtola, S.; Head-Gordon, M.; Jónsson, H. Complex Orbitals, Multiple Local Minima, and Symmetry Breaking in Perdew–Zunger Self-Interaction Corrected Density Functional Theory Calculations. *J. Chem. Theory Comput.* **2016**, *12*, 3195–3207, DOI: doi:[10.1021/acs.jctc.6b00347](https://doi.org/10.1021/acs.jctc.6b00347).
- (236) Schwalbe, S.; Schulze, W. T.; Trepte, K.; Lehtola, S. Ensemble Generalization of the Perdew–Zunger Self-Interaction Correction: A Way Out of Multiple Minima and Symmetry Breaking. *J. Chem. Theory Comput.* **2024**, *20*, 7144–7154, DOI: doi:[10.1021/acs.jctc.4c00694](https://doi.org/10.1021/acs.jctc.4c00694).
- (237) Cernatic, F.; Senjean, B.; Robert, V.; Fromager, E. Ensemble Density Functional Theory of Neutral and Charged Excitations. *Top. Curr. Chem.* **2022**,

- 380, 4, DOI: doi:[10.1007/s41061-021-00359-1](https://doi.org/10.1007/s41061-021-00359-1).
- (238) Levy, M.; Perdew, J. P. Hellmann-Feynman, virial, and scaling requisites for the exact universal density functionals. Shape of the correlation potential and diamagnetic susceptibility for atoms. *Phys. Rev. A* **1985**, *32*, 2010–2021, DOI: doi:[10.1103/PhysRevA.32.2010](https://doi.org/10.1103/PhysRevA.32.2010).
- (239) Levy, M. Density-functional exchange correlation through coordinate scaling in adiabatic connection and correlation hole. *Phys. Rev. A* **1991**, *43*, 4637–4646, DOI: doi:[10.1103/PhysRevA.43.4637](https://doi.org/10.1103/PhysRevA.43.4637).
- (240) Görling, A.; Levy, M. Correlation-energy functional and its high-density limit obtained from a coupling-constant perturbation expansion. *Phys. Rev. B* **1993**, *47*, 13105–13113, DOI: doi:[10.1103/PhysRevB.47.13105](https://doi.org/10.1103/PhysRevB.47.13105).
- (241) Seidl, M.; Perdew, J. P.; Levy, M. Strictly correlated electrons in density-functional theory. *Phys. Rev. A* **1999**, *59*, 51–54, DOI: doi:[10.1103/PhysRevA.59.51](https://doi.org/10.1103/PhysRevA.59.51).
- (242) Seidl, M. Strong-interaction limit of density-functional theory. *Phys. Rev. A* **1999**, *60*, 4387–4395, DOI: doi:[10.1103/PhysRevA.60.4387](https://doi.org/10.1103/PhysRevA.60.4387).
- (243) Seidl, M.; Perdew, J. P.; Kurth, S. Density functionals for the strong-interaction limit. *Phys. Rev. A* **2000**, *62*, 012502, DOI: doi:[10.1103/PhysRevA.62.012502](https://doi.org/10.1103/PhysRevA.62.012502).
- (244) Seidl, M.; Perdew, J. P.; Kurth, S. Erratum: Density functionals for the strong-interaction limit [Phys. Rev. A 62, 012502 (2000)]. *Phys. Rev. A* **2005**, *72*, 029904, DOI: doi:[10.1103/PhysRevA.72.029904](https://doi.org/10.1103/PhysRevA.72.029904).
- (245) Gori-Giorgi, P.; Seidl, M.; Vignale, G. Density-Functional Theory for Strongly Interacting Electrons. *Phys. Rev. Lett.* **2009**, *103*, 166402, DOI: doi:[10.1103/PhysRevLett.103.166402](https://doi.org/10.1103/PhysRevLett.103.166402).
- (246) Gori-Giorgi, P.; Seidl, M. Density functional theory for strongly-interacting electrons: perspectives for physics and chemistry. *Phys. Chem. Chem. Phys.* **2010**, *12*, 14405–14419, DOI: doi:[10.1039/C0CP01061H](https://doi.org/10.1039/C0CP01061H).
- (247) Macke, W. Über die Wechselwirkungen im Fermi-Gas. Polarisationserscheinungen, Correlationsenergie, Elektronencondensation. *Z. Naturforsch. A* **1950**, *5*, 192–208, DOI: doi:[10.1515/zna-1950-0402](https://doi.org/10.1515/zna-1950-0402).
- (248) DuBois, D. Electron interactions: Part II. Properties of a dense electron gas. *Ann. Phys.* **1959**, *8*, 24–77, DOI: doi:[10.1016/0003-4916\(59\)90062-4](https://doi.org/10.1016/0003-4916(59)90062-4).
- (249) Carr, W. J.; Maradudin, A. A. Ground-State Energy of a High-Density Electron Gas. *Phys. Rev.* **1964**, *133*, A371–A374, DOI: doi:[10.1103/PhysRev.133.A371](https://doi.org/10.1103/PhysRev.133.A371).
- (250) Gell-Mann, M.; Brueckner, K. A. Correlation Energy of an Electron Gas at High Density. *Phys. Rev.* **1957**, *106*, 364, DOI: doi:[10.1103/PhysRev.106.364](https://doi.org/10.1103/PhysRev.106.364).
- (251) Endo, T.; Horiuchi, M.; Takada, Y.; Yasuhara, H. High-density expansion of correlation energy and its extrapolation to the metallic density region. *Phys. Rev. B* **1999**, *59*, 7367–7372, DOI: doi:[10.1103/PhysRevB.59.7367](https://doi.org/10.1103/PhysRevB.59.7367).
- (252) Sun, J.; Perdew, J. P.; Seidl, M. Correlation energy of the uniform electron gas from an interpolation between high- and low-density limits. *Phys. Rev. B* **2010**, *81*, 085123, DOI: doi:[10.1103/PhysRevB.81.085123](https://doi.org/10.1103/PhysRevB.81.085123).
- (253) Sun, J.; Perdew, J. P.; Seidl, M. Erratum: Correlation energy of the uniform electron gas from an interpolation between high- and low-density limits [Phys. Rev. B 81, 085123 (2010)]. *Phys. Rev. B* **2018**, *98*, 079903, DOI: doi:[10.1103/PhysRevB.98.079903](https://doi.org/10.1103/PhysRevB.98.079903).

- (254) Wang, Y.; Perdew, J. P. Spin scaling of the electron-gas correlation energy in the high-density limit. *Phys. Rev. B* **1991**, *43*, 8911–8916, DOI: doi:[10.1103/PhysRevB.43.8911](https://doi.org/10.1103/PhysRevB.43.8911).
- (255) Hoffman, G. G. Correlation energy of a spin-polarized electron gas at high density. *Phys. Rev. B* **1992**, *45*, 8730–8733, DOI: doi:[10.1103/PhysRevB.45.8730](https://doi.org/10.1103/PhysRevB.45.8730).
- (256) Loos, P.-F.; Gill, P. M. W. Correlation energy of the spin-polarized uniform electron gas at high density. *Phys. Rev. B* **2011**, *84*, 033103, DOI: doi:[10.1103/PhysRevB.84.033103](https://doi.org/10.1103/PhysRevB.84.033103).
- (257) Bhattarai, P.; Patra, A.; Shahi, C.; Perdew, J. P. How accurate are the parametrized correlation energies of the uniform electron gas? *Phys. Rev. B* **2018**, *97*, 195128, DOI: doi:[10.1103/PhysRevB.97.195128](https://doi.org/10.1103/PhysRevB.97.195128).
- (258) Wigner, E. On the Interaction of Electrons in Metals. *Phys. Rev.* **1934**, *46*, 1002–1011, DOI: doi:[10.1103/PhysRev.46.1002](https://doi.org/10.1103/PhysRev.46.1002).
- (259) Carr, W. J.; Coldwell-Horsfall, R. A.; Fein, A. E. Anharmonic Contribution to the Energy of a Dilute Electron Gas—Interpolation for the Correlation Energy. *Phys. Rev.* **1961**, *124*, 747–752, DOI: doi:[10.1103/PhysRev.124.747](https://doi.org/10.1103/PhysRev.124.747).
- (260) Perdew, J. P.; Wang, Y. Accurate and simple analytic representation of the electron-gas correlation energy. *Phys. Rev. B* **1992**, *45*, 13244, DOI: doi:[10.1103/PhysRevB.45.13244](https://doi.org/10.1103/PhysRevB.45.13244).
- (261) Perdew, J. P.; Wang, Y. Erratum: Accurate and simple analytic representation of the electron-gas correlation energy [Phys. Rev. B 45, 13244 (1992)]. *Phys. Rev. B* **2018**, *98*, 079904, DOI: doi:[10.1103/PhysRevB.98.079904](https://doi.org/10.1103/PhysRevB.98.079904).
- (262) Aguilera-Navarro, V. C.; Baker, G. A.; de Llano, M. Ground-state energy of helium. *Phys. Rev. B* **1985**, *32*, 4502–4506, DOI: doi:[10.1103/PhysRevB.32.4502](https://doi.org/10.1103/PhysRevB.32.4502).
- (263) Engel, E.; Dreizler, R. *Density Functional Theory: An Advanced Course*; Theoretical and Mathematical Physics; Springer Berlin Heidelberg, 2013; DOI: doi:[10.1007/978-3-642-14090-7](https://doi.org/10.1007/978-3-642-14090-7).
- (264) Brack, M.; Jennings, B. K.; Chu, Y. H. On the extended Thomas–Fermi approximation to the kinetic energy density. *Phys. Lett. B* **1976**, *65*, 1–4, DOI: doi:[10.1016/0370-2693\(76\)90519-0](https://doi.org/10.1016/0370-2693(76)90519-0).
- (265) Perdew, J. P.; Sahni, V.; Harbola, M. K.; Pathak, R. K. Fourth-order gradient expansion of the fermion kinetic energy: Extra terms for nonanalytic densities. *Phys. Rev. B* **1986**, *34*, 686–691, DOI: doi:[10.1103/PhysRevB.34.686](https://doi.org/10.1103/PhysRevB.34.686).
- (266) Perdew, J. P.; Sahni, V.; Harbola, M. K.; Pathak, R. K. Erratum: Fourth-order gradient expansion of the fermion kinetic energy: Extra terms for nonanalytic densities. *Phys. Rev. B* **1988**, *37*, 4267–4267, DOI: doi:[10.1103/PhysRevB.37.4267](https://doi.org/10.1103/PhysRevB.37.4267).
- (267) Svendsen, P. S.; von Barth, U. Gradient expansion of the exchange energy from second-order density response theory. *Phys. Rev. B* **1996**, *54*, 17402–17413, DOI: doi:[10.1103/PhysRevB.54.17402](https://doi.org/10.1103/PhysRevB.54.17402).
- (268) van Leeuwen, R. Density gradient expansion of correlation functions. *Phys. Rev. B* **2013**, *87*, 155142, DOI: doi:[10.1103/PhysRevB.87.155142](https://doi.org/10.1103/PhysRevB.87.155142).
- (269) Lieb, E. H.; Simon, B. Thomas-Fermi Theory Revisited. *Phys. Rev. Lett.* **1973**, *31*, 681–683, DOI: doi:[10.1103/PhysRevLett.31.681](https://doi.org/10.1103/PhysRevLett.31.681).
- (270) Perdew, J. P.; Constantin, L. A.; Sagvolden, E.; Burke, K. Relevance of the Slowly Varying Electron Gas to Atoms, Molecules, and Solids. *Phys. Rev. Lett.* **2006**, *97*, 223002, DOI: doi:[10.1103/PhysRevLett.97.223002](https://doi.org/10.1103/PhysRevLett.97.223002).

- (271) Perdew, J. P.; Ruzsinszky, A.; Csonka, G. I.; Vydrov, O. A.; Scuseria, G. E.; Constantin, L. A.; Zhou, X.; Burke, K. Restoring the Density-Gradient Expansion for Exchange in Solids and Surfaces. *Phys. Rev. Lett.* **2008**, *100*, 136406, DOI: doi:[10.1103/PhysRevLett.100.136406](https://doi.org/10.1103/PhysRevLett.100.136406).
- (272) Perdew, J. P.; Ruzsinszky, A.; Csonka, G. I.; Vydrov, O. A.; Scuseria, G. E.; Constantin, L. A.; Zhou, X.; Burke, K. Erratum: Restoring the Density-Gradient Expansion for Exchange in Solids and Surfaces [Phys. Rev. Lett.100, 136406 (2008)]. *Phys. Rev. Lett.* **2009**, *102*, 039902, DOI: doi:[10.1103/PhysRevLett.102.039902](https://doi.org/10.1103/PhysRevLett.102.039902).
- (273) Elliott, P.; Burke, K. Non-empirical derivation of the parameter in the B88 exchange functional. *Can. J. Chem.* **2009**, *87*, 1485–1491, DOI: doi:[10.1139/V09-095](https://doi.org/10.1139/V09-095).
- (274) Constantin, L. A.; Fabiano, E.; Laricchia, S.; Della Sala, F. Semiclassical Neutral Atom as a Reference System in Density Functional Theory. *Phys. Rev. Lett.* **2011**, *106*, 186406, DOI: doi:[10.1103/PhysRevLett.106.186406](https://doi.org/10.1103/PhysRevLett.106.186406).
- (275) Vilhena, J. G.; Räsänen, E.; Marques, M. A. L.; Pittalis, S. Construction of the B88 Exchange-Energy Functional in Two Dimensions. *J. Chem. Theory Comput.* **2014**, *10*, 1837–1842, DOI: doi:[10.1021/ct4010728](https://doi.org/10.1021/ct4010728).
- (276) Sun, J.; Ruzsinszky, A.; Perdew, J. P. Strongly Constrained and Appropriately Normed Semilocal Density Functional. *Phys. Rev. Lett.* **2015**, *115*, 036402, DOI: doi:[10.1103/PhysRevLett.115.036402](https://doi.org/10.1103/PhysRevLett.115.036402).
- (277) Kunz, H.; Rueedi, R. Atoms and quantum dots with a large number of electrons: The ground-state energy. *Phys. Rev. A* **2010**, *81*, 032122, DOI: doi:[10.1103/PhysRevA.81.032122](https://doi.org/10.1103/PhysRevA.81.032122).
- (278) Daas, K. J.; Kooi, D. P.; Grooteman, A. J. A. F.; Seidl, M.; Gori-Giorgi, P. Gradient Expansions for the Large-Coupling Strength Limit of the Møller–Plesset Adiabatic Connection. *J. Chem. Theory Comput.* **2022**, *18*, 1584–1594, DOI: doi:[10.1021/acs.jctc.1c01206](https://doi.org/10.1021/acs.jctc.1c01206).
- (279) Argaman, N.; Redd, J.; Cancio, A. C.; Burke, K. Leading Correction to the Local Density Approximation for Exchange in Large- Z Atoms. *Phys. Rev. Lett.* **2022**, *129*, 153001, DOI: doi:[10.1103/PhysRevLett.129.153001](https://doi.org/10.1103/PhysRevLett.129.153001).
- (280) Burke, K.; Cancio, A.; Gould, T.; Pittalis, S. Locality of correlation in density functional theory. *J. Chem. Phys.* **2016**, *145*, 054112, DOI: doi:[10.1063/1.4959126](https://doi.org/10.1063/1.4959126).
- (281) Sharp, R. T.; Horton, G. K. A Variational Approach to the Unipotent Many-Electron Problem. *Phys. Rev.* **1953**, *90*, 317–317, DOI: doi:[10.1103/PhysRev.90.317](https://doi.org/10.1103/PhysRev.90.317).
- (282) Kümmel, S.; Kronik, L. Orbital-dependent density functionals: Theory and applications. *Rev. Mod. Phys.* **2008**, *80*, 3–60, DOI: doi:[10.1103/RevModPhys.80.3](https://doi.org/10.1103/RevModPhys.80.3).
- (283) Betzinger, M.; Friedrich, C.; Görling, A.; Blügel, S. Precise response functions in all-electron methods: Application to the optimized-effective-potential approach. *Phys. Rev. B* **2012**, *85*, 245124, DOI: doi:[10.1103/PhysRevB.85.245124](https://doi.org/10.1103/PhysRevB.85.245124).
- (284) Arbuznikov, A. V.; Kaupp, M. The self-consistent implementation of exchange-correlation functionals depending on the local kinetic energy density. *Chem. Phys. Lett.* **2003**, *381*, 495–504, DOI: doi:[10.1016/j.cplett.2003.10.009](https://doi.org/10.1016/j.cplett.2003.10.009).
- (285) Zahariev, F.; Leang, S. S.; Gordon, M. S. Functional derivatives of meta-generalized gradient approximation (meta-GGA) type exchange-correlation density functionals. *J.*

- Chem. Phys.* **2013**, *138*, 244108, DOI: doi:[10.1063/1.4811270](https://doi.org/10.1063/1.4811270).
- (286) Eich, F. G.; Hellgren, M. Derivative discontinuity and exchange-correlation potential of meta-GGAs in density-functional theory. *J. Chem. Phys.* **2014**, *141*, 224107, DOI: doi:[10.1063/1.4903273](https://doi.org/10.1063/1.4903273).
- (287) Yang, Z.-h.; Peng, H.; Sun, J.; Perdew, J. P. More realistic band gaps from meta-generalized gradient approximations: Only in a generalized Kohn–Sham scheme. *Phys. Rev. B* **2016**, *93*, 205205, DOI: doi:[10.1103/PhysRevB.93.205205](https://doi.org/10.1103/PhysRevB.93.205205).
- (288) Körzdörfer, T.; Kümmel, S.; Mundt, M. Self-interaction correction and the optimized effective potential. *J. Chem. Phys.* **2008**, *129*, 014110, DOI: doi:[10.1063/1.2944272](https://doi.org/10.1063/1.2944272).
- (289) Yamamoto, Y.; Baruah, T.; Chang, P.-H.; Romero, S.; Zope, R. R. Self-consistent implementation of locally scaled self-interaction-correction method. *J. Chem. Phys.* **2023**, *158*, 064114, DOI: doi:[10.1063/5.0130436](https://doi.org/10.1063/5.0130436).
- (290) Grüning, M.; Marini, A.; Rubio, A. Density functionals from many-body perturbation theory: The band gap for semiconductors and insulators. *J. Chem. Phys.* **2006**, *124*, 154108, DOI: doi:[10.1063/1.2189226](https://doi.org/10.1063/1.2189226).
- (291) Riemelmoser, S.; Kaltak, M.; Kresse, G. Optimized effective potentials from the random-phase approximation: Accuracy of the quasiparticle approximation. *J. Chem. Phys.* **2021**, *154*, 154103, DOI: doi:[10.1063/5.0045400](https://doi.org/10.1063/5.0045400).
- (292) Pitts, T.; Contant, D.; Hellgren, M. Self-consistent random phase approximation and optimized hybrid functionals for solids. *Phys. Rev. B* **2025**, *112*, 085137, DOI: doi:[10.1103/1ymj-3ycc](https://doi.org/10.1103/1ymj-3ycc).
- (293) Seidl, A.; Görling, A.; Vogl, P.; Majewski, J. A.; Levy, M. Generalized Kohn–Sham schemes and the band-gap problem. *Phys. Rev. B* **1996**, *53*, 3764–3774, DOI: doi:[10.1103/PhysRevB.53.3764](https://doi.org/10.1103/PhysRevB.53.3764).
- (294) Fukutome, H. Unrestricted Hartree–Fock theory and its applications to molecules and chemical reactions. *Int. J. Quantum Chem.* **1981**, *20*, 955–1065, DOI: doi:[10.1002/qua.560200502](https://doi.org/10.1002/qua.560200502).
- (295) Löwdin, P.-O.; Mayer, I. In *Some Studies of the General Hartree-Fock Method*; Löwdin, P.-O., Ed.; Advances in Quantum Chemistry; Academic Press, 1992; Vol. 24; pp 79–114, DOI: doi:[10.1016/S0065-3276\(08\)60101-X](https://doi.org/10.1016/S0065-3276(08)60101-X).
- (296) Hammes-Schiffer, S.; Andersen, H. C. The advantages of the general Hartree–Fock method for future computer simulation of materials. *J. Chem. Phys.* **1993**, *99*, 1901–1913, DOI: doi:[10.1063/1.465305](https://doi.org/10.1063/1.465305).
- (297) Small, D. W.; Sundstrom, E. J.; Head-Gordon, M. A simple way to test for collinearity in spin symmetry broken wave functions: General theory and application to generalized Hartree Fock. *J. Chem. Phys.* **2015**, *142*, 094112, DOI: doi:[10.1063/1.4913740](https://doi.org/10.1063/1.4913740).
- (298) Neumann, R.; Nobes, R. H.; Handy, N. C. Exchange functionals and potentials. *Mol. Phys.* **1996**, *87*, 1–36, DOI: doi:[10.1080/00268979600100011](https://doi.org/10.1080/00268979600100011).
- (299) Ferrighi, L.; Madsen, G. K. H.; Hammer, B. Self-consistent meta-generalized gradient approximation study of adsorption of aromatic molecules on noble metal surfaces. *J. Chem. Phys.* **2011**, *135*, 084704, DOI: doi:[10.1063/1.3624529](https://doi.org/10.1063/1.3624529).
- (300) Sun, J.; Marsman, M.; Csonka, G. I.; Ruzsinszky, A.; Hao, P.; Kim, Y.-S.; Kresse, G.; Perdew, J. P. Self-consistent meta-generalized gradient approximation

- within the projector-augmented-wave method. *Phys. Rev. B* **2011**, *84*, 035117, DOI: doi:[10.1103/PhysRevB.84.035117](https://doi.org/10.1103/PhysRevB.84.035117).
- (301) Womack, J. C.; Mardirossian, N.; Head-Gordon, M.; Skylaris, C.-K. Self-consistent implementation of meta-GGA functionals for the ONETEP linear-scaling electronic structure package. *J. Chem. Phys.* **2016**, *145*, 204114, DOI: doi:[10.1063/1.4967960](https://doi.org/10.1063/1.4967960).
- (302) Yao, Y.; Kanai, Y. Plane-wave pseudopotential implementation and performance of SCAN meta-GGA exchange-correlation functional for extended systems. *J. Chem. Phys.* **2017**, *146*, 224105, DOI: doi:[10.1063/1.4984939](https://doi.org/10.1063/1.4984939).
- (303) Doumont, J.; Tran, F.; Blaha, P. Implementation of self-consistent MGGA functionals in augmented plane wave based methods. *Phys. Rev. B* **2022**, *105*, 195138, DOI: doi:[10.1103/PhysRevB.105.195138](https://doi.org/10.1103/PhysRevB.105.195138).
- (304) Doumont, J.; Tran, F.; Blaha, P. Erratum: Implementation of self-consistent MGGA functionals in augmented plane wave based methods [Phys. Rev. B 105, 195138 (2022)]. *Phys. Rev. B* **2022**, *106*, 159901, DOI: doi:[10.1103/PhysRevB.106.159901](https://doi.org/10.1103/PhysRevB.106.159901).
- (305) Liu, R.; Zheng, D.; Liang, X.; Ren, X.; Chen, M.; Li, W. Implementation of the meta-GGA exchange-correlation functional in numerical atomic orbital basis: With systematic testing on SCAN, rSCAN, and r²SCAN functionals. *J. Chem. Phys.* **2023**, *159*, 074109, DOI: doi:[10.1063/5.0160726](https://doi.org/10.1063/5.0160726).
- (306) Sham, L. J.; Schlüter, M. Density-functional theory of the band gap. *Phys. Rev. B* **1985**, *32*, 3883–3889, DOI: doi:[10.1103/PhysRevB.32.3883](https://doi.org/10.1103/PhysRevB.32.3883).
- (307) Baerends, E. J. From the Kohn–Sham band gap to the fundamental gap in solids. An integer electron approach. *Phys. Chem. Chem. Phys.* **2017**, *19*, 15639–15656, DOI: doi:[10.1039/C7CP02123B](https://doi.org/10.1039/C7CP02123B).
- (308) Görling, A. Exchange-correlation potentials with proper discontinuities for physically meaningful Kohn–Sham eigenvalues and band structures. *Phys. Rev. B* **2015**, *91*, 245120, DOI: doi:[10.1103/PhysRevB.91.245120](https://doi.org/10.1103/PhysRevB.91.245120).
- (309) Trushin, E.; Betzinger, M.; Blügel, S.; Görling, A. Band gaps, ionization potentials, and electron affinities of periodic electron systems via the adiabatic-connection fluctuation-dissipation theorem. *Phys. Rev. B* **2016**, *94*, 075123, DOI: doi:[10.1103/PhysRevB.94.075123](https://doi.org/10.1103/PhysRevB.94.075123).
- (310) Perdew, J. P.; Yang, W.; Burke, K.; Yang, Z.; Gross, E. K. U.; Scheffler, M.; Scuseria, G. E.; Henderson, T. M.; Zhang, I. Y.; Ruzsinszky, A.; Peng, H.; Sun, J.; Trushin, E.; Görling, A. Understanding band gaps of solids in generalized Kohn–Sham theory. *Proc. Natl. Acad. Sci. U.S.A.* **2017**, *114*, 2801–2806, DOI: doi:[10.1073/pnas.1621352114](https://doi.org/10.1073/pnas.1621352114).
- (311) Tran, F.; Doumont, J.; Blaha, P.; Marques, M. A. L.; Botti, S.; Bartók, A. P. On the calculation of the bandgap of periodic solids with MGGA functionals using the total energy. *J. Chem. Phys.* **2019**, *151*, 161102, DOI: doi:[10.1063/1.5126393](https://doi.org/10.1063/1.5126393).
- (312) Perdew, J. P.; Parr, R. G.; Levy, M.; Balduz, J. L. Density-Functional Theory for Fractional Particle Number: Derivative Discontinuities of the Energy. *Phys. Rev. Lett.* **1982**, *49*, 1691–1694, DOI: doi:[10.1103/PhysRevLett.49.1691](https://doi.org/10.1103/PhysRevLett.49.1691).
- (313) Yang, W.; Zhang, Y.; Ayers, P. W. Degenerate Ground States and a Fractional Number of Electrons in Density and Reduced Density Matrix Functional Theory. *Phys. Rev. Lett.* **2000**, *84*, 5172–5175, DOI: doi:[10.1103/PhysRevLett.84.5172](https://doi.org/10.1103/PhysRevLett.84.5172).

- (314) Marques, M. A. L.; Vidal, J.; Oliveira, M. J. T.; Reining, L.; Botti, S. Density-based mixing parameter for hybrid functionals. *Phys. Rev. B* **2011**, *83*, 035119, DOI: doi:[10.1103/PhysRevB.83.035119](https://doi.org/10.1103/PhysRevB.83.035119).
- (315) Kraisler, E.; Kronik, L. Piecewise Linearity of Approximate Density Functionals Revisited: Implications for Frontier Orbital Energies. *Phys. Rev. Lett.* **2013**, *110*, 126403, DOI: doi:[10.1103/PhysRevLett.110.126403](https://doi.org/10.1103/PhysRevLett.110.126403).
- (316) Kraisler, E.; Kronik, L. Fundamental gaps with approximate density functionals: The derivative discontinuity revealed from ensemble considerations. *J. Chem. Phys.* **2014**, *140*, 18A540, DOI: doi:[10.1063/1.4871462](https://doi.org/10.1063/1.4871462).
- (317) Sun, J.; Ruzsinszky, A.; Perdew, J. P. Strongly Constrained and Appropriately Normed Semilocal Density Functional. *Phys. Rev. Lett.* **2015**, *115*, 036402, DOI: doi:[10.1103/PhysRevLett.115.036402](https://doi.org/10.1103/PhysRevLett.115.036402).
- (318) Lebeda, T.; Aschbrock, T.; Kümmel, S. Balancing the Contributions to the Gradient Expansion: Accurate Binding and Band Gaps with a Nonempirical Meta-GGA. *Phys. Rev. Lett.* **2024**, *133*, 136402, DOI: doi:[10.1103/PhysRevLett.133.136402](https://doi.org/10.1103/PhysRevLett.133.136402).
- (319) Grüning, M.; Marini, A.; Rubio, A. Effect of spatial nonlocality on the density functional band gap. *Phys. Rev. B* **2006**, *74*, 161103, DOI: doi:[10.1103/PhysRevB.74.161103](https://doi.org/10.1103/PhysRevB.74.161103).
- (320) Kuisma, M.; Ojanen, J.; Enkovaara, J.; Rantala, T. T. Kohn–Sham potential with discontinuity for band gap materials. *Phys. Rev. B* **2010**, *82*, 115106, DOI: doi:[10.1103/PhysRevB.82.115106](https://doi.org/10.1103/PhysRevB.82.115106).
- (321) Castelli, I. E.; Olsen, T.; Datta, S.; Landis, D. D.; Dahl, S.; Thygesen, K. S.; Jacobsen, K. W. Computational screening of perovskite metal oxides for optimal solar light capture. *Energy Environ. Sci.* **2012**, *5*, 5814–5819, DOI: doi:[10.1039/C1EE02717D](https://doi.org/10.1039/C1EE02717D).
- (322) Tran, F.; Ehsan, S.; Blaha, P. Assessment of the GLLB-SC potential for solid-state properties and attempts for improvement. *Phys. Rev. Mater.* **2018**, *2*, 023802, DOI: doi:[10.1103/PhysRevMaterials.2.023802](https://doi.org/10.1103/PhysRevMaterials.2.023802).
- (323) Guandalini, A.; Rozzi, C. A.; Räsänen, E.; Pittalis, S. Fundamental gaps of quantum dots on the cheap. *Phys. Rev. B* **2019**, *99*, 125140, DOI: doi:[10.1103/PhysRevB.99.125140](https://doi.org/10.1103/PhysRevB.99.125140).
- (324) Guandalini, A.; Ruini, A.; Räsänen, E.; Rozzi, C. A.; Pittalis, S. Density functional approach to the band gaps of finite and periodic two-dimensional systems. *Phys. Rev. B* **2021**, *104*, 085110, DOI: doi:[10.1103/PhysRevB.104.085110](https://doi.org/10.1103/PhysRevB.104.085110).
- (325) Bastard, G. *Wave Mechanics Applied to Semiconductor Heterostructures*; Monographies de physique; Wiley, 1988.
- (326) Kim, Y.-H.; Lee, I.-H.; Nagaraja, S.; Leburton, J.-P.; Hood, R. Q.; Martin, R. M. Two-dimensional limit of exchange-correlation energy functional approximations. *Phys. Rev. B* **2000**, *61*, 5202–5211, DOI: doi:[10.1103/PhysRevB.61.5202](https://doi.org/10.1103/PhysRevB.61.5202).
- (327) Pollack, L.; Perdew, J. P. Evaluating density functional performance for the quasi-two-dimensional electron gas. *J. Phys.: Condens. Matter* **2000**, *12*, 1239, DOI: doi:[10.1088/0953-8984/12/7/308](https://doi.org/10.1088/0953-8984/12/7/308).
- (328) Räsänen, E.; Pittalis, S.; Proetto, C. R.; Gross, E. K. U. Electronic exchange in quantum rings: Beyond the local-density approximation. *Phys. Rev. B* **2009**, *79*, 121305, DOI: doi:[10.1103/PhysRevB.79.121305](https://doi.org/10.1103/PhysRevB.79.121305).
- (329) Chiodo, S.; Russo, N.; Sicilia, E. LANL2DZ basis sets recontracted in the framework of density functional theory.

- J. Chem. Phys.* **2006**, *125*, 104107, DOI: doi:10.1063/1.2345197.
- (330) Putaja, A.; Räsänen, E.; van Leeuwen, R.; Vilhena, J. G.; Marques, M. A. L. Kirzhnits gradient expansion in two dimensions. *Phys. Rev. B* **2012**, *85*, 165101, DOI: doi:10.1103/PhysRevB.85.165101.
- (331) Vilhena, J. G.; Räsänen, E.; Marques, M. A. L.; Pittalis, S. Correction to Construction of the B88 Exchange-Energy Functional in Two Dimensions. *J. Chem. Theory Comput.* **2015**, *11*, 5054–5054, DOI: doi:10.1021/acs.jctc.5b00860.
- (332) Haymaker, R. W.; Rau, A. R. P. Supersymmetry in quantum mechanics. *Am. J. Phys.* **1986**, *54*, 928–936, DOI: doi:10.1119/1.14794.
- (333) Javanainen, J.; Eberly, J. H.; Su, Q. Numerical simulations of multiphoton ionization and above-threshold electron spectra. *Phys. Rev. A* **1988**, *38*, 3430–3446, DOI: doi:10.1103/PhysRevA.38.3430.
- (334) Casula, M.; Sorella, S.; Senatore, G. Ground state properties of the one-dimensional Coulomb gas using the lattice regularized diffusion Monte Carlo method. *Phys. Rev. B* **2006**, *74*, 245427, DOI: doi:10.1103/PhysRevB.74.245427.
- (335) Mermin, N. D. Thermal Properties of the Inhomogeneous Electron Gas. *Phys. Rev.* **1965**, *137*, A1441–A1443, DOI: doi:10.1103/PhysRev.137.A1441.
- (336) Greiner, M.; Carrier, P.; Görling, A. Extension of exact-exchange density functional theory of solids to finite temperatures. *Phys. Rev. B* **2010**, *81*, 155119, DOI: doi:10.1103/physrevb.81.155119.
- (337) Pittalis, S.; Proetto, C. R.; Floris, A.; Sanna, A.; Bersier, C.; Burke, K.; Gross, E. K. U. Exact Conditions in Finite-Temperature Density-Functional Theory. *Phys. Rev. Lett.* **2011**, *107*, 163001, DOI: doi:10.1103/PhysRevLett.107.163001.
- (338) Dufty, J. W.; Trickey, S. B. Scaling, bounds, and inequalities for the noninteracting density functionals at finite temperature. *Phys. Rev. B* **2011**, *84*, 125118, DOI: doi:10.1103/physrevb.84.125118.
- (339) Dufty, J. W.; Trickey, S. Finite temperature scaling in density functional theory. *Mol. Phys.* **2015**, *114*, 988–996, DOI: doi:10.1080/00268976.2015.1122844.
- (340) Burke, K.; Smith, J. C.; Grabowski, P. E.; Pribram-Jones, A. Exact conditions on the temperature dependence of density functionals. *Phys. Rev. B* **2016**, *93*, 195132, DOI: doi:10.1103/PhysRevB.93.195132.
- (341) Sharma, S.; Dewhurst, J. K.; Ambrosch-Draxl, C.; Kurth, S.; Helbig, N.; Pittalis, S.; Shallcross, S.; Nordström, L.; Gross, E. K. U. First-Principles Approach to Noncollinear Magnetism: Towards Spin Dynamics. *Phys. Rev. Lett.* **2007**, *98*, 196405, DOI: doi:10.1103/PhysRevLett.98.196405.
- (342) Scalmani, G.; Frisch, M. J. A New Approach to Noncollinear Spin Density Functional Theory beyond the Local Density Approximation. *J. Chem. Theory Comput.* **2012**, *8*, 2193–2196, DOI: doi:10.1021/ct300441z.
- (343) Bulik, I. W.; Scalmani, G.; Frisch, M. J.; Scuseria, G. E. Noncollinear density functional theory having proper invariance and local torque properties. *Phys. Rev. B* **2013**, *87*, 035117, DOI: doi:10.1103/PhysRevB.87.035117.
- (344) Eich, F. G.; Gross, E. K. U. Transverse Spin-Gradient Functional for Noncollinear Spin-Density-Functional Theory. *Phys. Rev. Lett.* **2013**, *111*, 156401, DOI: doi:10.1103/PhysRevLett.111.156401.

- (345) Eich, F. G.; Pittalis, S.; Vignale, G. Transverse and longitudinal gradients of the spin magnetization in spin-density-functional theory. *Phys. Rev. B* **2013**, *88*, 245102, DOI: doi:10.1103/PhysRevB.88.245102.
- (346) Ullrich, C. A. Density-functional theory for systems with noncollinear spin: Orbital-dependent exchange-correlation functionals and their application to the Hubbard dimer. *Phys. Rev. B* **2018**, *98*, 035140, DOI: doi:10.1103/PhysRevB.98.035140.
- (347) Dewhurst, J.; Sanna, A.; Sharma, S. Effect of exchange-correlation spin-torque on spin dynamics. *Eur. Phys. J. B* **2020**, *18*, 25, 218, DOI: doi:doi.org/10.1140/epjb/e2018-90146-1.
- (348) Petrone, A.; Williams-Young, D. B.; Sun, S.; Stetina, T. F.; Li, X. An efficient implementation of two-component relativistic density functional theory with torque-free auxiliary variables. *Eur. Phys. J. B* **2018**, *91*, 1–14, DOI: doi:10.1140/epjb/e2018-90170-1.
- (349) Goings, J. J.; Egidi, F.; Li, X. Current development of noncollinear electronic structure theory. *Int. J. Quantum Chem.* **2018**, *118*, e25398, DOI: doi:10.1002/qua.25398.
- (350) Desmarais, J. K.; Komorovsky, S.; Flament, J.-P.; Erba, A. Spin-orbit coupling from a two-component self-consistent approach. II. Noncollinear density functional theories. *J. Chem. Phys.* **2021**, *154*, 204110, DOI: doi:10.1063/1.5114902.
- (351) Hill, D.; Shotton, J.; Ullrich, C. A. Magnetization dynamics with time-dependent spin-density functional theory: Significance of exchange-correlation torques. *Phys. Rev. B* **2023**, *107*, 115134, DOI: doi:10.1103/PhysRevB.107.115134.
- (352) Pu, Z.; Li, H.; Zhang, N.; Jiang, H.; Gao, Y.; Xiao, Y.; Sun, Q.; Zhang, Y.; Shao, S. Noncollinear density functional theory. *Phys. Rev. Res.* **2023**, *5*, 013036, DOI: doi:10.1103/PhysRevResearch.5.013036.
- (353) Tancogne-Dejean, N.; Rubio, A.; Ullrich, C. A. Constructing semilocal approximations for noncollinear spin density functional theory featuring exchange-correlation torques. *Phys. Rev. B* **2023**, *107*, 165111, DOI: doi:10.1103/PhysRevB.107.165111.
- (354) Tancogne-Dejean, N.; Rubio, A.; Ullrich, C. A. Erratum: Constructing semilocal approximations for noncollinear spin density functional theory featuring exchange-correlation torques [Phys. Rev. B 107, 165111 (2023)]. *Phys. Rev. B* **2024**, *110*, 199902, DOI: doi:10.1103/PhysRevB.110.199902.
- (355) Moore, G. C.; Horton, M. K.; Kaplan, A. D.; Ashour, O. A.; Griffin, S. M.; Persson, K. A. Noncollinear ground states of solids with a source-free exchange correlation functional. *Phys. Rev. B* **2025**, *111*, 094417, DOI: doi:10.1103/PhysRevB.111.094417.
- (356) von Barth, U.; Hedin, L. A local exchange-correlation potential for the spin polarized case. i. *J. Phys. C: Solid State Phys.* **1972**, *5*, 1629, DOI: doi:10.1088/0022-3719/5/13/012.
- (357) Capelle, K.; Vignale, G.; Györffy, B. L. Spin Currents and Spin Dynamics in Time-Dependent Density-Functional Theory. *Phys. Rev. Lett.* **2001**, *87*, 206403, DOI: doi:10.1103/PhysRevLett.87.206403.
- (358) Perdew, J. P.; Savin, A.; Burke, K. Escaping the symmetry dilemma through a pair-density interpretation of spin-density functional theory. *Phys. Rev. A* **1995**, *51*, 4531–4541, DOI: doi:10.1103/PhysRevA.51.4531.

- (359) Vignale, G.; Rasolt, M. Density-functional theory in strong magnetic fields. *Phys. Rev. Lett.* **1987**, *59*, 2360–2363, DOI: doi:[10.1103/PhysRevLett.59.2360](https://doi.org/10.1103/PhysRevLett.59.2360).
- (360) Vignale, G.; Rasolt, M. Density-Functional Theory in Strong Magnetic Fields. *Phys. Rev. Lett.* **1989**, *62*, 115–115, DOI: doi:[10.1103/PhysRevLett.62.115](https://doi.org/10.1103/PhysRevLett.62.115).
- (361) Vignale, G.; Rasolt, M. Current- and spin-density-functional theory for inhomogeneous electronic systems in strong magnetic fields. *Phys. Rev. B* **1988**, *37*, 10685–10696, DOI: doi:[10.1103/PhysRevB.37.10685](https://doi.org/10.1103/PhysRevB.37.10685).
- (362) Vignale, G.; Rasolt, M. Erratum: Current- and spin-density-functional theory for inhomogeneous electronic systems in strong magnetic fields. *Phys. Rev. B* **1989**, *39*, 5475–5475, DOI: doi:[10.1103/PhysRevB.39.5475.2](https://doi.org/10.1103/PhysRevB.39.5475.2).
- (363) Bencheikh, K. Spin-orbit coupling in the spin-current-density-functional theory. *J. Phys. A* **2003**, *36*, 11929, DOI: doi:[10.1088/0305-4470/36/48/002](https://doi.org/10.1088/0305-4470/36/48/002).
- (364) Huebsch, M.-T.; Tran, F.; Marsman, M. Capturing spin-torque effects with a semilocal exchange-correlation functional. *arXiv* **2025**, 2501.04124, DOI: doi:[10.48550/arXiv.2501.04124](https://doi.org/10.48550/arXiv.2501.04124).
- (365) Desmarais, J. K.; Erba, A.; Vignale, G.; Pittalis, S. Meta-Generalized Gradient Approximation Made Magnetic. *Phys. Rev. Lett.* **2025**, *134*, 106402, DOI: doi:[10.1103/PhysRevLett.134.106402](https://doi.org/10.1103/PhysRevLett.134.106402).
- (366) Desmarais, J. K.; Bencheikh, K.; Vignale, G.; Pittalis, S. Physical Spin Torques from Exactly Constrained Exchange-Correlation Torques. *Phys. Rev. Lett.* **2026**, *136*, 016403, DOI: doi:[10.1103/lt1f-8pz2](https://doi.org/10.1103/lt1f-8pz2).
- (367) Stoll, H.; Pavlidou, C.; Preuß, H. On the calculation of correlation energies in the spin-density functional formalism. *Theor. Chim. Acta* **1978**, *49*, 143–149, DOI: doi:[10.1007/BF02399063](https://doi.org/10.1007/BF02399063).
- (368) Stoll, H.; Golka, E.; Preuß, H. Correlation energies in the spin-density functional formalism. *Theor. Chim. Acta* **1980**, *55*, 29–41, DOI: doi:[10.1007/BF00551408](https://doi.org/10.1007/BF00551408).
- (369) Gori-Giorgi, P.; Perdew, J. P. Spin resolution of the electron-gas correlation energy: Positive same spin contributions. *Phys. Rev. B* **2004**, *69*, 041103, DOI: doi:[10.1103/PhysRevB.69.041103](https://doi.org/10.1103/PhysRevB.69.041103).
- (370) Becke, A. D. Density-functional thermochemistry. V. Systematic optimization of exchange-correlation functionals. *J. Chem. Phys.* **1997**, *107*, 8554, DOI: doi:[10.1063/1.475007](https://doi.org/10.1063/1.475007).
- (371) Ceperley, D. M.; Alder, B. J. Ground State of the Electron Gas by a Stochastic Method. *Phys. Rev. Lett.* **1980**, *45*, 566–569, DOI: doi:[10.1103/PhysRevLett.45.566](https://doi.org/10.1103/PhysRevLett.45.566).
- (372) Ortiz, G.; Ballone, P. Correlation energy, structure factor, radial distribution function, and momentum distribution of the spin-polarized uniform electron gas. *Phys. Rev. B* **1994**, *50*, 1391, DOI: doi:[10.1103/PhysRevB.50.1391](https://doi.org/10.1103/PhysRevB.50.1391).
- (373) Ortiz, G.; Ballone, P. Erratum: Correlation energy, structure factor, radial distribution function, and momentum distribution of the spin-polarized uniform electron gas [Phys. Rev. B 50, 1391 (1994)]. *Phys. Rev. B* **1997**, *56*, 9970, DOI: doi:[10.1103/PhysRevB.56.9970](https://doi.org/10.1103/PhysRevB.56.9970).
- (374) Benites, M.; Rosado, A.; Manousakis, E. Accurate electron correlation energy functional: Expansion in the interaction renormalized by the random-phase approximation. *Phys. Rev. B* **2024**, *110*, 195151, DOI: doi:[10.1103/PhysRevB.110.195151](https://doi.org/10.1103/PhysRevB.110.195151).

- (375) Gáspár, R. Über eine Approximation des Hartree-Fock'schen Potentials Durch eine Universelle Potentialfunktion. *Acta Phys. Hung.* **1954**, *3*, 263, DOI: doi:[10.1103/PhysRevA.45.6891](https://doi.org/10.1103/PhysRevA.45.6891).
- (376) Rae, A. I. M. A theory for the interactions between closed shell systems. *Chem. Phys. Lett.* **1973**, *18*, 574–577, DOI: doi:[10.1016/0009-2614\(73\)80469-5](https://doi.org/10.1016/0009-2614(73)80469-5).
- (377) Engel, E.; Keller, S.; Bonetti, A. F.; Müller, H.; Dreizler, R. M. Local and nonlocal relativistic exchange-correlation energy functionals: Comparison to relativistic optimized-potential-model results. *Phys. Rev. A* **1995**, *52*, 2750–2764, DOI: doi:[10.1103/PhysRevA.52.2750](https://doi.org/10.1103/PhysRevA.52.2750).
- (378) Helbig, N.; Fuks, J. I.; Casula, M.; Verstraete, M. J.; Marques, M. A. L.; Tokatly, I. V.; Rubio, A. Density functional theory beyond the linear regime: Validating an adiabatic local density approximation. *Phys. Rev. A* **2011**, *83*, 032503, DOI: doi:[10.1103/PhysRevA.83.032503](https://doi.org/10.1103/PhysRevA.83.032503).
- (379) Finzel, K.; Baranov, A. I. A simple model for the Slater exchange potential and its performance for solids. *Int. J. Quantum Chem.* **2017**, *117*, 40–47, DOI: doi:[10.1002/qua.25312](https://doi.org/10.1002/qua.25312).
- (380) Clementi, E.; Roetti, C. Roothaan–Hartree–Fock atomic wavefunctions: Basis functions and their coefficients for ground and certain excited states of neutral and ionized atoms, $Z \leq 54$. *At. Data Nucl. Data Tables* **1974**, *14*, 177–478, DOI: doi:[10.1016/S0092-640X\(74\)80016-1](https://doi.org/10.1016/S0092-640X(74)80016-1).
- (381) Borlido, P.; Aull, T.; Huran, A. W.; Tran, F.; Marques, M. A. L.; Botti, S. Large-Scale Benchmark of Exchange–Correlation Functionals for the Determination of Electronic Band Gaps of Solids. *J. Chem. Theory Comput.* **2019**, *15*, 5069–5079, DOI: doi:[10.1021/acs.jctc.9b00322](https://doi.org/10.1021/acs.jctc.9b00322).
- (382) Borlido, P.; Schmidt, J.; Huran, A. W.; Tran, F.; Marques, M. A. L.; Botti, S. Exchange-correlation functionals for band gaps of solids: benchmark, reparametrization and machine learning. *npj Comput. Mater.* **2020**, *6*, 96, DOI: doi:[10.1038/s41524-020-00360-0](https://doi.org/10.1038/s41524-020-00360-0).
- (383) Wigner, E. Effects of the electron interaction on the energy levels of electrons in metals. *Trans. Faraday Soc.* **1938**, *34*, 678, DOI: doi:[10.1039/TF9383400678](https://doi.org/10.1039/TF9383400678).
- (384) Wilson, L. C.; Ivanov, S. A new Wigner-like correlation-energy functional from coordinate scaling requirements. *Int. J. Quantum Chem.* **1998**, *69*, 523, DOI: doi:[10.1002/\(SICI\)1097-461X\(1998\)69:4<523::AID-QUA9>3.0.CO;2-X](https://doi.org/10.1002/(SICI)1097-461X(1998)69:4<523::AID-QUA9>3.0.CO;2-X).
- (385) Stewart, P. A.; Gill, P. M. W. Becke–Wigner: a simple but powerful density functional. *J. Chem. Soc., Faraday Trans.* **1995**, *91*, 4337–4341, DOI: doi:[10.1039/FT9959104337](https://doi.org/10.1039/FT9959104337).
- (386) Gáspár, R.; Nagy, A. $X\alpha$ method with theoretically determined parameter α -exchange parameters α and ionisation energies of multiply charged ions. *J. Phys. B: At. Mol. Phys.* **1987**, *20*, 3631, DOI: doi:[10.1088/0022-3700/20/15/012](https://doi.org/10.1088/0022-3700/20/15/012).
- (387) Zope, R. R.; Dunlap, B. I. Slater's Exchange Parameters α for Analytic and Variational $X\alpha$ Calculations. *J. Chem. Theory Comput.* **2005**, *1*, 1193–1200, DOI: doi:[10.1021/ct050166w](https://doi.org/10.1021/ct050166w).
- (388) Carr, W. J.; Maradudin, A. A. Ground-State Energy of a High-Density Electron Gas. *Phys. Rev.* **1964**, *133*, A371–A374, DOI: doi:[10.1103/PhysRev.133.A371](https://doi.org/10.1103/PhysRev.133.A371).
- (389) Gombás, P. Pseudopotentials. *Fortschr. Phys.* **1965**, *13*, 137–156, DOI: doi:[10.1002/prop.19650130402](https://doi.org/10.1002/prop.19650130402).
- (390) Gombás, P. *Pseudopotentials*; Springer-Verlag: New York, 1967.

- (391) Hedin, L.; Lundqvist, B. I. Explicit local exchange-correlation potentials. *J. Phys. C: Solid State Phys.* **1971**, *4*, 2064, DOI: doi:[10.1088/0022-3719/4/14/022](https://doi.org/10.1088/0022-3719/4/14/022).
- (392) Singwi, K. S.; Sjölander, A.; Tosi, M. P.; Land, R. H. Electron Correlations at Metallic Densities. IV. *Phys. Rev. B* **1970**, *1*, 1044–1053, DOI: doi:[10.1103/PhysRevB.1.1044](https://doi.org/10.1103/PhysRevB.1.1044).
- (393) Gordon, R. G.; Kim, Y. S. Theory for the Forces between Closed-Shell Atoms and Molecules. *J. Chem. Phys.* **1972**, *56*, 3122–3133, DOI: doi:[10.1063/1.1677649](https://doi.org/10.1063/1.1677649).
- (394) McWeeny, R. Present Status of the Correlation Problem. The New World of Quantum Chemistry. Boston, 1976; pp 3–31, DOI: doi:[10.1007/978-94-010-1523-3.1](https://doi.org/10.1007/978-94-010-1523-3.1).
- (395) Brual Jr., G.; Rothstein, S. M. Rare gas interactions using an improved statistical method. *J. Chem. Phys.* **1978**, *69*, 1177–1183, DOI: doi:[10.1063/1.436705](https://doi.org/10.1063/1.436705).
- (396) Vosko, S. H.; Wilk, L.; Nusair, M. Accurate spin-dependent electron liquid correlation energies for local spin density calculations: a critical analysis. *Can. J. Phys.* **1980**, *58*, 1200, DOI: doi:[10.1139/p80-159](https://doi.org/10.1139/p80-159).
- (397) Stephens, P. J.; Devlin, F. J.; Chabalowski, C. F.; Frisch, M. J. Ab Initio Calculation of Vibrational Absorption and Circular Dichroism Spectra Using Density Functional Force Fields. *J. Phys. Chem.* **1994**, *98*, 11623, DOI: doi:[10.1021/j100096a001](https://doi.org/10.1021/j100096a001).
- (398) Hertwig, R. H.; Koch, W. On the parameterization of the local correlation functional. What is Becke-3-LYP? *Chem. Phys. Lett.* **1997**, *268*, 345–351, DOI: doi:[10.1016/s0009-2614\(97\)00207-8](https://doi.org/10.1016/s0009-2614(97)00207-8).
- (399) Ceperley, D. Ground state of the fermion one-component plasma: A Monte Carlo study in two and three dimensions. *Phys. Rev. B* **1978**, *18*, 3126–3138, DOI: doi:[10.1103/PhysRevB.18.3126](https://doi.org/10.1103/PhysRevB.18.3126).
- (400) Misawa, S. Ferromagnetism of an Electron Gas. *Phys. Rev.* **1965**, *140*, A1645–A1648, DOI: doi:[10.1103/PhysRev.140.A1645](https://doi.org/10.1103/PhysRev.140.A1645).
- (401) Lehtola, S.; Marques, M. A. L. Many recent density functionals are numerically ill-behaved. *J. Chem. Phys.* **2022**, *157*, 174114, DOI: doi:[10.1063/5.0121187](https://doi.org/10.1063/5.0121187).
- (402) Barbiellini, B.; Jarlborg, T. A simple approach towards non-local potentials: theory and applications. *J. Phys. Condens. Matter* **1989**, *1*, 8865–8876, DOI: doi:[10.1088/0953-8984/1/45/012](https://doi.org/10.1088/0953-8984/1/45/012).
- (403) Perdew, J. P.; Wang, Y. Erratum: Accurate and simple analytic representation of the electron-gas correlation energy [Phys. Rev. B 45, 13244 (1992)]. *Phys. Rev. B* **2018**, *98*, 079904, DOI: doi:[10.1103/physrevb.98.079904](https://doi.org/10.1103/physrevb.98.079904).
- (404) Proynov, E. I.; Salahub, D. R. Simple but efficient correlation functional from a model pair-correlation function. *Phys. Rev. B* **1994**, *49*, 7874, DOI: doi:[10.1103/PhysRevB.49.7874](https://doi.org/10.1103/PhysRevB.49.7874).
- (405) Proynov, E. I.; Salahub, D. R. Erratum: Simple but efficient correlation functional from a model pair-correlation function [Phys. Rev. B 49, 7874 (1994)]. *Phys. Rev. B* **1998**, *57*, 12616–12616, DOI: doi:[10.1103/PhysRevB.57.12616](https://doi.org/10.1103/PhysRevB.57.12616).
- (406) Curtiss, L. A.; Raghavachari, K.; Trucks, G. W.; Pople, J. A. Gaussian-2 theory for molecular energies of first- and second-row compounds. *J. Chem. Phys.* **1991**, *94*, 7221–7230, DOI: doi:[10.1063/1.460205](https://doi.org/10.1063/1.460205).
- (407) Gill, P. M.; Johnson, B. G.; Pople, J. A.; Frisch, M. J. The performance of the Becke-Lee-Yang-Parr (B-LYP) density functional theory with various basis sets. *Chem. Phys. Lett.* **1992**,

- 197, 499–505, DOI: doi:[10.1016/0009-2614\(92\)85807-M](https://doi.org/10.1016/0009-2614(92)85807-M).
- (408) Liu, S.; Parr, R. G. Expansions of the correlation-energy density functional $E_c[\rho]$ and its kinetic-energy component $T_c[\rho]$ in terms of homogeneous functionals. *Phys. Rev. A* **1996**, *53*, 2211–2219, DOI: doi:[10.1103/PhysRevA.53.2211](https://doi.org/10.1103/PhysRevA.53.2211).
- (409) Liu, S.; Parr, R. Homogeneities in density of various LDA energy functionals. *J. Mol. Struct.: THEOCHEM* **2000**, *501–502*, 29–34, DOI: doi:[10.1016/S0166-1280\(99\)00410-8](https://doi.org/10.1016/S0166-1280(99)00410-8).
- (410) Savin, A. Expression of the exact electron-correlation-energy density functional in terms of first-order density matrices. *Phys. Rev. A* **1995**, *52*, R1805–R1807, DOI: doi:[10.1103/PhysRevA.52.R1805](https://doi.org/10.1103/PhysRevA.52.R1805).
- (411) Grabo, T.; Gross, E. Density-functional theory using an optimized exchange-correlation potential. *Chem. Phys. Lett.* **1995**, *240*, 141 – 150, DOI: doi:[10.1016/0009-2614\(95\)00500-4](https://doi.org/10.1016/0009-2614(95)00500-4).
- (412) Morrison, R. C.; Zhao, Q. Solution to the Kohn–Sham equations using reference densities from accurate, correlated wave functions for the neutral atoms helium through argon. *Phys. Rev. A* **1995**, *51*, 1980–1984, DOI: doi:[10.1103/PhysRevA.51.1980](https://doi.org/10.1103/PhysRevA.51.1980).
- (413) Attaccalite, C.; Moroni, S.; Gori-Giorgi, P.; Bachelet, G. B. Correlation Energy and Spin Polarization in the 2D Electron Gas. *Phys. Rev. Lett.* **2002**, *88*, 256601, DOI: doi:[10.1103/PhysRevLett.88.256601](https://doi.org/10.1103/PhysRevLett.88.256601).
- (414) Attaccalite, C.; Moroni, S.; Gori-Giorgi, P.; Bachelet, G. B. Erratum: Correlation Energy and Spin Polarization in the 2D Electron Gas [Phys. Rev. Lett. 88, 256601 (2002)]. *Phys. Rev. Lett.* **2003**, *91*, 109902, DOI: doi:[10.1103/PhysRevLett.91.109902](https://doi.org/10.1103/PhysRevLett.91.109902).
- (415) Rajagopal, A. K.; Kimball, J. C. Correlations in a two-dimensional electron system. *Phys. Rev. B* **1977**, *15*, 2819–2825, DOI: doi:[10.1103/PhysRevB.15.2819](https://doi.org/10.1103/PhysRevB.15.2819).
- (416) Ragot, S.; Cortona, P. Correlation energy of many-electron systems: A modified Colle–Salvetti approach. *J. Chem. Phys.* **2004**, *121*, 7671, DOI: doi:[10.1063/1.1792153](https://doi.org/10.1063/1.1792153).
- (417) Colle, R.; Salvetti, O. Approximate calculation of the correlation energy for the closed shells. *Theor. Chim. Acta* **1975**, *37*, 329, DOI: doi:[10.1007/BF01028401](https://doi.org/10.1007/BF01028401).
- (418) Perdew, J. P.; Wang, Y. Pair-distribution function and its coupling-constant average for the spin-polarized electron gas. *Phys. Rev. B* **1992**, *46*, 12947–12954, DOI: doi:[10.1103/PhysRevB.46.12947](https://doi.org/10.1103/PhysRevB.46.12947).
- (419) Tognetti, V.; Cortona, P.; Adamo, C. A new parameter-free correlation functional based on an average atomic reduced density gradient analysis. *J. Chem. Phys.* **2008**, *128*, 034101, DOI: doi:[10.1063/1.2816137](https://doi.org/10.1063/1.2816137).
- (420) Tognetti, V.; Cortona, P.; Adamo, C. Increasing physical constraints and improving performances in a parameter-free GGA functional. *Chem. Phys. Lett.* **2008**, *460*, 536, DOI: doi:[10.1016/j.cplett.2008.06.032](https://doi.org/10.1016/j.cplett.2008.06.032).
- (421) Pittalis, S.; Räsänen, E.; Marques, M. A. L. Local correlation functional for electrons in two dimensions. *Phys. Rev. B* **2008**, *78*, 195322, DOI: doi:[10.1103/PhysRevB.78.195322](https://doi.org/10.1103/PhysRevB.78.195322).
- (422) Proynov, E.; Kong, J. Analytic form of the correlation energy of the uniform electron gas. *Phys. Rev. A* **2009**, *79*, 014103, DOI: doi:[10.1103/PhysRevA.79.014103](https://doi.org/10.1103/PhysRevA.79.014103).
- (423) Proynov, E.; Kong, J. Erratum: Analytic form of the correlation energy of the uniform electron gas [Phys. Rev. A 79, 014103 (2009)]. *Phys.*

- Rev. A* **2017**, *95*, 059904, DOI: doi:[10.1103/PhysRevA.95.059904](https://doi.org/10.1103/PhysRevA.95.059904).
- (424) Proynov, E. Simple analytic form of the correlation energy of the uniform electron gas. *J. Mol. Struct.: THEOCHEM* **2006**, *762*, 139–145, DOI: doi:[10.1016/j.theochem.2005.07.033](https://doi.org/10.1016/j.theochem.2005.07.033).
- (425) Loos, P.-F. High-density correlation energy expansion of the one-dimensional uniform electron gas. *J. Chem. Phys.* **2013**, *138*, 064108, DOI: doi:[10.1063/1.4790613](https://doi.org/10.1063/1.4790613).
- (426) Loos, P.-F.; Gill, P. M. W. Uniform electron gases. I. Electrons on a ring. *J. Chem. Phys.* **2013**, *138*, 164124, DOI: doi:[10.1063/1.4802589](https://doi.org/10.1063/1.4802589).
- (427) Fogler, M. M. Ground-State Energy of the Electron Liquid in Ultrathin Wires. *Phys. Rev. Lett.* **2005**, *94*, 056405, DOI: doi:[10.1103/PhysRevLett.94.056405](https://doi.org/10.1103/PhysRevLett.94.056405).
- (428) Cioslowski, J. Robust interpolation between weak- and strong-correlation regimes of quantum systems. *J. Chem. Phys.* **2012**, *136*, 044109, DOI: doi:[10.1063/1.3679657](https://doi.org/10.1063/1.3679657).
- (429) Lee, R. M.; Drummond, N. D. Ground-state properties of the one-dimensional electron liquid. *Phys. Rev. B* **2011**, *83*, 245114, DOI: doi:[10.1103/PhysRevB.83.245114](https://doi.org/10.1103/PhysRevB.83.245114).
- (430) Loos, P.-F.; Ball, C. J.; Gill, P. M. W. Uniform electron gases. II. The generalized local density approximation in one dimension. *J. Chem. Phys.* **2014**, *140*, 18A524, DOI: doi:[10.1063/1.4867910](https://doi.org/10.1063/1.4867910).
- (431) Chachiyo, T. Simple and accurate uniform electron gas correlation energy for the full range of densities. *J. Chem. Phys.* **2016**, *145*, 021101, DOI: doi:[10.1063/1.4958669](https://doi.org/10.1063/1.4958669).
- (432) Karasiev, V. V. Comment on “Communication: Simple and accurate uniform electron gas correlation energy for the full range of densities” [J. Chem. Phys. **145**, 021101 (2016)]. *J. Chem. Phys.* **2016**, *145*, 157101, DOI: doi:[10.1063/1.4964758](https://doi.org/10.1063/1.4964758).
- (433) Ruggeri, M.; Ríos, P. L.; Alavi, A. Correlation energies of the high-density spin-polarized electron gas to meV accuracy. *Phys. Rev. B* **2018**, *98*, 161105, DOI: doi:[10.1103/PhysRevB.98.161105](https://doi.org/10.1103/PhysRevB.98.161105).
- (434) Chachiyo, T.; Chachiyo, H. Understanding electron correlation energy through density functional theory. *Comput. Theor. Chem.* **2020**, *1172*, 112669, DOI: doi:[10.1016/j.comptc.2019.112669](https://doi.org/10.1016/j.comptc.2019.112669).
- (435) Xie, Q.-X.; Wu, J.; Zhao, Y. Accurate correlation energy functional for uniform electron gas from an interpolation ansatz without fitting parameters. *Phys. Rev. B* **2021**, *103*, 045130, DOI: doi:[10.1103/PhysRevB.103.045130](https://doi.org/10.1103/PhysRevB.103.045130).
- (436) Azadi, S.; Drummond, N. D.; Vinko, S. M. Correlation energy of the paramagnetic electron gas at the thermodynamic limit. *Phys. Rev. B* **2023**, *107*, 1121105, DOI: doi:[10.1103/physrevb.107.1121105](https://doi.org/10.1103/physrevb.107.1121105).
- (437) Azadi, S.; Drummond, N. D.; Vinko, S. M. Correlation energy of the spin-polarized electron liquid studied using quantum Monte Carlo simulations. *Phys. Rev. B* **2023**, *108*, 115134, DOI: doi:[10.1103/physrevb.108.115134](https://doi.org/10.1103/physrevb.108.115134).
- (438) Lee, C.; Parr, R. G. Exchange-correlation functional for atoms and molecules. *Phys. Rev. A* **1990**, *42*, 193–200, DOI: doi:[10.1103/PhysRevA.42.193](https://doi.org/10.1103/PhysRevA.42.193).
- (439) Fuentealba, P. Exchange-correlation functional from a correlation-factor model. *Phys. Rev. A* **1992**, *45*, 6891–6894, DOI: doi:[10.1103/PhysRevA.45.6891](https://doi.org/10.1103/PhysRevA.45.6891).
- (440) Goedecker, S.; Teter, M.; Hutter, J. Separable dual-space Gaussian pseudopotentials

- tials. *Phys. Rev. B* **1996**, *54*, 1703, DOI: doi:[10.1103/PhysRevB.54.1703](https://doi.org/10.1103/PhysRevB.54.1703).
- (441) Zhao, Q.; Levy, M.; Parr, R. G. Applications of coordinate-scaling procedures to the exchange-correlation energy. *Phys. Rev. A* **1993**, *47*, 918–922, DOI: doi:[10.1103/PhysRevA.47.918](https://doi.org/10.1103/PhysRevA.47.918).
- (442) Zhao, Q.; Morrison, R. C.; Parr, R. G. From electron densities to Kohn–Sham kinetic energies, orbital energies, exchange-correlation potentials, and exchange-correlation energies. *Phys. Rev. A* **1994**, *50*, 2138–2142, DOI: doi:[10.1103/PhysRevA.50.2138](https://doi.org/10.1103/PhysRevA.50.2138).
- (443) Parr, R. G.; Liu, S.; Kugler, A. A.; Nagy, A. Some identities in density-functional theory. *Phys. Rev. A* **1995**, *52*, 969–976, DOI: doi:[10.1103/PhysRevA.52.969](https://doi.org/10.1103/PhysRevA.52.969).
- (444) Tozer, D. J.; Handy, N. C.; Green, W. H. Exchange-correlation functionals from ab initio electron densities. *Chem. Phys. Lett.* **1997**, *273*, 183, DOI: doi:[10.1016/S0009-2614\(97\)00586-1](https://doi.org/10.1016/S0009-2614(97)00586-1).
- (445) Jarlborg, T. Pair correlation functions for exchange and correlation in uniform spin densities. *Phys. Lett. A* **1999**, *260*, 395–399, DOI: doi:[10.1016/s0375-9601\(99\)00528-9](https://doi.org/10.1016/s0375-9601(99)00528-9).
- (446) Karasiev, V. V.; Sjoström, T.; Dufty, J.; Trickey, S. B. Accurate Homogeneous Electron Gas Exchange-Correlation Free Energy for Local Spin-Density Calculations. *Phys. Rev. Lett.* **2014**, *112*, 076403, DOI: doi:[10.1103/PhysRevLett.112.076403](https://doi.org/10.1103/PhysRevLett.112.076403).
- (447) Karasiev, V. V.; Dufty, J. W.; Trickey, S. B. Nonempirical Semilocal Free-Energy Density Functional for Matter under Extreme Conditions. *Phys. Rev. Lett.* **2018**, *120*, 076401, DOI: doi:[10.1103/PhysRevLett.120.076401](https://doi.org/10.1103/PhysRevLett.120.076401).
- (448) Spink, G. G.; Needs, R. J.; Drummond, N. D. Quantum Monte Carlo study of the three-dimensional spin-polarized homogeneous electron gas. *Phys. Rev. B* **2013**, *88*, 085121, DOI: doi:[10.1103/PhysRevB.88.085121](https://doi.org/10.1103/PhysRevB.88.085121).
- (449) Brown, E. W.; Clark, B. K.; DuBois, J. L.; Ceperley, D. M. Path-Integral Monte Carlo Simulation of the Warm Dense Homogeneous Electron Gas. *Phys. Rev. Lett.* **2013**, *110*, 146405, DOI: doi:[10.1103/PhysRevLett.110.146405](https://doi.org/10.1103/PhysRevLett.110.146405).
- (450) Perrot, F.; Dharma-wardana, M. W. C. Spin-polarized electron liquid at arbitrary temperatures: Exchange-correlation energies, electron-distribution functions, and the static response functions. *Phys. Rev. B* **2000**, *62*, 16536–16548, DOI: doi:[10.1103/PhysRevB.62.16536](https://doi.org/10.1103/PhysRevB.62.16536).
- (451) Perrot, F.; Dharma-wardana, M. W. C. Erratum: Spin-polarized electron liquid at arbitrary temperatures: Exchange-correlation energies, electron-distribution functions, and the static response functions [Phys. Rev. B 62, 16 536 (2000)]. *Phys. Rev. B* **2003**, *67*, 079901, DOI: doi:[10.1103/PhysRevB.67.079901](https://doi.org/10.1103/PhysRevB.67.079901).
- (452) Entwistle, M. T.; Hodgson, M. J. P.; Wetherell, J.; Longstaff, B.; Ramsden, J. D.; Godby, R. W. Local density approximations from finite systems. *Phys. Rev. B* **2016**, *94*, 205134, DOI: doi:[10.1103/PhysRevB.94.205134](https://doi.org/10.1103/PhysRevB.94.205134).
- (453) Groth, S.; Dornheim, T.; Sjoström, T.; Malone, F. D.; Foulkes, W. M. C.; Bonitz, M. Ab initio Exchange-Correlation Free Energy of the Uniform Electron Gas at Warm Dense Matter Conditions. *Phys. Rev. Lett.* **2017**, *119*, 135001, DOI: doi:[10.1103/PhysRevLett.119.135001](https://doi.org/10.1103/PhysRevLett.119.135001).
- (454) Herman, F.; Dyke, J. P. V.; Ortenburger, I. B. Improved Statistical Exchange Approximation for Inhomogeneous Many-Electron Systems.

- Phys. Rev. Lett.* **1969**, *22*, 807, DOI: doi:[10.1103/PhysRevLett.22.807](https://doi.org/10.1103/PhysRevLett.22.807).
- (455) Vosko, S. H.; Macdonald, L. D. *Condensed Matter Theories*; Springer US, 1987; pp 101–111, DOI: doi:[10.1007/978-1-4613-0917-8_12](https://doi.org/10.1007/978-1-4613-0917-8_12).
- (456) DePristo, A. E.; Kress, J. D. Rational function representation for accurate exchange energy functionals. *J. Chem. Phys.* **1987**, *86*, 1425, DOI: doi:[10.1063/1.452230](https://doi.org/10.1063/1.452230).
- (457) Lee, H.; Lee, C.; Parr, R. G. Conjoint gradient correction to the Hartree–Fock kinetic- and exchange-energy density functionals. *Phys. Rev. A* **1991**, *44*, 768, DOI: doi:[10.1103/PhysRevA.44.768](https://doi.org/10.1103/PhysRevA.44.768).
- (458) Perdew, J. P. Proceedings of the 75. WE-Heraeus-Seminar and 21st Annual International Symposium on Electronic Structure of Solids. Berlin, 1991; p 11.
- (459) Perdew, J. P.; Chevary, J. A.; Vosko, S. H.; Jackson, K. A.; Pederson, M. R.; Singh, D. J.; Fiolhais, C. Atoms, molecules, solids, and surfaces: Applications of the generalized gradient approximation for exchange and correlation. *Phys. Rev. B* **1992**, *46*, 6671, DOI: doi:[10.1103/PhysRevB.46.6671](https://doi.org/10.1103/PhysRevB.46.6671).
- (460) Perdew, J. P.; Chevary, J. A.; Vosko, S. H.; Jackson, K. A.; Pederson, M. R.; Singh, D. J.; Fiolhais, C. Erratum: Atoms, molecules, solids, and surfaces: Applications of the generalized gradient approximation for exchange and correlation. *Phys. Rev. B* **1993**, *48*, 4978, DOI: doi:[10.1103/PhysRevB.48.4978.2](https://doi.org/10.1103/PhysRevB.48.4978.2).
- (461) Adamo, C.; Barone, V. Exchange functionals with improved long-range behavior and adiabatic connection methods without adjustable parameters: The mPW and mPW1PW models. *J. Chem. Phys.* **1998**, *108*, 664, DOI: doi:[10.1063/1.475428](https://doi.org/10.1063/1.475428).
- (462) Engel, E.; Chevary, J. A.; Macdonald, L. D.; Vosko, S. H. Asymptotic properties of the exchange energy density and the exchange potential of finite systems: relevance for generalized gradient approximations. *Z. Phys. D: At., Mol. Clusters* **1992**, *23*, 7–14, DOI: doi:[10.1007/BF01436696](https://doi.org/10.1007/BF01436696).
- (463) Engel, E.; Vosko, S. H. Exact exchange-only potentials and the virial relation as microscopic criteria for generalized gradient approximations. *Phys. Rev. B* **1993**, *47*, 13164–13174, DOI: doi:[10.1103/PhysRevB.47.13164](https://doi.org/10.1103/PhysRevB.47.13164).
- (464) van Leeuwen, R.; Baerends, E. J. Exchange-correlation potential with correct asymptotic behavior. *Phys. Rev. A* **1994**, *49*, 2421–2431, DOI: doi:[10.1103/PhysRevA.49.2421](https://doi.org/10.1103/PhysRevA.49.2421).
- (465) Krieger, J. B.; Li, Y.; Iafrate, G. J. Construction and application of an accurate local spin-polarized Kohn–Sham potential with integer discontinuity: Exchange-only theory. *Phys. Rev. A* **1992**, *45*, 101–126, DOI: doi:[10.1103/PhysRevA.45.101](https://doi.org/10.1103/PhysRevA.45.101).
- (466) Gaiduk, A. P.; Staroverov, V. N. How to tell when a model Kohn–Sham potential is not a functional derivative. *J. Chem. Phys.* **2009**, *131*, 044107, DOI: doi:[10.1063/1.3176515](https://doi.org/10.1063/1.3176515).
- (467) Karolewski, A.; Armiento, R.; Kümmel, S. Polarizabilities of Polyacetylene from a Field-Counteracting Semilocal Functional. *J. Chem. Theory Comput.* **2009**, *5*, 712–718, DOI: doi:[10.1021/ct8005198](https://doi.org/10.1021/ct8005198).
- (468) Ugalde, J. M.; Sarasola, C.; Aguado, M. Exchange energy from Gaussian-type basis sets. *J. Phys. B: At., Mol. Opt. Phys.* **1994**, *27*, 423–427, DOI: doi:[10.1088/0953-4075/27/3/009](https://doi.org/10.1088/0953-4075/27/3/009).
- (469) Fuentealba, P.; Reyes, O. Further evidence of the conjoint correction to

- the local kinetic and exchange energy density functionals. *Chem. Phys. Lett.* **1995**, *232*, 31, DOI: doi:[10.1016/0009-2614\(94\)01321-L](https://doi.org/10.1016/0009-2614(94)01321-L).
- (470) Ou-Yang, H.; Levy, M. Approximate noninteracting kinetic energy functionals from a nonuniform scaling requirement. *Int. J. Quantum Chem.* **1991**, *40*, 379, DOI: doi:[10.1002/qua.560400309](https://doi.org/10.1002/qua.560400309).
- (471) Lembarki, A.; Rogemond, F.; Chermette, H. Gradient-corrected exchange potential with the correct asymptotic behavior and the corresponding exchange-energy functional obtained from the virial theorem. *Phys. Rev. A* **1995**, *52*, 3704–3710, DOI: doi:[10.1103/PhysRevA.52.3704](https://doi.org/10.1103/PhysRevA.52.3704).
- (472) The exact value is implemented in Libxc.
- (473) Gill, P. M. W. A new gradient-corrected exchange functional. *Mol. Phys.* **1996**, *89*, 433, DOI: doi:[10.1080/002689796173813](https://doi.org/10.1080/002689796173813).
- (474) Filatov, M.; Thiel, W. A new gradient-corrected exchange-correlation density functional. *Mol. Phys.* **1997**, *91*, 847, DOI: doi:[10.1080/002689797170950](https://doi.org/10.1080/002689797170950).
- (475) Perdew, J. P.; Burke, K.; Ernzerhof, M. Perdew, Burke, and Ernzerhof Reply. *Phys. Rev. Lett.* **1998**, *80*, 891–891, DOI: doi:[10.1103/PhysRevLett.80.891](https://doi.org/10.1103/PhysRevLett.80.891).
- (476) Dion, M.; Rydberg, H.; Schröder, E.; Langreth, D. C.; Lundqvist, B. I. Van der Waals Density Functional for General Geometries. *Phys. Rev. Lett.* **2004**, *92*, 246401, DOI: doi:[10.1103/PhysRevLett.92.246401](https://doi.org/10.1103/PhysRevLett.92.246401).
- (477) Dion, M.; Rydberg, H.; Schröder, E.; Langreth, D. C.; Lundqvist, B. I. Erratum: Van der Waals Density Functional for General Geometries [Phys. Rev. Lett. 92, 246401 (2004)]. *Phys. Rev. Lett.* **2005**, *95*, 109902, DOI: doi:[10.1103/PhysRevLett.95.109902](https://doi.org/10.1103/PhysRevLett.95.109902).
- (478) Hamprecht, F. A.; Cohen, A. J.; Tozer, D. J.; Handy, N. C. Development and assessment of new exchange-correlation functionals. *J. Chem. Phys.* **1998**, *109*, 6264, DOI: doi:[10.1063/1.477267](https://doi.org/10.1063/1.477267).
- (479) Hammer, B.; Hansen, L. B.; Nørskov, J. K. Improved adsorption energetics within density-functional theory using revised Perdew–Burke–Ernzerhof functionals. *Phys. Rev. B* **1999**, *59*, 7413, DOI: doi:[10.1103/PhysRevB.59.7413](https://doi.org/10.1103/PhysRevB.59.7413).
- (480) Gilbert, A. T.; Gill, P. M. Decomposition of exchange-correlation energies. *Chem. Phys. Lett.* **1999**, *312*, 511–521, DOI: doi:[10.1016/S0009-2614\(99\)00836-2](https://doi.org/10.1016/S0009-2614(99)00836-2).
- (481) Schipper, P. R. T.; Gritsenko, O. V.; van Gisbergen, S. J. A.; Baerends, E. J. Molecular calculations of excitation energies and (hyper)polarizabilities with a statistical average of orbital model exchange-correlation potentials. *J. Chem. Phys.* **2000**, *112*, 1344, DOI: doi:[10.1063/1.480688](https://doi.org/10.1063/1.480688).
- (482) Proynov, E.; Chermette, H.; Salahub, D. R. New τ -dependent correlation functional combined with a modified Becke exchange. *J. Chem. Phys.* **2000**, *113*, 10013–10027, DOI: doi:[10.1063/1.1321309](https://doi.org/10.1063/1.1321309).
- (483) Adamson, R. D.; Gill, P. M. W.; Pople, J. A. Empirical density functionals. *Chem. Phys. Lett.* **1998**, *284*, 6, DOI: doi:[10.1016/S0009-2614\(97\)01282-7](https://doi.org/10.1016/S0009-2614(97)01282-7).
- (484) Proynov, E. I.; Sirois, S.; Salahub, D. R. Extension of the LAP functional to include parallel spin correlation. *Int. J. Quantum Chem.* **1997**, *64*, 427–446, DOI: doi:[10.1002/\(SICI\)1097-461X\(1997\)64:4<427::AID-QUA5>3.0.CO;2-Y](https://doi.org/10.1002/(SICI)1097-461X(1997)64:4<427::AID-QUA5>3.0.CO;2-Y).
- (485) Vitos, L.; Johansson, B.; Kollár, J.; Skriver, H. L. Exchange energy in

- the local Airy gas approximation. *Phys. Rev. B* **2000**, *62*, 10046, DOI: doi:[10.1103/PhysRevB.62.10046](https://doi.org/10.1103/PhysRevB.62.10046).
- (486) Kohn, W.; Mattsson, A. E. Edge Electron Gas. *Phys. Rev. Lett.* **1998**, *81*, 3487–3490, DOI: doi:[10.1103/PhysRevLett.81.3487](https://doi.org/10.1103/PhysRevLett.81.3487).
- (487) Handy, N. C.; Cohen, A. J. Left-right correlation energy. *Mol. Phys.* **2001**, *99*, 403, DOI: doi:[10.1080/00268970010018431](https://doi.org/10.1080/00268970010018431).
- (488) Adamo, C.; Barone, V. Physically motivated density functionals with improved performances: The modified Perdew–Burke–Ernzerhof model. *J. Chem. Phys.* **2002**, *116*, 5933, DOI: doi:[10.1063/1.1458927](https://doi.org/10.1063/1.1458927).
- (489) Harbola, M. K.; Sen, K. D. Improved Becke88 and PW91 exchange potentials. *J. Phys. B At. Mol. Opt. Phys.* **2002**, *35*, 4711–4718, DOI: doi:[10.1088/0953-4075/35/22/312](https://doi.org/10.1088/0953-4075/35/22/312).
- (490) Keal, T. W.; Tozer, D. J. The exchange-correlation potential in Kohn–Sham nuclear magnetic resonance shielding calculations. *J. Chem. Phys.* **2003**, *119*, 3015, DOI: doi:[10.1063/1.1590634](https://doi.org/10.1063/1.1590634).
- (491) Xu, X.; Goddard, W. A. The extended Perdew–Burke–Ernzerhof functional with improved accuracy for thermodynamic and electronic properties of molecular systems. *J. Chem. Phys.* **2004**, *121*, 4068, DOI: doi:[10.1063/1.1771632](https://doi.org/10.1063/1.1771632).
- (492) Mortensen, J. J.; Kaasbjerg, K.; Frederiksen, S. L.; Nørskov, J. K.; Sethna, J. P.; Jacobsen, K. W. Bayesian Error Estimation in Density-Functional Theory. *Phys. Rev. Lett.* **2005**, *95*, 216401, DOI: doi:[10.1103/PhysRevLett.95.216401](https://doi.org/10.1103/PhysRevLett.95.216401).
- (493) Armiento, R.; Mattsson, A. E. Functional designed to include surface effects in self-consistent density functional theory. *Phys. Rev. B* **2005**, *72*, 085108, DOI: doi:[10.1103/PhysRevB.72.085108](https://doi.org/10.1103/PhysRevB.72.085108).
- (494) Mattsson, A. E.; Armiento, R. Implementing and testing the AM05 spin density functional. *Phys. Rev. B* **2009**, *79*, 155101, DOI: doi:[10.1103/PhysRevB.79.155101](https://doi.org/10.1103/PhysRevB.79.155101).
- (495) Mattsson, A. E.; Armiento, R.; Mattsson, T. R. Comment on “Restoring the Density-Gradient Expansion for Exchange in Solids and Surfaces”. *Phys. Rev. Lett.* **2008**, *101*, 239701, DOI: doi:[10.1103/PhysRevLett.101.239701](https://doi.org/10.1103/PhysRevLett.101.239701).
- (496) Mattsson, A. E.; Armiento, R.; Paier, J.; Kresse, G.; Wills, J. M.; Mattsson, T. R. The AM05 density functional applied to solids. *J. Chem. Phys.* **2008**, *128*, 084714, DOI: doi:[10.1063/1.2835596](https://doi.org/10.1063/1.2835596).
- (497) Wu, Z.; Cohen, R. E. More accurate generalized gradient approximation for solids. *Phys. Rev. B* **2006**, *73*, 235116, DOI: doi:[10.1103/PhysRevB.73.235116](https://doi.org/10.1103/PhysRevB.73.235116).
- (498) Madsen, G. K. H. Functional form of the generalized gradient approximation for exchange: The PBE α functional. *Phys. Rev. B* **2007**, *75*, 195108, DOI: doi:[10.1103/PhysRevB.75.195108](https://doi.org/10.1103/PhysRevB.75.195108).
- (499) Perdew, J. P.; Ruzsinszky, A.; Csonka, G. I.; Vydrov, O. A.; Scuseria, G. E.; Constantin, L. A.; Zhou, X.; Burke, K. Perdew *et al.* Reply:. *Phys. Rev. Lett.* **2008**, *101*, 239702, DOI: doi:[10.1103/PhysRevLett.101.239702](https://doi.org/10.1103/PhysRevLett.101.239702).
- (500) Zhao, Y.; Truhlar, D. G. Construction of a generalized gradient approximation by restoring the density-gradient expansion and enforcing a tight Lieb–Oxford bound. *J. Chem. Phys.* **2008**, *128*, 184109, DOI: doi:[10.1063/1.2912068](https://doi.org/10.1063/1.2912068).
- (501) Zupan, A.; Perdew, J. P.; Burke, K.; Causà, M. Density-gradient analysis for density functional theory: Application to atoms. *Int. J. Quantum Chem.* **1997**, *61*,

- 835–845, DOI: doi:[10.1002/\(SICI\)1097-461X\(1997\)61:5<835::AID-QUA9>3.0.CO;2-X](https://doi.org/10.1002/(SICI)1097-461X(1997)61:5<835::AID-QUA9>3.0.CO;2-X).
- (502) Zupan, A.; Burke, K.; Ernzerhof, M.; Perdew, J. P. Distributions and averages of electron density parameters: Explaining the effects of gradient corrections. *J. Chem. Phys.* **1997**, *106*, 10184–10193, DOI: doi:[10.1063/1.474101](https://doi.org/10.1063/1.474101).
- (503) Pittalis, S.; Räsänen, E.; Vilhena, J. G.; Marques, M. A. L. Density gradients for the exchange energy of electrons in two dimensions. *Phys. Rev. A* **2009**, *79*, 012503, DOI: doi:[10.1103/PhysRevA.79.012503](https://doi.org/10.1103/PhysRevA.79.012503).
- (504) Tognetti, V.; Adamo, C. Optimized GGA Functional for Proton Transfer Reactions. *J. Phys. Chem. A* **2009**, *113*, 14415, DOI: doi:[10.1021/jp903672e](https://doi.org/10.1021/jp903672e).
- (505) Curtiss, L. A.; Raghavachari, K.; Redfern, P. C.; Pople, J. A. Assessment of Gaussian-2 and density functional theories for the computation of enthalpies of formation. *J. Chem. Phys.* **1997**, *106*, 1063–1079, DOI: doi:[10.1063/1.473182](https://doi.org/10.1063/1.473182).
- (506) Murray, E. D.; Lee, K.; Langreth, D. C. Investigation of Exchange Energy Density Functional Accuracy for Interacting Molecules. *J. Chem. Theory Comput.* **2009**, *5*, 2754, DOI: doi:[10.1021/ct900365q](https://doi.org/10.1021/ct900365q).
- (507) Lee, K.; Murray, E. D.; Kong, L.; Lundqvist, B. I.; Langreth, D. C. Higher-accuracy van der Waals density functional. *Phys. Rev. B* **2010**, *82*, 081101, DOI: doi:[10.1103/PhysRevB.82.081101](https://doi.org/10.1103/PhysRevB.82.081101).
- (508) Pedroza, L. S.; da Silva, A. J. R.; Capelle, K. Gradient-dependent density functionals of the Perdew–Burke–Ernzerhof type for atoms, molecules, and solids. *Phys. Rev. B* **2009**, *79*, 201106, DOI: doi:[10.1103/PhysRevB.79.201106](https://doi.org/10.1103/PhysRevB.79.201106).
- (509) Ruzsinszky, A.; Csonka, G. I.; Scuse-ria, G. E. Regularized Gradient Expansion for Atoms, Molecules, and Solids. *J. Chem. Theory Comput.* **2009**, *5*, 763, DOI: doi:[10.1021/ct8005369](https://doi.org/10.1021/ct8005369).
- (510) Constantin, L. A.; Ruzsinszky, A.; Perdew, J. P. Exchange-correlation energy functional based on the Airy-gas reference system. *Phys. Rev. B* **2009**, *80*, 035125, DOI: doi:[10.1103/PhysRevB.80.035125](https://doi.org/10.1103/PhysRevB.80.035125).
- (511) Vela, A.; Medel, V.; Trickey, S. B. Variable Lieb–Oxford bound satisfaction in a generalized gradient exchange-correlation functional. *J. Chem. Phys.* **2009**, *130*, 244103, DOI: doi:[10.1063/1.3152713](https://doi.org/10.1063/1.3152713).
- (512) Swart, M.; Solá, M.; Bickelhaupt, F. M. Switching between OPTX and PBE exchange functionals. *J. Comput. Methods Sci. Eng.* **2009**, *9*, 69, DOI: doi:[10.3233/JCM-2009-0230](https://doi.org/10.3233/JCM-2009-0230).
- (513) Swart, M.; Solá, M.; Bickelhaupt, F. M. A new all-round density functional based on spin states and S_N2 barriers. *J. Chem. Phys.* **2009**, *131*, 094103, DOI: doi:[10.1063/1.3213193](https://doi.org/10.1063/1.3213193).
- (514) Grimme, S. Accurate description of van der Waals complexes by density functional theory including empirical corrections. *J. Comput. Chem.* **2004**, *25*, 1463–1473, DOI: doi:[10.1002/jcc.20078](https://doi.org/10.1002/jcc.20078).
- (515) Grimme, S. Semiempirical GGA-type density functional constructed with a long-range dispersion correction. *J. Comput. Chem.* **2006**, *27*, 1787, DOI: doi:[10.1002/jcc.20495](https://doi.org/10.1002/jcc.20495).
- (516) Schwinger, J. Thomas-Fermi model: The leading correction. *Phys. Rev. A* **1980**, *22*, 1827–1832, DOI: doi:[10.1103/PhysRevA.22.1827](https://doi.org/10.1103/PhysRevA.22.1827).
- (517) Schwinger, J. Thomas-Fermi model: The second correction. *Phys. Rev.*

- A **1981**, *24*, 2353–2361, DOI: doi:[10.1103/PhysRevA.24.2353](https://doi.org/10.1103/PhysRevA.24.2353).
- (518) Odashima, M. M.; Capelle, K.; Trickey, S. B. Tightened Lieb–Oxford Bound for Systems of Fixed Particle Number. *J. Chem. Theory Comput.* **2009**, *5*, 798–807, DOI: doi:[10.1021/ct8005634](https://doi.org/10.1021/ct8005634).
- (519) Cooper, V. R. Van der Waals density functional: An appropriate exchange functional. *Phys. Rev. B* **2010**, *81*, 161104, DOI: doi:[10.1103/PhysRevB.81.161104](https://doi.org/10.1103/PhysRevB.81.161104).
- (520) Thonhauser, T.; Cooper, V. R.; Li, S.; Puzder, A.; Hyldgaard, P.; Langreth, D. C. Van der Waals density functional: Self-consistent potential and the nature of the van der Waals bond. *Phys. Rev. B* **2007**, *76*, 125112, DOI: doi:[10.1103/PhysRevB.76.125112](https://doi.org/10.1103/PhysRevB.76.125112).
- (521) Jurecka, P.; Sponer, J.; Cerny, J.; Hobza, P. Benchmark database of accurate (MP2 and CCSD(T) complete basis set limit) interaction energies of small model complexes, DNA base pairs, and amino acid pairs. *Phys. Chem. Chem. Phys.* **2006**, *8*, 1985–1993, DOI: doi:[10.1039/B600027D](https://doi.org/10.1039/B600027D).
- (522) Klimeš, J.; Bowler, D. R.; Michaelides, A. Chemical accuracy for the van der Waals density functional. *J. Phys.: Condens. Matter* **2010**, *22*, 022201, DOI: doi:[10.1088/0953-8984/22/2/022201](https://doi.org/10.1088/0953-8984/22/2/022201).
- (523) Fabiano, E.; Constantin, L. A.; Della Sala, F. Generalized gradient approximation bridging the rapidly and slowly varying density regimes: A PBE-like functional for hybrid interfaces. *Phys. Rev. B* **2010**, *82*, 113104, DOI: doi:[10.1103/PhysRevB.82.113104](https://doi.org/10.1103/PhysRevB.82.113104).
- (524) Swart, M.; Solá, M.; Bickelhaupt, F. M. Inter- and intramolecular dispersion interactions. *J. Comput. Chem.* **2011**, *32*, 1117–1127, DOI: doi:[10.1002/jcc.21693](https://doi.org/10.1002/jcc.21693).
- (525) Swart, M.; Solá, M.; Bickelhaupt, F. M. Corrigendum: Inter- and intramolecular dispersion interactions. *J. Comput. Chem.* **2013**, *34*, 2401–2402, DOI: doi:[10.1002/jcc.23386](https://doi.org/10.1002/jcc.23386).
- (526) Csonka, G. I.; Ruzsinszky, A.; Perdew, J. P.; Grimme, S. Improved Description of Stereoelectronic Effects in Hydrocarbons Using Semilocal Density Functional Theory. *J. Chem. Theory Comput.* **2008**, *4*, 888–891, DOI: doi:[10.1021/ct800003n](https://doi.org/10.1021/ct800003n).
- (527) Tkatchenko, A.; Scheffler, M. Accurate Molecular Van Der Waals Interactions from Ground-State Electron Density and Free-Atom Reference Data. *Phys. Rev. Lett.* **2009**, *102*, 073005, DOI: doi:[10.1103/PhysRevLett.102.073005](https://doi.org/10.1103/PhysRevLett.102.073005).
- (528) Gaiduk, A. P.; Staroverov, V. N. Construction of integrable model Kohn–Sham potentials by analysis of the structure of functional derivatives. *Phys. Rev. A* **2011**, *83*, 012509, DOI: doi:[10.1103/PhysRevA.83.012509](https://doi.org/10.1103/PhysRevA.83.012509).
- (529) Lee, D.; Constantin, L. A.; Perdew, J. P.; Burke, K. Condition on the Kohn–Sham kinetic energy and modern parametrization of the Thomas–Fermi density. *J. Chem. Phys.* **2009**, *130*, 034107, DOI: doi:[10.1063/1.3059783](https://doi.org/10.1063/1.3059783).
- (530) Haas, P.; Tran, F.; Blaha, P.; Schwarz, K. Construction of an optimal GGA functional for molecules and solids. *Phys. Rev. B* **2011**, *83*, 205117, DOI: doi:[10.1103/PhysRevB.83.205117](https://doi.org/10.1103/PhysRevB.83.205117).
- (531) Peverati, R.; Zhao, Y.; Truhlar, D. G. Generalized Gradient Approximation That Recovers the Second-Order Density-Gradient Expansion with Optimized Across-the-Board Performance. *J. Phys. Chem. Lett.* **2011**, *2*, 1991, DOI: doi:[10.1021/jz200616w](https://doi.org/10.1021/jz200616w).
- (532) Klimeš, J.; Bowler, D. R.; Michaelides, A. Van der Waals density functionals applied to solids.

- Phys. Rev. B* **2011**, *83*, 195131, DOI: doi:[10.1103/PhysRevB.83.195131](https://doi.org/10.1103/PhysRevB.83.195131).
- (533) Brémond, É.; Pilard, D.; Ciofini, I.; Chermette, H.; Adamo, C.; Cortona, P. Generalized gradient exchange functionals based on the gradient-regulated connection: a new member of the TCA family. *Theor. Chem. Acc.* **2012**, *131*, 1184, DOI: doi:[10.1007/s00214-012-1184-0](https://doi.org/10.1007/s00214-012-1184-0).
- (534) Grüning, M.; Gritsenko, O. V.; van Gisbergen, S. J. A.; Baerends, E. J. Shape corrections to exchange-correlation potentials by gradient-regulated seamless connection of model potentials for inner and outer region. *J. Chem. Phys.* **2001**, *114*, 652–660, DOI: doi:[10.1063/1.1327260](https://doi.org/10.1063/1.1327260).
- (535) Vela, A.; Pacheco-Kato, J. C.; Gázquez, J. L.; del Campo, J. M.; Trickey, S. B. Improved constraint satisfaction in a simple generalized gradient approximation exchange functional. *J. Chem. Phys.* **2012**, *136*, 144115, DOI: doi:[10.1063/1.3701132](https://doi.org/10.1063/1.3701132).
- (536) Liu, S.; Parr, R. G. Expansions of density functionals in terms of homogeneous functionals: Justification and nonlocal representation of the kinetic energy, exchange energy, and classical Coulomb repulsion energy for atoms. *Phys. Rev. A* **1997**, *55*, 1792–1798, DOI: doi:[10.1103/PhysRevA.55.1792](https://doi.org/10.1103/PhysRevA.55.1792).
- (537) del Campo, J. M.; Gázquez, J. L.; Trickey, S. B.; Vela, A. Non-empirical improvement of PBE and its hybrid PBE0 for general description of molecular properties. *J. Chem. Phys.* **2012**, *136*, 104108, DOI: doi:[10.1063/1.3691197](https://doi.org/10.1063/1.3691197).
- (538) Chiodo, L.; Constantin, L. A.; Fabiano, E.; Della Sala, F. Nonuniform Scaling Applied to Surface Energies of Transition Metals. *Phys. Rev. Lett.* **2012**, *108*, 126402, DOI: doi:[10.1103/PhysRevLett.108.126402](https://doi.org/10.1103/PhysRevLett.108.126402).
- (539) Constantin, L. A. Dimensional crossover of the exchange-correlation energy at the semilocal level. *Phys. Rev. B* **2008**, *78*, 155106, DOI: doi:[10.1103/PhysRevB.78.155106](https://doi.org/10.1103/PhysRevB.78.155106).
- (540) Pittalis, S.; Räsänen, E.; Proetto, C. R. Becke–Johnson-type exchange potential for two-dimensional systems. *Phys. Rev. B* **2010**, *81*, 115108, DOI: doi:[10.1103/PhysRevB.81.115108](https://doi.org/10.1103/PhysRevB.81.115108).
- (541) Armiento, R.; Kümmel, S. Orbital Localization, Charge Transfer, and Band Gaps in Semilocal Density-Functional Theory. *Phys. Rev. Lett.* **2013**, *111*, 036402, DOI: doi:[10.1103/PhysRevLett.111.036402](https://doi.org/10.1103/PhysRevLett.111.036402).
- (542) Swart, M. A new family of hybrid density functionals. *Chem. Phys. Lett.* **2013**, *580*, 166–171, DOI: doi:[10.1016/j.cplett.2013.06.045](https://doi.org/10.1016/j.cplett.2013.06.045).
- (543) Grimme, S. Density functional theory with London dispersion corrections. *Wiley Interdiscip. Rev. Comput. Mol. Sci.* **2011**, *1*, 211–228, DOI: doi:[10.1002/wcms.30](https://doi.org/10.1002/wcms.30).
- (544) Berland, K.; Hyldgaard, P. Exchange functional that tests the robustness of the plasmon description of the van der Waals density functional. *Phys. Rev. B* **2014**, *89*, 035412, DOI: doi:[10.1103/PhysRevB.89.035412](https://doi.org/10.1103/PhysRevB.89.035412).
- (545) Langreth, D. C.; Vosko, S. In *Density Functional Theory of Many-Fermion Systems*; Löwdin, P.-O., Ed.; Advances in Quantum Chemistry; Academic Press, 1990; Vol. 21; pp 175 – 199, DOI: doi:[10.1016/S0065-3276\(08\)60597-3](https://doi.org/10.1016/S0065-3276(08)60597-3).
- (546) Burke, K.; Cancio, A.; Gould, T.; Pittalis, S. Atomic correlation energies and the generalized gradient approximation. *ArXiv e-prints* **2014**,
- (547) Hamada, I. van der Waals density functional made accurate. *Phys. Rev. B* **2014**, *89*, 121103, DOI: doi:[10.1103/PhysRevB.89.121103](https://doi.org/10.1103/PhysRevB.89.121103).

- (548) Hamada, I. Erratum: van der Waals density functional made accurate [Phys. Rev. B 89, 121103(R) (2014)]. *Phys. Rev. B* **2015**, *91*, 119902, DOI: doi:[10.1103/PhysRevB.91.119902](https://doi.org/10.1103/PhysRevB.91.119902).
- (549) Carmona-Espíndola, J.; Gázquez, J. L.; Vela, A.; Trickey, S. B. Generalized gradient approximation exchange energy functional with correct asymptotic behavior of the corresponding potential. *J. Chem. Phys.* **2015**, *142*, 054105, DOI: doi:[10.1063/1.4906606](https://doi.org/10.1063/1.4906606).
- (550) Yu, H. S.; Zhang, W.; Verma, P.; He, X.; Truhlar, D. G. Nonseparable exchange-correlation functional for molecules, including homogeneous catalysis involving transition metals. *Phys. Chem. Chem. Phys.* **2015**, *17*, 12146–12160, DOI: doi:[10.1039/C5CP01425E](https://doi.org/10.1039/C5CP01425E).
- (551) Sarmiento-Pérez, R.; Botti, S.; Marques, M. A. L. Optimized Exchange and Correlation Semilocal Functional for the Calculation of Energies of Formation. *J. Chem. Theory Comput.* **2015**, *11*, 3844–3850, DOI: doi:[10.1021/acs.jctc.5b00529](https://doi.org/10.1021/acs.jctc.5b00529).
- (552) Stevanović, V.; Lany, S.; Zhang, X.; Zunger, A. Correcting density functional theory for accurate predictions of compound enthalpies of formation: Fitted elemental-phase reference energies. *Phys. Rev. B* **2012**, *85*, 115104, DOI: doi:[10.1103/PhysRevB.85.115104](https://doi.org/10.1103/PhysRevB.85.115104).
- (553) Brémond, E.; Ciofini, I.; Adamo, C. Gradient-regulated connection-based correction for the PBE exchange: the PBEtrans model. *Mol. Phys.* **2016**, *114*, 1059–1065, DOI: doi:[10.1080/00268976.2015.1132788](https://doi.org/10.1080/00268976.2015.1132788).
- (554) Brémond, E. A power series revisit of the PBE exchange density-functional approximation: The PBEpow model. *J. Chem. Phys.* **2016**, *145*, 244102, DOI: doi:[10.1063/1.4972815](https://doi.org/10.1063/1.4972815).
- (555) Constantin, L. A.; Terentjevs, A.; Della Sala, F.; Cortona, P.; Fabiano, E. Semiclassical atom theory applied to solid-state physics. *Phys. Rev. B* **2016**, *93*, 045126, DOI: doi:[10.1103/PhysRevB.93.045126](https://doi.org/10.1103/PhysRevB.93.045126).
- (556) Pacheco-Kato, J. C.; del Campo, J. M.; Gázquez, J. L.; Trickey, S. B.; Vela, A. A PW91-like exchange with a simple analytical form. *Chem. Phys. Lett.* **2016**, *651*, 268–273, DOI: doi:[10.1016/j.cplett.2016.03.028](https://doi.org/10.1016/j.cplett.2016.03.028).
- (557) Karasiev, V. V.; Mihaylov, D. I.; Hu, S. X. Meta-GGA exchange-correlation free energy density functional to increase the accuracy of warm dense matter simulations. *Phys. Rev. B* **2022**, *105*, 1081109, DOI: doi:[10.1103/physrevb.105.1081109](https://doi.org/10.1103/physrevb.105.1081109).
- (558) Carmona-Espíndola, J.; Gázquez, J. L.; Vela, A.; Trickey, S. B. Generalized Gradient Approximation Exchange Energy Functional with Near-Best Semilocal Performance. *J. Chem. Theory Comput.* **2019**, *15*, 303–310, DOI: doi:[10.1021/acs.jctc.8b00998](https://doi.org/10.1021/acs.jctc.8b00998).
- (559) The value in Libxc is implemented with much more accuracy.
- (560) Gráfová, L.; Pitoňák, M.; Řezáč, J.; Hobza, P. Comparative Study of Selected Wave Function and Density Functional Methods for Noncovalent Interaction Energy Calculations Using the Extended S22 Data Set. *J. Chem. Theory Comput.* **2010**, *6*, 2365–2376, DOI: doi:[10.1021/ct1002253](https://doi.org/10.1021/ct1002253).
- (561) Chachiyo, T.; Chachiyo, H. Simple and Accurate Exchange Energy for Density Functional Theory. *Molecules* **2020**, *25*, 3485, DOI: doi:[10.3390/molecules25153485](https://doi.org/10.3390/molecules25153485).
- (562) Albavera-Mata, A.; Botello-Mancilla, K.; Trickey, S. B.; Gázquez, J. L.; Vela, A.

- Generalized gradient approximations with local parameters. *Phys. Rev. B* **2020**, *102*, 035129, DOI: doi:[10.1103/PhysRevB.102.035129](https://doi.org/10.1103/PhysRevB.102.035129).
- (563) Rasolt, M.; Geldart, D. J. W. Exchange and correlation energy in a nonuniform fermion fluid. *Phys. Rev. B* **1986**, *34*, 1325–1328, DOI: doi:[10.1103/PhysRevB.34.1325](https://doi.org/10.1103/PhysRevB.34.1325).
- (564) Cancio, A.; Chen, G. P.; Krull, B. T.; Burke, K. Fitting a round peg into a round hole: Asymptotically correcting the generalized gradient approximation for correlation. *J. Chem. Phys.* **2018**, *149*, 084116, DOI: doi:[10.1063/1.5021597](https://doi.org/10.1063/1.5021597).
- (565) Carmona-Espíndola, J.; Flores, A.; Gázquez, J. L.; Vela, A.; Trickey, S. B. Hardness of molecules and bandgap of solids from a generalized gradient approximation exchange energy functional. *J. Chem. Phys.* **2022**, *157*, 114109, DOI: doi:[10.1063/5.0096678](https://doi.org/10.1063/5.0096678).
- (566) Kovács, P.; Tran, F.; Blaha, P.; Madsen, G. K. H. What is the optimal mGGA exchange functional for solids? *J. Chem. Phys.* **2022**, *157*, 094110, DOI: doi:[10.1063/5.0098787](https://doi.org/10.1063/5.0098787).
- (567) Bhattacharjee, S.; Koshi, N. A.; Lee, S.-C. Customizing PBE exchange-correlation functionals: a comprehensive approach for band gap prediction in diverse semiconductors. *Phys. Chem. Chem. Phys.* **2024**, *26*, 26443–26452, DOI: doi:[10.1039/D4CP03260H](https://doi.org/10.1039/D4CP03260H).
- (568) Langreth, D. C.; Mehl, M. J. Beyond the local-density approximation in calculations of ground-state electronic properties. *Phys. Rev. B* **1983**, *28*, 1809–1834, DOI: doi:[10.1103/PhysRevB.28.1809](https://doi.org/10.1103/PhysRevB.28.1809).
- (569) Langreth, D. C.; Mehl, M. J. Erratum: Beyond the local-density approximation in calculations of ground-state electronic properties. *Phys. Rev. B* **1984**, *29*, 2310, DOI: doi:[10.1103/PhysRevB.29.2310.2](https://doi.org/10.1103/PhysRevB.29.2310.2).
- (570) Hu, C. D.; Langreth, D. C. A Spin Dependent Version of the Langreth–Mehl Exchange-Correlation Functional. *Phys. Scr.* **1985**, *32*, 391, DOI: doi:[10.1088/0031-8949/32/4/024](https://doi.org/10.1088/0031-8949/32/4/024).
- (571) Perdew, J. P. Density-functional approximation for the correlation energy of the inhomogeneous electron gas. *Phys. Rev. B* **1986**, *33*, 8822, DOI: doi:[10.1103/PhysRevB.33.8822](https://doi.org/10.1103/PhysRevB.33.8822).
- (572) Perdew, J. P. Erratum: Density-functional approximation for the correlation energy of the inhomogeneous electron gas. *Phys. Rev. B* **1986**, *34*, 7406–7406, DOI: doi:[10.1103/PhysRevB.34.7406](https://doi.org/10.1103/PhysRevB.34.7406).
- (573) Geldart, D. J. W.; Rasolt, M. Exchange and correlation energy of an inhomogeneous electron gas at metallic densities. *Phys. Rev. B* **1976**, *13*, 1477–1488, DOI: doi:[10.1103/PhysRevB.13.1477](https://doi.org/10.1103/PhysRevB.13.1477).
- (574) Hu, C. D.; Langreth, D. C. Beyond the random-phase approximation in nonlocal-density-functional theory. *Phys. Rev. B* **1986**, *33*, 943–959, DOI: doi:[10.1103/PhysRevB.33.943](https://doi.org/10.1103/PhysRevB.33.943).
- (575) Lee, C.; Yang, W.; Parr, R. G. Development of the Colle–Salvetti correlation-energy formula into a functional of the electron density. *Phys. Rev. B* **1988**, *37*, 785, DOI: doi:[10.1103/PhysRevB.37.785](https://doi.org/10.1103/PhysRevB.37.785).
- (576) Miehlich, B.; Savin, A.; Stoll, H.; Preuss, H. Results obtained with the correlation energy density functionals of Becke and Lee, Yang and Parr. *Chem. Phys. Lett.* **1989**, *157*, 200, DOI: doi:[10.1016/0009-2614\(89\)87234-3](https://doi.org/10.1016/0009-2614(89)87234-3).
- (577) Wilson, L. C.; Levy, M. Nonlocal Wigner-like correlation-energy density functional through coordinate scaling. *Phys. Rev. B* **1990**, *41*, 12930, DOI: doi:[10.1103/PhysRevB.41.12930](https://doi.org/10.1103/PhysRevB.41.12930).

- (578) Fuentealba, P.; Savin, A. A test for the Wilson–Levy correlation energy functional. *Chem. Phys. Lett.* **1994**, *217*, 566 – 570, DOI: doi:[10.1016/0009-2614\(93\)E1422-D](https://doi.org/10.1016/0009-2614(93)E1422-D).
- (579) Burke, K.; Perdew, J. P.; Wang, Y. In *Electronic Density Functional Theory: Recent Progress and New Directions*; Dobson, J. F., Vignale, G., Das, M. P., Eds.; Plenum: NY, 1997; p 81.
- (580) Fuentealba, P. A correlation-energy functional from a correlation-factor model. *Int. J. Quantum Chem.* **1994**, *49*, 549–557, DOI: doi:[10.1002/qua.560490417](https://doi.org/10.1002/qua.560490417).
- (581) Wilson, L. C. Development of non-local Wigner-like correlation-energy density functionals through coordinate scaling requirements and evaluation of constraint obedience in the construction of density functionals. *Chem. Phys.* **1994**, *181*, 337–353, DOI: doi:[10.1016/0301-0104\(93\)E0444-Z](https://doi.org/10.1016/0301-0104(93)E0444-Z).
- (582) Filatov, M.; Thiel, W. A nonlocal correlation energy density functional from a Coulomb hole model. *Int. J. Quantum Chem.* **1997**, *62*, 603, DOI: doi:[10.1002/\(SICI\)1097-461X\(1997\)62:6<603::AID-QUA4>3.0.CO;2-#](https://doi.org/10.1002/(SICI)1097-461X(1997)62:6<603::AID-QUA4>3.0.CO;2-#).
- (583) Gritsenko, O.; Bagaturjants, A.; Kazansky, V. Model universal coulomb hole function for many-electron systems. *Int. J. Quant. Chem.* **1986**, *29*, 1799–1813, DOI: doi:[10.1002/qua.560290612](https://doi.org/10.1002/qua.560290612).
- (584) Gritsenko, O.; Zhidomirov, G. Correlation energy correction as a density functional. A model of the pair distribution function and its application to the first- and second-row atoms and hydrides. *Chem. Phys.* **1987**, *116*, 21 – 32, DOI: doi:[10.1016/0301-0104\(87\)80064-2](https://doi.org/10.1016/0301-0104(87)80064-2).
- (585) Thakkar, A. J.; Smith, V. H. Compact and accurate integral-transform wave functions. I. The $1S1$ state of the helium-like ions from H^- through $Mg1+$. *Phys. Rev. A* **1977**, *15*, 1–15, DOI: doi:[10.1103/PhysRevA.15.1](https://doi.org/10.1103/PhysRevA.15.1).
- (586) Tsuneda, T.; Suzumura, T.; Hirao, K. A new one-parameter progressive Colle–Salvetti-type correlation functional. *J. Chem. Phys.* **1999**, *110*, 10664, DOI: doi:[10.1063/1.479012](https://doi.org/10.1063/1.479012).
- (587) Tsuneda, T.; Suzumura, T.; Hirao, K. A reexamination of exchange energy functionals. *J. Chem. Phys.* **1999**, *111*, 5656–5667, DOI: doi:[10.1063/1.479954](https://doi.org/10.1063/1.479954).
- (588) Yan, Z.; Perdew, J. P.; Kurth, S. Density functional for short-range correlation: Accuracy of the random-phase approximation for isoelectronic energy changes. *Phys. Rev. B* **2000**, *61*, 16430–16439, DOI: doi:[10.1103/PhysRevB.61.16430](https://doi.org/10.1103/PhysRevB.61.16430).
- (589) Yan, Z.; Perdew, J. P.; Kurth, S. Erratum: Density functional for short-range correlation: Accuracy of the random-phase approximation for isoelectronic energy changes [Phys. Rev. B 61, 16430 (2000)]. *Phys. Rev. B* **2010**, *81*, 169902, DOI: doi:[10.1103/PhysRevB.81.169902](https://doi.org/10.1103/PhysRevB.81.169902).
- (590) Cohen, A. J.; Handy, N. C. Dynamic correlation. *Mol. Phys.* **2001**, *99*, 607, DOI: doi:[10.1080/00268970010023435](https://doi.org/10.1080/00268970010023435).
- (591) Handy, N. C.; Cohen, A. J. A dynamical correlation functional. *J. Chem. Phys.* **2002**, *116*, 5411–5418, DOI: doi:[10.1063/1.1457432](https://doi.org/10.1063/1.1457432).
- (592) Proynov, E. I.; Thakkar, A. J. Is combining meta-GGA correlation functionals with the OPTX exchange functional useful? *Int. J. Quantum Chem.* **2006**, *106*, 436–446, DOI: doi:[10.1002/qua.20758](https://doi.org/10.1002/qua.20758).
- (593) Boese, A. D.; Handy, N. C. New exchange-correlation density functionals: The role of the kinetic-energy density. *J. Chem. Phys.* **2002**, *116*, 9559, DOI: doi:[10.1063/1.1476309](https://doi.org/10.1063/1.1476309).

- (594) Perdew, J. P.; Ruzsinszky, A.; Csonka, G. I.; Constantin, L. A.; Sun, J. Workhorse Semilocal Density Functional for Condensed Matter Physics and Quantum Chemistry. *Phys. Rev. Lett.* **2009**, *103*, 026403, DOI: doi:10.1103/PhysRevLett.103.026403.
- (595) Perdew, J. P.; Ruzsinszky, A.; Csonka, G. I.; Constantin, L. A.; Sun, J. Erratum: Workhorse Semilocal Density Functional for Condensed Matter Physics and Quantum Chemistry [Phys. Rev. Lett. 103, 026403 (2009)]. *Phys. Rev. Lett.* **2011**, *106*, 179902, DOI: doi:10.1103/PhysRevLett.106.179902.
- (596) Sun, J.; Xiao, B.; Ruzsinszky, A. Communication: Effect of the orbital-overlap dependence in the meta-generalized gradient approximation. *J. Chem. Phys.* **2012**, *137*, 051101, DOI: doi:10.1063/1.4742312.
- (597) Sun, J.; Haunschild, R.; Xiao, B.; Bulik, I. W.; Scuseria, G. E.; Perdew, J. P. Semilocal and hybrid meta-generalized gradient approximations based on the understanding of the kinetic-energy-density dependence. *J. Chem. Phys.* **2013**, *138*, 044113, DOI: doi:10.1063/1.4789414.
- (598) Sun, J.; Perdew, J. P.; Ruzsinszky, A. Semilocal density functional obeying a strongly tightened bound for exchange. *Proc. Natl. Acad. Sci. U. S. A.* **2015**, *112*, 685–689, DOI: doi:10.1073/pnas.1423145112.
- (599) Thakkar, A. J.; McCarthy, S. P. Toward improved density functionals for the correlation energy. *J. Chem. Phys.* **2009**, *131*, 134109, DOI: doi:10.1063/1.3243845.
- (600) Chakravorty, S. J.; Davidson, E. R. Refinement of the Asymptotic Z Expansion for the Ground-State Correlation Energies of Atomic Ions. *J. Phys. Chem.* **1996**, *100*, 6167–6172, DOI: doi:10.1021/jp952803s.
- (601) Constantin, L. A.; Fabiano, E.; Della Sala, F. Improving atomization energies of molecules and solids with a spin-dependent gradient correction from one-electron density analysis. *Phys. Rev. B* **2011**, *84*, 233103, DOI: doi:10.1103/PhysRevB.84.233103.
- (602) Lynch, B. J.; Truhlar, D. G. Small Representative Benchmarks for Thermochemical Calculations. *J. Phys. Chem. A* **2003**, *107*, 8996–8999, DOI: doi:10.1021/jp035287b.
- (603) Lynch, B. J.; ; Truhlar, D. G. Small Representative Benchmarks for Thermochemical Calculations. *J. Phys. Chem. A* **2004**, *108*, 1460–1460, DOI: doi:10.1021/jp0379190.
- (604) The approximate value is the one implemented in Libxc.
- (605) Constantin, L. A.; Fabiano, E.; Della Sala, F. Semilocal dynamical correlation with increased localization. *Phys. Rev. B* **2012**, *86*, 035130, DOI: doi:10.1103/PhysRevB.86.035130.
- (606) Wood, B.; Hine, N. D. M.; Foulkes, W. M. C.; García-González, P. Quantum Monte Carlo calculations of the surface energy of an electron gas. *Phys. Rev. B* **2007**, *76*, 035403, DOI: doi:10.1103/PhysRevB.76.035403.
- (607) Constantin, L. A.; Chiodo, L.; Fabiano, E.; Bodrenko, I.; Sala, F. D. Correlation energy functional from jellium surface analysis. *Phys. Rev. B* **2011**, *84*, 045126, DOI: doi:10.1103/PhysRevB.84.045126.
- (608) Constantin, L. A.; Fabiano, E.; Della Sala, F. Spin-dependent gradient correction for more accurate atomization energies of molecules. *J. Chem. Phys.* **2012**, *137*, 194105, DOI: doi:10.1063/1.4766324.

- (609) Fabiano, E.; Trevisanutto, P. E.; Terentjevs, A.; Constantin, L. A. Generalized Gradient Approximation Correlation Energy Functionals Based on the Uniform Electron Gas with Gap Model. *J. Chem. Theory Comput.* **2014**, *10*, 2016–2026, DOI: doi:[10.1021/ct500073b](https://doi.org/10.1021/ct500073b).
- (610) Krieger, J. B.; Chen, J.; Iafrate, G. J.; Savin, A. In *Electron Correlations and Materials Properties*; Gonis, A., Kioussis, N., Ciftan, M., Eds.; Springer US: Boston, MA, 1999; pp 463–477, DOI: doi:[10.1007/978-1-4615-4715-0_28](https://doi.org/10.1007/978-1-4615-4715-0_28).
- (611) Rey, J.; Savin, A. Virtual space level shifting and correlation energies. *Int. J. Quantum Chem.* **1998**, *69*, 581–590, DOI: doi:[10.1002/\(SICI\)1097-461X\(1998\)69:4<581::AID-QUA16>3.0.CO;2-2](https://doi.org/10.1002/(SICI)1097-461X(1998)69:4<581::AID-QUA16>3.0.CO;2-2).
- (612) Kurth, S.; Perdew, J. P.; Blaha, P. Molecular and solid-state tests of density functional approximations: LSD, GGAs, and meta-GGAs. *Int. J. Quantum Chem.* **1999**, *75*, 889–909, DOI: doi:[10.1002/\(SICI\)1097-461X\(1999\)75:4/5<889::AID-QUA54>3.0.CO;2-8](https://doi.org/10.1002/(SICI)1097-461X(1999)75:4/5<889::AID-QUA54>3.0.CO;2-8).
- (613) Toulouse, J.; Savin, A.; Adamo, C. Validation and assessment of an accurate approach to the correlation problem in density functional theory: The Kriger–Chen–Iafrate–Savin model. *J. Chem. Phys.* **2002**, *117*, 10465–10473, DOI: doi:[10.1063/1.1521432](https://doi.org/10.1063/1.1521432).
- (614) Fabiano, E.; Constantin, L. A.; Cortona, P.; Della Sala, F. Global Hybrids from the Semiclassical Atom Theory Satisfying the Local Density Linear Response. *J. Chem. Theory Comput.* **2015**, *11*, 122–131, DOI: doi:[10.1021/ct500902p](https://doi.org/10.1021/ct500902p).
- (615) Lynch, B. J.; Truhlar, D. G. Robust and Affordable Multicoefficient Methods for Thermochemistry and Thermochemical Kinetics: The MCCM/3 Suite and SAC/3. *J. Phys. Chem. A* **2003**, *107*, 3898–3906, DOI: doi:[10.1021/jp0221993](https://doi.org/10.1021/jp0221993).
- (616) Patra, B.; Jana, S.; Constantin, L. A.; Samal, P. Relevance of the Pauli kinetic energy density for semilocal functionals. *Phys. Rev. B* **2019**, *100*, 155140, DOI: doi:[10.1103/PhysRevB.100.155140](https://doi.org/10.1103/PhysRevB.100.155140).
- (617) Margraf, J. T.; Kunkel, C.; Reuter, K. Towards density functional approximations from coupled cluster correlation energy densities. *J. Chem. Phys.* **2019**, *150*, 244116, DOI: doi:[10.1063/1.5094788](https://doi.org/10.1063/1.5094788).
- (618) Čížek, J. On the Correlation Problem in Atomic and Molecular Systems. Calculation of Wavefunction Components in Ursell-Type Expansion Using Quantum-Field Theoretical Methods. *J. Chem. Phys.* **1966**, *45*, 4256–4266, DOI: doi:[10.1063/1.1727484](https://doi.org/10.1063/1.1727484).
- (619) Čížek, J. Origins of coupled cluster technique for atoms and molecules. *Theor. Chim. Acta* **1991**, *80*, 91–94, DOI: doi:[10.1007/bf01119616](https://doi.org/10.1007/bf01119616).
- (620) Tozer, D. J.; Handy, N. C. The development of new exchange-correlation functionals. *J. Chem. Phys.* **1998**, *108*, 2545, DOI: doi:[10.1063/1.475638](https://doi.org/10.1063/1.475638).
- (621) Davidson, E. R.; Hagstrom, S. A.; Chakravorty, S. J.; Umar, V. M.; Fischer, C. F. Ground-state correlation energies for two- to ten-electron atomic ions. *Phys. Rev. A* **1991**, *44*, 7071–7083, DOI: doi:[10.1103/PhysRevA.44.7071](https://doi.org/10.1103/PhysRevA.44.7071).
- (622) Pople, J. A.; Head-Gordon, M.; Fox, D. J.; Raghavachari, K.; Curtiss, L. A. Gaussian-1 theory: A general procedure for prediction of molecular energies. *J. Chem. Phys.* **1989**, *90*, 5622–5629, DOI: doi:[10.1063/1.456415](https://doi.org/10.1063/1.456415).
- (623) Tozer, D. J.; Handy, N. C. Development of New Exchange-Correlation Functionals. 2. *J. Phys. Chem. A* **1998**, *102*, 3162, DOI: doi:[10.1021/jp980259s](https://doi.org/10.1021/jp980259s).

- (624) Handy, N. C.; Tozer, D. J. The development of new exchange-correlation functionals: 3. *Mol. Phys.* **1998**, *94*, 707, DOI: doi:[10.1080/002689798167863](https://doi.org/10.1080/002689798167863).
- (625) Curtiss, L. A.; Jones, C.; Trucks, G. W.; Raghavachari, K.; Pople, J. A. Gaussian-3 theory of molecular energies for second-row compounds. *J. Chem. Phys.* **1990**, *93*, 2537–2545, DOI: doi:[10.1063/1.458892](https://doi.org/10.1063/1.458892).
- (626) Boese, A. D.; Doltsinis, N. L.; Handy, N. C.; Sprik, M. New generalized gradient approximation functionals. *J. Chem. Phys.* **2000**, *112*, 1670–1678, DOI: doi:[10.1063/1.480732](https://doi.org/10.1063/1.480732).
- (627) Boese, A. D.; Martin, J. M. L.; Handy, N. C. The role of the basis set: Assessing density functional theory. *J. Chem. Phys.* **2003**, *119*, 3005–3014, DOI: doi:[10.1063/1.1589004](https://doi.org/10.1063/1.1589004).
- (628) Cohen, A. J.; Handy, N. C. Assessment of exchange correlation functionals. *Chem. Phys. Lett.* **2000**, *316*, 160, DOI: doi:[10.1016/S0009-2614\(99\)01273-7](https://doi.org/10.1016/S0009-2614(99)01273-7).
- (629) Boese, A. D.; Handy, N. C. A new parametrization of exchange-correlation generalized gradient approximation functionals. *J. Chem. Phys.* **2001**, *114*, 5497, DOI: doi:[10.1063/1.1347371](https://doi.org/10.1063/1.1347371).
- (630) Curtiss, L. A.; Redfern, P. C.; Raghavachari, K.; Pople, J. A. Assessment of Gaussian-2 and density functional theories for the computation of ionization potentials and electron affinities. *J. Chem. Phys.* **1998**, *109*, 42–55, DOI: doi:[10.1063/1.476538](https://doi.org/10.1063/1.476538).
- (631) Menconi, G.; Wilson, P. J.; Tozer, D. J. Emphasizing the exchange-correlation potential in functional development. *J. Chem. Phys.* **2001**, *114*, 3958, DOI: doi:[10.1063/1.1342776](https://doi.org/10.1063/1.1342776).
- (632) Boese, A. D.; Chandra, A.; Martin, J. M. L.; Marx, D. From ab initio quantum chemistry to molecular dynamics: The delicate case of hydrogen bonding in ammonia. *J. Chem. Phys.* **2003**, *119*, 5965, DOI: doi:[10.1063/1.1599338](https://doi.org/10.1063/1.1599338).
- (633) Xu, X.; Goddard, W. A. The X3LYP extended density functional for accurate descriptions of nonbond interactions, spin states, and thermochemical properties. *Proc. Natl. Acad. Sci. U. S. A.* **2004**, *101*, 2673, DOI: doi:[10.1073/pnas.0308730100](https://doi.org/10.1073/pnas.0308730100).
- (634) Keal, T. W.; Tozer, D. J. A semiempirical generalized gradient approximation exchange-correlation functional. *J. Chem. Phys.* **2004**, *121*, 5654–5660, DOI: doi:[10.1063/1.1784777](https://doi.org/10.1063/1.1784777).
- (635) Dahlke, E. E.; Truhlar, D. G. Improved Density Functionals for Water. *J. Phys. Chem. B* **2005**, *109*, 15677, DOI: doi:[10.1021/jp052436c](https://doi.org/10.1021/jp052436c).
- (636) Díaz, C.; Pijper, E.; Olsen, R. A.; Busnengo, H. F.; Auerbach, D. J.; Kroes, G. J. Chemically Accurate Simulation of a Prototypical Surface Reaction: H₂ Dissociation on Cu(111). *Science* **2009**, *326*, 832–834, DOI: doi:[10.1126/science.1178722](https://doi.org/10.1126/science.1178722).
- (637) Chuang, Y.-Y.; Radhakrishnan, M. L.; Fast, P. L.; Cramer, C. J.; Truhlar, D. G. Direct Dynamics for Free Radical Kinetics in Solution: Solvent Effect on the Rate Constant for the Reaction of Methanol with Atomic Hydrogen. *J. Phys. Chem. A* **1999**, *103*, 4893–4909, DOI: doi:[10.1021/jp990969d](https://doi.org/10.1021/jp990969d).
- (638) Goerigk, L.; Grimme, S. A General Database for Main Group Thermochemistry, Kinetics, and Noncovalent Interactions – Assessment of Common and Reparameterized (meta-)GGA Density Functionals. *J. Chem. Theory Comput.* **2010**, *6*, 107, DOI: doi:[10.1021/ct900489g](https://doi.org/10.1021/ct900489g).
- (639) Korth, M.; Grimme, S. "Mindless" DFT Benchmarking. *J. Chem. The-*

- ory Comput. **2009**, *5*, 993–1003, DOI: doi:10.1021/ct800511q.
- (640) Nattino, F.; Díaz, C.; Jackson, B.; Kroes, G.-J. Effect of Surface Motion on the Rotational Quadrupole Alignment Parameter of D_2 Reacting on Cu(111). *Phys. Rev. Lett.* **2012**, *108*, 236104, DOI: doi:10.1103/PhysRevLett.108.236104.
- (641) Wellendorff, J.; Lundgaard, K. T.; Møgelhøj, A.; Petzold, V.; Landis, D. D.; Nørskov, J. K.; Bligaard, T.; Jacobsen, K. W. Density functionals for surface science: Exchange-correlation model development with Bayesian error estimation. *Phys. Rev. B* **2012**, *85*, 235149, DOI: doi:10.1103/PhysRevB.85.235149.
- (642) Bishop, C. M. *Pattern Recognition and Machine Learning*; Springer: New York, 2006.
- (643) Zheng, J.; Zhao, Y.; Truhlar, D. G. The DBH24/08 Database and Its Use to Assess Electronic Structure Model Chemistries for Chemical Reaction Barrier Heights. *J. Chem. Theory Comput.* **2009**, *5*, 808, DOI: doi:10.1021/ct800568m.
- (644) Verma, P.; Truhlar, D. G. HLE16: A Local Kohn–Sham Gradient Approximation with Good Performance for Semiconductor Band Gaps and Molecular Excitation Energies. *J. Phys. Chem. Lett.* **2017**, *8*, 380–387, DOI: doi:10.1021/acs.jpcclett.6b02757.
- (645) Brandenburg, J. G.; Bannwarth, C.; Hansen, A.; Grimme, S. B97-3c: A revised low-cost variant of the B97-D density functional method. *J. Chem. Phys.* **2018**, *148*, 064104, DOI: doi:10.1063/1.5012601.
- (646) Grimme, S.; Antony, J.; Ehrlich, S.; Krieg, H. A consistent and accurate ab initio parametrization of density functional dispersion correction (DFT-D) for the 94 elements H–Pu. *J. Chem. Phys.* **2010**, *132*, 154104, DOI: doi:10.1063/1.3382344.
- (647) Sure, R.; Grimme, S. Corrected small basis set Hartree–Fock method for large systems. *J. Comput. Chem.* **2013**, *34*, 1672–1685, DOI: doi:10.1002/jcc.23317.
- (648) Rehman, A. U.; Szalewicz, K. Dispersionless Nonhybrid Density Functional. *J. Chem. Theory Comput.* **2025**, *21*, 1098–1118, DOI: doi:10.1021/acs.jctc.4c00941.
- (649) Jedwabny, W.; Dyguda-Kazimierowicz, E.; Pernal, K.; Szalewicz, K.; Patkowski, K. Extension of an Atom-Atom Dispersion Function to Halogen Bonds and Its Use for Rational Design of Drugs and Biocatalysts. *J. Phys. Chem. A* **2021**, *125*, 1787–1799, DOI: doi:10.1021/acs.jpca.0c11347.
- (650) Lehtola, S.; Marques, M. A. L. Meta-Local Density Functionals: A New Rung on Jacob’s Ladder. *J. Chem. Theory Comput.* **2021**, *17*, 943–948, DOI: doi:10.1021/acs.jctc.0c01147.
- (651) Ernzerhof, M.; Scuseria, G. E. Kinetic energy density dependent approximations to the exchange energy. *J. Chem. Phys.* **1999**, *111*, 911, DOI: doi:10.1063/1.479374.
- (652) Negele, J. W.; Vautherin, D. Density-Matrix Expansion for an Effective Nuclear Hamiltonian. *Phys. Rev. C* **1972**, *5*, 1472–1493, DOI: doi:10.1103/PhysRevC.5.1472.
- (653) Koehl, R. M.; Odom, G. K.; Scuseria, G. E. The use of density matrix expansions for calculating molecular exchange energies. *Mol. Phys.* **1996**, *87*, 835–843, DOI: doi:10.1080/00268979600100561.
- (654) Campi, X.; Bouyssy, A. A simple approximation for the nuclear density matrix. *Phys. Lett. B* **1978**, *73*, 263–266, DOI: doi:10.1016/0370-2693(78)90509-9.

- (655) Ghosh, S. K.; Parr, R. G. Phase-space approach to the exchange-energy functional of density-functional theory. *Phys. Rev. A* **1986**, *34*, 785–791, DOI: doi:[10.1103/PhysRevA.34.785](https://doi.org/10.1103/PhysRevA.34.785).
- (656) Manby, F. R.; Knowles, P. J. An exchange functional for accurate virtual orbital energies. *J. Chem. Phys.* **2000**, *112*, 7002, DOI: doi:[10.1063/1.481298](https://doi.org/10.1063/1.481298).
- (657) Ghosh, S. K.; Berkowitz, M.; Parr, R. G. Transcription of ground-state density-functional theory into a local thermodynamics. *Proc. Natl. Acad. Sci. U. S. A.* **1984**, *81*, 8028–8031, DOI: doi:[10.1073/pnas.81.24.8028](https://doi.org/10.1073/pnas.81.24.8028).
- (658) Becke, A. D.; Roussel, M. R. Exchange holes in inhomogeneous systems: A coordinate-space model. *Phys. Rev. A* **1989**, *39*, 3761, DOI: doi:[10.1103/PhysRevA.39.3761](https://doi.org/10.1103/PhysRevA.39.3761).
- (659) Neumann, R.; Handy, N. C. Investigations using the Becke–Roussel exchange functional. *Chem. Phys. Lett.* **1995**, *246*, 381–386, DOI: doi:[10.1016/0009-2614\(95\)01143-2](https://doi.org/10.1016/0009-2614(95)01143-2).
- (660) Becke, A. D.; Johnson, E. R. A simple effective potential for exchange. *J. Chem. Phys.* **2006**, *124*, 221101, DOI: doi:[10.1063/1.2213970](https://doi.org/10.1063/1.2213970).
- (661) Tran, F.; Blaha, P.; Schwarz, K. How Close Are the Slater and Becke-Roussel Potentials in Solids? *J. Chem. Theory Comput.* **2015**, *11*, 4717–4726, DOI: doi:[10.1021/acs.jctc.5b00675](https://doi.org/10.1021/acs.jctc.5b00675).
- (662) Johnson, E. R.; Wolkow, R. A.; DiLabio, G. A. Application of 25 density functionals to dispersion-bound homomolecular dimers. *Chem. Phys. Lett.* **2004**, *394*, 334 – 338, DOI: doi:[10.1016/j.cplett.2004.07.029](https://doi.org/10.1016/j.cplett.2004.07.029).
- (663) Tsuneda, T.; Hirao, K. Parameter-free exchange functional. *Phys. Rev. B* **2000**, *62*, 15527–15531, DOI: doi:[10.1103/PhysRevB.62.15527](https://doi.org/10.1103/PhysRevB.62.15527).
- (664) Tao, J. Exchange energy density of an atom as a functional of the electron density. *J. Chem. Phys.* **2001**, *115*, 3519–3530, DOI: doi:[10.1063/1.1388047](https://doi.org/10.1063/1.1388047).
- (665) Adamo, C.; Ernzerhof, M.; Scuseria, G. E. The meta-GGA functional: Thermochemistry with a kinetic energy density dependent exchange-correlation functional. *J. Chem. Phys.* **2000**, *112*, 2643–2649, DOI: doi:[10.1063/1.480838](https://doi.org/10.1063/1.480838).
- (666) Rabuck, D. A.; Scuseria, E. G. Performance of recently developed kinetic energy density functionals for the calculation of hydrogen binding strengths and hydrogen-bonded structures. *Theor. Chem. Acc.* **2000**, *104*, 439–444, DOI: doi:[10.1007/s002140000163](https://doi.org/10.1007/s002140000163).
- (667) Becke, A. D.; Edgecombe, K. E. A simple measure of electron localization in atomic and molecular systems. *J. Chem. Phys.* **1990**, *92*, 5397–5403, DOI: doi:[10.1063/1.458517](https://doi.org/10.1063/1.458517).
- (668) Savin, A.; Nesper, R.; Wengert, S.; Fässler, T. F. ELF: The Electron Localization Function. *Angew. Chem., Int. Ed. Engl.* **1997**, *36*, 1808–1832, DOI: doi:[10.1002/anie.199718081](https://doi.org/10.1002/anie.199718081).
- (669) Aschebrock, T.; Armiento, R.; Kümmel, S. Orbital nodal surfaces: Topological challenges for density functionals. *Phys. Rev. B* **2017**, *95*, 245118, DOI: doi:[10.1103/PhysRevB.95.245118](https://doi.org/10.1103/PhysRevB.95.245118).
- (670) Zhao, Y.; Truhlar, D. G. A new local density functional for main-group thermochemistry, transition metal bonding, thermochemical kinetics, and noncovalent interactions. *J. Chem. Phys.* **2006**, *125*, 194101, DOI: doi:[10.1063/1.2370993](https://doi.org/10.1063/1.2370993).
- (671) Zhao, Y.; Schultz, N. E.; Truhlar, D. G. Exchange-correlation functional with broad accuracy for metallic and nonmetallic compounds, kinetics, and noncovalent interactions. *J.*

- Chem. Phys.* **2005**, *123*, 161103, DOI: doi:[10.1063/1.2126975](https://doi.org/10.1063/1.2126975).
- (672) Wang, Y.; Jin, X.; Yu, H. S.; Truhlar, D. G.; He, X. Revised M06-L functional for improved accuracy on chemical reaction barrier heights, non-covalent interactions, and solid-state physics. *Proc. Natl. Acad. Sci. U. S. A.* **2017**, *114*, 8487–8492, DOI: doi:[10.1073/pnas.1705670114](https://doi.org/10.1073/pnas.1705670114).
- (673) Lehtola, S. Atomic Electronic Structure Calculations with Hermite Interpolating Polynomials. *J. Phys. Chem. A* **2023**, *127*, 4180–4193, DOI: doi:[10.1021/acs.jpca.3c00729](https://doi.org/10.1021/acs.jpca.3c00729).
- (674) Perdew, J. P.; Ruzsinszky, A.; Tao, J.; Csonka, G. I.; Scuseria, G. E. One-parameter optimization of a nonempirical meta-generalized-gradient-approximation for the exchange-correlation energy. *Phys. Rev. A* **2007**, *76*, 042506, DOI: doi:[10.1103/PhysRevA.76.042506](https://doi.org/10.1103/PhysRevA.76.042506).
- (675) Pittalis, S.; Räsänen, E.; Helbig, N.; Gross, E. K. U. Exchange-energy functionals for finite two-dimensional systems. *Phys. Rev. B* **2007**, *76*, 235314, DOI: doi:[10.1103/PhysRevB.76.235314](https://doi.org/10.1103/PhysRevB.76.235314).
- (676) Krieger, J. B.; Li, Y.; Iafrate, G. J. Derivation and application of an accurate Kohn–Sham potential with integer discontinuity. *Phys. Lett. A* **1990**, *146*, 256–260, DOI: doi:[10.1016/0375-9601\(90\)90975-T](https://doi.org/10.1016/0375-9601(90)90975-T).
- (677) Krieger, J.; Li, Y.; Iafrate, G. Systematic approximations to the optimized effective potential: Application to orbital-density-functional theory. *Phys. Rev. A* **1992**, *46*, 5453–5458, DOI: doi:[10.1103/PhysRevA.46.5453](https://doi.org/10.1103/PhysRevA.46.5453).
- (678) Proynov, E.; Gan, Z.; Kong, J. Analytical representation of the Becke–Roussel exchange functional. *Chem. Phys. Lett.* **2008**, *455*, 103–109, DOI: doi:[10.1016/j.cplett.2008.02.039](https://doi.org/10.1016/j.cplett.2008.02.039).
- (679) Ruzsinszky, A.; Sun, J.; Xiao, B.; Csonka, G. I. A meta-GGA Made Free of the Order of Limits Anomaly. *J. Chem. Theory Comput.* **2012**, *8*, 2078–2087, DOI: doi:[10.1021/ct300269u](https://doi.org/10.1021/ct300269u).
- (680) Tran, F.; Blaha, P. Accurate Band Gaps of Semiconductors and Insulators with a Semilocal Exchange–Correlation Potential. *Phys. Rev. Lett.* **2009**, *102*, 226401, DOI: doi:[10.1103/PhysRevLett.102.226401](https://doi.org/10.1103/PhysRevLett.102.226401).
- (681) Tran, F.; Blaha, P.; Schwarz, K. Band gap calculations with Becke–Johnson exchange potential. *J. Phys.: Condens. Matter* **2007**, *19*, 196208, DOI: doi:[10.1088/0953-8984/19/19/196208](https://doi.org/10.1088/0953-8984/19/19/196208).
- (682) Tran, F.; Doumont, J.; Kalantari, L.; Huran, A. W.; Marques, M. A. L.; Blaha, P. Semilocal exchange–correlation potentials for solid-state calculations: Current status and future directions. *J. Appl. Phys.* **2019**, *126*, 110902, DOI: doi:[10.1063/1.5118863](https://doi.org/10.1063/1.5118863).
- (683) Räsänen, E.; Pittalis, S.; Proetto, C. R. Universal correction for the Becke–Johnson exchange potential. *J. Chem. Phys.* **2010**, *132*, 044112, DOI: doi:[10.1063/1.3300063](https://doi.org/10.1063/1.3300063).
- (684) Oliveira, M. J. T.; Räsänen, E.; Pittalis, S.; Marques, M. A. L. Toward an All-Around Semilocal Potential for Electronic Exchange. *J. Chem. Theory Comput.* **2010**, *6*, 3664–3670, DOI: doi:[10.1021/ct100448x](https://doi.org/10.1021/ct100448x).
- (685) Peverati, R.; Truhlar, D. G. M11-L: A Local Density Functional That Provides Improved Accuracy for Electronic Structure Calculations in Chemistry and Physics. *J. Phys. Chem. Lett.* **2012**, *3*, 117, DOI: doi:[10.1021/jz201525m](https://doi.org/10.1021/jz201525m).
- (686) Peverati, R.; Truhlar, D. G. An improved and broadly accurate local approximation to the exchange–correlation

- density functional: The MN12-L functional for electronic structure calculations in chemistry and physics. *Phys. Chem. Chem. Phys.* **2012**, *14*, 13171, DOI: doi:[10.1039/C2CP42025B](https://doi.org/10.1039/C2CP42025B).
- (687) Koller, D.; Tran, F.; Blaha, P. Improving the modified Becke–Johnson exchange potential. *Phys. Rev. B* **2012**, *85*, 155109, DOI: doi:[10.1103/PhysRevB.85.155109](https://doi.org/10.1103/PhysRevB.85.155109).
- (688) del Campo, J. M.; Gázquez, J. L.; Trickey, S. B.; Vela, A. A new meta-GGA exchange functional based on an improved constraint-based GGA. *Chem. Phys. Lett.* **2012**, *543*, 179–183, DOI: doi:[10.1016/j.cplett.2012.06.025](https://doi.org/10.1016/j.cplett.2012.06.025).
- (689) Staroverov, V. N.; Scuseria, G. E.; Perdew, J. P.; Tao, J.; Davidson, E. R. Energies of isoelectronic atomic ions from a successful metageneralized gradient approximation and other density functionals. *Phys. Rev. A* **2004**, *70*, 012502, DOI: doi:[10.1103/PhysRevA.70.012502](https://doi.org/10.1103/PhysRevA.70.012502).
- (690) Haunschild, R.; Klopper, W. Theoretical reference values for the AE6 and BH6 test sets from explicitly correlated coupled-cluster theory. *Theor. Chem. Acc.* **2012**, *131*, 1–7, DOI: doi:[10.1007/s00214-012-1112-3](https://doi.org/10.1007/s00214-012-1112-3).
- (691) Zhao, Y.; Lynch, B. J.; Truhlar, D. G. Development and Assessment of a New Hybrid Density Functional Model for Thermochemical Kinetics. *J. Phys. Chem. A* **2004**, *108*, 2715, DOI: doi:[10.1021/jp049908s](https://doi.org/10.1021/jp049908s).
- (692) Constantin, L. A.; Fabiano, E.; Della Sala, F. Meta-GGA Exchange-Correlation Functional with a Balanced Treatment of Nonlocality. *J. Chem. Theory Comput.* **2013**, *9*, 2256, DOI: doi:[10.1021/ct400148r](https://doi.org/10.1021/ct400148r).
- (693) Constantin, L. A.; Pitarke, J. M.; Dobson, J. F.; Garcia-Lekue, A.; Perdew, J. P. High-Level Correlated Approach to the Jellium Surface Energy, without Uniform-Gas Input. *Phys. Rev. Lett.* **2008**, *100*, 036401, DOI: doi:[10.1103/PhysRevLett.100.036401](https://doi.org/10.1103/PhysRevLett.100.036401).
- (694) Wellendorff, J.; Lundgaard, K. T.; Jacobsen, K. W.; Bligaard, T. mBEEF: An accurate semi-local Bayesian error estimation density functional. *J. Chem. Phys.* **2014**, *140*, 144107, DOI: doi:[10.1063/1.4870397](https://doi.org/10.1063/1.4870397).
- (695) Curtiss, L. A.; Raghavachari, K.; Redfern, P. C.; Pople, J. A. Assessment of Gaussian-3 and density functional theories for a larger experimental test set. *J. Chem. Phys.* **2000**, *112*, 7374–7383, DOI: doi:[10.1063/1.481336](https://doi.org/10.1063/1.481336).
- (696) Hao, P.; Fang, Y.; Sun, J.; Csonka, G. I.; Philipsen, P. H. T.; Perdew, J. P. Lattice constants from semilocal density functionals with zero-point phonon correction. *Phys. Rev. B* **2012**, *85*, 014111, DOI: doi:[10.1103/PhysRevB.85.014111](https://doi.org/10.1103/PhysRevB.85.014111).
- (697) Jishi, R. A.; Ta, O. B.; Sharif, A. A. Modeling of Lead Halide Perovskites for Photovoltaic Applications. *J. Phys. Chem. C* **2014**, *118*, 28344–28349, DOI: doi:[10.1021/jp5050145](https://doi.org/10.1021/jp5050145).
- (698) Perdew, J. P.; Ruzsinszky, A.; Sun, J.; Burke, K. Gedanken densities and exact constraints in density functional theory. *J. Chem. Phys.* **2014**, *140*, 18A533, DOI: doi:[10.1063/1.4870763](https://doi.org/10.1063/1.4870763).
- (699) Konrad Patkowski, C.-M. F., Garold Murdachaew; Szalewicz, K. Accurate ab initio potential for argon dimer including highly repulsive region. *Mol. Phys.* **2005**, *103*, 2031–2045, DOI: doi:[10.1080/00268970500130241](https://doi.org/10.1080/00268970500130241).
- (700) Almeida, L. M.; Perdew, J. P.; Fiolhais, C. Surface and curvature energies from jellium spheres: Density functional hierarchy and quantum Monte Carlo. *Phys. Rev. B* **2002**, *66*, 075115, DOI: doi:[10.1103/PhysRevB.66.075115](https://doi.org/10.1103/PhysRevB.66.075115).

- (701) de Silva, P.; Corminboeuf, C. Communication: A new class of non-empirical explicit density functionals on the third rung of Jacob’s ladder. *J. Chem. Phys.* **2015**, *143*, 111105, DOI: doi:10.1063/1.4931628.
- (702) Yu, H. S.; He, X.; Truhlar, D. G. MN15-L: A New Local Exchange-Correlation Functional for Kohn–Sham Density Functional Theory with Broad Accuracy for Atoms, Molecules, and Solids. *J. Chem. Theory Comput.* **2016**, *12*, 1280–1293, DOI: doi:10.1021/acs.jctc.5b01082.
- (703) Tao, J.; Mo, Y. Accurate Semilocal Density Functional for Condensed-Matter Physics and Quantum Chemistry. *Phys. Rev. Lett.* **2016**, *117*, 073001, DOI: doi:10.1103/PhysRevLett.117.073001.
- (704) Constantin, L. A.; Fabiano, E.; Pitarke, J. M.; Della Sala, F. Semilocal density functional theory with correct surface asymptotics. *Phys. Rev. B* **2016**, *93*, 115127, DOI: doi:10.1103/PhysRevB.93.115127.
- (705) Lewin, M.; Lieb, E. H. Improved Lieb-Oxford exchange-correlation inequality with a gradient correction. *Phys. Rev. A* **2015**, *91*, 022507, DOI: doi:10.1103/PhysRevA.91.022507.
- (706) Feinblum, D. V.; Kenison, J.; Burke, K. Communication: Testing and using the Lewin-Lieb bounds in density functional theory. *J. Chem. Phys.* **2014**, *141*, 241105, DOI: doi:10.1063/1.4904448.
- (707) Lundgaard, K. T.; Wellendorff, J.; Voss, J.; Jacobsen, K. W.; Bligaard, T. mBEEF-vdW: Robust fitting of error estimation density functionals. *Phys. Rev. B* **2016**, *93*, 235162, DOI: doi:10.1103/PhysRevB.93.235162.
- (708) Loos, P.-F. Exchange functionals based on finite uniform electron gases. *J. Chem. Phys.* **2017**, *146*, 114108, DOI: doi:10.1063/1.4978409.
- (709) Jana, S.; Samal, P. Semilocal Exchange Energy Functional for Two-Dimensional Quantum Systems: A Step Beyond Generalized Gradient Approximations. *J. Phys. Chem. A* **2017**, *121*, 4804–4811, DOI: doi:10.1021/acs.jpca.7b03686.
- (710) Mejía-Rodríguez, D.; Trickey, S. B. Deorbitalization strategies for meta-generalized-gradient-approximation exchange-correlation functionals. *Phys. Rev. A* **2017**, *96*, 052512, DOI: doi:10.1103/PhysRevA.96.052512.
- (711) Mejía-Rodríguez, D.; Trickey, S. B. Erratum: Deorbitalization strategies for meta-generalized-gradient-approximation exchange-correlation functionals [Phys. Rev. A 96, 052512 (2017)]. *Phys. Rev. A* **2025**, *111*, 029901, DOI: doi:10.1103/PhysRevA.111.029901.
- (712) Mejía-Rodríguez, D.; Trickey, S. B. Deorbitalized meta-GGA exchange-correlation functionals in solids. *Phys. Rev. B* **2018**, *98*, 115161, DOI: doi:10.1103/PhysRevB.98.115161.
- (713) Perdew, J. P.; Constantin, L. A. Laplacian-level density functionals for the kinetic energy density and exchange-correlation energy. *Phys. Rev. B* **2007**, *75*, 155109, DOI: doi:10.1103/PhysRevB.75.155109.
- (714) Cancio, A. C.; Redd, J. J. Visualisation and orbital-free parametrisation of the large- Z scaling of the kinetic energy density of atoms. *Mol. Phys.* **2017**, *115*, 618–635, DOI: doi:10.1080/00268976.2016.1246757.
- (715) Francisco, H.; Cancio, A. C.; Trickey, S. B. Removing Orbital-Dependence to Improve Exchange-Correlation Functional Accuracy. *J. Phys. Chem. A* **2025**, *129*, 10240–10250, DOI: doi:10.1021/acs.jpca.5c04829.
- (716) Bienvenu, A. V.; Knizia, G. Efficient Treatment of Local Meta-generalized

- Gradient Density Functionals via Auxiliary Density Expansion: The Density Fitting J + X Approximation. *J. Chem. Theory Comput.* **2018**, *14*, 1297–1303, DOI: doi:[10.1021/acs.jctc.7b01083](https://doi.org/10.1021/acs.jctc.7b01083).
- (717) Garza, A. J.; Bell, A. T.; Head-Gordon, M. Nonempirical Meta-Generalized Gradient Approximations for Modeling Chemisorption at Metal Surfaces. *J. Chem. Theory Comput.* **2018**, *14*, 3083–3090, DOI: doi:[10.1021/acs.jctc.8b00288](https://doi.org/10.1021/acs.jctc.8b00288).
- (718) Mezei, P. D.; Csonka, G. I.; Kállay, M. Simple Modifications of the SCAN Meta-Generalized Gradient Approximation Functional. *J. Chem. Theory Comput.* **2018**, *14*, 2469–2479, DOI: doi:[10.1021/acs.jctc.8b00072](https://doi.org/10.1021/acs.jctc.8b00072).
- (719) Furness, J. W.; Sun, J. Enhancing the efficiency of density functionals with an improved iso-orbital indicator. *Phys. Rev. B* **2019**, *99*, 041119, DOI: doi:[10.1103/PhysRevB.99.041119](https://doi.org/10.1103/PhysRevB.99.041119).
- (720) Traoré, B.; Boudier, G.; Lafargue-Dit-Hauret, W.; Rocquefelte, X.; Katan, C.; Tran, F.; Kepenekian, M. Efficient and accurate calculation of band gaps of halide perovskites with the Tran-Blaha modified Becke–Johnson potential. *Phys. Rev. B* **2019**, *99*, 035139, DOI: doi:[10.1103/PhysRevB.99.035139](https://doi.org/10.1103/PhysRevB.99.035139).
- (721) Jana, S.; Sharma, K.; Samal, P. Improving the Performance of Tao–Mo Non-empirical Density Functional with Broader Applicability in Quantum Chemistry and Materials Science. *J. Phys. Chem. A* **2019**, *123*, 6356–6369, DOI: doi:[10.1021/acs.jpca.9b02921](https://doi.org/10.1021/acs.jpca.9b02921).
- (722) Patra, B.; Jana, S.; Constantin, L. A.; Samal, P. Efficient band gap prediction of semiconductors and insulators from a semilocal exchange–correlation functional. *Phys. Rev. B* **2019**, *100*, 045147, DOI: doi:[10.1103/PhysRevB.100.045147](https://doi.org/10.1103/PhysRevB.100.045147).
- (723) Bartók, A. P.; Yates, J. R. Regularized SCAN functional. *J. Chem. Phys.* **2019**, *150*, 161101, DOI: doi:[10.1063/1.5094646](https://doi.org/10.1063/1.5094646).
- (724) Mejía-Rodríguez, D.; Trickey, S. B. Comment on "Regularized SCAN functional" [J. Chem. Phys. 150, 161101 (2019)]. *J. Chem. Phys.* **2019**, *151*, 207101, DOI: doi:[10.1063/1.5120408](https://doi.org/10.1063/1.5120408).
- (725) Bartók, A. P.; Yates, J. R. Response to "Comment on 'Regularized SCAN functional'" [J. Chem. Phys. 151, 207101 (2019)]. *J. Chem. Phys.* **2019**, *151*, 207102, DOI: doi:[10.1063/1.5128484](https://doi.org/10.1063/1.5128484).
- (726) Furness, J. W.; Kaplan, A. D.; Ning, J.; Perdew, J. P.; Sun, J. Accurate and Numerically Efficient r²SCAN Meta-Generalized Gradient Approximation. *J. Phys. Chem. Lett.* **2020**, *11*, 8208–8215, DOI: doi:[10.1021/acs.jpcclett.0c02405](https://doi.org/10.1021/acs.jpcclett.0c02405).
- (727) Furness, J. W.; Kaplan, A. D.; Ning, J.; Perdew, J. P.; Sun, J. Correction to "Accurate and Numerically Efficient r²SCAN Meta-Generalized Gradient Approximation". *J. Phys. Chem. Lett.* **2020**, *11*, 9248–9248, DOI: doi:[10.1021/acs.jpcclett.0c03077](https://doi.org/10.1021/acs.jpcclett.0c03077).
- (728) Patra, A.; Jana, S.; Myneni, H.; Samal, P. Laplacian free and asymptotic corrected semilocal exchange potential applied to the band gap of solids. *Phys. Chem. Chem. Phys.* **2019**, *21*, 19639–19650, DOI: doi:[10.1039/C9CP03356D](https://doi.org/10.1039/C9CP03356D).
- (729) Smeets, E. W. F.; Voss, J.; Kroes, G.-J. Specific Reaction Parameter Density Functional Based on the Meta-Generalized Gradient Approximation: Application to H₂ + Cu(111) and H₂ + Ag(111). *J. Phys. Chem. A* **2019**, *123*, 5395–5406, DOI: doi:[10.1021/acs.jpca.9b02914](https://doi.org/10.1021/acs.jpca.9b02914).
- (730) Aschebrock, T.; Kümmel, S. Ultranonlocality and accurate band gaps from a meta-generalized

- gradient approximation. *Phys. Rev. Res.* **2019**, *1*, 033082, DOI: doi:[10.1103/PhysRevResearch.1.033082](https://doi.org/10.1103/PhysRevResearch.1.033082).
- (731) Lebeda, T.; Aschebrock, T.; Kümmel, S. First steps towards achieving both ultranonlocality and a reliable description of electronic binding in a meta-generalized gradient approximation. *Phys. Rev. Res.* **2022**, *4*, 023061, DOI: doi:[10.1103/PhysRevResearch.4.023061](https://doi.org/10.1103/PhysRevResearch.4.023061).
- (732) Ahmed, U.; Johansson, M. P.; Lehtola, S.; Sundholm, D. Density functional benchmark for quadruple hydrogen bonds. *Phys. Chem. Chem. Phys.* **2025**, *27*, 8706, DOI: doi:[10.1039/d5cp00836k](https://doi.org/10.1039/d5cp00836k).
- (733) Rauch, T.; Marques, M. A. L.; Botti, S. Local Modified Becke–Johnson Exchange–Correlation Potential for Interfaces, Surfaces, and Two-Dimensional Materials. *J. Chem. Theory Comput.* **2020**, *16*, 2654–2660, DOI: doi:[10.1021/acs.jctc.9b01147](https://doi.org/10.1021/acs.jctc.9b01147).
- (734) Rauch, T.; Marques, M. A. L.; Botti, S. Accurate electronic band gaps of two-dimensional materials from the local modified Becke–Johnson potential. *Phys. Rev. B* **2020**, *101*, 245163, DOI: doi:[10.1103/physrevb.101.245163](https://doi.org/10.1103/physrevb.101.245163).
- (735) Rauch, T.; Marques, M. A. L.; Botti, S. Erratum: Accurate electronic band gaps of two-dimensional materials from the local modified Becke–Johnson potential [Phys. Rev. B 101, 245163 (2020)]. *Phys. Rev. B* **2020**, *102*, 119902, DOI: doi:[10.1103/physrevb.102.119902](https://doi.org/10.1103/physrevb.102.119902).
- (736) Hastrup, S.; Strange, M.; Pandey, M.; Deilmann, T.; Schmidt, P. S.; Hinsche, N. F.; Gjerding, M. N.; Torelli, D.; Larsen, P. M.; Riis-Jensen, A. C.; Gath, J.; Jacobsen, K. W.; Mortensen, J. J.; Olsen, T.; Thygesen, K. S. The Computational 2D Materials Database: high-throughput modeling and discovery of atomically thin crystals. *2D Mater.* **2018**, *5*, 042002, DOI: doi:[10.1088/2053-1583/aacfc1](https://doi.org/10.1088/2053-1583/aacfc1).
- (737) Mejía-Rodríguez, D.; Trickey, S. B. Meta-GGA performance in solids at almost GGA cost. *Phys. Rev. B* **2020**, *102*, 121109, DOI: doi:[10.1103/PhysRevB.102.121109](https://doi.org/10.1103/PhysRevB.102.121109).
- (738) Patra, A.; Jana, S.; Samal, P. A way of resolving the order-of-limit problem of Tao–Mo semilocal functional. *J. Chem. Phys.* **2020**, *153*, 184112, DOI: doi:[10.1063/5.0025173](https://doi.org/10.1063/5.0025173).
- (739) Furness, J. W.; Sengupta, N.; Ning, J.; Ruzsinszky, A.; Sun, J. Examining the order-of-limits problem and lattice constant performance of the Tao–Mo functional. *J. Chem. Phys.* **2020**, *152*, 244112, DOI: doi:[10.1063/5.0008014](https://doi.org/10.1063/5.0008014).
- (740) Neupane, B.; Tang, H.; Nepal, N. K.; Adhikari, S.; Ruzsinszky, A. Opening band gaps of low-dimensional materials at the meta-GGA level of density functional approximations. *Phys. Rev. Mater.* **2021**, *5*, 063803, DOI: doi:[10.1103/PhysRevMaterials.5.063803](https://doi.org/10.1103/PhysRevMaterials.5.063803).
- (741) Tran, F.; Doumont, J.; Kalantari, L.; Blaha, P.; Rauch, T.; Borlido, P.; Botti, S.; Marques, M. A. L.; Patra, A.; Jana, S.; Samal, P. Bandgap of two-dimensional materials: Thorough assessment of modern exchange–correlation functionals. *J. Chem. Phys.* **2021**, *155*, 104103, DOI: doi:[10.1063/5.0059036](https://doi.org/10.1063/5.0059036).
- (742) Brown, K.; Maimaiti, Y.; Trepte, K.; Bligaard, T.; Voss, J. MCML: Combining physical constraints with experimental data for a multi-purpose meta-generalized gradient approximation. *J. Comput. Chem.* **2021**, *42*, 2004–2013, DOI: doi:[10.1002/jcc.26732](https://doi.org/10.1002/jcc.26732).
- (743) Heyd, J.; Scuseria, G. E.; Ernzerhof, M. Hybrid functionals based on a screened Coulomb potential. *J. Chem. Phys.* **2003**, *118*, 8207, DOI: doi:[10.1063/1.1564060](https://doi.org/10.1063/1.1564060).

- (744) Heyd, J.; Scuseria, G. E.; Ernzerhof, M. Erratum: "Hybrid functionals based on a screened Coulomb potential" [J. Chem. Phys. 118, 8207 (2003)]. *J. Chem. Phys.* **2006**, *124*, 219906, DOI: doi:[10.1063/1.2204597](https://doi.org/10.1063/1.2204597).
- (745) Krukau, A. V.; Vydrov, O. A.; Izmaylov, A. F.; Scuseria, G. E. Influence of the exchange screening parameter on the performance of screened hybrid functionals. *J. Chem. Phys.* **2006**, *125*, 224106, DOI: doi:[10.1063/1.2404663](https://doi.org/10.1063/1.2404663).
- (746) Holzwarth, N. A. W.; Torrent, M.; Charraud, J.-B.; Côté, M. Cubic spline solver for generalized density functional treatments of atoms and generation of atomic datasets for use with exchange-correlation functionals including meta-GGA. *Phys. Rev. B* **2022**, *105*, 125144, DOI: doi:[10.1103/PhysRevB.105.125144](https://doi.org/10.1103/PhysRevB.105.125144).
- (747) Furness, J. W.; Kaplan, A. D.; Ning, J.; Perdew, J. P.; Sun, J. Construction of meta-GGA functionals through restoration of exact constraint adherence to regularized SCAN functionals. *J. Chem. Phys.* **2022**, *156*, 034109, DOI: doi:[10.1063/5.0073623](https://doi.org/10.1063/5.0073623).
- (748) Trepte, K.; Voss, J. Data-driven and constrained optimization of semi-local exchange and nonlocal correlation functionals for materials and surface chemistry. *J. Comput. Chem.* **2022**, *43*, 1104–1112, DOI: doi:[10.1002/jcc.26872](https://doi.org/10.1002/jcc.26872).
- (749) Sabatini, R.; Gorni, T.; de Gironcoli, S. Nonlocal van der Waals density functional made simple and efficient. *Phys. Rev. B* **2013**, *87*, 041108, DOI: doi:[10.1103/PhysRevB.87.041108](https://doi.org/10.1103/PhysRevB.87.041108).
- (750) Kaplan, A. D.; Perdew, J. P. Laplacian-level meta-generalized gradient approximation for solid and liquid metals. *Phys. Rev. Materials* **2022**, *6*, 083803, DOI: doi:[10.1103/PhysRevMaterials.6.083803](https://doi.org/10.1103/PhysRevMaterials.6.083803).
- (751) Tran, F.; Stelzl, J.; Blaha, P. Rungs 1 to 4 of DFT Jacob's ladder: Extensive test on the lattice constant, bulk modulus, and cohesive energy of solids. *J. Chem. Phys.* **2016**, *144*, 204120, DOI: doi:[10.1063/1.4948636](https://doi.org/10.1063/1.4948636).
- (752) Francisco, H.; Cancio, A. C.; Trickey, S. B. Reworking the Tao–Mo exchange-correlation functional. I. Reconsideration and simplification. *J. Chem. Phys.* **2023**, *159*, 214102, DOI: doi:[10.1063/5.0167868](https://doi.org/10.1063/5.0167868).
- (753) Francisco, H.; Cancio, A. C.; Trickey, S. B. Reworking the Tao–Mo exchange-correlation functional. II. De-orbitalization. *J. Chem. Phys.* **2023**, *159*, 214103, DOI: doi:[10.1063/5.0167873](https://doi.org/10.1063/5.0167873).
- (754) Francisco, H.; Cancio, A. C.; Trickey, S. B. Reworking the Tao–Mo Exchange–Correlation Functional. III. Improved Deorbitalization Strategy and Faithful Deorbitalization. *J. Phys. Chem. A* **2024**, *128*, 6010–6018, DOI: doi:[10.1021/acs.jpca.4c02635](https://doi.org/10.1021/acs.jpca.4c02635).
- (755) Aschebrock, T.; Lebeda, T.; Brütting, M.; Richter, R.; Schelter, I.; Kümmel, S. Exact exchange-like electric response from a meta-generalized gradient approximation: A semilocal realization of ultranonlocality. *J. Chem. Phys.* **2023**, *159*, 234107, DOI: doi:[10.1063/5.0173776](https://doi.org/10.1063/5.0173776).
- (756) Cai, Y.; Michiels, R.; De Luca, F.; Neyts, E.; Tu, X.; Bogaerts, A.; Gerrits, N. Improving Molecule-Metal Surface Reaction Networks Using the Meta-Generalized Gradient Approximation: CO₂ Hydrogenation. *J. Phys. Chem. C* **2024**, *128*, 8611–8620, DOI: doi:[10.1021/acs.jpcc.4c01110](https://doi.org/10.1021/acs.jpcc.4c01110).
- (757) Ramasamy, A.; Hou, L.; Bazantes, J. V.; Irons, T. J. P.; Wibowo-Teale, A. M.; Lebeda, T.; Sun, J. Tackling the one-electron self-interaction error within the semilocal density functional framework.

- Phys. Rev. B* **2025**, *112*, L161112, DOI: doi:10.1103/dkf7-jkb4.
- (758) Becke, A. D. Thermochemical tests of a kinetic-energy dependent exchange-correlation approximation. *Int. J. Quantum Chem.* **1994**, *52*, 625–632, DOI: doi:10.1002/qua.560520855.
- (759) Proynov, E. I.; Vela, A.; Salahub, D. R. Nonlocal correlation functional involving the Laplacian of the density. *Chem. Phys. Lett.* **1994**, *230*, 419–428, DOI: doi:10.1016/0009-2614(94)01189-3.
- (760) Proynov, E. I.; Vela, A.; Salahub, D. R. Nonlocal correlation functional involving the Laplacian of the density (Chem. Phys. Letters 230 (1994) 419). *Chem. Phys. Lett.* **1995**, *234*, 462, DOI: doi:10.1016/0009-2614(95)00113-i.
- (761) Proynov, E. I.; Ruiz, E.; Vela, A.; Salahub, D. R. Determining and extending the domain of exchange and correlation functionals. *Int. J. Quantum Chem.* **1995**, *56*, 61–78, DOI: doi:10.1002/qua.560560808.
- (762) Tsuneda, T.; Hirao, K. A new spin-polarized Colle-Salvetti-type correlation energy functional. *Chem. Phys. Lett.* **1997**, *268*, 510–520, DOI: doi:10.1016/S0009-2614(97)00201-7.
- (763) Carravetta, V.; Clementi, E. Water-water interaction potential: An approximation of the electron correlation contribution by a functional of the SCF density matrix. *J. Chem. Phys.* **1984**, *81*, 2646–2651, DOI: doi:10.1063/1.447973.
- (764) Krieger, J. B.; Chen, J.; Kurth, S. Construction and application of an accurate self-interaction-corrected correlation energy functional based on an electron gas with a gap. *AIP Conf. Proc.* **2001**, *577*, 48–69, DOI: doi:10.1063/1.1390178.
- (765) Proynov, E.; Kong, J. Improved meta-GGA Correlation Functional of the Lap Family. *J. Chem. Theory Comput.* **2007**, *3*, 746–754, DOI: doi:10.1021/ct600372t.
- (766) Proynov, E.; Kong, J. An Improved meta-GGA Correlation Functional of the Lap Family. *J. Chem. Theory Comput.* **2012**, *8*, 1514–1514, DOI: doi:10.1021/ct2009076.
- (767) Taut, M. Two electrons in an external oscillator potential: Particular analytic solutions of a Coulomb correlation problem. *Phys. Rev. A* **1993**, *48*, 3561–3566, DOI: doi:10.1103/PhysRevA.48.3561.
- (768) Zhao, Y.; Truhlar, D. G. Exploring the Limit of Accuracy of the Global Hybrid Meta Density Functional for Main-Group Thermochemistry, Kinetics, and Noncovalent Interactions. *J. Chem. Theory Comput.* **2008**, *4*, 1849, DOI: doi:10.1021/ct800246v.
- (769) Gräfenstein, J.; Izotov, D.; Cremer, D. Avoiding singularity problems associated with meta-GGA (generalized gradient approximation) exchange and correlation functionals containing the kinetic energy density. *J. Chem. Phys.* **2007**, *127*, 214103, DOI: doi:10.1063/1.2800011.
- (770) Schmidt, T.; Kraisler, E.; Makmal, A.; Kronik, L.; Kümmel, S. A self-interaction-free local hybrid functional: Accurate binding energies vis-à-vis accurate ionization potentials from Kohn–Sham eigenvalues. *J. Chem. Phys.* **2014**, *140*, 18A510, DOI: doi:10.1063/1.4865942.
- (771) Perdew, J. P.; Tao, J.; Staroverov, V. N.; Scuseria, G. E. Meta-generalized gradient approximation: Explanation of a realistic nonempirical density functional. *J. Chem. Phys.* **2004**, *120*, 6898, DOI: doi:10.1063/1.1665298.
- (772) Ivanov, S.; Levy, M. Connections between High-Density Scaling Limits of DFT Correlation Energies and

- Second-Order Z-1 Quantum Chemistry Correlation Energy. *J. Phys. Chem. A* **1998**, *102*, 3151–3156, DOI: doi:[10.1021/jp9731415](https://doi.org/10.1021/jp9731415).
- (773) Jana, S.; Behera, S. K.; Śmiga, S.; Constantin, L. A.; Samal, P. Improving the applicability of the Pauli kinetic energy density based semilocal functional for solids. *New J. Phys.* **2021**, *23*, 063007, DOI: doi:[10.1088/1367-2630/abfd4d](https://doi.org/10.1088/1367-2630/abfd4d).
- (774) Jana, S.; Behera, S. K.; Śmiga, S.; Constantin, L. A.; Samal, P. Accurate density functional made more versatile. *J. Chem. Phys.* **2021**, *155*, 024103, DOI: doi:[10.1063/5.0051331](https://doi.org/10.1063/5.0051331).
- (775) Jana, S.; Constantin, L. A.; Samal, P. Density functional applications of jellium with a local gap model correlation energy functional. *J. Chem. Phys.* **2023**, *159*, 114109, DOI: doi:[10.1063/5.0160961](https://doi.org/10.1063/5.0160961).
- (776) Cancio, A. C.; Chou, M. Y. Beyond the local approximation to exchange and correlation: The role of the Laplacian of the density in the energy density of Si. *Phys. Rev. B* **2006**, *74*, 081202, DOI: doi:[10.1103/PhysRevB.74.081202](https://doi.org/10.1103/PhysRevB.74.081202).
- (777) Hood, R. Q.; Chou, M. Y.; Williamson, A. J.; Rajagopal, G.; Needs, R. J.; Foulkes, W. M. C. Quantum Monte Carlo Investigation of Exchange and Correlation in Silicon. *Phys. Rev. Lett.* **1997**, *78*, 3350–3353, DOI: doi:[10.1103/PhysRevLett.78.3350](https://doi.org/10.1103/PhysRevLett.78.3350).
- (778) Hood, R. Q.; Chou, M. Y.; Williamson, A. J.; Rajagopal, G.; Needs, R. J. Exchange and correlation in silicon. *Phys. Rev. B* **1998**, *57*, 8972–8982, DOI: doi:[10.1103/PhysRevB.57.8972](https://doi.org/10.1103/PhysRevB.57.8972).
- (779) Schwabe, T.; Grimme, S. Double-hybrid density functionals with long-range dispersion corrections: higher accuracy and extended applicability. *Phys. Chem. Chem. Phys.* **2007**, *9*, 3397–3406, DOI: doi:[10.1039/B704725H](https://doi.org/10.1039/B704725H).
- (780) Mardirossian, N.; Head-Gordon, M. Mapping the genome of meta-generalized gradient approximation density functionals: The search for B97M-V. *J. Chem. Phys.* **2015**, *142*, 074111, DOI: doi:[10.1063/1.4907719](https://doi.org/10.1063/1.4907719).
- (781) Vydrov, O. A.; Van Voorhis, T. Non-local van der Waals density functional: The simpler the better. *J. Chem. Phys.* **2010**, *133*, 244103, DOI: doi:[10.1063/1.3521275](https://doi.org/10.1063/1.3521275).
- (782) Verma, P.; Truhlar, D. G. HLE17: An Improved Local Exchange–Correlation Functional for Computing Semiconductor Band Gaps and Molecular Excitation Energies. *J. Phys. Chem. C* **2017**, *121*, 7144–7154, DOI: doi:[10.1021/acs.jpcc.7b01066](https://doi.org/10.1021/acs.jpcc.7b01066).